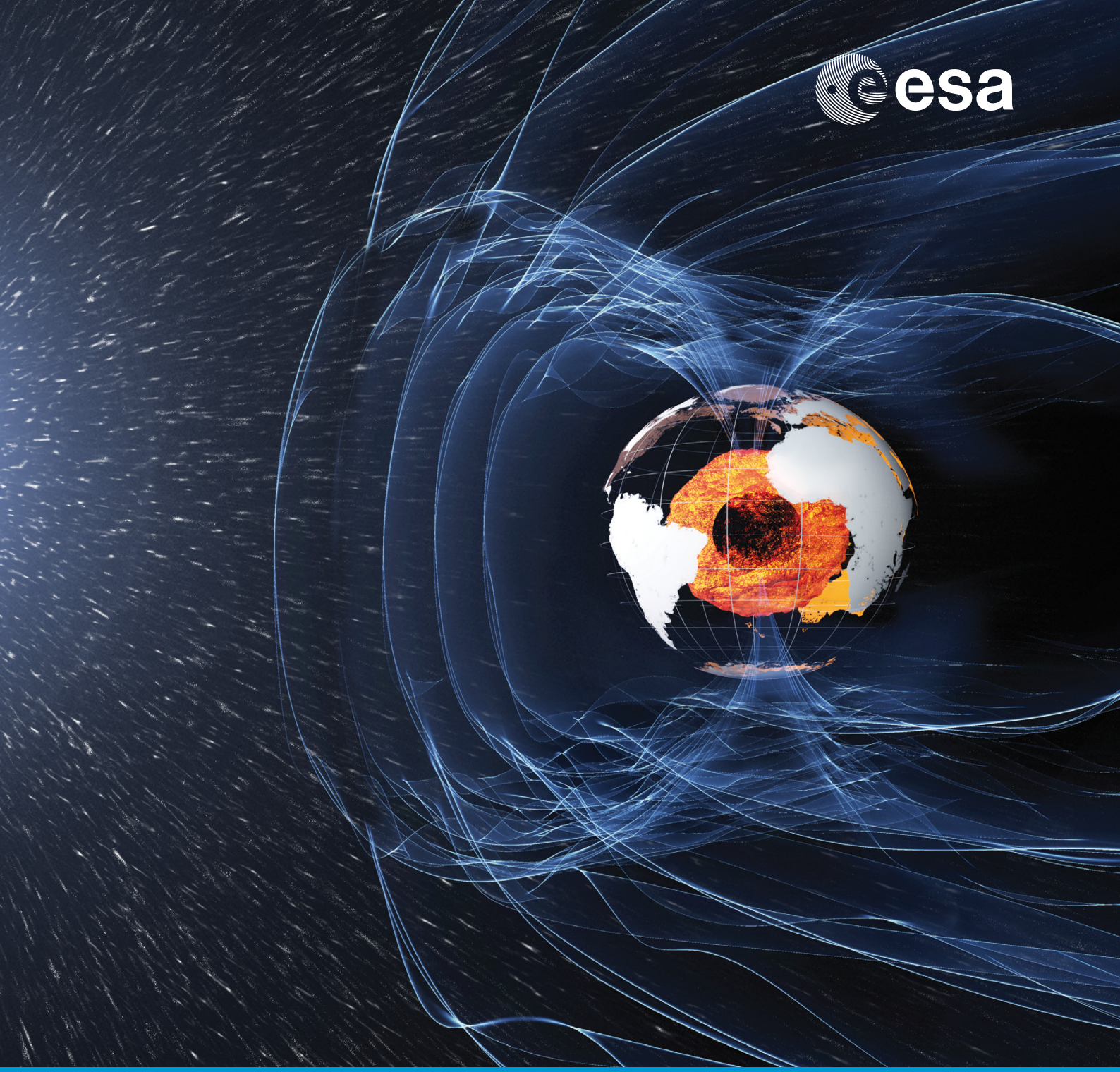

→ ESA'S REPORT TO THE 39TH COSPAR MEETING

Mysore, India, July 2012

www.esa.int

European Space Agency

SP-1323
June 2012

→ ESA'S REPORT TO THE 39TH COSPAR MEETING

Mysore, India, July 2012

European Space Agency

Acknowledgements

This report on the scientific activities of the European Space Agency was written by members of the Directorate of Earth Observation, the Directorate of Human Spaceflight and Operations and the Directorate of Science and Robotic Exploration. Special thanks go to M. Rast, J. Weems, R. Schulz and C. Bingham.

The authors acknowledge the use of published and unpublished material supplied by experimenters, observers and colleagues.

The report was completed in June 2012.

Communications should be addressed to the scientific editor:
M. McCaughrean
Research & Scientific Support Department
European Space Research and Technology Centre (ESTEC)
Postbus 299
NL-2200 AG Noordwijk
The Netherlands
Tel: +31 71 565-3552
Email: Mark.McCaughrean@esa.int

Cover: Artist's impression of the interaction of the solar wind with Earth's magnetic field. (ESA/AOES Medialab)

An ESA Communications Production

Publication *ESA's Report to the 39th COSPAR Meeting* (ESA SP-1323, June 2012)

Project Leader K. Fletcher

Scientific Editor M. McCaughrean

Editing/Layout Contactivity bv, Leiden, the Netherlands

Publisher ESA Communications
ESTEC, PO Box 299, 2200 AG Noordwijk, the Netherlands
Tel: +31 71 565 3408 Fax: +31 71 565 5433 www.esa.int

ISBN 978-92-9221-421-0

ISSN 0379-6566

Foreword

It may seem obvious, but it is worth underlining nonetheless: science is a key component of the European Space Agency's activities. ESA has an impressive track record when it comes to space science and Earth sciences. There is a broad emphasis within ESA programmes on the advancement of knowledge, the science of the Universe, exploration of the Solar System, fundamental physics, Earth sciences, our environment, plus a whole range of scientific activities that make use of space as a laboratory, on the International Space Station (ISS) in particular.

ESA's Science Programme is a backbone activity. Since the last COSPAR Scientific Assembly, held in 2010 in Bremen, Germany, there have been plenty of fresh mission results and scientific findings. Since its launch, coupled with that of Herschel in May 2009, the Planck mission has been taking the most accurate measurements ever of the cosmic microwave background radiation left over after the Big Bang. These investigations are helping us learn more about the birth, evolution and ultimate fate of the Universe.

In early 2011, scientists from ESA and several European astronomy institutes presented early data and results from Planck. Thousands of galaxy clusters and dense clouds in the Milky Way were detected at radio to far-infrared wavelengths, and the catalogue released to the public. The Herschel infrared observatory has revealed hitherto hidden details of star formation and shown that the water in comet 103P/Hartley 2 has the same deuterium-to-hydrogen ratio as the oceans on Earth, providing a tantalising clue to a hotly-debated scientific question: the origin of water on our planet. While the Rosetta probe cruises on towards a rendezvous with its target comet in 2014, scientists have been busy analysing the treasure trove of data collected during its 2010 flyby of asteroid (21) Lutetia. The results suggest that underneath its cold and cracked exterior, the asteroid may once have harboured a molten metallic core. Many other space science missions have contributed to extending our knowledge of the Universe. In addition, ESA has made significant progress on its upcoming space science missions, promising a future every bit as exciting.

Science is also a key component of many of ESA's Earth observation programmes, starting with the series of Earth Explorer missions. CryoSat-2, a satellite devoted to studying ice cover on our planet, was launched in 2010. Thanks to this mission, and two others launched in 2009, ESA has become the space agency currently devoting the greatest efforts to studying climate change. SMOS has delivered results on soil moisture and ocean salinity, while GOCE gave us its first global gravity model in 2010. ESA is actively working for enhanced international cooperation on understanding and tackling global-scale environmental challenges. Earth observation data are increasingly being used for such purposes. Today, Europe is at the forefront of Earth observation endeavours, thanks to the success of ESA's satellite programmes.

With the ISS, and in particular ESA's Columbus laboratory, Europe has access to a unique research facility in low-Earth orbit. In May 2011, ESA astronaut Roberto Vittori and his five crewmates carried out a mission to deliver to the ISS the Alpha Magnetic Spectrometer, a highly sophisticated international instrument designed to identify the cosmic fingerprints left by antimatter and dark matter in the Universe.

While astronauts attract much attention, we should not forget that most of the people working on or making use of the ISS are based not out there in space, but firmly on the ground. A wide variety of research projects is being supported by the European Programme for Life and Physical Sciences in Space (ELIPS). Europe's large science community and research institutions are actively pushing back the boundaries of science and technology, further strengthening Europe's already strong position in research. In doing so, they are building on the capabilities already in place on the ISS, in particular

Columbus, as well as other research platforms, including ground-based drop towers, parabolic flights and sounding rockets.

Science is clearly a key component of ESA's programmes. The Agency is investing effort in pursuing a 'science-led, one-ESA' vision. This involves taking an Agency-wide coherent and comprehensive approach to science and technology as a whole, encouraging and mapping out the route for cross-directorate synergies in science and science-related activities throughout the organisation. This vision also embraces more recent programmatic fields of scientific relevance, notably satellite navigation. It emphasises the interrelationship between science and technology. And it aims to look ahead – beyond currently approved programmes – to ensure that the Agency paves the way for a future full of new scientific discoveries and breakthroughs in knowledge.

Jean-Jacques Dordain
Director General
European Space Agency

Contents

→ EARTH OBSERVATION

Contents

→ INTRODUCTION

1. Introduction

ESA's Earth Observation Programme plays an essential role in advancing science and ensuring that Europe keeps pace with the challenges of a changing world. From their vantage points in space, satellites offer the only means of monitoring the entire planet. Carrying novel observational capabilities, they are able to deliver critical information to explore and understand the complexities of how Earth works as a system, and detect the changes taking place. To improve our understanding of natural Earth processes, this robust programme harnesses the relationship between science and technology to forge innovative missions that address the most urgent scientific questions of our time.

For understanding the mechanisms and interactions between the different compounds of Earth's system, the availability of precise and regularly updated data is essential. This basic information includes atmospheric circulation dynamics, its chemistry and its interactions with land and ocean surfaces, as well as their respective interactions with solar radiation and gravity. ESA will continue to provide reliable key data for this important research.

To be able to respond to these requirements, new technological developments have been made and will be carried out in the future in a large cooperation effort between European research institutions and space industries. These efforts also ensure high-class research and development, as well as excellence in education and training capacities being further extended.

In the framework of global change, there is a need to better understand critical parameters such as clouds and how they affect Earth's thermal budget, the carbon storage capacity of biomass and soils, the impacts of changing concentrations of certain atmospheric gases as well as variations in the water cycle. The next generation of ESA's 'Earth Explorer' missions will need to address these knowledge and data gaps.

Earth observation data are now systematically used for global climate change models and forecasts in Intergovernmental Panel on Climate Change (IPCC) reports. Through the Global Climate Observing System (GCOS), the international science community requests the provision of long time-series of critical global and regional information. ESA started pioneering in this field by providing the requested 'Essential Climate Variables' to the science community.

International cooperation is a prerequisite for deploying the complex monitoring systems needed for Earth science. The high level of performance in space and Earth science activities, which is evidenced by the key scientific achievements of the series of Earth Explorer missions, is based on the unbiased process in which missions are selected. These state-of-the-art satellites are filling specific gaps in our knowledge. The relation with the science community as users and as a source of proposals for future payloads needs sustained efforts on the ESA side to involve the new generation of scientists, encourage networking among the science community, and maintain its impact on upfront scientific endeavours such as IPCC reporting.

The Earth Observation Programme draws on existing findings to identify gaps in our knowledge and to make sure that new satellite missions provide complementary information. This approach offers new opportunities for exploiting synergies and developing new applications.

The success of the programme places Europe at the forefront of Earth observation. It also lays the foundation for international cooperation for a collaborative approach to understanding and tackling global environmental challenges.

A better knowledge of how Earth works and how it is changing relies on sustained commitment, to which Europe can respond through ESA's Earth Observation Envelope Programme. Many of the quantitative indicators that

Table 1.1. Earth observation operational missions, status May 2012.

Satellite	Launch date	End of operational life	Mission
Meteosat-1	23 November 1977	25 November 1979	Meteorology, climatology
Meteosat-2	19 June 1981	11 August 1988	Meteorology, climatology
Meteosat-3	15 June 1988	31 May 1995	Meteorology, climatology
Meteosat-4	6 March 1989	4 February 1994	Meteorology, climatology
Meteosat-5	2 March 1991	16 April 2007	Meteorology, climatology, atmospheric dynamics, water and energy cycles
ERS-1	17 July 1991	10 March 2000	Earth resources, physical oceanography, ice and snow, land surface, meteorology, environmental monitoring
Meteosat-6	20 November 1993	15 April 2011	Meteorology, climatology, atmospheric dynamics/water and energy cycles.
ERS-2	21 April 1995	4 July 2011	Earth resources, physical oceanography, ice and snow, land surface, meteorology, geodesy, environmental monitoring, atmospheric chemistry
Meteosat-7	2 September 1997	December 2013	Meteorology, climatology, atmospheric dynamics/water and energy cycles.
Proba	22 October 2001	December 2012	Earth resources science and applications
Envisat	1 March 2002	8 April 2012	Oceanography, land surface, ice and snow, atmospheric chemistry and dynamics, water and energy cycles, environment, climatology
MSG-1 (Meteosat-8)	28 August 2002	August 2012	Meteorology, climatology, atmospheric dynamics/water and energy cycles.
MSG-2 (Meteosat-9)	21 December 2005	December 2015	Meteorology, climatology, atmospheric dynamics/water and energy cycles.
MetOp-A	19 October 2006	December 2013	Meteorology, climatology
GOCE	17 March 2009	December 2012 (extension possible)	Earth's gravity field and geoid, ocean circulation, Earth interior
SMOS	2 November 2009	November 2012 (extension possible)	Global observations of soil moisture and ocean salinity, vegetation water content, snow and ice.
CryoSat-2	8 April 2010	October 2013 (extension possible)	Mass of land and marine ice fields

will be discussed at Rio+20 in June 2012 with regard to the progress over the last 20 years will have been derived largely or exclusively from satellite Earth observation data.

ESA's Earth Observation Programme offers a solid base for Europe to further science and develop superior technology, and thus to secure a solid heritage for future missions for scientific as well as operational purposes.

Table 1.2. Earth observation planned missions, status May 2012.

Satellite	Launch date	Mission
MetOp-B	2012	Meteorology, climatology
MSG-3 (Meteosat-10)	2012	Meteorology, climatology, atmospheric dynamics/ water and energy cycles.
Swarm	2012	Geomagnetic field, Earth interior and climate
Sentinel-1A	2013	Operational monitoring of sea ice, marine environment, land surface
Sentinel-3A	2014	Global land and ocean monitoring services
Sentinel-2A	2014	Land monitoring related services
SeoSat-Ingenio	2014	Cartography, land use, urban management, water management, environmental monitoring, risk management and security.
ADM-Aeolus	2014	Global 3D wind field, atmospheric dynamics
Sentinel-3B	2015	Global land and ocean monitoring services
MSG-4 (Meteosat-11)	2015	Meteorology, climatology, atmospheric dynamics/ water and energy cycles.
Sentinel-1B	2015	Operational monitoring of sea ice, marine environment, land surface
Sentinel-2B	2015	Land monitoring related services
Sentinel-5 precursor	2015	Supporting global atmospheric composition and air quality monitoring services. It will bridge the gap between Envisat and Sentinel-5
EarthCARE	2015	Atmospheric cloud–aerosol interactions and radiative balance
MetOp-C	2017	Meteorology, climatology
MTG-I1 (Imager)	2017	Meteorology, climatology, atmospheric dynamics/ water and energy cycles, air quality including Sentinel-4 for atmospheric chemistry monitoring on each of the MTG Sounder satellites
MTG-S1 (Sounder)	2019	
Sentinel-4A	2019	
Sentinel-5A	2020	
MTG-I2 (Imager)	2022	
MTG-I3 (Imager)	2026	
MTG-S2 (Sounder)	2028	
MTG-I4 (Imager)	2030	
MetOp-SG A1	2020	Meteorology, climatology, including Sentinel-5 for atmospheric chemistry monitoring on each of the MetOp-SG A satellites
MetOp-SG B1	2022	
MetOp-SG A2	2027	
MetOp-SG B2	2029	
MetOp-SG A3	2034	
MetOp-SG B3	2036	
Jason-CS A	2018	Low-inclination ocean surface topography
Jason-CS B	2023	Low-inclination ocean surface topography

→ THE LIVING PLANET PROGRAMME

2. The Living Planet Programme

ESA has been observing Earth from space since the launch of its first meteorological satellite, Meteosat, in 1977. Following the success of this mission, the subsequent series of Meteosat satellites, the European Remote Sensing (ERS) satellites ERS-1 and ERS-2, and Envisat have provided a wealth of valuable data about Earth, its climate and changing environment.

Monitoring our planet is crucial both to improve understanding of the Earth system and its processes, especially in the context of global change, and to predict the effects of climate change.

In response to the growing need for knowledge and for accurate satellite data for numerous practical applications, ESA created the Living Planet Programme. This comprises two elements: a science and research element, which includes the Earth Explorer missions, and an Earth Watch element, which is designed to facilitate the delivery of Earth observation (EO) data for use in operational services.

The Earth Explorer Element

The Earth Explorer missions are designed to address key data needs or gaps in knowledge that are identified by the science community (Fig. 2.1), while demonstrating breakthrough technologies and observing techniques. For each new mission, a number of candidate ideas or concepts are proposed, which go through a phased selection process and feasibility studies until one

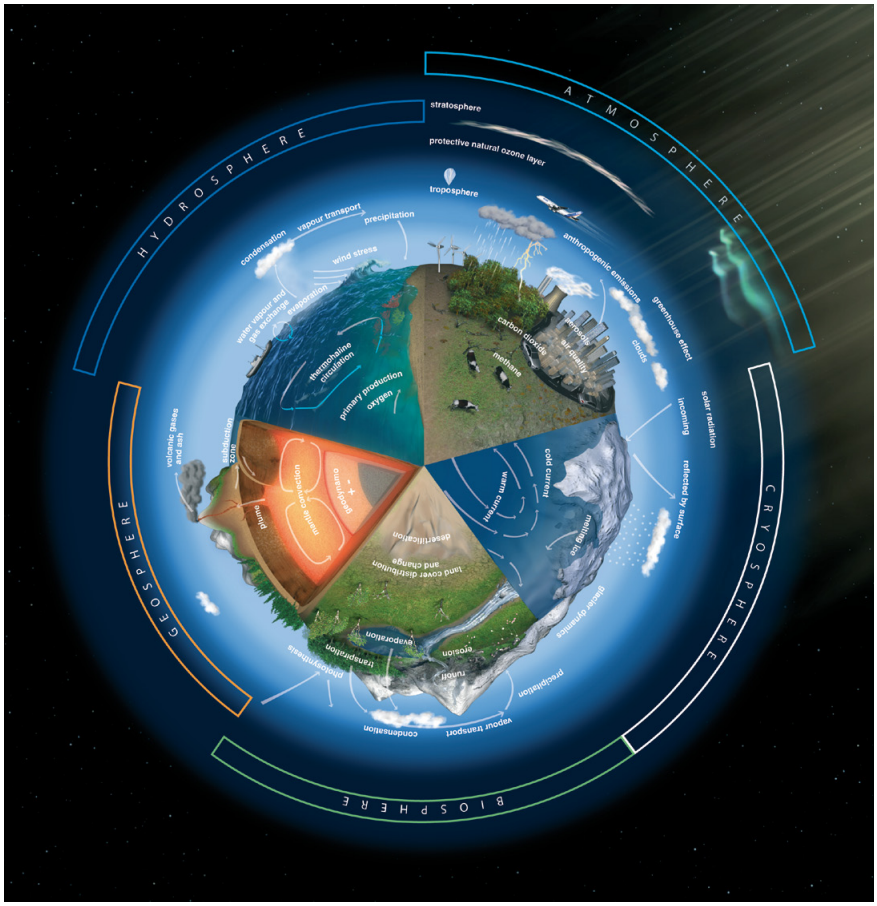

Figure 2.1. Scientific challenges for ESA's Living Planet Programme. (ESA/AOES Medialab)

Further information about ESA's Living Planet Programme can be found at *www.esa.int/esaLP*

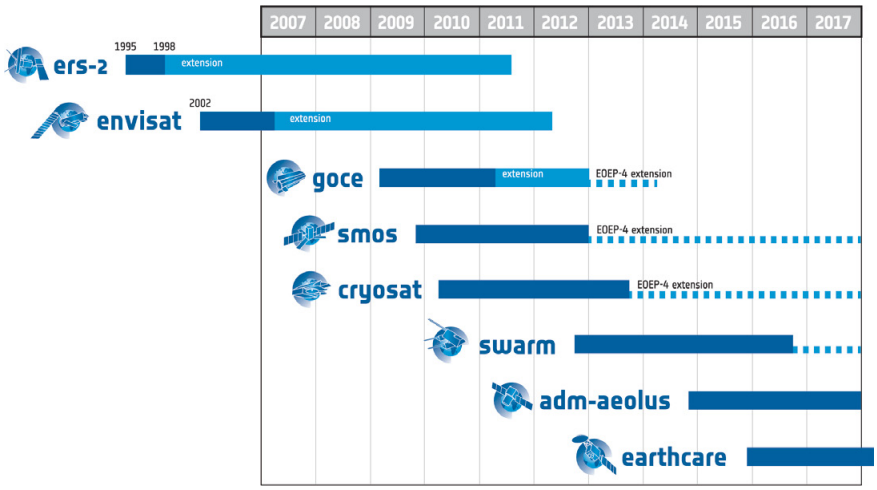

Figure 2.2. Timelines of ERS-2, Envisat and the Earth Observation Envelope Programme missions. (ESA)

candidate is selected. From the outset, the science community is involved in the definition of these new missions and in the peer-reviewed selection process to ensure that each mission is developed efficiently and provides the exact data required by users. This approach provides excellent opportunities for international cooperation, both in the scientific domain and in the technological development of new missions (Fig. 2.2).

The six Earth Explorer missions currently in orbit or in development are:

— Gravity field and steady-state Ocean Circulation Explorer (GOCE): ESA's gravity mission;
— Soil Moisture and Ocean Salinity mission (SMOS): ESA's water mission;
— CryoSat: ESA's ice mission;
— Swarm: ESA's magnetic field mission;
— Atmospheric Dynamics Mission (ADM)-Aeolus: ESA's wind mission; and
— Earth Cloud, Aerosol and Radiation Explorer (EarthCARE).

For the next two missions, provisionally known as Earth Explorers 7 and 8, five candidates are currently undergoing feasibility studies:

— Earth Explorer 7: Following ESA's Call for Ideas in 2005, three missions were selected for further study in 2009: Biomass, the Cold Regions Hydrology High-Resolution Observatory ($CoReH_2O$) and the Process Exploration through Measurement of Infrared and millimetre-wave Emitted Radiation (PREMIER). The final selection is expected in 2013.

— Earth Explorer 8: As a result of the Call for Proposals released in October 2009, two missions – CarbonSat and the Florescence Explorer (FLEX) – were approved to move forward as candidate missions to be studied at the level of Phase-A/B1 in 2012–13.

More detailed descriptions of the Earth Explorer 7 and 8 candidate missions can be found in section 3.3, Missions under study.

The Earth Watch Element

The Earth Watch element of the Living Planet Programme includes the operational satellite systems developed in partnership with the European Organisation for the Exploitation of Meteorological Satellites (Eumetsat), the European Community and public and private stakeholders. It covers the classical Phase-B studies involving identified industry partners who are prepared to contribute to a mission, and participate in additional activities necessary to define such a programme. The definition of an Earth Watch type

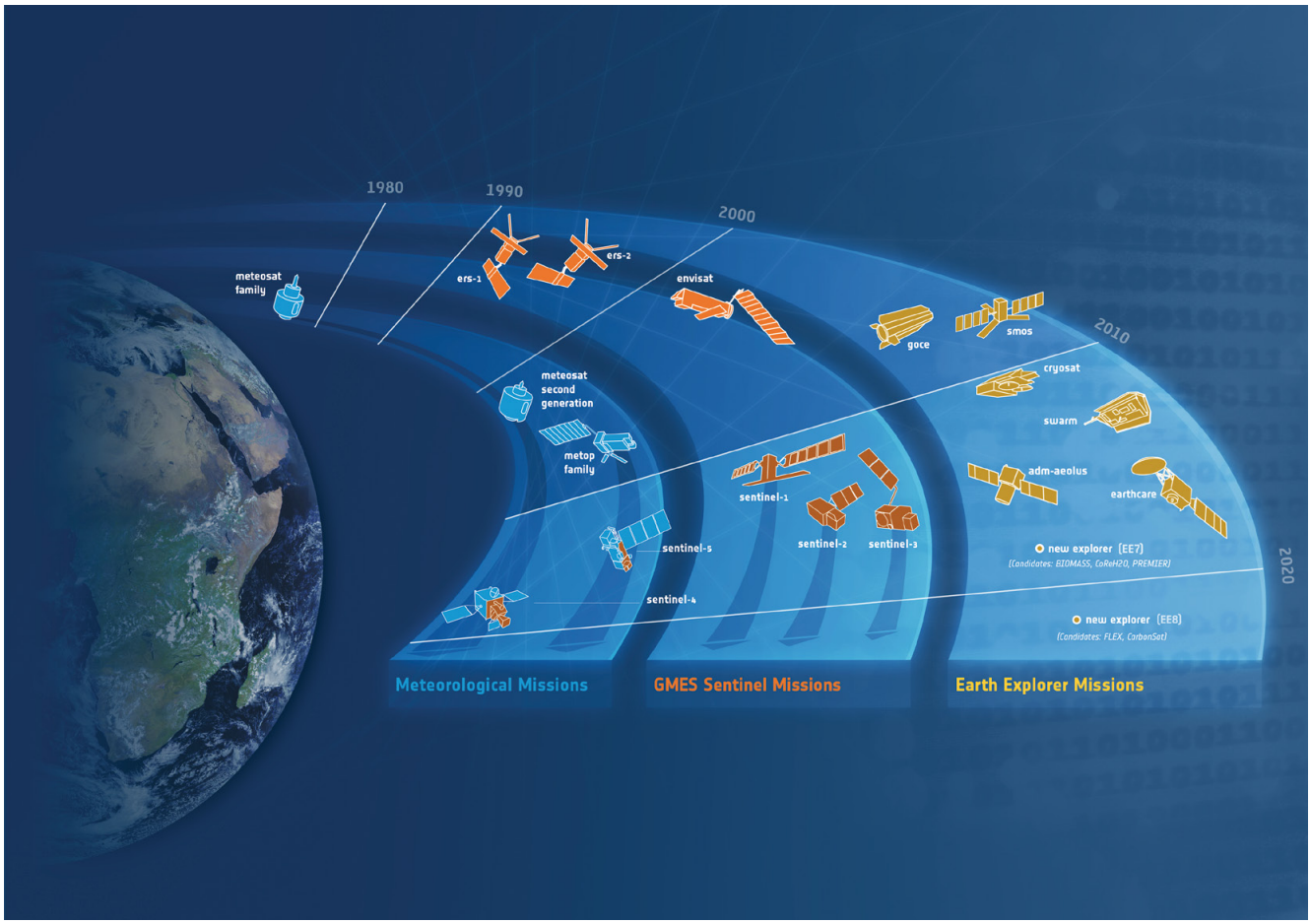

Figure 2.3. The Living Planet Programme. (ESA/EOGB)

Earth observation satellite mission concludes with a dossier specifying the end-to-end mission concept, partnership arrangements and a solid business case, where relevant.

The Global Monitoring for Environment and Security (GMES) initiative between ESA and the European Union (EU) features the Sentinel missions, which form part of the GMES Space Component (Fig. 2.3). The Sentinel missions will gather robust, long-term climate-relevant datasets that will be combined with other satellite data in archives and used to produce 'essential climate variables' for monitoring, modelling and prediction.

Reference

ESA (2006). *The Changing Earth: The Scientific Challenges for ESA's Living Planet Programme*. ESA SP-1304. European Space Agency, Noordwijk, the Netherlands. *http://esamultimedia.esa.int/docs/SP-1304.pdf*

2.1 The Earth Observation Envelope Programme

The Earth Observation Envelope Programme (EOEP) is a major contributor to the implementation of the Living Planet Strategy. Its strategic objectives are to pursue scientific knowledge, enhance the quality of life, create an independent European capability as the key to cooperation, and promote innovation, value-added services and industry in Europe.

Based on these objectives, EOEP aims to advance the scientific agenda of the Earth science community, and to respond to the challenges of global change and anthropogenic effects on the environment through the development and exploitation of appropriate new monitoring tools. The programme will also ensure the continuity of data provided by existing missions, thereby assisting governments to meet their commitments to protect the environment by:

— bulding strategic capabilities for independent European information gathering by supporting the early development of Earth Watch type operational missions;
— guaranteeing easy access to Earth observation data, including higher-level products for scientific use and for the development of applications;
— supporting Europe's position as a frontline player in the Earth observation scene and fostering international cooperation;
— ensuring the maximum scientific return on ESA's investments in Earth observation; and
— strengthening the competitiveness of European Earth observation industries and securing employment for highly qualified professionals.

EOEP's strategic objectives and the specific goals were confirmed for the second (2003–07) and third (2008–12) phases of the programme, in line with the European Strategy for Space defined jointly by ESA and the European Commission, including the GMES initiative.

Based on this strategy, EOEP provides a unique framework that enables ESA to respond quickly and effectively to the requirements and priorities of EO data users within a long-term planning horizon.

2.1.1 Components of EOEP

The Earth Observation Envelope Programme comprises two main components. First, the Earth Explorer component covers the definition, development, launch and operation of missions, including the platforms, payloads and their associated ground segments. Second, the development and exploitation component includes:

— preparatory activities for Earth Explorer and Earth Watch missions;
— instrument predevelopment for user-driven candidates for Earth Explorer and Earth Watch type missions;
— definition of Earth Watch type missions and the preparation of dedicated programme proposals for optional programmes; and
— mission exploitation/market development.

There are two types of Earth Explorer mission: core or major missions led by ESA that address its primary research objectives, and smaller opportunity missions that provide a rapid reaction capability. These latter missions contribute to and exploit the cross-fertilisation between research (Earth Explorer) and applications (Earth Watch).

The Earth Explorer missions are science driven, while the Earth Watch missions are user/market driven. All mission themes and partnership arrangements are based on the needs of a wide range of users, including scientists, the European

Union, Eumetsat and other European and national agencies, industry, commercial companies, etc.

All Earth Explorer and Earth Watch missions are based on coordination and cooperation among ESA, the European Community and Eumetsat, where ESA plays a valuable role in the coordination and progressive integration of European-level Earth observation activities. EOEP also takes into account of the need for coordination between ESA's and Member States' Earth observation strategies and programmes. It further supports, in particular through the Earth Explorer missions, international cooperation on a global scale and Europe's role in Earth observation, including making the necessary provisions for cooperation with developing countries.

Earth Explorer Component

The Earth Explorer component of the programme is intended to respond directly to the increasing public concerns about Earth, its environment and mankind's impact upon it, and to raise public awareness of global threats such as climate change, stratospheric ozone and tropospheric pollution, as well as regional phenomena such as El Niño events, forest fires and floods.

Effective responses to such concerns require a better understanding of the complex interaction processes within the Earth system. The Earth Explorer component contributes by addressing the research and associated demonstration requirements. At the outset of the programme, in consultation with researchers and user community, four interdisciplinary themes were identified: Earth's interior, the physical climate, the geosphere–biosphere, and anthropogenic impacts on the atmosphere and the marine environment.

The Earth Explorer mission concepts can be summarised as follows:

— Each mission is designed for a nominal operational period, in line with its scientific and/or demonstration objectives. Any extension of a mission after this nominal operational period requires detailed justification and must be implemented in the most cost-effective way. This, combined with cost capping, leads to small, cost-effective missions.

— The mission selection process is science driven.

— Within the agreed cost of an Earth Explorer mission, the programme funds the development of the complete satellite, including its payload, launch, the ground segment (satellite operations and data processing) and its operation during its nominal period.

— Following each Announcement of Opportunity (AO), the programme seeks contributions, e.g. instruments or platforms, from ESA Member States or international partners in order to reduce the overall cost of a mission, and thus provide value for money.

— In parallel with the research activities, the development and exploitation component of the programme investigates possible applications of Earth Explorer data.

— The ground segment associated with each mission is based as far as possible on existing multi-mission infrastructures already available to ESA programmes in order to minimise both investment and exploitation costs. The data processing by ESA, in support of the provision of data and associated services to the user community, may range from Level-0 to Level-2, and higher levels as approved.

Whereas the Earth Explorer core missions led by ESA address the agreed primary research objectives, the Earth Explorer opportunity missions can be of different types, such as:

— providing instruments for international, European national or other ESA programmes within agreed cooperation frameworks;
— small (including micro-) satellite Earth research missions; and
— small missions to demonstrate new Earth observation technologies and techniques.

The Earth Explorer component of the programme funds Phase-B, C, D, E and F (disposal at end of life) activities of Earth Explorer missions, with some flexibility as needed to accommodate the expected international cooperation.

Preparatory activities (pre-Phase-A and Phase-A/B1) for new Earth Explorer missions are undertaken within the development and exploitation component of EOEP.

Development and Exploitation Component

The development and exploitation component of the programme is divided into six interconnected elements: Earth observation preparatory activities, Earth Watch definition activities, instrument predevelopment, and support to the science, data user, value-adding and market development elements.

The for each new Earth observation mission, pre-Phase-A and Phase-A/B1 activities include:

— establishing the scientific objectives of the mission in consultation with the scientific community (Earth Explorer);
— establishing service requirements and potential partnership arrangements in consultation with industry, EU institutions and agencies, Eumetsat, EU Member States and user communities (Earth Watch concept);
— defining the mission and system requirements;
— supporting market evaluation activities;
— undertaking instrument, satellite system and mission feasibility or concept studies;
— identifying critical technology requirements for the space and ground segments;
— initiating, in consultation with other programmes, critical technology developments and evaluations, and ensuring the visibility of ESA's overall technology development activities to the Earth Observation Programme Board;
— establishing instrument predevelopment requirements with a view to reducing costs and risks;
— identifying opportunities for cooperation and cost sharing with other ESA programmes (Earth Explorer missions);
— identifying programme costs, schedules and risks and preparing proposals for selection by the Programme Board for either the Earth Explorer component or for submission to Earth Watch definition studies; and
— supporting scientific and campaign activities.

The Earth Watch definition activities include:

— studies to elaborate concepts for the next generation of European operational missions, including next-generation GMES studies;
— studies of the possible operationalisation of (in-orbit proven) Earth Explorer missions, whose operational value is confirmed by the EO user community;
— concepts that could be considered for future meteorological programmes; and
— early phase studies of new missions that that would address a future (pre-) operational monitoring capability.

The instrument predevelopment activities involve studies of identified and agreed user-driven candidates for Earth Explorer and Earth Watch type missions. These activities include the development and testing of critical instrument elements to a sufficient level to demonstrate overall performance against clearly defined requirements, and before committing such instruments to a full satellite programme.

The support for science and innovation provides a flexible mechanism to address the scientific needs and requirements of the Earth system science community in terms of novel observations, new algorithms and products, and innovative results by:

- exploring novel mission concepts to address major observational gaps identified by the Earth science community;
- developing advanced algorithms and innovative products that may exploit the ESA's increasing multimission capacity, with special attention to the Earth Explorer missions and ESA's Earth observation data archives;
- promoting new scientific results by supporting the synergic use of ESA data by the Earth science community with special attention to the next generation of young European scientists; and
- expanding the use of ESA data within new Earth system science communities by reinforcing ESA's contribution to the major global Earth science programmes.

The data user element transfers scientifically proven EO research results into an operational context by producing high-quality data and information products that meet the needs of international organisations and public authorities in ESA Member States. The data user element aims to bridge the gap between validated EO capabilities that are accessible only to the expert EO research community, and the much larger communities of non-expert users who wish to access such information.

The value-adding element aims to strengthen the competitive position of both small companies and institutional suppliers of marketable EO services in Europe and Canada, by building on the achievements of service industries using the ERS, Envisat, Earth Explorer and European and Canadian national missions.

Finally, the market development element encompasses two types of activity. It provides support to industry by offering new products and services derived from the data from ESA missions, possibly combined with data from other missions and/or sources, and by building on past experiences within ESA, in national organisations in Member States and in the European Community. Market development also involves fostering the transfer of technology from R&D activities (AOs, pilot projects) to other activities aimed at establishing and providing reliable and sustainable services to industry.

2.1.2 EOEP Review 2011

In accordance with EOEP's Implementing Rules, the programme was reviewed in 2011 in order to assess its achievements and the status of activities. The review thus helped to prepare for the ESA Ministerial Council in late 2012 when a proposal to continue the programme will be presented to ESA Member States. If approved, this will be the fourth programme period; the first was approved in 1999, and was followed by EOEP-2 (2003–07) and EOEP-3 (2008–12).

The review was conducted by an independent panel of internationally recognised scientific experts under the chairmanship of the Director of the World Climate Research Programme (WCRP). In its *Science Review Report* (Fig. 2.1.1), the panel found that EOEP has continued to achieve the science, technology and overall strategic objectives of the Living Planet Programme. That programme's scientific priorities and requirements, developed in dialogue

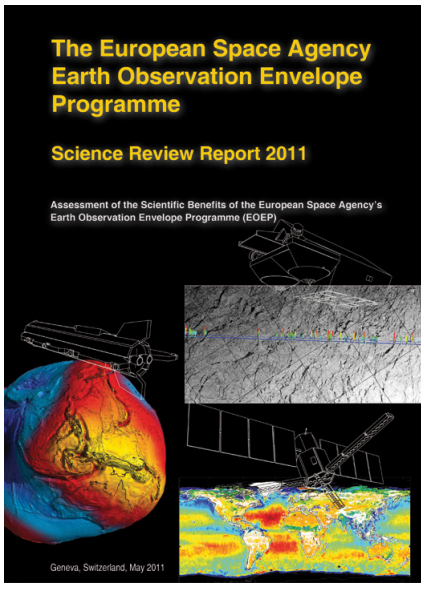

Figure 2.1.1. EOEP Science Review Report 2011. (ESA)

with European scientists and international partners, continue to guide the evolution and implementation of EOEP.

The review found that EOEP had made progress towards achieving its science objective of providing innovative space-based observations of the atmosphere, oceans, cryosphere, solid Earth and terrestrial ecosystems. Observations from the recently launched Earth Explorer missions, as well as legacy missions such as ERS and Envisat, are enabling European scientists to explore and understand many aspects of Earth's natural systems.

The open process of soliciting new ideas, together with rigorous expert review and evaluation processes that ESA has put in place for definition, selection and implementation of EOEP has served both ESA and the European scientific and technical community very well by identifying the most innovative ideas and technologies and developing them to the point that they enable successful missions.

2.2 Meteorological Programmes

ESA's meteorological programmes include the geostationary (Meteosat) and low-Earth polar orbit Meteorological Operational (MetOp) satellites, both of which have been developed in cooperation with Eumetsat. Within this cooperation, Eumetsat is responsible for defining the end user requirements and the overall system, for providing the ground segment, satellite operations and data retrieval, and for data processing and dissemination. ESA is responsible for the design and development of the space segment elements and for the procurement, launch and commissioning of the satellites.

Following on from the success of the first Meteosat programme, the Meteosat Second Generation (MSG) and MetOp satellites are now fully operational, with some satellites deployed in orbit and others in storage awaiting launch.

Looking to the future, ESA has begun the detailed design and development of the Meteosat Third Generation (MTG) satellite, to be launched in 2017, and preparations for the MetOp Second Generation satellite are well advanced.

2.2.1 Meteosat Second Generation

The Meteosat Second Generation satellites acquire images of the Earth through the Spinning Enhanced Visible and Infrared Imager (SEVIRI) instrument (Fig. 2.2.1). SEVIRI provides 12 spectral channels (with 3 km sampling distance for 11 standard channels, and 1 km sampling distance for the High-Resolution Visible (HRV) channel), with a repeat cycle of 15 min for full-disc scanning services and down to 2.5 min for local area scanning services.

The main characteristics of the MSG satellites are as follows:

— satellite type: spin stabilised (100 rpm);
— launch mass: 2000 kg;
— payload: SEVIRI, Geostationary Earth Radiation Budget (GERB) instruments and a Data Collection System (DCS)/Search and Rescue package;
— orbit: geostationary; altitude 35 800 km;
— inclination: nominal 0°, operational to ±1°;
— nominal design lifetime: 7 years.

SEVIRI is the main instrument on the MSG satellites, and is accompanied by the GERB experiment, which is contributing to climate change studies by measuring the amount of solar radiation arriving on Earth and the amounts leaving as heat and scattered and reflected solar radiation. Each satellite also carries a transponder in support of the global search and rescue mission.

To fulfil the operational availability criteria, two MSG satellites are in geostationary orbit at any one time. The primary satellite operates at 0° longitude, directly above equatorial West Africa, and provides full-disc scanning coverage. The backup satellite is placed at 9.5°E and, under nominal conditions, provides the rapid scanning services.

The first MSG satellite was launched from Kourou in French Guiana in 2002, entered into service with Eumetsat in early 2004 and was renamed Meteosat-8. The second satellite, launched on 21 December 2005, was renamed Meteosat-9. Two further satellites are currently on the ground with a third scheduled for launch in mid-2012. The fourth and final MSG satellite is in storage awaiting launch in 2015.

Further information about the Meteosat Second Generation satellites can be found at *www.esa.int/specials/msg/*

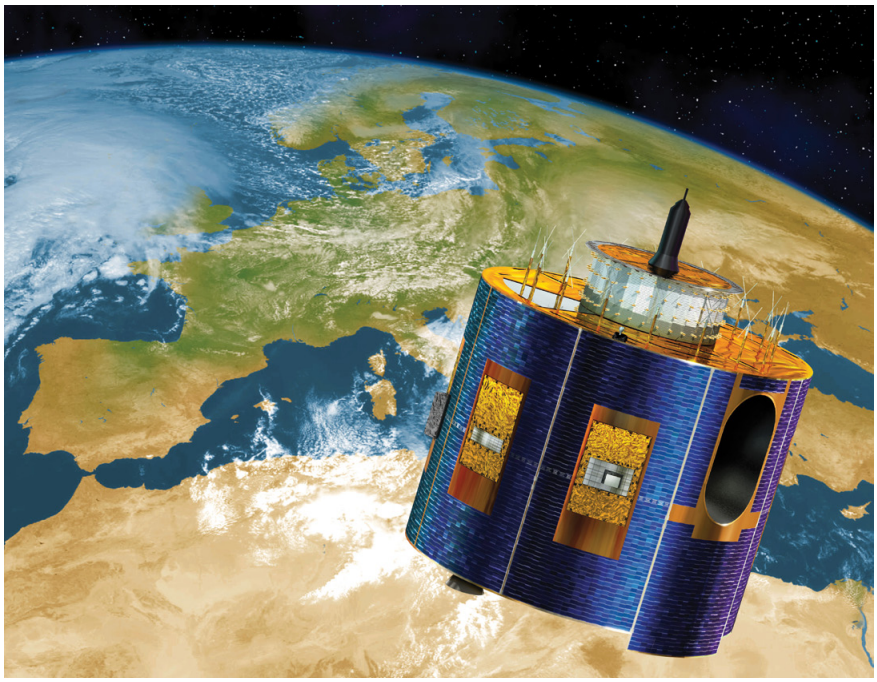

Figure 2.2.1. Meteosat Second Generation. (ESA/Eumetsat)

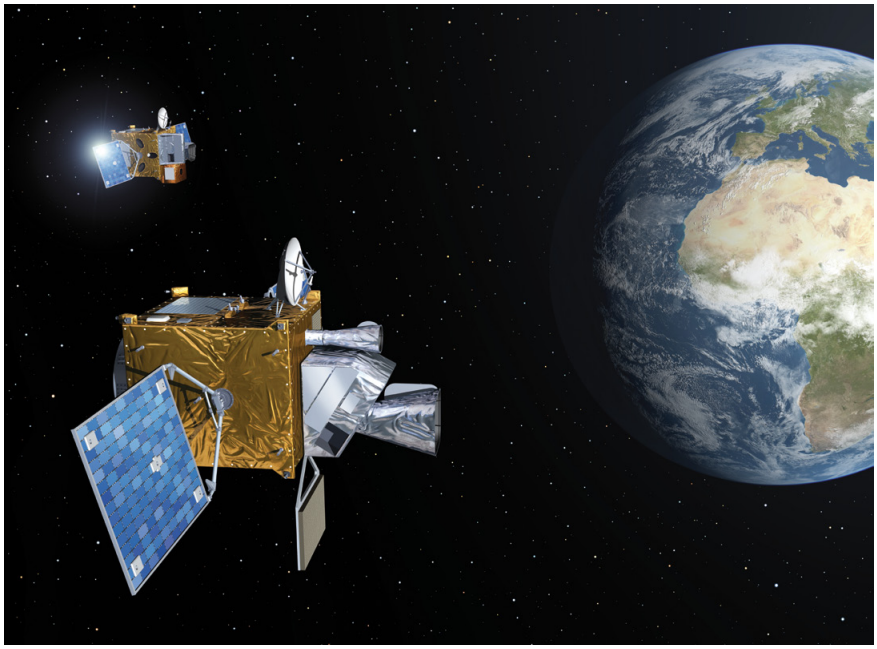

Figure 2.2.2. Meteosat Third Generation satellites. (ESA/Eumetsat)

2.2.2 Meteosat Third Generation

The Meteosat Third Generation satellites are under development, and will succeed the MSG family of satellites that have been in operation since 2002, with a first launch scheduled for 2017. The MTG will build on the imaging capabilities of MSG and provide new capabilities including infrared sounding (from geostationary orbit) and global lightning imaging.

The MTG Space Segment will comprise two types of satellite, both based on a common high-performance 3-axis stabilised platform (Fig. 2.2.2):

Further information about the Meteosat Third Generation satellites can be found at *www.esa.int/esaLP/LPmeteomiss.html*

— The MTG Imaging satellite (MTG-I) will offer advanced imaging capabilities through the Flexible Combined Imager (FCI) and the Lightning Imager (LI), providing 16 channels with spatial resolution of between 2 km and 0.5 km at nadir. It will also provide both global and local area coverage with repeat cycles of 10 min and 2.5 min, respectively.

— The MTG Sounding satellite (MTG-S) will offer the new capability provided by the Infrared Sounding Instrument (IRS). It will also accommodate the Sentinel-4/UVN (Ultraviolet/Visible/Near-infrared) instrument being developed in the framework of the GMES programme. The MTG-S will provide high-resolution atmospheric soundings in the long- and medium-wave infrared with a spatial sampling of 4 km, a channel interval of 0.625 cm^{-1} and a global repeat cycle of 15 min.

The main characteristics of the MTG satellites are as follows:

— satellite type: 3-axis stabilised
— launch mass: 3000–3500 kg
— payloads: MTG-I, Flexible Combined Imager and Lightning Imager; MTG-S, Infrared Sounder and the Sentinel-4/UVN instrument;
— orbit: geosationary, altitude 35 800 km
— nominal location: 0° with a nominal operating range 10°E to 10°W (extended operating range 70°E to 50°W)
— nominal design lifetime: 8.5 years.

In total, four imaging satellites and two sounding satellites are currently under contract; they will provide a nominal 20-year operational imaging mission and a 15.5-year sounding mission.

2.2.3 Meteorological Operational (MetOp) Satellites

The MetOp satellites constitute the space segment of the Eumetsat Polar System (EPS), which has been developed in conjunction with the US National Oceanic and Atmospheric Administration (NOAA) under an international cooperation known as the Initial Joint Polar-Orbiting Operational Satellite System (IJPS).

MetOp has been designed to work in conjunction with the NOAA satellite system, with MetOp occupying the ‘morning orbit’ and the NOAA satellite the ‘afternoon orbit’ in a Sun-synchronous polar orbit at an altitude of approximately 820 km. This global observing system is able to provide meteorological data from polar orbit to users within 2 h 15 min of the measurements being taken and full global coverage within 6 h.

While the MetOp and NOAA satellites accommodate a common suite of heritage instruments, MetOp also carries several new European developments, offering enhanced remote-sensing capabilities through microwave and infrared sounding. These instruments provide high-resolution vertical temperature and humidity profiles, and temperatures of land and ocean surfaces on a global basis. MetOp also monitors atmospheric ozone levels and a scatterometer determines wind speeds and direction over the oceans. Finally, the payload includes support elements for the global Advanced Data Collection System and search and rescue missions.

Further information about the MetOp programme can be found at *www.esa.int/esaLP/LPmetop.html*

Figure 2.2.3. MetOp. (ESA/Eumetsat)

The main characteristics of the MetOp satellite (Fig. 2.2.3) are as follows:

- satellite type: 3-axis stabilised
- launch mass: 4100 kg
- payload (instruments marked with an asterisk are common to MetOp and US satellites):
  - Advanced Scatterometer (ASCAT)
  - Advanced Infrared Sounder (IASI)
  - Microwave Humidity Sounder (MHS*) and Advanced Microwave Sounding Units (AMSU-A1* and AMSU-A2*) and
  - Advanced Very-High-Resolution Radiometer (AVHRR) *
  - High-resolution Infrared Radiation Sounder (HIRS) *
  - Global Ozone Monitoring Experiment (GOME-2)
  - Global Navigation Satellite System (GNSS) Receiver for Atmospheric Sounding (GRAS)
  - Advanced Data Collection System (A-DCS) and Search and Rescue Package
- orbit: polar orbit at 820 km (orbit repeat ~100 min)
- inclination: 98.7°
- nominal design lifetime: 5 years.

The first in the series, MetOp-A, was launched in October 2006 from the Baikonur Cosmodrome in Kazakhstan on a Soyuz/ST Fregat rocket operated by Starsem. MetOp-B is scheduled for launch in summer 2012, while the third flight model remains in storage with the earliest anticipated launch in 2017–18.

2.2.4 MetOp Second Generation

The MetOp Second Generation (MetOp-SG) series of satellites will ensure the continuity and enhancement of observations of the first MetOp series, starting in 2020 with a target of 21 years of operational service (Fig.2.2.3).

MetOp-SG will consist of two series of satellites, A and B, both in the same Sun-synchronous orbit as the first-generation satellites. The MetOp-SG satellites will constitute the space segment of the Second Generation of the Eumetsat Polar System, and will carry a series of instruments developed by ESA, CNES and DLR.

As of mid-2012, funding for the MetOp-SG satellites is awaiting approval by both ESA and Eumetsat.

2.3 Operational Programmes: GMES and the Sentinels

The Global Monitoring for Environment and Security is a joint EU/ESA initiative that is intended as Europe's response to the need for joined-up information about the environment, as well as to understand climate change and to contribute to the security of European citizens.

Through a unique combination of satellite, atmospheric and Earth-based monitoring systems and models to convert observation data into information services, GMES will provide new insights into the state of the land, sea and air, providing policy makers, scientists, businesses and the public with accurate, up-to-date, global information.

To accomplish its objectives GMES has been divided into three components: the Space, *in situ* and Services components.

GMES Space Component

The Space Component, led by ESA, comprises five new types of satellite – the Sentinels – that are being developed to meet the observation requirements of GMES services (Fig. 2.3.1). In addition, access to data from the Contributing Missions will ensure that the European space infrastructure is fully utilised for GMES. An integrated Ground Segment infrastructure will ensure access to data from the Sentinels and the Contributing Missions.

The Sentinel mission satellites will carry a range of technologies, including radar and multispectral imaging instruments for land, ocean and atmospheric monitoring.

The Sentinel-1 constellation is a pair of C-band Synthetic Aperture Radar (SAR) imaging satellites, the first of which will be launched in 2013 (ESA, 2012a). The SAR sensor will be operated in two main modes, Interferometric Wide Swath and Wave Mode, the first having a swath width of 250 km and 5 × 20 m ground resolution. It will also ensure the continuity of C-band SAR data and build on the heritage and experience with the ERS and Envisat satellites. These two modes will satisfy most existing service requirements. Two other mutually exclusive modes will be provided to ensure continuity with other SAR missions and to accommodate emerging user requirements.

Sentinel-1 applications will include ice/ocean observations, land monitoring/management, hydrology, disaster management, oil spill monitoring, and ship detection for maritime security. With two satellites, the global revisit time of Sentinel-1 will be 6 days, with 1–3 day coverage of areas such as Europe, Canada and the main northern shipping routes.

The pair of Sentinel-2 satellites will routinely provide high-resolution optical images globally. Sentinel-2 aims at ensuring the continuity of multispectral data provided by the SPOT and Landsat satellites (ESA, 2012b).

The MultiSpectral Instrument (MSI) on Sentinel-2 will measure Earth-reflected radiance through the atmosphere in 13 spectral bands from the Visible and Near Infrared (VNIR) to the Short-Wave Infrared (SWIR). The mean altitude of the Sentinel-2 satellites will be approximately 800 km, with the first planned for launch in 2014. The revisit time, with two satellites in orbit, will be 5 days at the equator and 2–3 days at mid-latitudes. The mission is dedicated to the full and systematic coverage of all land surfaces (including major islands) from –56°S (South America) to +83°N (northern Greenland), with a swath width of 290 km. The acquired data will be available in tiles of 100 × 100 km.

The increased swath width, together with the short revisit time, will allow the monitoring of rapid changes such as vegetation characteristics

Further information about GMES and the Sentinel missions can be found at *www.esa.int/esaLP/LPgmes.html*

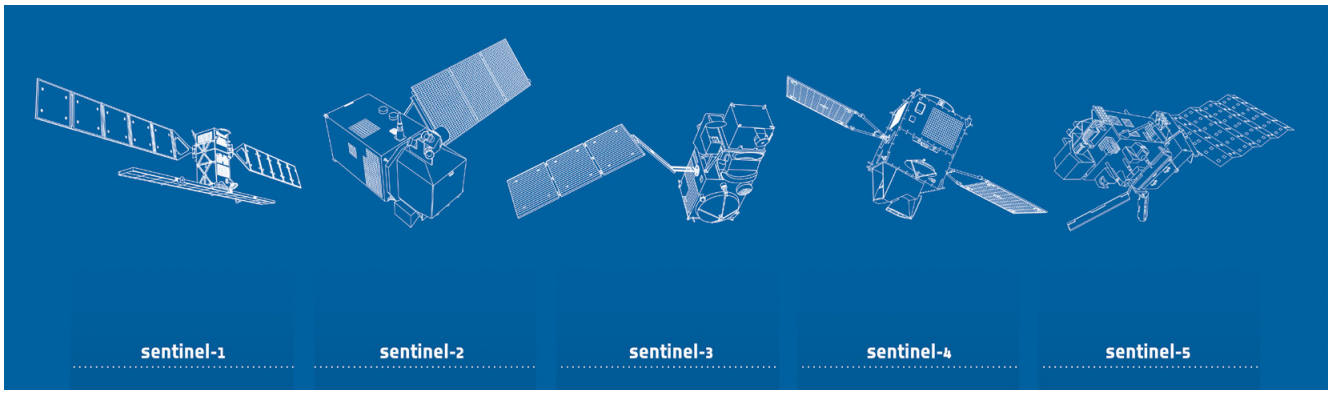

Figure 2.3.1. The Sentinel satellites. (ESA)

during the growing season and improved change detection techniques. Data from Sentinel-2 will benefit European and national services in areas such as land management, agriculture and forestry, as well as disaster control and humanitarian relief operations. The satellites will also acquire images of extreme events such as floods, volcanic eruptions and landslides.

The objective of the Sentinel-3 mission is to determine parameters such as sea-surface topography, sea- and land-surface temperatures, as well as ocean- and land-surface colour with high-end accuracy and reliability (ESA, 2012c). The Sentinel-3 satellites will carry several instruments, benefiting from their proven heritage on ERS-2 and Envisat:

— A Sea and Land Surface Temperature Radiometer (SLSTR), based on heritage from Envisat's Advanced Along Track Scanning Radiometer (AATSR). The SLSTR will use a dual viewing technique and will operate across nine wavelength bands (plus two additional fire channels) supporting atmospheric correction. The spectral range of these channels will be: 0.55, 0.66, 0.86, 1.37, 1.61, 2.25, 3.74, 10.95 and 12 µm, plus the two fire channels at 3.74 µm and 10.95 µm. It will provide a swath width of 750 km in dual view and 1420 km in single view. The SLSTR will have a spatial resolution in the visible bands of 500 m.

— An Ocean and Land Colour Instrument (OLCI), based on heritage from Envisat's Medium-Resolution Imaging Spectrometer (MERIS), but with improved wavelength bands (21 compared with 15 on MERIS) and Sun-glint effects reduction.

— A topography system, including a dual-band Ku- and C-band altimeter, based on technologies used on ESA's Earth Explorer CryoSat mission, a microwave radiometer for atmospheric correction and a Doppler Orbitography and Radio Positioning Integrated by Satellite (DORIS) receiver for orbit positioning. It will feature advanced discrimination of ocean and sea ice, and of the transitions from land to sea in coastal areas or inland water bodies. It will measure the topography of all types of surfaces, including seas, coastal areas, sea ice, ice sheets, ice margins and inland waters with high coverage and accuracy.

The revisit times of the Sentinel-3 instruments will be very short, even with only one satellite in orbit: less than 3 days for OLCI, less than 2 days for SLSTR and 27 days for the topography package. In combination, the OLCI and SLSTR instruments will provide global daily coverage with the nominal two-satellite configuration.

Sentinel-3 will provide support services relating to the marine environment, with capabilities to serve numerous land-, atmosphere- and cryosphere-based areas of application. The marine part will be operated by Eumetsat, while the

land part will be operated by ESA. The first Sentinel-3 satellite is expected to be launched in 2014.

Unlike the first three Sentinel missions, Sentinel-4 and Sentinel-5 will be payloads embarked on meteorological satellites operated by Eumetsat. Both of these missions, and the Sentinel-5 precursor mission, will be dedicated to monitoring Earth's atmosphere, providing data related to air quality, climate change, stratospheric ozone and solar radiation for the GMES atmosphere monitoring service.

There will be two families of atmospheric chemistry monitoring instruments:

— The Sentinel-4 payload (a UVN spectrometer) will be carried on the two Meteosat Third Generation–Sounder (MTG-S) satellites, planned for launch in 2019 and 2028, in geostationary orbit. In addition, a Thermal Infrared (TIR) sounder on the same platform, and a cloud imager on the MTG-Imager (MTG-I) platform will be exploited by the Sentinel-4 services.

— The Sentinel-5 payload will be carried on the MetOp Second Generation satellites (planned for launch in 2020 and currently awaiting approval by ESA and Eumetsat) in a Sun-synchronous low-Earth orbit at a mean altitude of about 800 km. Sentinel-5 will consist of an UV–VIS–NIR and Shortwave Infrared Spectrometer, which will also house a TIR sounder and imager.

To avoid gaps in the data between Envisat – in particular the SCanning Imaging Absorption spectrometer for Atmospheric CartograpHY (SCIAMACHY) instrument – and Sentinel-5, and thus to ensure the continuity of atmospheric monitoring services, a precursor mission, similar to Sentinel-5 but with no TIR sounder or imager, will be launched in 2015.

Also included in the evolution of GMES Space Component (GSC) is the low-inclination altimetry mission Jason-CS, a further development of Cryosat-2 for high-precision ocean topography. This mission will continue the series of measurements made by ERS and Envisat, and will complement the Radar Altimeter on Sentinel-3.

ESA is responsible for ensuring the integrity and coordination of the GSC. Within the GSC Core Ground Segment, ESA is responsible for:

— the overall technical coordination related to access to EO data, including interfaces with the GMES Contributing Missions and for coordinating the development of Ground Segment interfaces/standards;
— the operations of the Core Ground Segment for the Sentinel-1, Sentinel 2 and Sentinel-3 missions (for the land user community) and the operations of the Coordinated Data Access System, which will be performed by existing facilities or industry under contract with ESA;
— ensuring the technical integration of new missions and the technical evolution of the Core Ground Segment, while maintaining its operational services; and
— coordinating the work of the Ground Segment and Eumetsat for the marine part of the Sentinel-3 mission, and for the Sentinel-4 and Sentinel-5 missions.

GMES *In Situ* Component

The GMES *In Situ* Component, coordinated by the European Environment Agency (EEA), manages the environmental monitoring data gathered by European and international organisations and networks using a multitude of *in situ* sensors on the ground, at sea or in the air, including field instruments, shipping vessels, aircraft or observation balloons. GMES provides a unified system through which vast amounts of data are fed into a range of thematic information services that benefit the environment, assist humanitarian efforts and contribute to effective policy-making.

GMES Services Component

The European Commission is in charge of implementing the GMES Services Component and of leading GMES politically. GMES services provide essential information in six main domains: atmosphere, ocean and land monitoring, as well as emergency response and security. Climate change has recently been added as a new GMES service that will cut across all of these domains. In terms of security, GMES is a purely civil system that addresses civil security needs.

With GMES, Europe is ensuring access to reliable, traceable and sustainable information on environment and security. It is also contributing, through the Global Earth Observation System of Systems (GEOSS) initiative, to the building of global observation datasets. The GMES programme will enter its operational phase in 2014, when the first dedicated satellites, the Sentinel missions, will be in orbit. The main challenge will be to ensure the programme's long-term sustainability.

References

ESA (2012a) *Sentinel-1: ESA's Radar Observatory Mission for GMES Operational Services*. ESA SP-1322/1. European Space Agency, Noordwijk, the Netherlands.

ESA (2012b) *Sentinel-2: ESA's Optical High-Resolution Mission for GMES Operational Services*. ESA SP-1322/2. European Space Agency, Noordwijk, the Netherlands.

ESA (2012c) *Sentinel-3: ESA's Medium-Resolution Land and Ocean Mission for GMES Operational Services*. ESA SP-1322/3. European Space Agency, Noordwijk, the Netherlands (in press).

→ THE EARTH EXPLORER MISSIONS

3. The Earth Explorer Missions

The Earth Explorer missions constitute the core of the ESA's Earth Observation Envelope Programme. This section describes the family of six Earth Explorer satellites, three of which are currently in operation and a further three are under development. Five candidate missions for EE-6 and EE-7 are now under study.

3.1 Missions in Operation

Three Earth Explorer missions are currently in operation: GOCE, CryoSat and SMOS.

3.1.1 Gravity Field and Steady-State Ocean Circulation Explorer (GOCE)

GOCE, ESA's gravity mission, was launched from Plesetsk Cosmodrome in the Russian Federation on 17 March 2009. The first in the Earth Explorer family of satellites within ESA's Living Planet Programme, GOCE aims to improve understanding of the Earth system.

The main objective of the GOCE mission is to determine Earth's gravity field and geoid with high accuracy and maximum spatial resolution, which will contribute to studies of ocean circulation and ocean transport and sea-level research (Fig. 3.1.1). The geoid, combined with the de facto mean ocean surface derived from more than 20 years of satellite radar altimetry, yields the global dynamic ocean topography. GOCE geoid heights allow the conversion of Global Positioning System (GPS) heights to high-precision heights above sea level.

Gravity anomalies and also gravity gradients from GOCE are used for gravity-to-density inversion and, in particular, for studies of Earth's lithosphere and upper mantle. GOCE is the first satellite to carry a gravitational gradiometer and, in order to achieve its challenging mission objectives, a number of world-first technologies. In essence, the satellite, together with its sensors, can be regarded as a spaceborne gravimeter.

Figure 3.1.1. Mean dynamic ocean topography and geostrophic surface velocities derived from GOCE, without the need for buoys or drifters in the ocean. (ESA/HPF/GUT)

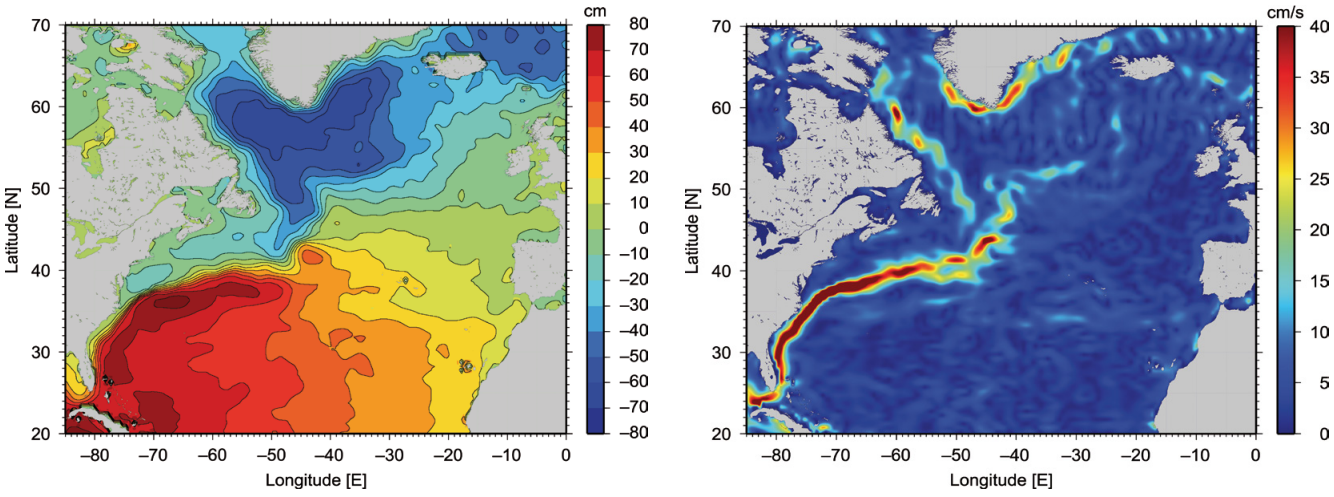

Further information about the GOCE mission can be found at *http://earth.esa.int/goce*

GOCE is determining geoid heights with centimetre-level accuracy and variations in gravity to one part per million (ppm), in both cases with a (half-wavelength) spatial resolution of 100 km on Earth's surface.

The mission objectives complement those of the US–German Gravity Recovery and Climate Experiment (GRACE) mission, which is measuring temporal variations in Earth's gravity field caused by the transport of masses and their redistribution in the Earth system. While the goal of GOCE is maximum spatial resolution, the GRACE mission aims at maximum temporal precision at some expense in terms of spatial resolution.

The two types of gravity field information are complementary and vastly important for Earth system science. Datasets from the two missions are therefore often exploited together. The GRACE time series reveal the paths and, to some extent, the size of mass movements related to and caused by processes such as melting ice sheets, the global seasonal water cycle, sea-level variations, post-glacial mass readjustments, etc. GOCE, on the other hand, provides one global and detailed map of spatial gravity and geoid variations. In short, the GOCE mission aims to provide the best possible snapshot of the spatial structure of Earth's gravity field.

New Technology

Mapping the gravity field with high accuracy and at fine spatial scales requires the space-based observing platform to orbit at the lowest possible altitude. At such altitudes, the near-Earth environment exerts significant aerodynamic forces and torques on the satellite. On the other hand, the environment in which the instrument acquires its measurements must be as 'quiet' as possible, and ideally free of any disturbances from non-gravitational forces.

The specific requirements applicable to the GOCE satellite could only be satisfied by embarking a number of novel technologies, including various 'firsts', making the GOCE mission a major technological challenge (and achievement). These technologies include: full drag-free control along the flight direction using modulated electric propulsion, electrostatic gravity gradiometry and triple-junction gallium arsenide (GaAs) solar cells, as well as large, three-dimensional carbon–carbon honeycomb structures that provide the extreme mechanical stability of the gradiometer instrument. All parts and components that could potentially cause micro-disturbances were strictly screened during the manufacturing process.

Literally the centrepiece of the GOCE satellite, the Electrostatic Gravity Gradiometer (EGG) is the first of its kind (Figs 3.1.2 and 3.1.3). The EGG consists of three orthogonal pairs of capacitive accelerometers mounted on an ultra-stable carbon–carbon honeycomb support structure. The principle of operation of these accelerometers is that a proof mass is kept levitated in the centre of

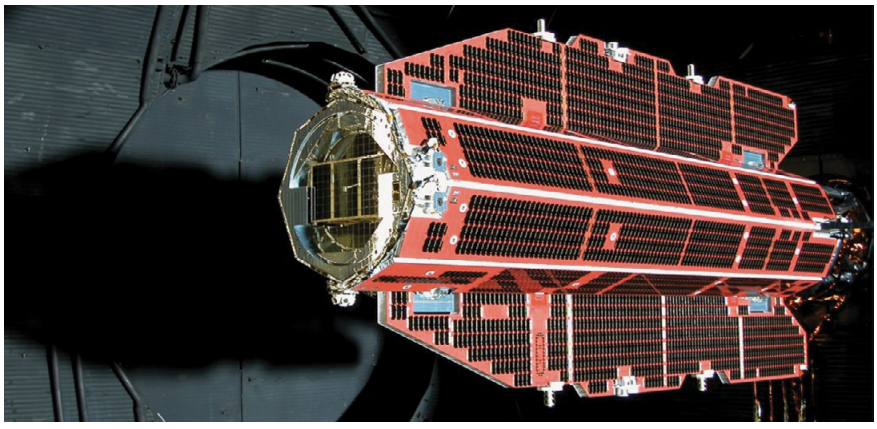

Figure 3.1.2. The GOCE satellite. (ESA)

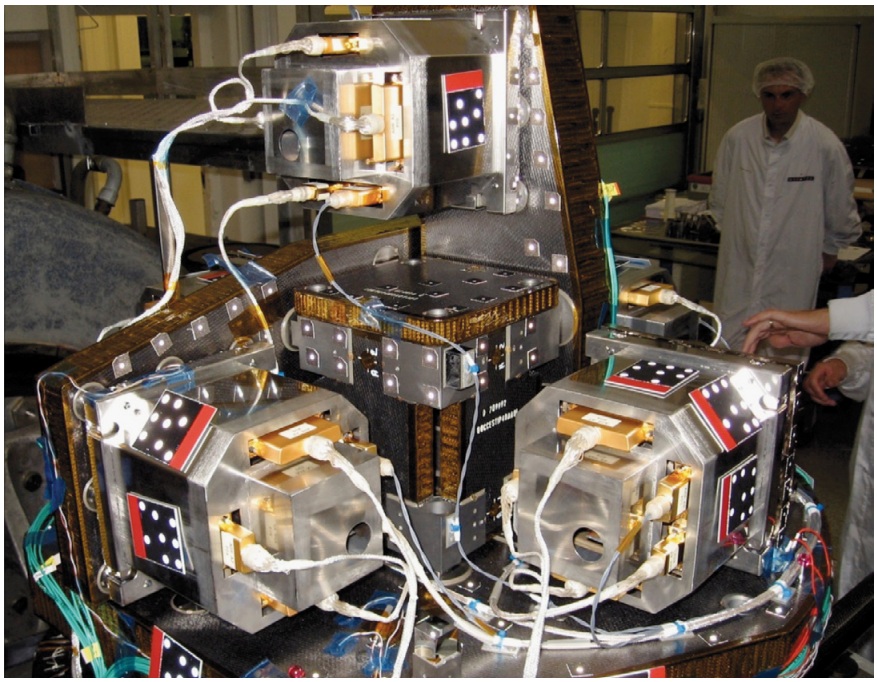

Figure 3.1.3. The core of the gradiometer instrument on GOCE, including the ultra-sensitive accelerometers. (ESA)

a slightly larger cage by electrostatic forces, i.e. by applying control voltages between the (eight) electrode pairs embedded in the cage and the different faces of the parallelepiped proof mass. These voltages are representative of the accelerations seen by the proof mass and are the initial input to an elaborate chain of processing steps that, ultimately, lead to a full-fledged model of the gravity field.

The requirements for the gradiometer are severe and stringent. The acceleration measured by each accelerometer within a band-limited frequency range of 5–100 mHz can be as small as one part in 10^{-13} of the gravity experienced on Earth. The GOCE accelerometers are therefore about 100 times more sensitive than any previously flown, such as the Super Space Three-axis Accelerometer for Research (SuperSTAR) on GRACE. The distance between each sensor pair must vary by no more than 1% of an angstrom (roughly the diameter of an atom) over a time interval of about 3 min. Realistically, this can only be achieved by using structural design technologies based on 3D carbon–carbon panels and central stiffeners. Two accelerometers of the same pair are mounted 50 cm apart and form a gradiometric arm. Along the satellite orbit the two proof masses of any pair of accelerometers have the tendency to move under the influence of Earth's gravity field and its spatial variations. The gradiometer measures this tendency, expressed as a differential acceleration between accelerometer pairs, for all six accelerometers and each of them in six degrees of freedom (three linear and three rotational accelerations).

In order to measure gravity gradients, a differential observation technique is used. The measurements from two accelerometers in one arm are subtracted from each other, removing noise and disturbing forces that affect both of them, in a process called 'common mode rejection'. What remains is the difference in acceleration due to Earth's gravitation, measured at two locations separated by 50 cm. This difference is directly linked to the gravity gradient and is the main scientific product of GOCE. The difference between the accelerations measured by the two accelerometers belonging to the same arm therefore represents the basic scientific product of the gradiometer.

The other main payload of GOCE is a 12-channel, geodetic quality GPS receiver that provides centimetre-level positioning information and long-wavelength gravity field information. It is known as the high–low Satellite-to-Satellite Tracking Instrument (SSTI).

Operations

Its complex and unique design features mean that the GOCE flight operations plan developed by the flight control team is extensive, containing a total of 977 procedures for operating the satellite in both routine and contingency scenarios. On the other hand, from a satellite operations perspective, the complexity of the routine science operations activities is limited.

Unlike most other missions, there is no need for involved payload operations activities to perform the routine mission. Once the satellite has attained a stable and quiet drag-free mode, the acquisition of the science data requires (simplistically put) only that GOCE maintains the same stable configuration. The only science-related routine operation is to acquire special diagnostics sampling the measured accelerations at a higher frequency. Apart from this, the gradiometer is calibrated every two months.

Routinely, six passes per day are taken on the Kiruna ground station in northern Sweden, augmented by one or two passes on the SvalSat station (located on Svalbard, Norway). Most notably, due to the low orbit, the pass durations are much shorter than for a typical low-Earth orbiter. As a consequence, the routine pass activities are automated to the maximum extent possible, with virtually all pass-related activities (e.g. connection of links to ground stations, starting and stopping mass memory playback) performed through an automatic release-based stack running on the mission control system, or by time-tagged commands from the onboard mission timeline.

Once acquired at Kiruna station, the mission data are then transferred via the European Space Operations Centre (ESOC) in Darmstadt, Germany, to the science data processing facility at the European Space Research Institute (ESRIN) in Frascati, Italy, for Level-1b product generation, archiving and data distribution. The Level-1b data are distributed to the so-called High-level Processing Facility (HPF) for processing to Level-2, i.e. gravity field models and ultra-precise satellite orbits. The HPF is a distributed facility involving 10 world-renowned scientific partners in seven European countries. All final mission products are distributed to the user community using ESA user service facilities.

GOCE Data Products

The official GOCE data products provided by ESA are as follows:

— Level-1b EGG product: full history of all processing steps from accelerometer control voltages to gravity gradients, including attitude, angular rate and angular acceleration, calibrated and non-calibrated.

— Level-1b SSTI product: full history of all processing steps from accelerometer control voltages to gravity gradients, including attitude, angular rate and angular acceleration, calibrated and non-calibrated.

— Level-2 products: global gravity field models with a spatial resolution of about 80 km, parameterised in spherical harmonics; global grid of gravity field functionals such as geoid heights, gravity anomalies and deflections of the vertical; full error variance–covariance information; gravity gradients fully calibrated and geophysically corrected, in the instrument frame as well as in an Earth-fixed local north–east-down frame; and ultra-precise positioning information based on reduced-dynamic and kinematic techniques.

All GOCE products are reversible in the sense that they contain all the corrections applied at each processing step.

3.1.2 Soil Moisture and Ocean Salinity (SMOS)

The SMOS mission, launched on 2 November 2009, is a direct response to the lack of global observations of soil moisture and ocean salinity. Such observations are needed to further our knowledge of the water cycle, and to contribute to better weather and extreme-event forecasting and seasonal climate predictions. The variability of soil moisture and ocean salinity is due to the continuous exchange of water between the oceans, the atmosphere and the land – Earth's water cycle.

Soil moisture is a key variable in the hydrological cycle. SMOS observations will therefore further our knowledge of processes in the water and energy fluxes at the land surface–atmosphere interface and will provide information on the storage of water, water uptake by vegetation, fluxes at the interface and their effects on runoff. This knowledge is important for improving meteorological and hydrological modelling and forecasting, water resource management, monitoring plant growth, and forecasting hazardous weather events such as floods.

Ocean salinity is a key variable for characterising global ocean circulation and its seasonal and inter-annual variability, and is thus an important constraint in ocean and ocean–atmosphere models. SMOS observations will therefore contribute to improving predictions of seasonal to inter-annual climate conditions (e.g. El Niño/La Niña–Southern Oscillation, ENSO), estimates of ocean rainfall, and thus global hydrological budgets. They will also help to improve monitoring of large-scale salinity events and of sea-surface salinity variability. The latter is needed to better understand and characterise the distribution of biogeochemical parameters in the ocean's surface and upper layers.

Mission Objectives

Soil moisture content is a measure of the amount of water within a given volume of material, usually expressed as a percentage. From space, the SMOS instrument can measure as little as 4% moisture in surface soil, which is about the same as being able to detect less than one teaspoonful of water mixed into a handful of dry soil. The mission objective is to measure soil moisture with an accuracy of 4% volumetric soil moisture, at a spatial resolution of 35–50 km, with a revisit time of 1–3 days (Fig. 3.1.4).

Ocean salinity describes the concentration of dissolved salts in 1 litre of water. It is measured in practical salinity units (psu), which express a conductivity ratio. The average salinity of the oceans is 35 psu, which is equivalent to 35 g of salt in 1 litre of water. SMOS aims to observe salinity down to 0.1 psu (averaged over 10–30 days and an area of 200 × 200 km), which is about the same as detecting 0.1 g of salt in a litre of water. The mission objective is to measure ocean salinity with an accuracy of 0.5–1.5 practical psu for a single observation, with an accuracy of 0.1 psu for a 10–30 day average for an open ocean area of 200 × 200 km.

New technology

Providing soil moisture and ocean salinity data from space represents a real technical challenge. The instrument on SMOS, the Microwave Imaging Radiometer using Aperture Synthesis (MIRAS) operates in the L-band at 1.4 GHz and measures brightness temperatures as a function of polarisation and angle. It applies interferometry to provide a spatial resolution suitable for

Further information about the SMOS mission can be found at *www.esa.int/specials/smos*

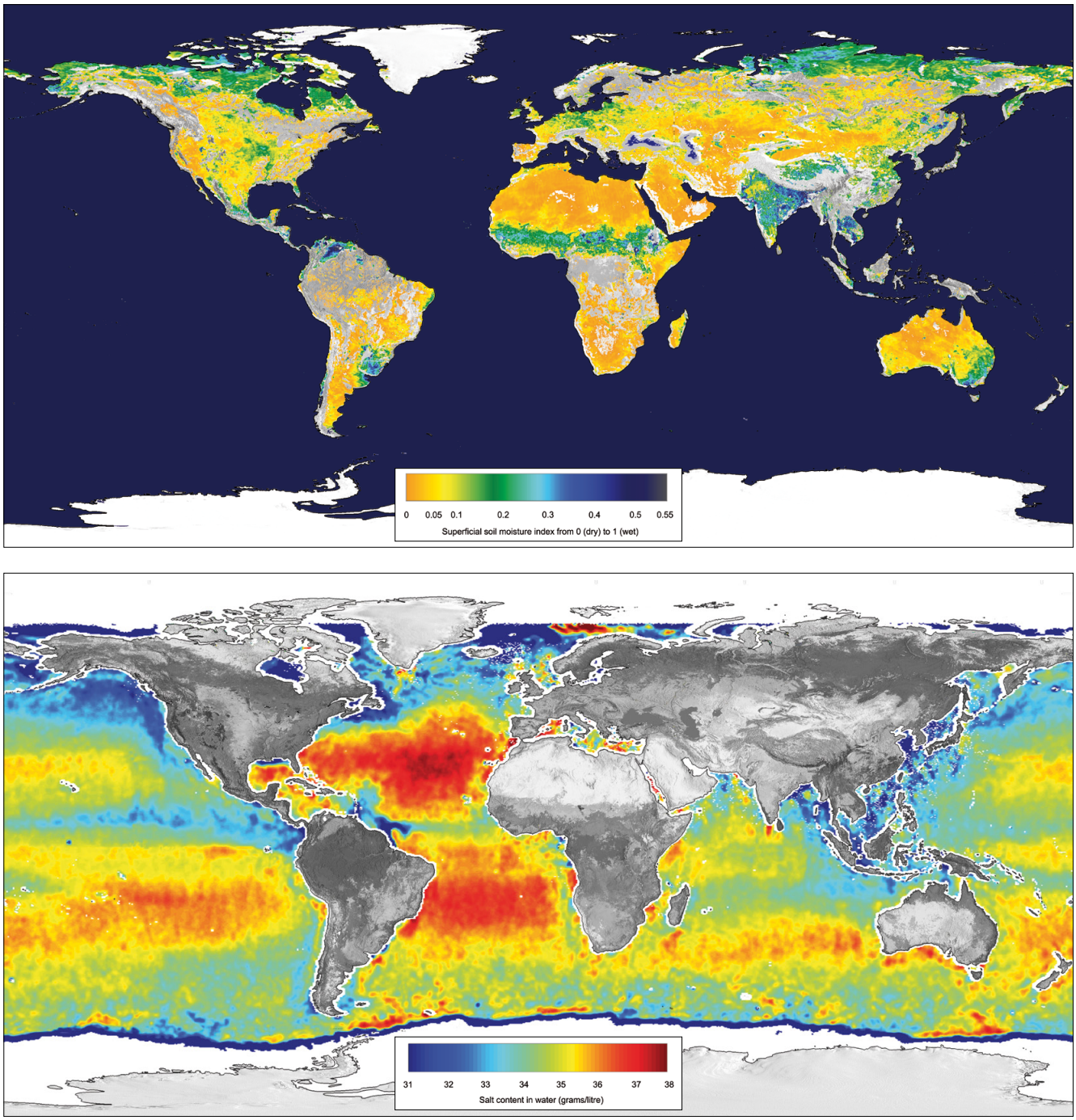

Figure 3.1.4. Global maps of soil moisture (*top*) and ocean salinity (*bottom*) as seen by SMOS. (CESBIO, IFREMER, CATDS)

the global measurements required. SMOS is the first mission to apply such a technology in space.

To make this concept work, the MIRAS instrument has had to overcome a number of technical challenges: the 69 individual receivers that form the elements of the interferometric array have to be as 'identical' as possible in their amplitude over frequency response. For all receivers, the time sampling has to be the same within 0.5 ns, requiring the first use in space of a distributed fibre optical harness. Also, each of the three arms of the array, spanning more than 4 m, that accommodate the rows of receivers could only be carried on a satellite if folded during launch and deployed on arrival in orbit (Fig. 3.1.5).

Figure 3.1.5. The SMOS satellite. (ESA/AOES Medialab)

Operations

The programmatic setup of SMOS has been just as challenging as the technology. As the Earth Observation Envelope Programme explicitly allows inter-agency cooperation, SMOS has been conceived from the outset as a collaboration between ESA, the French space agency CNES, and the Spanish Centro para el Desarrollo Tecnológico Industrial (CDTI). While the contribution of CDTI was mainly at the programmatic level by providing complementary funding through the General Support Technology Programme (GSTP), the CNES cooperation involved the provision of an adapted Proteus platform and its generic flight operations ground segment. Furthermore, ESA and CNES equally shared and managed the tasks of system engineering and satellite assembly, integration and testing up to and including the launch campaign. Finally, CNES is responsible for the operation of the satellite and is supporting the ground segment throughout the mission lifetime, while ESA maintains responsibility for the overall management of the mission and its operations.

The main stations that keep SMOS running day-to-day are at ESAC in Villafranca, Spain, which hosts the main part of the Data Processing Ground Segment (DPGS), and at CNES in Toulouse, which hosts the Satellite Operations Ground Segment (SOGS), with their respective receiving stations (Fig. 3.1.6). Global soil moisture data are important variables for operational meteorological applications. ESA Member States therefore approved in 2006 an add-on to the original mission configuration by introducing another X-band receiving station at Svalbard, Norway, which guarantees this service. The near-realtime (NRT) data are provided to operational agencies such as the European Centre for Medium-Range Weather Forecasts (ECMWF), which are working on integrating these data in their predictive models, and assessing the improvements SMOS data will be able to make to meteorological forecasts.

There is a variety of activities happening on ground. Once the SMOS data reach the DPGS at ESAC they are calibrated, processed, archived in the Fast Processing Centre and disseminated to users. There are two parallel processing chains for the scientific and NRT data products, the latter being distributed to the operational users within 3 h of sensing. The DPGS also hosts facilities to check the performance of the overall system, as well as the products to ensure that the quality of SMOS data provided to users is appropriate.

There are strong national efforts to develop Level-3 (global, single-instrument) and Level-4 (global, multi-instrument) SMOS data products at the French Centre

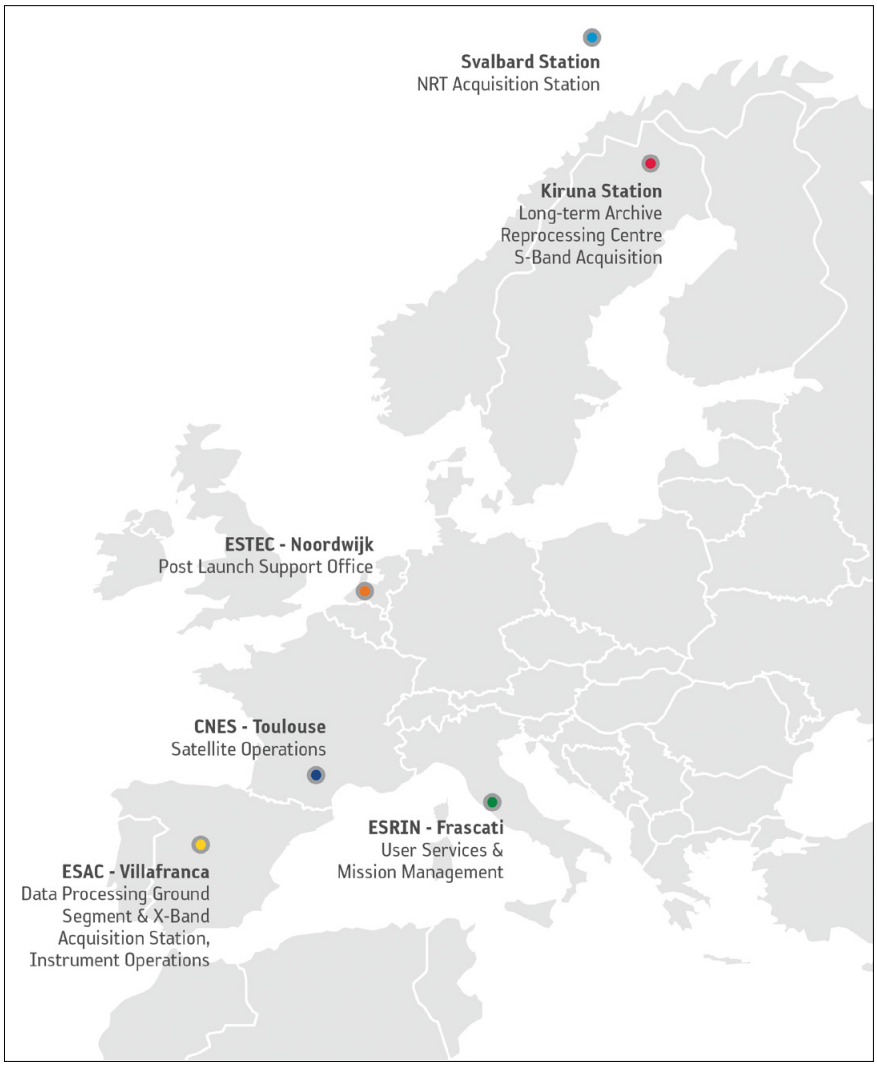

Figure 3.1.6. SMOS Ground Segment elements. In addition to ESA facilities, various functionalities are supported by industrial contractors.

Aval de Traitement des Donnees SMOS (CATDS, *www.catds.fr*) and the Spanish SMOS Level-3/4 Processing Centre (CP34, *www.cp34-users.cmima.csic.es*).

SMOS Data Products

The following SMOS data products are available:

— Level-1a product: calibrated visibilities between receivers prior to applying image reconstruction.

— Level-1b product: output of the image reconstruction of the observations, comprising the Fourier component of the brightness temperature in the antenna polarisation reference frame.

— Level-1c product: multi-angular brightness temperatures at the top of the atmosphere, geolocated in an equal-area grid system. Two Level-1c products are generated according to the surface type: one containing only sea, and the other only land pixels. Two sets of information are available: pixel-wise and snapshot-wise. For each Level-1c product there is also a browse product containing brightness temperatures for an incidence angle of 42.5°.

— Level-2 soil moisture product: it contains not only the soil moisture retrieved, but also a series of ancillary data derived from the processing (nadir optical thickness, surface temperature, roughness parameter, dielectric constant and brightness temperature retrieved at the top of the atmosphere and on the surface), with the corresponding uncertainties.

— Level-2 ocean salinity product: it contains three different ocean salinity values derived from retrieval algorithms using different assumptions for the surface roughness correction and the brightness temperature retrieved at the top of atmosphere and on the sea surface, with the corresponding uncertainties.

— Near-realtime full data product: similar to the Level-1c product but adjusted to the requirements of operational meteorological agencies such as the ECMWF and MétéoFrance, available 3 h after sensing. It contains brightness temperatures at the top of the atmosphere on an Icosahedral Snyder Equal Area (ISEA) grid with reduced spatial resolution.

— Near-realtime reduced data product: a reduced full NRT product, geolocated on a gaussian grid (T511/N256) for land pixels only, but keeping full angular resolution; pixels consolidated in a full-dump orbit segment (100 min sensing time) with a maximum size of about 30 MB per half-orbit.

3.1.3 CryoSat

CryoSat-2 was launched on 8 April 2010 by a Russian Dnepr rocket from Baikonur Cosmodrome in Kazakhstan. The launch came four and half years after the original CryoSat satellite was destroyed when the Russian Rockot launch vehicle failed to achieve orbit and the satellite fell into the Arctic Ocean. The current satellite is therefore CryoSat-2, but the mission is known simply as CryoSat.

CryoSat orbits the planet at an altitude of 720 km with a retrograde orbit inclination of 92° and a repeat cycle of 369 days (30-day subcycle). This offers high-density coverage over the polar regions. The orbit is not Sun-synchronous and allows the orbit plane to drift naturally around the Sun direction by about 0.75°/day. Thanks to this orbit geometry, CryoSat is able to reach latitudes up to 88°, and to cover more than 4.6 million km^2 of unexplored areas over the poles, which has not been possible with previous altimeters.

ESA's third Earth Explorer satellite, CryoSat is the first European mission dedicated to observing changes in ice masses to the limit allowed by natural variability, on spatial scales varying over three orders of magnitude. The mission is thus providing scientists with the data they need to improve their understanding of the relationship between ice, climate and sea level (Francis, 2010).

Scientific Objectives

The cryosphere plays a central role in Earth's radiation budget. As a consequence, a loss of sea ice is predicted to cause greater greenhouse-gas warming in the Arctic than elsewhere on Earth. Ice sheets and glaciers together comprise one of the largest uncertainties in the potential sources of global sea-level rise and have a significant influence on sea-level variations. The CryoSat mission has been designed to contribute to resolving many of the hotly debated environmental issues related to global warming and its effects on the cryosphere (ESA, 2003).

Further information about the CryoSat mission can be found at *http://earth.esa.int/cryosat*

Table 3.1.1. CryoSat mission performance requirements.

Requirements	Sea ice (10^5 km^2)	Ice sheets (10^4 km^2)		Ice sheets (13.8×10^6 km^2)
Minimum latitude	50°	72°		63°
Required performance	1.6 cm yr^{-1}	3.3 cm yr^{-1}		0.7 cm yr-$^{-1}$
Predicted performance	1.2 cm yr^{-1}	2.7 cm yr^{-1}	3.3 cm yr^{-1}	0.12 cm yr^{-1}
SIRAL mode	SAR	LRM	SARin	LRM/SARin

The CryoSat mission has two important goals: to build a detailed picture of the trends and natural variability in Arctic sea ice, and to observe the trends in the thinning rate of the great ice sheets of Antarctica and Greenland.

During the first three years of the mission lifetime, CryoSat will be able to determine whether the observed changes in sea ice are signalling important long-term trends in the Arctic climate, and to reduce the uncertainty in the ice sheet contribution to sea level to a magnitude similar to that associated with other sources of sea-level rise. In most cases, this will be accomplished with an order of magnitude improvement with respect to previous missions.

The performance of a satellite is assessed simply as the uncertainty that remains at the end of the mission. CryoSat was conceived to ensure that the residual uncertainty in ice trends is no more than 10% greater than the limit of natural variability. Loosely speaking, the mission has been designed so that the measurement error is much smaller than the variation in the ice sheets themselves, and has led to the mission performance requirements presented in Table 3.1.1.

CryoSat also takes extensive measurements of seasonal sea ice fields and provides measurements over ice caps and glaciers that have not been possible with previous altimeter systems (Wingham, 2005).

Satellite and Science Instruments

The CryoSat-2 satellite is part of the system that makes the measurements. The fundamental measure is the distance from the satellite to Earth's surface below, and for this a radar altimeter is used. The primary payload on CryoSat-2 is in fact a Synthetic Aperture Radar/Interferometric Radar Altimeter (SIRAL), which is derived from the conventional pulse-width-limited altimeter called Poseidon-2 and the US–French Jason missions. SIRAL is a single-frequency Ku-band radar, featuring some new design characteristics that enable it to provide data that can be more elaborately processed on the ground (Ratier et al., 2005).

The SIRAL instrument can be operated in three main modes. As well as the conventional pulse-width-limited low-resolution mode (LRM), which offers continuity with earlier altimeter missions (like ERS and Envisat), SIRAL can also operate in synthetic aperture mode (SAR). This increases the along-track resolution, enabling it to more readily distinguish the narrow leads of open water between sea-ice floes (Fig. 3.1.7). Over the rough terrain at the edges of the major ice sheets, this increased along-track resolution is further augmented by across-track Synthetic Aperture Interferometry (SARIn) using the second antenna and receiving channel mounted on the same optical bench. The derived angle of arrival of the radar echoes allows precise identification of the source of the echoes.

SIRAL takes very precise measurements of the range to the surface, each with an uncertainty of just a few tens of centimetres. Thanks to the high-density sampling, the averaging of many such measurements brings the system performance to the level needed to satisfy the mission objectives. However, the precise measurement of range alone is insufficient. The exact position of the satellite at the time of each measurement is needed to convert this simple measurement of range into something scientifically meaningful, which is the

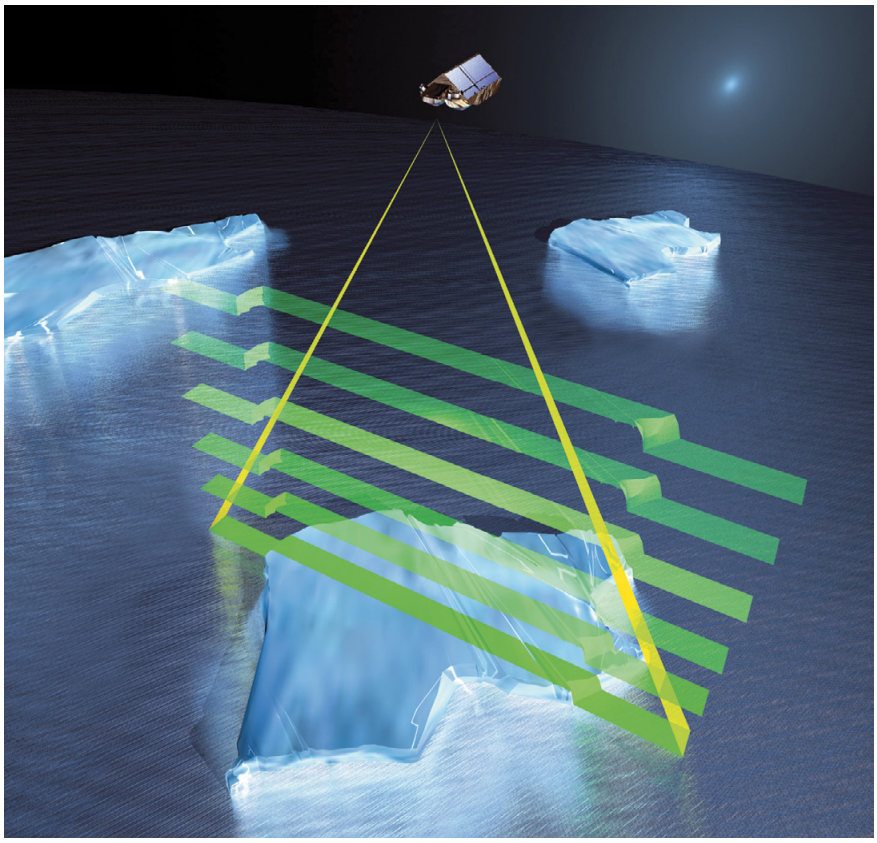

Figure 3.1.7. SIRAL in SAR mode over ice floes. (ESA/AOES Medialab)

height of the surface above some known reference. To achieve this, CryoSat-2 flies a DORIS (Doppler Orbitography and Radiopositioning Integrated by Satellite), a special radio receiver that picks up signals from a network of more than 50 transmitting stations evenly spread around Earth. By measuring the Doppler shifts of these signals, the range-rate to each one can be determined. The DORIS receiver is augmented by a passive laser retro-reflector, which allows precise range measurements to be taken by ground-based laser-ranging stations.

The final item in this collection of high-precision payload equipment is a set of three identical startrackers, which are needed to complement the SIRAL interferometer measurements and identify the baseline orientation with high accuracy. The startrackers are also the principal three-axis attitude measurement sensors in the nominal operating mode. They are lightweight, low-power-consuming, fully autonomous devices. They are accommodated so that the Sun and Moon can each blind only one head at any time, making the whole sensor system single-failure tolerant.

CryoSat-2 is an unusual satellite in that it has virtually no moving parts, the only exceptions being a couple of valves in the propulsion system. One area where this lack of moving parts is particularly noticeable is in the attitude and orbit control subsystem, where gyroscopes and reaction wheels are usually commonplace. Attitude control for CryoSat-2 is innovative since it exploits two of the payload equipment items. The startrackers provide realtime measurements of the satellite's orientation with respect to the stars, which, together with the time and orbit information from DORIS, allows the onboard software to calculate the satellite's orientation with respect to Earth.

Scientific measurements require a precise attitude control system that can turn the satellite as needed to keep it Earth-pointing within the required tolerance. CryoSat's main means of generating such torques is to use electromagnets interacting with Earth's magnetic field. A small set of cold-gas thrusters of 10 mN guards against excessive pointing errors and provides the necessary yaw steering rotation.

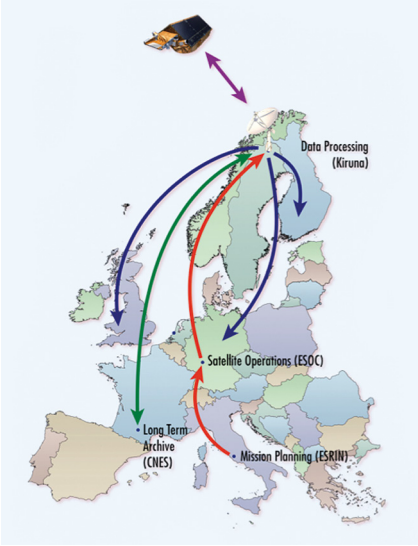

Figure 3.1.8. CryoSat Ground Segment. (R. Francis, ESA)

The attitude-control system has other sensors, which were used during the initial stabilisation after separation from the launcher, and can be used in emergencies. These are a set of magnetometers and an ingenious sensor, the combined Earth–Sun sensor, which measures the difference in temperature between a black and a mirrored surface on each face of the satellite. A clever piece of software then calculates the directions to both the Sun and Earth.

Mission Operations and Data Products

The architecture of the ground systems has been kept simple. The main parts of the system are the planning facility at ESRIN (Italy), the Mission Control Centre at ESOC (Germany), the Long-Term Archive and reprocessing facility at the Centre National d'Études Spatiales (CNES, France) and the single ground station at Kiruna (Sweden) (Fig. 3.1.8). As well as providing the link to the satellite, the Kiruna station hosts the data processing and dissemination system. From here, the scientific data (3 GB/day) are distributed directly to users.

The planning of CryoSat operations is very static and largely automated. The key to this is that the exploitation of the three different measurement modes of the SIRAL instrument can be planned well in advance. In addition to the baseline geographical zones, which stemmed from the original proposal, a number of Announcements of Opportunity (AOs) have been issued giving scientists the chance to define additional regions or zones they want to study using specific SIRAL modes, even beyond the original mission objectives. These have been added along with some specific regions that are used for calibration and validation measurements. The resulting patchwork (mode mask) of zones forms the heart of the mission planning system (Fig. 3.1.9).

All of the data generated by CryoSat's scientific payload are recorded onboard as the satellite is only in contact with Kiruna station for brief periods. Typically there are 10 passes of 5–10 min duration each day, occurring on consecutive orbits where the data is downlinked at 100 Mbit/s. These contacts are followed by a gap of 3 or 4 blind orbits where there is no contact with the ground and the data are accumulated in the onboard solid-state recorder. As mentioned earlier, the required orbit is not Sun-synchronous; every day the orbital plane shifts to almost 3 min earlier with respect to the Sun and therefore the blind orbits are not fixed in time but drift through all local times across the year. This means that there are times in the year when the orbits are acquired only outside normal working hours.

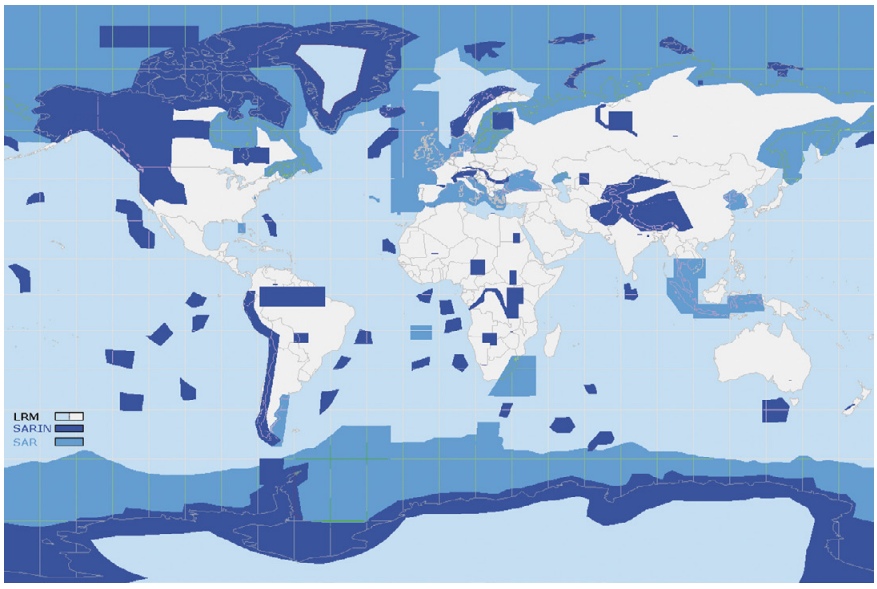

Figure 3.1.9. CryoSat SIRAL mode mask. (T. Parrinello/ESA)

There are other data flows in the system since CryoSat, like any altimeter mission, needs auxiliary data from a variety of sources. For example, the precise orbits are computed by an expert group at CNES in Toulouse, France. They need to get the data from the DORIS instrument as soon as it is available, and it takes around 30 days to compute and check the orbits to the highest accuracy. These data are sent back to Kiruna and incorporated into the CryoSat data products.

To the scientists using CryoSat data, the system appears extremely simple: all the science data generated onboard and processed on the ground are available to them through an FTP server (*ftp://science-pds.cryosat.esa.int*).

CryoSat generates about 50 Gb per day of science data (Level-0) that is processed on the ground as soon as all the input (auxiliary) files become available. The processing typically starts around 30 days after acquisition when the precise orbit files become available.

The first step is to generate a product of the same size as the Level-0, but containing the coherent synthetic radar beams; this is the so-called full-bit-rate product. The data volume and the complexity of applying the necessary calibration corrections make this product attractive only to a handful of highly specialised radar laboratories, and is not generally distributed.

The initial volume of Level-0 data is reduced to about 3 GB per day, whereby all of the synthetic radar beams illuminating a given strip of Earth's surface are combined into one composite radar echo, a process that is called multi-looking. These echoes, which include phase information for the SARIn mode, have been calibrated and constitute the Level-1b products – one product type per instrument mode. The final step in the data processing at Kiruna takes the Level-1b products and applies specific retracking of power and phase to generate a product that can be used directly by geoscientists rather than radar scientists. Level-2 products contain measurements of the surface elevation along the ground-track, corrected for atmospheric and geophysical effects. Level-2 products are also packaged as a single file per orbit called geophysical data records (GDRs).

There is a further dedicated product to satisfy the needs of the community of meteorologists and oceanographers who require a subset of altimeter data in near-realtime, i.e. within 3 h of measurement. This fast delivery mode (FDM) product is processed in the same way as other products but using the realtime orbit solution computed by DORIS that is normally used for onboard satellite control. This product contains mainly ocean elevation, wind speed and wave height data, and is only made from the SIRAL low-resolution mode (LRM) data over the oceans. Clearly, it is not always available in near-realtime because of the 3–4 blind orbits. Table 3.1.2 summarises the main SIRAL products available to the user community.

Table 3.1.2. CryoSat SIRAL products.

Products	Main characteristics	Volume	Distribution
Level-1b Full bit rate	Time-ordered, coherent synthetic radar beams for raw SAR and SARIn modes. In LRM, echoes are incoherently multi-looked onboard the satellite prior to download.	50 Gb/day	Limited
Level-1b Multi-look wave	Multi-look echoes. SARIn data contain multi-look phase. Full engineering and geophysical corrections are applied.	2.5 GB/day	To all users
Level-2 GDRs	These are consolidated products per orbit containing LRM, SAR and SARIn data. These are time-ordered elevation values (of ice, ocean or land) and, in the case of sea ice, ice thickness.	60 MB/day	To all users
Level-2 FDM	Fast delivery mode ocean data for meteorological uses.	35 MB/day	To all users

Status of the CryoSat Mission

The status of the satellite, instruments and ground segment remain excellent. Operations have been approved until 31 October 2013, but an extension is expected as part of the next Earth Observation Envelope Programme (EOEP-4). The satellite is being operated on all its prime hardware chains and no redundancy has had to be used so far. Onboard consumables are sufficient to operate the satellite for at least 10 years.

Soon after launch, the Launch and Early Operations Phase (LEOP) activities were carried out with no major issues and confirmed that all onboard systems were in very good condition. On 12 April 2010, the main payload SIRAL was switched on and the first echoes proved that it was in excellent health. The commissioning phase was carried out according to plan. A number of minor anomalies were detected on the platform and instrument, which were well understood and solved throughout the upload of new versions of the onboard software.

Quite unusual for commissioning activities was the checkout on the redundant chain of the main instrument. In fact, the active SIRAL was switched several times between the nominal (A) and redundant (B) chains. This deliberate switching, for periods of 15 days at a time, was done to provide interleaved datasets that will be used for cross-calibration in the event that the nominal chain fails, forcing a permanent switch to the redundant chain. This activity led to some important characterisation of the redundant chain with respect to the nominal one.

In July 2010, three months after launch, the first set of scientific data (Level-1b) was released to the Calibration and Validation (Cal/Val) teams for preliminary validation and troubleshooting. The result of this was the implementation of a new version of the ground processors, which became operational in January 2011, followed by the release of data to the user community a month later.

In October 2010, the first space debris collision avoidance manoeuvre was performed. Two additional major alerts had already been considered, but in those cases no manoeuvres were needed since the objects ultimately proved to be quite some distance away.

After six months of commissioning, the mission formally entered the operational phase in November 2010. Since then, the mission has been working seamlessly with the exception of two major anomalies: a safe mode due to a bug in the onboard software, and the latch of electronic protection of the SIRAL due to highly charged cosmic particles. Both problems were well understood and had a marginal impact on the systematic generation of science data.

The release of new ground processors is planned for mid-2012, which will cure a number of bugs in the software of the ground processors discovered thanks to the contributions of the expert teams and the user community. The number of users has doubled during the last year, confirming the great interest of the scientific community in this remarkable mission.

Preliminary Scientific Highlights

As described in the previous sections, CryoSat's primary goal is to acquire accurate measurements of the thickness of floating sea ice so that annual variations can be detected, and to survey the surface of ice sheets accurately enough to detect small changes. Therefore, the whole mission has been designed to identify trends and changes in Earth's ice fields rather than to measure absolute quantities of ice. This means that achieving the mission objectives will require at least two years (but probably much longer) of high-quality acquisitions. The process of putting together critical datasets has begun, and CryoSat has already produced two important results, as described below.

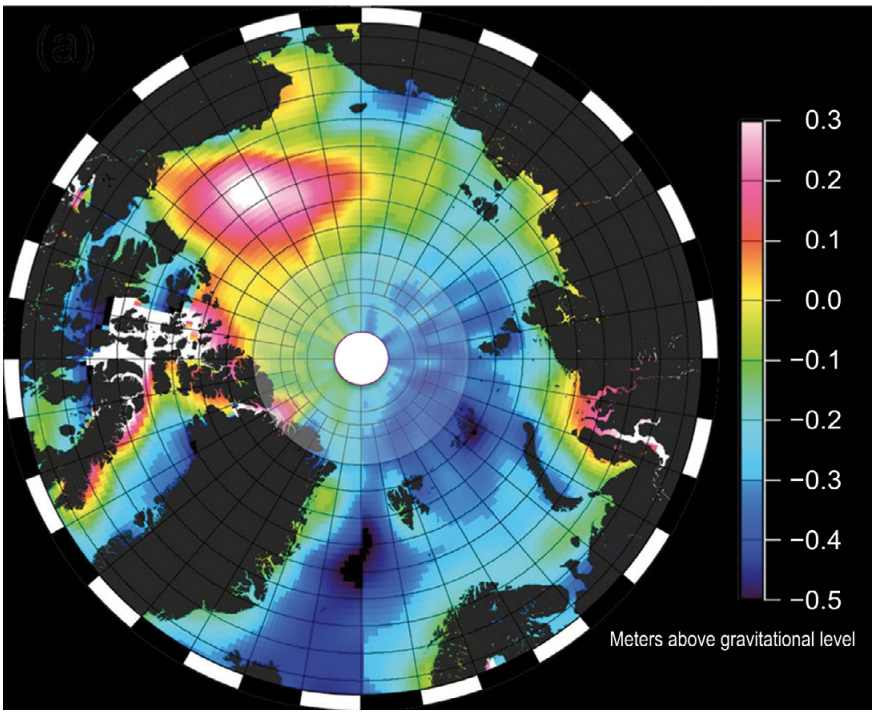

Figure 3.1.10. Ocean dynamic topography and currents. (CPOM/UCL/ESA)

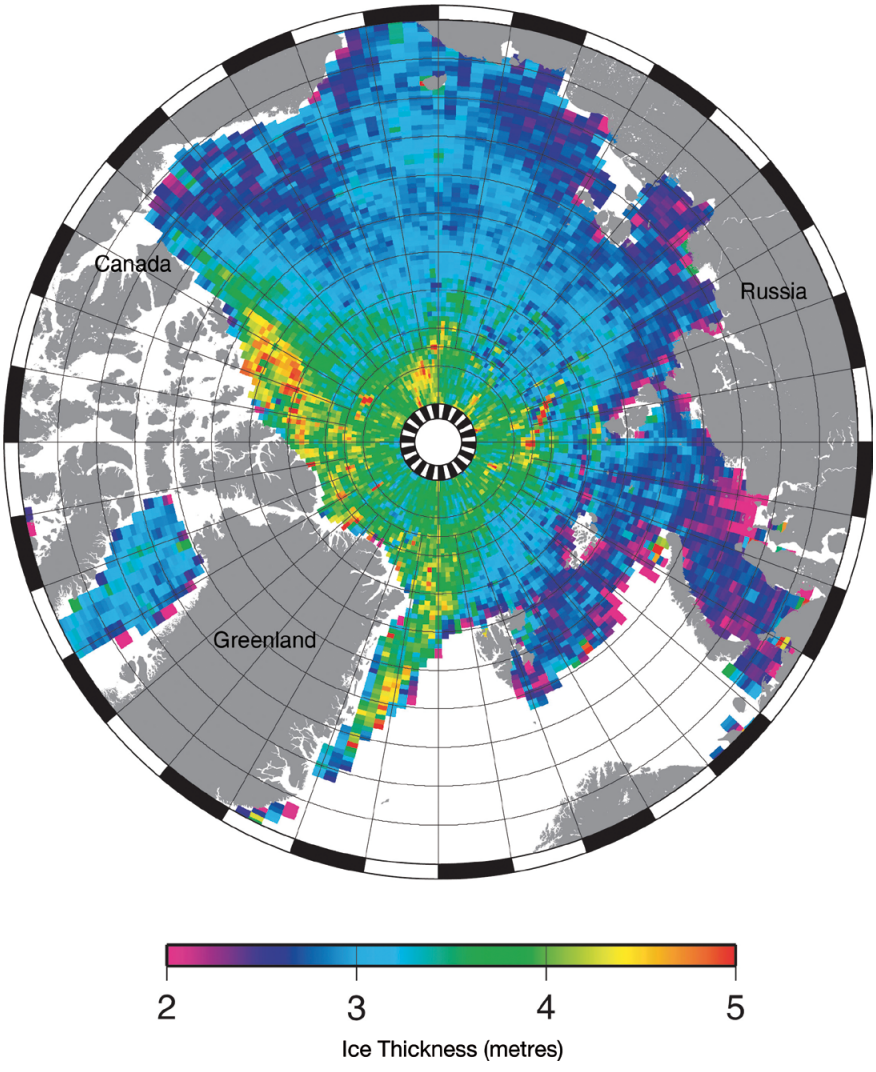

Figure 3.1.11. Sea-ice thickness in the Arctic basin. (CPOM/UCL/ESA)

Measurements from the SIRAL altimeter were used to generate a map of ocean circulation across the Arctic basin. In addition to measuring sea-ice thickness, the instrument is able to map the shape of the sea surface, providing insights into how the Arctic currents are changing as a result of the fact that winds are able to blow more easily on ice-free waters (Fig. 3.1.10). In sensing the surface of the water, CryoSat also becomes a powerful tool for studying ocean behaviour, particularly at latitudes never reached by an altimeter mission. Indeed, the oceanography community has been very interested in the CryoSat mission since it was conceived. There are plans to extend the CryoSat data portfolio to include oceanographic products.

By measuring the difference in height between ice floes and open water, CryoSat is able to work out the height of the freeboard of the floating ice and, using a relatively simple calculation, to work out the overall thickness (i.e. volume) of the marine ice cover in the Artic basin. In June 2010, the CryoSat mission delivered the first sea-ice map relative to January–February 2011 (Fig. 3.1.11). This was the first fully processed map of Arctic sea ice using CryoSat data that confirmed the potential of the SIRAL instrument. The information on the sea-ice thickness was validated with a number of independent *in situ* and airborne measurements showing very good matches.

References

ESA (2003). *CryoSat Science Report*. ESA SP-1272. European Space Agency, Noordwijk, the Netherlands.

Francis, R. (2010). ESA's ice mission. CryoSat: more important than ever. *ESA Bull*. **141**.

Ratier, G. et al. (2005). The CryoSat system: The satellite and its radar altimeter. *ESA Bull*. **122**.

Wingham, D. (2005). CryoSat: A mission to the ice fields of Earth. *ESA Bull*. **122**.

3.2 Missions under Development

In addition to GOCE, SMOS and CryoSat, three further Earth Explorer missions are being developed for launch in the timeframe 2012–15: Swarm, ADM-Aeolus and EarthCARE.

3.2.1 Swarm

Swarm, ESA's magnetic field mission, will provide the most detailed survey of Earth's magnetic field and how it changes over time, providing new insights into our planet's interior and climate. Swarm was selected as the fourth Earth Explorer mission in ESA's Living Planet Programme, and is expected to be launched in July 2012.

The powerful and complicated magnetic field created deep inside the planet provides protection from the continuous flow of charged particles, the solar wind, before it reaches the atmosphere. The field is generated by the turbulent motions of molten iron in the outer core, and acts like a dynamo. The dominant axial dipole component, however, is weakening ten times faster than it would naturally decay if the dynamo were switched off. It has fallen by almost 8% over the last 150 years, a rate comparable with those seen at times of magnetic

Figure 3.2.1. The interplay between the geomagnetic field and the solar wind (*top*). *Bottom left:* The magnetic field strength at Earth's surface. The South Atlantic anomaly is evident from the weak field (blue). The white dots indicate where the Topex/Poseidon satellite suffered radiation upsets. *Bottom right:* The changes in field strength over 20 years (from Magsat to Ørsted) shown as percentages. (ESA)

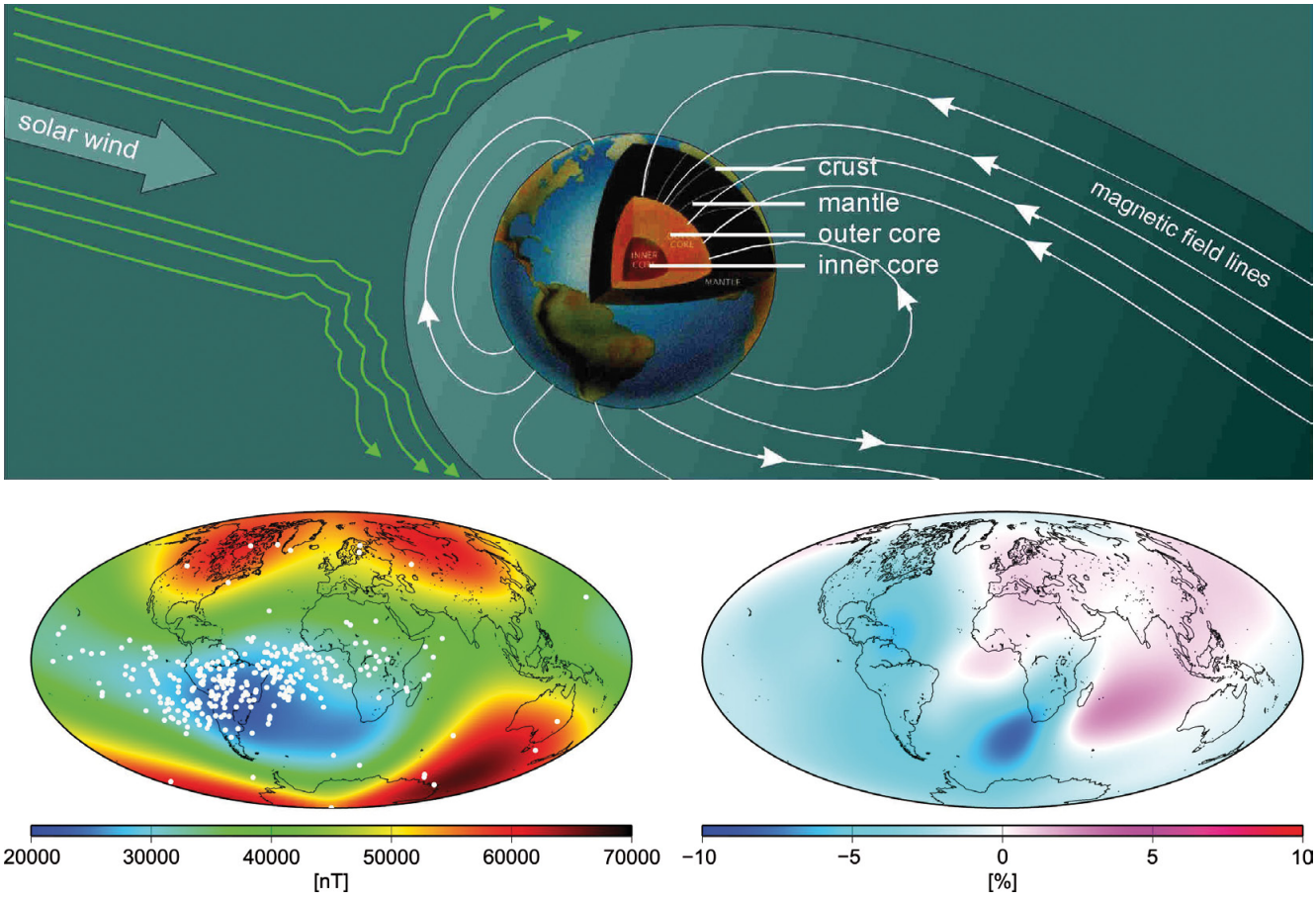

Further information about the Swarm mission can be found at *www.esa.int/esaLP/LPswarm.html*

Figure 3.2.2. The Swarm constellation of three identical satellites. (ESA/AOES Medialab)

reversal. In some regions, such as the South Atlantic anomaly, the field has weakened remarkably rapidly in recent decades (Fig. 3.2.1).

Swarm will use a constellation of three identical satellites in polar orbit at initial altitudes of 460 km and 530 km for high-precision and high-resolution measurements of the strength and direction of the magnetic field (Fig. 3.2.2). Swarm will take full advantage of a new generation of magnetometers for measurements over different regions of Earth simultaneously. GPS receivers, an accelerometer and an electric field instrument will provide supplementary information for studying the interaction of Earth's magnetic field with the solar wind.

Scientific Objectives

Swarm will address a number of scientific issues:

— In conjunction with recent advances in numerical and experimental dynamos, better mapping of the geomagnetic field with time will provide new insights into field generation and diffusion, and mass and wave motions in Earth's fluid core. Progress in geomagnetic research requires moving beyond simple extrapolation of the field with time to forecasting that field via a better understanding of the underlying physics.

— The magnetism of the lithosphere, which tells us about the history of the global field and geological activity, could be determined with much higher resolution. This will form a bridge between knowledge of the lower crust from previous satellite missions, and of the upper crust from aeromagnetic surveys. The changing field might also have affected the climate over history by affecting the escape to space of atmospheric gases.

— Global 3D images of the mantle's electrical conductivity will be possible for the first time. These images could provide clues to the chemical composition and temperature of the mantle, which are fundamentally important for understanding its properties and dynamics.

— The magnetic field is of primary importance for Earth's external environment, providing information about the Sun–Earth system.

— The conductive ocean produces a relatively weak magnetic signature, which contains independent data on ocean circulation.

Magnetic sensors on or near Earth's surface measure a combination of the core field entangled with other fields from magnetised rocks in the crust, electrical currents flowing in the ionosphere, magnetosphere and oceans, and currents induced in the Earth by external fields. The challenge is to separate the magnetic field from all these other sources, each with its own spatial and temporal characteristics (see Fig. 3.2.3).

The core field and, in particular, how it changes with time are among the very few means available for probing Earth's liquid core. Variations with time directly reflect the fluid flows in the outermost core and provide a unique experimental constraint on geodynamo theory. But investigations of internal processes over months to years are seriously limited by the lack of knowledge of the effects of external magnetic sources that contribute on timescales up to the 11-year solar cycle. This clearly shows the need for a comprehensive separation and understanding of external and internal processes.

Recent studies have greatly improved our knowledge of the global and regional magnetisation of the crust and uppermost mantle. However, fundamental questions about the magnetic field of the lithosphere and the electrical conductivity of the mantle remain unresolved. Answering these

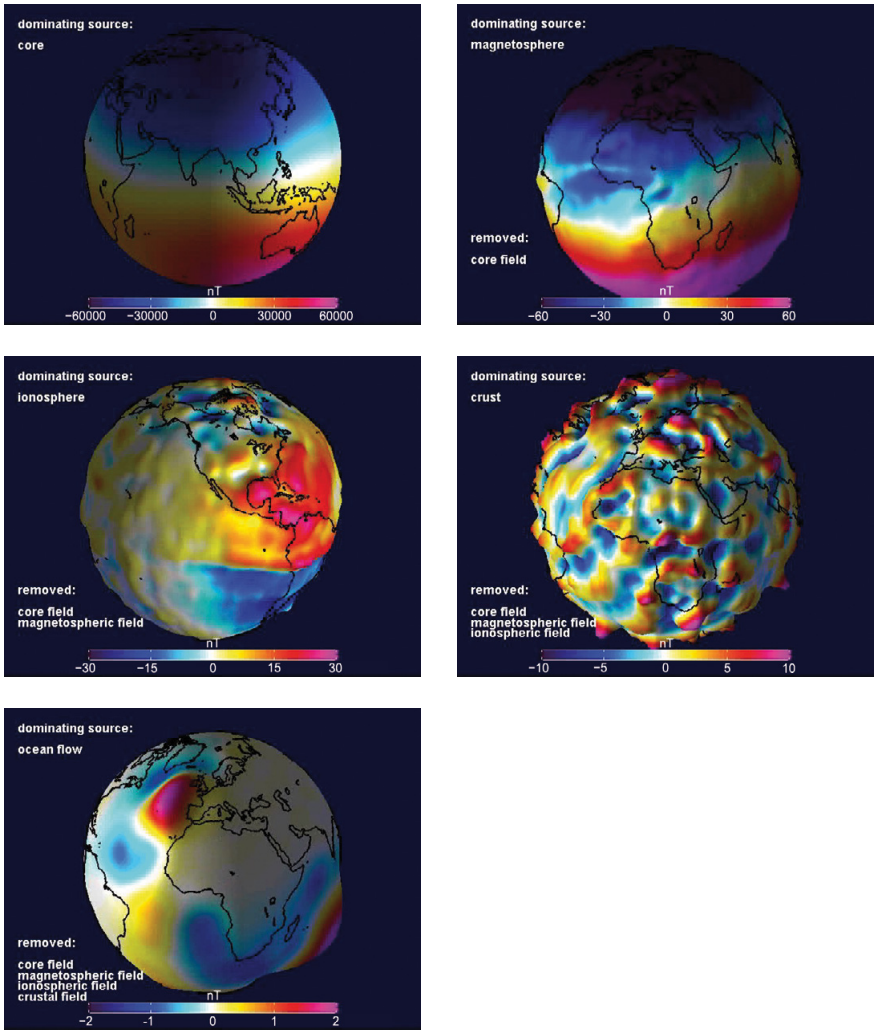

Figure 3.2.3. Simulated results from Swarm at 400 km altitude. With the progressive removal of each dominant field effect, weaker sources are revealed. *From top left:* The core, magnetosphere, ionosphere, crust and ocean currents. (ESA)

questions requires high-resolution measurements in space and time on global and regional scales.

The geomagnetic field is important not only for learning about the origin and evolution of our planet. While it is well known that the air density in the thermosphere is statistically related to geomagnetic activity, recent results suggest that it is also locally affected by geomagnetic activity in a way that is still poorly understood. Furthermore, the magnetic field is a shield against high-energy particles from the Sun and deeper space. It controls the location of the radiation belts, and also the paths of incoming cosmic ray particles, which reflect the physical state of the heliosphere. The interplanetary medium controls the energy input into Earth's magnetosphere and the development of magnetic storms, in short: space weather. Possible correlations between solar activity and climate variations are frequently reported, but are still poorly understood.

No other single physical quantity can be used for such a variety of studies related to our planet. Highly accurate and frequent measurements of the magnetic field will provide new insights into Earth's formation, dynamics and environment, stretching all the way from the core to the Sun.

Mission Status

Swarm has reached the end of Phase-C/D and is expected to be launched in July 2012 from Plesetsk Cosmodrome in the Russian Federation on a Rockot launch vehicle. Following release from the launcher, the three satellites will be manoeuvred into a constellation with two satellites separated east–west by 150 km at the equator in a lower orbit (460 km) and one in a higher orbit (530 km).

The orbits of all satellites decay slowly from their initial altitudes due to atmospheric drag. The lower Swarm satellites will have polar orbits with an inclination different from that of the higher one, which causes a relative drift with time. This will allow good spacetime mapping of the magnetic field during the mission. The nominal mission will last for 4.5 years. The mission control for the satellites will be at ESOC via Kiruna, and the data will be processed and archived at ESRIN.

The three Swarm satellites are identical. The configuration for each satellite needs to be as magnetically clean as possible, with the magnetic field instruments on a deployed boom (Fig. 3.2.4). Each satellite payload includes the same set of instruments:

— An Absolute Scalar Magnetometer (ASM) located on the boom measures the magnetic field strength and calibrates the VFM to maintain absolute accuracy during the multi-year mission.

— A Vector Field Magnetometer (VFM) measures the magnetic field vector. It is located on the boom, together with startracker for precise attitude measurement.

— An Electrical Field Instrument (EFI) measures the local ion density, drift velocity and electric field, and is also used for plasma density mapping in conjunction with GPS.

— An Accelerometer (ACC) measures non-gravitational acceleration, such as air drag, winds and solar radiation.

— A GPS Receiver (GPS) determines the precise position, speed and time and the Total Electron Content (TEC).

— A Laser Retroreflector (LRR) is used for orbit determination to centimetre accuracy by laser ranging.

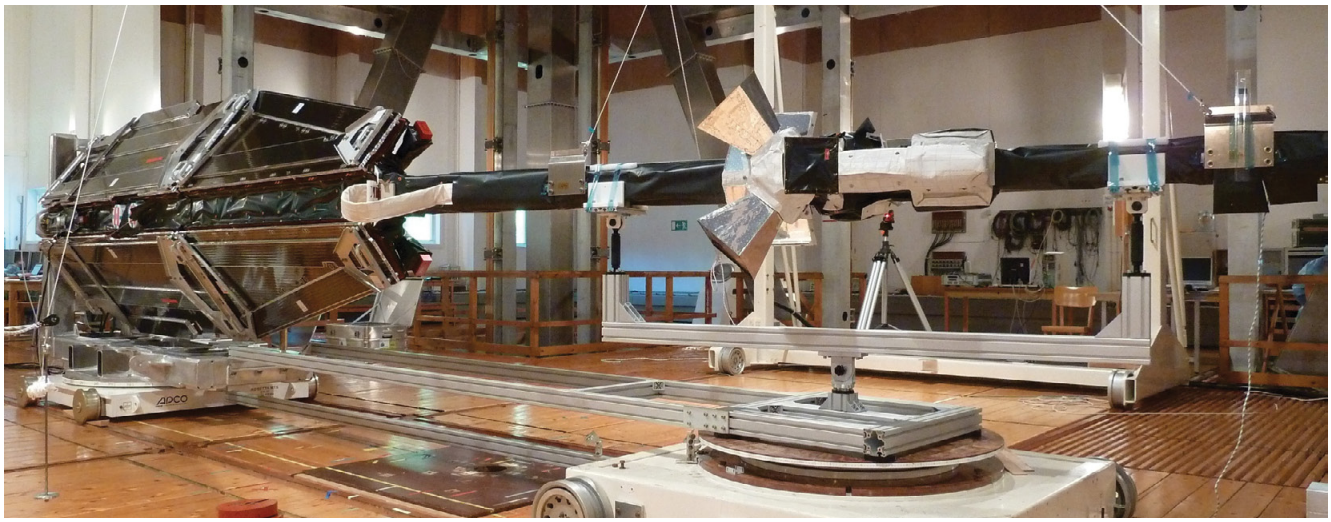

Figure 3.2.4. A Swarm satellite at IABG (Industrieanlagen-Betriebsgesellschaft mbH), Germany, for magnetic characterisation (ESA/R. Bock)

The specific constellation of three satellites, together with the different set of instruments on each one, will make it possible to address the various scientific objectives of the mission. For analyses of the measurements of the constellation new methodologies have been designed and implemented, offering the wider user community Level-2 products such as global magnetic field models.

3.2.2 Atmospheric Dynamics Mission (ADM)-Aeolus

ADM-Aeolus will be the first mission to acquire profiles of the wind on a global scale. These near-realtime observations will improve the accuracy of numerical weather and climate prediction models and advance our understanding of tropical dynamics and processes relevant to climate variability.

Together with temperature, pressure and humidity, wind is one of the basic variables describing the state of the atmosphere. Wind is generally the result of parts of Earth receiving more heat from the Sun than other areas, leading to differences in air pressure, which in turn cause the air to move, creating wind. The planetary movement of air generates the atmospheric circulation, transporting warm air from equatorial regions to the poles and returning cooler air to the tropics, due to the high temperatures over the equator and low temperatures over the poles. Because Earth rotates, the consequent Coriolis forces cause the main circulation pattern to be split in latitude into three cell zones – the Hadley, Ferrel and polar cells. High-speed wind fields, known as jets, are associated with large temperature differences. This general circulation of the atmosphere is depicted in Fig. 3.2.5.

Wind speed and direction observations are needed in support of Numerical Weather Predictions (NWPs) and for the prediction of long-term climate change. Improved knowledge of the global wind field is widely recognised as fundamental for advancing understanding and predicting weather and climate. Wind profiles are measured by ground-based networks, but due to their limited coverage (mostly in the northern hemisphere, outside the tropics) satellite measurements are essential to obtain a more uniform global coverage.

The possibility of measuring global wind profiles from space has been studied using various techniques. It was concluded that only an active optical system

Further information about the ADM-Aeolus mission can be found at *www.esa.int/esaLP/LPadmaeolus.html*

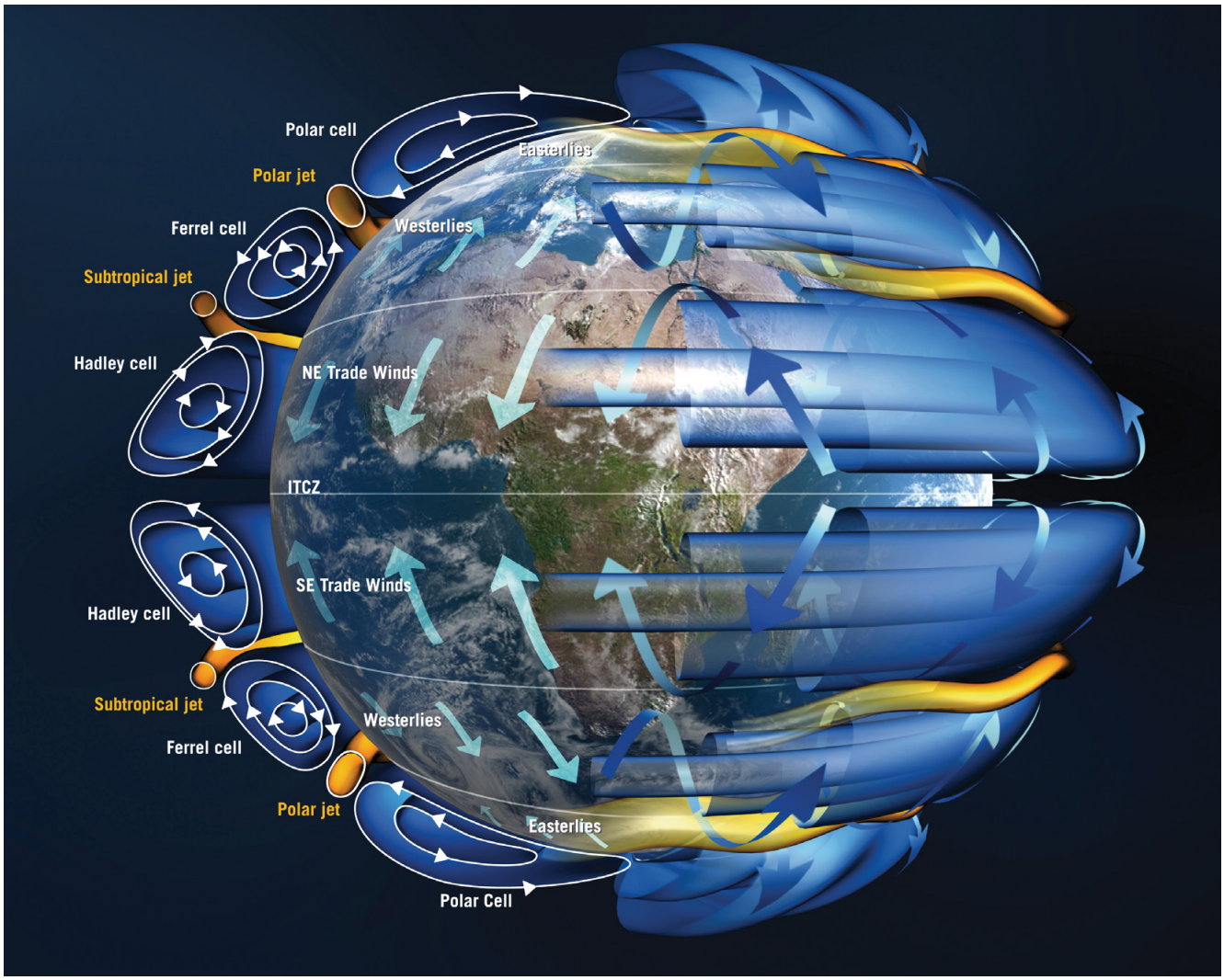

Figure 3.2.5. The general circulation of the atmosphere. (ESA/AOES Medialab)

(Light Detection And Ranging, lidar) could provide global data of the required accuracy. Scientific studies were performed to assess the impact of Doppler Wind Lidar (DWL) observations on data assimilation systems widely used for NWP models. The results of studies conducted by national meteorological services supported the basic idea that a wind lidar providing single-component wind measurements could provide useful information in the context of a data assimilation system, while complementing other existing observations.

ESA has been evaluating the prospects of using space-borne DWL for measurements of global wind fields over the past 15 years. Successive advisory committees, composed of meteorologists and lidar scientists, have helped direct the work, and many supporting contracts for lidar research and technology development have been placed with European research institutes and industry.

A first assessment of the potential of a DWL was carried out in the frame of the atmospheric laser Doppler instrument report in 1989, and the ideas carried forward were presented at a workshop in 1995. The workshop results, together with the 1989 report, laid the foundations for the *Atmospheric Dynamics Mission: Report for Assessment* (ESA, 1996), which presented a first feasibility assessment for a demonstration mission to test the use of a space-borne DWL for meteorological applications. Technological capabilities, World Meteorological Organization (WMO) user requirements and the experience with existing ground-based wind profile measurements made measurement

accuracy and reliability the main mission drivers. The observation rate was set so as to achieve more uniform global wind profile observation coverage, in order to be able to demonstrate beneficial meteorological impacts.

Scientific Objectives

The current lack of homogeneous sampling of the 3D wind field in large parts of the tropics and over the major oceans has led to major difficulties in studying key processes in coupled climate systems and in further improving NWPs. It has been shown that direct wind profile measurements over the oceans and in the tropics are essential for improving short-range forecasts of severe weather and for a correct representation of wind dynamics in the tropics.

The WMO has also emphasised the need for more uniformly distributed wind profile measurements, particularly in the tropicsl and polar regions. In the 1980s, various studies looked into which satellite-based remote sensing techniques would be most suitable for global wind profiling. It was demonstrated that an active optical system (lidar) could provide global measurements at the required level accuracy. Recommendations from the scientific and NWP community therefore led to the selection of the Aeolus space-based lidar as ESA's second Earth Explorer core mission in 1999 (ESA, 1999).

The primary aim of Aeolus is to provide global observations of vertical wind profiles from the surface throughout the troposphere and lower stratosphere. Spin-off products from Aeolus will include optical properties profiles, information on cloud/aerosol layers, optical densities, backscatter and extinction coefficients, lidar and scattering ratios. These spin-off products could be useful for including aerosols in NWP models, perhaps acting as a gap-filler between the dedicated aerosol observations of the CloudSat and Cloud–Aerosol Lidar and Infrared Pathfinder Satellite Observation (Calipso) missions, and the Earth Clouds, Aerosols and Radiation Explorer (EarthCARE) missions. However, because the optical properties products will be retrieved from backscattered light at one wavelength but with no information about its polarisation, the distinction between clouds and aerosols will rely on the high-spectral-resolution capability of the instruments. Furthermore, the vertical and horizontal resolution of the optical products will be coarser than those of dedicated aerosol lidars.

Mission Concept

Aeolus is a direct detection Doppler wind lidar for measuring wind from space. The pulsed high-spectral-resolution ultraviolet (UV) lidar will deliver horizontally projected, single line-of-sight tropospheric and lower stratospheric wind profiles in clear and particle-rich air (aerosol layers and transparent clouds) and down to the top of optically dense clouds. The measurements will be delivered in near-realtime (within 3 h) and quasi-realtime (QRT, within 30 min) for the region close to the data downlink station, for direct processing and ingestion into operational NWP models.

The selection of the Aeolus mission was motivated by the need for more abundant direct wind profile measurements in the Global Observing System (GOS), which is used by NWP models, for example. In the current GOS, direct wind profile measurements are obtained from radiosondes, commercial aircraft ascends and descends, and ground-based wind lidar and radar. The distribution of the measurements is not homogeneous, however, with most observations taken over land in the northern hemisphere. Winds can also be inferred from temperature soundings, abundant provided by satellites. However, the wind field can only be estimated from temperature measurements

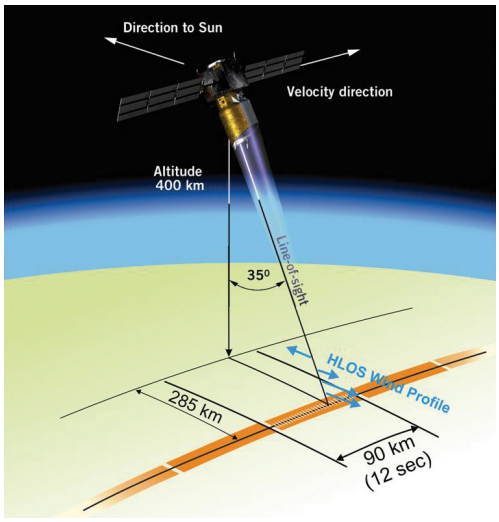

Figure 3.2.6. The Aeolus orbit, pointing and sampling characteristics. (ESA)

when the flow is in geostrophic balance, which means that only large-scale winds outsider the tropics can be obtained.

Air motion vectors also provide valuable wind observations from cloud and aerosol tracking, although these measurements are limited by the difficulty in performing accurate height assignments. It is therefore expected that the Aeolus mission will make a significant contribution to improving predictions of small-scale flows and forecasts in observation-sparse regions.

Aeolus will carry a single instrument, a high-spectral-resolution Doppler Wind Lidar ALADIN (Atmospheric LAser Doppler INstrument). ALADIN is a pulsed UV lidar (355 nm, 50 Hz, circularly polarised), operated in continuous mode. This means that the instrument is measuring continuously along the track, as illustrated in Fig. 3.2.6. Its high-spectral-resolution capability is the separate detection of the molecular (Rayleigh) and particle (Mie) backscattered signals in two channels, which makes it possible for Aeolus to track winds in both clear and (partly) cloudy conditions down to optically thick clouds.

The height of the wind measurements in the atmosphere is calculated from the time it takes for the laser pulse to travel from the emitter to the backscatter altitude and back to the receiving telescope (Fig. 3.2.7). The backscatter signals are also time-averaged, resulting in layer-averaged measurements from 24 vertical bins per channel. The emitted laser pulse is frequency shifted and broadened by the motion of the scattering media before it reenters the instrument and the instrument detectors. The frequency shift of the backscattered signal is proportional to the velocity of the scattering media along the instrument line-of-sight (LOS). The instrument is pointing perpendicular to the flight direction in order to remove any Doppler shift associated with the velocity of the spacecraft. After signal calibration and processing, the LOS wind speed can be retrieved and projected down to the horizontal (HLOS).

Aeolus will be launched in a Sun-synchronous dawn-to-dusk orbit, with a descending equatorial crossing time at 06:00. A quasi-global coverage is achieved daily (by ~16 orbits, evenly distributed around the globe), and the orbit repeat cycle is 109 (7 days).

The Aeolus Wind Lidar mission is scheduled for launch in autumn 2013, and will provide global wind profile observations in near-realtime for direct ingestion into NWP models. Recently, however, the mission measurement strategy had to be adapted in order to meet strict user requirements in terms of stability and measurement accuracy. As a consequence, the wind observation profiles are now 100 km horizontal averages with no spacing, rather than the earlier 50 km horizontal averages with 200 km spacing. This results in a change in the spatial representativity of the data.

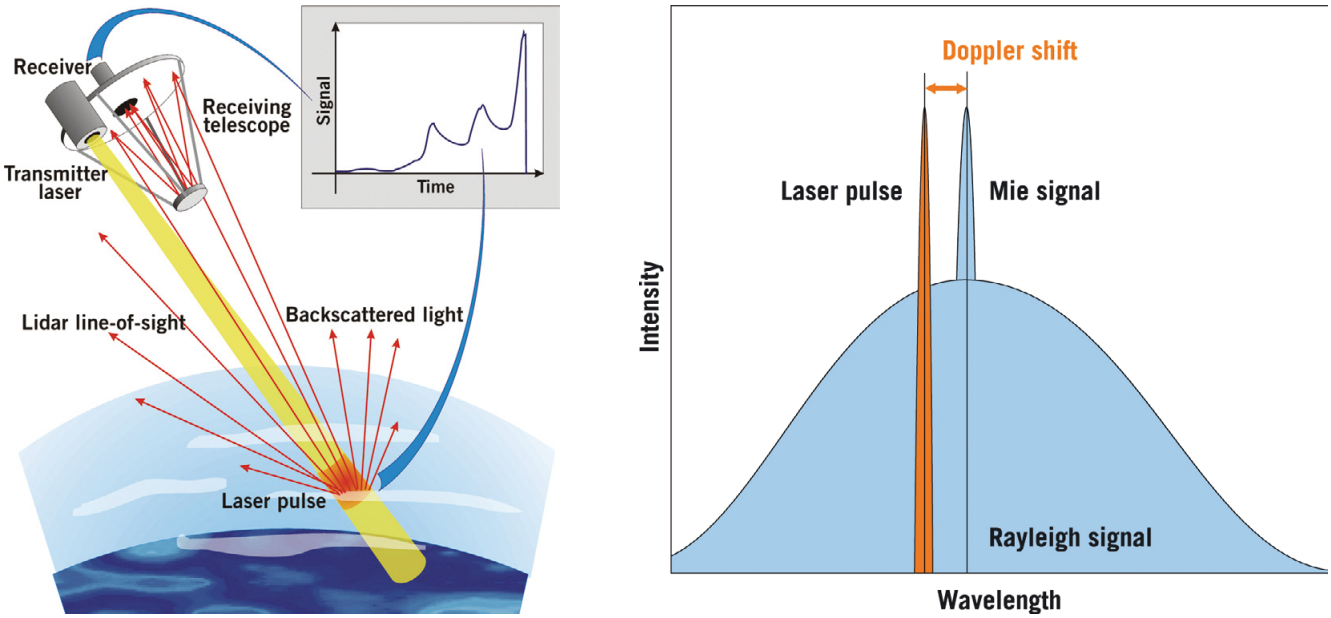

Figure 3.2.7. The Aeolus lidar measurement concept. The instrument's emit and receive path is monostatic. The laser emits narrow pulses at 355 nm at a frequency of 50 Hz, which are backscattered by molecules (Rayleigh scattering) and particles (Mie scattering) at various altitudes in the atmosphere (left). The movement of molecules or particles along the laser line-of-sight cause a Doppler shift of the emitted laser light (right). The frequency shift is measured by the CCD detectors, allowing estimates of the local wind speed. The backscattered laser light is also detected as a function of time (left, inset), allowing the retrieval of wind profiles. The signals are time-averaged, resulting in layer-averaged measurements from 250 m (near the surface) up to 2 km (in the stratosphere). (ESA)

Ongoing impact studies show that the observation representativeness error is now smaller, but the need to average the data over larger distances to achieve the same accuracy requirements leads to a loss of small-scale information. However, the laser now provides twice the amount of measurements per 200 km due to its continuous operation, which could compensate for the loss of horizontal resolution. This will be established after impact experiments using an Ensemble Data Assimilation system.

References

ESA (1996). *Atmospheric Dynamics Mission: Report for Assessment*. ESA SP-1196(4). European Space Agency, Noordwijk, the Netherlands.

ESA (1999). *The Four Candidate Earth Explorer Core Missions: Atmospheric Dynamics*. ESA SP-1233(4). European Space Agency, Noordwijk, the Netherlands.

3.2.3 Earth Cloud, Aerosol and Radiation Explorer (EarthCARE)

Scheduled for launch in 2015, EarthCARE will advance our understanding of the role of clouds and aerosols in reflecting incident solar radiation back into space and trapping infrared radiation emitted from Earth's surface. EarthCARE will quantify the interactions between clouds, aerosols and radiation so that they may be included correctly in climate and numerical weather forecasting models.

Earth's climate is driven by the balance of the energy from incoming solar radiation, the portion of it reflected back into space and the thermal

Further information about the EarthCARE mission can be found at *www.esa.int/esaLP/LPearthcare.html*

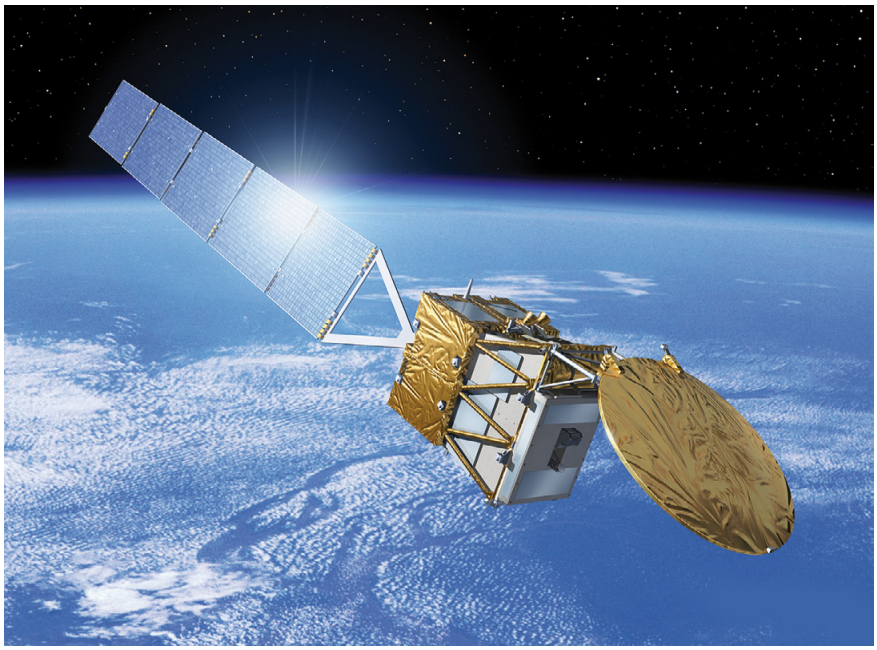

Figure 3.2.8. The EarthCARE satellite. (ESA)

radiation emitted from Earth. Greenhouse gases, clouds and aerosols regulate the absorption and reflection of the radiation inside the atmosphere. While greenhouse gases trap energy and heat in the atmosphere, the effects of clouds and aerosols are more complex as they reflect both incoming and outgoing radiation. In addition, aerosols affect the life cycle of clouds, further increasing their radiative effect.

Clouds and aerosols are the biggest uncertainties in our understanding of the atmospheric conditions that drive the climate system. An improved understanding and better modelling of the relationship between clouds, aerosols and radiation is therefore among the highest priorities in climate research and weather prediction. For this purpose, global data on the occurrence, structure and physical properties of clouds and aerosols, together with collocated measurements of solar and thermal radiation, are required.

EarthCARE was jointly proposed by European and Japanese scientists and selected in 2004 for implementation as the sixth Earth Explorer mission (ESA, 2004). By acquiring vertical profiles of clouds and aerosols, as well as the radiances at the top of the atmosphere, EarthCARE aims to quantify the relationships between them. EarthCARE is the largest and most complex Earth Explorer mission to date, and is being developed as a joint venture between ESA and the Japan Aerospace Exploration Agency (JAXA) (Fig. 3.2.8).

Scientific Objectives

EarthCARE will quantify the interactions between clouds, aerosols and radiation so that they may be included correctly in climate and numerical weather forecasting models. The scientific objectives of the mission are to:

- observe vertical profiles of natural and anthropogenic aerosols on a global scale, their radiative properties and interaction with clouds;
- observe vertical distributions of atmospheric liquid water and ice on a global scale, their transport by clouds and their radiative impact;
- observe cloud distribution, cloud–precipitation interactions and the characteristics of vertical motions within clouds; and
- retrieve profiles of atmospheric radiative heating and cooling through the combination of the retrieved aerosol and cloud properties.

In combination, EarthCARE measurements will link cloud and aerosol radiation at a target accuracy of 10 W m^{-2}.

Mission Concept

The EarthCARE mission will achieve its science objectives by taking global measurements of the vertical structure and horizontal distribution of cloud and aerosol fields together with outgoing radiation. In order to achieve its observational objectives, the satellite will carry four instruments:

- a lidar for observing aerosols and thin clouds;
- a radar for observing vertical cloud profiles (including the optically thick region of clouds where lidar signals are fully attenuated) with Doppler capability for observing vertical motions within clouds;
- an imager for deriving scene context information in the across-ground track direction; and
- a broadband radiometer to measure the collocated top-of-atmosphere (TOA) reflected solar and emitted thermal radiation of the observed cloud and aerosol scenes.

The first instrument is the Atmospheric Lidar (ATLID), a high-spectral-resolution lidar that transmits linearly polarised laser signals at a wavelength of 355 nm. The signal backscattered on air molecules is broadened according to the Rayleigh scattering function, while light backscattered on particles only has a very small broadening and follows, in the case of backscatter on spherical particles, Mie scattering functions. The lidar receiver is a so-called high-spectral-resolution receiver, which means that it is equipped with a very narrow wavelength filter separating the spectrally narrow particle backscatter signal from the much broader molecular backscatter signal. By this means, the signal extinction of cloud and aerosols can be distinguished from clear air extinction. Furthermore, depending on the structure of the backscattering particle, the polarisation of the incident light changes when backscattered. The receiver is equipped with the additional functionality to measure the degree of change in the polarisation of the backscattered signal, which allows the data analysis to distinguish different types of scattering particles. The fixed lidar viewing direction is tilted off-nadir by 3° backwards in order to minimise specular reflection on ice cloud particles. The spatial sampling will be 285 m horizontally and 100 m vertically.

EarthCARE's second instrument is the Cloud Profiling Radar (CPR), a millimetre-wave cloud radar. With its very high sensitivity the CPR will be able to retrieve accurate profiles of high ice clouds that impact Earth's radiation budget. It will be the first cloud radar in space equipped with the capability to measure the Doppler shift of the backscattered radar signal. The CPR will operate at a frequency of 94.05 GHz, with a pulse width of 3.3 µs and a variable pulse repetition frequency of 6100–7500 Hz. Its high-accuracy offset antenna has an aperture diameter of 2.5 m. The minimum sensitivity is –35 dBZ. The Doppler range is ±10 m s^{-1}, with an accuracy of 1 m s^{-1}. The CPR is a contribution from JAXA in collaboration with the Japanese National Institute of Information and Communications Technology (NICT).

The third payload instrument is the MultiSpectral Imager (MSI), which will take images with a fixed nadir-viewing direction and swath of 150 km and a pixel size of 500 m. The swath is slightly tilted eastwards (on the day side) to minimise regions contaminated by Sun glint. It covers 35 km on one side to 115 km on the other side of the ATLID and CPR observations. The instrument has seven channels, four solar channels (0.67, 0.865, 1.65 and 2.21 µm) and three thermal channels (8.80, 10.80 and 12.00 µm). While ATLID and CPR will provide vertical profiles along the satellite flight direction, the MSI will provide images of clouds and aerosols in the across-track direction. With

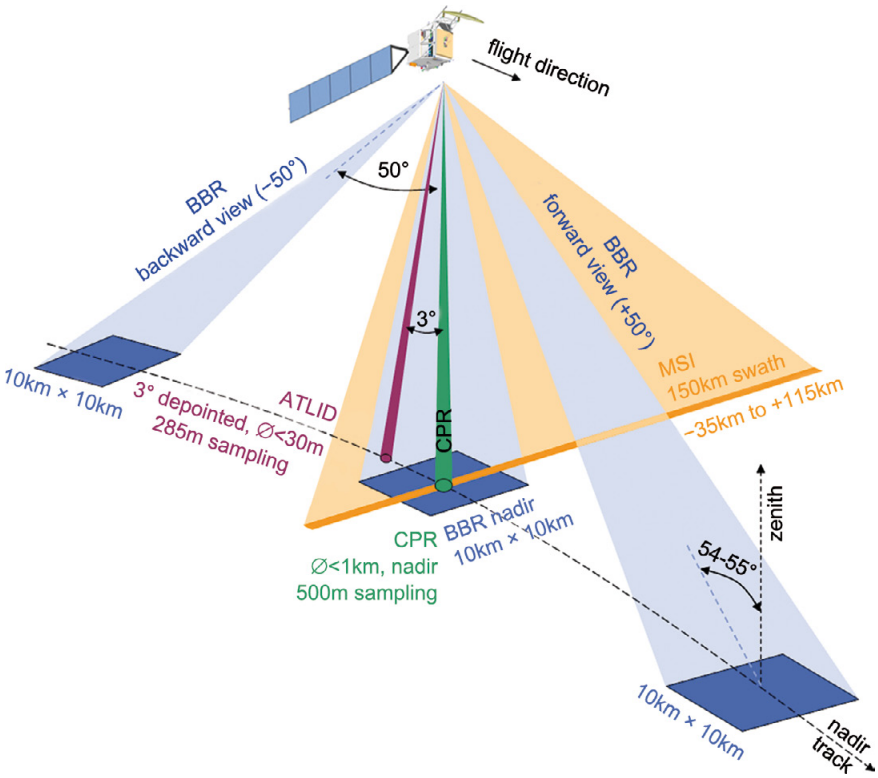

Figure 3.2.9. EarthCARE viewing geometry. (ESA)

the combination of ATLID, CPR and MSI observations it will be possible to construct 3D scenes of clouds and aerosols. Furthermore, the scene information derived from the MSI will be an important input to the algorithms estimating the TOA radiative fluxes from the BBR measurements (see below).

EarthCARE's fourth instrument, the Broad-Band Radiometer (BBR) will measure the TOA reflected total radiance (0.25≥50 μm) and short-wave radiance (0.25–4 μm), from which the solar and emitted thermal radiances will be derived. The BBR has three independent, fixed telescopes, observing each scene in forward, nadir and backward viewing directions with a ground pixel size of 10×10 km for each view. The combination of these three observations in the data processing, together with scene inhomogeneity information from the MSI imagery, will allow accurate TOA solar and thermal flux estimates linked to the simultaneously observed cloud and aerosol scenes.

Figure 3.2.9. illustrates the observational geometry of the four instruments.

Since global coverage is required, EarthCARE's orbit will be near-polar with a mean solar local equator crossing time of 14:00 (descending node), a mean spherical altitude of 393 km and a repeat cycle of 25 days for routine operations and 9 days for calibration/validation.

The EarthCARE mission is scheduled for launch in autumn 2015. It has a design lifetime of three years, including a six-month commissioning phase.

Data Products

ESA will produce calibrated Level-1b data for the ATLID, MSI and BBR instruments, while JAXA will produce Level-1b data for the CPR. Instrument Level-1b data will include:

— ATLID: attenuated backscatter signals in three channels (Rayleigh channel, copolar and cross-polar Mie);
— MSI: top of the atmosphere radiances for four solar channels and brightness temperatures for the three thermal channels;

— BBR: top of the atmosphere short- and long-wave and total-wave radiances; and
— CPR: radar reflectivity and Doppler profiles;

Level-2 data products are geophysical products retrieved from Level-1b data plus auxiliary data, such as meteorological data (ECMWF). Both ESA and JAXA will produce and exchange Level-2 data products for dissemination to their respective user communities.

The particular strength of the EarthCARE mission is the simultaneous use of four instruments with collocated fields-of-view. Consequently, the geophysical data products contain synergistically retrieved cloud, aerosol and radiation products and allow for the reconstruction of 3D scenes, in addition to data products derived independently from the individual instruments. The Level-2 data products will include:

— properties of aerosol layers: occurrence, extinction profiles, boundary layer heights, distinction between aerosol types;
— properties of cloud fields: cloud boundaries and multilayer clouds, height-resolved fractional cloud cover and overlap, occurrence of liquid/ice/supercooled layers, vertical profiles of ice water content and effective particle size, vertical profiles of liquid water and effective droplet size, and small-scale fluctuations of these properties;
— vertical velocities to characterise cloud convective motion and ice sedimentation;
— drizzle rain rates and estimates of heavier rainfall rates;
— reflected solar and emitted thermal TOA radiances and fluxes derived from BBR observations; and
— radiation parameters (including heating rates, up- and downwelling solar and thermal fluxes) calculated by 1D and 3D radiative transfer models from the retrieved 3D cloud and aerosol scenes, including, for comparison, parameters equivalent to the TOA radiances and fluxes derived from the BBR observations.

EarthCARE is the most complex of ESA's Earth Explorer missions to date. It will be built in cooperation with Japan, which will provide the CPR instrument and cooperate in the development of the ground segment and scientific data products, and in the validation and science exploitation of the mission. Valuable experience in the preparation of validation and exploitation will also be gained from the cooperation with the science communities of NASA's CloudSat and Calipso missions and their synergistic use within the A-train.

Once in orbit in autumn 2015, EarthCARE will provide global 3D cloud, aerosol and radiation observations with unprecedented accuracy, as well as novel features such as the first space-borne cloud radar Doppler observations and high-spectral-resolution lidar measurements. The synergistic exploitation of the ATLID, CPR and MSI observations will allow the construction of complex 3D cloud and aerosol scenes for which radiation parameters can be modelled and directly compared with those measured independently by the BBR. EarthCARE data will be used to improve the representation of cloud, convection, aerosol and radiation processes in climate and weather forecast and air quality models.

Reference

ESA (2004). *EarthCARE: Earth Clouds, Aerosols and Radiation*. ESA SP-1279(1). European Space Agency, Noordwijk, the Netherlands.

3.3 Missions under Study

Looking beyond the first six Earth Explorer missions, studies of candidate missions for EE-7 and EE-8 are currently being conducted. For Earth Explorer 7 there are three candidates. For Earth Explorer 8, ESA is studying two concepts, FLEX and CarbonSat. These mission concepts are described below.

3.3.1 Earth Explorer 7

The three candidates for the seventh Earth Explorer mission are Biomass, CoReH$_2$O and PREMIER.

Biomass

The purpose of the Biomass mission will be to provide spatially detailed observations of global forest ecosystems. Measurements from a low-frequency (P band) fully polarimetric, interferometric SAR will provide fundamental first observations of the global distribution of forest biomass and heights at a resolution and accuracy compatible with the needs of international reporting on carbon stocks for use in terrestrial carbon models. The mission will exploit the unique sensitivity of P-band SAR to forest biomass and will employ advanced retrieval methods to map forest biomass globally across the whole range of biomass found in tropical, temperate and boreal forests. Biomass will also provide the first opportunity to explore Earth's surface at the P-band wavelength (see Table 3.3.1).

The primary environmental science challenge in the early 21st century is to improve our understanding of how global change will affect the Earth system and the feedbacks in this system, in order that human societies can assess their likely impacts and adopt ways to mitigate and adapt to them. Deeply embedded in the functioning of the Earth system is the carbon cycle, which consists of intermeshed processes by which carbon is exchanged between the atmosphere, land and ocean (Fig. 3.3.1). Quantifying this global scale cycle is fundamental to understanding many of the dramatic changes taking place on Earth, because of its close connection with both to fossil fuel burning and land use change. These are the two most significant drivers of global change, leading to increases in atmospheric carbon dioxide (CO_2) and the associated global warming (IPCC, 2007).

Mission characteristics	
Aim	To observe global forest biomass and forest heights for a better understanding of the carbon cycle
Mission duration	5 years
Orbit	Sun-synchronous, local time 06:00
Coverage	Global coverage of forested areas in less than 6 months.
Instrument	P-band (435 MHz) Synthetic Aperture Radar
Polarisation	Fully polarimetric
Interferometry	Temporal baseline of 21 days
Resolution	50 × 50 m (4 looks)

Table 3.3.1. The Biomass mission.

Further information about the Earth Explorer candidate missions can be found at *www.esa.int/esaLP/LPearthexp.html* and *www.esa.int/esaLP/LPfuturemis.html*

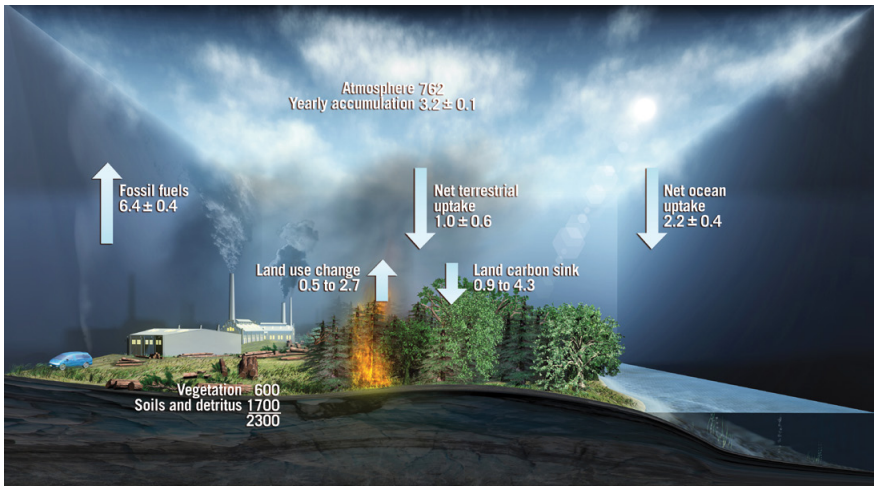

Figure 3.3.1. The global carbon cycle, showing estimates of atmospheric, ocean and terrestrial carbon pools (in Gt C), and the net annual fluxes between them (in Gt C yr^{-1}; IPCC, 2007). A small carbon run-off term from land to ocean has been omitted. (ESA/AOES Medialab)

Terrestrial processes play a crucial role in the carbon cycle through carbon uptake and respiration associated with plant growth, emissions due to the disturbance of natural processes (e.g. wildfires) and anthropogenic land use change. There is strong evidence that over the last 50 years the terrestrial biosphere has acted as a net carbon sink, removing from the atmosphere approximately one third of the CO_2 emitted in the process of fossil fuel combustion (Canadell et al., 2007). However, the status, dynamics and evolution of the terrestrial biosphere are the least well understood and most uncertain elements of the carbon cycle.

These uncertainties span a wide range of temporal scales. The inter-annual variability of atmospheric CO_2 is mainly controlled by the terrestrial biosphere, while the Intergovernmental Panel on Climate Change (IPCC, 2007) identified the effects of coupling between the terrestrial carbon cycle and climate as one of the main areas of uncertainty in climate change over decadal to century time scales. Spatially, there are major uncertainties in the distribution of carbon stocks and carbon exchange in the estimates of carbon emissions due to forest disturbance and in the uptake of carbon due to forest growth. A fundamental parameter characterising the spatial distribution of carbon in the biosphere is biomass, which is the quantity of living organic matter in a given space, usually measured as the mass per unit area. Half of biomass is carbon, so it represents a basic accounting unit for carbon. Forests contain ~80% of the terrestrial above-ground biomass.

The UN Framework Convention on Climate Change (UNFCCC) has identified biomass as an Essential Climate Variable (ECV) that is needed to reduce uncertainties in our knowledge of the climate system (GCOS, 2004). While global observation programmes for most terrestrial ECVs are advanced or evolving, there is currently no such effort for biomass (Houghton et al., 2009). In addition, sequestration of carbon in forest biomass is the only mechanism for mitigating climate change recognised under the Kyoto Protocol, other than reduced emissions. Arising from the UNFCCC, the United Nations plan for Reducing Emissions through Degradation and Deforestation (REDD; *www.un-redd.org*) is a unique international activity that is designed to assign proper values to forest resources. The REDD programme aims to encourage sustainable management of forests, maintain their carbon stores, reduce emissions of CO_2 from forest loss, and thereby mitigate climate change. Obtaining global, spatially explicit and consistent knowledge of biomass is therefore a basic requirement for understanding and managing the processes involved in the carbon cycle, and supporting REDD and other international policies for climate change mitigation and adaptation.

Scientific objectives

The Biomass mission addresses a fundamental gap in our understanding of the land component of the Earth system, which is the status and the dynamics of the Earth's forests, as represented by the distribution of forest biomass and its changes. With accurate, frequent and global information on these forest properties at a spatial scale of around 100 m, it will be possible to address a range of critical issues with far-reaching scientific and societal consequences. In particular, the Biomass mission will help to:

— reduce the large uncertainties in the carbon flux due to changes in land use;
— provide scientific support for international treaties and agreements such as REDD;
— improve understanding and predictions of landscape-scale carbon dynamics;
— provide observations to initialise and test the land element of Earth system models;
— provide key information for forest resources management and ecosystem services; and
— support biodiversity studies and conservation efforts.

The Biomass mission will explore Earth's surface at the P-band wavelength, making observations that could have a wide range of as yet unforeseen applications, such as for mapping subsurface geological features in deserts in support of palaeo-hydrological studies, the surface topography of areas under dense vegetation, and glacier and ice sheet velocities.

Mission Concept

The space component of Biomass is envisaged as a P-band polarimetric SAR mission with controlled inter-orbit distances (baselines) between successive revisits to the same site. At each acquisition, the radar will measure the scattering matrix, from which the backscattering coefficients (equivalent to radar intensity) will be derived in each of the different linear polarisation combinations, i.e. HH, VV, HV and VH, and the inter-channel complex correlation. For interferometric image pairs, the system will provide the complex interferometric correlation between the images at each linear polarisation, from which tree heights can be directly inferred.

Compared with existing and planned satellite missions, the anticipated Biomass mission concept marks a major step forward because of the unique capabilities of P-band SAR, including:

— the highest sensitivity of backscatter intensity to biomass out of all frequencies that can be exploited from space;
— its high temporal coherence over repeat passes, allowing the use of Polarimetric Interferometry (Pol-InSAR) to retrieve forest heights and, for the first time, forest vertical structure from space during an experimental tomographic phase; and
— its high sensitivity to disturbances and temporal changes in biomass.

Parallel studies of the Phase-A system and payload are addressing all elements of the mission architecture, including the space segment (platform and payload), ground segment, operations and exploitation. Throughout these studies, special attention is being paid to minimising the end-to-end cost of the mission. In addition, a number of scientific activities have been launched to study concepts related to the retrieval of biomass and tree height data, the correction of ionospheric effects on the P-band signal, the exploitation of data in models and for international treaties, and the prospect of applications of the

mission data other than for forest mapping. Dedicated airborne and ground-based campaigns have been conducted to collect P-band data over tropical and boreal forests to support the scientific assessment of the concept and to consolidate the mission requirements.

References

Canadell, J.G., Quere, C., Le Raupach, M.R., Field, C.B., Buitenhuis, E.T., Ciais, P., Conway, T.J., Gillett, N.P., Houghton, R.A. & Marland, G. (2007). Contributions to accelerating atmospheric CO_2 growth from economic activity, carbon intensity, and efficiency of natural sinks. *Proc. Nat. Acad. Sci.* **104**, 18866–18870.

GCOS (2004) *Implementation Plan for the Global Observing System for Climate in Support of the UNFCCC*. GCOS–92, WMO Technical Document No. 1219. World Meteorological Organization, Geneva, Switzerland. *www.wmo.int/pages/prog/gcos*

Houghton, R.A., Hall, F. & Goetz, S.J. (2009). Importance of biomass in the global carbon cycle. *J. Geophys. Res.* **114**, G00E03.

IPCC (2007). *Climate Change 2007: The Physical Science Basis* (Eds. S. Solomon et al.), Contribution of Working Group I to the Fourth Assessment Report of the Intergovernmental Panel on Climate Change. Cambridge University Press, Cambridge, UK.

UN-REDD. *UN Collaborative Programme on Reducing Emissions from Deforestation and Forest Degradation in Developing Countries*. FAO, UNDP, UNEP. *www.un-redd.org*

$CoReH_2O$

The second candidate Earth Explorer 7 mission is the Cold Regions Hydrology High-Resolution Observatory ($CoReH_2O$), which aims to provide spatially detailed observations of key snow, ice and water cycle parameters that are necessary for understanding land surface, atmosphere and ocean processes and their interactions. Measurements from a high-frequency SAR will provide fundamental data for detailed modelling of surface processes and surface/atmosphere exchange mechanisms in regions where snow and ice play a major role in the water and energy cycles, as well as in biospheric processes (ESA, 2008; see Table 3.3.2). Seasonal snow covers up to 50 million km^2, affecting atmospheric circulation and climate from regional to global scales.

Snow cover and glaciers are vital sources of fresh water in high-latitude regions and in many densely populated areas in the mid and low latitudes. Climate change is seriously threatening the abundance of these non-renewable resources, and immediate action is needed to improve understanding of its effects on the water cycle and to assist in the implementation of emergency

Mission characteristics	
Aim	To provide observations of key snow, ice and water cycle parameters
Mission duration	5 years
Orbit	Sun-synchronous, local time 06:00
Coverage	Test sites and dedicated areas (phase-1); global coverage of snow and ice areas (phase-2)
Revisit time	3 days (phase-1); ≥15 days (phase-2)
Instrument	dual-frequency (X-band 9.6 GHz/Ku-band 17.2 GHz) SAR
Polarisation	dual (vertical–vertical; vertical–horizontal)
Resolution	50 × 50 m (≥4 looks)
Swath width	≥100 km

Table 3.3.2. The $CoReH_2O$ mission.

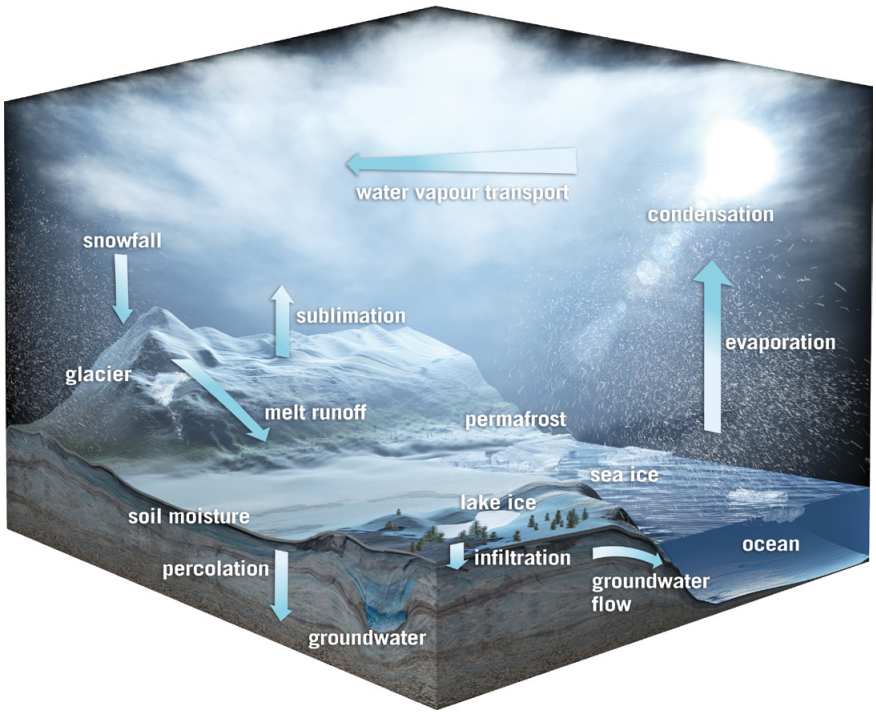

Figure 3.3.2. The CoReH$_2$O mission will address major sources of uncertainty in the global climate and water cycles: snow, glaciers, lake ice and sea ice. (ESA/AOES Medialab)

measures. Among the climate-related themes of the CoReH$_2$O mission, the supply of fresh water to high-latitude oceans and its relation to the heat and mass balance of sea ice and the thermohaline circulation is of particular interest. The mission will provide a new type of high-quality observations, which will be used to initialise, run and validate numerical water, weather and climate models for prediction and environmental monitoring applications.

For quantifying the interactions between the major components of the Earth system – the atmosphere, the hydrosphere, the cryosphere, land surfaces and the biosphere – and for assessing anthropogenic impacts on climate and ecosystems, it is necessary to develop realistic models and parameterisation schemes for the main subsystems and processes. Such models are also essential for assessing the current availability and the climate-induced changes in vital resources such as fresh water that can be expected in the future.

Although understanding of climatic and environmental processes has advanced in recent years, there is still a significant need for a more complete characterisation of dominant processes and feedbacks. The importance of improved snow and ice observations for climate research and modelling, for numerical weather prediction, for water management and ecology, and for supporting adaptation to climate change has been highlighted in many recent reports, including the IPCC's Climate Change 2007 (IPCC, 2007a,b), UNEP's Global Outlook for Ice and Snow (UNEP, 2007) and the Arctic Climate Impact Assessment (ACIA, 2005).

Snow and ice are particularly sensitive to changes in temperature and precipitation, and interact with other climate variables through complex feedbacks (Fig. 3.3.2). They also play an important role in biogeochemical cycles, particularly in the supply of water and nutrients to terrestrial and aquatic ecosystems, and have dominant influence on annual cycles. Moreover, snow and glacier melt provide basic water resources for many densely populated areas, and their abundance is seriously threatened by climate change. Accurate inventories of snow and ice masses and their dynamics, as well as improved parameterisations and modelling of water and energy exchange processes are therefore necessary to advance understanding of climate change and assess anthropogenic perturbations.

Improved process models, to be developed in the context of the $CoReH_2O$ mission, will also be of great relevance for improved management of water resources and the mitigation of water shortages.

Earth observation from space is particularly suitable for studying and monitoring snow and ice from regional to global scales because of their large spatial extent and temporal variability. Although various components of the cryosphere have been observed by non-dedicated satellite missions for many years, and a dedicated ESA mission, CryoSat, has observed fluctuations in the masses of ice sheets and sea ice, there are still large gaps in spatially detailed observations of key parameters and processes of global snow and ice masses and the high-latitude environment. The $CoReH_2O$ mission aims to fill these gaps, by providing high-resolution data on the extent, mass, melt and metamorphic state of snow and ice at regular repeat intervals over extended areas.

Scientific objectives

A set of key scientific objectives has been defined for the $CoReH_2O$ mission, which will directly address four of the five components of the Earth System highlighted in ESA's Living Planet Programme (ESA, 2006): the cryosphere (including water budgets), the land surface, the ocean and the atmosphere (through surface–atmosphere exchange processes).

The $CoReH_2O$ mission objectives related to water and climate include:

- quantifying the amount and variability of fresh water stored in terrestrial snow packs and snow accumulation on glaciers;
- validate and improve predictive hydrological models in order to reduce uncertainties in streamflow forecasts;
- validating and improving the representation of snow and ice processes and feedbacks in regional and global climate models in order to reduce the uncertainty in predictions; and
- evaluating high-resolution snow distributions and assessing their relationship to climate model grid scales in order to support the development of improved downscaling techniques for local–regional climate models.

In relation to snow and ice processes, the mission objectives include:

- exploring the distribution of snow properties in high-latitude regions with focus on the implications for terrestrial carbon cycling, trace gas exchanges and permafrost;
- evaluating the mass balance of a broad sampling of glaciers and ice caps worldwide in order to understand recent changes and place them into historical context;
- validating and improving lake ice process models with observations of ice properties in order to reduce model uncertainty and assess the effects of lake ice on surface energy exchanges; and
- exploring the magnitude and distribution of snow on sea ice and thin sea ice in order to understand their role in sea ice thermodynamics and mass balance.

The primary parameters to be observed are Snow Water Equivalent (SWE, i.e. the amount of water stored in a snow pack), snow extent and winter snow accumulation on glaciers. Secondary parameters include other features of snow (extent of melting snow, snow depth), glaciers (glacier facies types, terminus positions, glacial lakes), lake and river ice (area, freezing and melting rates, onset of melting) and sea ice (SWE, snowmelt onset, snowmelt area, type and the thickness of thin ice).

Mission concept

The mission will focus on making detailed observations of important snow, ice and water cycle parameters. Producing this geophysical information depends on backscatter measurements from a synthetic aperture radar instrument in the X- and Ku-bands, at 9.6 GHz and 17.2 GHz, respectively, transmitting with vertical linear polarisation and receiving backscattered signals from Earth's surface with vertical and horizontal linear polarisation. The Ku-band is more sensitive to shallow dry snow, while the X-band provides greater penetration of deeper snow layers and larger snow grains. The combination of observations at the two frequencies and polarisations would improve the accuracy of information about snow and provide a high level of information on sea ice, ice sheets and glaciers.

Measurements of the polarisation of the reflected radar pulses are important for separating surface and volume scattering and for estimating the snow water equivalent. The dual-frequency SAR will image a swath of 100 km in a side-looking configuration with incidence angles between 30° and 45°. The ScanSAR mode of operation has been selected, with 6–7 sub-swaths covering the 100 km swath at a spatial resolution of 50 × 50 m with four effective looks.

The mission will be based on a single satellite in a near-polar Sun-synchronous dawn–dusk orbit to observe the global snow and ice areas at high spatial resolution. A Sun-synchronous orbit with a local time early in the morning is proposed to avoid the effects of daily warming and melting. The mission will be divided into two distinct operational phases. In the first phase, lasting two years, the orbit at 666 km altitude with a 3-day repeat period over selected test areas will allow matching of the cycles of synoptic meteorological systems. These frequent visits will be at the expense of coverage. During the second phase, lasting three years, the orbit will be changed to one with a 15-day repeat cycle and 645 km altitude, allowing near-global coverage of snow and ice areas.

Parallel studies of the Phase-A system and payload are addressing all elements of the mission architecture, namely the space segment (platform and payload), ground segment, operations and exploitation. Throughout these studies, special attention is being paid to minimising the end-to-end cost of the mission. In addition, a number of scientific activities have been launched to study retrieval concepts of snow and ice parameters, ensuring the synergy of $CoReH_2O$ measurements with those of other sensors, and the assimilation of snow water equivalent measurements of in operational analyses. In analysing the mission concept, dedicated campaigns have been conducted to collect backscattered signals at the $CoReH_2O$ frequencies on the ground and with airborne sensors over several winters and under different snow regimes.

References

ACIA (2005). *Arctic Climate Impact Assessment*. Arctic Council and the International Arctic Science Committee (ACIA) Scientific Report. Cambridge University Press, Cambridge, UK. *www.acia.uaf.edu/pages/scientific.html*

ESA (2006). *The Changing Earth: New Scientific Challenges for ESA's Living Planet Programme*. ESA SP-1304. European Space Agency, Noordwijk, the Netherlands. *http://esamultimedia.esa.int/docs/SP-1304.pdf*

ESA (2008). *$CoReH_2O$: Cold Regions Hydrology High-Resolution Observatory. Candidate Earth Explorer Core Missions – Report for Assessment*. ESA SP-1313(3). European Space Agency, Noordwijk, the Netherlands. *www.congrex.nl/09c01/SP1313-3_COREH2O.pdf*

IPCC (2007a). *Climate Change 2007: Impacts, Adaptation and Vulnerability – Summary for Policymakers* (Eds. M.L. Parry et al.), Contribution of Working Group II to the Fourth Assessment Report of the Intergovernmental Panel on Climate Change. Cambridge University Press, Cambridge, UK, pp.7–22.

IPCC (2007b). *Climate Change 2007: The Physical Science Basis* (Eds. S. Solomon et al.), Contribution of Working Group I to the Fourth Assessment Report of the Intergovernmental Panel on Climate Change. Cambridge University Press, Cambridge, UK.

UNEP (2007). *Global Outlook for Ice and Snow* (Ed. J. Eamer), UNEP/GRID-Arendal, Norway.

PREMIER

Climate change is one of the biggest challenges facing society. The report The Changing Earth (ESA, 2006) highlighted several tasks for the scientific community, including gaining a better qualitative and quantitative understanding of the role of the atmosphere in the climate system. The IPCC's Fourth Assessment Report (IPCC, 2007) and the WMO's *Scientific Assessment of Ozone Depletion Report* (WMO/UNEP, 2010) also recognised the important but poorly understood interactions between atmospheric composition and climate.

The area between the upper troposphere and lower stratosphere (UTLS), at about 6 km and 25 km altitude, is particularly important for climate as it is the region where most of the thermal infrared (TIR) radiation escapes to space and where cirrus clouds trap significant amounts of outgoing TIR. Furthermore, couplings between radiative, dynamical and chemical feedbacks in this region modulate the surface climate and the atmospheric general circulation on decadal to century time scales. Interactions of the radiation field with water vapour, ozone, cirrus clouds and the distribution of aerosols in the UTLS leads to important although poorly quantified climate feedbacks.

Figure 3.3.3 illustrates some of the key radiative, chemical and dynamic processes that need to be better quantified for inclusion in climate models, such as rapid vertical transport by convective clouds, turbulent mixing related to wave breaking, gravity wave drag, ice microphysics and heterogeneous chemistry. These processes, which affect the lifetime of greenhouse gases, tend to occur on short time scales. Understanding of these processes is limited because of lack of necessary observations in the UTLS region with sufficiently high spatial and temporal resolution and accuracy.

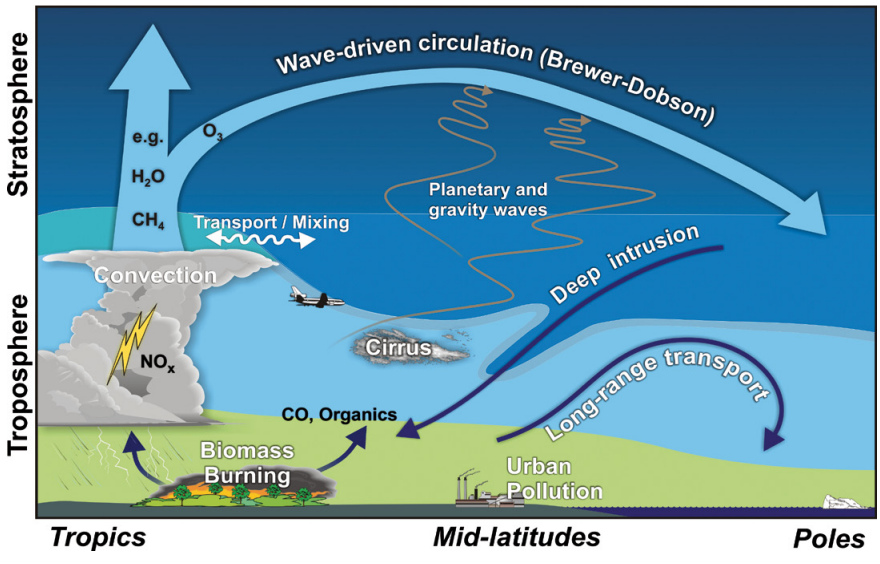

Figure 3.3.3. The structure of the upper troposphere and lower stratosphere. The tropopause (thick grey line) is the boundary between the troposphere and the stratosphere. The broad light-blue arrow indicates the wave-driven Brewer–Dobson circulation, the main transport pathway in the stratosphere. Tropospheric air enters the stratosphere (medium and dark blue) predominantly in the tropics, and is transported poleward and downwards at high latitudes. Outside the tropics, exchanges between the lowermost stratosphere (medium blue) and the free troposphere (light blue) are bidirectional. Pollution from industrial processes or biomass burning (NO_x, CO and volatile organic compounds) from the planetary boundary layer (light green) can be transported quickly into the free troposphere through convection or long-range transport. Other sources of NO_x in the free troposphere are lightning and aircraft emissions. (P. Preusse)

Scientific objectives

The PRocess Exploration through Measurement of Infrared and millimetre-wave Emitted Radiation (PREMIER) mission will provide data on the temperature and atmospheric composition of the UTLS with much improved vertical and horizontal resolution as well as 3D coverage.

The scientific objectives of the PREMIER mission are to quantify:

— the impact of UTLS variability and general circulation on the surface climate. The distributions of radiatively active gases in the UTLS affect surface climate directly through radiative forcing. They also affect the thermal structure and winds of this region, which impact surface climate indirectly through dynamic couplings between the tropospheric and stratospheric circulations. PREMIER will observe the fine-scale structure and variability in the distribution of radiatively active gases, cirrus clouds and temperature to investigate these radiative and dynamical couplings and to quantify their impact on surface climate.

— exchanges of trace gases between the troposphere and stratosphere. Exchanges of air between the stratosphere and troposphere, while poorly understood, play a major role in the budgets and distributions of water vapour, ozone and other radiatively active gases in the UTLS. The mission will measure transport tracers and temperature fields in 3D with the spatial resolutions needed to quantify quasi-horizontal transport, vertical transport by convection and gravity wave breaking, and the influence of the Brewer–Dobson circulation.

— the impacts of convection, pyroconvection and their outflow on the composition of the UTLS. Surface emissions of trace gases, particulates and water vapour can be lifted rapidly to the upper troposphere in convective or pyroconvective events. PREMIER will observe indicators of convective, pyrogenic, biogenic and volcanic sources in the outflow plumes to differentiate sources and quantify their impacts on ozone production and the composition of the UTLS.

— processes linking the composition of the UTLS and the lower troposphere. The composition of the lower troposphere is governed by surface emissions, chemical transformations, both wet and dry removal processes and transport occurring on a range of scales. By combining collocated observations from PREMIER with those from MetOp/MetOp Second Generation satellites it will be possible to extend profiles the of ozone, precursors and methane into the lower troposphere, improve estimates of the tropospheric ozone budget, surface emissions and the influence of long-range pollutant transport on air quality.

Mission concept

The PREMIER mission will address the limitations of horizontal and vertical resolution by dense sampling along-track (line-of-sight) and also across-track using an Infrared Limb Sounder (IRLS), thereby effectively producing a 3D view of the atmosphere (Fig. 3.3.4). In addition, dense along-track sampling with a millimetre-wave limb sounder (Stratosphere–Troposphere Exchange and Climate Monitor Radiometer, STEAMR) will be used to probe deeper into the troposphere in the presence of cirrus clouds. Finally, the mission will fly in tandem with the MetOp/MetOp-SG satellites in order to generate synergy between the limb and nadir measurements on the two platforms.

The PREMIER space segment will consist of a single satellite flying in formation with a MetOp/MetOp-SG satellite in a Sun-synchronous orbit at an altitude of 817 km with 09:30 local time at the descending node. The satellite will fly about 8 min ahead of MetOp and observe the limb in a rearward-

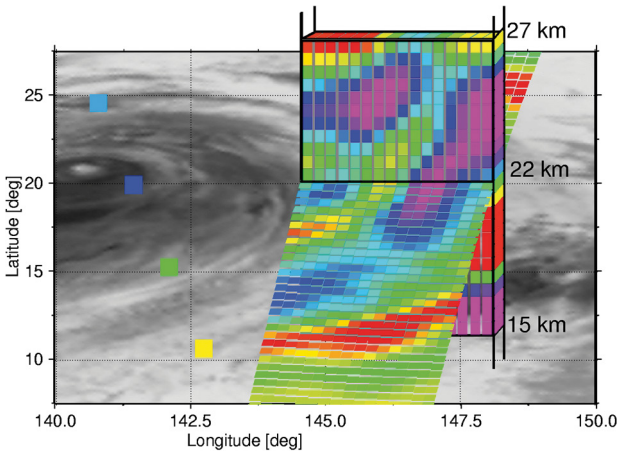

Figure 3.3.4. PREMIER sampling of 3D gravity wave temperature structures (horizontal and vertical cross-sections). For comparison, Michelson Interferometer for Passive Atmospheric Sounding (MIPAS) measurement points are indicated on the left. (L. Hoffmann and P. Preusse)

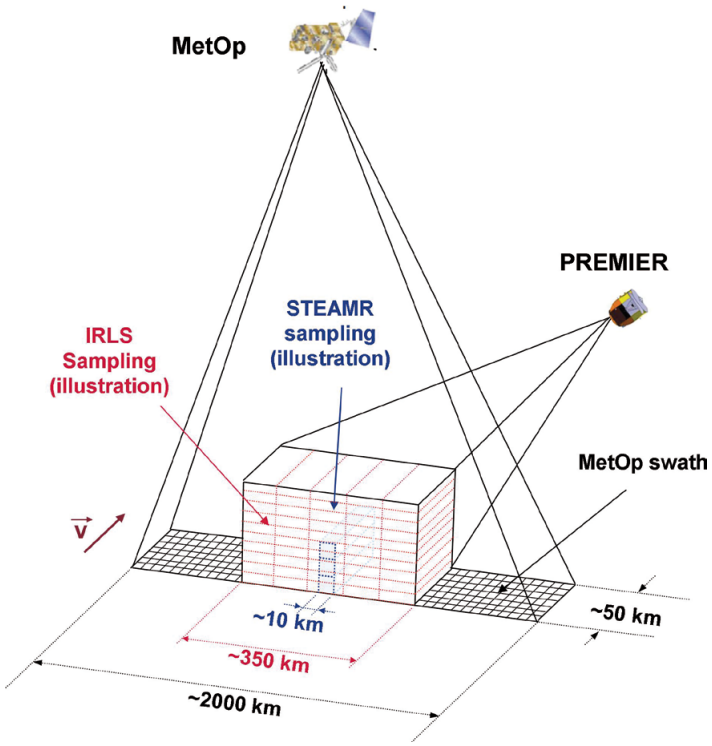

Figure 3.3.5. PREMIER and MetOp (SG) satellites in loose formation. (ESA)

looking geometry in order to exploit synergy with the nadir observations from the MetOp instruments (see Fig. 3.3.5).

References

ESA (2006). *The Changing Earth: New Scientific Challenges for ESA's Living Planet Programme*. ESA SP-1304, European Space Agency, Noordwijk, the Netherlands. *http://esamultimedia.esa.int/docs/SP-1304.pdf*

ESA (2008). *PREMIER: PRocess Exploitation through Measurements of Infrared and Millimetre-wave Emitted Radiation, Candidate Earth Explorer Core Missions – Report for Assessment*. ESA SP-1313(5), European Space Agency, Noordwijk, the Netherlands. *www.congrex.nl/09c01/SP1313-5_PREMIER.pdf*

IPCC (2007). *Climate Change 2007: The Physical Science Basis* (Eds. S. Solomon et al.). Contribution of Working Group I to the Fourth Assessment Report of the Intergovernmental Panel on Climate Change. Cambridge University Press, Cambridge, UK.

WMO/UNEP (2010). *Scientific Assessment of Ozone Depletion: 2010*, Global Ozone Research and Monitoring Project Report No. 52. World Meteorological Organization, Geneva, Switzerland.

3.3.2 Earth Explorer 8

The two candidates for eighth Earth Explorer mission are the Carbon Monitoring Satellite (CarbonSat) and the Fluorescence Explorer (FLEX).

CarbonSat

Based on experiences and lessons learnt with instruments such as SCIAMACHY on Envisat, CarbonSat has been proposed as a candidate for the eighth Earth Explorer mission. CarbonSat would be optimised to monitor carbon dioxide and methane with significantly greater spatial resolution than those of earlier instruments.

CO_2 and CH_4 are the two most important anthropogenic ('man-made') greenhouse gases responsible for climate change. Despite their importance, there are significant gaps in our knowledge of their variable natural and

Figure 3.3.6. Global average radiative forcing (RF) estimates and ranges in 2005 for anthropogenic CO_2, CH_4, N_2O and other important agents and mechanisms, together with the typical geographical extent (spatial scale) of the forcing and the assessed Level Of Scientific Understanding (LOSU). The net anthropogenic radiative forcing and its range are also shown. (IPCC, 2007).

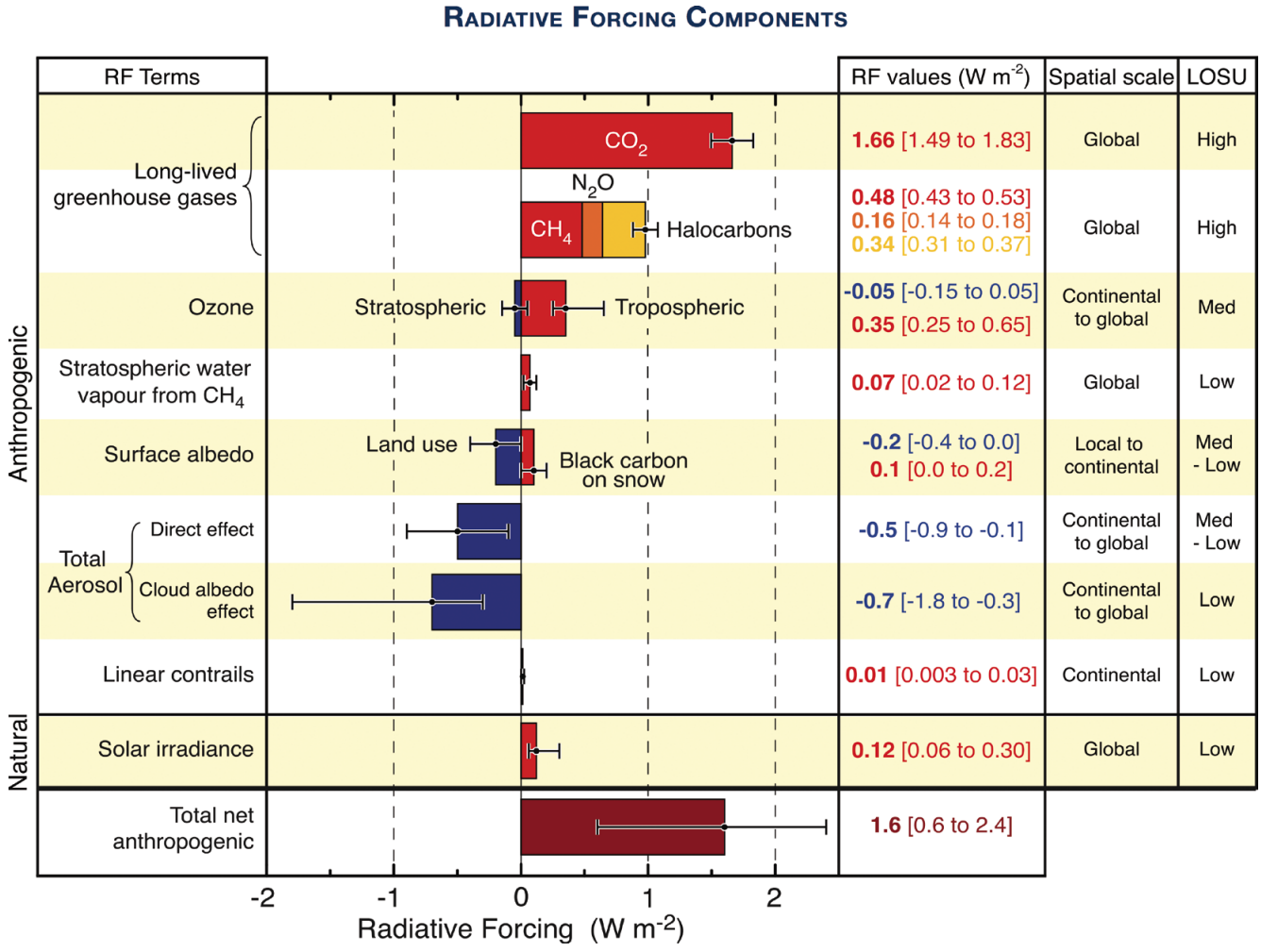

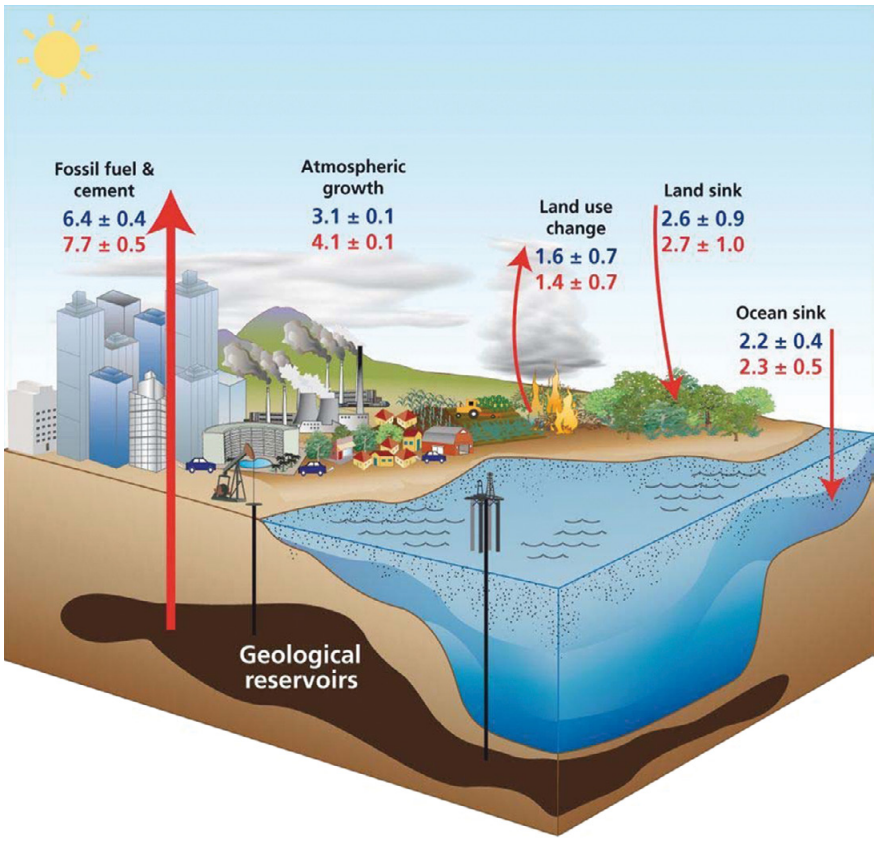

Figure 3.3.7. Global carbon dioxide budgets (Gt C yr^{-1}) in 1990–2000 (blue) and 2000–2008 (red). (IGBP/GCP)

anthropogenic sources and sinks. Appropriate knowledge about these sources and sinks is essential for reliable predictions of the future climate of our planet. Satellites can add important missing information inherent to their global coverage. This requires highly accurate CO_2 and CH_4 atmospheric measurements, with sensitivity to near-surface concentrations, and appropriate inverse modelling schemes to convert the atmospheric concentrations into surface fluxes and hence link to sources and sinks. In its Fourth Assessment Report, the IPCC (2007) pointed out that CO_2 and CH_4 are by far the two most significant long-lived greenhouse gases being released to the troposphere by anthropogenic activity (see Fig. 3.3.6).

The increasing atmospheric loading of these radiatively active gases is the dominant process that is driving global climate change. The key scientific issue is to understand the regional consequences of global climate change taking place now, and to make accurate predictions of future changes that can be used to support policies for mitigation, adaptation and management of ecosystem services in a changing climate. Despite the importance of these gases, our knowledge of the variability of natural sources and sinks, which are determined by the underlying biogeochemical cycles and feedbacks, is inadequate. This results in large uncertainties in predictions of global climate change. Figure 3.3.7 provides an overview of the global carbon cycle, and compares the global CO_2 budgets in 1990–2000 and 2000–08.

Mission Objectives

The CarbonSat mission aims to quantify and monitor CO_2 and CH_4 sources and sinks at regional to local scales, in order to understand the processes that control the carbon cycle dynamics. It will also provide independent estimates of local greenhouse gas emissions (fossil fuels, geological CO_2 and CH_4, etc.) in the context of international treaties. This latter will be achieved by frequent,

high-spatial-resolution passive remote sensing combined with inverse modelling techniques.

The CarbonSat mission will provide key data for greenhouse gas monitoring from space identified by the WMO's Global Climate Observing System (GCOS), the Integrated Global Observing Strategy (IGOS) and Global Atmospheric Chemistry Observations (IGACO) and will also serve the data needs of the GMES Atmospheric Greenhouse Gas service chain.

The mission will quantify the natural carbon budget, including terrestrial and oceanic CO_2 sinks, and assess the feedbacks between Earth's surface and the atmosphere. It will also measure methane in the most vulnerable regions, such as tropical and Siberian wetlands, permafrost areas and the continental shelf, especially those areas where methane hydrate deposits might be destabilised.

As a result of its high spatial resolution measurements, and in addition to its scientific objectives, CarbonSat will contribute to important applications for policymakers by providing quantification of strong local sources of greenhouse gases, thereby contributing to independent monitoring, verification and reporting of emissions of CO_2 and CH_4.

With CarbonSat, CO_2 emissions from local sources such as coal-fired power plants, industrial complexes, urban areas and other large sources, can be objectively assessed at a global scale. Similarly, it will become feasible to monitor leakages from natural gas pipelines and compressor stations, and to detect and quantify substantial geological CH_4 emission sources such as seeps, volcanoes and mud volcanoes will be achieved for the first time.

To establish the link between the regional and local scales, CarbonSat needs to determine very accurately the atmospheric concentrations of CO_2 and CH_4 with high spatial resolution and coverage in a unique way.

The various elements of the CarbonSat mission are building on the heritage and lessons learnt during missions such as SCIAMACHY, the Greenhouse Gases Observing Satellite (GOSAT) and the Orbiting Carbon Observatory (OCO) to make strategically important measurements of the amounts and distributions of CO_2 and CH_4 in the context of climate change.

Mission Concept

As an Earth Explorer candidate mission, CarbonSat is expected to have observational capabilities in the Near-Infrared (NIR) and Short-Wave Infrared (SWIR) part of the spectrum. This covers bands with strong absorption features of CO_2 and CH_4 and provides information on clouds and aerosols for atmospheric corrections. It is expected that data interpretation will benefit from auxiliary CO measurements such as those provided by MetOp's Infrared Atmospheric Sounding Interferometer (IASI) and MetOp-SG, including Sentinel-5.

Following the successes of SCIAMACHY and GOSAT, the challenge for the new measurement systems will be to retrieve the dry column amounts of CO_2 and CH_4 at high spatial resolution and temporal sampling. CarbonSat will meet this challenge by requiring a high spatial resolution (2×2 km) combined with sufficient spatial coverage, ideally with a 500 km swath. High spatial resolution is essential in order to maximise the probability of clear-sky observations and to identify flux hot spots.

CarbonSat's primary instrument is expected to be an imaging NIR/SWIR spectrometer that will measure CO_2 and CH_4 in combination with O_2 to yield their dry column amounts. Spectral absorptions of CO_2 in the 1.6 µm and 2 µm bands, O_2 in the 760 nm and CH_4 in the 1.65 µm spectral ranges, measured with high spectral resolution of the order of 0.03–0.3 nm and a high signal-to-noise ratio. The objective is to measure CO_2 columns at 1 ppm and methane columns at 1 ppb for single measurements.

CarbonSat is currently being studied at the feasibility level, and various implementation options are under review. System as well as scientific studies

are about to start, leading to an optimisation and consolidation of the CarbonSat observational and system concept.

Reference

IPCC (2007). *Climate Change 2007: The Physical Science Basis* (Eds. S. Solomon et al.). Contribution of Working Group I to the Fourth Assessment Report of the Intergovernmental Panel on Climate Change. Cambridge University Press, Cambridge, UK.

Fluorescence Explorer (FLEX)

The first FLEX mission concept was presented in response to the call for proposals for the seventh Earth Explorer, and was selected for Phase-0 study. After an assessment, FLEX was not selected for Phase-A study, but in 2009 the Earth Science Advisory Committee (ESAC) recommended a detailed investigation of the options for a tandem mission comprising a stand-alone fluorescence spectrometer and an approved mission. The new EE-8 FLEX mission concept features a small satellite carrying a Fluorescence Imaging Spectrometer (FLORIS) flying in tandem with a GMES Sentinel-3 satellite.

Photosynthesis

The carbon that is released by anthropogenic activities has been increasing monotonically in recent decades. The net amount of carbon that is fixed each year in natural ecosystems, however, is highly variable. Photosynthetic CO_2 fixation is the first key process that removes carbon from the atmosphere and there are currently great uncertainties about the mechanisms underlying these dramatic year-to-year variations. The annual uptake of atmospheric carbon by terrestrial ecosystems (120 Gt) is much larger than the amount of carbon released in fossil fuel combustion (6–7 Gt). Hence, even small alterations in the terrestrial carbon balance are likely to have major impacts on atmospheric CO_2 concentrations. The large year-to-year variations in carbon removed from the atmosphere highlight the enormous role of the biogenic carbon cycle, where plant photosynthesis constitutes a key process in determining gross primary production (GPP). Small changes in GPP will unavoidably have major impacts on the entire carbon cycle, with unpredictable impacts on carbon storage in the short, medium and long term.

Photosynthesis is a complex physiological process that consists of nearly 100 biophysical subprocesses and chemical reactions. Even though plants look green even when environmental conditions are sub-optimal, their internal processes constantly adjust the assembly of the pigments and related physiological processes, such that the actual photosynthetic efficiency of plant tissues varies over a wide range. While most of these mechanisms are well known at the leaf or canopy levels, the understanding of all such mechanisms at larger scales, covering biomes or even continents, is still very poor.

The main reason for this is the lack of indicators at such large scales that can reflect the dynamics of photosynthesis. The boreal forests, for example, represent a significant fraction of the amount of carbon assimilated by vegetation. The photosynthetic capacity of boreal forests – both deciduous trees (which regrow their canopy every spring) and evergreen conifers (due to dormancy, frozen soil or damage to the photosynthetic machinery) – varies considerably during the annual cycle. These restrictions can have a drastic influence on the carbon balance of boreal coniferous stands, and calculations

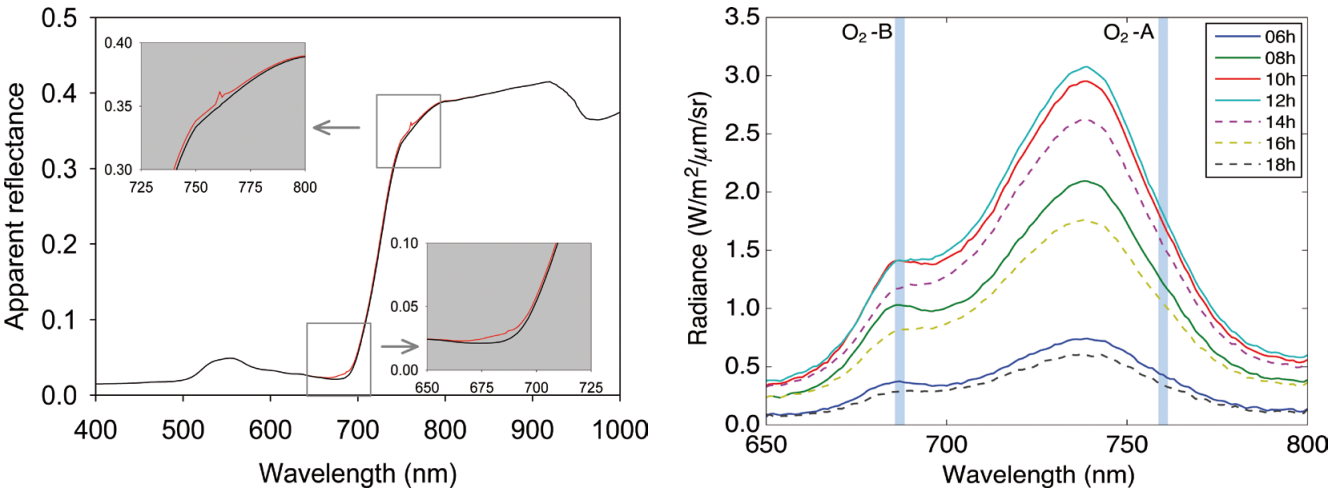

Figure 3.3.8. *Left:* Contribution of spectral fluorescence emissions over the background reflectance (Meroni et al., 2009). *Right:* Laboratory-measured vegetation fluorescence spectra under varying illumination conditions, filtering out the reflected component (Amoros-Lopez et al., 2008).

of GPP may result in overestimates of up to 40% if these restrictions on photosynthesis are not taken into account.

Until now, most of the information acquired by remote sensing of vegetation conditions and photosynthetic activity has come from 'reflected' light in the solar domain. There is, however, one additional source of information about vegetation photosynthesis in the optical and near-infrared wavelength range that has not yet been exploited by any satellite mission. It is related to the 'emission' of fluorescence from the chlorophyll of leaves: part of the energy absorbed by chlorophyll is not used for carbon fixation, but is re-emitted at longer wavelengths as fluorescence.

Analysis of the fluorescence signals provides information about photosynthetic efficiency, making fluorescence a sensitive bioindicator of photosynthetic perturbation and stress. Solar-induced fluorescence can be measured by passive techniques, making use of strong atmospheric absorption bands in narrow regions of the spectrum, where apparent vegetation reflectance is mostly contributed by chlorophyll fluorescence. Recent studies have demonstrated that the weak fluorescence signal (Fig. 3.3.8) is indeed detectable from a satellite system at relevant spatial resolution, and with the accuracy required by ecosystem models, providing a link between atmospheric CO_2 observations and the detailed knowledge of leaf physiology, and making the most direct possible measurement of photosynthesis processes on land at representative regional to global scales.

Mission Objectives

By quantifying and monitoring vegetation photosynthesis at the global scale, the FLEX mission will provide data of fundamental interest to climate change researchers:

— FLEX will be used to create a database of global remote measurements of fluorescence derived under a range of environmental conditions and types of vegetation. The database will include monitoring data for different plant species, C3 and C4 dynamics, different age structures, seasonal fluorescence patterns and year-to-year differences in fluorescence behaviour. Such a library will provide an invaluable foundation for developing and testing physiological applications.

— By combining measurements from FLORIS and the GMES Sentinel-3 instruments, the mission will provide accurate and reliable information on photosynthetic activity.

— Fluorescence signals address directly the initial photochemical events of photosynthesis, specifically related to photosystems I and II – the so-called light reactions – which have a direct bearing on the overall process of photosynthesis. The FLEX results may therefore be evaluated as inputs for improving estimates of photosynthesis, including gross primary production.

— The early responsiveness of fluorescence to biotic and abiotic stresses makes it a powerful bioindicator of health status of vegetation.

Decades of research have already established the sensitivity of near-field fluorescence to atmospheric perturbations, soil composition effects, plant water balance, atmospheric chemistry, insect and disease attacks and the effects of human land use. FLEX will advance this work to the remote scale for identifying and tracking the effects of such stresses on terrestrial vegetation. In particular, the use of fluorescence in quantifying photosynthetic strain, resilience and recovery will be assessed. Currently, vegetation stress is poorly described in numerical models since hardly any observations at regional to continental scales have been available. A particular advantage of fluorescence is its capacity to serve as a pre-visual indicator of stress effects before damage is irreversible and detectable through reflectance measurements.

Mission Concept

To reduce the complexity of the mission and the associated implementation costs, a tandem mission concept is foreseen for FLEX. The most critical information required from the tandem partner mission is related to the characterisation of the state of the atmosphere (cloudiness, aerosols and atmospheric water vapour) and land surface characteristics (land cover type, biophysical parameters and surface temperature). This information will be available on a routine operational basis from systems that are not constrained by the lifetime and launch date of an Explorer-type satellite. This is only possible if the partner satellite is an operational mission designed to provide continuous data over an extended period. In this context, the GMES Sentinel missions are ideal candidates. Sentinel-3 could deliver the required auxiliary datasets and is therefore the baseline companion for the tandem mission.

Optimal retrievals are obtained when using a full spectral range from 500 nm to 780 nm, which includes:

— the two main oxygen absorption bands and the red-edge in between driving surface reflectance variations for vegetation targets;
— the spectral region associated with Photochemical Reflectance Index (PRI) between 500 nm and 600 nm; and
— the region of chlorophyll absorption with or without very low fluorescence emission from 600 nm to 67 nm.

To demonstrate the usefulness of fluorescence measurements from space, at least three full vegetation growing cycles will be needed to obtain statistical significance in inter-annual variability versus seasonal cycles over both hemispheres, giving minimum target mission duration of 3.5 years. The mission will provide global access over all vegetation-covered land surfaces between latitudes 56°S and 75°N, including islands larger than 100 km^2 and coastal zones within 50 km of land. As a balance between maximum fluorescence emission and maximum solar illumination, the observation time should be around

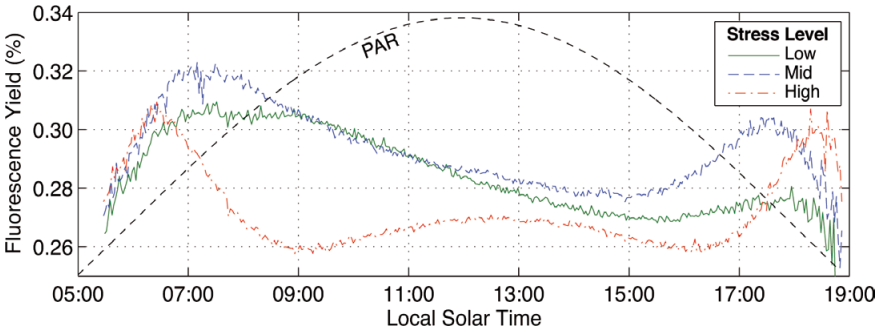

Figure 3.3.9. Typical variations in the fluorescence yield of vegetation during a diurnal cycle under environmental conditions that induce different levels of vegetation stress. PAR: Photosynthetically Active Radiation (Amoros-Lopez et al., 2008).

9:30–10:00 local solar time (Fig. 3.3.9). The spatial resolution at the ground should be comparable to that provided for the Sentinel-3 data, i.e. 300 m.

Phase-A of the FLEX mission is expected to start in 2012.

References

Amoros-Lopez, J., Gomez-Chova, L., Vila-Frances, J., Alonso, L., Calpe, J., Moreno J. & Del Valle-Tascon, S. (2008). Evaluation of remote sensing of vegetation fluorescence by the analysis of diurnal cycles, *Int. J. Rem. Sens.* **29**(17-18).

Meroni, M., Rossini, M., Guanter, L., Alonso, L., Rascher, U., Colombo, R. & Moreno, J. (2009). Remote sensing of solar induced chlorophyll fluorescence: Review of methods and applications, *Rem. Sens. Env.* **113** (10), 2037–2051.

→ ERS AND ENVISAT

4. ERS and Envisat

4.1 20 Years of the ERS Programme

The European Remote Sensing (ERS) programme included two satellites, ERS-1 and ERS-2, launched on 17 July 1991 and on 21 April 1995. The programme resulted from a well-planned strategy initiated in the early 1970s by the European Space Research Organisation (ESRO), the predecessor of ESA, to explore the potential of remote sensing from space for the management of Earth resources and monitoring the Earth environment. This section presents an overview of the history of the ERS programme, from the early definition phase of ERS-1 in the early 1980s to the deorbiting phase and passivation of ERS-2 in September 2011.

4.1.1 ERS-1

An important event in the decision process for the ESA remote sensing satellite programme was the launch of Seasat in July 1978. Despite its short lifetime (106 days), Seasat provided large amounts of data of interest to the world's oceanographic community. The success of Seasat encouraged ESA to consider alternative Coastal Oceans Monitoring Satellite System (COMSS) payloads, and follow-on trade-off studies performed in 1980 considered the inclusion of a radar altimeter, wind scatterometer and other instruments for measuring Earth's radiation budget. Those studies determined that the ERS mission objectives, covering land, ice and oceans, could be accomplished by a single satellite using the multi-mission SPOT-2 platform (proposed by France as a 'contribution in kind').

The ERS programme was set up at about the same time as a number of global climate and ocean monitoring programmes, such as the World Climate Research Programme's World Ocean Circulation Experiment and Tropical Ocean–Global Atmosphere observing system. There were also growing concerns among politicians, decision makers and the public about climate change and possible human interactions and contributions, which required an improved scientific understanding of the climate system. The ERS was to be primarily a scientific research mission, while also to a certain extent supporting commercial applications, with the following objectives:

— to increase scientific understanding of coastal zones, global oceans and polar regions, and provide support for government policies related to the environment and climate change;
— to develop and promote economic and commercial applications, using ERS-1 as a demonstration mission and a 'market opener' for downstream/value-adding industries; and
— to explore the potential of radar data for studies of land processes and other applications.

The proposed ERS payload consisted of an Active Microwave Instrument (AMI), including SAR and wind scatterometer modes, both operating in the C-band (5.3 GHz) and sharing common electronic hardware. The SAR mode was designed to operate as a 'wave scatterometer' over the open ocean (SAR Wave mode) and as a high-resolution imaging radar (SAR imaging mode) over land, coastal zones and polar regions. The payload would also include a Radar Altimeter operating in the Ku-band.

Further information about the ERS programme can be found at *http://earth.esa.int/ers*

Table 4.1.1. ERS-1 mission phases (ESA, 1999).

Phase	Repeat cycle	Mean altitude	Dates
A: Commissioning phase	3 days	785 km	July to December 1991
B: 1st Ice phase	3 days	785 km	December 1991 to March 1992
C: 1st Multidisciplinary phase	35 days	782 km	April 1992 to December 1993
D: 2nd Ice phase	3 days	785 km	January to April 1994
E: 1st Geodetic phase	168 days	770 km	April to September 1994
F: 2nd Geodetic phase	168 days	770 km	October 1994 to March 1995
G: 2nd Multidisciplinary phase	35 days	782 km	April 1995 to end of mission

Following an Announcement of Opportunity, three instruments were selected: the Along-Track Scanning Radiometer (ATSR) provided by the United Kingdom and Australia, the Microwave Radiometer (MWR) provided by France, and the Precise Range and Range Rate Experiment (PRARE) provided by Germany.

ERS-1 Orbit Configuration

In order to meet the requirements of the various user communities (land, ice, ocean, coastal zones, geodesy) in terms of revisit frequency, as well as those for commissioning phase activities (requiring a fast revisit frequency over calibration sites), several trade-offs had to be made. Various studies were conducted, leading to the orbit configuration described in Table 4.1.1.

The adoption of the sequence of repeat cycles shown in the table generated lively discussions, in particular for the geodetic Phase-D, which required a long repeat cycle to allow a dense spatial sampling of the marine geoid with the Radar Altimeter. The other user communities (land, ice, etc.) raised concerns about the implications of such a repeat cycle, and these became even stronger when a second geodetic phase (interleaved with the first) was proposed and adopted, doubling the spatial sampling density of the geoid (16 km at the equator). The user communities reached a compromise by implementing a ‘pseudo-repeat cycle’ within this 168 day cycle.

Throughout its mission lifetime, from 1995 to 2011, ERS-2 was operated in the 35 day repeat orbit, except for the last four months before deorbiting (10 March to 4 July 2011), when the satellite was operated in the 3-day repeat orbit configuration.

ERS-1 Ground Segment

The complete ERS-1 ground segment included the telemetry, tracking and command (TT&C) operations performed under the responsibility of ESOC, and the payload data management by ESRIN, near Rome, Italy. The ground segment for the payload data handling consisted of two parts: the near-realtime (NRT) part, which was responsible for generating and distributing an agreed set of products (geophysical parameters and SAR imagery) within 3 h of observation, and an offline part, which was responsible for generating, archiving and distributing more elaborate products.

The low-bit-rate data recorded by ERS-1 were downlinked to ESA’s network of receiving stations, which included Kiruna (Sweden), Maspalomas (Spain), Gatineau (Canada) and Prince Albert (Canada). The data were also disseminated in NRT to meteorological offices and research institutes. For the SAR data, the receiving stations at Kiruna, Maspalomas and Fucino (Italy) were selected. For the offline activities, four national Processing and Archiving Facilities (PAFs) were selected: DFVLR (now the German Aerospace Center,

DLR) at Oberpfaffenhofen in Germany; the Institut Français de Recherche pour l'Exploitation de la Mer (IFREMER) in Brest, France; Matera in Italy; and Farnborough in the UK, each with well-defined responsibilities and mandates.

User Communities

ESA has devoted considerable effort and resources to the development of user communities, which in the early 1980s were still embryonic and not well structured, except for the meteorological community.

In 1986 an Announcement of Opportunity for scientific research experiments and application pilot projects was released. It generated considerable interest and 140 responses, which were regrouped into 276 individual proposals covering all ERS areas of research and applications. More than 100 Principal Investigators (PIs) were selected, each representing a team of scientists, some of them very large. The PIs played a key role in the development of user communities and in raising awareness of ESA's Earth observation programmes, and the ERS in particular. This and later AO processes during the lifetime of ERS-1 and ERS-2 resulted in thousands of peer-reviewed publications. These reported on scientific research, application demonstrations, to the exploitation of ERS-1/ERS-2 tandem data collected after the launch of ERS-2 in 1995. Regular ERS symposia were organised, and attracted increasing interest. The number of participants rose from 400 at the first symposium in Cannes, France, in 1992, to 1200 at the final symposium in Bergen, Norway, in June 2010.

ESA set up several expert groups to advise on ERS instruments (SAR, Wind Scatterometer, Radar Altimeter) and data products. These groups, which included European and Canadian experts, contributed to the definition and preparation of sensor calibration and product validation activities, and of processing algorithms needed to generate the geophysical parameters derived from the engineering data. They also assisted the project team in the definition of airborne campaigns to support the calibration and validation activities.

The Association of Remote Sensing Laboratories (EARSeL), whose members include more than 200 laboratories and institutes, played an active role in expanding the user communities by conducting specialised studies financed by ESA and organising workshops and symposia. The creation of the European Association of Remote Sensing Companies (EARSC) in 1989 also provided an impetus for the development of operational/commercial applications using ERS data. By 2010 the EARSC network had grown to 67 companies and small and medium enterprises (SMEs).

ESA has continued its activities to promote and raise awareness of the ERS programme, including making presentations at important events, symposia and specialised workshops, as well as thematic events. International cooperation with foreign countries and/or organisations also provides opportunities to promote the ERS programme.

Figure 4.1.1. One of the first SAR images acquired by ERS-1, covering the calibration site of Flevoland, the Netherlands. (ESA)

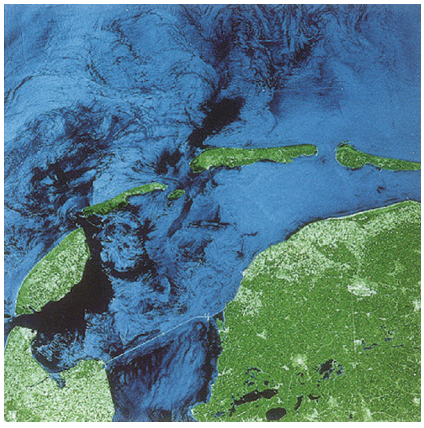

ERS Launch and Early Exploitation Phase

ERS-1 was delivered to the planned orbit with such accuracy that only 10 kg of hydrazine fuel was required for final orbit acquisition, leaving a healthy fuel margin to support a long lifetime in service. ERS-1 was designed for a nominal two-year lifetime and consumables sized for three years, but it remained in service for nine years, until March 2000.

The first SAR images were taken over Spitsbergen and the Frisian islands in the North Sea (Fig. 4.1.1) on 27 July 1991, 10 days after launch and switch-on of all instruments (except for PRARE, which failed after just five days over the South Atlantic anomaly).

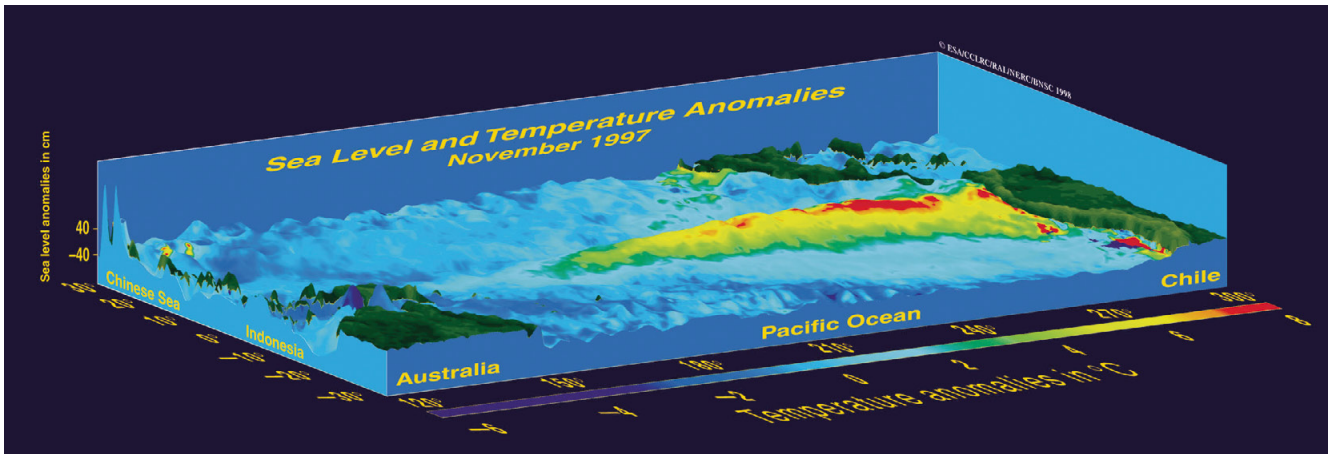

Figure 4.1.2. 3D ERS-2 image of sea level and temperature anomalies in the Pacific during the 1997–98 El Niño event, based on simultaneous ATSR and RA data acquired in November 1997. (ESA/CEOS)

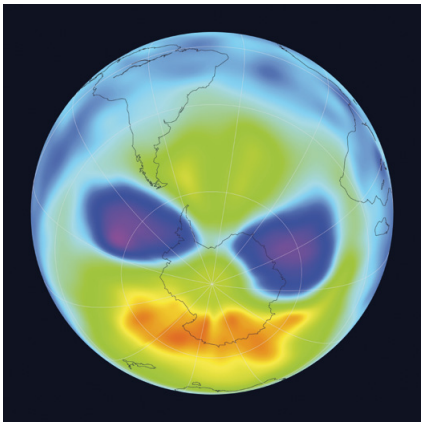

Figure 4.1.3. An atypical split in the ozone hole over Antarctic monitored by GOME in 2002. (ESA/DLR)

ERS-2 was launched in 1995 and injected into the same orbital plane as ERS-1. It supported observations of the 1997–98 El Niño event with simultaneous measurements by the ATSR and the Radar Altimeter (RA). This El Niño had enormous impacts worldwide, with increased rainfall causing floods in the United States and Peru, and drought in the western Pacific. Figure 4.1.2 presents a 3D image of the Pacific in November 1997, showing measured deviations from the 'normal' ocean state with changes in sea-surface height of between –40 cm and +40 cm and in temperature of –6°C (blue) to 8°C (red).

The Global Ozone Monitoring Experiment (GOME) on ERS-2 monitored the ozone layer and other atmospheric trace gases for 16 years. Figure 4.1.3 shows the total ozone measured by GOME in September 2002 showing an atypical split in the ozone hole over the Antarctic due to the unusual meteorological conditions at that time. GOME led the way in the use of space instrumentation for monitoring air quality.

ERS-1 Routine Exploitation

The ERS-1 exploitation phase continued until the failure of the satellite on 10 March 2000. During its nine years in service, ERS-1 completed 45 000 orbits and collected 1.5 million individual SAR images. In 1992, the members of the ERS consortium – SPOT Image, Eurimage and Radarsat International – signed an agreement to promote and distribute ERS-1 products, with ESA retaining responsibility for distributing products free of charge to selected PIs.

During that period additional AOs were released, fostering an ever-growing user community. ESA negotiated numerous Memoranda of Understanding (MOUs) for the acquisition of ERS-1 SAR data with the United States, Israel, countries in Asia (Japan, China, Taiwan, Singapore, Indonesia and Thailand), in Africa (South Africa and Kenya), South America (Argentina and Ecuador) and Antarctica (Syowa, McMurdo and O'Higgins stations). Other MOUs related to the deployment of mobile/transportable receiving stations were negotiated with Gabon, Mongolia and Bangladesh. These international agreements (for some 20 receiving stations) have extended the use of ERS data and have helped raise awareness of the programme.

ESA, either alone or in association with UN agencies, has organised numerous education and training courses in developing countries and at ESRIN, and has collaborated with many international organisations, in particular the United Nations Educational, Scientific and Cultural Organization (UNESCO), the UN Environment Programme (UNEP), the UN International Drug

Control Program (UNDCP), the UN Office for Outer Space Affairs (UNOOSA), the World Meteorological Organization (WMO), the UN Food and Agriculture Organization (FAO), the Intergovernmental Oceanographic Commission (IOC), as well as the World Bank and the Asian and African Development Banks. Such cooperation has been extremely fruitful, helping to promote and expand the use of ERS data and products (e.g. funding from the Asian Development Bank was used to upgrade the regional Bangkok receiving station).

4.1.2 ERS-2

The ERS-2 programme was approved in spring 1990. With the addition of the GOME instrument for stratospheric ozone measurements, the ERS-2 payload was further improved with the ATSR-2, which included three additional VIS channels, and PRARE-2 was completely redesigned.

4.1.3 ERS-1/ERS-2 Tandem Operations

Participants at several ERS-1 user meetings and symposia expressed interest in the simultaneous operation of ERS-1 and ERS-2. An ERS-1/ERS-2 tandem mission would provide many advantages and would benefit both research and applications. In particular, it would be possible to collect a unique SAR dataset for interferometry applications.

One objective of the tandem operation phase was to acquire, as quickly as possible, complete Earth coverage with ERS-1 and ERS-2 SAR data within the visibility of existing ERS-1 ground receiving stations (Fig. 4.1.4). The collection of a unique tandem dataset was considered to be an asset for the development of interferometry applications (such as Digital Elevation Models, DEMs) as well as differential interferometry applications allowing the detection of subcentimetre ground displacements/motion.

Just a few days after the launch of ERS-2, a number of SAR images were acquired using ERS-1 and ERS-2 in tandem mode, with each satellite observing the same target region at 24 h intervals. These data were quickly processed and

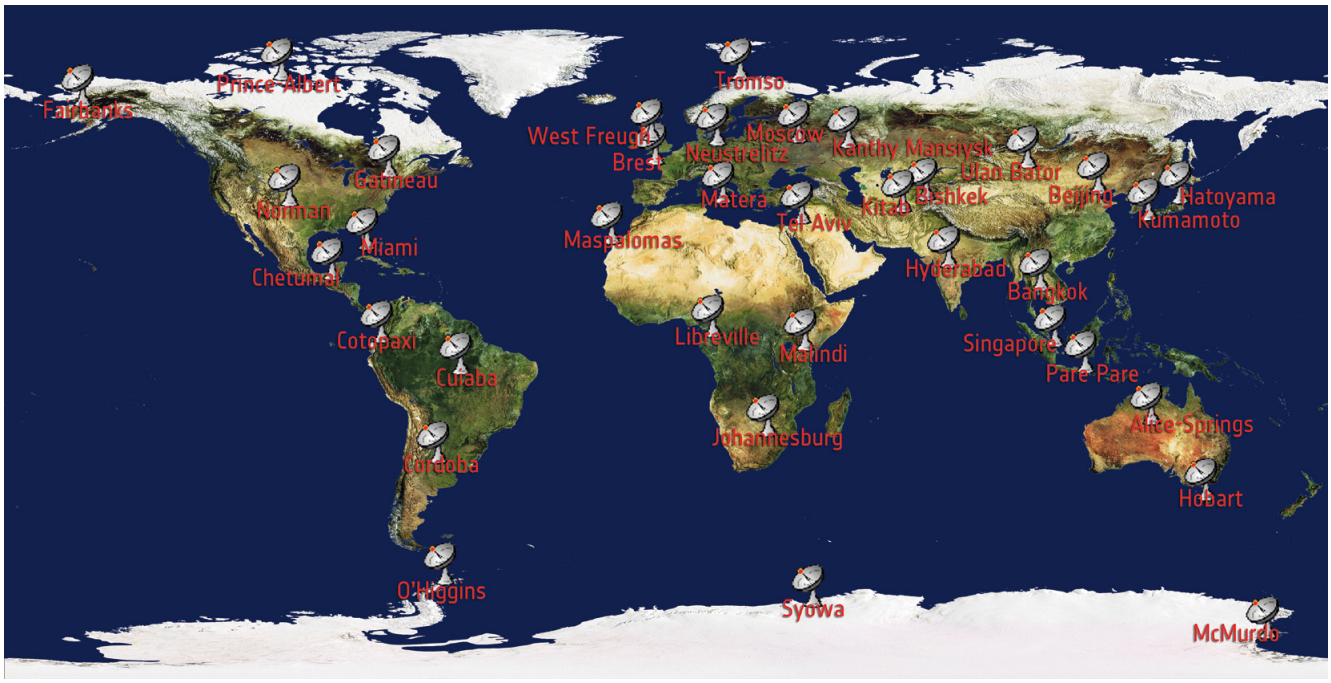

Figure 4.1.4. The global network of ERS receiving stations. (ESA)

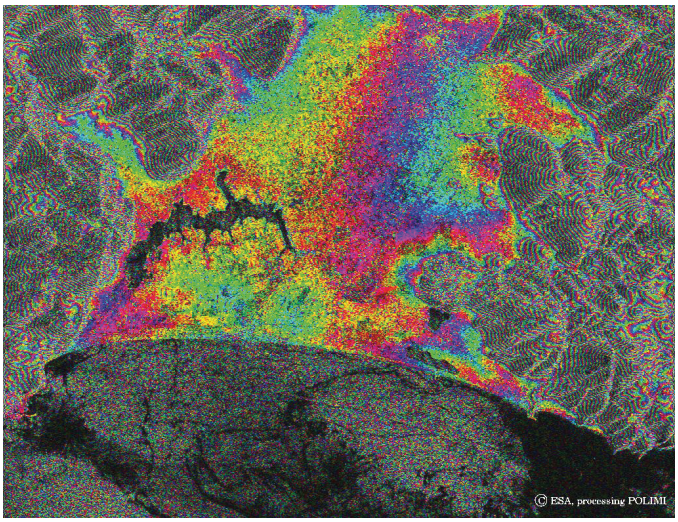

Figure 4.1.5. The first ERS-1/ERS-2 tandem interferogram, central Italy, May 1995. (ESA/PoliMi)

analysed by European experts to demonstrate some of the possibilities offered by SAR interferometry for the generation of DEMs.

Figure 4.1.5 shows the first example of a radar interferogram generated as the basis for a 3D map of Earth's surface, using the first ERS-2 SAR image acquired on 2 May 1995, combined with an ERS-1 image from the previous day.

One Mission across Three Platforms

The ERS instruments were the predecessors of Envisat's ASAR, Radar Altimeter-2, AATSR and SCIAMACHY instruments. The successors to the ERS Scatterometer and GOME are now flying on MetOp-A. By ensuring the continuity of time series observations over more than two decades, the ERS programme has fulfilled the requirement for cross-calibration specified in GCOS Climate Monitoring Principle 12 (GCOS, 2003). Throughout all the ERS missions, special emphasis was given to the determination and documentation of inter-satellite/instrument biases.

Furthermore, the ERS and equivalent Envisat instrument data products have been harmonised in terms of format and the retrieval algorithms used. This harmonisation is particularly important for reprocessing exercises using cross-satellite datasets. Data quality and homogeneity have been operationally assessed with the support of the European Centre for Medium-Range Weather Forecasts for the Scatterometer and Wave Mode missions. For the ATSR missions, the data quality has been monitored jointly by the Rutherford Appleton Laboratory (UK), the instrument provider, the PI team, and the UK Natural Environment Research Council (NERC), which funded the ATSR mission. The high quality of GOME mission data has been ensured by the DLR, which was responsible for operational processing and continuous improvement of data retrieval. This led to five data reprocessing exercises, as a result of which new trace gases have been derived with ever smaller error bars.

Long-term quality assurance and documentation have been essential elements of the ERS-2 mission. For routine operational monitoring, a consortium of instrument specialists monitored instrument performance on a daily basis. Quality Working Groups (QWGs), composed of European and Canadian specialists, evaluated the evolution of the instruments, analysed the retrieval algorithms and defined actions for further improvement. This setup ensured the constant evolution of products that would extend beyond the ERS mission lifetime. Further improvements in the data products have been made thanks to the close working relationships with user communities worldwide that provided inputs to ESA via workshops and symposia. For the instruments

jointly exploited with Eumetsat and the UK's NERC, the mechanism of Science Advisory Groups (SAGs) is being used to advance the science and to improve the instrument products. One example of this fruitful collaboration with the user community, the QWG, the Advanced Scatterometer Science Advisory Group (ASCAT SAG) and Eumetsat has been the creation of a Scatterometer Soil Moisture product, which after 20 years, enabled the use of 'ocean data' also for land applications.

The ERS, one of the longest multi-instrument missions ever flown, has in its operations scenario also considered the GCOS Climate Monitoring Principles. With the continuous mission extension approvals by Member States, ERS-2 had a five-year overlap with ERS-1, a nine-year overlap with Envisat and a five-year overlap with MetOp-A for the Scatterometer and GOME-2. Before deorbiting, a low-bit rate station was installed in Brazil to allow ERS Scatterometer and the MetOp ASCAT to make concurrent observations over a large, homogeneous target area in the Amazon rainforest covering all three beams, which contributed to the best possible cross-calibration of these twin instruments.

As a further example of the continuous evolution of the mission, chapter 2 of the WMO's *Scientific Assessment of Ozone Depletion* (WMO, 2010) assessed the measurements of the total ozone column retrieved from nadir sounding instruments. The report notes that GOME-1 had provided the most reliable and accurate dataset for analysing ozone trends for the morning orbit, which has become the standard in terms of reliability and accuracy. The SCIAMACHY and GOME-2 data records are now being combined with those of GOME-1 to provide full global coverage for trend analysis adapted to GOME-1.

ERS-2–Envisat Tandem Operations

The idea of exploiting the cross-satellite interferometry capabilities came from the Swiss company GAMMA Remote Sensing AG. Envisat was flying 28 min ahead of ERS-2, observing the same ground targets. However, the two satellites had a slightly different SAR centre frequency of 31 MHz. In order to obtain interferograms taking advantage of this short observation interval, the perpendicular baseline needed to be about 2 km (see Fig. 4.1.6). Since ERS-2 had ample fuel on board and Envisat had stringent GMES service commitments to fulfil, it was obvious that ERS-2 needed to be manoeuvred to implement the required baseline at specific observation targets.

Because the interferometry baselines could only be reached via slight changes in inclination, and thus only observation targets within a range of latitudes could be addressed, the ERS-2–Envisat tandem mission was divided

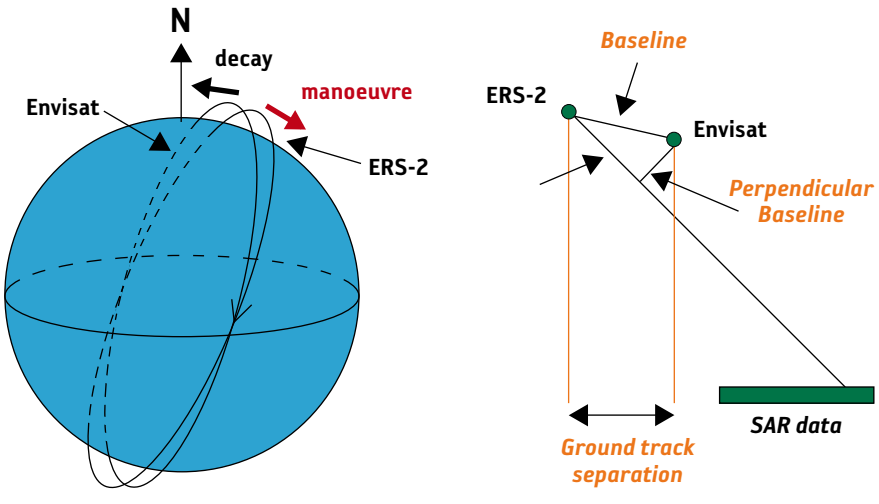

Figure 4.1.6. ERS-2–Envisat tandem operation orbital configuration. (GAMMA Remote Sensing AG)

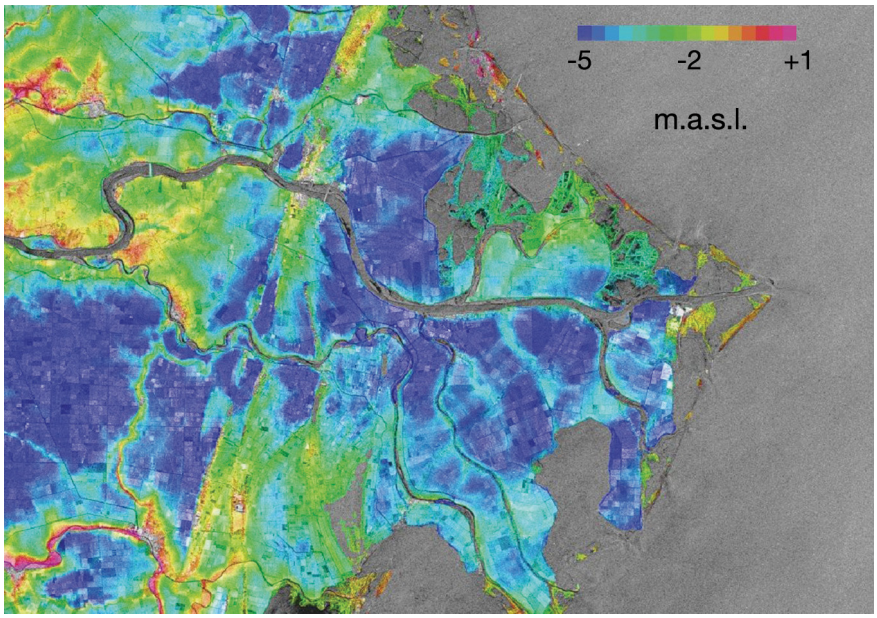

Figure 4.1.7. Digital Elevation Model of the Po delta, Italy, from the ERS-2–Envisat cross-InSAR; area covered 50 × 30 km; m.a.s.l.= mean altitude above sea level (ESA/GAMMA Remote Sensing AG)

into four campaigns, with the second and fourth campaigns addressing change detection over intermediate northern latitudes. The campaigns took place on the following dates:

— first campaign: September 2007 to February 2008, northern latitudes;
— second campaign: November 2008 to April 2009, intermediate northern latitudes;
— third campaign: February to April 2010, Antarctica;
— fourth campaign: July to October 2010, intermediate northern latitudes.

The exploitation of the unique dataset has been led by two Swiss companies, GAMMA Remote Sensing AG and Sarmap SA.

The ERS-2–Envisat tandem mission addressed numerous applications.

— For cryospheric applications, including monitoring changes in ice shelf grounding lines, locations in 1992, 1994 and 2011 were identified and the dynamics of fast-moving glaciers have been studied.

— Outstanding results have been achieved in the derivation of high-resolution DEMs (digital 3D representation of a terrain) over low-relief areas (see Fig. 4.1.7). The quality of these DEMs is equivalent to those derived from the Shuttle Radar Topography Mission (SRTM) flown in February 2000, although the SRTM data are restricted to latitudes ±60°.

— ERS-2, being a polar-orbiting satellite, has acquired unique datasets that complement the SRTM data with respect to coverage and change detection over certain areas.

— Outstanding results have been achieved for forest mapping in Siberia, on the largest scale so far observed.

— The ERS-2–Envisat satellite constellation has supported new applications for estimating biomass over low-relief areas.

For day-to-day operations, the centralised user services and mission planning at ESRIN have ensured that the synergy between ERS-2 and Envisat has been fully exploited. ERS-2, carrying the predecessor instrumentation, acquired

data where Envisat conflicts could not be resolved. For example, the ASAR on Envisat with its modes and different polarisations created conflicting demands. Therefore, whenever Envisat image mode swath 2 VV polarisation was requested within the ERS station coverage, ERS-2 was tasked with meeting that request while Envisat addressed different requirements.

ERS-2 Ice Phase

The ERS-2 Ice Phase was intended to repeat the 1992 and 1994 ERS-1 Ice Phases (see Fig. 4.1.8), even though the satellite had already been in operation for 16 years in space and had various problems, known and unknown. Therefore, ERS-2 could provide nominal support only for reduced duty cycles of 4–5 min per orbit in order to ensure the safety of the satellite in view of its degraded power system. During the Ice Phase, however, the ESOC Spacecraft Operations team, in cooperation with the ESRIN mission planners, optimised and closely monitored the power utilisation of the satellite, allowing maximum duty cycles of 10 min during eclipse periods to avoid depleting the batteries.

The Ice Phase or '3-day repeat' mission started on 10 March 2011, one day before the disastrous earthquake struck the Sendai area of northern Japan. Since the objective of the main mission phase was to observe the cryosphere, no pre-earthquake acquisitions had been made over this region. However, ERS-2, with its fast mission planning capacity, was rescheduled to make observations of Sendai three days after the earthquake until the end of the mission. Special manoeuvres ensured that a minimal baseline of maximum 70 m with respect to the reference scene was maintained until the end of the mission. Thanks to the low solar activity, the yaw accuracy was very stable, resulting in good data quality for interferometry for nearly all passes during the last phase of the mission.

During the ERS-2 Ice Phase unique data were acquired, providing excellent results in terms of changes in the grounding lines and in the ice mass balances of major glaciers over 16 years. Figure 4.1.9 shows that the grounding line of the Petermann Glacier in Greenland has retreated by 0.7–3.4 km since 1992.

Figure 4.1.8. ERS-2–Envisat tandem mission observation targets. (ESA)

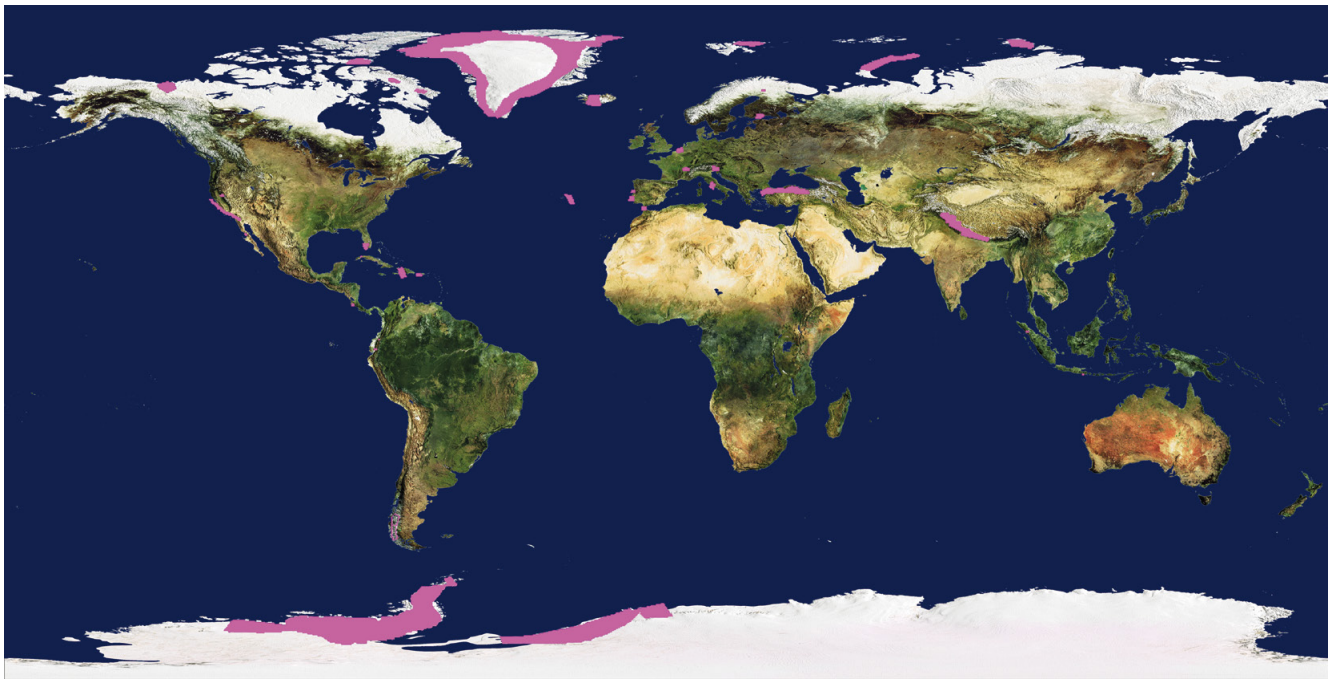

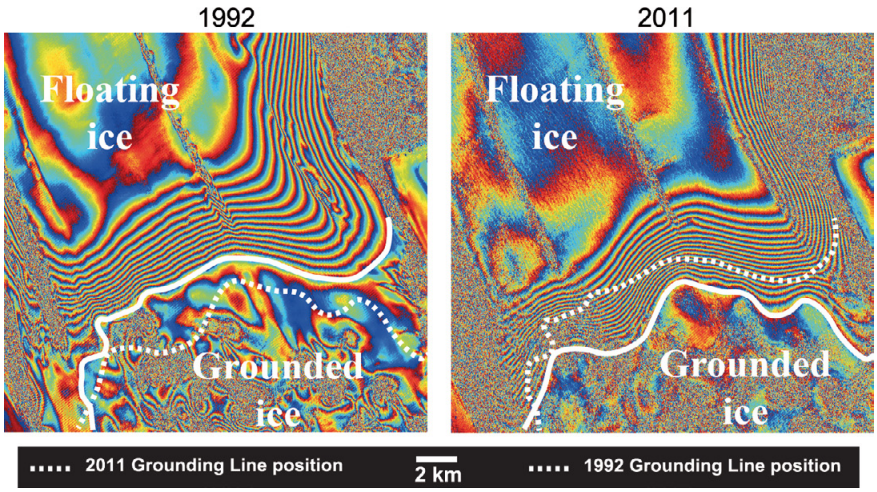

Figure 4.1.9. The Petermann glacier in Greenland, showing the retreat of the grounding line between 1992 and 2011. (ESA/A. Shepherd, University of Leeds, UK/N. Gourmelen, IPG, Strasbourg, France)

ERS-2 Operations Supporting Data Exploitation

Since 1995, the ERS-2 operations scenario has gradually evolved, adapting to the changing environment. The Ground Segment, beside the data acquisition systems at the stations, is composed of off-the-shelf computing hardware. The mission operations concept is strongly reliant on online services, as shown in the following examples of the modern operations scenario of the ERS-2 mission.

In 2007, ERS-2 became a major contributor to the GMES Service Element, Maritime Security Service (MARISS) project. In support of this project, the mission planning procedure was tuned to allow satellite tasking within 8 h after a request has been communicated. In many cases, data were made available to national authorities via the internet within 15 min after sensing. Even though systematic observations of the European coast were foreseen, in some cases rapid tasking and operations were still required. The best performance from a satellite tasking request to the receipt of data, via the internet, by the user is 6 h (mission planning, satellite tasking, acquisition, processing, data dissemination).

Following the earthquake in northern Japan in March 2011, ESA's existing cloud computing infrastructure, which became operational in 2008, was extended to Taiwan in less than 24 h, so that every three days, data covering the Sendai area could be provided to the geohazard science community in less than 3 h. In this ad hoc service setup, the Taiwan station (CSRSR) acquired the data and quickly put it on ESA's cloud computing assets, for which a Content Delivery Network (CDN) storage was set up on the US West coast within a day. The station in Miami (CSTARS) processed the data and put the results back on ESA's 'Virtual Archive' cloud. From there, the team at the Italian National Research Council/Institute for Electromagnetic Sensing of the Environment (CNR/IREA) in Naples picked up the low-level product to create interferograms. These high-level products provided information on the ground deformation triggered by the almost daily aftershocks in Japan (Fig. 4.1.10). The ERS-2 3-day repeat cycle became a unique observation tool that has helped to understand this extreme geophysical phenomenon.

ERS-1 (from ESA) and the first web page (from CERN) were launched in the same year, 1991. Since then, the evolution of the mission exploitation has been closely linked to the internet and the evolution of mass-market IT assets. Now, the science community is interconnected via the internet, and the online storage of large datasets (petabyte scale, or 10^{15} bytes) is affordable, allowing large-scale data sharing and supporting interdisciplinary research.

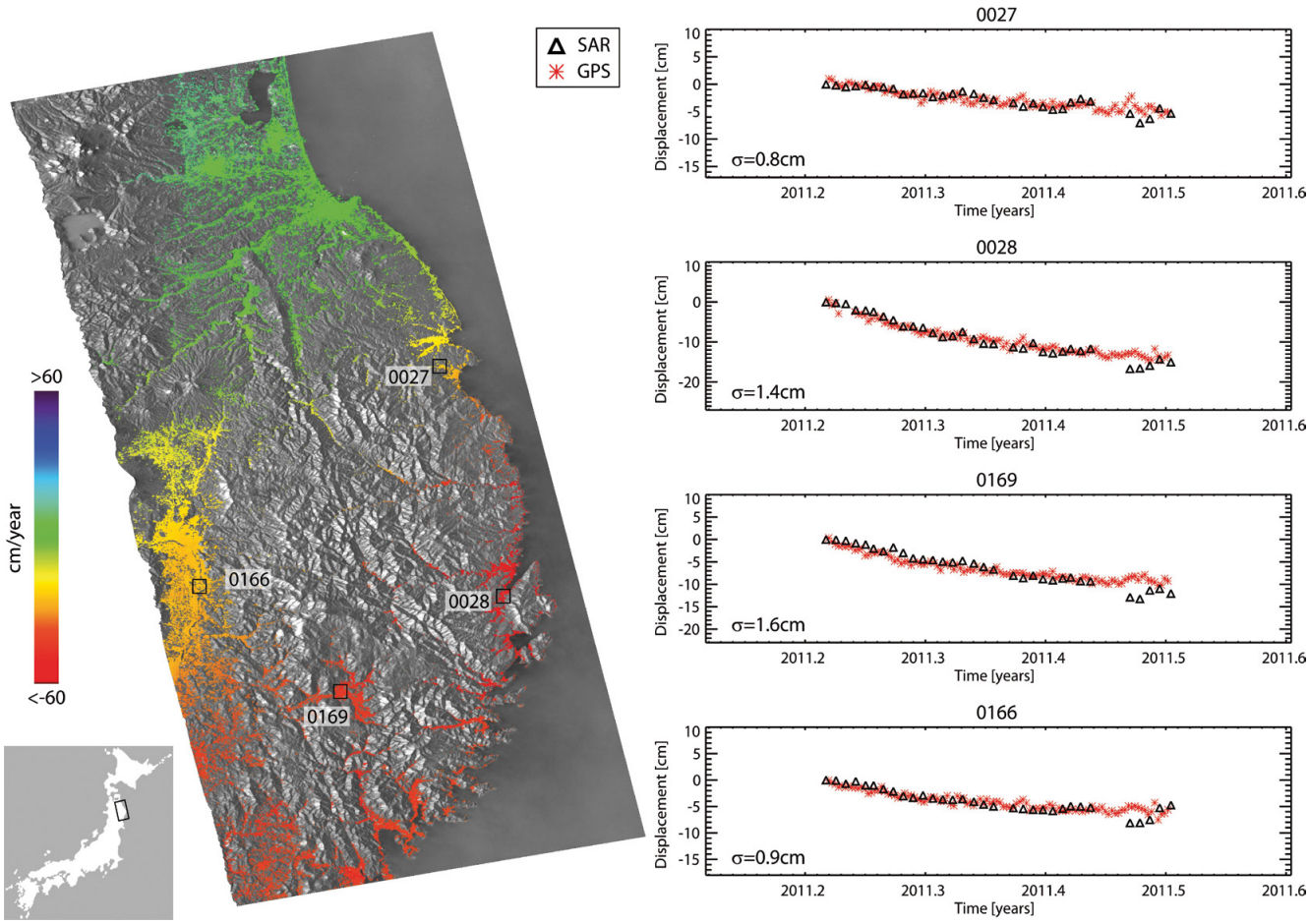

Figure 4.1.10. Monitoring of the Japan earthquake with ERS-2 operated in a 3-day repeat cycle using the Small Baseline Subset–Interferometric SAR (SBAS–InSAR) approach. (ESA, SAR data; CNR/IREA, SBAS–InSAR processing; GSI, GPS RINEX data; ARIA team at JPL and Caltech, GPS data processing).

ERS-2 Deorbiting

After 16 years of successful operation and a highly satisfactory output of scientific results and applications, the ERS-2 satellite was deorbited in summer 2011 and finally passivated on 5 September 2011.

The weakest point of the satellite was its power system. As far back as 2007 special measures were implemented to ensure that the satellite had enough power to recover a possible error condition during eclipse. Even though ERS had the same platform as SPOT-1 and SPOT-2, which were in operation for more than 16 years, problems with the ERS gyroscope and the ageing power system supporting the SAR, an instrument with very high power demands, were the main arguments for a controlled deorbiting in 2011.

For the deorbiting, ESA has to comply with the Inter-Agency Space Debris Mitigation Agreement, which requires signatory agencies to minimise satellite reentry time (around 25 years), free up 'busy' orbits in the low-Earth orbit region (900–700 km), and deactivate a satellite once it reaches its disposal orbit. ERS-2 is now flying in a circular orbit at about 570 km altitude. Its reentry into the atmosphere, where it will burn up, will take 15–20 years (depending on solar activity), well within the 25-year limit.

During its final months of activity, the ERS-2 satellite was dedicated to a specific Ice Phase (3-day repeat orbit), and acquired its last image on 4 July 2011 (Fig. 4.1.11).

Figure 4.1.11. The last image taken by ERS-2, on 4 July 2011, covering the Rome area. (ESA)

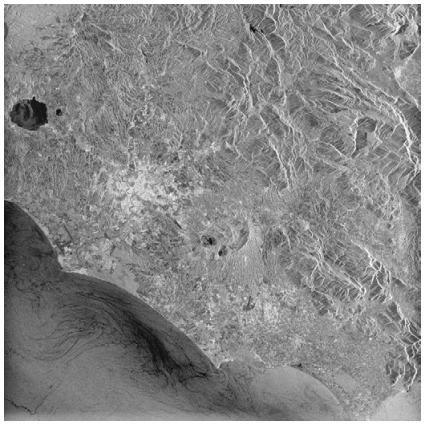

ESA Earth Observation Symposia

Even before the launch of ERS-1 many scientists and operational data users supported the ERS mission by participating in the definition of routine orbit phases, preparing the Calibration and Validation activities and developing retrieval algorithms. Many PhDs have been earned in preparation for the mission, as well as during the 20 years of operation. Since the beginning of the mission, members of this community have gathered at symposia organised by ESA every three or four years to exchange the latest research findings and to communicate requests to ESA to tune their operations and services in view of the advances made by the mission and to address new challenges.

Contributions to the symposia in terms of the numbers of participants, and of papers and posters submitted have continued to rise. The most recent 'Living Planet' symposium in Bergen, Norway, in 2010, was the largest since the launch of ERS-1, with 1200 participants from 44 countries who presented 1000 papers and posters.

Lessons Learnt and Follow-on Steps

The ERS programme has made major advances and achieved outstanding results over the last 20 years:

— Valuable data archives compiled over 20 years containing well calibrated, regularly reprocessed datasets that are essential for climate studies and other applications. These archives are important assets that remain to be fully exploited.

— The demonstration of the operational capability and potential of ERS instruments, such as the Wind Scatterometer and GOME, has enabled their transfer to the operational Eumetsat MetOp series of satellites.

— The ERS can be seen as an international cooperation tool through the establishment and negotiations of agreements for a global network of ground receiving stations and its participation in CEOS and other cooperation boards.

— The programme encouraged cooperation in developing applications and scientific research involving the United States, China, Japan, India, Russia, Australia, South Africa, etc., European and international organisations (ECMWF, FAO, UNESCO, UNDCP, UNOOSA, WMO, etc.), the worldwide scientific community, and innovative companies and SMEs.

— With the ERS, ESA (together with the French Center for Space Studies (CNES) with its SPOT satellites) was at the centre of efforts to introduce the International Charter on Space and Major Disasters, launched in response to Hurricane Mitch in 1998, the most powerful of the season with wind speeds of ~300 km h^{-1}, which caused ~20 000 fatalities.

Although ERS is no longer an active mission, it will continue to pioneer future satellite mission operations, collaborations and data exploitation schemes, based on its archive compiled over 20 years covering all fields of Earth science. It has proven its capacity to adapt to changing environments by building on the technical and structural heritages and partnerships.

Supported by ESA's 'open and free' data policy, the ERS will continue to contribute to innovative online exploitation platforms, with their potential to create new opportunities for commercial companies and Earth observation data providers, and for telecommunications and IT businesses.

In conclusion, the ERS programme has been a complete European success, which has paved the way for the Envisat, MetOp and Sentinel missions.

References

GCOS (2003). *GCOS Climate Monitoring Principles*. World Meteorological Organization, Geneva, Switzerland.
www.wmo.int/pages/prog/gcos/index.php?name=ClimateMonitoringPrinciples

WMO/UNEP (2010). *Scientific Assessment of Ozone Depletion: 2010*, Global Ozone Research and Monitoring Project Report No. 52. World Meteorological Organization, Geneva, Switzerland.
http://ozone.unep.org/Assessment_Panels/SAP/

The specific achievements of the ERS programme have been described in various ESA publications. The reports listed below represent but a small fraction of the thousands of publications and hundreds of services derived from the ERS mission:

ESA (1995). *Scientific Achievements of ERS-1*, ESA SP-1176/I. European Space Agency, Noordwijk, the Netherlands.

ESA (1996). *Applications Achievements of ERS-1*, ESA SP-1176/II.

ESA (1985). *Further Achievements of the ERS Missions*, ESA SP-1228.

ESA (1992). *Space at the Service of Our Environment*, 1st ERS-1 Symposium, Cannes, France, ESA SP-359, vols 1&2.

ESA (1993). *Space at the Service of our Environment*, 2nd ERS-1 Symposium, Hamburg, Germany, ESA SP-361, vols 1&2.

ESA (1994). *First Workshop on ERS-1 Pilot Projects*, Toledo, USA, ESA SP-365.

ESA (1995). *Second ERS Application Workshop*, London, UK, ESA SP-383.

ESA (1997). *Third ERS Scientific Symposium*, Florence, Italy, ESA SP-414.

ESA (1997). *New Views of the Earth: Engineering Achievements of ERS-1*. ESA SP 1176/III.

ESA (2000). *ERS–Envisat Symposium*, Göteborg, Sweden, ESA SP-461.

ESA (2005). *Envisat and ERS Symposium*, Salzburg, Austria, September 2004, ESA SP 572.

ESA (2007). *Envisat Symposium*, Montreux, Switzerland, ESA SP-636.

ESA (2010). *ESA Living Planet Symposium*, Bergen, Norway, ESA SP-686.

4.2 Envisat

Envisat, the largest and most complex satellite ever built in Europe, was launched in 2002 and had been monitoring Earth for 10 years – twice its planned lifetime – when a major anomaly stopped the satellite operations on 8 April 2012. Envisat was a unique mission, with its combination of 10 instruments using very different techniques, and with its numerous user communities ranging from many fields of the Earth sciences (atmosphere, cryosphere, oceanography, land use and land movements) to operational applications.

As a package, Envisat's capabilities exceeded those of any previous or planned Earth observation satellite. The payload included three sounding instruments designed for monitoring atmospheric chemistry, including measuring ozone concentrations in the stratosphere. The Advanced Synthetic Aperture Radar instrument collected high-resolution images with a variable viewing geometry, with new wide-swath and selectable dual polarisation capabilities. Envisat also carried an imaging spectrometer for ocean colour and vegetation monitoring, as well as improved versions of the ERS radar altimeter, a microwave radiometer and visible/near-IR radiometers, together with a very precise orbit measurement system.

Envisat observed many factors related to changes in atmospheric composition. The results of these changes included the enhanced greenhouse effect, increased levels of UVB radiation reaching the ground and changes in atmospheric composition.

The oceans exert a major influence on Earth's meteorology and climate through their interaction with the atmosphere. Understanding the transfer of moisture and energy between ocean and atmosphere, as well as the transfer of energy by the oceans themselves, are matters of scientific priority. Envisat contributed to this area by providing information on ocean topography and circulation, winds and waves, ocean waves and internal waves, atmospheric effects on the sea surface, sea-surface temperatures, coastal bathymetry and sediment movements, as well as the biophysical properties of oceans.

The land surface is a critical component of the Earth system because it carries more than 90% of the biosphere. It is the location of most human activity and is therefore where the human impacts are most visible. Within the biosphere, vegetation is fundamentally important because it supports the bulk of human and animal life and largely controls the exchanges of water and carbon between the land and the atmosphere. Yet our understanding of the many processes involved is limited. Envisat observations characterised and measured vegetation parameters, surface water and soil moisture, surface temperature, elevation and topography, and provided critical datasets for improving climate models.

Last, but not least, the cryosphere is a key component of the climate system. It includes the ice sheets, sea ice and snow cover. Here, Envisat's all-weather capabilities were exploited to the full as the remoteness, winter darkness, hostile weather conditions and frequent cloud cover of high-latitude ice/snow-covered regions make the use of remote sensing mandatory. Envisat provided important information on seasonal and long-term variations in the extent and thickness of sea ice, and the evolution of ice sheets and snow cover, all of which affect the climate system, and may be highly sensitive indicators of climate change.

4.2.1 The Envisat Payload

Envisat's payload complement was mounted on the satellite's Polar Platform. Details of the ten instruments are given in Table 4.2.1.

Further information about the Envisat mission can be found at *http://earth.esa.int/envisat*

Table 4.2.1. The Envisat payload.

Instrument	Details
Advanced Synthetic Aperture Radar (ASAR)	A radar instrument with several imaging modes to observe land, sea and ice surfaces. Developed from its predecessor on ERS.
Advanced Along-Track Scanning Radiometer (AATSR)	A conical-scan imaging radiometer in the visible, near and thermal infrared wavebands to measure sea surface temperatures and observe dry land. Developed from its predecessor on ERS.
Radar Altimeter (RA-2)	A device used specifically to measure changes in sea level. Developed from its predecessor on ERS.
Microwave Radiometer (MWR)	A passive microwave radiometer to determine the water content of the atmosphere to improve the precision of the RA-2 altimeter.
Doppler Orbitography and Radio Positioning Integrated by Satellite (DORIS)	A measuring instrument to determine the orbit of the satellite with high precision.
Laser Retro Reflector (LRR)	An optical square used for high-precision optical orbit measurements with a ground-based laser.
Medium-Resolution Imaging Spectrometer (MERIS)	An imaging wide-angle spectrometer of medium geometrical resolution used to observe ocean and land surfaces in the visible and near-infrared spectral range.
Scanning Imaging Absorption Spectrometer for Atmospheric Chartography (SCIAMACHY)	A spectrometer in the ultraviolet, visible and near-infrared wavebands, for observing the concentrations of a large number of trace gases and substances. It could be directed at the horizon as well as directly down to Earth. Developed from the GOME instrument on the ERS-2 mission.
Global Ozone Monitoring by Occultation of Stars (GOMOS)	A spectrometer directed at the horizon that operated in the UV, visible and NIR wavebands to measure the concentrations of ozone and other gases in the atmosphere with the aid of star spectra.
Michelson Interferometer for Passive Atmospheric Sounding (MIPAS)	This passive Michelson interferometer was directed at the horizon, and operated in the mid-infrared waveband to study atmospheric trace gases.

Some of these instruments – ASAR, AATSR and RA-2 – ensured the continuity of data from the ERS satellites, with the MWR, DORIS and LRR as supporting instruments. Observation of ocean and coastal waters – with the retrieval of marine biology constituent information – was the primary objective of MERIS. Following on from GOME on ERS-2, the ability to observe the atmosphere was significantly enhanced by three complementary instruments: SCIAMACHY, GOMOS and MIPAS. They could detect a large number of atmospheric trace gas constituents by analysing absorption lines, and could characterise atmospheric layers by complementary limb and nadir observations.

4.2.2 Envisat Results

Over the last decade numerous findings demonstrated the value of the Envisat mission to the Earth science community. Each Envisat symposium, held every three years, brought together more than 1000 participants, who often announced major results, such as:

— Salzburg 2004: evidence of global sea-level rise of ~3 mm yr^{-1} and an increase in sea surface temperature of ~0.1°C since 1992 (Envisat and ERS missions); evidence of growing air pollution in China since 1995 (Envisat and ERS missions); and the identification of the blind tectonic fault at the epicentre of the earthquake in Bam, Iran, in December 2003.

— Montreux 2007: the first global measurements of greenhouse gases by Envisat's SCIAMACHY demonstrating the increasing concentration of CO_2

and seasonal variations in methane concentrations in the atmosphere. Other results include measurements of the increased velocity of large glaciers in Greenland and Antarctica by ERS and Envisat SAR instruments, and the first description of a very large magma intrusion event between two tectonic plates in Ethiopia.

— Bergen 2010: evidence of the rapid reduction in the extent of Arctic sea ice in the last five years, monitoring data showing the break-up of several ice shelves (e.g. Larsen and Wilkins) in Antarctica since 2002, and observations of the Eyjafjöll eruption in Iceland in April 2010.

ESA regularly organises dedicated workshops that form an important element of the interactions between ESA and the science user communities with the aim of optimising the exploitation of Envisat mission data.

Many remarkable results based on Envisat and ERS SAR interferometry were presented at ESA's 8th Fringe workshop, 'Advances in the Science and Applications of SAR Interferometry', in September 2011. Among these were the first Antarctica ice velocity map, based on SAR data acquired during the International Polar Year, produced in coordination between ESA (Envisat), the Canadian Space Agency (Radarsat) and JAXA (Advanced Land Observing Satellite, ALOS).

Over the years, the demand for Envisat data for scientific and operational uses grew steadily, requiring continuous adaptations of the ground segment facilities to improve the quality and delivery of data.

An orbit change of the Envisat satellite was performed in October 2010. This major change, after eight years of operation, was needed to allow the satellite to operate for a few more years, well beyond its originally planned five-year lifetime. Unfortunately, in April 2012, just a few weeks after celebrating its tenth anniversary in space, a major anomaly suddenly interrupted Envisat's data acquisition.

Envisat's instruments had continued to perform well until the end. In 2011, for example, the mission made a number of key observations:

— following the disastrous earthquake in Japan in March 2011, Envisat data were used to produce a detailed map of ground displacements along an area extending for 800 km using the SAR Interferometry technique;
— based on Envisat SAR observations, Brunt et al. (2011) reported the first evidence that a tsunami in the northern hemisphere (such as the one generated by the 2011 earthquake in Japan) can trigger ice-shelf calving in Antarctica, more than 13 000 km away;
— using the SCIAMACHY and MERIS instruments, the Envisat mission provided remarkable images of the Grimsvötn volcanic eruption in Iceland in May 2011; and
— in September 2011, Envisat observed the extent of Arctic sea ice at its minimum, very close to the previous minimum record of September 2007.

Some of Envisat's many other successes over the last decade are presented in the following paragraphs.

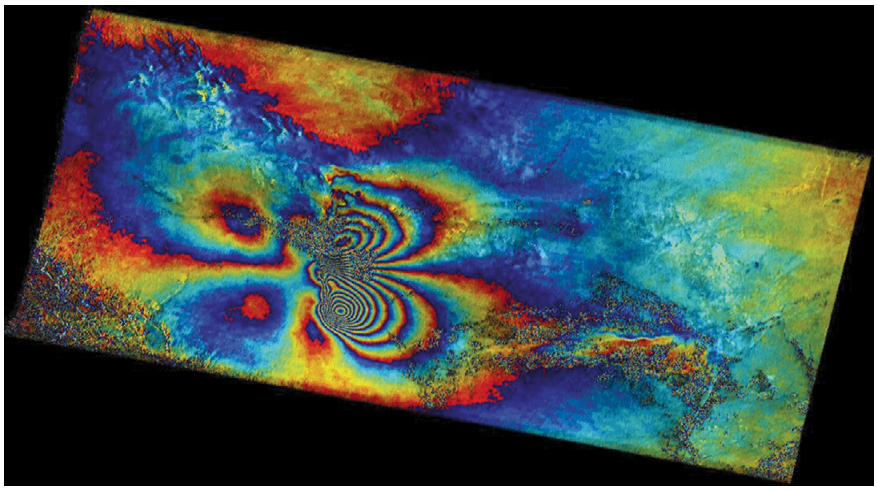

Figure 4.2.1. Interferogram showing ground displacements in the area near Bam, Iran, following the earthquake in December 2003. (PoliMi/PoliBa)

Bam Earthquake, Iran, 2003

The interferogram in Fig. 4.2.1 shows the contours of ground displacements towards and away from the Envisat satellite following the earthquake in Bam, Iran, in December 2003. The four-quadrant pattern is consistent with a near-vertical strike–slip fault oriented north–south. The ground moved approximately 30 cm towards the satellite in the southeast quadrant, and approximately 15 cm away from it in the northeast quadrant.

The black areas in the image indicate locations where the ground surface had moved, preventing the measurement of displacements. Those around the city of Bam (image centre) and neighbouring towns were caused by damage to buildings and by vegetation. The narrow linear black band extending south of the centre of Bam is the surface expression of the fault, previously hidden, on which the earthquake occurred.

NO_2 Measurements over China, 2003–04

Rapid industrialisation in China has led to a dramatic increase in emissions of air pollutants, in particular nitrogen oxides and particulates. Figure 4.2.2 shows a map of the tropospheric nitrogen dioxide vertical column density over China as measured by Envisat's SCIAMACHY instrument, averaged between December 2003 and November 2004.

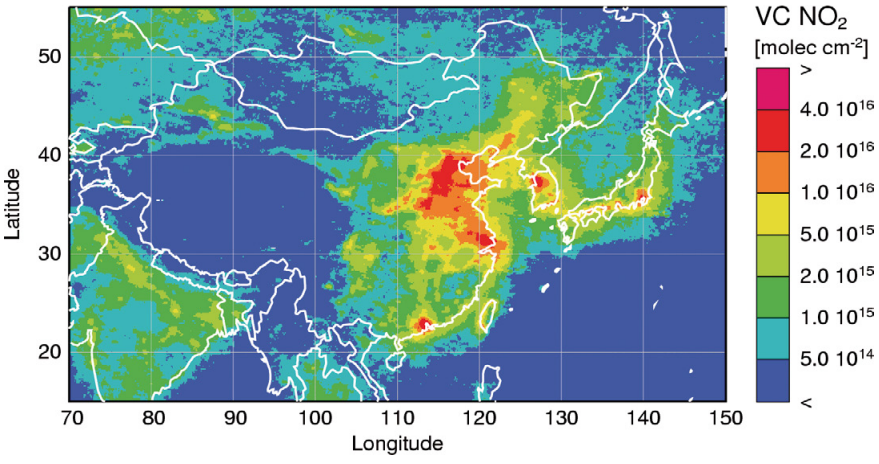

Figure 4.2.2. Map of tropospheric NO_2 vertical column density over China between December 2003 and November 2004. (Institute of Environmental Physics, University of Bremen, Germany)

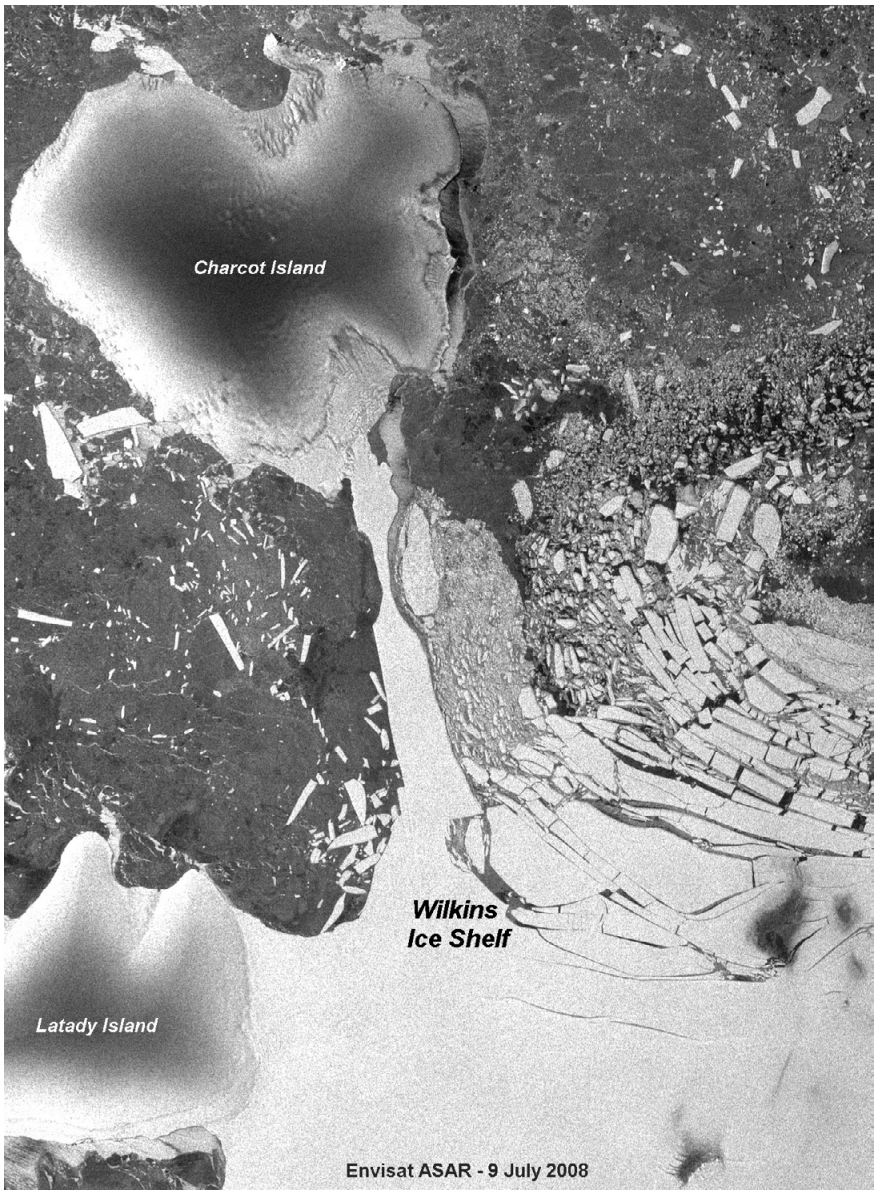

Figure 4.2.3. Envisat ASAR image of the Wilkins ice shelf in Antarctica, 9 July 2008. (ESA)

Wilkins Ice Shelf Break-up, 2008

Figure 4.2.3 shows an image of the Wilkins ice shelf in Antarctica, acquired on 9 July 2008 by Envisat's ASAR instrument. It shows the ice bridge that connected Charcot Island and Latady Island (bottom left) until the ice shelf finally broke up in April 2009.

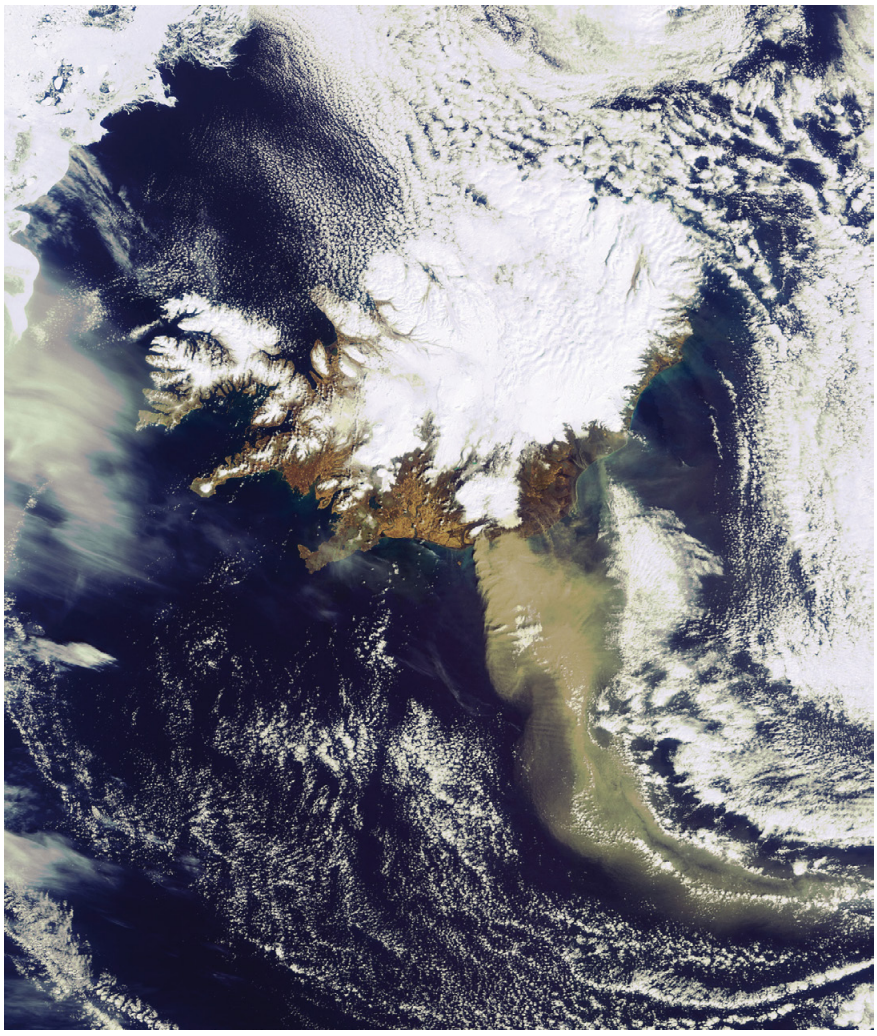

Figure 4.2.4. Envisat MERIS image of the Eyjafjöll volcano in Iceland, acquired on 19 April 2010. (ESA)

Eyjafjöll Volcano Eruption, Iceland, 2010

Figure 4.2.4 shows an image of the Eyjafjöll volcano in Iceland, acquired by Envisat's MERIS sensor on 19 April 2010. A heavy plume of volcanic ash can be seen moving in a roughly southeasterly direction. The plume, visible in brownish-grey, is approximately 400 km long.

Perhaps the two most important Envisat science results in 2011 are presented in Figs 4.2.5 and 4.2.6. Figure 4.2.5 shows the first map of ice velocity over the entire continent of Antarctica, mainly derived from Envisat, Radarsat-2 and ALOS SAR data, with contributions from ERS-1/ERS-2 and Radarsat-1 data. These findings are critical for studies of the global impact of sea-level rise resulting from the more rapid flow of ice into the ocean.

Figure 4.2.6 shows ground displacements in northern Japan following the earthquake of March 2011 (Envisat ASAR).

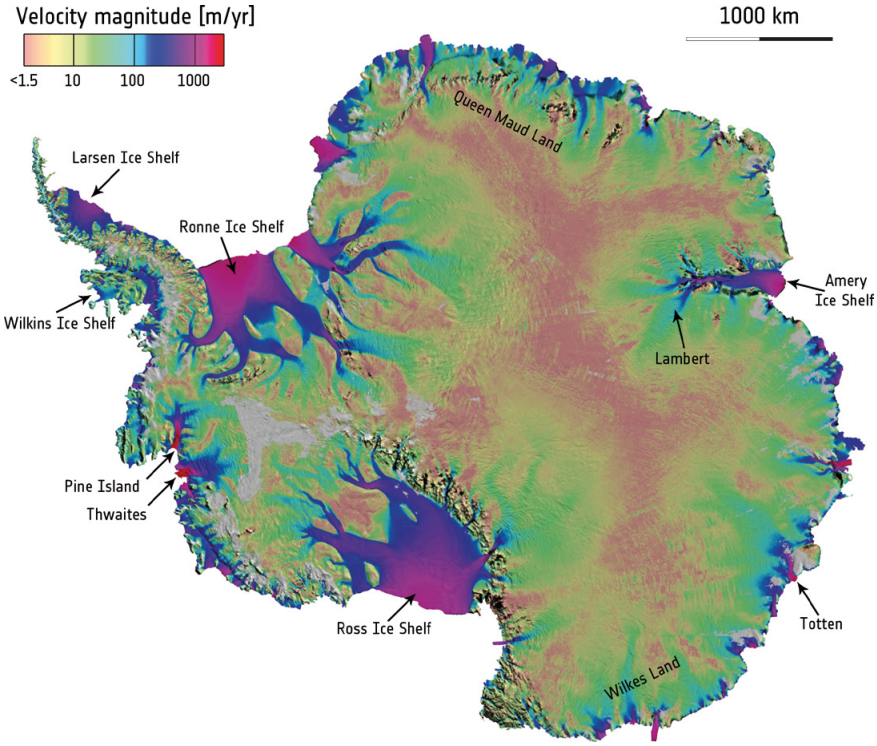

Figure 4.2.5. The first map of ice velocity over Antarctica. (E. Rignot et al., 2011)

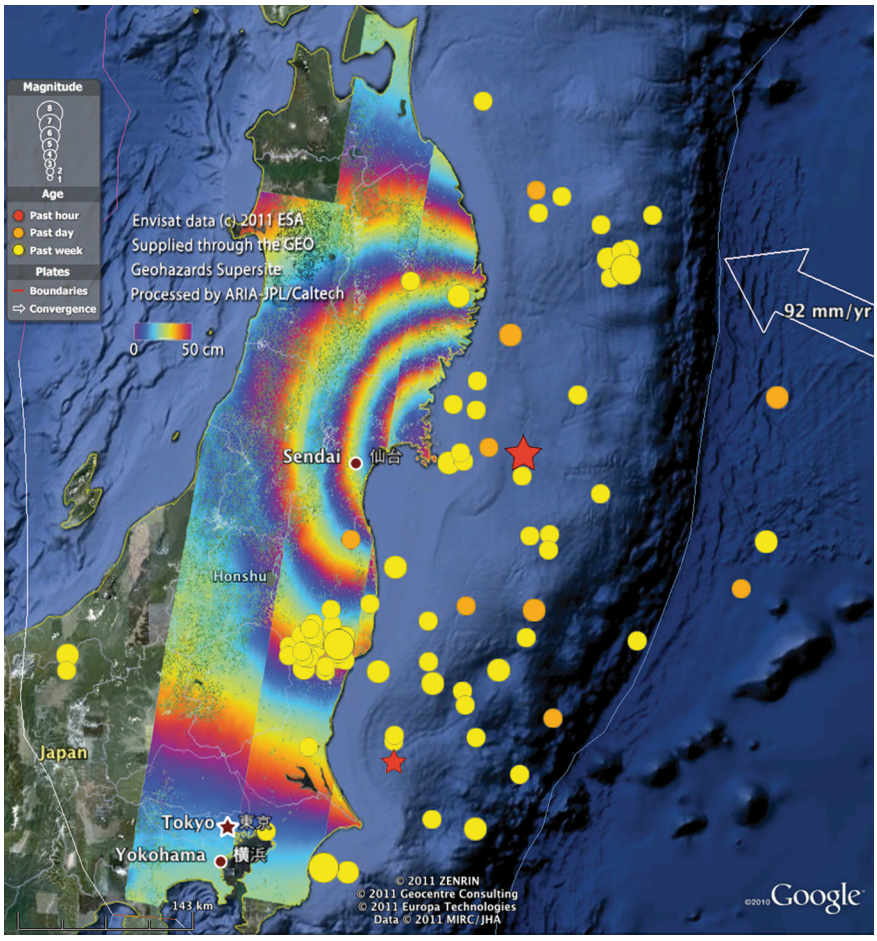

Figure 4.2.6. Ground displacements in northern Japan following the earthquake of March 2011. (Envisat data, ESA, supplied through the GEO Geohazards Supersite, processed by ARIA-JPL/Caltech; ZENRIN; Geocentre Consulting; Europa Technologies; Data MIRC/JHA; Google)

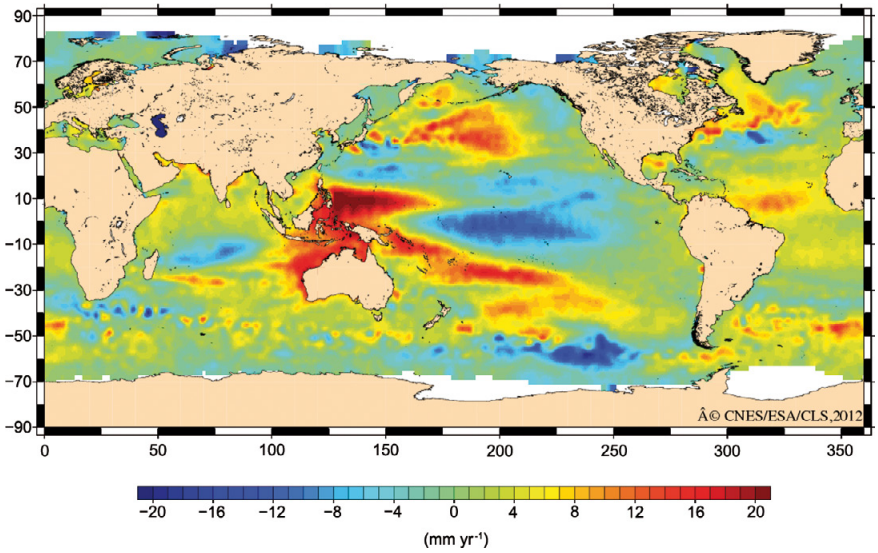

Figure 4.2.7. Envisat Radar Altimeter observations of changes in global mean sea level (in mm yr^{-1}) between December 2003 and December 2011 (cycles 22–109). (Inverted barometer correction applied/wet troposphere: radiometer-derived, seasonal signal removed.) (© CNES/ESA/CLS)

Changes in Global Sea Level, 2003–11

Figure 4.2.7 shows a map based on Envisat Radar Altimeter observations of changes in sea level between December 2003 and December 2011. Although the global trend indicates a rise in mean sea level of about 3 mm yr^{-1}, there are marked regional differences of ±20 mm yr^{-1}. These spatial patterns of changing sea level are not stationary, so that patterns observed by satellite altimetry are transient features.

Phytoplankton Bloom in the Barents Sea, 2011

Figure 4.2.8 shows an Envisat MERIS image of a phytoplankton bloom stretching across the Barents Sea off the coast of mainland Europe's most northerly point, Cape Nordkinn. The southern area of this deep shelf sea – with an average depth of 230 m – remains mostly ice-free due to the warm North Atlantic Drift. This contributes to its high biological production compared with other oceans at the same latitude.

Free-floating phytoplankton highlight the whirls of ocean currents in spectacular shades of blue and green. These microscopic marine organisms, which drift at or near the surface, have been called 'the grass of the sea' because they are form the base of the marine food chain, and play a role similar to that of terrestrial plants in the photosynthetic process. Phytoplankton are able to convert inorganic compounds such as water, nitrogen and CO_2 into complex organic materials. With their ability to 'digest' these compounds, they are credited with removing as much CO_2 from the atmosphere as their 'cousins' on land, and thus can have a profound influence on climate.

Although most individual phytoplankton are microscopic, they collect in such vast numbers that the chlorophyll they use for photosynthesis colours the surrounding ocean waters. These tiny organisms can then be detected from space with dedicated 'ocean colour' sensors such as MERIS.

The MERIS instrument has also been used to measure the average chlorophyll concentration in the seas around Denmark, as shown in Fig. 4.2.9.

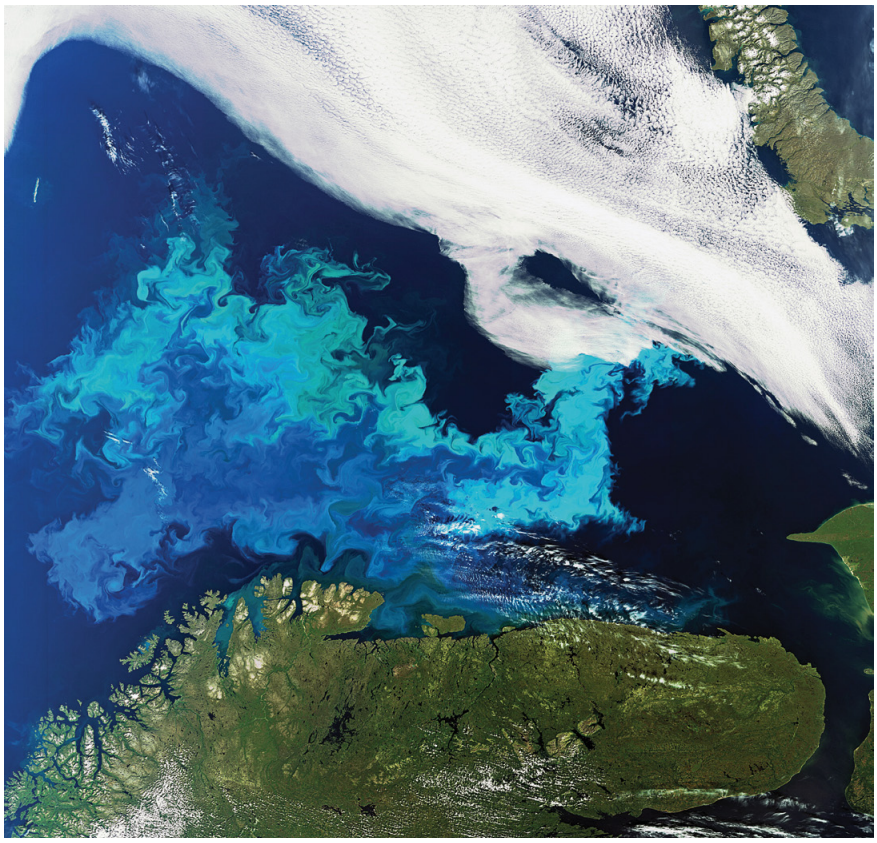

Figure 4.2.8. Phytoplankton bloom in the Barents Sea, acquired by Envisat's MERIS instrument, 17 August 2011.

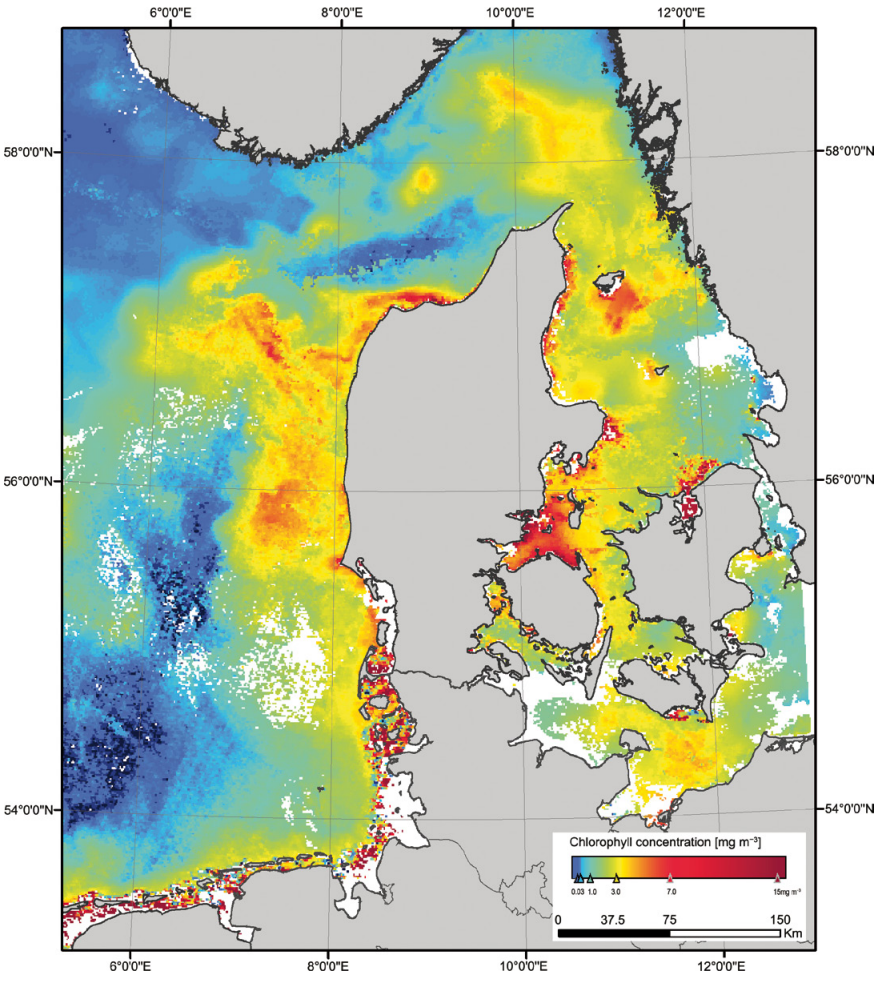

Figure 4.2.9. Weekly average chlorophyll concentration (mg m^{-3}) in the seas around Denmark, measured by Envisat's MERIS instrument, 13–19 March 2006. (Brockmann Consult)

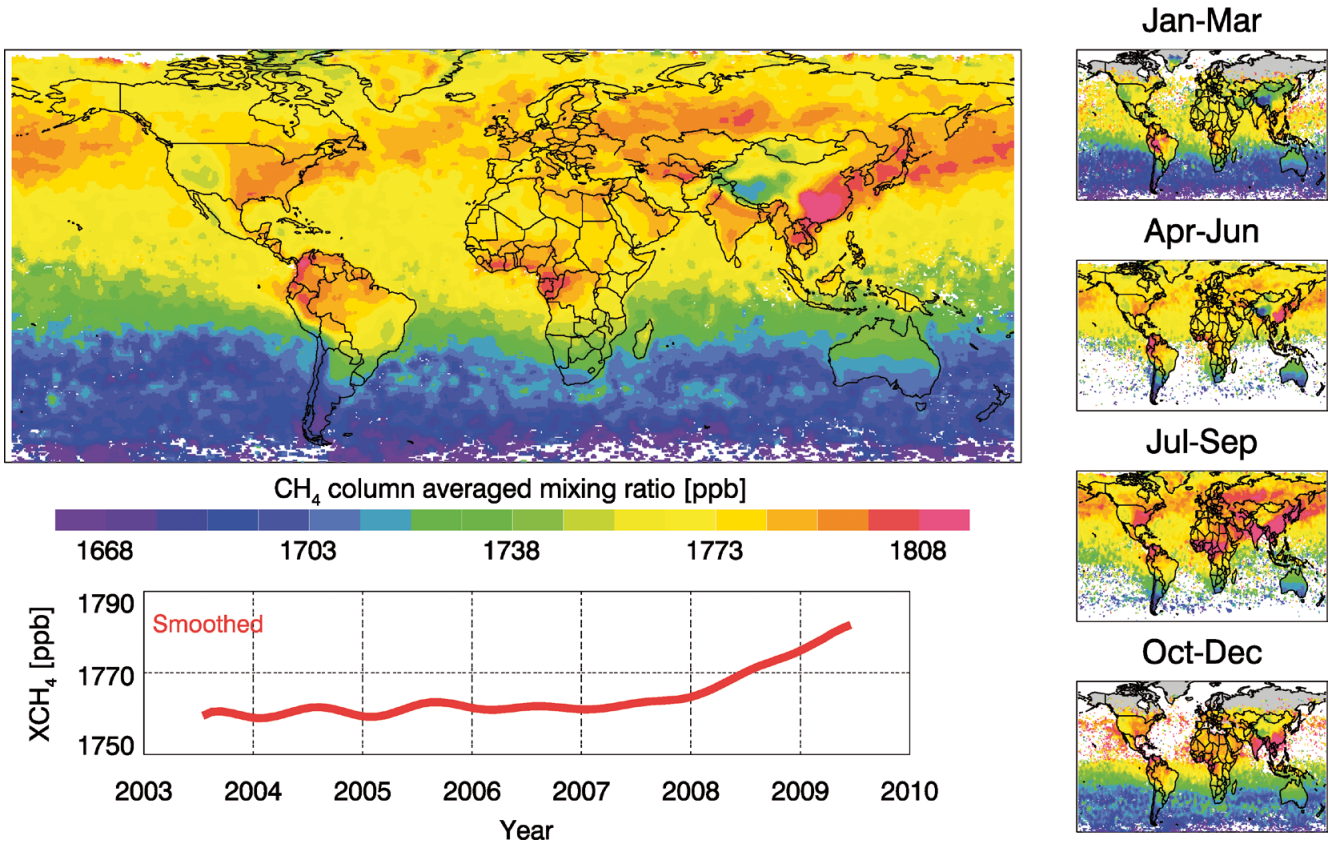

Figure 4.2.10. Global and seasonal maps of atmospheric methane concentrations retrieved from Envisat SCIAMACHY measurements. (University of Bremen, IUP/IFE)

Atmospheric Methane Measurements

Carbon dioxide and methane are the two most important anthropogenic greenhouse gases and contributors to global warming. Reliable predictions of future atmospheric greenhouse gas concentrations and associated climate change require an adequate understanding of their (natural and anthropogenic) sources and sinks.

Figure 4.2.10 presents global and seasonal maps of atmospheric methane concentrations retrieved from Envisat's SCIAMACHY measurements. SCIAMACHY is the first satellite instrument whose measurements contain information on the vertical columns of both gases due to high measurement sensitivity down to Earth's surface where the major sources and sinks of these greenhouse gases are located. The vertical column density of a gas is the number of molecules of this gas located in an air column extending from Earth's surface to the top of the atmosphere per surface area (molecules/cm^2). For CH_4 and CO_2 the columns are normalised with the corresponding (measured) number of air molecules (obtained using O_2 measurements) to obtain the dry air column-averaged mixing ratios or mole fractions of the greenhouse gases (unit: ppb for CH_4).

The red curve in the bottom panel of Fig. 4.2.10 is a smoothed time series. The atmospheric CH_4 concentration was relatively stable until about 2007 but has started to increase in recent years, for reasons that are not yet fully understood. High values typically indicate major sources of methane, such as wetlands, rice paddies, ruminants, waste handling, coal mining, etc. As methane is long-lived, atmospheric transport is very important. Therefore, high values may also appear far from source regions, especially when those regions are poorly sampled, perhaps due to persistent cloud cover. Interpretation of the maps is therefore not straightforward and is typically done using complex models.

References

ESA (1997) *New Views of the Earth: Engineering Achievements of ERS-1*, ESA SP-1176/III. European Space Agency, Noordwijk, the Netherlands.

Rignot, E., Mouginot, J. & Scheuchl, B. (2011). Ice flow of the Antarctic ice sheet, *Science* **333**(6048), 1427–1430.

→ HUMAN SPACEFLIGHT AND OPERATIONS

Contents

→ INTRODUCTION

1. Introduction

As the European organisation for space, ESA is doing its utmost to push the boundaries of science in all areas. The Human Spaceflight and Operations Directorate is one of ESA's key sectors facilitating many of these activities. From a research perspective the science undertaken within the directorate covers the most diverse areas of enquiry, and is pursuing some of the most important questions facing human society, from understanding the physiological processes behind osteoporosis and other health issues, to the development of new lighter and stronger materials by improving industrial casting models and enhancing the recycling of materials, etc. The objectives of this scientific programme are being achieved through ESA's management of top research and industrial teams across Europe and the world. The science teams are developing relevant scientific proposals, while the industrial teams are developing state-of-the-art space hardware to facilitate research in the required environment.

Research supported by the European Programme for Life and Physical Sciences in Space (ELIPS) covers many fields, from fundamental to applied research, and across all areas of the physical and life sciences. In much of this research, one of the principal questions is how gravity (weightlessness) affects various processes. This research can also help to reveal the influence of other processes on Earth that are masked by gravity and are thus very difficult to study outside a weightless environment.

To make optimal use of available resources, ESA supports this research across a host of platforms on the ground and in space (see Table 1.1). Ground-based research, including simulations such as bedrest campaigns and isolation studies, is helping to test and develop measures to counteract certain psychological and physiological effects of spaceflight. Weightless platforms include drop towers, parabolic flights, sounding rockets and, above all, the International Space Station (ISS).

The ISS, with ESA's Columbus laboratory, is the pinnacle and focus of current research in low-Earth orbit. It offers continuous access to weightless conditions in space and facilitates science in all areas: biology and physiology, fluids and materials science, plasma physics, astrobiology, solar and radiation research, as well as testing new technologies.

The aim of these endeavours is not only to improve daily life on Earth and the ongoing endeavours of astronauts and systems in low-Earth orbit. These activities are also paving the way for future human spaceflight missions beyond low-Earth orbit, to the Moon, Mars and further into the Solar System. At the same time, we are also looking back at our planet. The ISS provides an ideal platform from which to undertake extensive research with long-term monitoring of both space and Earth phenomena.

Table 1.1. Research on the International Space Station and other platforms. The table includes research projects carried out in the period 2010–11, and additional projects from early 2012. Some projects from 2009 have also been included for context.

Research Area	Project/experiment
International Space Station	
Human Research	*Cardiopulmonary*. Five long-term experiments covering cardiovascular adaptation and changes in cardiovascular regulation (CARD, Sympatho, Vessel Imaging, EKE, Thermolab)
	Musculoskeletal. Two long-term experiments covering effects of sodium on bone mass reduction and early detection of osteoporosis (SOLO, EDOS)
	Neuroscience. Eight long-term experiments covering various areas, including altered (visual) perception in weightlessness, effects of weightlessness on systems that affect balance, and assessing measures to counter these effects, such as centrifugation (NeuroSpat [2], Passages, 3D-Space, Otolith, Space Headaches, Spin, Zag)
	Immunology. One long- and two short-term experiments to determine the mechanisms behind suppression of immune response in weightlessness (Immuno, PADIAC, ROALD-2)
Biology Research	*Plant biology*. Four plant-growth experiments covering levels of, and mechanisms behind, gravity response in various species, in particular *Arabidopsis thaliana* (WAICO, Genara-A, Multigen, Gravi)
	Cell/Molecular biology. Three experiments covering the effects of weightlessness on cellular organisation and function (Yeast In No Gravity, SPHINX, Coloured Fungi in Space)
Fluid Physics Research	Eight experiments covering areas such as planetary modelling, fluid processes in oil fields, influence of vibrations on fluids, colloidal science and foams and emulsions research (Geoflow [2], SODI Colloid [2], SODI DSC, SODI IVIDIL, Foam Stability, FOCUS)
Materials Research	Four long-term experiments covering solidification processes in metal alloys (CETSOL/MICAST/SETA) and fundamental studies of crystal growth from solutions (Protein Crystallisation Diagnostics Facility)
Complex Plasma Research	One experiment covering the effects of weightlessness on complex plasmas (PK-3 plus)
Radiation Research	Five long-term experiments to determine radiation levels in low-Earth orbit, the effects of shielding materials on radiation levels, and the neurophysiological effects of radiation on humans (ALTEA-Shield, Matroshka, EuCPDs, DOSIS, R3D)
Technology Research	Five technology demonstrations ranging from maritime navigation to 3D technologies (Vessel Identification System, ERB-2, WEAR, Flywheel Exercise Device, GTS-2)
Solar Research (Solar facility)	Three long-term experiments measuring solar spectral irradiance across the full spectrum (SolACES, SOLSPEC, SOVIM)
Space Exposure Research	*Astrobiology*. Numerous long-term experiments on the EuTEF (Adapt, LIFE, Protect, Seeds, PROCESS) and Expose-R (AMINO, ENDO, OSMO, SPORES, PHOTO, SUBTIL, PUR, ORGANIC, IBMP) facilities to assess the ability of various organisms to survive the conditions in open space – the findings are relevant to issues such as panspermia and planetary protection
	Materials exposure. One long-term experiment covering the effects of the space environment on material properties (MEDET)
	Space environment monitoring. Five experiments monitoring different aspects of the space environment: space debris, radiation, atomic oxygen, electrostatic charging and temperature (DEBIE-2, DOSTEL, FIPEX, PLEGPAY, EuTEMP)
	Tribology. One long-term experiment related to the science of friction and lubrication (Tribolab)
	Technology. One long-term technology demonstration (Earth Viewing Camera)

Research Area	Project/experiment
Sounding Rockets (short duration, ~6–12 min weightlessness)	
Materials Research	Six materials experiments (2009 [3], 2010 [2], 2012 [1]) covering solidification processes in metallic and semiconductor alloys, including steel, palladium/silicon, titanium aluminide, other Al-based alloys, and silicon/germanium. One further experiment studying agglomeration in evaporated nickel nanoparticles (2010)
Combustion Research	One experiment in 2009 studying combustion properties of a partially premixed/ prevaporised droplet array (PHOENIX)
Fluids Research	One experiment studying dynamic heat transfer mechanisms in flow boiling and condensation (SOURCE-2), and one studying fluid flow in blood through biomimicry (BIOMICS-2) (both in 2012)
Biology Research	Three experiments, one covering gravity sensitivity in Characean algae (2010) and two covering the immune response in weightlessness (MicImmun, STIM; 2012)
Parabolic Flight Campaigns (short-duration, ~20 s weightlessness per parabola)	
Physical Sciences	28 experiments during the 52nd–55th Parabolic Flight Campaigns (2010–11)*
Life Sciences	25 experiments during the 52nd–55th Parabolic Flight Campaigns (2010–11)*
Technology	One experiment during the Joint European Partial-g Parabolic Flight Campaign (2011)
Student Research	Four experiments during the 54th Parabolic Flight Campaign (2011)
Drop Towers (very short-duration, ~5–10 s weightlessness per drop)	
Physical Sciences	Four experiments in 2010–11 studied turbulent bubble suspensions in microgravity (BUBSUS), the combustion synthesis of metal oxide nanoparticles (CoSyMONa) and aspects related to planet formation (Chondrule-2, ICAPS/IPE)
Student research ('Drop Your Thesis' campaign)	One experiment in 2010 investigated the interaction of bubble jets in weightlessness, and another in 2011 studied sensitivity to gravity and signalling in plant roots
Ground-based Research: Life Sciences	
Bedrest Campaigns	Three campaigns in 2010–11 looked at measures to counter the effects of simulated weightlessness: the use of potassium bicarbonate as a dietary supplement (DLR, Germany, 2 × 21 days); artificial gravity with centrifugation on short-arm centrifuge (MEDES, France, 3 × 5 days); and the effectiveness of a specific exercise protocol performed during centrifugation (DLR, Germany, 3 × 5 days)
Isolation and Confinement Studies	*Mars500*. Studies of the psychological/physiological effects on a six-person crew of a simulated 520-day mission to Mars, and of measures to counter the effects of isolation, and tests of new technologies (IBMP, Russia, June 2010–November 2011).
	Concordia. Isolation studies during winter at the Antarctic station Concordia to prepare for future missions to the Moon or Mars. Includes psychological/ physiological monitoring and testing new technologies, especially water recycling. (February–November each year)
Biological Effects of Radiation	*IBER:* Assessing the risks related to radiation in various exploration scenarios through a programme of experiments on biological materials using the particle accelerator facility at the GSI Helmholtz Centre, Germany (ongoing)
Ground-based Research: Physical Sciences	
Intermetallic Materials Processing	IMPRESS: Studies of families of intermetallics – titanium aluminides and nickel aluminides – relevant to improving the production of high-performance gas turbine blades and industrial catalysts. EU project, coordinated by ESA (various locations, 2004–10)

* Includes the Joint European Partial-*g* Parabolic Flight Campaign.

→ OVERVIEW: COLUMBUS AND ISS FACILITIES

2. Overview: Columbus and ISS Facilities

2.1 ESA and the ISS

The International Space Station is one of the most extensive civil engineering projects ever undertaken. It is the principal platform for scientists and technology developers worldwide to gain access to the environmental conditions in space for undertaking research projects across all scientific domains and provides an important tool for education and public relations.

The Columbus module (Fig. 2.1.1) is ESA's and Europe's largest single contribution to the ISS and its permanent deployment in February 2008 greatly increased Europe's research potential on the station. It is equipped with a suite of flexible, multi-user research facilities that offer extensive capabilities.

The Columbus laboratory houses the following ESA research facilities: Biolab (for biological research), the Fluid Science Laboratory (for fluid physics research), the European Physiology Modules facility (for physiological and neurological research), the European Drawer Rack (for housing subrack payloads across various research disciplines), and the Muscle Atrophy Research and Exercise System (for neuromuscular and exercise research).

In addition, Columbus hosts two NASA Human Research Facility racks for supporting physiology research, a NASA rack that incorporates ESA's European Modular Cultivation System for biological research, and the European Transport Carrier, which acts as a research stowage locker. The tenth and final rack location in Columbus housed the European-built Microgravity Science Glovebox (see Fig. 2.3.1) for undertaking a variety of materials, combustion, fluids and biotechnology experiments, although this was relocated to the US Laboratory following the arrival of the Muscle Atrophy Research and Exercise System (MARES).

The full spectrum of major European research facilities inside the ISS is completed by the Materials Science Laboratory (Fig. 2.1.2), which is the principal element of NASA's Materials Science Research Rack in the US Laboratory. There are also three European-built Minus Eighty-degree Laboratory Freezer for the ISS (MELFI) units for the cold storage of samples.

The external surface of the ISS offers great potential for undertaking a broad range of exposure research and technology demonstrations in areas such as astrobiology, materials science and Earth observation. Columbus offers four external payload locations (Fig. 2.1.3) exposed to the vacuum of

Figure 2.1.1. ESA astronaut Hans Schlegel working outside the Columbus module in February 2008, two days after its installation on the ISS as part of the STS-122 mission. (NASA)

Figure 2.1.2. ESA astronaut and ISS Expedition 21 Commander Frank De Winne, working with the Materials Science Laboratory in October 2009. (NASA)

Figure 2.1.3. Columbus laboratory's External Payload Facility (upper and lower sections) in March 2011. The Solar facility is positioned at the top of the upper section. (NASA)

space, with an unhindered view of Earth and space, and supplied with relevant resources (power, data, etc.). One external payload, the European Technology Exposure Facility (EuTEF) was returned to Earth in September 2009 following the completion of 18 months' exposure to open space (see section 4.9, Space Exposure Research). Another, the Solar facility (see section 4.8, Solar Research), was installed outside Columbus in February 2008 and will remain in orbit until 2013 and possibly beyond.

Figure 2.2.1. The Columbus Control Centre in Oberpfaffenhofen, Germany.

2.2 The European Control Centre Network

To harness the diverse European involvement in the ISS, Europe (via ESA) has established a network of ground control centres across the continent to control Europe's infrastructure on the ISS. The focus of this is the Columbus Control Centre at the German Aerospace Center (DLR), in Oberpfaffenhofen, near Munich, which operates the Columbus laboratory, and is in close contact with the other ISS partner control centres. The Columbus Control Centre coordinates all Columbus systems and research activities. It provides the ground services for Columbus operations, including communication services (voice, video and data) to all sites responsible for control and coordination of individual European facilities and experiments on the ISS, including a network of nine user support and operations centres across Europe, industrial support sites, and ESA management and associated ESA locations.

ESA also has an Automated Transfer Vehicle (ATV) Control Centre based at the Centre National d'Etudes Spatiales (CNES), the French space agency, in Toulouse, France, which is responsible for operating the ATVs, Europe's logistics supply vehicles for delivering research equipment and supplies to the ISS.

2.3 Supporting ISS Research: Astronauts and Logistics

The ISS partners rely on the permanent presence of astronauts on the ISS who carry out their research activities and maintain the station. This is in turn supported by the ongoing logistics effort to supply the station with the necessary research samples and equipment as well as supplies for the astronauts and the station such as food, water, air and propellants.

Since 2001, nine ESA astronauts have served on short-duration missions to the ISS; two of them, Christer Fuglesang and Roberto Vittori, have flown on more than one mission. These short missions have played a vital role in the overall ISS logistics and assembly effort, serving to build the system and research infrastructure of the ISS up to its current levels, as well as transporting necessary supplies.

However, 2006 marked a stepping stone for ESA with its first long-duration crewmember, Thomas Reiter, who served as the first European and ESA astronaut as a member of an Expedition crew (Expedition 13) as well as undertaking a full programme of research activities as part of the European Astrolab mission. Reiter's presence on the ISS for almost six months was significant in that it again increased the number of permanent crewmembers on the station to three (following the STS-107 *Columbia* accident), allowing the crew to devote more time to (European) research activities in addition to their standard ISS crew duties.

European research activities were further enabled during the STS-122 mission in February 2008. This mission included ESA astronauts Hans Schlegel and Léopold Eyharts who played important roles in installing the Columbus laboratory on the ISS and undertaking numerous tasks to commission Europe's ISS laboratory. Schlegel returned at the end of the Shuttle mission, although Eyharts continued his work on the station for a further five weeks as a member of the Expedition 16 crew.

Since 2009 five ESA astronauts have served on missions to the ISS, three of them for five or six months. These missions included extensive experimental programmes covering research into human physiology, biology, fluid physics, materials science, radiation dosimetry, solar research, astrobiology and technology demonstrations, as well as related education activities to increase the interest of schoolchildren and students in science-related subjects. The other two astronauts served as Shuttle Mission Specialists.

Frank De Winne (Fig. 2.1.2) arrived on the station as an ISS Expedition 20 Flight Engineer with two additional crewmembers in May 2009 (and became ISS Expedition 21 Commander in October 2009). The arrival of Expeditions 20/21 increased the number of ISS crewmembers from three to six for the first time, which was significant as it allowed more time to be spent on research, not only due to more astronauts being on board but also each one had to spend less time on standard ISS maintenance activities.

During De Winne's OasISS mission, which landed on 1 December 2009, a total of 50 experiments covering life and physical sciences, technology and education were undertaken. The research potential of the ISS expanded with the delivery and installation of the External Platform of the Japanese laboratory for exposure research (during the STS-127 Shuttle *Endeavour* mission in July 2009). De Winne was a primary robotic arm operator for the docking of the first Japanese H-II Transfer Vehicle (HTV-1) with the ISS in September 2009 and for transferring scientific payloads from HTV-1 to the Japanese External Platform. The HTV is the Japanese unmanned logistics vehicle for the ISS.

Between STS-127 and HTV-1, the STS-128 Shuttle *Discovery* mission to the ISS was undertaken with ESA astronaut Christer Fuglesang as Mission Specialist. As part of the mission De Winne and Fuglesang were instrumental in the installation of NASA's Materials Science Research Rack (with ESA's Materials Science Laboratory). This expanded the potential of materials research on the ISS. One final highlight of the OasISS mission was the launch

Figure 2.3.1. ESA astronaut Paolo Nespoli preparing to install experimental hardware in the Microgravity Science Glovebox in March 2011. (NASA)

and attachment of the Russian 'Poisk' Mini Research Module 2 to the Russian segment of the ISS. Poisk was a new docking compartment to facilitate increased Soyuz/Progress dockings associated with six-member crews, thus further supporting the research effort on the Station.

Paolo Nespoli (Fig. 2.3.1) was the next ESA Expedition crewmember on the ISS from December 2010 to May 2011. During his mission (called MagISStra) a total of 31 ESA experiments covering life and physical sciences, technology and education were undertaken. Like Frank De Winne, Nespoli was a primary robotic arm operator for docking the Japanese HTV-2 to the ISS and participated in the docking of the second Automated Transfer Vehicle (ATV-2), Europe and ESA's ISS logistics vehicle and currently the largest servicing vehicle for the ISS. The Permanent Multipurpose Module loaded with about 2.7 tonnes of research equipment and logistics supplies was permanently attached to the ISS (during the STS-133 mission in February/March 2011) to increase its working volume. Nespoli was still serving on the ISS when the STS-134 Shuttle mission was undertaken (May/June 2011) which included ESA astronaut Roberto Vittori as a Shuttle Mission Specialist. This mission attached the Alpha Magnetic Spectrometer, the most complex scientific instrument ever fitted to the ISS, which is detecting and cataloguing cosmic rays in the search for antimatter and investigating the fundamental nature of matter.

In December 2011, André Kuipers was launched to the ISS on a long-duration mission (called PromISSe) as a member of ISS Expedition 30/31. During the mission a total of 33 ESA experiments covering the physical and life sciences, technology and education are scheduled to take place. In relation to the logistics vehicles that support ISS research, he was a prime crewmember responsible for the rendezvous and docking operations of ATV *Edoardo Amaldi*, ESA's third ATV, at the end of March 2012. ATV-3 delivered essential research equipment and cargo, has performed regular ISS orbit reboosts, and attitude control manoeuvres, and enables debris-avoidance manoeuvres if necessary. Kuipers was also involved in berthing the new visiting logistics vehicle Dragon (SpaceX) as part of NASA's commercial resupply programme for the ISS.

In addition to the astronaut missions, ATV-2 arrived at the ISS on 24 February 2011, eight days after launch (Fig. 2.3.2). The logistics vehicle delivered about seven tonnes of dry cargo (including research equipment and supplies), propellants and air; removed 1200 kg of old equipment and waste; carried out a debris-avoidance manoeuvre in April 2011; and reboosted the ISS in June 2011 by about 40 km to a higher orbit.

Figure 2.3.2. ATV-2 docking with the ISS on 24 February 2011. (NASA)

→ FUNDING EUROPE'S ISS RESEARCH: ELIPS

3. Funding Europe's ISS Research: ELIPS

ESA's research activities on the International Space Station are governed by the European Programme for Life and Physical Sciences (ELIPS). ELIPS ensures that Europe's investment in the development and exploitation of the ISS produces the best scientific results. To this end, ELIPS promotes global cooperation, international peer review of research proposals and European coordination in the development of facilities and the use of resources. It covers a broad range of scientific disciplines, including physics, chemistry, biology, physiology, psychology and related topics.

The ELIPS programme is financed by 14 ESA Member States: Austria, Belgium, Czech Republic, Denmark, France, Germany, Greece, Ireland, Italy, the Netherlands, Norway, Spain, Sweden and Switzerland, plus Canada, which has a cooperation agreement with ESA.

The programme is unique in that its orientations are based on inputs from the scientific and industrial user communities in Europe in a process supervised by the European Science Foundation. The ELIPS scientific and industrial user community is of the highest international quality. The programme makes use of all possible research platforms, in addition to the ISS itself (Fig. 3.1.1), including ground-based facilities, drop towers, parabolic aircraft flights, sounding rockets (Fig. 3.1.2) and unmanned orbital capsules. All of these platforms offer very specific operational and physical environments, especially weightlessness.

Weightlessness provides a unique environment for scientific research, giving an unusual opportunity to answer questions that would be impossible to tackle on Earth. Many more processes in physics, chemistry, biology or physiology that are relevant for biological, physical or industrial processes on Earth are affected by gravity than was expected in the early days of spaceflight. Research in weightlessness has led to high-level discoveries or changes of commonly accepted scientific understandings. Even Nobel Prize-winning hypotheses, like eye movement reflexes, have been found to be partly erroneous thanks to experiments performed by astronauts during spaceflight missions.

In terms of the subjects of experiments on the ISS, the ELIPS programme is organised into research 'cornerstones'.

The cornerstones of ELIPS in the life sciences include biological research, focusing on the effects of gravity on fundamental processes in plant and animal cells. From this research a better understanding is evolving of how cells adapt to their environment, which in turn could be exploited in medical

Figure 3.1.1. The ISS photographed from STS-133 Shuttle *Discovery* following undocking on 7 March 2011. (NASA)

Figure 3.1.2. Launch of the Texus-49 sounding rocket from the Esrange launch site near Kiruna, Sweden, on 29 March 2011. (Astrium GmbH)

and biotechnological applications, and in studies of the immune system, food production, etc.

Human physiology research includes studies of a number of age-related health problems such as osteoporosis, cardiovascular and respiratory diseases and equilibrium disorders, which are induced or accelerated in weightlessness. The results may be relevant for new diagnostics and medical treatments on Earth, as well as for the design of effective measures to maintain the fitness of astronauts in preparation for long-duration space missions.

In fundamental physics, novel states of matter such as complex plasmas, solid/liquid dust particles and cold atoms are being examined within the ELIPS programme. Careful studies of these systems require weightlessness, since on Earth they are influenced by gravitational effects. Such fundamental studies may lead to new theories regarding physical processes. However, practical studies are also envisaged, such as very stable atomic clocks that can be used in future navigation systems.

In materials science, the space environment is being used to measure thermophysical properties of metals and alloys with unprecedented accuracy. These properties are being used by industry in numerical models to optimise production processes and even to develop new materials with advanced properties. With EU funding, the extensive five-year Intermetallic Materials Processing in Relation to Earth and Space Solidification (IMPRESS) research project has been carried out within the ELIPS programme for the development of more efficient aircraft engines and hydrogen fuel cells. Additional materials science projects are in the pipeline.

In fluid physics, the weightless environment on the ISS helps in studying the physics of fluids and interfaces in an undisturbed way (Fig. 3.1.3). Apart from the theoretical importance of such studies, the results may be used to optimise chemical industrial processes or combustion processes in power plants or car engines. The close link between materials and fluids research is leading to substantial advances in our understanding of physical processes.

Finally, experiments in the field of astrobiology are addressing fundamental questions related to the origin, evolution and distribution of life in the Solar System and beyond, as well as on Earth.

ESA's research activities on the ISS are fully embedded in the overall context and in the various cornerstones of the ELIPS programme. The selection of scientific experiments to be conducted on the ISS and on the ground is driven primarily by the physical and life sciences and applications, and by research undertaken in preparation for human space exploration missions.

Figure 3.1.3. Frank De Winne installing the Selectable Optical Diagnostic Instrument (SODI) in the Microgravity Science Glovebox on the ISS in September 2009. SODI is involved in three ESA fluid science projects. (NASA)

→ RESEARCH ON THE ISS

4. Research on the ISS

4.1 Human Research

Human research on the ISS focuses on maintaining the health of astronauts and improving medical care on Earth. The human body is highly complex array of systems that science is still striving to understand in its entirety. Previous research in (and exposure to) space as well as simulation campaigns on Earth have shown that weightlessness and the conditions in orbiting spacecraft affect the human body in unique ways. Understanding these effects and developing ways to counter them will be beneficial for maintaining the health of astronauts now and in the future. They may also contribute to our understanding of many medical conditions prevalent on Earth and could help improve rehabilitation procedures.

The development of new medical diagnostic tools for use in human long-duration spaceflight will be essential as the crews will need to be self-reliant. These new tools will also find significant applications on Earth, such as in providing medical assistance in areas that do not have easy or rapid access to medical services, and medical monitoring for personnel with critical occupations, such as pilots, air traffic controllers, nuclear facility operators and firefighters. They could also be beneficial for the chronically ill or the aged, allowing them to be cared for at home.

4.1.1 Cardiopulmonary Research

On Earth, gravity plays an important role in blood circulation, assisting in maintaining blood flow to the lower parts of the body, which is countered by the blood pressure control system. An everyday example is when someone faints, i.e. there is a failure in blood pressure control. Simply standing up increases blood pressure in the lower parts of the body. This in itself can induce constriction and structural thickening of the walls of arteries and may contribute to hypertension and cardiovascular disease.

Although the indications exist, the influence of gravity on disease development and the consequences of removing it are unclear. One effect of weightlessness is cardiovascular deconditioning, which can lead to a serious postflight condition known as orthostatic intolerance, i.e. the inability to maintain an upright posture for a long period of time. This orthostatic intolerance is experienced by 20% of astronauts following short-duration missions (<15 days), and by up to 80% of crewmembers after longer missions. Understanding and countering the mechanisms underlying this condition is of considerable significance for the success of future space exploration missions.

Establishing a better understanding of how gravity influences blood pressure control and the sympathetic nervous system over the course of a spaceflight mission will also shed light on certain cardiovascular conditions on Earth. This will in turn impact the treatment and rehabilitation of patients suffering from hypertension and other cardiovascular diseases. The cost of cardiovascular disease was estimated at around €170 billion in the EU in 2003. This indicates the importance of this area of research, not only from a financial perspective, but also from the social perspective of the debilitating effects of such diseases.

Orthostatic intolerance is the most obvious symptom of cardiovascular deconditioning caused by exposure to weightlessness, and is characterised by a large fall in stroke volume (the volume of blood pumped from the ventricles) and tachycardia (a high heart rate) in the upright position. The mechanisms responsible for this intolerance after space travel have been investigated extensively. Various hypotheses have been put forward, many of them focusing

Figure 4.1.1. ISS Expedition 19 flight engineer and JAXA astronaut Koichi Wakata, preparing to use the Pulmonary Function System as part of the CARD experiment. (NASA)

on the alteration of vascular and circulatory function (fluid shifting to the chest and head), but also on the autonomic nervous system impairment of cardiovascular control.

Changes in Cardiovascular Regulation

CARD (A Model for Investigating Mechanisms of Heart Disease) is an experiment programme that began during ISS Expedition 14 and completed activities on orbit during Expedition 30/31. On Earth, increased activity in the sympathetic nervous system and increased cardiac output are normally associated with increased blood pressure. However, it has been observed that during exposure to weightlessness, cardiac output and activity in the sympathetic nervous system (which normally constricts arteries) increases while blood pressure falls (caused by dilated arteries). The CARD experiment is examining these effects in order to provide a thorough picture of how the circulatory system changes during a prolonged periods of weightlessness.

At different points before, during and after an astronaut's ISS mission, 24 h blood pressure measurements are taken, and blood samples are tested for biochemical markers of increased activity in the sympathetic nervous system. Urine samples are also taken to measure renal sodium output, and cardiac output is measured using the ESA/NASA Pulmonary Function System (Fig. 4.1.1).

The CARD programme includes a separate experiment called Sympatho-2, which is a study of adrenal activity of the sympathetic nervous system in weightlessness. Sympatho-2 builds on the results of ESA's first Sympatho experiment, undertaken between 2002 and 2005, which showed a rather conflicting increase in activity in the sympathetic nervous system in weightlessness through an increase in thrombocyte noradrenaline in analysed samples. As one example of how the results of this kind of research can be translated to Earth-based applications, heart failure patients have been shown to benefit if they are immersed in thermoneutral water, so that the cardiovascular system is almost weightless.

The Vessel Imaging Experiment, which started in June 2010, is another ESA experiment that is adding to our knowledge of cardiovascular function by providing information on the properties of blood vessels during weightlessness. The experiment is evaluating the changes in the properties and cross-sectional areas of central and peripheral blood vessel walls in long-term ISS crewmembers. Measurements are taken during and after long-term exposure to weightlessness using ultrasound scans of major arteries/veins combined with electrocardiogram and heart rate measurements. The experiment is the result of the suggestion that long-term exposure to microgravity will induce changes in the properties of blood vessel walls, as well as in vessel size and blood flow, with effects similar to those seen in bedrest studies.

If continued research determines that long-duration spaceflight increases cardiac output and induces dilation of peripheral arteries, this suggests that it is actually healthy for the cardiovascular system. If confirmed, this finding may have an impact not only on how astronauts are prepared and future long-duration missions are planned, but also on the treatment and rehabilitation of patients suffering from hypertension and other cardiovascular diseases.

Cardiovascular Adaptation and Endurance

ESA's Assessment of Endurance Capacity by Gas Exchange and Heart Rate Kinetics (EKE) experiment, which began during ISS Expedition 19, is looking into ways to reduce the time spent assessing endurance capacity in orbit. Although this is important for assessing the health status of astronauts, it will increase the time they can devote to other research activities. Thermolab is another

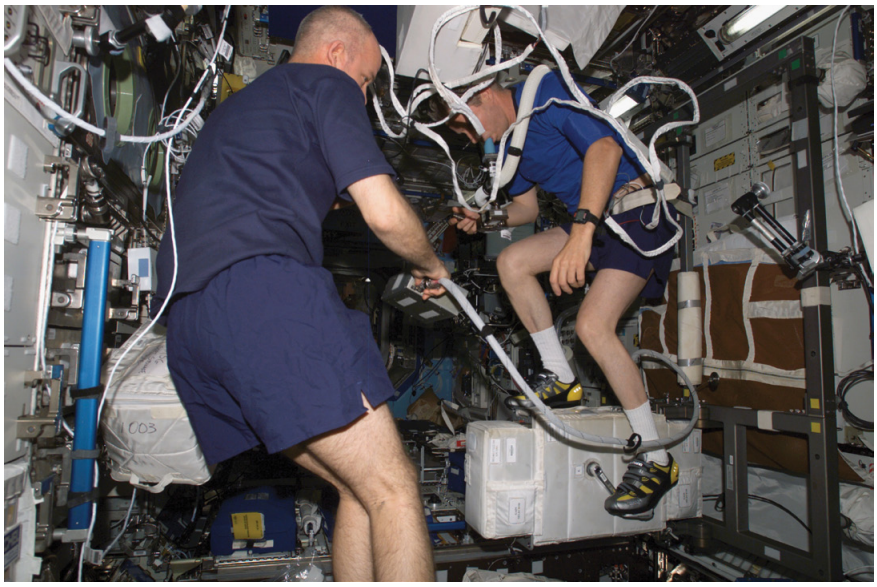

Figure 4.1.2. ESA astronaut Thomas Reiter, assisted by ISS Flight Engineer Jeff Williams, performing a periodic fitness evaluation with oxygen uptake measurements during ISS Expedition 13. A similar protocol is used to measure VO_2 Max. (NASA)

ESA experiment that is looking into thermoregulatory and cardiovascular adaptations during rest and exercise in the course of long-term weightlessness. Both of these experiments are using the portable Pulmonary Function System for measuring oxygen uptake and cardiac output during various levels of exercise (Fig. 4.1.2), and the data are being shared with NASA's Maximum Volume of Oxygen used during exhaustive exercise (VO_2 Max) experiment.

For the EKE experiment, numerous ISS crewmembers have already been the subjects of tests to assess their endurance capacity by measuring gas exchange and heart rate kinetics during physical exercise. Preserving astronauts' aerobic capacity is a major goal of exercise countermeasures during space missions. VO_2 max is a widely used measure of maximum work capacity. To reduce the frequency of such tests, EKE is looking at a potential alternative method for determining the rate of changes in pulmonary oxygen uptake (VO_2) and heart rate responses during changes in workload. Specific goals include the development of a diagnostic tool for assessing endurance capacity from oxygen uptake and heart rate in response to changes in exercise intensity, and of a physiological model to explore the transport of oxygen from the lungs to muscle cells.

The Thermolab experiment has involved numerous crewmembers since it started during Expedition 21 in October 2009. The experiment is based on the hypothesis that heat balance, thermoregulation and circadian temperature rhythms are altered in humans during long-term space flights because of changes in the natural convective heat transfer from the body, fluid shifts throughout the body, the cardiovascular and autonomous nervous system and changes in body composition (fat and muscle mass, body water). Thermolab is combined with the VO_2 Max protocol as these factors are cross-linked with each other, particularly during exercise. The information obtained by this study will lead to a better basic understanding of heat transfer and thermal regulation in humans under microgravity conditions.

Although these experiments are under way, and the data obtained so far are very promising.

4.1.2 Musculoskeletal Research

One of the most important areas of ESA's human physiology research involves studies of bone mass reduction and related medical conditions in astronauts. On Earth, the most prevalent of these conditions is osteoporosis. It has been estimated that in Europe the treatment of bone fractures costs €25 billion

Figure 4.1.3. Frank De Winne taking body mass measurements in the Columbus laboratory, as part of the SOLO experiment in 2009. (NASA)

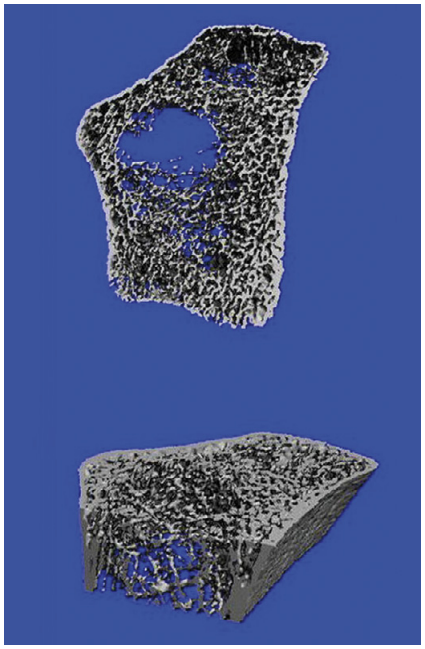

Figure 4.1.4. 3DpQCT image of osteoporotic bone. (Scanco Medical AG)

per year (EU, 2003), a figure that is set to rise as the elderly population increases, and underestimates the total cost to society. Europe's average annual contribution to the ISS programme is only around 1% of the amount spent each year on osteoporosis treatment.

During space missions, astronauts exhibit bone loss similar to osteoporosis, losing about 1% of bone mass per month, particularly in the lower parts of the body. This makes the ISS a perfect testbed for carrying out research in this field.

ESA is helping to develop innovative tools to detect, monitor and combat the effects of osteoporosis in two experiments: the SOdium LOading in Microgravity (SOLO) and Early Detection of Osteoporosis in Space (EDOS).

SOLO has been studying the mechanisms of fluid and salt retention in space and related human physiology effects since October 2008, based on data from various crewmembers (Fig. 4.1.3). The link with bone loss may not be obvious to the layman, but it is suspected that weightlessness may lead to the activation of sodium-retaining hormones, resulting in higher than normal levels of sodium in the body. In addition, sodium has a pH-lowering effect, which could also have a negative impact on bone metabolism. An average or high sodium intake in weightlessness may exacerbate the rise in the rate of bone resorption by the body.

In the SOLO experiment the astronaut subjects participate in a two-phase study following a diet of constant either low or normal sodium levels with the same daily calorie intake and fairly high fluid consumption. In this metabolically controlled study, blood and urine samples are collected from the subjects during each diet period, and are analysed after return to ground for relevant biochemical markers to indicate the effects on bone metabolism.

ESA's research into bone mass reduction with SOLO is supported by the EDOS experiment, which uses a technique called Three-Dimensional peripheral Quantitative Computed Tomography (3DpQCT) (Fig. 4.1.4) to detect bone structure, and to provide a detailed evaluation of the kinetics of bone recovery after flight. This enhanced scanner is providing high-quality 3D images of living bone structures (wrist and ankle) as part of the ground-based experiment, which is backed up by analysis of bone biochemical markers in blood samples.

One important outcome of ESA's research into bone loss in space has been the successful commercialisation of the 3DpQCT scanner. ESA supported the development of the enhanced 3D scanner by the Swiss company Scanco Medical and the Institute for Biomedical Engineering in Zürich, as a non-invasive/*in vivo* technique for observing bone structure.

Reference

EU (2003). *Osteoporosis in the European Community: Action Plan*. European Union Osteoporosis Consultation Panel.

4.1.3 Neuroscience Research

For orientation on Earth people rely heavily on visual perception and cues from the vestibular system, and in particular the perception of gravity, which normally defines our frame of reference. In contrast, in the weightlessness of space the gravity-sensitive vestibular sensors in the inner ear are no longer stimulated by gravity. Astronauts must therefore adapt their sensory and motor activities to their free-floating 3D environment, and rely heavily on their visual perception to maintain spatial orientation.

Astronauts initially experience a sensory mismatch or conflict in space that can cause space adaptation syndrome or space sickness. This occurs to varying degrees in as many as two-thirds of astronauts and can adversely affect their performance. Fortunately, the neurovestibular system is able to adapt to

these weightless conditions within the first few days in space, although some astronauts may continue to experience disorientation.

Besides the potential benefits of this research in reducing the discomfort felt by many astronauts, this field of research has many implications for mainstream laboratory research. Possible areas of research include studies of the balance system to improve diagnosis and treatment of patients with dizziness and equilibrium disorders, including the development of new methods for evaluating their ability to use visual and pressure cues for maintaining balance and orientation; motor function development in children; and with regard to aerospace technology, in refining the design of flight simulator and virtual reality vision systems.

ESA is undertaking three experiments to improve understanding of spatial orientation and perception: the Study of Spatial Cognition, Novelty Processing and Sensorimotor Integration (NeuroSpat), Scaling Body-Related Actions in the Absence of Gravity (Passages) and the Mental Representation of Spatial Cues during Space Flight (3D-Space) experiments.

NeuroSpat

Following the launch of the Columbus laboratory in February 2008, Neurospat was the first major neurological experiment to make full use of the European Physiology Modules facility in June 2009, with Frank De Winne (Fig. 4.1.5) and Canadian Space Agency astronaut Robert Thirsk as the first test subjects. More recently, Paolo Nespoli in 2011 (Fig. 4.1.6) and André Kuipers in 2012 were subjects in NeuroSpat, which is a study of spatial cognition, novelty processing and sensorimotor integration. The experiment includes two parts, NeuroCog-2 (Effect of gravitational context on brain processing), an extension of the NeuroCog experiment that began in 2002, and PreSpat (Prefrontal brain functions and Spatial cognition).

PreSpat and NeuroCog-2 were originally separate experiment proposals. PreSpat uses physiological and behavioural measures to assess changes in general activation, prefrontal brain function and perceptual reorganisation. Prefrontal brain function is known to be especially important for the higher organisation of behaviour and is particularly vulnerable to stresses such as fatigue, lack of sleep or hypoxia. Different measurements have been taken during spatial orientation tasks using devices such as a multichannel electroencephalogram (EEG).

Figure 4.1.5. Frank De Winne undertaking the NeuroSpat experiment on the ISS in June 2009. (NASA)

Figure 4.1.6. Paolo Nespoli having gel injected into an EEG cap prior to undertaking the NeuroSpat experiment in December 2010. (ESA/NASA)

The NeuroCog-2 part is studying the brain activities underlying cognitive processes involved in four tasks that humans on Earth (and astronauts in orbit) may perform on a daily basis: visuo-motor tracking, the perception of self-orientation, 3D navigation and the discrimination of the orientation of objects.

In short, NeuroSpat has been investigating how crewmembers' perceptions of 3D objects and space are affected by long periods in weightlessness. The Multi-Electrode Encephalogram Measurement Module (MEEMM), one of the science modules of the European Physiology Modules used during NeuroSpat, proved successful and high-quality EEG signals were obtained. The NeuroSpat experiment is part of the Supporting the Use of Research Evidence (SURE) project, supported by the European Commission.

In the context of the NeuroSpat experiment, it is expected that some indication will be obtained of the mechanisms involved in altered behaviour in weightlessness, and the location of the specific areas of the cerebral cortex involved.

Following on from NeuroSpat, ESA's Passages experiment, which started in January 2010, also utilised the NeuroSpat hardware and the European Physiology Modules facility to test how astronauts interpret visual information in weightlessness. It is studying the effects of microgravity on the use of a specific neural strategy for estimating allowed actions in an environment, and whether this might decrease after long exposure to weightlessness. The experiment was performed by ten crewmembers, and the science team is nearing completion. Although it is too early to draw any conclusions, the data look promising.

3D Space

3D Space was the first neuroscience experiment to take place in the Columbus laboratory. It has been investigating whether the absence of gravity during spaceflight is responsible for alterations in distance and depth perception in astronauts. Such alterations could impact the perception and localisation of objects in the space environment, and consequently spatial orientation and reliable performance of tasks. The objective of this experiment is to identify the problems associated with distance and depth perception in astronauts with the goal of developing measures to alleviate any associated performance risk.

Since 2008 the 3D Space experiment has been performed by nine astronauts, with ESA's Paolo Nespoli (Fig. 4.1.7) and NASA's Catherine Coleman as the final subjects in 2011.

Figure 4.1.7. Paolo Nespoli undertaking the 3D Space experiment on the ISS in January 2011. (ESA/NASA)

Measurements included three science objectives. First, the subjects use a trackball to adjust the shape of 2D geometric illusions and 3D objects presented via a headset as an element of depth perception. Second, the subjects write or draw objects from memory on a digitising tablet using an electronic pen, while following instructions presented in the head-mounted display. Finally, their distance perception is assessed with natural or computer-generated 3D scenes presented in the display. The subjects estimate and report absolute distances or adjust the distances between objects using the trackball.

The results of the 3D Space experiment have shown that: a 3D cube looks 'normal' if it is shorter and wider than a normal cube. The height effect is significant; hand-drawn objects are wider and shorter than on the ground, while words written vertically in zero gravity are shorter (total vertical length of the word) than preflight, but longer immediately after return. Also, the perceived asymmetry between vertical and horizontal distance seen on Earth, where vertical distance is overestimated, disappears late inflight. Shorter distances ranging from 30–300 m, however, are underestimated (G. Clément, personal communication).

The Vestibulo–Oculomotor System

Three experiments on the ISS – Otolith Assessment during Postflight Readaptation (Otolith), Validation of Centrifugation as a Countermeasure for Otolith Deconditioning during Spaceflight (Spin), and the Z-axis Aligned Gravito-inertial force (Zag) – aim to increase our understanding of the vestibulo–oculomotor system. The coordination of the vestibular system (which regulates balance, orientation and posture) and eye movements allows humans to fix on a stationary object while moving around. The vestibular system provides precise information about how the head is moving, and this is relayed within a few milliseconds to the eye muscles, so that compensatory eye movements are made to keep the 'eye on the ball'. This is known as the vestibulo–ocular reflex.

Since the vestibular frame of reference is governed by gravity, understanding how the system adapts to the absence of gravity and subsequently readapts to it is crucially important for basic research, including the exact mechanisms involved in disorders like space sickness. This type of research also provides insights into clinical vestibular disorders involving vertigo, disorientation and nausea.

Ground-Based Neuroscience

Numerous ESA experiments are also performed on the ground, with procedures pre- and post- flight, including Otolith, Spin and Zag. While Otolith is assessing otolith–ocular responses to determine neural pathway communication between the otoliths of the inner ear and the central nervous system, Spin has been evaluating centrifugation as a countermeasure for otolith deconditioning during spaceflight using a centrifuge and a standardised tilt test. If a correlation is found between postflight otolith deconditioning and orthostatic intolerance, this would prove highly significant, necessitating the provision of an artificial gravity countermeasure for future long-duration space missions.

The Zag experiment is investigating the influence of weightlessness on astronauts' perceptions of translation and tilt, based on their performance before and immediately after spaceflight. It also evaluates whether a specially developed vibrotactile vest can improve perception and performance. On landing day it was shown during tests that manual control performance without any vibrotactile feedback was reduced by more than 30%, suggesting that a vibrotactile aid improves the ability to null out tilt motion within a range of motion disturbances.

As of 2011 both the Otolith and Zag experiments had gathered sufficient data from the allotted number of test subjects.

Reference

ICHD-II (2004). *International Classification of Headache Disorders*, 2nd edn. International Headache Society/Blackwell, Oxford, UK.

4.1.4 Immunology Research

Research in this area has built on extensive research dating back decades. Analysis of blood samples taken from the Apollo astronauts after the 1973 Skylab mission showed that more than 50% had experienced either bacterial or viral infections during the mission and later on their return to Earth.

The immune system is extremely complex, reacting to all manner of 'threats' to the human body. Beyond barriers such as skin, mucus and stomach acid, invading microbes are faced with the innate immune system, which includes phagocytes (a type of white blood cell) that engulf and destroy pathogenic bacteria, virus-infected cells and other foreign substances. They also face the adaptive immune system, which includes other types of white blood cell, such as B- and T-lymphocytes (Fig. 4.1.8), which react specifically to the microbe itself, identify it, produce specific antibodies and eliminate it (the principle harnessed for developing immunity through vaccination).

Figure 4.1.8. Constituents of blood. L is a lymphocyte, a white blood cell that plays an important role in the body's immune system. E is an erythrocyte or red blood cell and P is a blood platelet. (NASA)

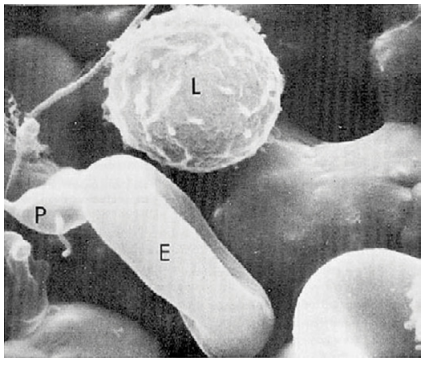

Several factors, such as exposure to weightlessness and stress, can adversely influence how the immune system functions in space. For example, ground studies have shown that increased stress (and hence increased levels of stress hormones) is accompanied by modulation and suppression of immune functions, altering the activity of critically important immune cells, which can lead to the reactivation of viruses such as Epstein–Barr and *Herpes simplex*, and can adversely affect physiological functions such as the healing of wounds. By carrying out this research and getting a better understanding of how our immune system works in space, it may be possible to determine appropriate measures to counter adverse effects, whether by pharmaceutical treatment or environmental manipulation (such as the use of artificial gravity). More sophisticated preventive methods lie in the remote future, such as the manipulation of gene sequences that trigger gravity-dependent immune cell dysfunction as well as those that offer protection against radiation.

Figure 4.1.9. ESA astronaut André Kuipers working with the Role of Apoptosis in Lymphocyte Depression 2 (ROALD-2) experiment in the Kubik-3 incubator in the Columbus laboratory in December 2011. (NASA)

In addition to the crucial task of maintaining astronaut health, this research will also benefit patients on Earth with the potential for targeted drug treatments, vaccinations and other therapies. These achievements could be implemented into the treatment of any patient, of any age, at any location, from the local clinic to the ISS.

In order to characterise the immunological changes in astronauts, ESA is undertaking an extensive research programme. The Immuno experiment, which started during Expedition 12, aims to determine changes in stress and immune responses during and after a stay on the ISS. This includes sampling saliva, blood and urine for dopamine, epinephrine and cortisol, hormones associated with stress. Thomas Reiter was one of the ESA astronauts to undertake the experiment as part of the Astrolab mission.

In addition, ESA has undertaken a series of experiments with immune cells on the ISS, which although relatively small scale, have provided a host of data on behaviour of elements of the immune system under spaceflight conditions. Over the past five years this set of ESA experiments has been performed in transportable Kubik incubators (Fig. 4.1.9) designed in the frame of the ISS Soyuz missions for biology experiments.

The most recent investigation in this series was the PAthway DIfferent Activators (PADIAC) experiment, which took place in October 2010 using two Kubik incubators. PADIAC is studying the activation in space of T-cells with different activator cocktails to stimulate various activation pathways, and analysing the differences in gene expression among these different conditions.

PADIAC was expanding on the research undertaken in a previous series of experiments, including:

— the Motion and Interact (MIA) experiment (2006), which studied the effects of weightlessness on the motion of monocyte white blood cells and their interaction with T-lymphocytes. The results may provide an indication of the mechanisms responsible for inhibited immune cell activation in microgravity;
— the Leukin experiment, which focused on testing whether inhibited T-cell activity was due to lack of expression of a receptor (IL-2) responsible for eliciting an immune response from T-lymphocytes;
— the Pkinase experiment (October 2007), which studied the protein kinase C family of enzymes that have many functions in the human body and are central in turning monocytes into macrophages – white blood cells that engulf and digest cellular debris and pathogens; and

— the ROle of Apoptosis in Lymphocyte Depression (ROALD) experiment (2008), which studied the process of programmed cell death (apoptosis), a normal function in human and animal cells, and whether stimulation of this process in lymphocytes was responsible for inhibited activation of these white blood cells.

At the end of 2011, the ROALD-2 experiment (see Fig. 4.1.9) was performed in the Kubik incubators, with its experiment containers secured in a Minus Eighty-Degree Laboratory Freezer for the ISS (MELFI) until their return for analysis in April 2012. Anandamide (AEA) is the main representative of a family of polyunsaturated fatty acid amides and esters, called endocannabinoids. The project investigated gene expression of the proteins involved in the metabolic control of AEA tone, in order to determine the role of this lipid in the regulation of immune processes and in the cell cycle under microgravity conditions. In fact, AEA is a signal for the cells to make a choice between life and death, and might be responsible for the immune deficit observed in astronauts in space. The experiment expanded on the objectives of the ROALD experiment using a similar protocol.

4.2 Biology Research

ESA's biological research on the ISS continues to improve our understanding of a variety of biological processes. These encompass plant biology, focusing on the mechanisms behind gravity perception and the impact on human exploration missions and plant growth processes on Earth; developmental biology, including studies of organisms/ecosystems that could form a part of Environmental Control and Life Support Systems and increase our knowledge of immune system behaviour; and cell and molecular biology, including biotechnology experiments (cells, tissue bacterial growth) with potential applications in medicine, agriculture and environmental management (e.g. biological air filters and biosensors).

4.2.1 Plant Biology: Plant Growth Processes

Plant biology research has been undertaken for many decades in space, and for ESA since 2003 on the ISS. One of the principal areas of research focuses on the mechanisms by which plants sense gravity, and how these mechanisms are altered in weightlessness. Which strains of specific plants are better able to deal with the stress of growing under weightless or low-gravity conditions is also of great importance. This applies not only to individual plants but also to successive generations of plants and how they adapt with each generation. This research is crucial for future human exploration missions where greater self-sufficiency with respect to growing food will have a positive effect on mission planning and cost, as will the development of plant-based life support systems that will contribute to carbon dioxide recycling.

Beyond the impacts of this research for future human spaceflight missions, increased knowledge of plant growth processes and how these are altered by different environmental conditions can only help to improve our understanding of plant growth processes on Earth, and hence will have a positive impact on cultivation and production processes.

In the past two years ESA's plant biology research on the ISS has been extended with additional studies of species such as *Arabidopsis thaliana* (thale cress), which is an important model organism that has been well characterised from the physiological down to the genetic level. *A. thaliana* has a fully characterised genome, can develop under variable conditions and shows a wide range of morphological variations depending on the environment. Increasing our knowledge of this species of plant can also help shed light on the growth processes in other species and in plants in general. ESA's most recent Arabidopsis research on the ISS has included experiments such as Waving and Coiling of Arabidopsis Roots at Different *g*-levels (WAICO) and Gravity-Related Genes in Arabidopsis (Genara), the last runs of which were undertaken in 2010. These experiments built on previous research and data, and the results obtained will help to drive further experiments in the future.

The WAICO experiments were the first to take place in the Biolab facility in the Columbus laboratory in 2008 (and thereafter in 2010). These experiments studied the interaction between circumnutation (spiralling motion) of the growing tips of the stems and roots of Arabidopsis, and gravitropism (the tendency to grow toward or away from gravity). For comparative purposes, the specimens (Fig. 4.2.1) were exposed to weightlessness and 1-*g* environments.

Genara-A was the most recent ESA Arabidopsis experiment to take place (in the European Modular Cultivation System) on the ISS, in 2010, and samples were returned from orbit on STS-133 in March 2011. Undertaken in two parts, Genara-A aims to identify gravity-regulated genes by assessing protein synthesis expression in Arabidopsis seedlings, while Genara-B will analyse root system development and determine the distribution of auxin (an important plant growth

Figure 4.2.1. *Arabidopsis thaliana* plants growing during the WAICO experiment in the Biolab facility in the Columbus laboratory (ESA)

hormone) in the seedlings. For purposes of comparison, normal and mutated type seedlings are used. As of mid-2012, the analysis was still ongoing.

Based on the results obtained from experiments on the ground, it is expected to see an increase in root development in seedlings grown under weightless conditions in space compared with those grown at 1 *g*. It is also expected that some differences in protein synthesis will be seen between seedlings grown under weightlessness and 1-*g* space conditions.

Another experiment that first took place in the European Modular Cultivation System (Fig. 4.2.2) in 2007 is the Molecular and Plant Physiological Analyses of the Microgravity Effects on Multigeneration Studies of *Arabidopsis thaliana* (Multigen) experiment. A follow-up Multigen experiment is currently under discussion, with the potential to maximise the use of ISS resources by developing a joint scenario together with the Genara-B experiment. The results of the first Multigen experiment were published in 2009 (Johnsson et al., 2009).

This purpose of this multigeneration plant experiment is to test how plants behave at different stages of development under weightless conditions, and ultimately to produce viable seeds from plants grown in space.

Figure 4.2.2. Exchanging the experiment container on the ISS during Expedition 14. (NASA)

During the first part of the experiment, the plants were grown from seed in 0-*g* and in 1-*g* centrifuged conditions on the ISS, and in 1-*g* conditions on the ground (at the Norwegian User Support and Operations Centre in Trondheim). The plants took 2–3 months to grow from seed to mature seed-bearing plants on the ISS, and the process was recorded using time-lapse video (Fig. 4.2.3). The plants were observed with regard to growth, development and production of flowers and seeds with special emphasis on spiralling growth (circumnutation) in the shoots.

Under the initial pure weightless conditions most of the movements of the side shoots of the plants were random, but there was some rhythmic movement, albeit very small, compared with the samples when gravity was introduced by activating a centrifuge.

Once the force of gravity was introduced the periods of circumnutation could be clearly measured (60 min periods during light growth periods and around 85 min periods during the dark growth periods). The present results extend previous observations and confirm the existence of circumnutational movements in weightlessness although with fewer cycles and smaller amplitudes. The importance of gravity in amplifying these minute oscillatory movements in weightlessness into high-amplitude circumnutations was also demonstrated.

The results obtained in this study unequivocally reveal several new features of circumnutation movements in *A. thaliana* stems in weightlessness (Johnsson

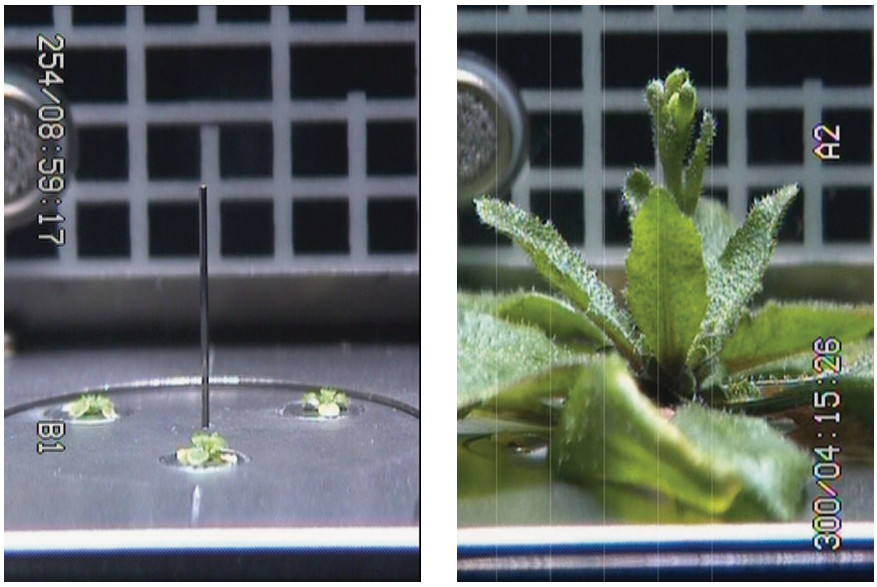

Figure 4.2.3. The Multigen experiment. *Arabidopsis thaliana* seedlings just after germination (*left*) and after seven weeks (*right*). (ESA)

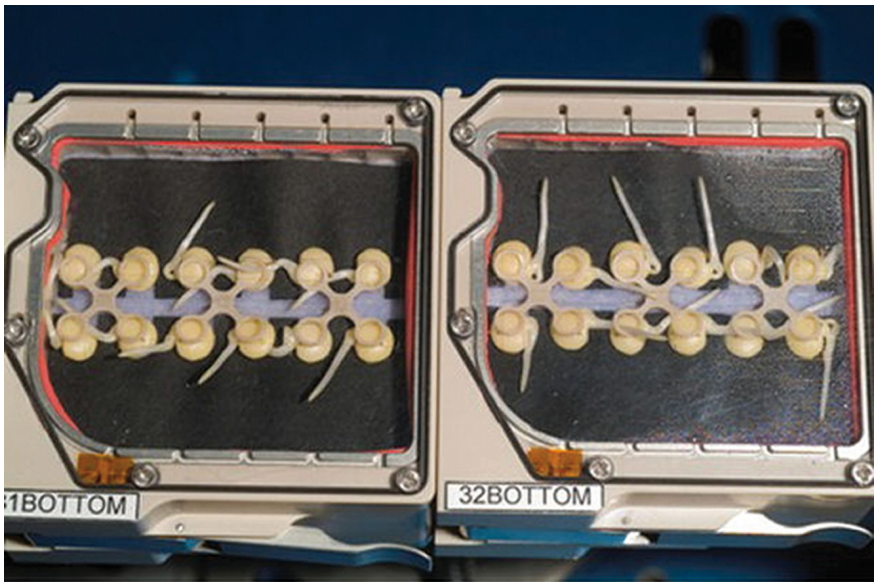

Figure 4.2.4. Cultivation chambers from the Gravi-1 experiment in the US laboratory, carrying out research to determine the gravity perception threshold in lentil seedlings. (NASA)

et al., 2009; Solheim et al., 2009). To take research in this field one step further, future experiments will focus on how gravity amplifies circumnutation.

The experiments also provided unequivocal demonstrations of periodic, self-sustained rhythmic movements in the rosette leaves of *A. thaliana* in weightlessness.

Beyond the Arabidopsis research, another study of plant growth is Gravi, a series of experiments that is also looking into gravitational responses in plants using lentil seedlings (Fig. 4.2.4), specifically what level of gravity initiates a directional growth response in the seedlings and what degree of response is generated. The Gravi experiments also take place in the European Modular Cultivation System. Although there have been no in-orbit activities on the ISS in the last two years, the results of the first Gravi experiment in 2007 were significant, and helped in the development of the follow-up scenario for the Gravi-2 experiment. Gravi-2 will analyse the free calcium distribution and the localisation of calcium-targeted proteins in root cap cells. Intracellular calcium deposits in the root caps are known to influence the sensation of gravity in plants, although the mechanisms behind this are still unclear.

Figure 4.2.5. Frank De Winne installing experiment containers into Biolab incubator in Columbus on 2 October 2009. (NASA)

Gravi-1 produced significant results related to gravity perception in lentils, and in plants in general (Driss-Ecole et al., 2008). Following in-orbit activities during which different seedlings were exposed to gravity levels as low as 0.003 *g* and up to 0.2 *g*, it was discovered that lentil roots grown in weightlessness are more sensitive to stimulation than those grown under 1-*g* conditions. The gravity threshold perceived by these plants was determined to be between 0 *g* and 0.002 *g*. In addition, by using a hyperbolic model, the gravity perception threshold was estimated to be 1.4×10^{-5} *g*.

4.2.2 Cell and Molecular Biology

The ISS is being used for biotechnology experiments on the growth of cells, tissues and bacteria, with potential applications in medicine, agriculture and environmental management (e.g. biological air filters and biosensors). Research in space has advanced our understanding of the role of gravity in life processes at various levels: genes, cells, organs and entire organisms. Changes in the functioning of plants, animals and humans in microgravity have been studied, as well as the underlying molecular, genetic and cellular mechanisms.

Cell and molecular biology is the area of biology in which the majority of ESA experiments have taken place in the past. ESA's yeast research has been under way on the ISS since 2001. In October 2009 ESA's first ISS Commander Frank De Winne processed the Yeast In No Gravity (YING-B) experiment in the Biolab facility (Fig. 4.2.5). This continued the YING-A experiment on the ISS in 2006 with ESA astronaut Thomas Reiter. The YING experiment studies the influence of weightlessness on Flo proteins, which regulate the flocculation (clumping together) and adhesion of cells. The goal is to obtain a detailed insight into the importance of weightlessness on the formation of organised cell structures, and on Flo processes, which are of considerable interest for fundamental science, industry and the field of medicine.

4.2.3 Physiology-related Experiments

There have been many biology experiments that have a direct link to human physiology problems although using different sample organisms. One of the most recent ESA experiments on the ISS, in late 2010, was the SPaceflight of Huvec: an Integrated EXperiment (SPHINX), which used the European Drawer Rack and the Kubik 6 incubator. The objective of the SPHINX experiment is to determine how Human Umbilical Vein Endothelial Cells (HUVECs) modify their behaviour when exposed to real weightlessness. This could provide better knowledge of endothelial cell function, which could be useful for clinical applications. Endothelial cells line the interior of the heart and blood vessels and are important in many aspects of vascular function. Postflight activities are still under way.

4.2.4 Microbial Adaptation in Space

In relation to the presence/adaptation of microbes in space, another recent ESA experiment is the Coloured Fungi in Space experiment, which will help determine the effects of weightlessness and cosmic radiation on the growth and survival of coloured fungal species. This work may be relevant to efforts to prevent fungal contamination of spacecraft.

The fungal species chosen for the experiment belong to four genera selected as organic material decomposers, possible contaminants of materials destined for interplanetary travel, and aggressive biodeteriogens of works of art and wooden buildings. All the samples for the experiment were flown to the ISS on

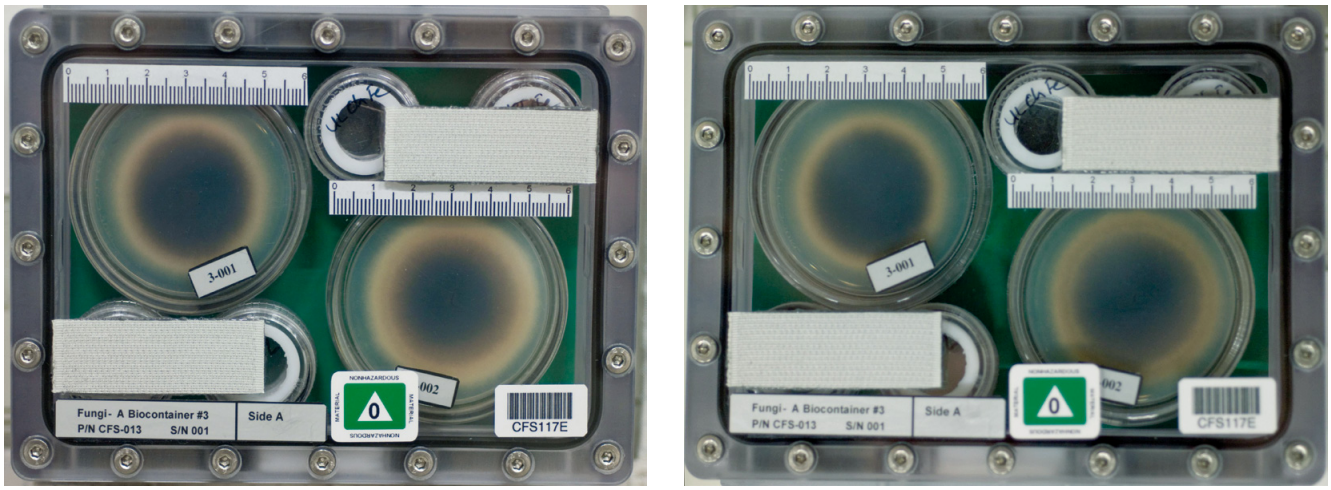

Figure 4.2.6. The Coloured Fungi in Space experiment: live cultures on Flight Day 5 (left) and Flight Day 9 (right) during the STS-133 mission. (I. Gomoiu, Romanian Academy Institute of Biology)

STS-133 in February 2011. The live samples (Fig. 4.2.6) were returned on STS-133 in March 2011, and the dry spore samples on STS-135 in July 2011. The science team has already carried out postflight analysis of the returned samples, and observed different growth rates.

References

Driss-Ecole, D., Legué, V., Carnero-Diaz, E. & Perbal, G. (2008). Gravisensitivity and automorphogenesis of lentil seedling roots grown on board the International Space Station. *Physiologia Plantarum* **134**, 191–201.

Johnsson, A., Solheim, B.G.B. & Iversen. T.-H. (2009). Gravity amplifies and microgravity decreases circumnutations in *Arabidopsis thaliana* stems: results from a space experiment. *New Phytologist* **182**, 621–629.

Solheim, B.G.B., Johnsson, A. & Iversen. T.-H. (2009). Ultradian rhythms in *Arabidopsis thaliana* leaves in microgravity. *New Phytologist* **183**, 1043–1052.

4.3 Fluid Physics Research

Fluid physics is an area of research that is helping to tackle some extremely important issues on Earth. The absence of gravity on the ISS helps to remove the disturbing influence of gravity-induced convection and hence allows us to study different aspects of fluid motion that are heavily masked on Earth. The aim is to improve mathematical modelling of fluid and geophysical processes that could benefit, for example, many industrial processes involving fluid systems. This work could help reduce CO_2 emissions in the oil industry, produce new lightweight metallic foams for industry, promote advances in optics and improve our knowledge of the fundamental laws of the universe.

4.3.1 Planetary Modelling: The Geoflow Experiment

Our planet is a very complex system, not only on the surface but also beneath the surface where complex fluid systems are at work. Furthering our knowledge of spherical fluid systems could improve understanding of the processes at work on Earth (and other planets) and, one day, help to build accurate geophysical models that are currently not available.

Geoflow was the first experiment to take place in ESA's Fluid Science Laboratory, between August 2008 and January 2009, and numerous runs were executed before the hardware was returned to Earth. The series of experiments continued with Geoflow-2 in 2011. The experiment container for Geoflow is a representation of a planet. The experiment is investigating the flow of a viscous incompressible fluid between two concentric spheres maintained at different temperatures and rotating around a common axis. An electric field between the spheres simulates a central force field just like gravity around a planet. This supports the testing of numerical models of astrophysical and geophysical problems, such as the convection of Earth's liquid outer core, global-scale flows in the atmosphere, the oceans and in the liquid nuclei of planets. The parameters that were varied in the first Geoflow series of experiments were the rotational speed and the temperature difference between the spheres.

The wealth of in-orbit benchmark data is proving invaluable for the validation and improvement of numerical models describing such convection flows in spherical systems (Fig. 4.3.1). From the numerous experiment runs taken with a variation of different parameters it was possible to observe different convective patterns.

The Geoflow-2 experiment, which was flown to the ISS on ATV-2 in February 2011, uses nonanol as a liquid instead of silicon oil, and is providing data that complement the first data set. The viscosity of nonanol has the distinct characteristic of changing significantly with temperature, thereby providing

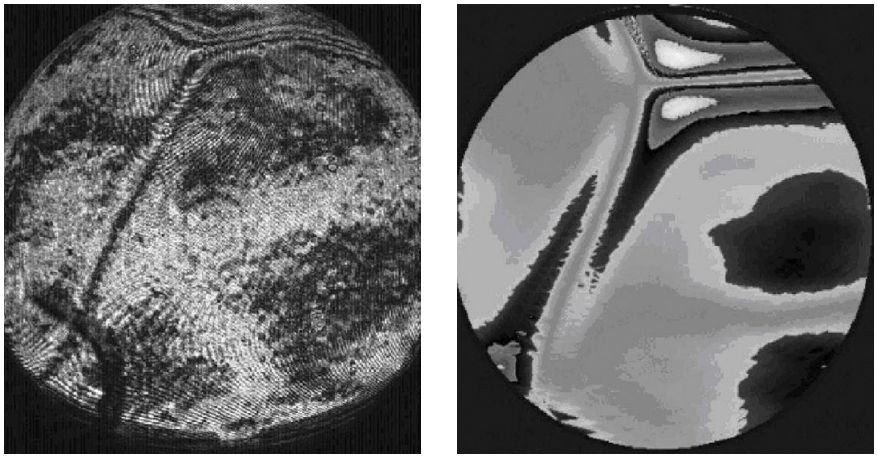

Figure 4.3.1. Comparison of an interferometric image taken from the first Geoflow experiment (*left*) and an image generated from a numerical model (*right*), both with the same temperature and rotational parameters. (BTU Cottbus)

an extra degree of complexity in the whole fluid system. Geoflow-2 started an extensive series of experiment processing from March 2011 and completed in-orbit activities in May 2012.

In terms of results, the Geoflow experiment has already provided a wealth of benchmark data highlighting different convective profiles for a variety of temperature/rotational regimes and for testing/improving numerical models on convection flow in spherical systems.

One interesting result to come from the in-orbit data is the confirmation of the octahedral convective flow formation generated by a numerical model under conditions of no rotation and an intermediate convective regime (Fig. 4.3.2). In the figure, the dark areas are the hot spots, i.e. fluid flowing towards the surface, while the lighter areas represent internal flows away from the surface.

Figure 4.3.2. Graphic image generated from a Geoflow numerical model of spherical convective regimes. This octahedral pattern is generated in conditions of no rotation and a medium-temperature gradient profile. (BTU Cottbus)

4.3.2 Influence of Vibrations: SODI IVIDIL

The potential of ESA's fluid physics research was expanded in 2009 with the launch of the Selectable Optical Diagnostic Instrument (SODI), an advanced optical instrument equipped with two Mach–Zehnder interferometers that can be operated at different wavelengths. The experiments with the SODI instrument took place over the period 2009–11 within the ESA-built Microgravity Science Glovebox (see Fig. 4.3.5), which has been a workhorse of ISS research since 2002.

The first experiment to utilise SODI was the Influence of Vibrations on Diffusion in Liquids (IVIDIL) experiment, from October 2009 to January 2010, which was an ESA project in collaboration with the Canadian Space Agency. The effect of vibration on inhomogeneous fluid mixtures is masked on Earth by gravity, making the ISS the perfect environment to study this phenomenon. Extensive experimental runs were undertaken for more than three months in orbit, in which the frequency/amplitude of vibrations as well as temperature gradients were varied across the experiment cells.

The experimental results exceeded all expectations. The data received allowed, for the first time, observation of flow patterns generated exclusively by controlled vibrations (Fig. 4.3.3). The experiment has been able to trace a variation in concentration of about 0.03% from the initial composition, making it possible to demonstrate vibrational effects and to quantify their impact on the measurement of thermodiffusion coefficients (thermodiffusion is the diffusion that occurs in a mixture due to the presence of a temperature gradient). In addition, with the unavoidable presence of 'g-jitter' present on orbiting platforms due to such influences as equipment, movement of crewmembers, etc., this research has confirmed the negligible influence of g-jitter on measurements, which will be helpful for data analysis across all areas of research.

The wealth of data coming from IVIDIL may help to advance fundamental physics and many everyday chemical processes in the future.

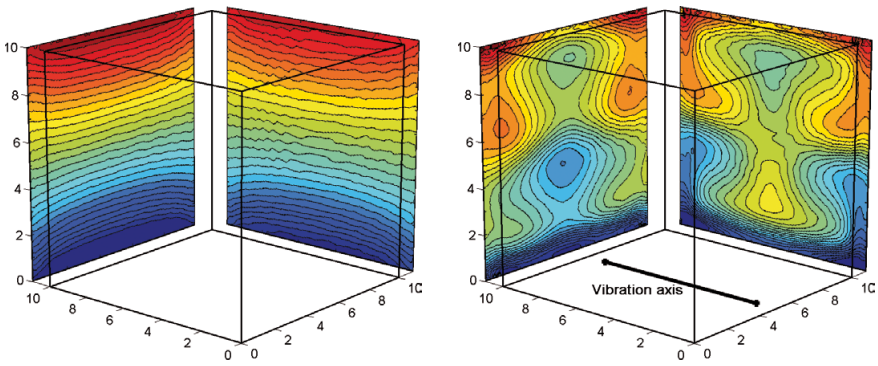

Figure 4.3.3. Comparison of convection flow without vibration (*left*) and with strong vibration (*right*) from the IVIDIL experiment. (V. Shevtsova, ULB)

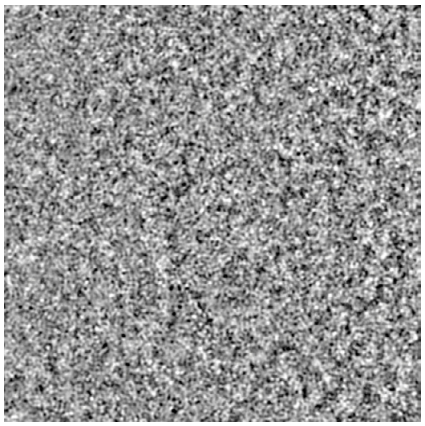

Figure 4.3.4. Image from the Colloid experiment showing aggregation in a colloidal solution. (University of Amsterdam/University of Milan)

4.3.3 Advances in Optics: SODI Colloid

Colloids represent an important area of fluid research. Developments in colloidal science may eventually contribute to the design of new types of material for applications in optics, for example.

After IVIDIL, the next SODI experiment to take place was the Colloid experiment, which generated extensive data for analysis in September 2010, and the Colloid-2 experiment in November 2011. These experiments are studying the growth of colloidal structures from solution in an aggregation process that can be easily controlled experimentally. While the focus is on the still not fully understood physical mechanisms that govern this process, the experiments may lead to interesting applications in photonics, and especially photonic crystals, which possess appealing properties and make them promising candidates for new types of optical components. Although the data analysis is still ongoing, the set of images and data studied so far are extremely promising, providing the first evidence of temperature-controlled aggregation (Fig. 4.3.4).

Once the complete dataset has been analysed it should be possible to determine the size and structure of the aggregates formed in the colloidal solutions. From this it will be possible to correlate the structure of the aggregates with the strength of the aggregating forces and elucidate the mechanisms behind the process. The results are expected to be of interest beyond the field of colloidal science, with impacts on crystal growth from solutions in general, and on self-organisation in complex fluids.

4.3.4 Oil Recovery and Carbon Sequestration: SODI-DSC

Improving the efficiency of oil recovery is currently a major challenge. At about 4000 m below ground level, hydrocarbon fluids are highly sensitive to applied forces, not only gravity, but also temperature and pressure gradients. The prediction of hydrocarbon composition is an important factor that contributes to the choice of reservoir exploitation strategies. Since the cost of extracting resources increases with depth, oil companies are interested in reliable thermodynamic models that will allow the characterisation of an entire reservoir using a reduced number of exploratory wells.

One major area of research involves the observation of thermodiffusion in fluids (also known as the Soret effect), and the determination of thermodiffusion (Soret) coefficients. Thermodiffusion plays a crucial role in many naturally occurring processes, ranging from convection in oceans to component segregation in solidifying volcanic lava, and can seriously affect industrial processes such as the manufacture of semiconductors and oil-in-water emulsions.

ESA has undertaken numerous thermodiffusion experiments in the past decade, which have yielded significant amounts of data. This research is being expanded with the SODI Diffusion and Soret Coefficient Measurements (DSC) experiment (Fig. 4.3.5), which took place at the end of 2011 as the final experiment in the triple SODI experiment series. The DSC experiment will accurately determine four isothermal and two thermal diffusion coefficients for five samples that contain systems representing the three main families of crude oil. These coefficients will be used to validate and update simulation models and establish rules for extrapolating to more complex systems. Further studies of the effects of vibrations on various configurations of inhomogeneous fluids are also in preparation.

The basic principle of the experiment is to expose representative liquid mixtures to a temperature gradient in weightlessness where gravity-driven convection is avoided. On the ISS, when a stable liquid composition profile is reached, measurements of the variations in density caused by the Soret effect

Figure 4.3.5 SODI-DSC hardware installed inside the Microgravity Science Glovebox in the Columbus laboratory. (NASA)

are performed by interferometry. The experiment can then be repeated several times to obtain meaningful statistics.

Once the Soret coefficients are determined for different samples, the scientific community will be better able to model the distribution of components within underground reservoirs.

4.3.5 Foams and Emulsions Research

Foams and emulsions are common in nature; milk is an emulsion, for example. They are also used in the manufacture of products with specific properties for targeted applications such as foams for firefighting, spray foam insulation or metallic foams. However, their production and stability pose a wide range of problems, many of which are as yet poorly understood. Systematic studies of foams and emulsions on Earth are complicated by the influence of gravity, which causes drainage. On the ISS, gravity-driven drainage is prevented and the purely diffusive environment allows long-term studies of the dynamics of surface adsorption phenomena with high accuracy.

Several industries are partners to the ESA projects, numerous of which have been undertaken as part of parabolic flight campaigns and sounding rocket missions. ESA's research in this area began on the ISS with the successful Foam Stability experiment in September 2009 and the FOam Casting and Utilisation in Space (FOCUS) experiment in February 2010. The results may have significant applications in areas such as the physical chemistry of food, the hydrodynamics of complex fluids, the handling of crude oil and related instrumentation for process control. There are obvious applications of foams and emulsions in the food industry, and industrial partners are interested in the role of proteins as natural surfactants.

With the FOAM-Stability (FOAM-S) instrument, the foaming ability of a priori non-foaming liquids such as pure water was studied. Weightlessness offers the opportunity to investigate 'wet' foams, which cannot be stabilised on Earth because of drainage. The physics of wet foams is currently not well known. The experiment thus studied how long these foams remained stable in weightlessness and how the foamability of these solutions was enhanced by the addition of solid particles, which were expected to strongly modify the elastic and viscous properties of wet foams. The observations from this experiment are being compared with ground-based experiments.

The FOCUS experiment is studying foam formation and stability in weightlessness with a view to the future development of ultralight and strong metallic foams. The presence of foam was confirmed in all three experiment cartridges flown. The analysis of samples was very positive and activities deriving from the experiments are under way. These experiments are helping to answer fundamental questions relevant to the development of new foams for industrial applications. Metallic foams have numerous important industrial applications, such as in heat exchangers, energy absorption, flow diffusion, lightweight optics and high-temperature filters in the chemical industry. Advances in this area could result in improvements in production processes and in the development of new lightweight metallic foams for industrial applications.

Two new experiments, the Fundamental and Applied Studies of Emulsion Stability (FASES; Fig. 4.3.6) and the Facility for Adsorption and Surface Tension (FASTER), will be flown to the ISS in 2012. They will study the mechanisms of stabilisation or destabilisation of emulsions using various combinations of surfactants, polymers and particles. The systems will be investigated at various scales, from microscopic to macroscopic. The FOAM-Coarsening (FOAM-C) instrument, which is linked to the FOAM-S experiment, will be a precise study of the coarsening phenomenon and derive the dynamics of growth of bubbles.

From the foams and emulsions experiments on the ISS, instrument manufacturers are expecting results that will to help improve the analytical

Figure 4.3.6. An emulsion of hexane in water from ground-based tests of the FASES experiment. The black dots, which are due to light diffusion, provide the position and the velocity of the drops. (University of Marseille, France)

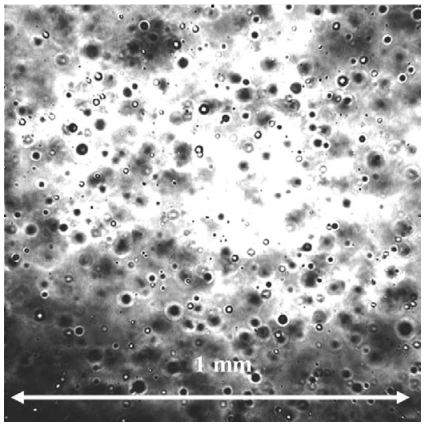

capability of products such as tensiometers and surface rheometers. Other applications will benefit from studies of the mechanisms of destabilisation and coarsening of crude oil, which is actually a mixture of oil, water, asphaltene and particles. Software companies also share an interest in numerical simulations of the complex flow of emulsified systems.

4.4 Materials Science Research

The world is facing many ecological and economic challenges. ESA's materials science research aims to address these challenges as part of a world-class programme involving hundreds of international partners from academia and industry. The main goal of this research is to increase understanding of material solidification processes in order to develop new, stronger lightweight materials that will have a significant impact on industry, and to help resolve some of the most pressing issues facing the planet, such as improving fuel efficiency and the consumption and recycling of materials.

The results of this research will be crucial to economic success, with cost-reducing effects across numerous industries and in turn making them more competitive and attractive to investors. They will also stimulate the growth of existing and new industries such as aerospace, transportation, electronics, computing, power generation, telecommunications, the environment and healthcare.

ESA's materials science research activities on the ISS are supported by extensive activities on the ground within ESA projects and involving the use of other weightless platforms such as sounding rockets. With the delivery of the Materials Science Laboratory (the principal payload inside NASA's Materials Science Research Rack 1) to the ISS on flight STS-128 in September 2009, ESA is now undertaking unique long-term materials research in space, providing data that cannot be obtained on Earth. This work will help to shed light on solidification phenomena that will contribute to improving casting processes.

4.4.1 Solidification Research: CETSOL and MICAST

The first experiments to take place inside the Materials Science Laboratory are the Columnar-to-Equiaxed Transition in Solidification Processing (CETSOL) and Microstructure Formation in Casting of Technical Alloys under Diffusive and Magnetically Controlled Convective Conditions (MICAST) projects. These complementary experiments involve European and US scientists, with the coordinated support of ESA and NASA. The influence of convection on processes involved during the solidification of different aluminium-based alloys is being analysed with a view to validating/updating numerical models, which will enable industry to optimise casting processes. The determination of the internal (micro) structure in processed metal samples is of great importance in these experiments, as the microstructure influences an alloy's characteristic properties such as strength, flexibility and resistance to fatigue.

The MICAST project is investigating the effects of controlled convection on the columnar dendritic or tree-like structures (Fig. 4.4.1) that can form in solidifying aluminium-based alloys under specific conditions. CETSOL is focusing on how these tree-like structures evolve into randomly oriented 'branches', the equiaxed structure, and the parameters that influence this transition. The existence of these non-uniform dendritic forms in an alloy microstructure implies that the mechanical properties of the alloy can vary considerably through the sample. This non-uniformity makes matching the specific casting of an alloy with the appropriate application much more complex, especially in high-end industry.

The first set of CETSOL/MICAST samples (13 in total) has already been processed (Fig. 4.4.2) under varying parameters in the Materials Science Laboratory on the ISS. Most of these samples were first processed in the Low-Gradient Furnace, and following their return to Earth are now undergoing microscopic and X-ray analysis by the relevant science teams. Very interesting preliminary results have already been presented by scientists (see 'Selected Results' below). Following the transfer to the Solidification and Quenching Furnace, the final sample was processed and returned to Earth on STS-133 Shuttle *Discovery* in March 2011 and is undergoing similar analysis.

Figure 4.4.1. Columnar dendritic or tree-like growth during solidification from solid (*bottom*) to molten metal (*top*) using real-time X-ray topography. (R. Mathiesen, Trondheim University of Science and Technology, Norway)

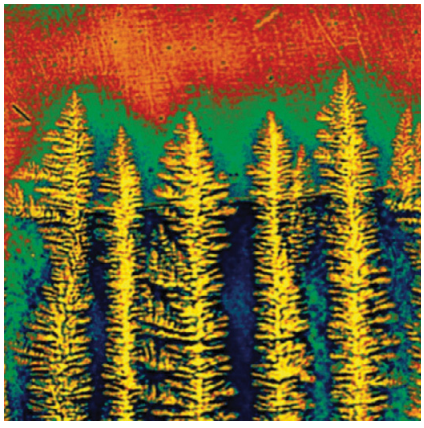

Fig 4.4.2. Frank De Winne during procedures to exchange samples before inserting them into the Materials Science Laboratory for processing. (NASA)

The research within the CETSOL/MICAST projects is being expanded with a second batch of samples, the first of which were transported to the ISS on the final Shuttle flight (STS-135) in July 2011, along with samples for the Solidification along a Eutectic path in Ternary Alloys (SETA) project. The SETA experiment will look into a specific type of eutectic growth in alloys of aluminium, manganese and silicon. The processing of the combined set of samples has begun. Additional samples for CETSOL/MICAST are scheduled for launch in summer 2012, with additional samples for SETA to follow.

The casting industry, especially for high-end industry such as aerospace, is coming to rely more heavily on the benefits of using numerical models to determine casting methods and conditions needed in anticipation of producing materials with specific performance characteristics that are tailored to particular applications. CETSOL and MICAST are helping to validate these casting models with the vital benchmark data needed from space experiments where gravity-induced convection does not mask certain physical phenomena that occur in molten liquids, such as multiphase fluid flow, diffusion, capillarity effects and heat transport that affect the properties of materials. Analyses of the CETSOL/MICAST samples are providing data to help understand and master these effects for improving casting and hence materials, and to drive the direction of future materials research.

Selected Results

The first experiments performed with the Materials Science Laboratory on the ISS have proved that constant solidification conditions can be established that meet the predefined scientific requirements for sample processing (Enz et al., 2011).

As an example, MICAST-4 was one of the first CETSOL/MICAST samples to be returned to Earth for analysis. MICAST-4 was studying the directional solidification of a particular aluminium–silicon alloy with a well-defined temperature gradient and fixed solidification velocity. The first part of the sample was solidified under purely weightless conditions, while for the second part of the sample a rotating magnetic field was activated to stimulate controlled stirring in the molten metal.

A numerical model was developed to predict solidification in orbit. The data gathered in orbit were compared with this numerical model. It was shown that the numerical model agrees with experimental data obtained on the ground, but showed deficiencies when predicting in-orbit experiments, even after the boundary conditions were modified. Heat transport along the axis of the sample was systematically overestimated although none of the modifications tested was able to resolve this issue. Therefore the software tool is valuable for identifying an initial set of process parameters.

For the processed MICAST-4 sample, two cuts (for analysis) were made through the sample: one within the section of the sample that went through solidification under purely weightless conditions within the experimental parameters. The second cut was made in the section of the sample that had the same conditions and parameters except for the addition of a rotating magnetic field acting on the sample to induce controlled stirring in the melt. These two sections of the sample demonstrate the basic differences between the microstructures that developed under diffusive conditions and those under forced convection induced by magnetic stirring of the melt (Fig. 4.4.3).

Without the rotating magnetic field being active a very uniform microstructure is observed. Dark regions correspond to dendritic structures primarily formed from the beginning of solidification. They are arranged in periodic rectangular patterns. With ongoing dendrite formation the amount of aluminium remaining in the residual molten metal decreases until eutectic solidification occurs, filling the areas between the dendrites (bright regions in Fig. 4.4.3). The microstructure changes significantly when the rotating magnetic field is acting on the sample. A complex flow field between the dendrites is induced which carries the residual

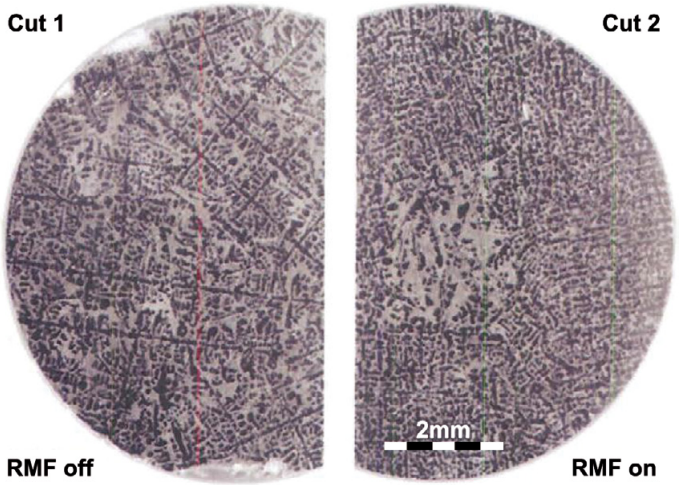

Figure 4.4.3. Metallographic sections of the processed MICAST-4 sample prepared at positions 135 mm (cut 1) and 190 mm (cut 2). *Left:* Diffusive conditions yielded periodic rectangular patterns of dendritic structures (dark regions) equally distributed across the sample. *Right:* Forced convection induced by magnetic stirring carried residual melt with eutectic composition (bright regions) from the mushy zone towards the centre of the sample. (RMF: rotating magnetic field.)

melt enriched with silicon from the mushy zone (consisting of both solid and liquid structures) towards the centre of the sample. Thus, the eutectic structures formed at the minimum temperature for the alloy are not equally distributed across the sample but are concentrated through the centre of the sample.

This result is consistent with those of similar experiments performed on sounding rocket missions. Careful quantitative microstructure analysis will follow, emphasising the evaluation of the dendrite arm spacing as a function of solidification time.

All the materials science projects implemented in the Materials Science Laboratory are supported by international teams of scientists from Europe and the United States.

4.4.2 The ElectroMagnetic Levitator

ESA's materials science research on the ISS will be extended with the ElectroMagnetic Levitator (EML), which will investigate properties of metal alloys under weightlessness, supporting basic and industrial research.

Starting in 2013, the EML, developed by ESA and DLR, will enable the container-less processing of materials. This work will make it possible to melt electrically conductive samples, and stimulate them to test their properties and eventually their solidification, all without the need for (and influence from) a sample container, under a much wider range of ultra-high vacuum or high gas purity conditions than those achievable on the ground. Samples will be heated and positioned by electromagnetic fields generated by a coil system (Fig. 4.4.4). The EML will support research into metastable states and phases and provide highly accurate measurements of the thermophysical properties of liquid metallic alloys at temperatures up to 2000°C. The former will include investigations of nucleation and solidification kinetics in undercooled melts and microstructure formation, for instance. Here again, a large international group of scientists from Europe, the United States, Canada, the Russian Federation and Japan is defining the scientific objectives and the utilisation of the EML. They will contribute to the preparation of the experiments and analysis of the samples and data, and will jointly publish the consolidated results.

Figure 4.4.4. Free-floating molten metal in the ElectroMagnetic Levitator. (DLR)

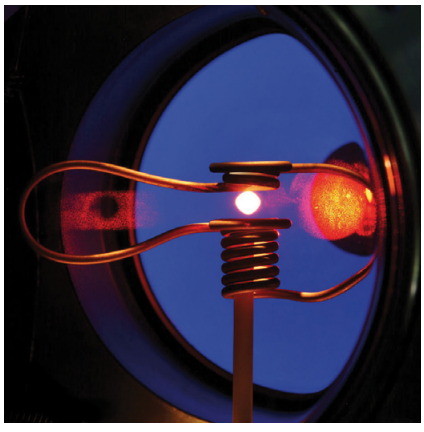

4.4.3 The X-ray Monitoring System

With the advent of new high-tech microfocus X-ray sources and high-sensitivity high-speed detectors, it is now possible to perform experiments in a laboratory environment that until recently were only possible at synchrotron sources.

Such instruments enable real-time observations of the solidification process in opaque metallic samples, and provide much more critical information on the process than the analysis of wholly solidified samples.

In particular, dynamic aspects of the solidification process can be investigated, providing a much better insight into the role of gravity or controlled convection on the microstructures and thus the mechanical properties of alloys. Such a high-resolution real-time imaging system is already available for sounding rocket experiments with which the transient phases will be studied. The feasibility of implementing such a system on the ISS to enable investigations of processes at steady state will be the subject of future studies.

4.4.4 Crystallisation Research

Within the field of materials science, studies of the crystallisation of minerals such as zeolites have important applications in the petrochemical industry. Zeolites are crystalline microporous aluminosilicates that have interesting catalytic and molecular sieving properties, with various applications as catalysts, sensors and absorbent materials. Although zeolites can be found in nature, their real advantage lies in their potential to be synthesised in the laboratory and to control the manner of synthesis in order to develop zeolites on an industrial scale with chosen characteristics for use in specific applications. To optimise the synthesis of zeolites, the effects of convection and sedimentation must be controlled. Weightlessness provides ideal conditions for experiments to create complex structures from the aggregation of nanoscopic particles.

ESA's Protein Crystallisation Diagnostics Facility was the first experiment payload to be installed in the European Drawer Rack in the Columbus laboratory in 2009. It provided a means for the scientific community to undertake fundamental studies of crystal growth from solutions in order to provide insights into nucleation (early stages of crystal formation) and crystallisation processes, and to quantify how they depend on the experimental conditions and on gravity in particular. The facility also enabled the science team on the ground to undertake series of experiments covering different conditions inside the growth reactors in orbit, while varying the concentrations of precipitants and the amounts of impurities, and triggering nucleation, crystallisation and finally redissolution by applying accurate temperature changes.

These conditions can be controlled from the ground and varied in real time. The nucleation process, crystal growth, and determination of the concentration of species in the solution around the crystals were all observed. Following the conclusion of the experiment and the return of samples to the Belgian User Support and Operations Centre (responsible for facilitating many of the solution crystallisation experiments for ESA) in August 2009, the samples and all data recorded during the flight underwent extensive analysis in the European science laboratories collaborating in this project.

The aggregation process is of particular importance in colloid physics, with the objectives of producing functional materials, however, here again, the influence of gravitational effects was demonstrated to be of paramount importance.

Reference

Enz, T., Steinbach, S., Simicic, D., Kasperovich, G. & Ratke L. (2011). First experiment using the Materials Science Laboratory on board the International Space Station: Experiment preparations, execution, and first results. *Microgravity Sci. Technol.* **23**(3), 345–353.

4.5 Complex Plasma Research

Plasma has many uses, such as in plasma displays by the lighting industry, and in the production of many microelectronic or electronic devices such as semiconductors. Plasma is also used in the manufacture of transmitters for microwaves or high-temperature films, in work with minerals such as diamond, and in extracting economically valuable metals from rock.

A plasma is an ionised gas consisting of electrons and ions. The importance of their study is evident since more than 99% of the visible matter in the Universe is in the plasma state. 'Complex (dusty) plasmas' include an additional component: microparticles or 'dust'.

Under certain conditions the particles in complex plasmas accumulate charges and start to interact. These interactions can lead to strong coupling of the particles, resembling a fluid phase, and even to behaviour reminiscent of atomic 'crystallisation', but with the advantage of presenting a scale size that is much easier to observe and study than at the atomic level.

Due to the strong influence of gravity on the microparticles, most experiments on complex plasmas are strongly distorted or even impossible on Earth and require weightless conditions (Fig. 4.5.1). Complex plasmas in flight experiments are a unique model system to study various generic processes in physics occurring in gases, fluids and solids on Earth. They provide an enabling technology for new fundamental research. This includes research in thermodynamics to identify the origin of the scaling and universality at the critical point, and investigations of the dynamics of phase transitions at the kinetic level, especially at the triple point where the three phases of a substance (gas, liquid and solid) can coexist in thermodynamic equilibrium under specific temperature and pressure conditions.

Plasma research also focuses on understanding the origins of instabilities and the development of turbulence in hydrodynamics and the development of nonlinear wave transport phenomena. It also addresses technical aspects, such as particle growth in plasma chambers used for microchip production.

Plasma experiments have been performed on the ISS as part of a German–Russian collaboration since 2001. The Plasma-Kristall (PK-3 Plus) experiments (Fig. 4.5.2), which were still operating on the ISS in 2012, led to the discovery of electro-rheological plasmas, which macroscopically mimic (and allow observation of) electro-rheological fluids. These fluids change their viscosity as a function of the electric field strength applied; for example, they change from solid to liquid state with and without an applied electric field. PK-3 Plus has also allowed major advances in the study of the dynamics of lane formation, i.e. where the particles line up, one behind another, making kinds of lanes.

At the heart of the PK-3 Plus hardware is a vacuum chamber into which a neutral gas (neon or argon) and associated microparticles are pumped. Electrode plates situated at the top and bottom of the chamber allow for variations in the frequency (in hertz) and amplitude (in volts) at the electrodes. Other parameters, such as the size of the microparticles, pressure, etc., can also be changed.

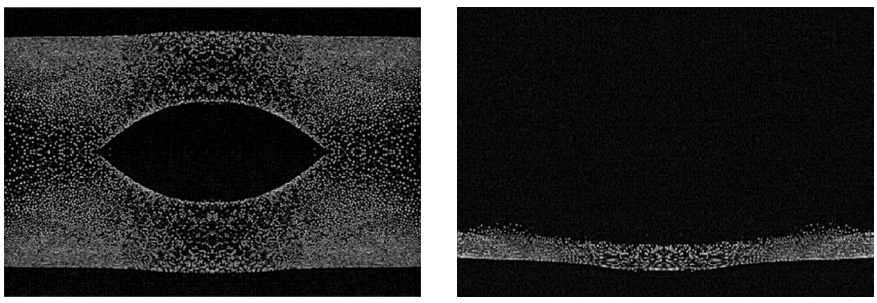

Figure 4.5.1. Electrically charged plasma in an experiment chamber in weightlessness, with a 'void' at its centre (*left*), and in an experiment chamber under gravity conditions (*right*). (DLR)

Figure 4.5.2. Russian cosmonaut Oleg Kotov working with the PK-3 Plus experiment payload on the ISS in 2010. (RKK-Energia)

Selected Results

From the PK-3 Plus experiments, the difference between using argon or neon as the neutral gas is clear to see. The argon plasma showed a brighter glow, corresponding to a higher ionisation rate, close to the electrodes, while the neon plasma showed a homogeneous distribution of the glow between the two electrodes. Although one could imagine that a homogeneous plasma distribution would cause a similar distribution in a complex plasma, the experiments showed the opposite. The argon distribution provided the best conditions for a homogeneous, void-free complex plasma, while the neon glow distribution unexpectedly resulted in a large void for identical gas and electrical parameters. The physical reason for this difference is not yet clear. There are a number of important differences between complex plasma parameters in neon and argon, such as the ion mass and mean free path, plasma density, electron temperature, etc.

PK-3 Plus showed that the 'void' at the centre of the complex plasma cloud could be easily closed under certain conditions, thus providing much better homogeneity of the complex plasma, a result rarely achieved before. This is a very promising result, as homogeneity is essential for many precision studies and offers new manipulation possibilities for future experiments.

Instabilities in the plasma (e.g. heartbeat instability, which causes continuous contraction and expansion of the void that the microparticles follow) appear at high microparticle densities and are strongly related to changes in the plasma glow. However, although a homogeneous and void-free plasma is advantageous for modelling solid (crystalline), fluid and gas phases and transitions between different phases, the reason for the appearance of the void in the neon distribution has itself created an interesting field of study for the future (Thomas et al., 2008).

Reference

Thomas, H.M. et al. (2008). Complex plasma laboratory PK-3 Plus on the International Space Station, *New J. Phys.* **10**, 033036, and references therein.

4.6 Radiation Research

In order to ensure the safety of astronauts during missions, whether inside the ISS or during spacewalks, it is essential to understand and monitor the radiation environment around Earth. In addition to monitoring radiation levels in orbit, ESA is determining the radiation absorbed by astronauts, its effect on the central nervous system, and the use of shielding materials as a means to reduce the effect of radiation on astronauts during missions. The continued development and testing of new lightweight shielding materials is important not only for use in low-Earth orbit, but also for future human exploration missions to the Moon or Mars where Earth's magnetic field no longer provides protective shielding.

New shielding materials will help extend the life of future satellites in orbit by reducing the effects of solar and galactic radiation, which can damage satellite electronics. Such shielding can be applied on Earth where cosmic rays penetrating the atmosphere cause errors in integrated circuits, including data corruption in memory devices and incorrect performance of central processing units (CPUs), which are more susceptible as they decrease in size. This area is already being investigated by various industries.

This type of research is providing a detailed picture of the radiation environment in low-Earth orbit. It is contributing to our understanding of how the planet works and how Earth's radiation environment affects the climate, and is thus helping to improve climate models.

Finally, results from this research may also have benefits on Earth, such as in neuroscience, and the use of ion therapies to treat brain tumours. Carbon ion therapy, for example, is proving more effective than traditional radiotherapy in localising irradiation at tumour sites and killing cancer cells with minimal damage to normal tissues.

ESA's radiation research on the ISS has built on decades of previous research on the Mir Space Station and Space Shuttle, and ESA's Spacelab. To date, ISS research has revealed that the radiation dose increases by 60% from the front to the back of the ISS, and variations in radiation dose of up to 50% have been measured within individual ISS modules due to differences in shielding. Shielding also accounts for variations in radiation dose from the inside to the outside of the ISS. Variations in radiation dose are also influenced by variations in the ISS altitude, the solar cycle, and as the ISS passes through the South Atlantic anomaly (Fig. 4.6.1; Berger, 2008; Narici, 2008; Reitz et al., 2009; Durante et al., 2006). This research makes use of a variety of radiation sensors that detect different parts of the radiation spectrum, in order to build on previous research and to provide details of the radiation environment in orbit.

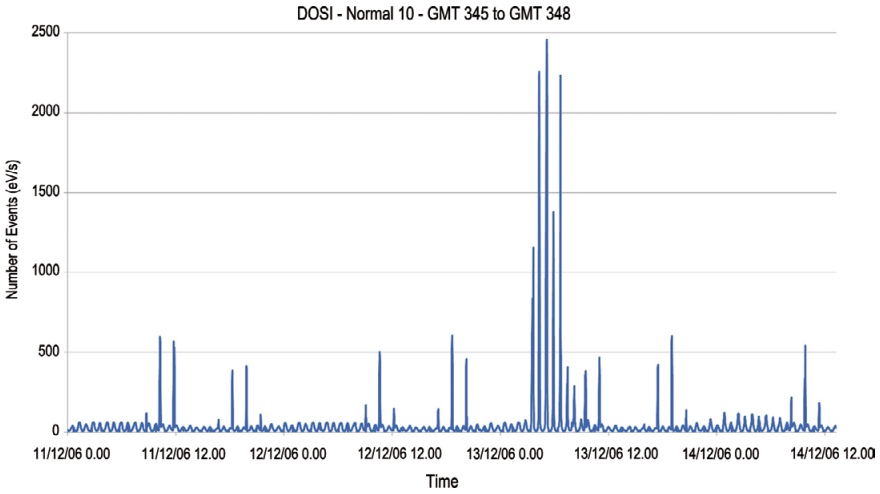

Figure 4.6.1. Data from the ALTEA experiment in 2006. The radiation dose during a solar flare event (highest peaks) in 2006 was up to 4–5 times higher than the other intermittent peaks recorded as the ISS passed through the South Atlantic anomaly. The ALTEA-Shield experiment is building on such findings, providing additional information on temporal fluctuations in the radiation environment inside the ISS as well as testing the effectiveness of different shielding materials. Note that ALTEA detects mainly heavy ions. (L. Narici)

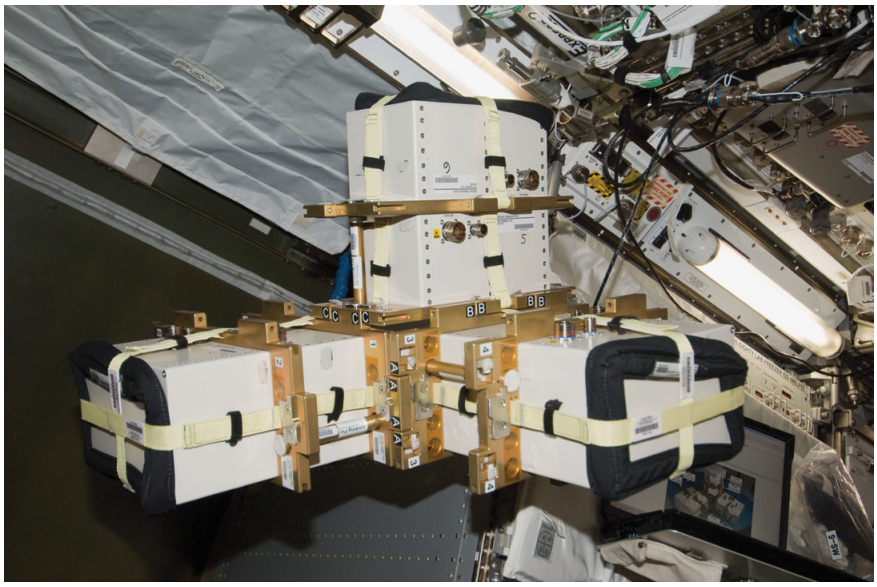

Figure 4.6.2. In-orbit hardware for ESA's ALTEA-Shield experiment. (NASA)

4.6.1 Radiation and the Central Nervous System: ALTEA-Shield

The Anomalous Long Term Effects in Astronauts' Central Nervous System – Shield (ALTEA-Shield) experiment is an ESA-sponsored project that builds on the previous ALTEA series of experiments and is providing data on the radiation environment inside the ISS. The data obtained will be used to test radiation models and help in extrapolating results to outer space. In the first part of the experiment, started in 2010, the hardware completed a 3D survey of the radiation environment at three locations within the ISS (Fig. 4.6.2).

The second part of ALTEA-Shield will test different materials covering the detectors to determine their effectiveness in shielding against cosmic particles. In the third and final part of the experiment, an astronaut will wear a headset covered with six silicon radiation detectors to monitor cosmic particles passing through the brain and their effects on the perception of light flashes and other transient electrophysiological changes in the retina and brain. At the same time, a 32-channel EEG will measure brain activity and a visual stimulator and a pushbutton will be used to determine visual performance and occurrence of light flashes. This will be carried out both with and without shielding materials.

The results of the ALTEA-Shield experiment are particularly relevant in view of the increasing length of human operations on the ISS, and the prospect of long journeys to Mars. The work is focusing on the design of appropriate radiation protection, including new lighter shielding materials or active shielding solutions.

4.6.2 Radiation Absorbed by the Body: Matroshka

Owing to the complex nature and density of different parts of the human body, it is vitally important to quantify how much radiation is absorbed by astronauts and specifically which areas or organs are most susceptible. As it is obviously not feasible to insert radiation sensors into the organs of the astronauts themselves, ESA developed the Matroshka series of experiments, named after the Russian doll. The experiments utilise a simulated upper torso called the Phantom, which contains natural bone and materials equivalent to human tissue to simulate the different muscles and organs of the body, with a lower-density material simulating the lungs. The Phantom is covered with a material equivalent to skin that in turn can be mounted in a carbon fibre casing to simulate the space suits worn by astronauts during spacewalks.

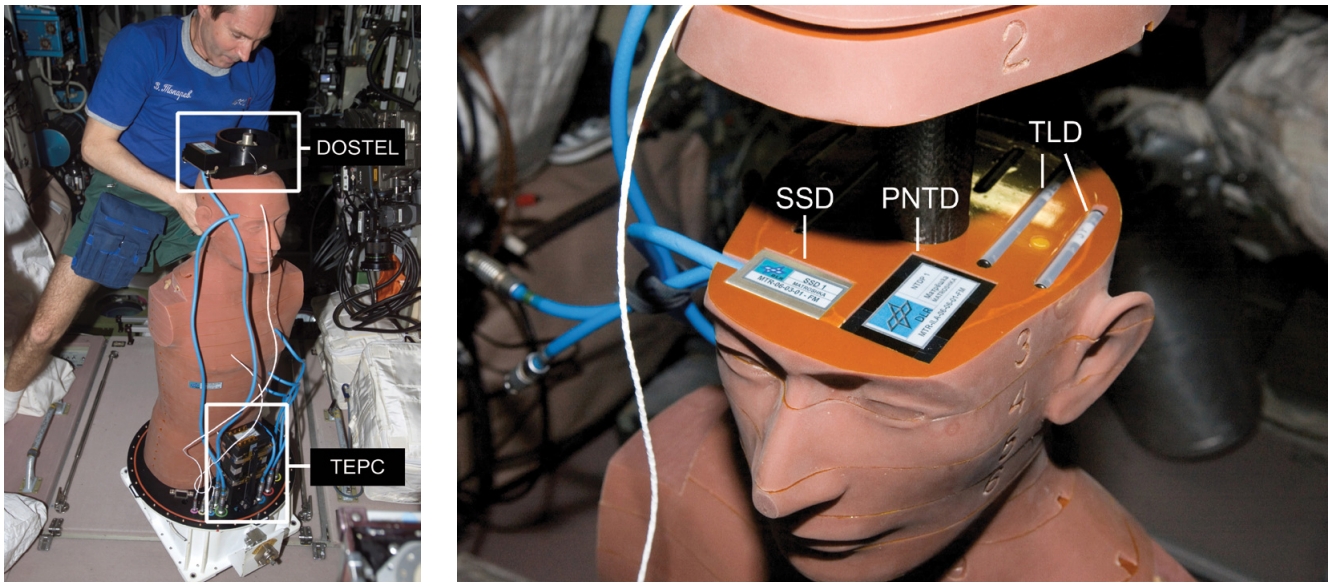

Figure 4.6.3. The Matroshka experiment. (NASA)

Table 4.6.1. The Matroshka radiation detectors.

Detector	
Dosimetric Telescope (DOSTEL)	This charged particle telescope uses three sandwiched silicon detectors to monitor the number of particles passing through the detectors (particle flux), the amount of radiation absorbed by the detectors per unit time (dose rate) and the amount of energy transferred to the silicon detectors (linear energy transfer, LET) from the particles of radiation from the Van Allen belts, deep space and the Sun.
Tissue-Equivalent Proportional Counter (TEPC)	A low-pressure ionisation chamber surrounded by 1.9 mm of tissue-equivalent material that measures all types of radiation and can record one LET spectrum per minute.
High-LET Radiation Spectrometer (HiLRS)	A dosimeter that measures the energy deposited in p–n junctions, with dimensions similar to (and simulating) a biological cell. It measures preferentially the high-LET particles.
Silicon Scintillator Device (SSD)	A plastic scintillator cube covered with silicon detectors. The light output from the cube is proportional to the radiation dose. This dosimeter discriminates against charged particles and thus measures the neutron dose.
Plastic Nuclear Track Detector (PNTD)	Particle radiation produces tracks that can be made visible by an etching process. From these, it is possible to generate LET spectra, particle fluxes and spectra that can be used to identify the particles.
Thermoluminescence Dosimeter (TLD)	Electrons and protons are trapped in lattice imperfections in the TLD crystal under the impact of radiation. When heated, the crystal's luminescence signal is proportional to the radiation dose. The dosimeters are distributed 2.5 cm apart to give depth–dose profiles within the Phantom.

Measuring the complex radiation field calls for a range of active and passive radiation detectors (see Fig. 4.6.3 and Table 4.6.1). Divided into many 25 mm-thick layers, the Phantom is fitted with hundreds of passive radiation detectors at key organ sites such as the stomach, lungs, kidney, colon, eyes and skin, and in the simulated spacesuit, from which it is possible to estimate the quantities of cosmic particles absorbed throughout the body.

Following an extended run of Matroshka outside the ISS to determine the radiation experienced by astronauts during spacewalks, and two extended runs inside the Russian segment of the ISS in 2006 and 2007–09, in May 2010 the facility was moved to the Japanese Kibo laboratory to continue mapping radiation levels experienced by astronauts in different parts of the ISS. This extended run of the experiment continued until March 2011 using only passive

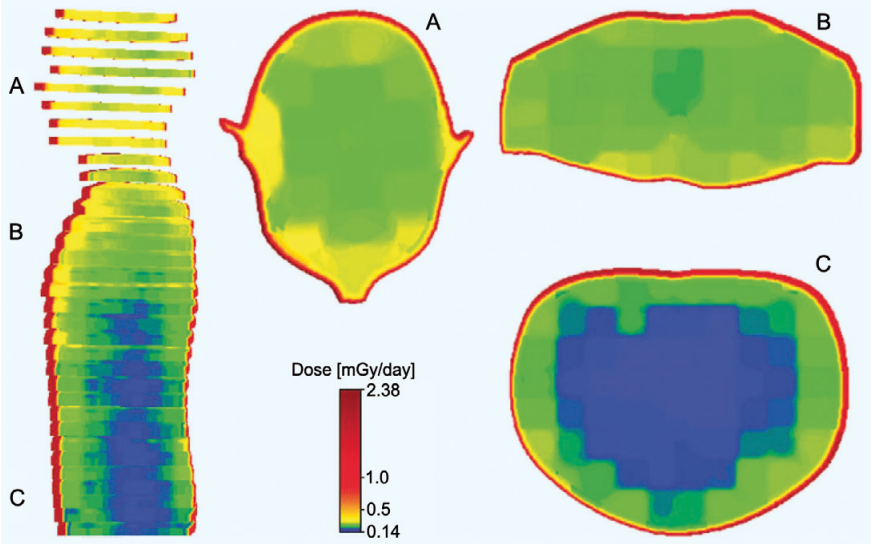

Figure 4.6.4. Results of the Matroshka experiment: absorbed radiation doses around the body (blue, lowest dose; red, highest dose). The highest dose is absorbed by the skin, with the internal organs receiving the lowest doses.

Table 4.6.2. Organ dose rates measured by the Matroshka experiment.

Organ	Dose rate (mGy per day)
Skin	0.94
Eyeball, lens	0.54, 0.58
Salivary glands, breast	0.33, 0.39
Thymus, thyroid, trachea, brain	0.28–0.30
Lungs, bones	0.26, 0.28
Oesophagus, testes	0.24, 0.26
Colon, stomach, liver, red bone marrow, heart	0.22–0.24
Kidneys, gall bladder, small intestine, spleen, pancreas, prostate	0.20–0.22

detectors. In the long term, Matroshka may again be accommodated on an external ISS platform to measure cosmic radiation levels in low-Earth orbit that are of relevance for astronauts engaged in extravehicular activities.

With the cooperation of 20 research institutes, universities and space agencies, Matroshka is the largest international effort engaged in gathering scientific data on radiation depth dose, organ dose and skin dose distribution. The Matroshka experiments were developed for ESA by the German Aerospace Center (DLR), and the science team is led by G. Reitz.

Data from the Matroshka series of experiments have revealed that radiation levels are 2.4 times higher than those measured inside the ISS (see Fig. 4.6.4 and Table 4.6.2). This is due to the shielding of the hull of the ISS, which blocks some of the radiation entering the station. This factor increased to 3.5 as the ISS passed through the South Atlantic anomaly.

4.6.3 European Crew Personal Dosimeters (EuCPDs)

Since 2006, ESA astronauts on the ISS have worn European Crew Personal Dosimeters (EuCPDs) to measure their exposure to radiation during their flights (Fig. 4.6.5). Astronauts working inside the station wear the dosimeters around their waist and left ankle, while those undertaking spacewalks wear them at the same locations above the liquid cooling garment inside the space suit. Each dosimeter is just 8 mm thick and consists of a stack of five passive radiation sensors, each of which measures different cosmic particles, including neutrons and heavy ions, as well as particle impact angles and the energy transfer from particles. All European astronauts will continue to wear EuCPDs for the foreseeable future.

Figure 4.6.5. Frank De Winne wearing an EuCPD belt on the ISS in 2009. (NASA)

4.6.4 Mapping Radiation inside the ISS

Area dosimetry is another important field of radiation research, using multiple sensors spread around the modules of the ISS to build a picture of the nature and distribution of the radiation field inside the station. This is a valuable method for verifying the shielding qualities of the ISS in different areas. The Dose Distribution inside the ISS (DOSIS) experiment is ESA's first experiment to determine gradients of the radiation across the Columbus laboratory, which has been in orbit since February 2008. The DOSIS experiment was undertaken from July 2009 to July 2011 when the hardware was uninstalled and returned on the final Shuttle flight, STS-135. In that time DOSIS collected valuable data on the radiation field across Columbus, which support similar measurements by international ISS partners to map the radiation across the whole station.

Measurements of heavy ions have been made using two active radiation detectors as well as sets of passive radiation dosimeters positioned at 11 locations in the Columbus module. The first set of passive dosimeters, swapped out by Frank De Winne in 2009, was returned to Earth for analysis, and the second set was returned in May 2010. The experiment's active DOSTEL radiation sensors were located in the European Physiology Modules facility until July 2011. This facility was used to transfer DOSIS experimental data to the Microgravity User Support Centre in Cologne, Germany, during in-orbit activities.

The DOSIS experiment includes additional information from the Dosimetry for Biological Experiments in Space (DOBIES) experiment, which aims to develop a standard method of measuring the radiation dosage experienced by biological samples in specific areas of the ISS using a combination of different dosimetric techniques. Similar radiation sensor packages have been located on the outside of the ISS as part of ESA's Expose-E (on the European EuTEF facility) and Expose-R (on the Russian module Zvezda) payloads.

4.6.5 Mapping Radiation outside the ISS

Comparisons of radiation levels inside and outside the ISS have provided invaluable information for determining the station's shielding capabilities. In isolation the external radiation data are also essential in the analysis of samples from exposure or exobiology experiments and how they react to the space environment.

ESA's suite of external radiation monitors has provided extensive data on the external radiation environment in low-Earth orbit. In 2011 the sample trays of the Expose-R facility, which had been located on the external surface of the Russian segment of the ISS since March 2009, were returned to Earth. Expose-R housed the Radiation Risks Radiometer–Dosimeter (R3D) for gathering radiation dose data. This backed up the data previously gathered by radiation dosimeters (EuTEF and Matroshka) outside the ISS. Data from R3D on Expose-R have provided invaluable information in connection with the Small Probes for Orbital Return of Experiments (SPORES) experiment on Expose-R, which looked into the effect of open space on biological samples.

References

Berger, T. (2008). Radiation dosimetry onboard the International Space Station (ISS), *Z. Med. Phys*. **18**(4), 265–275.

Durante, M., Kraft, G., O'Neill, P., Reitz, G., Sabatier, L. & Schneider, U. (2006) *Preparatory Study of Investigations into Biological Effects of Radiation*, Final Report, ITT/1-4948/05/NL/GM. European Space Agency.

Narici, L. (2008). Heavy ions light flashes and brain functions: recent observations at accelerators and in spaceflight. *New J. Phys*. **10**, 075010.

Reitz, G., Berger, T., Bilski, P. et al. (2009). Astronaut's organ doses inferred from measurements in a human phantom outside the International Space Station. *Radiation Res*. **171**, 225–235.

4.7 Technology Research

ESA has a rich history of demonstrating and testing new technologies on the ISS since the Andromède mission in 2001. These demonstrators encompass a wide range of technologies that could improve life in space and on Earth.

4.7.1 Monitoring Global Maritime Traffic

Space and navigation on Earth are now inextricably linked. Satellite navigation systems are used by global transportation industries such as shipping and airlines and by individuals in their cars. The ISS is a perfect testbed for testing navigation technologies such as those used for global tracking. Many industries could benefit from the global coverage and transmitting potential of the ISS for improving global services.

The Automatic Identification System (AIS), as specified by the International Maritime Organization (IMO), is a ship- and shore-based broadcast system. The AIS for Columbus (known as the Vessel Identification System), which operates in the VHF maritime band, is verifying the capability of the system to be used for tracking global maritime traffic from space. The ISS is in an ideal location, between 350 km and 400 km altitude, for space-based AIS signal reception that can be utilised by multiple users.

The AIS ground coverage from the ISS is between approximately 68°N and 68°S. The system, which has been active since June 2010, consists of two antenna assemblies that were mounted on the outside of Columbus during a spacewalk in November 2009 (Fig. 4.7.1), as well as data relay hardware – the Entwicklungsring Nord (ERNO) – and a receiver mounted inside Columbus. The two operational phases with the first receiver from Norway (NORAIS) have been extremely successful with data telemetry received by the Norwegian User Support and Operations Centre (N-USOC) in Trondheim, via the Columbus Control Centre in Germany. The results of the preliminary analyses are very good. In the first 118-day operation period, nearly 30 million AIS messages were received from more than 60 000 transponders, with between 200 000 and 400 000 decoded messages per day (Eriksen et al., 2011; Nordmo Skauen & Eriksen, 2011).

Data have been received by NORAIS in almost continuous operation and all modes of operation are working extremely well. This included digitising signals and sending them to ground for analysis of signal quality, which will be very helpful in making additional improvements/refinements to the system in crowded shipping areas where there is the possibility that signals can be lost or mixed.

The system is capable of receiving ship information such as identity, position, course, speed, ship particulars, cargo and voyage information to and from other vessels and shore. The ground-based system uses Self-Organising Time Division Multiple Access technology to meet high broadcast rates and ensure stable and reliable ship-to-ship and ship-to-shore operations within ~40 nautical miles (about 75 km). The system provides continuous operation and a high detection probability of AIS signals broadcast by maritime vessels.

Based on the payload designed for the Norwegian AIS Sat-1 satellite, which was launched into a near-polar orbit in July 2010 and also provides good data in the high north, the NORAIS receiver is a software-defined radio operating across the maritime band from 156 MHz to 163 MHz. The NORAIS receiver has been tuned to frequencies under consideration for allocation to space-based AIS. NORAIS took part in international tests of these two proposed frequencies in October 2010, arranged by US Coast Guard.

The main reason for covering more than the two current frequencies in use for AIS is to have the possibility to demonstrate the operational use of new channels in the maritime band being allocated to space-based AIS. Also, this configuration allows for characterisation of the maritime VHF spectrum with

Figure 4.7.1. The AIS antenna installed on the outside of Columbus. (NASA)

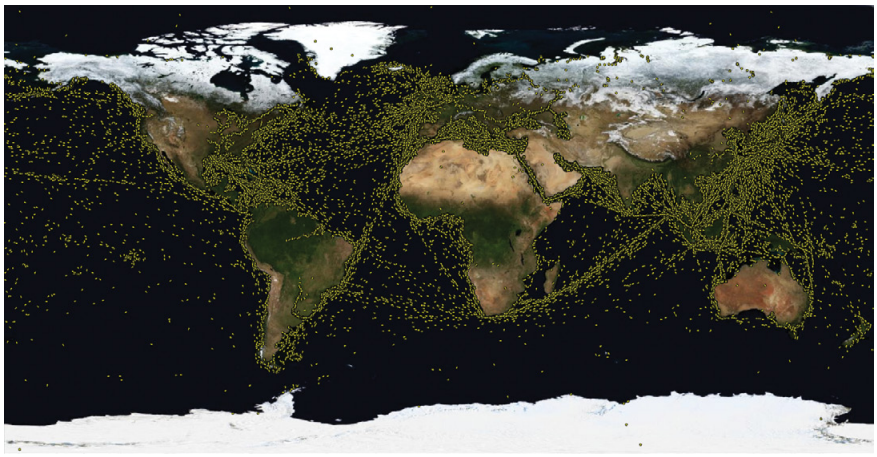

Figure 4.7.2. Plot of ship positions using AIS data from the Norwegian NORAIS receiver, which forms part of ESA's Vessel Identification System for tracking global maritime traffic. (FFI)

respect to occupancy and interference. The software implementation allows the receiver settings to be optimised in orbit and also new signal processing algorithms to be uploaded.

The current ground-based Automatic Identification Systems are designed to monitor maritime vessels in coastal waters. This capability will be greatly expanded by the Vessel Identification System on Columbus to incorporate maritime traffic in open waters (Fig. 4.7.2). The autonomous system will pick up signals from standard AIS transponders carried by all vessels over 300 gross tonnes engaged on international voyages, by other cargo vessels over 500 gross tonnes and all types of passenger ship mandated by the International Maritime Organization to carry AIS transponders.

The Vessel Identification System has been performing extremely well in monitoring global maritime traffic from the ISS. It could benefit many European organisations, particularly those involved in law enforcement, fishery control campaigns, maritime border control and maritime safety. The system could also benefit security services, especially in conducting marine pollution surveys, search and rescue missions and anti-piracy campaigns. Various services have already requested access to the VIS data that is continuously acquired on Columbus.

4.7.2 3D Technologies

ESA has been testing and developing various 3D technologies on the ISS since 2003, with all of the hardware working well in the difficult environmental conditions on the station. These technologies are helping to feed into astronaut training programmes, to improve ISS simulators, and to help stimulate public interest in the ISS.

Flown to the ISS in February 2010, the Erasmus Recording Binocular 2 (ERB-2) offers high-definition 3D video recording. Following commissioning, this video camera has already sent stunning 3D high-definition images back to Earth showing life on board the station (Fig. 4.7.3). These images will also be used in ESA's outreach programmes and to improve its 3D virtual reality simulators. The camera is an upgraded version of the Erasmus Recording Binocular, an easy-to-use digital 3D video camera that was tested by Thomas Reiter during the Astrolab Mission on the ISS in 2006.

In addition to providing the means to record high-definition 3D footage for downlinking to the ground, the Erasmus Recording Binocular 2 was used for the first ever 3D live streaming from space in August 2011. The uses of ERB-2 will continue expand in the future.

Figure 4.7.3. Expedition 27 Flight Engineer Paolo Nespoli filming ESA's ALTEA-Shield hardware on the ISS with the Erasmus Recording Binocular 2 in April 2011. (NASA)

4.7.3 Improving Astronaut Efficiency and Wellbeing

Conditions in space are demanding both physically and psychologically for astronauts. In view of the nature of the work of astronauts, any advances in technology to improve their efficiency and make their lives more comfortable in orbit, especially during long missions lasting six months, would benefit not only the wellbeing of the astronauts but would also to make optimal use of the resources available for important scientific research programmes. This could involve providing astronauts with aids for undertaking their daily work, developing new exercise devices for making in-orbit exercise even more efficient, developing new diagnostic devices for monitoring the health of crewmembers, or simply making their stay in the confined space of the ISS more comfortable.

Two such pieces of technology have been tested on the ISS in the past three years. The first was the Wearable Augmented Reality (WEAR) hardware (Fig. 4.7.4), which has shown great possibilities as a hands-free computer reference aid for astronauts during in-orbit activities. The second was the Flywheel Exercise Device, which was successfully tested as an advanced resistive exercise device. Both of these technology demonstrators were tested by Frank De Winne in September–October 2009.

Figure 4.7.4. Frank De Winne training with the WEAR system. (ESA)

WEAR combines multiple technologies such as object and speech recognition, barcode reading, augmented reality and the integration of multiple data sources such as the ISS Inventory Management System.

Astronauts are required to follow strict guidelines and rules when undertaking many of the complex activities on the ISS. The WEAR system eliminates the need for manuals or other hand-held media by providing a voice-controlled system that displays 3D graphics and data through a partially see-through viewing screen on a headset. De Winne successfully tested the system for opening up decking in the Columbus laboratory and replacing an internal filter.

Based on the success of the test, Space Applications, ESA's prime contractor for WEAR, is now considering firefighting as a non-space application of the system. In the space sector, it is being proposed to support operations inside ESA's test facilities. WEAR has built on ESA's experience in the development of numerous technologies to assist crewmembers on the ISS.

The Flywheel Exercise Device (Fig. 4.7.5) was successfully tested in a series of exercises at four different settings. The device uses a rotating flywheel that replaces weight plates and other means of resistance in training devices that

Figure 4.7.5. Frank De Winne testing the Flywheel Exercise Device in October 2009 (NASA)

rely on gravity. The device relies on concentric muscle action to accelerate the flywheel and eccentric action to decelerate it, which is advantageous as resistance exercise programmes using both concentric and eccentric muscle actions are more effective in increasing muscle strength and mass than training using concentric muscle actions alone.

4.7.4 Global Transmission Services

The Global Transmission Services (GTS) is a technology experiment on the ISS for the testing, validation and demonstration of radio transmission techniques for the synchronisation of Earth-based clocks and watches from the ISS (Fig. 4.7.6). Ultimately, GTS data services, based on a unique coding scheme, could lead to commercial services, such as blocking stolen cars or lost credit cards directly from space. The combination of nonlinear pseudo-noise spectrum signals, the large Doppler shift and the orbital information form a fingerprint that cannot be faked by carjackers on the ground.

Due to the orbital characteristics of the ISS, the GTS signal can be transmitted over almost the whole Earth every day with signals being received several times per day and lasting 5–12 min. The ISS is also ideal in that repairs to hardware can be made immediately.

The principal elements of the GTS system are the antenna unit attached to the outside of the Russian Zvezda module and the electronics unit installed inside it. The electronics unit has an ultra-stable quartz oscillator that provides an accuracy of 10–13 s, which is unprecedented among the station's applications if synchronised with an atomic clock on the ground.

Following an extended test phase when improvements were made to the ground hardware and a new electronics unit was launched to the ISS, a second-generation GTS operational test phase was started in summer 2007 and the Global Transmission Service was deactivated on 31 May 2009. Following negotiations with Russian representatives, however, the instrument has since been reactivated and functionally tested for continuation as a cooperative joint European–Russian experiment on the ISS.

Figure 4.7.6. Locations of the GTS antenna and electronics unit. (ESA)

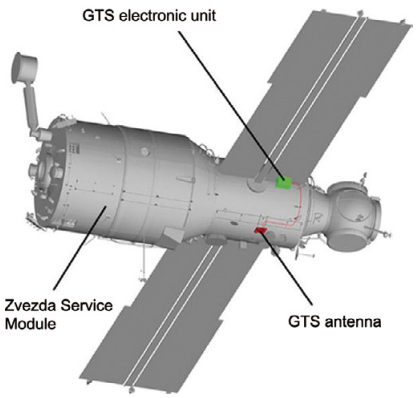

References

Eriksen, T., Nordmo Skauen, A., Narheim, B., Helleren, Ø. Olsen, Ø. & Olsen, R. (2011). *Tracking Ship Traffic with Space-Based AIS: Experience Gained in First Months of Operations*. 2nd International Waterside Security Conference, 2010. DOI: 10.1109/WSSC.2010.5730241.

Nordmo Skauen, A. & Eriksen, T. (2011). *AIS Receiving System for Columbus (COLAIS)*. Yearly Report 2010 for the COLAIS experiment with the NORAIS Receiver.

4.8 Solar Research

Solar activity can have significant effects not only on Earth but also on the satellites in orbit around it, which are now vital for communications and navigation on Earth. During high sunspot and increased solar activity, ultraviolet radiation increases dramatically, which can have a large effect on Earth's atmosphere and global climate. Solar radiation is one of the main elements that have the effect of heating the outer atmosphere, causing it to expand during periods of increased solar activity, which increases the drag on satellites orbiting Earth and thus reduces their lifetime in orbit.

Ultraviolet radiation emitted by solar flares can affect the ionosphere. These atmospheric changes, along with intense radio emissions during solar flares, can degrade the precision of GPS measurements. Since such data are used for landing planes or docking ships, it is important to measure the ultraviolet radiation affecting Earth's atmosphere.

Last but not least, solar-emitted radiation has demonstrated effects on human health, including certain skin and eye diseases.

Only by studying solar activity in more detail we can hope to understand the physical mechanisms at work in the Sun. Such data can be used to create models that better predict solar activity, and therefore we can be better prepared and develop methods to help deal with the negative effects.

Earth's atmosphere makes it difficult to study the wide range of solar electromagnetic emission spectra from the ground. This makes it necessary to undertake solar research in space, and the ISS provides an invaluable platform for observing the activity of the Sun over long periods of time.

Since 2008 the science instruments accommodated within the Solar facility (Fig. 4.8.1) have been studying the Sun's irradiation with extreme accuracy across most of its spectral range, and have produced excellent scientific data. The facility will continue to gather scientific data until at least February 2013, covering the expected upcoming period of increasing solar activity. If an extension of the safety certification beyond 2013 is granted, the Solar facility might operate until 2017. This extension will hopefully encompass the expected maximum level of activity in the 11-year solar cycle, when the occurrence of sunspots and solar flares will be at their maximum levels, and the Sun's magnetic field will be most powerful. This extension of the operations of the Solar facility will help to provide an even more detailed time-dependent picture of solar activity.

Figure 4.8.1. The Solar facility (*centre*) on the ISS in June 2008 during an STS-124 spacewalk. (NASA)

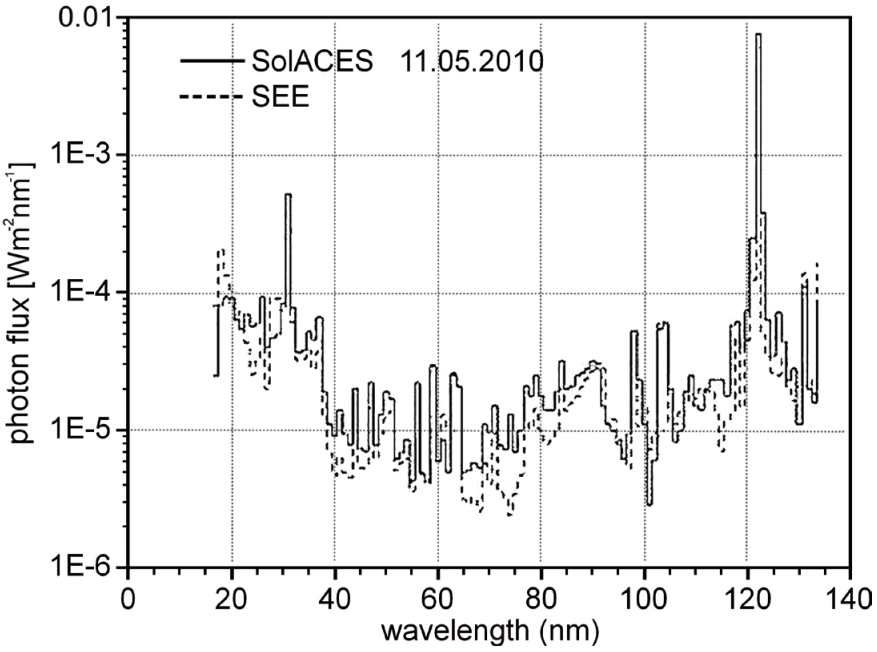

Figure 4.8.2. Example of a comparison of calibrated EUV spectra as measured by NASA's TIMED-SEE (Solar EUV Experiment) and SolACES for solar minimum conditions.

Located on the External Payload Facility of the Columbus laboratory since 15 February 2008, the Solar instruments will continue to measure the solar spectral irradiance of the full disc from 17 nm to 150 nm at 0.5 nm to 1.6 nm spectral resolution using the Solar Auto-Calibrating Extreme UV Spectrometer (SolACES), as well as the solar spectrum irradiance from 180 nm to 3000 nm using the Solar Spectral irradiance (SOLSPEC) instrument.

The set of the Solar science instruments is completed by the Solar Variability and Irradiance Monitoring (SOVIM) instrument, which is designed to measure the total and spectral irradiance of the Sun with high precision, high stability and high accuracy. The SOVIM instrument has not been active since late 2008, but prior to that had produced extensive scientific measurements complementing those made by SolACES and SOLSPEC.

Selected Results

Data from the Solar facility have already helped to validate improved models of the upper atmosphere. Recent results from NASA's Solar Radiation and Climate Experiment (SORCE) have shown that standard assumptions about the variability of the solar spectrum are incorrect (Unglaub et al., 2011).

A new method has now been developed that describes the effect of solar extreme ultraviolet (EUV) radiation on the ionosphere and its variability, called the EUV-Total Electron Content (or EUV-TEC) proxy. Comparisons have shown this method to be an improvement on conventional solar indices. In particular, for representing ionospheric variability, the new proxy performs better than the frequently used F10.7 radio flux.

Data from the Solar facility on the ISS, together with data from the Solar EUV Experiment (SEE) on NASA's Thermosphere, Ionosphere, Mesosphere Energetics and Dynamics (TIMED) satellite (which measures solar spectra in the wavelength range 0.1–200 nm) have helped to confirm the improvement in the EUV-TEC model (Fig. 4.8.2).

Figure 4.8.3 shows a comparison of EUV-TEC and F10.7, together with global mean TEC, from 2002 to 2009. Two SolACES data points are shown in the figure, which correspond well with the TIMED-SEE data.

There is a good correlation between EUV-TEC and F10.7 during periods of high solar activity. Comparing EUV-TEC and the global TEC index, the seasonal

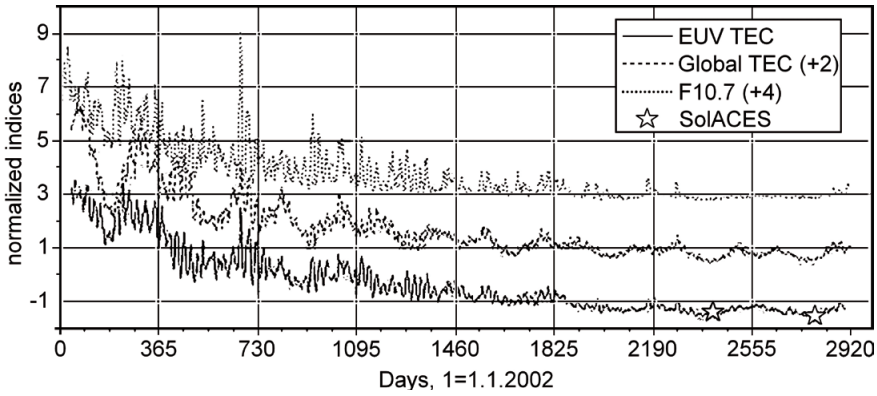

Figure 4.8.3. Time series of daily EUV-TEC indices, global mean TEC, and F10.7 solar radio flux over the period 2002–09. Two data points based on SolACES measurements are shown as open stars.

pattern at low solar activity is visible in both. One may conclude that F10.7 does not represent ionospheric variability as well as the EUV-TEC proxy does, in particular during times of low solar activity.

Note that the majority of data points refer to low solar activity conditions, essentially because the last solar minimum was very long, extending roughly from 2007 to 2009. The F10.7 index reaches an approximately constant value during solar minimum conditions, while the solar UV and EUV irradiance continues to decrease. This is one of the reasons why F10.7 is not a very good index for solar EUV variability during periods of low solar activity.

Reference

Unglaub, C., Jacobi, Ch., Schmidtke, G., Nikutowski, B. & Brunner, R. (2011). EUV-TEC proxy to describe ionospheric variability using satellite-borne solar EUV measurements: First results. *Adv. Space Res.* **47**(9), 1578–1584.

4.9 Space Exposure Research

The space environment is unique for carrying out various forms of research across many different scientific disciplines. It is important to monitor external surroundings of spacecraft to determine changes in environmental conditions (radiation, temperature, orbital debris, vacuum, etc.) and how they affect the spacecraft itself. This information is in turn helping to determine the shielding qualities of spacecraft against radiation (see also section 4.6, Radiation Research), as well as the levels of other possibly detrimental influences on the spacecraft hull such as atomic oxygen, or the buildup of electrical potential.

The space environment also offers opportunities to carry out research into new materials (and technologies) that could find their way into new satellites or spacecraft for future human exploration missions. The combined features present in orbit are difficult to simulate on Earth, making research on the ISS extremely valuable.

One of the most important areas of research in open space is astrobiology, which involves assessing the survivability of different organisms in orbit, outside Earth's protective environment, where they are exposed to full solar UV radiation, the vacuum of space, cosmic rays and extreme temperature variations as the ISS passes between areas of direct sunlight and the cold darkness of Earth's shadow. This kind of research can also shed light on the survivability of different organisms on other planets, whether they are able to build resistance when exposed to such harsh conditions, and help determine what protection measures will be necessary to restrict the possibility that surface probes sent from Earth contaminate another planetary body

4.9.1 The EuTEF and Expose-R Facilities

The launch of the Columbus laboratory in February 2008 provided Europe with a valuable means to undertake research requiring exposure to the open space environment. Columbus is fitted with an external payload facility that supplies utilities (power, data, etc.) to the attached payloads. In addition to the Solar payload facility (see section 4.8, Solar Research), the European Technology Exposure Facility (EuTEF) was also installed on the outside of Columbus (Fig. 4.9.1) in 2008.

EuTEF was a fully automated, multi-user external payload facility carrying a suite of experiments requiring exposure to open space, covering materials science, physics, astrobiology, astronomy and space technology. After more than 18 months of successful and continuous operations, EuTEF was deactivated and returned to Earth in September 2009 as part of the STS-128 mission. During the time in orbit, several EuTEF experiments were conducted under continuous monitoring and control from the Erasmus User Support and Operations Centre at the ESTEC facility in Noordwijk, the Netherlands. The preliminary results of these experiments were presented at the EuTEF Symposium at ESTEC in 2010 and are described below.

Continuing ESA's exposure research on the ISS, the Expose-R facility (Fig. 4.9.2) was retrieved from the outside of the Russian Zvezda Service Module during a Russian EVA on 21 January 2011 after almost two years of exposure to the harsh space environment. The sample trays from the facility were returned to Earth on the STS-133 Shuttle *Discovery* mission in March 2011. Expose-R hosted a suite of nine new astrobiology experiments (eight from ESA, one from the Institute for Biomedical Problems, IBMP, Moscow), including two investigations of chemical evolution, i.e. the behaviour of biochemical molecules exposed to full-spectrum solar UV radiation.

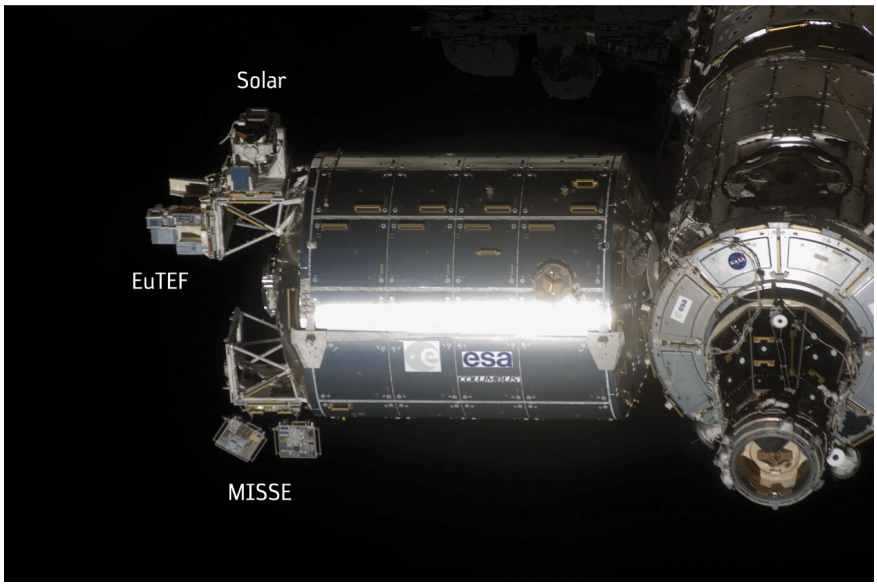

Figure 4.9.1. The Columbus module, showing the locations of three external payloads in June 2008, including ESA's Solar facility, the European Technology Exposure Facility (EuTEF) and two panels from NASA's Materials ISS Experiment (MISSE). (NASA)

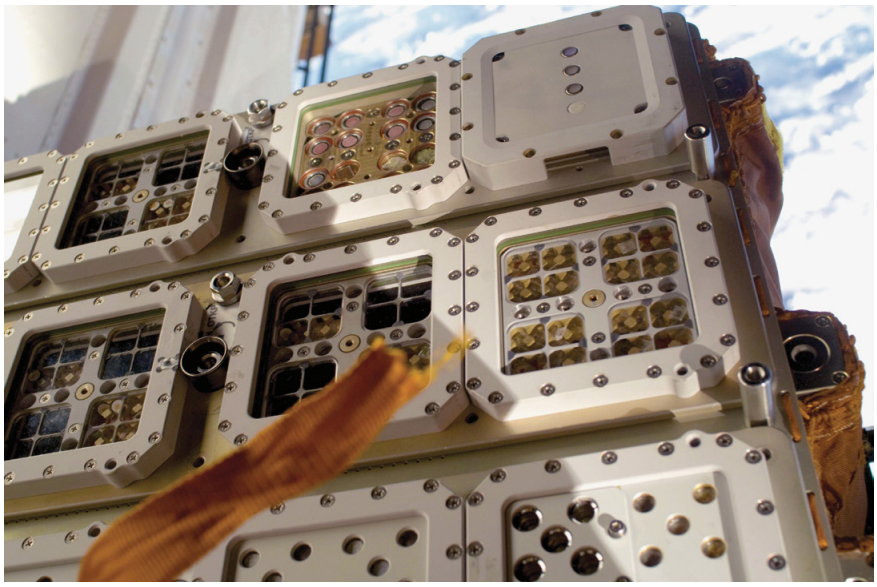

Figure 4.9.2. The Expose-R facility installed on the outside of Zvezda on the ISS in March 2009. (NASA)

4.9.2 Astrobiology

ESA-funded research has made major improvements in what is known in the field of astrobiology through ISS experiments on EuTEF and Expose-R as well as shorter-duration experiments (two weeks) on the Foton family of spacecraft.

Following earlier experiments with bacterial spores, the search for living organisms on other planets and the possibilities for transfer of life between planets have expanded to encompass more advanced organisms. Those experiments have already determined that lichens (Fig. 4.9.3) and water bears (tardigrades; Fig. 4.9.4) are able to survive approximately two weeks of exposure to the open space environment.

EuTEF's Expose-E platform was used to perform five astrobiology experiments (and three in radiation dosimetry) that provided an exposure time of 18 months. One part of the samples was exposed to open space conditions while the other part was exposed to modified conditions (low pressure, atmosphere mainly of CO_2 and an altered UV spectrum) to simulate conditions on Mars. During its mission Expose-E operated flawlessly with solar UV

radiation and temperature data were regularly downlinked to Earth (the results are presented below).

Several Expose-E (and Expose-R) experiments investigated to what extent particular terrestrial organisms were able to cope with extraterrestrial environmental conditions. Other Expose-E experiments tested how organic molecules, the building blocks of life, behave when subjected to unfiltered solar radiation for a prolonged period of time (a scientific domain called chemical evolution).

The Expose-R payload hosted a suite of nine astrobiology experiments, some of which could help understand how life originated on Earth. The experiments were accommodated in three special sample trays loaded with a variety of biological samples, including plant seeds and spores of bacteria, fungi and ferns.

The samples used in the individual Expose-R experiments have been returned and are now being analysed. The experiments were as follows:

- AMINO: photochemical processing of amino acids and other organic compounds in Earth orbit;
- ENDO: response of endolithic organisms to space conditions;
- OSMO: exposure of osmophilic microbes to the space environment;
- SPORES: spores in artificial meteorites;
- PHOTO: measurements of vacuum- and solar radiation-induced DNA damage within spores;
- SUBTIL: mutational spectra of *Bacillus subtilis* spores and plasmid DNA exposed to high vacuum and solar UV radiation in the space environment;
- PUR: responses of Phage T7, Phage DNA and polycrystalline uracil to the space environment;
- ORGANIC: the evolution of organic matter in space; and
- IBMP: exposure of the dormant stages of terrestrial organisms to space conditions.

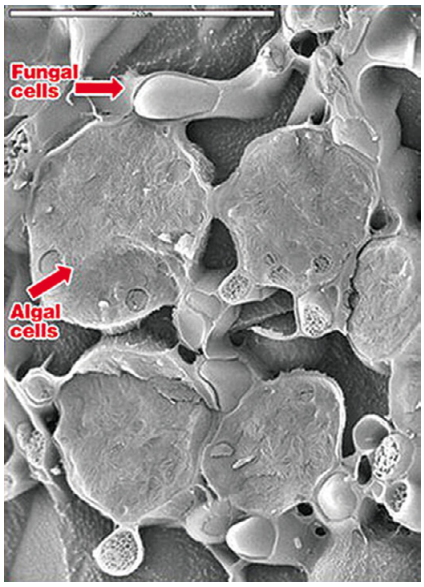

Figure 4.9.3. Microscopic image of a lichen showing fungal and algal cells. (L. Sancho)

Figure 4.9.4. Tardigrades or water bears are now known to be able to survive the harsh conditions of open space. (W. Gabriel and B. Goldstein)

Selected Results

Some of the results of experiments on the Expose-E platform on EuTEF were presented at ESTEC in Noordwijk, the Netherlands, in December 2010, and are summarised in the following.

The Adapt experiment (Fig. 4.9.5) investigated the capability of microorganisms to adapt to UV levels such as those on Earth and on Mars. Bacterial spores, cyanobacteria and halophilic archaea were exposed to open space conditions and to simulated martian conditions. Following analysis, the halophilic archaea *Halococcus dombrowskii* seemed tolerant to space conditions as many cells were still alive, their morphology was unchanged, and their enzymatic activities were still measurable.

The Lichens and Fungi Experiment (LIFE) followed up the short-term Foton experiments previously carried out by testing the survival rates of lithic fungi and lichens to exposure to space and simulated martian conditions for 18 months. Two samples (one lichen and one black fungus) resisted full solar irradiation, but almost all the dark samples shielded from UV light survived, although at different levels (from almost 100% to 2.5%). Interestingly, one sandstone sample contained a very high fraction of intact fungal cells even though they had been exposed to the full solar spectrum.

The Protect experiment (Fig. 4.9.5) addressed planetary protection issues. Spores of the bacterium *Bacillus subtilis*, which is resistant to non-UV space conditions, and *Bacillus pumilus* SAFR-032, which is notoriously resistant to sterilisation processes, were exposed to space and to martian conditions. The results showed that bacterial spores were able to survive a simulated journey to Mars if protected against solar UV-C. At the surface of Mars, they may survive

Figure 4.9.5. Flight sample carriers for the Adapt and Protect experiments after deintegration. (DLR)

for several years if shielded against direct solar irradiation. It is crucially important to measure the resistance of such organisms to space conditions in order to develop adequate decontamination procedures to counter the risk of planetary contamination by probes sent from Earth, especially in light of the search for extraterrestrial life *in situ*.

In the Seeds experiment, hundreds of plant seeds (of *Arabidopsis* and tobacco) were exposed to space conditions outside the ISS for 18 months. Plant seeds have frequently been tested in space, but never with full exposure to solar UV-C on a long-duration flight. When the germination of the seeds was studied on return to Earth, a remarkable number of seeds of both species survived, with higher rates for exposed seeds that were shielded against solar UV.

In the PRebiotic Organic ChEmistry on the Space Station (PROCESS) experiment (the final astrobiology experiment on Expose-E), selected organic molecules were exposed for 18 months to the full spectrum of solar light in order to investigate the chemical nature and evolution of organic molecules in extraterrestrial environments. The analysis of the samples is under way.

4.9.3 Materials Research

The Material Exposure and Degradation Experiment (MEDET), which took place on EuTEF (see Fig. 4.9.6), aimed to evaluate the effects of the complex low-orbit space environment on material properties and to investigate material degradation due to contamination. MEDET consisted of seven instruments, with active sensors and material samples. Most of the samples were exposed in the forward-facing ISS direction (i.e. the direction of travel), while others were pointing away from Earth (zenith direction). Data were frequently downlinked to the ground via EuTEF.

The material samples consisted of a selection of thermal control paints and foils, optical glasses, thin solar sail materials and metallic anodisations. There were 12 microcalorimeter samples and 20 spectrometer samples. In addition, the MEDET multilayer insulation and radiator surfaces were covered with Mapatox and Rigid Solar Reflector (RSR) atomic oxygen protection coatings (developed by the company MAP and the French space agency, CNES), which also formed part of the investigations.

Selected Results

Preliminary analysis of the data on material degradation from MEDET showed some trends in the material behaviour and ageing/degradation mechanisms (yellowing, erosion by atomic oxygen, etc.). However, more detailed modelling is required in order to acquire more accurate values for their thermo-optical properties.

The data from the environmental sensors on MEDET, in particular the pressure gauge, have been used to show the influence of ISS orbital manoeuvres and the docking of the Space Shuttle on the local ISS environment (Tighe et al., 2009).

Sample	Material type
SG121FD	White silicate thermal control paint
PCBE	White silicate thermal control paint
PSBN	White silicate thermal control paint
ITO/25 μm Kapton	Polyimide with conductive coating
25 μm Upilex S/VDA	Polyimide
Mapatox/25 μm Kapton HN/VDA	Polyimide with atomic oxygen protection coating
RSF/VDA/25 μm Kapton HN	Polysiloxane resin on aluminium-coated polyimide
RSR polished aluminium	Polysiloxane resin on polished aluminium
Keronite	Black thermal control coating
Plasmocer	Black thermal control coating
Second surface mirror	Silver-coated SiO2
Y100	Experimental polyimide

Table 4.9.1. Material samples analysed with the microcalorimeter in the Material Exposure and Degradation Experiment (MEDET).

During 2010 the analyses of the coatings tested in orbit were complemented with ground-based activities (environment simulations, calibration, chemical analysis, physical and optical properties). The preliminary results of the ground-based tests indicated some general trends in the behaviour of these materials (Table 4.9.1), as follows:

— there was no significant degradation of the white paints;
— there was no significant degradation of the Plasmocer;
— there was no significant degradation of the black bodies;
— complete erosion of the Upilex S occurred;
— darkening of the Y100 polyimide was followed by a decrease in absorptance;
— there was a small increase in the absorptance of the RSR, Mapatox and RSF coatings.

These results will need to be refined using more detailed analyses, and compared with the postflight measurements after the return of the samples.

4.9.4 Space Environment Monitoring

Orbital Debris

Orbital debris is an issue that must be seriously considered and monitored very closely for orbiting spacecraft, especially in view of the fact that the ISS itself is travelling at a speed of 8 km s^{-1}. For this reason, a great deal of thought goes into carefully protecting orbiting spacecraft and satellites with debris protection panels and methods of avoiding such debris.

Around 13 000 pieces of orbital debris larger than 10 cm across have been already catalogued. Some of these are large enough to be tracked by terrestrial radar so that the ISS and other satellites can manoeuvre out of their path. There are also many millions more pieces of debris too small to be monitored from the ground. These smaller items pose little threat to satellites but an understanding of their nature can be fed into future spacecraft design.

The DEBris In-orbit Evaluator-2 (DEBIE-2) was located on the EuTEF facility during its time in orbit. DEBIE-2 (Figs. 4.9.6 and 4.9.7) measured the impact energies and velocities of submillimetre micrometeoroids and space debris hitting its three aluminium foil panels, and thus provided some insight into this smaller type of orbital debris about which little is known. The micrometeoroids impact at hypersonic velocities briefly heating the aluminium foil locally to thousands of degrees kelvin, hotter than the surface of the Sun. This impact

Figure 4.9.6. View of the front face of the EuTEF showing the locations of four experiment payloads. (NASA)

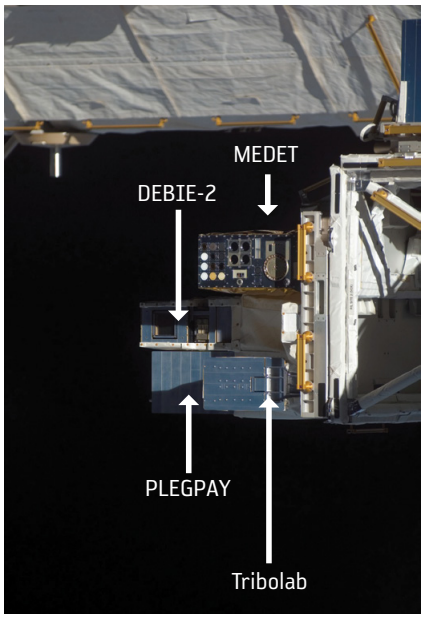

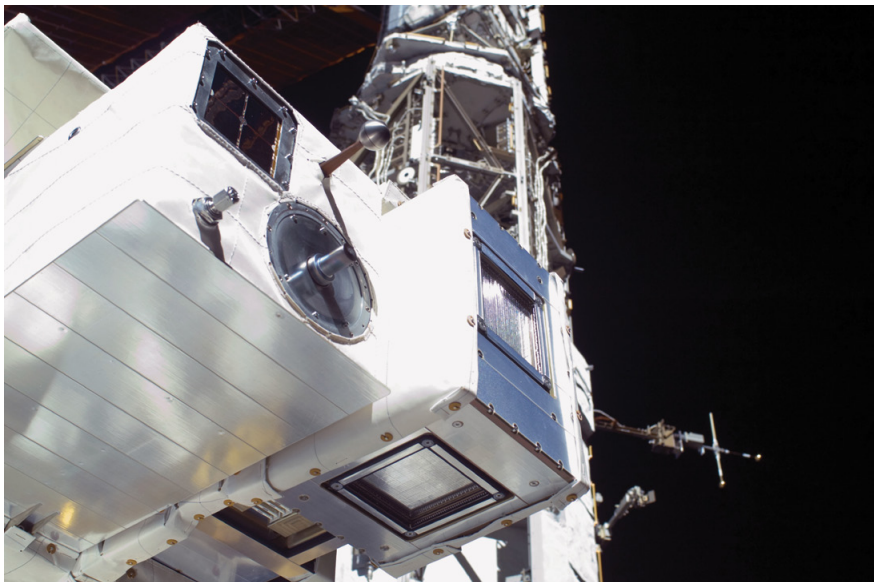

Figure 4.9.7. An in-orbit close-up of the DEBIE-2 and PLEGPAY payloads on EuTEF. (NASA)

creates a charged plasma cloud whose charge is measured by positive and negative plasma detectors adjacent to the foil.

Selected Results

After initial background noise filtering was undertaken, 931 events were identified as potential impact events in the period January–September 2009. From these data it was found that significantly more impacts occurred on the upward (zenith) facing sensor than on the forward-facing and starboard sensors. One surprising finding was that impact events came in clusters and were not randomly distributed. These peaks may be concentrated within perhaps 60–80 s at a time, indicating the existence of clouds of dust along the ISS orbit.

Radiation Research

Tying in with the majority of ESA's radiation research (see section 4.6), and the reasons for it, ESA had a radiation monitoring device installed on the EuTEF facility. The Advanced Dosimetric Telescope (DOSTEL) experiment was designed to monitor the cosmic radiation environment outside the ISS and the data were compared with measurements obtained inside the ISS. During all activation periods DOSTEL performed perfectly.

Selected Results

Preliminary results showed that dose rates outside the ISS are a factor of about two higher than those inside. These data have been compared with the results obtained from similar experiments previously sent to space, such as DOSIS and Matroshka, and have been used to build overall radiation models.

Figure 4.9.8 shows the trigger rates of DOSTEL from February to December 2008. The lower part of the Trigger profile shows the variations of dose due to the galactic cosmic ray environment, while the spikes are related to passing through the South Atlantic anomaly as well as to electrons from the horns of the radiation belts at higher latitudes.

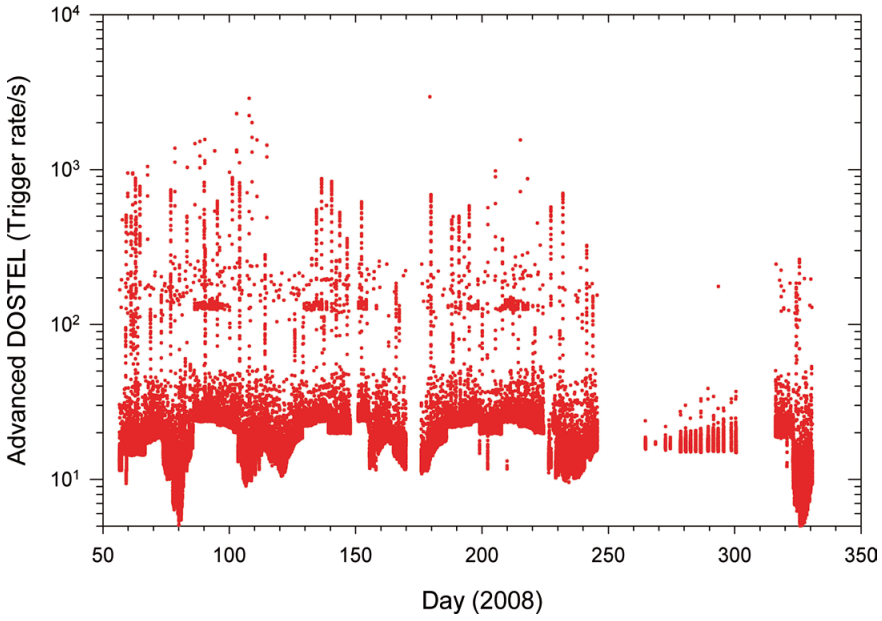

Figure 4.9.8. Trigger rates of the DOSTEL radiation detector, February to December 2008.

Other Instruments

Three additional instruments located on EuTEF were the Flux (Phi)-Probe-Experiment (FIPEX), the Plasma Electron Gun Payload (PLEGPAY) (Figs 4.9.6 and 4.9.7) and EuTEMP. FIPEX was a miniaturised atomic oxygen detector intended to measure the atomic oxygen flux as well as the oxygen molecules in the area surrounding the ISS. The objective of the PLEGPAY experiment was to study spacecraft/space environment interactions in low-Earth orbit with reference to electrostatic charging and discharging of gases, identifying a potentially fatal problem for spacecraft electronics. EuTEMP successfully recorded temperature data throughout the ascent into orbit, throughout its transfer phase from inside the Shuttle cargo bay and during its installation on Columbus, as well as during deinstallation and return to the Shuttle cargo bay at the conclusion of the mission, and for one additional day inside the Shuttle cargo bay.

Selected Results

The results from FIPEX showed that there is an increase in atomic oxygen soon after local sunrise and just before local sunset when the ISS is travelling along the orbit from south to north, reaching a peak when crossing the equator. The levels of atomic oxygen decrease as the ISS continues the orbit to higher latitudes, and reach a minimum when the ISS exits the night phase. The first runs of the first PLEGPAY experiment demonstrated the capability of the plasma contactor device to control the potential of a very large spacecraft such as the ISS through the biasing of the plasma contactor. Furthermore, the experiment demonstrated the capability to lock the ISS potential at around zero by small current emission, and the PLEGPAY Langmuir probe measurements were found to match those made independently by NASA's Floating Potential Measurement Unit.

4.9.5 Tribology

Tribology is the study of the science of friction and lubrication. This is of major importance for spacecraft systems. The Tribolab (Fig. 4.9.6) experiments on EuTEF covered both experiments in liquid and solid lubrication, such

as evaluations of fluid losses from surfaces and of the wear of polymer and metallic cages in weightlessness.

The first results from the 'pin on disc' tests in the Tribolab experiment showed that the behaviour of lubricants under microgravity and vacuum conditions in orbit is similar to that on Earth.

4.9.6 Technology Demonstration

In addition to the various scientific experiments, an Earth Viewing Camera was installed as a technology demonstrator, located on the external platform of Columbus module. The camera took photos of Earth to test the usability of commercial digital cameras for use in space.

Reference

Tighe, A.P., Iwanovsky, B. & van Eesbeek, M. (2009). Overview of results from the Materials Exposure and Degradation Experiment (MEDET) after 18 months in orbit on the ISS. *http://esmat.esa.int/Materials_News/ISME09/pdf/10-In-flight/S12%20-%20Tighe.pdf*

4.10 Education Activities

The need for education in an increasingly knowledge-based society is without question and forms a fundamental part of ESA's mandate. ESA is conscious that it can play a significant role in contributing to a scientifically literate and aware society, and that it has both a responsibility and a vested interest in doing so. The ISS Education Programme makes use of human spaceflight, and the ISS, as means to capture the attention and interest of students, to attract them to study, in particular, scientific and technical disciplines, and to appreciate and understand the benefits, challenges and importance of space for Europe.

ESA offers a range of education activities, materials and opportunities for primary and secondary and university students, and their teachers. This includes the development and dissemination of teaching materials, as well as supporting student experiments to be executed on the ISS and other spacecraft.

All of ESA's past, present and future human spaceflight missions to the ISS have an inherent education element encompassed in a detailed programme of activities tailored to each mission. These activities include live links with students and teachers on the ground, enabling students to question astronauts in orbit and to perform parallel experiments in space and in the classroom. These activities are backed up with educational materials produced by ESA, such as the ISS Education Kit for primary or secondary schoolchildren, additional online lessons and DVDs.

4.10.1 Amateur Radio on the ISS (ARISS)

One of the longest-running education activities involving the station is the Amateur Radio on the ISS (ARISS). ARISS is a volunteer working group set up by amateur radio societies in ISS partner countries. They have been entrusted with the task of organising radio voice contacts between the ISS and schools, and many radio contacts have been successfully established since 2001. When a contact is scheduled, volunteer amateur satellite operators set up a ground station in the selected school or location or a telebridge is connected to the school or location from a different ground station. During the 10-minute window as the ISS passes over the school, or ground station, an astronaut answers the questions prepared by the students. Some of the children chosen are the winners of national space-oriented competitions organised by ESA's ISS Education Office.

In recent years ESA has been extensively involved in ARISS activities. André Kuipers has been involved in activities in connection with the PromISSe mission to the ISS that was launched in December 2011. Paolo Nespoli was involved with ARISS contacts in 2010–11 as part of the MagISStra mission, and Frank De Winne was similarly involved as part of the OasISS mission in 2009. Additional ARISS contacts to date have included a special exhibition at the European Parliament in Brussels in April 2010 showing how ham radios on the ground and in space can help Europeans in many ways. These activities have built on numerous earlier contacts between European and partner astronauts on the ISS and students in countries across Europe and ESA Member States.

In 2010 ARISS was awarded the prestigious 2010 Boselli prize, recognising how ARISS has shown the importance of radio communications to hundreds of young students in Europe and beyond. The amateur radio station on the ISS was moved to the Columbus laboratory in summer 2011 and antennas for the radio station were placed outside the module.

Figure 4.10.1. Schoolchildren performing mass measurements on Earth during the 'Take your Classroom into Space' campaign. (ESA)

4.10.2 In-Orbit Science Demonstrations

During numerous ESA human spaceflight missions to the ISS, ESA's education programmes have included demonstrations of scientific principles in orbit to help engage primary and secondary schoolchildren by making science more stimulating. These demonstrations have either been undertaken as part of live links between astronauts and schoolchildren to make it truly interactive, or have been recorded for later use. Many of these demonstrations have been recorded on DVDs and made available to schools across Europe to be used as teaching tools within national science curricula.

In 2010, during the MagISStra mission, Paolo Nespoli carried out a plant growth experiment on the ISS in 2011 at the same time as children on the ground, and participants in the Mars500 isolation study. In 2009, Frank De Winne led the 'Take your Classroom into Space' activity on the ISS, which involved helping to demonstrate the difference between the concepts of weight and mass, and a second experiment to demonstrate capillary movement. Education kits containing equipment for the experiment were distributed to 1000 participating schools so that students aged 14–18 could perform the same experiment on the ground (Fig. 4.10.1) and compare their results with those obtained in orbit.

The activities during the 'Take your Classroom into Space' campaign were recorded and are now available on DVD. Additional DVDs have been produced with the help of European astronauts during their missions on the ISS. These form a series of DVDs that explain basic scientific concepts, fitting the European curricula, to pupils aged 12–18 years using the unique opportunity provided by the ISS to perform experiments in space.

Another in-orbit demonstration was 'Taste in Space', in November 2010, which aimed to demonstrate to primary students the differences in the sense of taste under weightless conditions and on Earth by comparing the results of blind tastings of six food items on the ground and in space. Video files of the demonstration will be used to produce online materials for primary school teachers and students aged 10–12 as part of the 'Lessons Online' series.

Live Links for Education Projects

In addition to their in-orbit science demonstrations, ESA astronauts have been involved in various education projects as part of their mission. By linking these projects to specific missions the material can be more relevant, as well

Figure 4.10.2. First training session to be as fit as an astronaut. (ESA/A. Le Floc'h)

as personal. The astronauts talk about their mission and introduce lessons and other activities, which may also involve live links between the astronauts and schoolchildren through the ARISS project.

One important education programme that began in January 2011 is the 'Mission-X: Train Like an Astronaut'. Mission-X is a worldwide initiative supported by ESA and the national space agencies of Austria, Belgium, Colombia, Czech Republic, France, Germany, Italy, Japan, the Netherlands, Spain, the UK and the USA, whose aim is to encourage children to adopt healthy and active lifestyles (Fig. 4.10.2). In the process, it is hoped that the children will become excited about the future in space and the opportunities available to them. Paolo Nespoli launched Mission-X in a video message from the ISS. Teams of primary school students (8–12 years) participate in training sessions in which they learn about the importance of healthy eating and exercise, and compete for points. Paolo finished the programme with a live call announcing the winning teams.

In February 2012 André Kuipers participated in a live call kicking off Mission-X 2012, during which thousands of children in the Netherlands, Portugal, Switzerland and Italy were able to speak with André about the programme. Mission-X concluded in April 2012.

As part of other activities, in 2009 Frank De Winne announced live from space the winner of the ESA/UNICEF Water Quiz. This was an online competition for 12–14 year-olds across Europe, which aimed to teach them about water on Earth and in space.

→ ONGOING RESEARCH USING OTHER PLATFORMS

5. Ongoing Research Using Other Platforms

5.1 Research on Sounding Rockets

The wide variety of sounding rockets provide great flexibility for European scientific, industrial, commercial and education communities. This makes them excellent platforms for performing experiments with stringent technological, safety, operations and sample logistics requirements, as well as providing a means of testing experiments and equipment to be undertaken or used as part of long-duration missions in orbit.

A sounding rocket is a sort of ballistic missile that can provide 6–12 min of weightlessness and can accommodate a payload of up to 800 kg. Three types of sounding rocket – Texus, Maser and Maxus – have been central to ESA's weightless research activities since 1982. They can reach altitudes ranging from 250 km to 750 km with excellent weightless conditions being achieved during the freefall phase. Sounding rocket missions are a valuable means to undertake experiments having stringent pre-/postflight experiment logistics and may involve the use of hazardous materials or equipment (e.g. radiation sources for *in situ* visualisation). They are also advantageous for high-temperature materials experiments as the heater/furnace materials degrade quickly and so can not be considered for long-term experiments on the ISS.

Most sounding rockets are launched from the Esrange launch site near Kiruna, Sweden, which is owned and managed by the Swedish Space Corporation (SSC). ESA is a regular user and major research partner along with other national organisations such as DLR. The location of the launch site, just within the Arctic Circle, is excellent for investigations of polar phenomena. ESA has recently been involved in three sounding rocket campaigns: Texus-46 in November 2009, Maxus-8 in March 2010 (Fig. 5.1.1) and Maser-12 in February 2012.

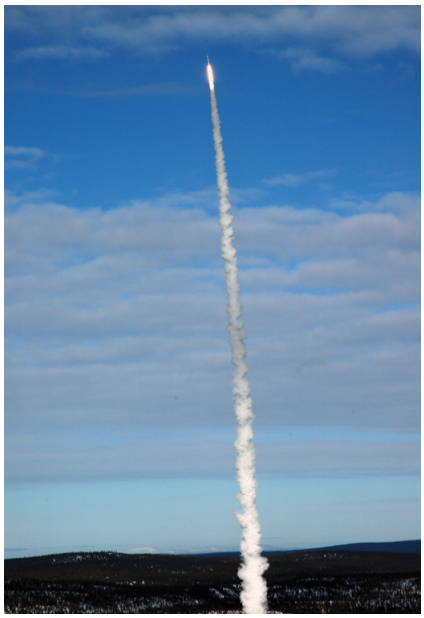

Figure 5.1.1. Launch of Maxus-8 in March 2010. (SSC)

5.1.1 Physical Science Research

The Texus-46 campaign in November 2009 included four experiments. Three of them, including one sponsored by DLR, made use of the ElectroMagnetic Levitator (EML), which involves container-less processing of molten metal alloy samples to enable measurement of their thermophysical properties at high temperature, as well as studies of solidification processes in undercooled samples, which are relevant for the casting industry. An EML will be flown to the ISS on a future flight.

Two of these three experiments looked into the properties of a steel sample and the influence of chill cooling on their thermomechanical properties, which are relevant for the continuous casting process employed by industry. The third experiment aimed to clarify whether the oscillating drop technique implemented in the EML, where the levitator itself generates a minimum level of convection in the molten sample, is capable of delivering precise viscosity data. A specific glass-forming alloy of palladium and silicon was the chosen sample. The viscosity of this alloy spans a large range of values as a function of temperature and reliable viscosity data were already available for comparative purposes, and it also enabled measurements of the glass transition temperature of this alloy.

The fourth experiment on Texus-46 was an ESA/JAXA collaboration to study the dynamics of flame propagation along a linear array of fuel droplets and on the burning efficiency as a function of the time of pre-vaporisation. This study supported current modelling efforts to predict nitrogen oxide emissions (which are directly harmful to humans) in fuel exhaust. The results suggested

that a high degree of vaporisation is required in order to achieve a substantial reduction in nitrogen oxide emissions.

The Maxus-8 mission in March 2010 included three materials science experiments as part of its research package. These experiments provided data that will help to improve industrial turbine blade casting models, and thus cost and fuel savings, across numerous aerospace and automotive industries. Two of the three experiments stemmed from the successful joint ESA/EU InterMetallic Processing in Relation to Earth and Space Solidification (IMPRESS) project, which involved 150 scientists and 40 partners including universities, research establishments and industry.

The first of these experiments addressed the solidification of new titanium–aluminium alloys under different conditions, and aimed to determine the influence of gravity on the transformation from liquid to solid, and thus on the microstructure of the alloys and ultimately their mechanical properties. The findings will help in the production of a new generation of lightweight and fuel-saving turbine blades for aircraft jet engines and ground-based turbines.

The second experiment examined the behaviour of nanoparticles of nickel formed by evaporation and then condensation in a laminar flow of inert gas in a specially designed reactor. The study focused on the efficient production of nickel nanoparticles and their clustering into strings or fractals. This research could lead to important concepts for the design of new catalysts, nanomagnets and particular classes of sensors.

The third materials science experiment on Maxus-8 attempted, for the first time, *in situ* X-ray monitoring of liquid diffusion in metallic and semiconductor alloys. The aim was to make direct measurements of diffusion coefficients with very high accuracy, but unfortunately the equipment malfunctioned.

The Maser-12 mission, launched in February 2012, included three physical science projects: X-ray Monitoring on sounding rockets (XRMON), SOUnding Rocket Compere Experiment-2 (SOURCE-2) and BIOMImetic and Cellular Systems (BIOMICS-2).

The XRMON project is making high-resolution *in situ* X-ray radiographic observations of directional solidification in metallic alloys such as aluminium–copper under microgravity and terrestrial conditions. On the ground, this technique demonstrated the pervasive effects of gravity on the stability of columnar dendrite arms and the drifting of equiaxed dendrite seeds. Observations performed without gravitational effects will enable scientists to separate individual processes and describe them more accurately in numerical models.

Following on from the SOURCE fluid science experiment on Maser-11 in 2008, SOURCE-2 is studying boiling along a superheated wall, pool boiling on a heated surface and boiling due to depressurisation, together with observations of the behaviour of the free gas–liquid interface and its interaction with the vapour bubbles and the wall. In contrast with the two-species system of the first SOURCE experiment, SOURCE-2 was performed using a single-species system.

The BIOMICS-2 experiment is also a follow-up to BIOMICS-1 on Maser-11, although it is concentrating in more detail on specific parameters from the first experiment. The aim of BIOMICS is to examine the dynamics of vesicles made of phospholipids in a shear flow. Since the vesicles mimic red blood cells, this study will improve understanding of their transport and mobility in blood vessels.

5.1.2 Life Sciences Research

The Maxus-8 research campaign included one plant biology experiment to study the mechanisms within cell structures to perceive both the intensity and direction of gravity in Characean algae (also known as stonewort or muskgrass). The cell structures being studied are rhizoids (root-like structures) that grow downwards to anchor the algae into lake sediment, and the protonemata that grow upwards towards light and are responsible for division

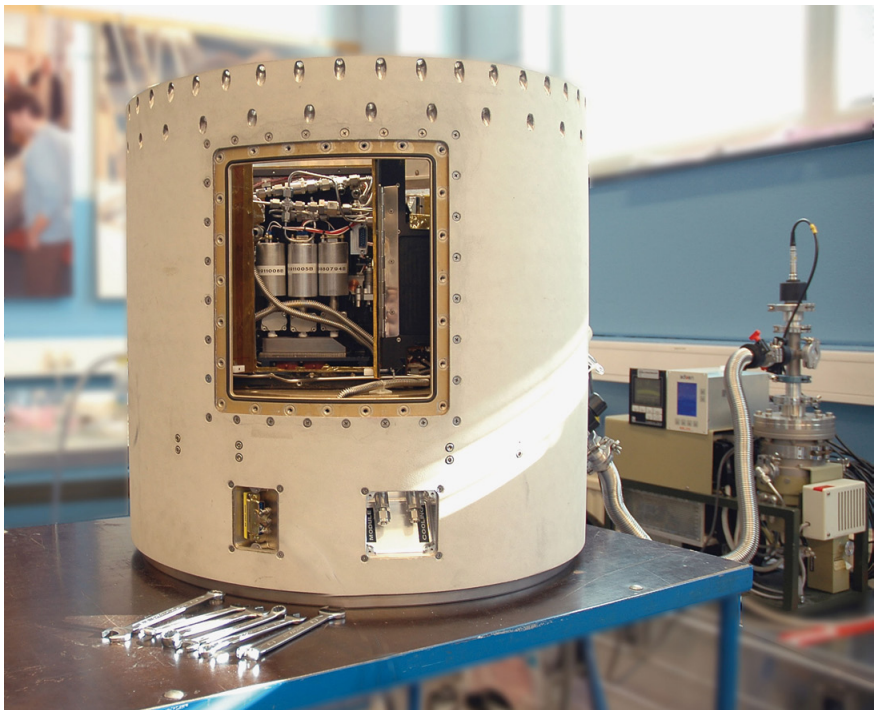

Figure 5.1.2. The XRMON-Diff module ready for Maxus-8 in March 2010. (SSC)

and regeneration. The purpose of the experiment was to test the hypothesis that the cell cytoskeleton, i.e. the cell's structural support, is involved in the gravity-sensing process, extending earlier studies indicating that lateral accelerations of between 0.05 *g* and 0.14 *g* caused a gravity response.

The launch of Maxus-9 is planned for 2014 with a complement of four physical sciences and biology experiments, including:

- a reflight of the XRMON module from Maxus-8 (Fig. 5.1.2);
- a study of the solidification of a peritectic aluminium–titanium alloy using the GRAvity DEpendence of Columnar-to-Equiaxed Transition (GRADECET) module;
- an experiment to study the combustion of a cloud of solid metal particles, as part of the joint ESA/Canadian Space Agency project PERWAVES (Percolating Reactive Waves in Particulate Suspensions); and
- a study of the sensitivity to gravity of *Euglena gracilis*, a unicellular photosynthesising organism, and the interaction between gravity/light-sensing mechanisms.

Two life science experiments flown on Maser-12 as part of the Biology in Microgravity (BIM-2) module involve *in vitro* research into the early immune response in weightlessness, which is known to be suppressed. The Signal Transduction in human T-cells In Microgravity (STIM) experiment is focusing on events that can be observed within minutes, even seconds after T-cells are presented with an effective stimulus. The Microgravity in adaptive Immunity (MicImmun) experiment is looking into monocyte and B-cell responses in weightlessness.

5.1.3 Education

The Rocket and Balloon Experiments for University Students (REXUS/BEXUS) programme is being conducted under a bilateral agreement between the German Aerospace Center (DLR) and the Swedish National Space Board (SNSB). The Swedish share of the payload has been made available to students from

other European countries through a collaboration with ESA. EuroLaunch, a cooperation between the Swedish Esrange Space Center and the DLR Mobile Rocket Base (MORABA), is responsible for the campaign management and operation of the launch vehicles. Experts from ESA, SSC and DLR provide technical support to the student teams throughout the project.

The REXUS rocket programme and the BEXUS high-altitude balloon programme are central components of ESA's education activities, offering opportunities for student experiments to be flown on sounding rockets and stratospheric balloons. Each flight carries a payload consisting solely of student experiments. In recent years flights have included the REXUS-7/-8 campaign in 2010, the REXUS-9/-10 campaign in 2011 and the REXUS-11/-12 campaign in 2012. Plans are also in the pipeline for future campaigns.

5.2 Research on Parabolic Flights

Aircraft parabolic flights are a useful tool for performing short-duration scientific and technological experiments in reduced gravity. The principal value of parabolic flights is that verification tests can be conducted prior to space experiments in order to improve their quality and success rates, and following space missions to confirm or invalidate (sometimes conflicting) results obtained from space experiments. For these purposes, since 1984 ESA has organised 55 parabolic flight campaigns in the frame of its Microgravity Programme. Since 1997, the Airbus A300 Zero-G aircraft has been used for short microgravity investigations, organised by Novespace (a subsidiary of CNES).

Parabolic flights for microgravity investigations have a number of advantages: the short turnaround time (typically a few months between the experiment proposal and its performance), the low cost involved (ESA provides flight opportunities free of charge to investigators), the flexibility of experiments (laboratory-type instrumentation is usually used), the possibility of direct intervention by investigators on the aircraft during and between parabolas, and the possibility to modify the experimental setup between flights.

Since 2010, Novespace has offered flights on the Airbus A300 Zero-G aircraft at gravity levels equivalent to those on the Moon and Mars for repeated periods of more than 20 s. These flights were introduced in response to requests from the European scientific community for opportunities to perform complementary research at partial-gravity levels, as well as to conduct studies and tests in the levels of gravity found on the Moon and Mars, in preparation for future human or robotic missions.

ESA conducted four microgravity research campaigns in 2010 and 2011. The 52nd campaign, in May 2010, included 13 experiments: six in the physical sciences, six in the life sciences, and one devoted to the training of new ESA astronauts selected in 2008.

The 53rd ESA campaign in October 2010 included 11 experiments, eight in the physical sciences and three in the life sciences, while the 54th campaign in May 2011 involved 13 experiments, seven in the physical sciences, two in the life sciences and four student experiments in the frame of the 'Fly Your Thesis' programme organised by ESA's Education Office. The 55th campaign in November 2011 included nine large experiments, three in the physical sciences and six in the life sciences. In addition, ESA, CNES and DLR organised a joint campaign at partial gravity in June 2011.

5.2.1 The Joint European Partial-*g* Parabolic Flight Campaign

In spring 2010, ESA, CNES and DLR organised the first Joint European Partial-g Parabolic Flight (JEPPF) campaign for partial-*g*, gravity-dependent and microgravity experiments that would need data at other partial-*g* levels. The three agencies launched a specific Announcement of Opportunity (1 June to 31 August 2010) inviting proposals for experiments that would take advantage of the several partial-*g* levels offered during flights.

A total of 42 proposals were received, including 18 at ESA, five at CNES, and 19 at DLR, covering the life sciences (30 proposals), the physical sciences and technology (12 proposals) from ten countries – Germany (17), France (7), Belgium (4), Switzerland (3), Italy (2), the Netherlands (2), USA (2), Austria (1), Spain (1) and the United Kingdom (1) – as well as one from ESA.

In September 2010, all but one of these proposals were submitted for independent external peer review organised by ESA. The other, a French experiment, was reviewed internally by CNES experts. Thirteen experiments were finally selected, five by ESA, and four each by CNES and DLR, covering the physical sciences (4), the life sciences (8) and technology (1).

The JEPPF campaign took place from 30 May to 10 June 2011, with three flights from the Bordeaux-Mérignac airport. Each flight included 31 parabolas in groups of seven and six, with the first two dedicated to Moon-gravity levels (13 parabolas), followed by two groups at Mars-gravity levels (12 parabolas), and a final group at zero-gravity (six parabolas), according to requests of investigators. All experiments were performed successfully.

5.2.2 Experiment Highlights

All of the 59 experiments performed during parabolic flights in 2010 and 2011 went very well. Among them, two were particularly interesting.

In the physical sciences, the experiment Interférometrie Cohérente pour l'Espace (ICE): Atom interferometry with cold atoms in microgravity (P. Bouyer of University Bordeaux 1, France, and his team) was conducted several times during parabolic flights. Atom interferometers have demonstrated excellent performance for precision acceleration and rotation measurements, and could be used to test fundamental physics.

In particular, the Weak Equivalence Principle states that two objects falling freely in a gravitational potential should undergo the same acceleration, whatever their mass or internal composition. However, some recent models have predicted violations of this principle at the quantum scale. The ICE experiment aimed to test the Weak Equivalence Principle with two atomic species (^{87}Rb and ^{39}K), by measuring their relative acceleration as they are in free-fall by atom interferometry. Microgravity allows for longer interrogation times, and higher sensitivities of the test. During these parabolic flight campaigns, it was demonstrated for the first time that it was possible to operate an atom accelerometer in flight and in microgravity. Simultaneous cooling of K and Rb atoms was also achieved, and a new robust laser source for onboard atom interferometry was constructed.

The last (55th) ESA campaign aimed to operate the Rb atom interferometer to characterise the instrument performance and carry out precision inertial measurements based on matter–wave interferometry. The ultimate goal is to contribute to ESA's Space–Time Explorer and Quantum Test of the Equivalence Principle (STE-QUEST) mission, which will test the Equivalence Principle in space at a level of 10^{-15}.

In the life sciences, an experiment to assess the influence of gravity on the dynamics of precision grip and the kinematics of upper limb movements (J.L. Thonnard, and P. Lefèvre of the University of Louvain, Belgium, and J. McIntyre of the University Paris Descartes, France) was performed several times during the microgravity and the JPPF campaigns over a period of ten years to investigate dexterous manipulation in various gravito-inertial environments (Fig 5.2.1). The central question is how the nervous system controls movements and forces when manipulating objects with the hand? Changes in gravity can be seen as perturbations to the performance of these tasks, which must somehow be compensated for through adaptive control. This is particularly so in the case of loads applied to the body by gravity because the muscle activities used to compensate for these loads appear to be programmed in a highly predictable way, perhaps based on a lifetime of experience in a normal 1-*g* environment.

Over the next few years, this experiment will be repeated in long-duration space missions on the ISS in an attempt to understand how the central nervous system adapts to an environment without gravity, and the consequences of long-term adaptation when an individual returns to a normal (Earth) or partial (Moon or Mars) gravitational field. A new instrument, the Dexterous Manipulation (DEX) payload, is now being defined and developed to conduct these experiments on the ISS. In parallel with the above scientific

Figure 5.2.1. Setup of 'The influence of gravity on the dynamics of precision grip and the kinematics of the upper limb movements' experiment during the 55th ESA parabolic flight campaign in November 2011. (ESA)

investigations, several DEX breadboards and subsystems have been intensively tested during parabolic flight campaigns over the last two years,

ESA's 56th microgravity campaign took place in May 2012 with 12 experiments, and the 57th campaign is planned for autumn 2012.

Prospective discussions have been held with CNES and DLR with a view to organising a second JEPPF campaign in 2013 or 2014 to allow European researchers to continue their investigations at partial gravity.

In view of the end of certification of the Airbus A300 Zero-G aircraft in mid-2014, discussions with CNES, DLR and Novespace are also under way to identify aircraft that could be used in the future in order to guarantee uninterrupted access to short-duration microgravity conditions for European scientists and engineers.

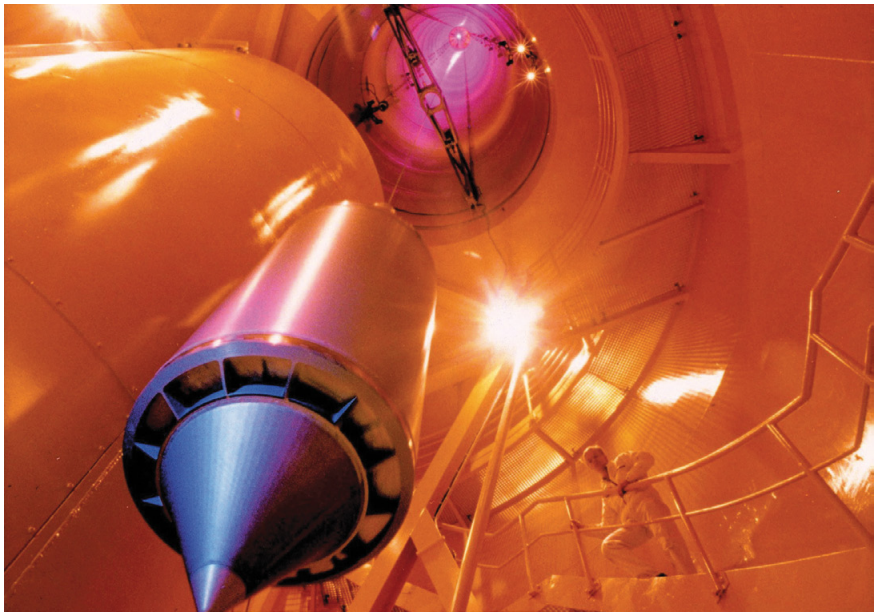

Figure 5.3.1. The experiment capsule being prepared at the ZARM drop tower in Bremen, Germany. (ZARM)

5.3 Research using Drop Towers

Drop towers offer short-duration free-fall conditions in which a variety of experiments can be undertaken in fields such as fluid dynamics, process engineering, combustion, materials science, biology and biotechnology. These experiments may require only limited exposure to weightlessness for up to a few seconds, either because this suits the experimental requirements, or they are precursors to experiments being flown on a different weightless platform.

In Europe, the principal exponent of this is the Center of Applied Space Technology and Microgravity (ZARM) at the University of Bremen, Germany (Fig. 5.3.1). Since 2009 ESA's education activities have included experiments using drop towers within the Drop Your Thesis programme (see below). The ZARM drop tower delivers 4.74 s of near-weightlessness for single drops up to three times a day. In order to double the microgravity time to 9.3 s, a catapult system has been included in the drop tower operation routine. With the drop tower catapult, the experiment capsule performs a vertical parabola instead of being dropped, i.e. the capsule is fired vertically up the tower by pneumatic piston so that the capsule first rises, stops and then falls down the drop tower tube.

Between January 2010 and December 2011, ESA funded some 127 drops at the ZARM drop tower, in more than 11 campaigns serving six experiments, including two Drop Your Thesis student campaigns, and scientific experiments addressing topics such as Turbulent Bubble Suspensions (BUBSUS), the Combustion Synthesis of Metal Oxide Nanoparticles processes (CoSyMONa) and the Photophoretic Motion of Chondrules (Chondrule-2). Breadboard experiments during 2010 and 2011 included the hardware development project Interactions in Cosmic and Atmospheric Particle Systems/ICAPS Precursor Experiment (ICAPS/IPE).

The BUBSUS experiment addressed the management and physics of turbulent bubble suspensions in microgravity. Its first aim was to develop the capability to generate a virtually homogeneous monodisperse bubble suspension carried by a turbulent pipe flow where the bubble size, mean bubble separation and Reynolds number of the flow were controlled separately. The second aim was to obtain data that will contribute to the understanding of bubble/turbulence interactions, the generation of large-scale structures in spatial bubble distributions and the statistics of bubble coalescence phenomena.

The CoSyMONa project investigated the versatile technique of flame spray pyrolysis on the production of tin dioxide nanoparticles due to their outstanding

properties related to gas sensing. Appropriate diagnostics were needed to gain insight into particle formation processes, which is essential for controlling primary particle and crystal sizes to gain optimum sensing properties. Temperature fields were also measured, since the local temperature distribution is an important process parameter affecting particle synthesis and aggregate growth. By undertaking these experiments in drop towers, the gravity-related effects of buoyancy that complicate this kind of research are removed.

The Chondrule-2 experiment is dedicated to the study of planet formation, one of the most active fields in astrophysics. About 700 extrasolar planets have been detected but the physical processes that determine these vast bodies remain partially unknown. The experiment is focusing on photophoresis, the thermodynamic process that can efficiently transport illuminated particles in the protoplanetary discs surrounding newly formed stars. In the Chondrule-1 experiment the photophoretic force was quantified for the first time using a special class of millimetre-sized particles called chondrules that are found in primitive meteorites. In Chondrule-2, the experimental parameters were changed, greatly increasing the accuracy of the measurements. From more than 200 particle trajectories the average photophoretic force acting on 33 particles has been analysed with outstanding accuracy. The variation in the trajectories of the different chondrules has led to a follow-up study of the dependence of the photophoretic force on mineralogical properties. In addition, the impact of the observed rotation of a number of particles is being analysed.

Following on from Chondrule-2, in 2011 ESA was involved in development and testing activities for the ICAPS payload, which will eventually be flown to the ISS. The experiment is designed to simulate dust agglomeration in molecular clouds and star-forming regions and to measure the light-scattering properties, such as intensity and polarisation, of these aggregates. The results of this research will help scientists to answer questions such as how the planets formed in the early Solar System, and to determine the nature of interplanetary and interstellar dust, as well as its mass, structure and motion in small aggregates.

One of the key technologies being developed for ICAPS is a thermophoretic trap, which facilitates the aggregation (and observation) of dust particles in weightlessness. The experimental runs (which used the ZARM catapult mode) have allowed for fine tuning of this hardware and the study of both full dust injection in zero gravity, and the effect of the thermophoretic trap on the particles and aggregates. Recent breadboard studies and analyses have focused on validating the parameters used in the thermophoretic trap numerical model (e.g. temperatures, frequencies, stability, gradients, squeezing time, etc.), for both the trapping and cloud manipulation functions.

As part of ESA's education activities (see section 4.10), the Drop Your Thesis! programme gives university students the opportunity to perform their own scientific experiments in weightless conditions, as part of their Masters or PhD research programme, by participating in an ESA-sponsored campaign at the ZARM drop tower. The 2010 programme (Fig. 5.3.2) included a fluid physics experiment that looked at the interactions between two bubble jets in weightlessness (Fig. 5.3.3). Such interactions could affect technologies based on multiphase flows for applications in thermal management, propulsion systems, solid waste management, water recovery and many other environmental control and life support systems.

In the 2011 campaign a plant biology experiment was selected to study the sensation of gravity and signalling in plant roots in weightlessness by analysing reactive oxygen species that are believed to be important signalling molecules that mediate many developmental and physiological processes.

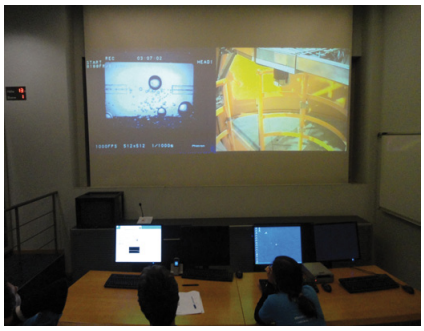

Figure 5.3.2. Control room at ZARM, Bremen, with members of the Drop Your Thesis 2010 team watching an inflight experiment on screen. (Drop Your Thesis 2010 team)

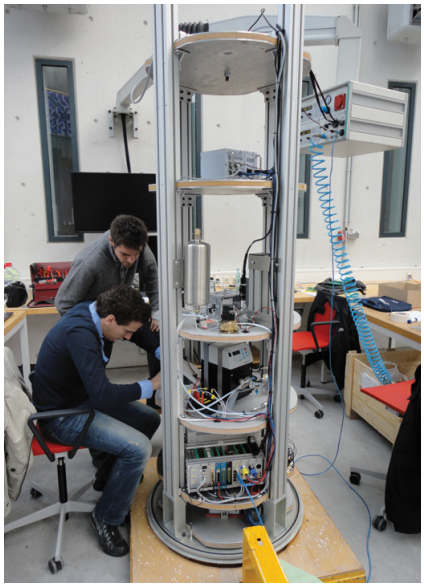

Figure 5.3.3. Two members of the Drop Your Thesis 2010 team inserting test hardware into a drop capsule during the bubble jet impingement experiment. (Drop Your Thesis 2010, Final Report)

5.4 Ground-Based Research

5.4.1 Life Sciences

Ground-based research is used to prepare for and support human spaceflight activities. Ground research is a cost-effective way to test measures to counter the physiological effects of extended stays in orbit through the use of bedrest campaigns. Ground-based isolation and confinement studies can also be used to assess the psychological (and also to a certain extent physiological) effects of confinement during long-duration missions. These activities are therefore useful for developing and testing techniques that will be used either on the ISS within the next decade and/or on future human exploration missions in space. The use of ground-based particle accelerators provides a further means to support future human exploration missions by testing the effects of radiation on biological materials.

5.4.2 Bedrest Campaigns

Bedrest studies are invaluable for simulating the effects of spaceflight on the human body. Lying on a bed tilted at 6° for an extended period with the head lower than the feet produces a number of physiological effects, including bone/muscle mass loss and fluid shifts, similar to those seen during spaceflight. Such studies are a cost-effective way to examine the mechanisms underlying these negative physiological effects and measures to alleviate them, including nutritional supplements, exercise protocols and equipment, or artificial gravity (Fig. 5.4.1).

For its bedrest studies, ESA uses the facilities at the DLR Institute of Aerospace Medicine in Cologne, Germany, and the Institute for Space Medicine and Physiology MEDES (known as the space clinic) in Toulouse, France. Depending on the location, these studies are organised in cooperation with DLR or CNES, respectively.

One topic pursued in 2010 was artificial gravity through centrifugation on a short-arm centrifuge. At MEDES, between March and July 2010, three 15-day study campaigns took place, each including five days of bedrest, to test different artificial gravity protocols. This work was complemented by a set of three similar campaigns at the DLR Institute (November 2010 to May 2011), with five days of bedrest to test the feasibility and effectiveness of an exercise

Figure 5.4.1. Exercise device used during a bedrest campaign with the subject tilted head down. (CNES/S. Levin)

protocol that could be performed during centrifugation. Further studies of artificial gravity will resume once necessary modifications to the short-arm human centrifuges are completed.

Another ESA research theme is nutrition. From February to September 2010, two campaigns including 21 days of bedrest were conducted at the DLR Institute, involving eight male subjects to test the use of potassium bicarbonate as a dietary supplement to mitigate the impact of spaceflight on bone and muscular metabolism. This line of investigation continued with two medium-duration (21 days) bedrest studies, also at the DLR Institute, the first of which took place in September/October 2011, combining potassium bicarbonate with whey protein supplements. Finally, starting in early 2012, three medium-term studies at MEDES will test to what extent this combined dietary supplement of potassium bicarbonate and whey protein increases the effectiveness of exercise on a vibration plate.

To ensure the consistency of results, the bedrest campaigns are required to comply with strict protocols with regard to the participants' activities and sleep patterns, diet and environmental conditions. Participants are regularly tested to determine changes in bone density, muscular strength, gait and balance, as well as to assess the impacts on the cardiovascular or neurosensory systems.

5.4.3 Isolation and Confinement Studies

Over the last two decades, the European scientific and technology community has gained considerable experience in assessing the risks to humans in the space environment, based on isolation studies, combined with other ground-based simulation facilities and data from low-Earth orbit space missions. Such research has helped to determine psychological aspects of spaceflight such as the psychology of group dynamics and the effects of isolation and confinement on individual performance. Combined with data from human spaceflight missions, this research has been invaluable in helping to understand how humans adapt to conditions in space, and in the development of support systems.

Mars500

In November 2011 the isolation period for the Mars500 study came to a successful conclusion. The principal finding was that a six-person international crew could cope with the psychological rigours of a long period (520 days) in an enclosed spacecraft environment.

The Mars500 study is one of the most extensive human spaceflight simulations ever undertaken, with a six-member crew – three Russians, one Chinese and two Europeans – being confined for 520 days in a purpose-built isolation facility at the Institute for Biomedical Problems (IBMP), in Moscow, Russian Federation. Many research protocols were implemented to see how an international crew would cope with such a long period of isolation, which simulated the journey to Mars and back, including orbiting the planet, and landing on the martian surface with associated spacewalks. To add to their isolation, communications with Mission Control were artificially delayed to mimic the natural delays over the great distance that a real Mars flight would involve.

The ESA research protocols focused on several areas, from psychology and physiology to technology demonstrations. The psychological protocols focused on the effects of such a long period in isolation on social adaptation and group structure/dynamics, as well as the impacts of confinement on coping strategies and increased feelings of stress and loneliness.

The physiological protocols focused on the physiological effects of confinement and the psychological influences on physiological processes. These included the

effects of inactivity and stress on cardiovascular deconditioning and immune response. Linked to immune response, an additional protocol involved microbial sampling inside the isolation facility, including testing a microbial probiotic food product.

In connection with the physiological (and psychological) wellbeing of the participants, some protocols tested the use of different measures to counter the effects of isolation. These included a test of a vibration exercise device on postural/locomotor muscles, a test of the effect of exercise with and without a dietary supplement on mental and physical performance, and an analysis of blood for levels of omega-3 fatty acids (important in many biological functions in the human body) in order to suggest an appropriate supplement to enhance psychological wellbeing. Another protocol involved stimulation with blue-enriched light to assess its effects on sleep–waking behaviour, sleep quality, subjective alertness levels and circadian rhythms.

The final set of ESA research protocols were linked to the testing of technologies and the retention of required skills during the isolation period. These included tests of training software related to complex spacecraft docking procedures, of refresher training courses and participants' theoretical and manual medical skills, as well as of a technology to support the crew in coping with unexpected situations.

The results of the research protocols during the Mars500 study will help in the development of pharmacological tools, dietary supplements and exercise programmes, as well as technologies, in order to optimise the health, wellbeing and performance of astronauts on future space exploration missions.

The Mars500 study was a joint project between IBMP and ESA. The 520-day isolation period started in June 2010 following an extensive period of candidate selection and training, and an initial 105-day study successfully undertaken in 2009. At the end of the isolation period, the crew underwent extensive medical checks and psychological evaluations until December 2011 in order to compile the final set of mission data for comparison and analysis.

Concordia

ESA has been cooperating with the Antarctic station Concordia (Fig. 5.4.2) since 2001. The location of the Italian/French Concordia base is considered to be one of the most hostile on Earth. The base and its 12–14 crewmembers are virtually inaccessible from February to November (the Antarctic winter). ESA's Directorate of Human Spaceflight and Operations is using Concordia's unique environment to prepare for future human missions to the Moon or Mars, and is supporting the French Institut Paul Emile Victor (IPEV) and the Italian Antarctic Programme with medical monitoring, operational validation of life-support technologies (especially water recycling) and psychological training.

ESA also coordinates regular Europe-wide Announcements of Opportunity to participate in all of Concordia's research in medicine, physiology and psychology. Based on these, experiments on a variety of topics are performed. In winter 2010, for example, studies investigated the positive effects of exercise on mood, medical skill maintenance, general physiological and psychological adaptation to this extreme environment, as well as the long-term effects of this stressful environment on the functioning of the immune system. Changes in microbial communities over time were also monitored.

During the winter of 2011, the research focused on sleep, cognitive performance, the effects of exercise as well as general physiological and psychological adaptation parameters. In addition, a new psychological questionnaire is being tested, that may provide a fairly complete overview of psychological effects of isolated and confined environments. The measurements will continue during winter 2012 for a second season of data gathering. New investigations of changes in the cardiovascular system and in

Figure 5.4.2. The Concordia Station in Antarctica in winter 2010. (IPEV)

team behaviour will be performed. On the technical side, elements of a crew support tool will be tested, which will support scheduling of activities and training, as well as some individual and team performance measurements. In future, these elements may become components of a mission support system for crews exploring the surface of other planets such as Mars.

5.4.4 Biological Effects of Radiation

When long-duration space exploration missions beyond low-Earth orbit become a reality, their crews will be exposed to significant doses of ionising radiation from galactic cosmic radiation and solar particle events. The secondary particles from the interaction of this radiation with spacecraft materials, planetary surfaces or a planetary atmosphere (in the case of Mars) have to be considered.

The Investigations into Biological Effects of Radiation (IBER) project is assessing the risks related to radiation in various exploration scenarios, with a programme of experiments on biological materials using the particle accelerator facility at the GSI Helmholtz Centre for Heavy Ion Research in Darmstadt, Germany. These experiments should contribute to improved risk assessments or to studies of countermeasures to allow the safe and stable human exploration of the Moon or Mars, for example, with an acceptable level risk of exposure to space radiation.

Following an Announcement of Opportunity released in 2008, 10 positively evaluated two-year projects were implemented. In a total of five beamtime windows, a variety of cells, tissues and detectors were irradiated. The research topics ranged from physics or the basic characterisation of cell damage and repair, to the effects of radiation on specific tissues such as the brain or photoreceptors, often using innovative tissue models.

In late 2010, as the 2008 experiments were approaching completion, ESA released another Announcement of Opportunity, which led to 15 proposals that have since passed scientific and feasibility evaluations.

The GSI Helmholtz Centre currently offers two heavy-ion accelerators: the low-energy Universal Linear Accelerator (UNILAC) (Fig. 5.4.3) and the high-energy Heavy-Ion Synchrotron (SIS). With the planned expansion of the facilities to incorporate the Facility for Antiproton and Ion Research (FAIR), ESA is uniquely placed to continue its research in support of future European exploration activities, and to undertake experiments that are not possible anywhere else.

Figure 5.4.3. The linear accelerator UNILAC – inner view of the Alvarez structure. (GSI Helmholtzzentrum für Schwerionenforschung GmbH)

5.5 Physical Sciences: IMPRESS

ESA's ground-based research in the physical sciences complements the activities undertaken on the ISS and other microgravity platforms. Intermetallic Materials Processing in Relation to Earth and Space Solidification (IMPRESS) was a €41 million integrated project involving 40 organisations in Europe and Russia, which was completed in 2010. This five-year EU project, coordinated by ESA, included a multidisciplinary team of 150 researchers with expertise in many fields, including physical metallurgy, chemistry, metrology, fluid science, space experimentation, computer modelling, environmental engineering and industrial product development relevant to turbomachinery, industrial catalysts and fuel cells.

Within IMPRESS, two specific families of intermetallics were studied, namely titanium aluminides and nickel aluminides. Titanium aluminide intermetallics have remarkable mechanical and physical properties at temperatures up to about 800°C. The combination of high melting point, high-temperature strength, creep resistance and low density makes titanium aluminides ideal for high-performance gas turbine blades. Nickel aluminide intermetallics, on the other hand, have good catalytic properties making them particularly useful for numerous hydrogenation reactions in the chemical industry, and as electrocatalysts in alkaline fuel cells.

5.5.1 Titanium Aluminide Turbine Blades

Cost-effective titanium aluminide blades (Fig. 5.5.1) were cast within the IMPRESS project. Prior to IMPRESS, many turbine and aero-engine producers had attempted this, at great expense but with little success. From a detailed assessment, it appears that the manufacturing technology developed within IMPRESS, supplemented by studies of the solidification fundamentals, led to significant improvements in the quality, yield and cost-effectiveness of titanium aluminide castings. Indeed, from the viewpoint of improving industrial casting models, IMPRESS has helped to create accurate thermophysical property databases for liquid intermetallics for the first time. These achievements have been made with the help of benchmark electromagnetic levitation experiments carried out in space.

In terms of materials development, following an alloy development programme, two titanium aluminide alloys were selected, one with added niobium (Ti–^{46}Al–^{8}Nb) and one with added tantalum (Ti–^{46}Al–^{8}Ta). These alloys permit a special heat treatment (developed within IMPRESS) and pressing sequence that produces a complex convoluted microstructure in the alloys, which in turn provides an excellent balance of mechanical properties in the turbine blades produced from them. Numerous other parts of gas turbines could benefit from these lightweight, high-strength materials, including high-pressure compressors, stator vanes, centrifugal impellers, as well as large turbochargers. In addition, a novel and commercially viable recycling route developed within the IMPRESS project is ready for industrial upscaling, and a new low-cost alternative for ingot production has been developed.

Figure 5.5.1. Centrifugally cast titanium aluminide alloy low-pressure turbine blades. (ACCESS, Germany)

This class of titanium aluminide alloys represent a 40–50% weight reduction for low-pressure turbine stages, compared with conventional nickel superalloys. If successfully implemented by industry, such a significant weight reduction could lead to aero-engines with improved thrust-to-weight ratios, higher efficiency, reduced fuel consumption and lower exhaust emissions. Industrial gas turbines also stand to benefit. Beyond IMPRESS, the next stage will focus on industrial upscaling, validation testing and supply chain management, to ensure that European industry and the environment benefit from these major technological advances.

5.5.2 Sponge Nickel Catalysts

Sponge nickel catalysts have been in use for over 80 years for many industrial reactions but the traditional processes have many limitations. Normally, these catalysts are prepared by casting and crushing nickel–aluminium ingots followed by caustic leaching in sodium hydroxide to remove the aluminium atoms and to create a large catalytically active surface area. Within the IMPRESS project, however, a cost-effective gas atomisation process was used to produce rapidly solidified spherical nickel aluminide powder with non-equilibrium structures (Fig. 5.5.2). More than 600 nickel aluminide gas-atomised samples were produced, tested and characterised. As a result it was realised that the microstructure of gas-atomised powder is important and can be tailored to give better catalytic performance after sodium hydroxide activation. For the first time in this field, within the IMPRESS project, a link between the process, structure and final catalytic properties has been defined.

The data from space-flown experiments are also contributing to the understanding of solidification fundamentals and providing thermophysical properties that are of great importance in improving computer models. To this end many multiscale structures are now being predicted.

The IMPRESS team has developed nickel catalysts an order of magnitude better than the current standard Raney composition catalysts for various industrial chemical reactions. The sponge nickel developed by the IMPRESS team has been extensively tested in alkaline fuel cells (Fig. 5.2.3), and the results are very promising, since sponge nickel provides excellent catalytic performance as part of anodic electrodes. Indeed, the performance of this nickel powder is better than conventional platinum–palladium catalysts, at a fraction of the cost, for well over 2000 h of operation. This development could offer commercial opportunities to bring more affordable and more reliable alkaline fuel cells to the market.

Successful scale-up trials have already been undertaken. By using such enhanced lower-cost catalysts, it is expected that there will be significant savings for the chemical and energy sectors in terms of cost, time, energy and CO_2 emissions. IMPRESS has made a significant scientific and technical contribution to achieving ‘sustainable chemistry’ in Europe.

IMPRESS has made substantial progress on all fronts, giving confidence that the new industrial prototypes will eventually be brought to the market by suppliers and end-users. The impact of this will be felt once prototypes are in service and are able to reduce greenhouse gas emissions, in particular CO_2.

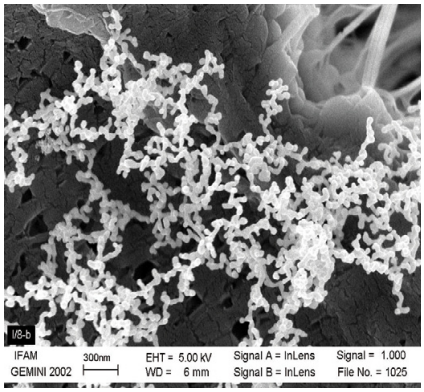

Figure 5.2.2. Metal nanoparticles produced in weightlessness via an evaporation–condensation process. (IFAM, Bremen, Germany)

Figure 5.2.3. A commercial alkaline fuel cell. (Hydrocell Oy, Finland)

→ PROJECTS UNDER DEVELOPMENT

6. Projects under Development

Announcements of Opportunity are released periodically by ESA in order to extend the boundaries of scientific knowledge and to ensure that the research facilities available on the International Space Station and other microgravity platforms are fully utilised. For some of the experiments chosen for their scientific value there may be quick turnaround times from selection to flight due to their size and simplicity, while for others there may be longer lead times to flight due to greater complexities involved in hardware development, refining experimental procedures, etc.

6.1 Life Sciences

In the area of the life sciences, ESA's International Life Science Research Announcement in 2009 has delivered many experiments in human research and biology that will define the pattern of research in the coming years.

6.1.1 Human Research

Analysis of exhaled air on the ISS using devices such as ESA's Portable Pulmonary Function System is proving valuable for research purposes, providing indications of specific physiological processes and conditions. This type of analysis will be utilised within ESA's cardiopulmonary research to support the evaluation of the mechanisms underlying oxygen uptake during exercise on the ISS, and to draw correlations between changes in oxygen uptake and work undertaken in weightlessness.

The research will also evaluate exhaled nitric oxide under normal pressure and reduced airlock pressure (used in preparation for spacewalks) to examine the mechanisms underlying the lower nitric oxide levels observed in weightlessness and at reduced pressure. This is an important issue for astronaut health and wellbeing, and continues from previous ISS research. Additional cardiopulmonary research will correlate cardiovascular parameters with parameters obtained using a method called ballisto-cardiography, which analyses 3D movements of the human body to provide new information on mechanical aspects of the cardiovascular system.

Figure 6.1.1. Frank De Winne using the advanced Resistive Exercise Device (aRED) on the ISS in June 2009. (NASA)

Within the area of musculoskeletal research, a key study is examining the effects of weightlessness on bone metabolism. ESA is planning a number of experiments to look into various aspects of these effects in the future. This work will include the use of the advanced Resistance Exercise Device (aRED) in Node 3 (Fig. 6.1.1) to quantify factors of bone and muscle loading such as the torque on human joints to improve exercise countermeasures; and the use of ESA's Muscle Atrophy Research and Exercise System (MARES) in the near future as part of musculoskeletal research activities. In addition, experiments using two complementary computed tomography devices pre/postflight will determine bone changes and recovery as a consequence of exposure to weightlessness. This will build on previous research and could be incorporated into the current Early Detection of Osteoporosis in Space (EDOS) project (see section 4.1.2, Musculoskeletal Research). The SOLO experiment will continue to determine the mechanisms and links between salt intake and bone metabolism and thus the development of measures to counter bone mass reduction, while a new experiment will assess cartilage degeneration and metabolism using MRI analysis.

The neurological effects of spaceflight represent an expanding field of research, and many research projects within ILSRA-09 will look into different aspects of neuroscience, ranging from the occurrence and characteristics of

headaches among astronauts to alterations in circadian rhythms in space. For astronauts, their hands are their principal means of locomotion and means to undertake work, and are more important in space than they are on Earth. One future project will look into the adaptation of grip force coordination in weightlessness and the interaction of different neurological cues in this process (a project from ILSRA-04). Another will aim to determine which neurological processes specifically influenced by gravity play a role in the action of reaching and grasping objects.

Other experiments in neuroscience will study altered visual perception in space by comparing proflight, inflight, and postflight observations of perspective-reversible figures; the navigation strategies used by astronauts during adaptation to weightlessness by measuring head-and-body acceleration using body sensors; and adaptive processes in the central nervous system while testing the effect of using a vibrotactile vest on spatial orientation, and using advanced MRI methods to examine neurovestibular and vestibulo-autonomic processes.

A final experiment will test the hypothesis that long-duration spaceflight significantly affects the synchronisation of the circadian rhythm in humans due to changes in the (non-) 24-hour light–dark cycle, reduced physical activity and body composition, as well as heat transfer and thermoregulation.

In the area of immunology, one of the experiments with a heritage in the Immuno experiment will investigate the interactions between stress and various biological stress-response systems on the ‘upstream’ (brain) and ‘downstream’ (immunity) functions, while another will test global functional cellular immunity.

A final human physiology project will study the ageing of skin in microgravity and consequently develop a mathematical model of ageing skin.

Several of these experiments, notably those concerned with bone loss, work capacity and neurovestibular function, are also important in the context of maintaining the health and performance of astronauts in future long-duration missions, such as activities in preparation for human space exploration. Studies related to work capacity, oxygen uptake during training and exercise kinematics, are also highly relevant for current and future medical operations and are planned and implemented together with astronaut trainers.

6.1.2 Biology Research

In addition to the Gravi-2 experiment (see section 4.2, Biology Research), ESA is planning and preparing a full spectrum of biological research to be flown on the ISS. Many of these studies will use facilities such as the Kubik incubators, Biolab and the European Modular Cultivation System.

Cellular biology is again the area that will command most attention in terms of the volume of experiments undertaken. The TripleLux A and B experiments will investigate cellular mechanisms involved in impaired immune response and enhanced response to radiation using rat macrophages (a type of white blood cell) focusing on the ability for the cells to engulf foreign material (phagocytosis), while the RHOCYT experiment will investigate the effect of weightlessness on Rho GTPase signalling proteins that control the cytoskeleton, and are important for cellular structure and function.

Looking further into the future, following the International Life Science Research Announcement in 2009, numerous cellular biology experiments will study the effects of weightlessness on, for example, immune cell activation (following up on the TripleLux experiments); mesenchymal stem cells (which can differentiate into bone, cartilage and fat cells); endothelial cells (which line the circulatory system) in relation to function and organisation; osteogenic cells (which differentiate into bone-forming cells, osteoblasts) and determining which are most sensitive to changes in gravity; fibroblasts (the most common

cells in connective tissue) with respect to cytoskeleton reorganisation; and gene expression in yeast cells.

Additional research projects will be carried out with zebrafish, medaka (ricefish), insect larvae and planarians (flatworms). Following on from these experiments, the ArtEMISS (*Arthrospira* sp. gene Expression and mathematical Modelling on the ISS) experiment will carry out research in closed ecological life support systems (of importance for future human exploration missions, for example) by determining the effect of spaceflight conditions on Arthrospira algae.

ESA's plant biology research will follow up on previous research on the ISS (ESA's Genara and NASA's Tropi experiments) to study Arabidopsis seedlings with respect to cellular responses to light stimulation in weightlessness, as well as following up on the PHOTO-II (Survival and Development of Photosynthetic Oxygenic Organisms Tolerant to Space Radiation and Production of Compounds with Anti-Oxidant Properties) experiment on the Foton-M3 mission with a study of the effect of space radiation on photosynthesis in specific algae.

Additional experiments in biology on the ISS will study the interactions between microorganisms and minerals with future applications in *in situ* mineral processing for future exploration missions (to the Moon and Mars); and microbial species on the ISS through interior sample collection and analysis. External experiments will involve *in situ* spectroscopic analyses of the evolution of organic compounds in the space environment and undertake global tracking of small animals using intelligent tags and the ISS as a data relay station.

6.1.3 Astrobiology Research

Following the completion of the experiments on Expose-E and Expose-R (see section 4.9, Space Exposure Research), a new set of experiments has been selected. Known as the Expose-R2 mission, implementation in collaboration with the Russian partners has commenced, with a planned launch in late 2012.

6.2 Physical Sciences

ESA is developing a number of major projects in the physical sciences, in addition to specific pieces of future hardware or experiments discussed in earlier chapters and ongoing experiments/projects such as the Solar facility and the Vessel ID system, which are scheduled to continue functioning for the foreseeable future. In the future, two major ESA facilities will be flown to the ISS and installed on the External Payload Facility of Columbus – the Atomic Clock Ensemble in Space (ACES) and the Atmospheric Space Interactions Monitoring Instrument (ASIM).

6.2.1 Atomic Clock Ensemble in Space (ACES)

ACES is being developed in cooperation with the French Space Agency (CNES) and will expand the range of research on the ISS. The ACES payload (Fig. 6.2.1) consists of two extremely complex, high-performance atomic clocks: PHARAO (Projet d'Horloge Atomique par Refroidissement d'Atomes en Orbite) and the Space Hydrogen Maser, which promise the most precise measurements of time in space. Together, they will be accurate to about one second in 300 million years.

The frequency reference generated on the ISS will be used by a worldwide network of ground terminals to perform comparisons with the best available atomic clocks on the ground. The most precise measurement of time yet in space will be used to probe our knowledge of the fundamental laws of physics governing the Universe. ACES will test Einstein's theory of General Relativity and alternative theories of gravitation. Taking full advantage of the microgravity environment and global coverage provided by the ISS, ACES will establish a stable and accurate onboard timescale which will be used to perform space-to-ground and ground-to-ground comparisons of best available atomic frequency standards. This is why measuring time as accurately as possible in space is of extreme interest.

This area of research will be expanded in the future with additional projects such as Space Optical Clocks (SOC) and Quantum test of the Weak Equivalence Principle (QWEP) on the ISS.

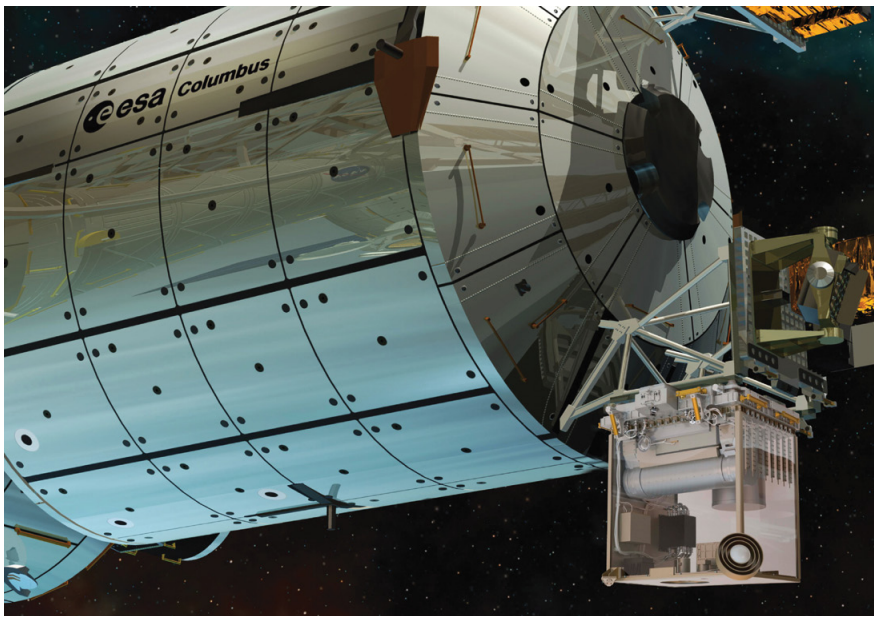

Figure 6.2.1. Artist's impression of the ACES payload attached to the Columbus module. (ESA/D. Ducros)

6.2.2 Atmosphere–Space Interactions Monitor (ASIM)

The ASIM facility is an external, observatory-type payload for Columbus that will study giant electrical discharges (lightning) in the high-altitude atmosphere above thunderstorms, and their role in Earth's climate. The instrument payload includes light detectors that are sensitive in the optical range (cameras, photometers) and in the X-ray to gamma-ray ranges (imaging spectrometer).

6.2.3 Materials Science Research

The very positive results of the IMPRESS project (section 5.5) have led to two further EU-funded projects coordinated by ESA – ThermoMag and Accelerated Metallurgy – which are now in the early stages of development.

The core concept of the ThermoMag project (€6 million) revolves around the development of new energy-harvesting thermoelectric materials and proof-of-concept modules based on nanostructured magnesium silicide. The thermoelectric materials developed will have attractive characteristics with respect to thermodynamic efficiency, operational temperature, melting point, thermal stability, corrosion, strength and toxicity, as well as their low density and the low cost of raw materials and manufacturing. In order to prove the concept works, the project will assemble demonstrator modules that integrate the new energy-harvesting nanostructured materials. These modules have widespread applications in the automotive, aerospace and manufacturing sectors, where waste heat can be usefully recovered, with clear environmental benefits.

The core concept of the Accelerated Metallurgy project (€24 million) is to deliver an integrated facility for synthesising and testing many thousands of unexplored alloys. This would be the first facility of its kind and would represent a significant advance for metallurgy. The novel technology to be employed in this facility is based on automated, direct laser deposition. The key feature of this technology is the way in which a mixture of elemental powders is accurately and directly fed into the laser's focal point, heated by the laser beam, and deposited on a substrate in the form of a melt pool, which finally solidifies to create a unique, fully dense alloy with a precise chemical composition.

This robotic alloy synthesis is 1000 times faster than conventional manual methods. Once produced, these discrete millimetre-sized alloy samples will be submitted to a range of automated, standardised tests to measure their chemical, physical and mechanical properties. The vast amount of information produced will be recorded in a 'Virtual Alloy Library' and coupled with computer codes such as neural network models, in order to extract and map out key trends linking process, composition, structure and properties. The most promising alloy formulations will be further tested, patented and exploited by end-users. Industrial interests include: new lightweight fuel-saving alloys for aerospace and automotive applications; high-temperature alloys for rockets, gas turbines, jet engines, nuclear fusion; high-temperature superconductor alloys for electrical applications; thermoelectric alloys with high thermodynamic efficiency for converting waste heat directly into electricity; magnetic and magnetocaloric alloys for motors and refrigerators; and phase-change alloys for high-density memory storage. The accelerated discovery of these alloy formulations will have a significant impact on society.

Turning from ground to in-orbit activities, research using the Materials Science Laboratory will continue in the future with projects such as the Solidification along a Eutectic Path in Ternary Alloys and Binary Alloys (SEBA-SETA) project, which will investigate the microstructures formed in binary and ternary eutectic alloys upon solidification; and the Metastable Solidification of Composites (METCOMP) project which will look at features forming in a bronze alloy by a peritectic reaction involving a liquid phase and solid to form yet another form of solid. The Materials Science Laboratory experiments will

be further complemented with the DIRectional SOLidification (DIRSOL) facility which will be positioned in the Microgravity Science Glovebox (MSG) and will be used for experiments on transparent materials using the Bridgman technique.

DIRSOL is a multi-user facility that will support *in situ* studies of solidification processes and other phenomena in transparent alloys. The samples are flat and rectangular in shape with variable heights and are pulled through the Bridgman assembly at variable speeds. The main diagnostics element of DIRSOL is optical observation with high resolution. The observation camera can observe the samples between the hot and cold zones of the Bridgman assembly at variable positions and viewing angles.

Future research in the field of solidification of metallic samples is supported by new advanced *in situ* diagnostic techniques employing X-rays that are already implemented in the Sounding Rocket programme and are candidates for deployment on the ISS.

ESA's research into zeolite crystallisation processes will be advanced in the future in order to observe the early steps of crystalline formation without the effect of gravity in orbit. This is a likely candidate for the use of an upgraded version of the Protein Crystallisation Diagnostics Facility which was flown to the ISS in 2009. Zeolites have interesting catalytic and molecular sieving properties, with various applications as catalysts, sensors and absorbent materials, particularly in the oil industry. In the future, once the processes influencing the aggregation of zeolite structures have been determined, this could lead to a better control of processes for varying porosity, so that zeolites could be tailored to different applications.

In the same area, a light-scattering instrument will be developed in the future to support studies of solidification of colloidal particles.

6.2.4 Fluid Science Research

Within the area of fluids research, two major projects are scheduled for launch in 2013. FASES and FASTER will study the mechanisms of stabilisation or destabilisation of emulsions using various combinations of surfactants, polymers and particles. FASES will take place inside the Fluid Science Laboratory in Columbus, while FASTER will take place inside the European Drawer Rack. The results of the FASES experiment are expected to be significant for oil extraction, chemical and food industries. FASTER research has applications in industrial domains and is linked to investigations such as foam stability, drainage and rheology. An additional project, called DCMIX, will continue the research undertaken within the SODI-DSC experiment related to the measurement of diffusion coefficients in liquid mixtures. The results of another SODI experiment (SODI-IVIDIL) will be used as the basis to extend studies of the effect of vibration on liquid systems within the VIPIL (VIbrational Phenomena In Liquids) project.

A major fluids experiment that will take place most likely in the 2012–13 timeframe is the Miller–Urey Experiment for the Microgravity Science Glovebox. This is based on the experiment conducted by Stanley Miller and Harold Urey at the University of Chicago in 1953, which simulated the conditions present in the early days of the planets, to figure out how organic compounds were formed from inorganic gases, when sufficient energy is available. In this experiment, vials will be filled with various gas mixtures and solid particles, into which a high-energy spark discharge will inject energy into the system to cause chemical reactions.

In the area of planetary science, the future ICAPS experiment will aim to understand the formation of planetesimals, or planet precursors, by studying dust particles and their agglomeration in conditions representative of pre-planetary conditions.

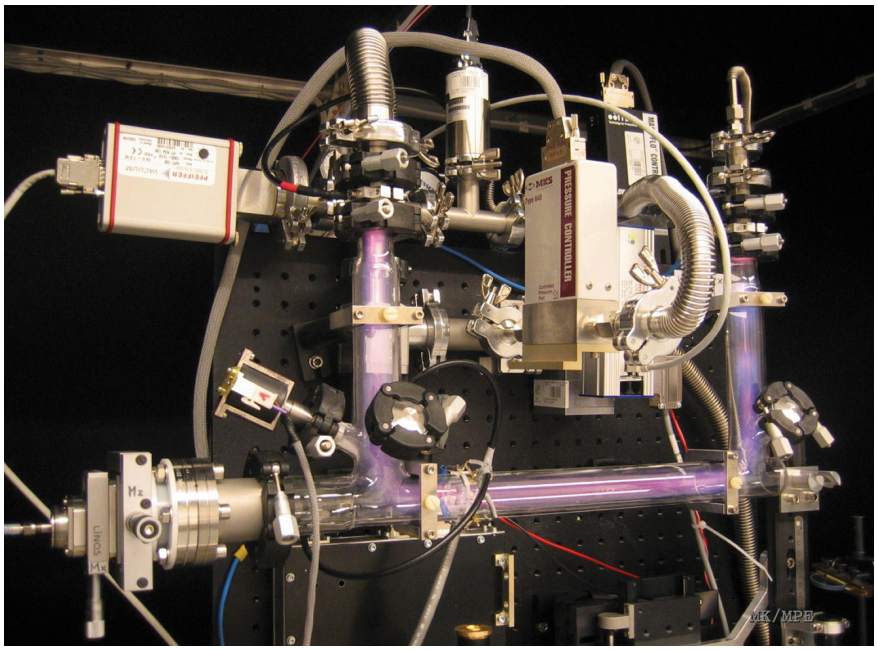

Figure 6.2.2. Plasma inside PK-4 hardware: the 'positive column' of a DC glow discharge. (MPE)

Further fluids experiments include the Convection and Interfacial Mass Exchange (CIMEX) programme, which will investigate fundamental and applied aspects of mass transfer through fluid interfaces; and the FOAM-C experiment, which will enable several studies, including the quiescent coarsening of foams as a function of the liquid fraction, the aggregation mechanisms in colloid solutions and the stress distribution in loosely compacted granular materials. The project focuses on very wet foams that cannot be studied on ground due to the drainage effect.

Further research in the field of heat transfer and boiling in particular are already in the planning with the instruments RUBI (Reference mUltiscale Boiling Investigation) and Thermal Platform I. Additional fluids experiments include an investigation into aspects of Marangoni convection called JEREMI (Japanese–European Research Experiments on Marangoni Instabilities) and a study of the dynamics and statistical mechanics of particles that dissipate due to collisions (Vibration-Induced Phenomena in GRANular media, VIP GRAN).

6.2.5 Plasma Research

In the area of complex plasma research, PK-4 is a successor to the PK-3 Plasma-Kristall space experiments discussed in section 4.5. The elongated geometry of the experiment chamber (Fig 6.2.2) will make it possible to focus on the study of fluid systems in contrast with the static plasma crystals addressed in the previous PK experimental setup. The effects that are planned to be studied at the kinetic level include laminar and turbulent flow, the transition between them, thermodynamics and self-organisation of complex plasma flows, solitons and shocks, interfaces and plasma instabilities, and agglomeration and disagglomeration, among others.

These advances in understanding the physics of the interactions of dust particles in gaseous plasmas have led an international team of scientists to conceive and propose a new generation of instruments that will allow them to shape the interactions such that they closely mimic molecular interactions. This instrument package is at the level of a feasibility study, which will take into account the experience gained with the PK series of instruments.

Even though PK-4 has not been yet flown to the ISS, plans for two follow-up experiments, PlasmaLab and PK-5, are already in the pipeline.

6.2.6 Radiation Research

In addition to the continuation of experiments such as ALTEA-Shield, ESA's radiation research will be strengthened with the 3D Silicon Detector Telescope (TriTel) and DOSIS 3D experiments. In one selected location in the Columbus laboratory, the TriTel instrument will detect radiation entering the station from all directions and record it with time resolution so that the dynamic fluctuations of the incoming radiation and full directionality can be assessed. This will be supported by the DOSIS 3D experiment, which will undertake a 3D mapping of radiation in all parts of the ISS.

6.3 Climate Change Activities

Understanding the causes and impacts of global changes in Earth's climate is crucial for humanity in the coming decades. Various natural physical processes modify the atmosphere, oceans and land surfaces on short and long time scales. However, in the past 150 years human activities have resulted in significant changes in many aspects of Earth's environment, including increasing greenhouse gas concentrations, modification of the nitrogen and phosphorus cycles, and major changes in land use (e.g. deforestation). In order to predict future changes in climate, it is important to understand the interactions between anthropogenic and natural environmental changes (Fig. 6.3.1).

ESA currently has an extensive programme of current and planned dedicated Earth observation missions which support studies of global change. Potentially, the ISS can be used as an Earth observation platform for instruments and experiments, supplementing ongoing and planned global climate change and Earth observations from dedicated satellites, and airborne and terrestrial platforms.

While it is not a dedicated Earth observation platform, the ISS provides a relatively stable platform for operation of observation instruments, as recently demonstrated with JAXA's Superconducting SubMIllimeter-wave Limb-Emission Sounder (SMILES) and NASA's Hyperspectral Imager for the Coastal Ocean (HICO) instruments. Furthermore, the space station has a versatile infrastructure to support instrument operation, including multiple internal and external mounting locations, with power and data connections. The ISS can therefore complement ongoing and planned dedicated Earth observation missions, taking advantage of the specific orbital characteristics – medium

Fig 6.3.1. Image of Egypt taken from the ISS in October 2010, featuring the bright lights of Cairo and Alexandria, the River Nile and its delta. Earth's atmosphere can be seen on the horizon. (NASA)

inclination (51.6°) and low-altitude orbit (350–400 km), regular observations of the tropical regions and observations at different local times of day.

An ESA user consultation in 2009 showed a high level of interest among the scientific community in using the ISS for observations related to climate change. An Announcement of Opportunity was therefore released in July 2011 to solicit proposals for flight experiments relevant to global climate change using the ISS. The evaluation process is still ongoing, based on standard and rigorous peer review, and the recommendations will be presented for approval in May 2012. After the selection, the definition work for initial studies and development of the instruments will begin. The final selection of flight experiments relevant to global climate change will complement ongoing projects in this field and will consolidate the research plan for ISS utilisation.

6.4 Upcoming Astronaut and Logistics Missions

In support of future research, ESA and its international partners are constantly planning and replanning experiment schedules in order to optimise the use of the ISS and its resources for research. These resources include power and data capabilities, the use of different research racks and experiment hardware, astronaut time and the upload and download capabilities on logistics spacecraft.

At the time of writing, André Kuipers was undertaking a six-month mission on the ISS as an Expedition 30/31 crewmember. During his mission Kuipers is undertaking a full complement of research activities for ESA (and other ISS partners), along with additional education and public relations activities as part of the PromISSe mission. Looking further into the future, Luca Parmitano will be the next ESA astronaut to visit the ISS as Flight Engineer and Expedition 36/37 crewmember in 2013. As in all ESA astronaut missions, Parmitano will undertake an extensive programme of research activities in addition to his tasks as an ISS Flight Engineer. Following on from Parmitano, ESA astronaut Alexander Gerst is scheduled to fly to the ISS in 2014, as an ISS Expedition 40/41 crewmember. Further plans for additional ESA astronauts to fly on missions to the ISS are being scheduled.

With regard to logistics spacecraft, ESA's third ATV, *Edoardo Amaldi*, was launched to the ISS, and docked with the Station at the end of March 2012. The ATV is one of the principal means of transporting research equipment and samples to the ISS, and also for ESA to contribute to the overall costs of the ISS. Beyond ATV-3, it is expected that the fourth ATV, *Albert Einstein*, will be launched in early 2013. As well as bringing research equipment food, water, air, propellants and additional essential supplies to the ISS, ESA's logistics vehicles will be used to carry out ISS attitude control, reboost the ISS to a higher orbital altitude to account for atmospheric drag, and carry out debris avoidance manoeuvres if that is deemed necessary at any point during the mission. The ATV will also be used to remove unwanted equipment and waste from the station at the end of its mission, undertaking a planned destructive reentry into the atmosphere after undocking from the ISS.

During 2012 the new unmanned US cargo vehicles Dragon (SpaceX) and Cygnus (Orbital Sciences) should become operational and allow for the return of samples from the ISS (currently this is only possible with Soyuz).

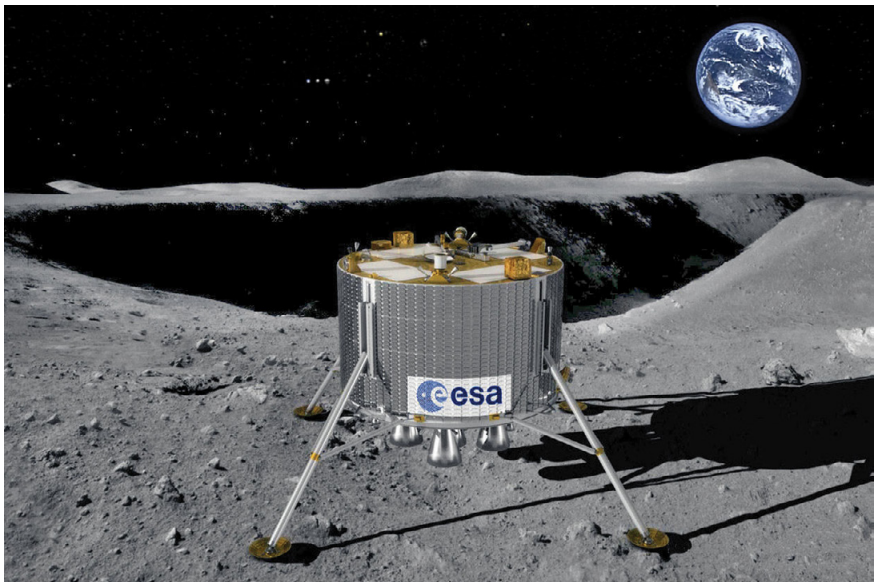

Fig 6.5.1 ESA's Lunar Lander at the lunar south pole. (ESA)

6.5 Lunar Lander: A Precursor Mission to Future Human Exploration

Recent years have seen a resurgence of international interest in further exploration of the Moon, with new missions being planned by several countries, including the United States, the Russian Federation, Japan, China and India. In Russia a new Moon exploration programme is taking shape with a Lunar Polar Sample Return as its main mission. The Moon is increasingly seen as an important target for future exploration, providing new and unique opportunities for scientific research that will yield both cultural and economic benefits.

In this context, ESA is preparing an unmanned Lunar Lander mission (Fig. 6.5.1), as a precursor to future human exploration of the Moon and beyond. The mission seeks to prepare Europe for participation in future human and robotic exploration efforts by developing and demonstrating new technologies, increasing the knowledge required to prepare future exploration programmes, and gaining experience of working and operating in the lunar environment. These aspects are achieved first by driving the development of key technologies for soft, safe precision landings, and second by operating payloads on the surface of the Moon. The target location for the mission is the lunar south pole, which has been highlighted as a favoured site for future human exploration activities and where favourable illumination conditions could enable an extended lifetime for surface operations.

The experiments in the Lander's payload will be focused on scientific investigations that will enable the exploration programmes of the future. These include investigations into the complex lunar environment and its effects on human explorers and surface systems, and exploring opportunities posed by the presence of resources (e.g. water and other volatiles) at the lunar poles.

With a distinct synergy with the Lunar Polar Sample Return mission, the European Lunar Lander may open the way for possible cooperation between ESA and the Russian Federation on Moon exploration in the near future.

6.5.1 Mission Outline

The launch of the Lunar Lander mission is planned for late 2018 on a Soyuz launcher from Centre Spatial Guyanais, Kourou. After launch, the Lander spacecraft will inject itself onto a transfer orbit to the Moon. Following a

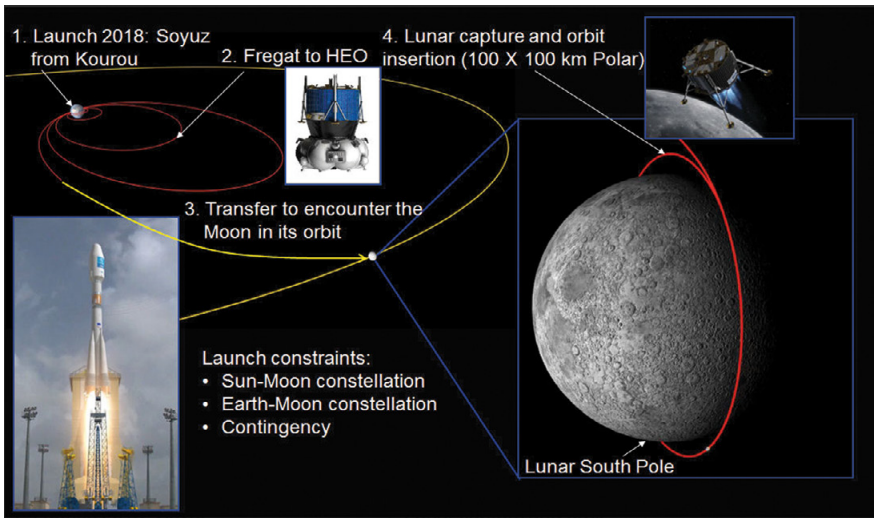

Figure 6.5.2. The Lunar Lander mission from launch to insertion into orbit around the Moon. HEO: highly elliptical orbit. (ESA)

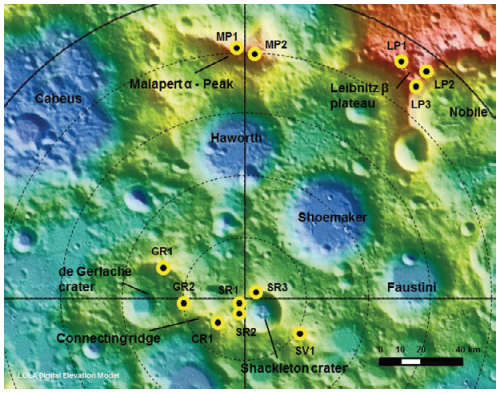

Figure 6.5.3. Potential landing sites with favourable illumination conditions identified near to the lunar south pole. Detailed analyses of the characteristics of these sites are under way. (ESA)

transfer of several weeks, the Lander spacecraft will reach a polar orbit around the Moon (Fig. 6.5.2). The Lander will then remain in orbit around the Moon for up to three months to allow checkout and calibration of the systems critical for landing, and to wait for the optimal orientation of Earth, Sun and Moon.

The descent and landing marks the demonstration of a key technology for the future of space exploration, and the primary objective of the mission, in which automated systems navigate and control the descent of the Lander from orbit to a precise landing with an accuracy of a few hundred metres. The landing site (Fig. 6.5.3) will be a topographic high point in the polar region, at which long periods of solar illumination can be used to extend the duration of surface operations beyond the 14 days typical of landing sites at lower latitudes.

6.5.2 Characterising Potential Landing Sites

The angle between the Moon's axis of rotation and the ecliptic plane results in small areas near the poles where the Sun very rarely sets. Their potential for near-continuous periods of illumination makes these sites highly attractive for exploration missions. In addition, nearby craters remain in continuous darkness and appear to be cold traps for volatiles and water ice, which may have future applications as resources that can be utilised to support exploration.

For the Lunar Lander mission the identification of sites that experience several months of sunlight is key to the overall mission preparations. The illumination conditions at these sites determine the duration of surface operations, and the sizes and properties of these sites define the engineering drivers for the landing. High-resolution topography and image datasets from

Table 6.5.1. Research areas and subjects of investigation for the Lunar Lander.

Research area	Investigation
Human health	Toxicity of lunar dust and the associated risks to humans. Radiation environment and likely hazards to humans.
Lunar environment and its effects	Characterisation of suitable landing sites for future exploration. The properties of dust and its effects on systems. The plasma environment and its coupling with charged dust and the lunar surface and resultant effects.
Resources	Availability and distribution of water, other volatiles and mineralogical species. Physical properties of potential resources and their source materials.
Preparations for future human activities	Characterisation of the surface bounded exosphere before it is permanently altered by human activities. Feasibility assessment of the Moon's surface for astronomical exploitation, particularly in radio.

the Lunar Reconnaissance Orbiter are key to performing these analyses. The analyses performed to date indicate that the size of 'well' illuminated landing sites is of the order of hundreds of metres.

6.5.3 Science to Enable Future Exploration

The wealth of data from recent lunar missions, reassessments of results from the Apollo era and analyses of lunar samples available on Earth using new techniques and technologies have had profound effects on our understanding of the Moon. The lunar environment is now understood to be dynamic, offering new opportunities for exploration, as well as challenging and complex. This is especially true in the regions near the poles, where abundant volatiles may be found and utilised, and where complex interactions between charged dust, plasma and electric fields pose unique challenges for systems and surface operations. Before developing a programme of sustainable lunar exploration a number of key gaps in our knowledge need to be filled to ensure that the human explorers and exploration systems of the future can be confident and prepared to overcome the challenges they will face.

A number of research areas have been highlighted to be addressed for the Lunar Lander mission (see Table 6.5.1). The identified subjects represent those of high priority, which are also considered feasible within the engineering boundary conditions presented by the mission.

6.5.4 Experiments under Consideration

A model payload is under investigation as part of the ongoing mission study (see Table 6.5.2), and is being used to inform the mission study in advance of a formal Announcement of Opportunity and selection, expected in early 2013.

The experiments in this model payload have been defined to address some of the many unknowns:

— The Lunar Dust Analysis Package (L-DAP) will perform *in situ* microscopy and compositional analysis of lunar dust and regolith. Lunar dust is both a hazard for lunar exploration and a potential asset. While potentially toxic to humans and hazardous to surface infrastructure, dust also contains potential resources that may be essential for the sustainability of future exploration.

— The Lunar Dust Environment and Plasma Package (L-DEPP) will determine the properties of the highly complex integrated dusty plasma environment at the lunar surface. This environment is poorly understood, in particular the charging, levitation and transport of lunar dust particles.

— The Lunar Volatiles Analysis Package (L-VRAP) will measure the species of volatiles present on the lunar surface, their abundance and distribution from a landed platform and demonstrate their extraction, as a precursor to future *in situ* resource utilisation. Recent observations have shown that extensive quantities of volatile elements and molecules are present near the lunar poles. These volatiles are potentially the most important resources on the Moon, enabling sustainable long-term exploration and potentially providing a source of fuel for exploration beyond the Moon.

— A stereo panoramic imager camera will acquire wide-angle stereo and narrow-angle monoscopic high-resolution imaging to characterise the landing site, monitor operations and provide information on the composition of rocks and soils.

— A radiation monitor will measure the radiation environment in which future explorers must live and operate, providing vital ground truth to validate radiation environment models.

— A Robotic Arm Camera will provide close-up, multispectral images of the lunar surface in the vicinity of the Lander.

— An experimental Mobile Payload Element is under investigation by DLR as a stand-alone robotic element to demonstrate robotics and mobility capabilities on the lunar surface.

The ESA Lunar Lander project offers a unique opportunity to address key, diverse scientific questions that can be enabling for the exploration programmes of the future. The science investigations are truly interdisciplinary in nature, combining disciplines from life sciences, physical sciences, space and planetary sciences and astronomy. Such an interdisciplinary approach is key to future exploration, in which humans and space systems must operate together in the complex environments that exist at the surface of the Moon, and especially at the poles.

Package	Instrument
Lunar Dust Analysis Package (L-DAP)	AFM
	Micro-Raman laser-Induced Breakdown Spectroscopy (LIBS)
	Microscope
	External Raman LIBS
Lunar Dust Environment and Plasma Package (L-DEPP)	Dust sensor
	Langmuir probes
	Radio antenna
	Ion/electron spectrometer
Lunar Volatile Resource Analysis Package (L-VRAP)	Gas chromatograph mass spectrometer
	Ion trap mass spectrometer
Experiments not studied within the above packages	Panoramic stereo camera
	High-resolution camera
	Robotic arm camera
	Radiation monitor
Mobile Payload	Mobile Payload experiment

Table 6.5.2. Experiments being considered for the Lunar Lander payload.

→ SCIENCE AND ROBOTIC EXPLORATION

Contents

→ INTRODUCTION

1. Introduction

This part of the report covers the studies, projects and missions of the Science and Robotic Exploration Directorate of ESA in the areas of astronomy, Solar System science, fundamental physics and the robotic exploration of Mars.

Since the last COSPAR meeting in 2010, no new missions have been launched, but a significant number of exciting scientific results have been returned from the broad array of missions currently in operation. The roster of space science missions where ESA is the sole, leading or junior partner now stands at 15, encompassing 18 individual spacecraft. Since the last report, the JAXA-operated Akari and CNSA-operated Double Star missions have ceased providing science data. Many of these missions are operating well beyond their originally foreseen lifetimes and further extensions are assessed on a biennial basis.

Substantial progress has been made towards the completion of ongoing projects in the mandatory Science Programme. Detailed studies of candidate missions in the Cosmic Vision 2015–25 programme have resulted in the selection of two new medium-class (M) missions (Solar Orbiter and Euclid) to be launched in the second half of the current decade. Finally, progress continues towards the launch of elements in the optional ExoMars programme, namely a Trace Gas Orbiter and an Entry, Descent and Landing demonstrator in 2016 and a surface rover in 2018 (see Table 1.1).

1.1 Highlights from Missions in Operation

Rosetta made its last major trajectory adjustment in February 2011 and entered its 2.5-year deep space hibernation phase in June 2011, ahead of its rendezvous with comet 67P/Churyumov–Gerasimenko in 2014. The main spacecraft will study the comet and its environment from close by as the comet travels into the inner Solar System, while the lander, Philae, will be deployed to the surface of the comet to study its composition and evolution as it activates in the presence of increased sunlight. En route to its rendezvous, Rosetta has had close encounters with Earth, Venus and Mars, as well as two asteroids, (2867) Steins in September 2008 and (21) Lutetia in July 2010. Key results from Rosetta's flyby of Lutetia were published in *Science* in 2011: imaging, imaging spectroscopy and radio science data combined to show that Lutetia is a primordial remnant of the formation of the Solar System, with a dense metallic core and a heavily weathered surface.

Herschel and Planck, two of ESA's most challenging astrophysics missions, have produced outstanding data and scientific results over the past two years. Launched together on an Ariane 5 ECA from Kourou in French Guiana in May 2009, they separated shortly afterwards and follow different orbital trajectories around the Sun–Earth L2 point. Herschel operates at far-infrared to submillimetre wavelengths, while Planck covers the submillimetre to centimetre range, and both use cryogenic coolants to achieve their required sensitivities. As a consequence, both have finite science operation phases and will reach the end of their useful lifetimes in the coming year.

Planck is the third-generation space explorer of the Cosmic Microwave Background (CMB), the all-sky remnant of the epoch of recombination that occurred some 300 000 years after the Big Bang. Spatial structure in the CMB in the form of temperature deviations from a perfect blackbody contains important clues as to the origin and early evolution of the Universe, as well as its fate. To reveal these tiny variations, Planck must observe and remove the bright foreground emission from dust and gas in the Milky Way to an extraordinarily high level of precision; these foreground data are nevertheless also of significant scientific interest in their own right to astronomers. Planck completed five all-sky surveys before its High-Frequency Instrument warmed

up in January 2012. Its Low-Frequency Instrument is expected to continue operating until at least the end of the year.

The first multi-wavelength image of the whole sky as seen by Planck and based on just one sky survey was released in July 2010 and garnered very wide media exposure. In January 2011, ESA made the Early Release Compact Source Catalogue available to the scientific community. Containing over 9000 sources detected in the first year of operations, the catalogue includes newly discovered cold, dense cores within molecular clouds, possible sites of future

Table 1.1. ESRO/ESA scientific missions.

Spacecraft	Launch date	End of operational life	Mission
Launched			
ESRO-II	17 May 1968	9 May 1971	Cosmic rays, solar X-rays
ESRO-IA	3 October 1968	26 June 1970	Auroral and polar-cap phenomena, ionosphere
HEOS-1	5 December 1968	28 October 1975	Interplanetary medium, bow shock
ESRO-IB	1 October 1969	23 November 1969	As ESRO-IA
HEOS-2	31 January 1972	2 August 1974	Polar magnetosphere, interplanetary medium
TD-1	12 March 1972	4 May 1974	Astronomy (UV, X- and gamma-ray)
ESRO-IV	26 November 1972	15 April 1974	Neutral atmosphere, ionosphere, auroral particles
Cos-B	9 August 1975	25 April 1982	Gamma-ray astronomy
Geos-1	20 April 1977	23 June 1978	Dynamics of the magnetosphere
ISEE-2	22 October 1977	26 September 1987	Sun/Earth relations and magnetosphere
IUE	26 January 1978	30 September 1996	Ultraviolet astronomy
Geos-2	24 July 1978	October 1985	Magnetospheric fields, waves and particles
Exosat	26 May 1983	9 April 1986	X-ray astronomy
FSLP	28 November 1983	8 December 1983	Multidisciplinary; First Spacelab Payload
Giotto	2 July 1985	23 July 1992	Comet Halley and Comet Grigg–Skjellerup encounters
Hipparcos	8 August 1989	15 August 1993	Astrometry
HST	24 April 1990		UV/optical/near-IR astronomy
Ulysses	6 October 1990	30 June 2009	Heliosphere
Eureka	31 July 1992	24 June 1993	Multidisciplinary
ISO	17 November 1995	8 April 1998	Infrared astronomy
SOHO	2 December 1995	31 December 2014	Sun (including interior) and heliosphere
Cassini-Huygens	15 October 1997	14 January 2005	Titan probe/Saturn orbiter
XMM-Newton	10 December 1999	31 December 2014	X-ray spectroscopy
Cluster	16 July/9 August 2000	31 December 2014	3D space plasma investigation
Integral	17 October 2002	31 December 2014	Gamma-ray astronomy
Mars Express	2 June 2003	31 December 2014	Mars exploration
SMART-1	27 September 2003	3 September 2006	Navigation with solar-electric propulsion
Rosetta	2 March 2004	December 2015	Comet rendezvous
Venus Express	9 November 2005	31 December 2014	Venus exploration
Herschel	14 May 2009	2013	Far-infrared and submillimetre astronomy
Planck	14 May 2009	2013	Cosmic microwave background
Proba-2	2 November 2009	2014	Technology testbed with solar instrumentation
Planned launches			
Gaia	2013		Next-generation astrometry mission
LISA Pathfinder	2014		LISA Technology Package
BepiColombo	2015		Mission to Mercury
ExoMars	2016 and 2018		Robotic exploration of Mars
Solar Orbiter	2017		Origin of the heliosphere
JWST	2018		Next-generation space telescope

star formation in the Milky Way, as well as clusters of galaxies in the more distant Universe detected via the Sunyaev–Zel'dovich effect. A broad array of non-CMB science results have been presented at two major Planck conferences, one in Paris in January 2011 and the other in Bologna in January 2012, with corresponding papers published in a special issue of *Astronomy & Astrophysics*. The first CMB results are due to be released in early 2013, and the full dataset and further scientific results a year later.

Herschel and its three scientific instruments (PACS, SPIRE and HIFI) have performed very well after overcoming an early electronics problem with the HIFI high-resolution spectrometer. They produce far-infrared data spanning a very wide range of scientific topics, from sources within the Solar System, out to the distant Universe. More than 98% of all Guaranteed Time and Open Time Key Programme observations have been completed, as have more than 70% of the top priority first round Open Time Programmes. A second and final Open Time call for proposals was completed at the end of 2011 and the selected projects will take Herschel to its end-of-mission, currently predicted to be in February–March 2013.

Over 400 refereed scientific papers based on Herschel data have been published to date. One of many highlights is a HIFI study of the isotopic composition of water in comet 103P/Hartley 2. Previous studies of other comets found a ratio of 'semi-heavy' water (HDO) to 'normal' water (H_2O) higher than found in Earth's oceans, leading scientists to conclude that comets could not have been the source of this water. However, the HIFI study of Hartley 2 showed it to have the same D/H ratio as Earth's oceans, reigniting the debate on whether a significant fraction of Earth's water could have been delivered by the impact of millions of Jupiter-family comets roughly 4 billion years ago, when Earth had cooled down sufficiently.

1.2 Other Missions in Operation

The Sun and the heliosphere play vital roles in our daily lives, and ESA operates or collaborates in a number of missions to study them. SOHO continues its long vigil at the Sun–Earth L1 point, monitoring and studying the Sun on a near-continuous basis following its launch in 1995, while the four spacecraft of the Cluster mission have been probing the relationship between the solar wind and Earth's magnetosphere since 2000. ESA is also a partner in the Japanese-led Hinode solar mission launched in 2006, and the ESA-led Proba-2 technology demonstration mission, launched in 2009, carries among other payload elements a solar EUV imager and UV irradiance radiometer.

In addition to Rosetta, ESA operates or collaborates in a several missions dedicated to the study of planets and their moons in the Solar System, providing insights into the atmospheric and surface evolution, and contributing to the science of comparative climatology. The NASA/ESA/ASI Cassini-Huygens mission to study the Saturn system was launched in 1997 and arrived in 2004, with the descent of the Huygens lander onto the surface of Titan in January 2005. Mars Express reached the Red Planet in 2003 and continues to deliver new insights into the formation and early evolution of Mars and its two small moons, Phobos and Deimos. Venus Express arrived at its destination in 2006 and has been returning results on the dense atmosphere and the extremely hot and weathered surface of Venus.

As well as Herschel and Planck, ESA operates and collaborates in astrophysical missions covering the electromagnetic spectrum in order to study the wider Universe, its contents and properties. The NASA/ESA Hubble Space Telescope was launched in 1990, but continues to deliver extraordinary scientific results in the optical–infrared wavelength range thanks to upgrades and repairs made possible by a number of refurbishment missions over the intervening period. Similarly, some 12 years after its launch, XMM-Newton has generated over 3000 scientific papers based on its X-ray observations. Since its launch in 2002, Integral has been observing the sky in gamma rays and has been building up a long-term view of highly variable sources in some key locations, including the galactic bulge. ESA also collaborates in the Japanese-led Suzaku X-ray mission launched in 2005 and the French-led COROT mission launched in 2006 to discover exoplanets using the transit method, as well as studying the interiors of stars via asteroseismology.

1.3 Missions in Implementation

Since the last COSPAR meeting, significant progress has been made on ESA's next space science missions, which now include Solar Orbiter and a contribution to JAXA's Astro-H.

Gaia follows on from ESA's successful Hipparcos mission. Gaia will provide 10–100 times better astrometric precision on stars up to 1000 times fainter, thus reaching roughly a billion stars in the Milky Way, some 10 000 times as many as Hipparcos. The resulting extremely precise and fundamental 3D map of these stars along with their space motions will allow us to decode the evolutionary history of the Galaxy. Gaia will also detect large numbers of exoplanets, brown dwarfs, white dwarfs and extragalactic supernovae, as well as providing precise tests of General Relativity. Launch on a Soyuz–Fregat from Kourou is planned for late 2013.

Astro-H is a Japanese X-ray mission employing a number of innovative instruments, including soft and hard X-ray imagers to provide imaging spectroscopy, a soft gamma-ray detector, and a high-spectral-resolution X-ray microcalorimeter. ESA will contribute hardware components and operations and user support, in return for observing time on the mission. NASA also contributes to the mission, which is due for launch on an H-IIA from the Tanegashima Space Centre in 2014.

LISA Pathfinder is a technology testbed for a future gravitational wave detection mission, in which one of its million km arms is compressed down to a few tens of cm in length. Interferometry between two drag-free test masses (i.e. decoupled from and shielded by the external spacecraft) should demonstrate that they follow pure geodesics, with residual parasitic accelerations smaller than the signal expected from gravitational waves. Launch is scheduled on a Vega from Kourou in 2014.

BepiColombo is a joint mission to Mercury, with ESA providing the Mercury Planetary Orbiter and JAXA providing the Mercury Magnetospheric Orbiter. These two separate but coordinated spacecraft will make a detailed study of the planet and its environment, and will help answer key questions regarding the origin of terrestrial planets. Launch on an Ariane 5 ECA from Kourou is due in 2015.

Solar Orbiter is the first Cosmic Vision mission to proceed to implementation. It is a collaborative ESA–NASA mission to conduct simultaneous *in situ* and remote observations from as close as 0.3 AU to the Sun and at ecliptic latitudes of up to 34°, in order to explore how the Sun creates and controls the heliosphere. Solar Orbiter is scheduled for launch from Cape Canaveral on an Atlas V in early 2017.

The NASA/ESA/CSA James Webb Space Telescope (JWST) is a large optical–infrared observatory, the successor to HST, ISO, Spitzer and Herschel. JWST has a 6.5 m-diameter mirror comprising 18 hexagonal beryllium segments. Behind a deployable sunshield at the Sun–Earth L2 point, the observatory will cool to around 40K, making it extremely sensitive over the wavelength range 0.6–28.5 μm. The European contribution to JWST includes leadership in two of the four science instruments (NIRSpec and MIRI), operations support at the Space Telescope Science Institute in Baltimore and launch on an Ariane 5 from Kourou in 2018.

1.4 Robotic Exploration

By the time of the last COSPAR meeting, responsibility for ESA's robotic exploration of Mars, an optional programme, had been transferred to the Science and Robotic Exploration Directorate. The ExoMars programme had been rescoped in the framework of a collaboration with NASA, centred on joint missions in 2016 and 2018, and a long-term goal of a Mars sample return mission in the mid- to late 2020s. However, in early 2012, NASA informed ESA that, for programmatic and funding reasons, it was no longer able to proceed with the collaboration. ESA is now pursuing a cooperation with Roscosmos instead, retaining much of the original programme architecture. The 2016 launch window foresees a Trace Gas Orbiter (TGO) to conduct highly sensitive observations of the martian atmosphere to confirm and locate sources of methane and other possible tracers of biogenic activity. The TGO will also act as a data relay for later missions and carry an instrumented Entry, Descent and Landing demonstrator to the surface of the planet. The 2018 mission will deliver the ExoMars rover to the surface, carrying a sophisticated scientific payload, including a drill capable of penetrating 2 m below the surface, in search of evidence for life in the past or present of Mars.

In addition, studies for candidate post-2018 Mars missions have been carried out in within the separate Mars Robotic Exploration Preparation programme. These include a mission to return samples from Phobos, a network of small landers to study the internal properties of Mars and a precision lander aimed at getting very close to key geological features of the planet. These missions are candidates for the new European Robotic Exploration Programme, which is in preparation for the ESA Council at Ministerial level, to be held in November 2012.

1.5 Cosmic Vision

The past two years have seen continued intense activity in the Cosmic Vision programme, which is intended to set a framework for ESA's space science programme in the period 2015–25 and beyond. The initial scientific themes for Cosmic Vision were established in 2005, covering the conditions for life and planetary formation, the origin and evolution of the Solar System, the fundamental laws of the cosmos, and the origin, structure and evolution of the Universe. The first call for mission proposals issued in 2007 resulted in 50 mission concepts, from which the Advisory Structure of the Science Programme selected a number of candidate medium and large mission concepts to be studied further.

After four years of study, the first Cosmic Vision missions were selected in October 2011, namely the first two medium-class (M) missions, Solar Orbiter as M1 and Euclid as M2. Solar Orbiter was also formally adopted for implementation and is thus described above. Euclid awaits formal adoption in June 2012, following a delta definition study phase to consolidate its scientific requirements. Comprising a 1.2 m-diameter telescope, an optical camera and a near-infrared camera/spectrometer, Euclid will survey a large fraction of the sky to use weak lensing and baryon acoustic oscillations as complementary tracers of dark matter and dark energy, unknown constituents that together make up some 96% of the energy–matter content of the Universe. Euclid is due for launch in 2019 on a Soyuz–Fregat from Kourou.

A contribution to the JAXA-led near- to far-infrared observatory SPICA has also been studied, and a decision on its continuation will be taken following completion of studies being carried out by JAXA. The proposed European contribution would be the telescope, based on Herschel heritage, support to the mission's operations, and an imaging FTS instrument, SAFARI, provided by a nationally funded consortium.

At the time of the previous COSPAR report, three large (L) missions were under study, namely EJSM–Laplace (a mission to Jupiter and its moons), IXO (a large X-ray observatory) and LISA (a gravitational wave observatory). All three were foreseen in the context of large ESA–NASA collaborations, with JAXA also involved in IXO. However, in early 2011, following the publication of the US National Research Council Decadal Surveys for astronomy and astrophysics and planetary sciences, NASA made it clear that they would be unable to participate in any of those missions in the near-term at a significant level.

To capitalise on the impetus behind and work done on the three missions, ESA then undertook three new studies covering the same scientific fields. The resulting mission candidates were JUICE (Jupiter Icy Moons Explorer), ATHENA (Advanced Telescope for High-Energy Astrophysics) and NGO (New Gravitational wave Observatory). All three were substantially reformulated with respect to the original L-mission concepts, such that they could be implemented as European-only or European-led missions. Compared with the two-spacecraft EJSM–Laplace, JUICE would now be a single-spacecraft mission, visiting Jupiter and three of its largest moons, Europa, Callisto and Ganymede, ending up in orbit around the latter; ATHENA would have a smaller collecting area and less complex instrument complement than IXO; NGO would implement two out of the three interferometer arms of LISA and over a 1 million km baseline rather than 5 million km.

Following the completion of the study activities and the customary selection process, in May 2012 the Science Programme Committee selected JUICE as the first L mission in the Cosmic Vision plan, for launch in 2022.

A new call for a medium-class mission (M3) to be launched in 2022 was issued in July 2010. From a total of 47 proposals, four were selected for study: EChO (an exoplanet transit spectroscopy mission), LOFT (a wide-field X-ray timing transient detection mission), MarcoPolo-R (an asteroid sample-return mission) and STE-QUEST (a fundamental physics mission carrying an atomic

clock and an atom interferometer to test various aspects of the Equivalence Principle to an unprecedented accuracy). The current timeline foresees a downselection towards mid-2013.

Finally, the first call for a new class of small (S) missions was made in March 2012. Over 50 Letters of Intent were received ahead of the mid-June proposal deadline.

1.6 Post-Operations and Archiving

Work is continuing on missions in their post-operational phase, i.e. after switch-off of the respective satellites. These activities are aimed at obtaining a full, homogeneous recalibration of the observations and the delivery of final archives to the scientific community. Lessons learned from previous missions are being applied to subsequent missions with the aim of bringing all astrophysics, heliophysics and planetary physics mission data under a unified archiving scheme at the European Space Astronomy Centre in Spain.

→ MISSIONS IN OPERATION

2. Missions in Operation

2.1 Hubble Space Telescope

Introduction

On 24 April 2011, Hubble celebrated the 21st anniversary of its launch. After the very successful Servicing Mission 4 in May 2009, Hubble is now at the peak of its scientific performance, with a full complement of operating instruments. Its observing efficiency remains high (~50%). Community interest in Hubble also continues to be very high, with a typical oversubscription of 6–7:1. In July 2011, Hubble took its 1 millionth science exposure. This observation was part of a Wide Field Camera 3 infrared grism observation of a planet transiting a nearby star named HAT-P-7b. When Hubble was launched, extrasolar planets had been predicted, but had not yet been discovered. In November 2011, Hubble achieved another milestone: the publication of the 10 000th refereed scientific paper based on Hubble data.

The Magellanic Stream

Gaseous inflow plays an important role in galaxy evolution, bringing in the fuel that powers new cycles of star formation. However, the chemical and physical properties of infalling clouds are poorly constrained. To address these properties in the Milky Way halo, Hubble observations have been taken of the Magellanic Stream, a long filament of gas stripped out of the Magellanic Clouds and falling toward the Galaxy.

By observing the absorption lines the Magellanic Stream imprints in the ultraviolet light from background galaxies, Hubble observers are piecing together the Stream's chemical composition and ionisation level (Fox et al., 2010). The abundance of oxygen in the Stream is found to be only one-tenth of the solar abundance (Fig. 2.1.1), indicating that the Stream likely originates in the Small Magellanic Cloud, rather than the Large Magellanic Cloud. Ongoing Hubble observations of other quasars behind the Stream will allow the abundance of several other chemical elements to be measured.

The Environments of Black Holes

A suite of space observatories including Hubble has shown unprecedented details in the environs of a supermassive black hole (Kaastra et al., 2012). Observations reveal 'bullets' of gas being driven away fast from the centre and a corona of very hot gas hovering above the disc of matter that is falling into the black hole. Astronomers have made use of data from ESA's XMM-Newton and Integral observatories (which study X-rays and gamma rays, respectively), Hubble (for ultraviolet observations with the Cosmic Origins Spectrograph, COS, instrument), NASA's Chandra (X-ray) and Swift (gamma and X-ray) satellites, as well as the ground-based William Herschel Telescope (WHT) and the Peters Automated IR Imaging Telescope (PAIRITEL).

The black hole investigated lies at the heart of the galaxy Markarian 509. This black hole is huge and is growing more massive every day as it continues to feed on surrounding matter, which glows brightly as it forms a rotating disc around the hole. Markarian 509 was chosen because it is known to vary in

Further information about the Hubble Space Telescope can be found at *http://sci.esa.int/hubble*

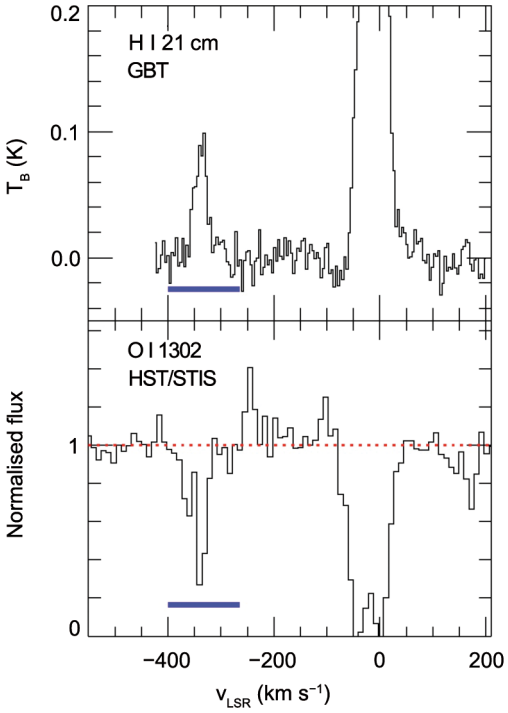

Figure 2.1.1. Abundance determination in the Magellanic Stream. HST/STIS spectra of neutral oxygen absorption and Green Bank Telescope (GBT) spectra of neutral hydrogen radio emissions are shown in the direction of the active galaxy NGC 7469. The relative strength of the two spectral lines at a velocity of −350 km s^{-1} (the blue shaded bars) indicates that the oxygen abundance in the Stream is one-tenth of the solar value. This suggests that the Stream originates in the Small, not the Large Magellanic Cloud.

brightness, which indicates that the flow of matter is turbulent. Using a large number of telescopes that are sensitive to different wavelengths of light gave astronomers the unprecedented coverage running from the infrared, through the visible, ultraviolet, X-rays and into the gamma-ray band.

Hubble has directly observed an accretion disc around a black hole in a distant quasar: HE 1104-1805. This study makes use of a novel technique that uses gravitational lensing to increase the power of the telescope. The incredible precision of the method has allowed astronomers to measure the disc's size directly and plot the temperature across different parts of the disc. They have done so by studying the gravitational lensing effect of stars in an intervening galaxy and using them as a scanning microscope to probe features in the quasar's disc that would otherwise be far too small to detect. As these stars move across the light from the quasar, gravitational effects amplify the light from different parts of the quasar, giving detailed colour information for a line that crosses through the accretion disc.

With this technique, astronomers were able to measure the size of the disc and to study the colours (and hence the temperatures) of different parts of the disc. They found that the disc is between four and eleven light-days across (approximately 100–300 billion km). While this measurement shows large uncertainties, it is still remarkably accurate for a small object at such a great distance, and the method holds great potential for increased accuracy in the future.

The Distant Universe

Using the amplifying power of a cosmic gravitational lens, astronomers have discovered a distant galaxy whose stars were born unexpectedly early in cosmic history (van der Wel, 2011). This result sheds new light on the formation of the first galaxies, as well as on the early evolution of the Universe. This distant galaxy began forming stars just 200 million years after the Big Bang, and is challenging theories of how soon galaxies formed and evolved in the first years of the Universe. It could even help to solve the mystery of how the hydrogen fog that filled the early Universe was cleared.

This distant galaxy is visible through a cluster of galaxies called Abell 383, whose powerful gravity bends the rays of light almost like a magnifying glass. The chance alignment of the galaxy, the cluster and Earth amplifies the light reaching us from this distant galaxy, allowing astronomers to make detailed observations. Without this gravitational lens, the galaxy would have been too faint to be observed even with today's largest telescopes. After detecting the galaxy in Hubble and Spitzer Space Telescope images, astronomers carried out spectroscopic observations with the Keck-II telescope in Hawaii, and were able to make detailed measurements of its redshift and infer information about the properties of its component stars.

The galaxy's redshift is 6.027, which means we see it as it was when the Universe was around 950 million years old. This does not make it the most remote galaxy ever detected – several have been confirmed at redshifts of more than 8, and one has an estimated redshift of around 10, placing it 400 million years earlier. However, the features of the newly discovered galaxy are dramatically different from those of other distant galaxies that have been observed, which generally display only young stars. In fact, the Spitzer infrared detection also indicated that the galaxy is made up of surprisingly old and relatively faint stars, already nearly 750 million years old – pushing back the epoch of its formation to about 200 million years after the Big Bang, much further than was expected.

The discovery has implications beyond the question of when galaxies first formed, and may help explain how the Universe became transparent to ultraviolet light in the first billion years after the Big Bang. In the early years of the cosmos, a diffuse fog of neutral hydrogen gas blocked ultraviolet light in the Universe. Some source of radiation must therefore have progressively ionised the diffuse gas, clearing the fog to make it transparent to ultraviolet rays as it is today – a process known as re-ionisation. Astronomers believe that the radiation that powered this re-ionisation must have come from galaxies. But so far, nowhere near enough of them have been found to provide the necessary radiation. This discovery may help solve this enigma.

Using its infrared vision to peer nine billion years back in time, Hubble has uncovered an extraordinary population of tiny, young galaxies that are rich in star formation. The galaxies are forming stars at such a rate that the number of stars in them would double in just ten million years. For comparison, the Milky Way has taken 1000 times longer to double its stellar population. These newly discovered dwarf galaxies are around 100 times smaller than the Milky Way (Fig. 2.1.2). Their star formation rates are extremely high, even for the young Universe, when most galaxies were forming stars at higher rates than they are today. They have turned up in the Hubble images because the radiation from young, hot stars has caused the oxygen in the gas surrounding them to light up. This rapid starbirth is believed to represent an important phase in the formation of dwarf galaxies, the most common galaxy type in the cosmos.

The observations were part of the Cosmic Assembly Near-infrared Deep Extragalactic Legacy Survey (CANDELS), an ambitious three-year survey to analyse the most distant galaxies in the Universe. Astronomers uncovered the 69 young dwarf galaxies in near-infrared and visible wavelength images taken with Hubble's Wide Field Camera 3 and Advanced Camera for Surveys. The observations concentrated on two regions of the sky called the Great Observatories Origins Deep Survey–South and the UKIDSS Ultra-Deep Survey (part of the UKIRT Infrared Deep Sky Survey). In addition to the images, Hubble has obtained spectra for a handful of these galaxies that show the detailed physics of what is happening within them and confirm their extreme star-forming nature.

Figure 2.1.2. Eighteen tiny galaxies discovered by Hubble (shown in the small panels, *bottom*), which existed 9 billion years ago and are brimming with new stars. They are typically 100 times less massive than the Milky Way galaxy but are churning out stars at such a furious pace that their stellar populations would double in just 10 million years. Hubble's Wide Field Camera 3 and Advanced Camera for Surveys detected the galaxies in a field called the Great Observatories Origins Deep Survey (GOODS). The locations of the galaxies in the GOODS field are marked in the large image (*top*).

A Dark Matter Census

Hubble has taken a remarkable image of galaxy cluster MACS J1206.2-0847 (Fig. 2.1.3) (Zitrin et al., 2012). The apparently distorted shapes of distant galaxies in the background are caused by dark matter, whose gravity bends

Figure 2.1.3 The galaxy cluster MACS J1206. Galaxy clusters like these have enormous mass, and their gravity is powerful enough to visibly bend the path of light, like a magnifying glass.

and distorts their light rays. MACS 1206 has been observed as part of a new survey of galaxy clusters using Hubble – the Cluster Lensing And Supernova survey with Hubble (CLASH) (Postman et al., 2012).

CLASH is probing, with unparalleled precision, the distribution of dark matter in 25 massive clusters of galaxies. So far, CLASH astronomers have observed six of the 25 clusters. Dark matter makes up the bulk of the mass of the Universe, yet it can only be detected by measuring how its gravity pulls on visible matter and warps the fabric of spacetime so that the light from distant objects is distorted. Galaxy clusters like MACS 1206 are perfect laboratories for studying the gravitational effects of dark matter because they are the most massive structures in the Universe to be held together by gravity.

Because of their immense gravitational pull, the clusters act like giant cosmic lenses, amplifying, distorting and bending any light that passes through them – an effect known as gravitational lensing. Lensing effects can also produce multiple images of the same distant object, as is evident in Fig. 2.1.3. In particular, the apparent numbers and shapes of the distant galaxies far beyond a galaxy cluster become distorted as the light passes through, yielding a visible measurement of how much mass there is in the intervening cluster, and how it is distributed. The substantial lensing distortions seen are proof that the dominant mass component of the clusters is dark matter. The distortions would be far weaker if the clusters' gravity came only from visible matter.

The CLASH survey will allow astronomers to construct the highly detailed dark matter maps of more galaxy clusters than ever before. These maps will be used to test previous surprising results that suggest that dark matter is more densely packed inside clusters than some models predict. This might mean that galaxy cluster assembly began earlier than commonly thought. MACS 1206 lies 4 billion light years from Earth. Hubble's keen vision has helped CLASH astronomers to uncover 47 multiple images of 12 newly identified faraway galaxies. Obtaining so many multiple images of a cluster is a unique capability of Hubble, and the CLASH survey is optimised to find them.

The new observations build on earlier work by Hubble and ground-based telescopes. Among the observations that complement Hubble's is a major project using the European Southern Observatory's Very Large Telescope (VLT). Unlike Hubble, which is making images of the clusters, the VLT is carrying out spectroscopic observations that will allow scientists to draw inferences about many of the properties of the cluster galaxies, including their distance and chemical makeup.

References

Fox, A., Wakker, B.P., Smoker, J.V., Richter, P., Savage, D. & Sembach, K. (2010). *Astrophys. J.* **718**, 1046.

Kaastra, J.S., Detmers, R.G., Mehdipour, M., Arav, N., Behar, E., Bianchi, S., Branduardi-Raymont, G., Cappi, M., Costantini, E., Ebrero, J. et al. (2012). *Astron. Astrophys.* **539**, 117.

Postman, M., Coe, D., Benítez, N., Bradley, L., Broadhurst, T., Donahue, M., Ford, H., Graur, O., Graves, G., Jouvel, S. et al. (2012). *Astrophys. J.* Suppl. **199**, 25.

Van der Wel, A.N., Rix, H.-W., Finkelstein, S.L., Koekemoer, A.M., Weiner, B.J., Wuyts, S., Bell, E.F., Faber, S.M., Trump, J.R. et al. (2011), *Astrophys. J.* **742**, 111.

Zitrin, A., Rosati, P., Nonino, M., Grillo, C., Postman, M., Coe, D., Seitz, S., Eichner, T., Broadhurst, T., Jouvel, S. et al. (2012). *Astrophys. J.* **749**, 97.

2.2 SOHO

Introduction

Since its launch on 2 December 1995, the joint ESA/NASA Solar and Heliospheric Observatory (SOHO) mission has provided a wealth of information about the Sun, from its interior, through the hot and dynamic atmosphere, to the solar wind and its interaction with the interstellar medium. Research using SOHO observations has revolutionised our understanding of the Sun, and science teams from around the world have made great strides towards a better understanding of 'the big three' areas of research that SOHO set out to tackle: the structure and dynamics of the solar interior, the heating of the solar corona, and the acceleration of the solar wind. The findings have been documented in an impressive and growing body of scientific literature and popular articles. SOHO enjoys a remarkable 'market share' in the worldwide solar physics community, with over 4200 papers in refereed journals, representing the work of more than 2500 scientists. At the same time, SOHO's easily accessible, spectacular data and basic science results have captured the imagination of the space science community and the general public alike.

SOHO's 12 instruments, which represent the most comprehensive set of solar and heliospheric instruments ever developed and carried on the same platform, are summarised in Table 2.2.1.

Mission Status

SOHO was launched by an Atlas IIAS from Cape Canaveral and inserted into its halo orbit around the L1 Lagrangian point on 14 February 1996. Normal science operations started in May 1996. While the original mission duration was only two years, ESA's Science Programme Committee has approved five mission extensions (in February 1997, February 2002, May 2006, November 2008 and November 2010). SOHO operations are currently approved through December 2014 (subject to a positive mid-term review in 2012). The satellite and payload are in good condition and there are no technical limitations that would prevent SOHO observing for several more years.

NASA's Solar Dynamics Observatory (SDO), which was launched on 11 February 2010, carries vastly improved versions of SOHO's Michelson Doppler Imager (MDI) and Extreme-ultraviolet Imaging Telescope (EIT) instruments (plus an EUV irradiance monitor). After the cross-calibration of the EIT with the SDO/Atmospheric Imaging Assembly (AIA), which provides images at a much higher resolution and time cadence for all EIT wavebands, as well as three other EUV wavelengths, at the end of July 2010 the EIT image cadence was reduced to two synoptic sets of images in all four wavelengths per day to track detector behaviour and to maintain the uniform dataset, spanning now almost one and a half solar cycles. The telemetry bandwidth previously used by EIT is now being used by the Large Angle and Spectrometric Coronagraph (LASCO) to improve the cadence of its observations of the fastest Coronal Mass Ejections (CMEs). After the completion of the cross-calibration with SDO's Helioseismic and Magnetic Imager (HMI), MDI was commanded to stop taking science data on 12 April 2011 at 23:22:31 UT. MDI has operated exceptionally well for more than 15 years and has produced data that form the basis of over 1500 papers in the refereed literature.

Further information about the SOHO mission can be found at *http://sci.esa.int/soho*

Table 2.2.1. Instruments on SOHO.

Investigation/PI	Measurements	Technique	Participants
Helioseismology			
Global Oscillations at Low Frequencies (GOLF) P. Boumier, IAS, Orsay, France	Global Sun velocity oscillations (l = 0–3)	Na-vapour resonant scattering cell, Doppler shift and circular polarisation	FR, ESA, DK, DE, CH, GB, NL, ES, US
Variability of solar IRradiance and Gravity Oscillations (VIRGO) C. Fröhlich, PMOD/WRC, Davos, Switzerland	Low-degree (l = 0–7) irradiance oscillations and solar constant	Global Sun and low-resolution (12-pixel) imaging and active cavity radiometers	CH, NO, FR, BE, ESA, ES
Michelson Doppler Imager (MDI) P.H. Scherrer, Stanford University, California, USA	Velocity oscillations high-degree modes (up to l = 4500)	Doppler shift with Fourier tachometer, 4 and 1.3 arcsec resolution	US, DK, GB
Solar atmosphere remote sensing			
Solar UV Measurements of Emitted Radiation (SUMER) W. Curdt, MPS, Lindau, Germany	Plasma flow characteristics (temperature, density, velocity); chromosphere through corona	Normal-incidence spectrometer, 50–160 nm, spectral resolution 20 000–40 000, angular resolution 1.2–1.5 arcsec	DE, FR, CH, US
Coronal Diagnostic Spectrometer (CDS) A. Fludra, RAL, Chilton, UK	Temperature and density: transition region and corona	Normal and grazing-incidence spectrometers, 15–80 nm, spectral resolution 1000–10 000, angular resolution 3 arcsec	UK, CH, DE, US, NO, IT
Extreme-ultraviolet Imaging Telescope (EIT) F. Auchère, IAS, Orsay, France	Evolution of chromospheric and coronal structures	Full-disc images (1024 × 1024 pixels in 42 × 42 arcmin) at lines of He II, Fe IX, Fe XII, Fe XV	FR, US, BE
UltraViolet Coronagraph Spectrometer (UVCS) J.L. Kohl, SAO, Cambridge, MA, USA	Electron and ion temperature densities, velocities in corona (1.3–10 $R_\odot$)	Profiles and/or intensity of selected EUV lines between 1.3 and 10 $R_\odot$	US, IT, CH, DE
Large Angle and Spectrometric COronagraph (LASCO) R. Howard, NRL, Washington DC, USA	Structures' evolution, mass, momentum and energy transport in corona (2–30 $R_\odot$)	Two externally occulted coronagraphs.	US, DE, FR, GB
Solar Wind ANisotropies (SWAN) E. Quémerais, IAS, Orsay, France	Solar wind mass flux anisotropies, temporal variations	Scanning telescopes with hydrogen absorption cell for Lyman-α	FR, FI, US
Solar wind '*in situ*'			
Charge, ELement and Isotope Analysis System (CELIAS) R. Wimmer-Schweingruber, Universität Kiel, Germany	Energy distribution and composition. Electrostatic deflection, time-of-flight (mass, charge, charge state) measurements and solid-state detectors (0.1–1000 keV/e)	CH, DE, USA, Russia	
Comprehensive SupraThermal Energetic Particle analyser (COSTEP) B. Heber, Universität Kiel, Germany	Energy distribution of ions (p, He) 0.04–53 MeV/n and electrons 0.04–5 MeV	Solid-state detector telescopes and electrostatic analysers	DE, US, JP, FR, ES, ESA, IE
Energetic and Relativistic Nuclei and Electron experiment (ERNE) E. Valtonen, University of Turku, Finland	Energy distribution and isotopic composition of ions (p-Ni) 1.4–540 MeV/n and electrons 5–60 MeV	Solid-state and plastic scintillation detectors	FI, GB

Operations

The SOHO Experimenters' Operations Facility (EOF), located at NASA's Goddard Space Flight Center (GSFC), served as the focal point for mission science planning and instrument operations. There, the experiment teams received realtime and playback telemetry, processed these data to determine instrument commands, and sent commands directly from their workstations through the ground system to their instruments, both in near-realtime and on a delayed execution basis. In response to budget pressures, the SOHO EOF and the SOHO Experimenters' Analysis Facility (EAF) at GSFC were closed at the end of November 2010. Most remote sensing instruments are now being operated remotely from the PIs' home institutions. The few remaining SOHO staff moved to new offices in the SOHO Bogart Operations Facility (BOF) in Building 21.

The SOHO satellite was originally designed for 24/7 manual operations. Starting in late 2006, SOHO engineers began an inhouse reengineering effort to automate SOHO satellite operations in an effort to reduce operating costs. This required the development of new ground software (pass generator, anomaly detection and notification) as well as modifications of the Central Onboard Software. Since September 2008, all Deep Space Network contacts (except nonroutine passes such as station keeping and momentum management manoeuvres) are automated.

Scientific Highlights

Solar Interior

The late onset of the new solar cycle and the unusually deep minimum between cycles 23 and 24 took all experts by surprise, which suggests that there is a fundamental lack in our understanding of the origin of the solar activity cycle. The Sun's meridional circulation, a massive flow pattern within the Sun that transports hot plasma near the surface from the solar equator to the poles and back to the equator in the deeper layers of the convection zone, is believed to play a key role in determining the strength of the Sun's polar magnetic field, which in turn determines the strength of the sunspot cycles.

One class of dynamo models predicts that a stronger meridional flow produces weaker polar fields, whereas another class of models predicts stronger polar fields (and a shorter sunspot cycle) for the same flow. Hathaway & Rightmire (2010) analysed more than 60 000 full-disc magnetograms registered by the MDI instrument on SOHO between May 1996 and June 2009. They measured the latitudinal profile of this flow and its variations over a solar cycle by tracking the motions of small-scale magnetic flux concentrations, which are carried away by the meridional flow like leaves on a river. They found an average flow that is poleward at all latitudes up to 75°, and that the flow was faster at sunspot cycle minimum than at maximum and substantially faster on the approach to the current minimum than it was at the last solar minimum (Fig. 2.2.1). This finding poses new constraints on solar dynamo models and may help to explain why the last solar minimum was so peculiar.

Ilonidis et al. (2011) for the first time succeeded in detecting sunspot regions in the deep interior of the Sun, 1–2 days before they appeared at the solar surface (Fig. 2.2.2). Their results, based on data from MDI, suggest that sunspots are generated at least 60 000 km below the surface and emerge from this depth at an average speed of 0.3–0.6 km s^{-1}.

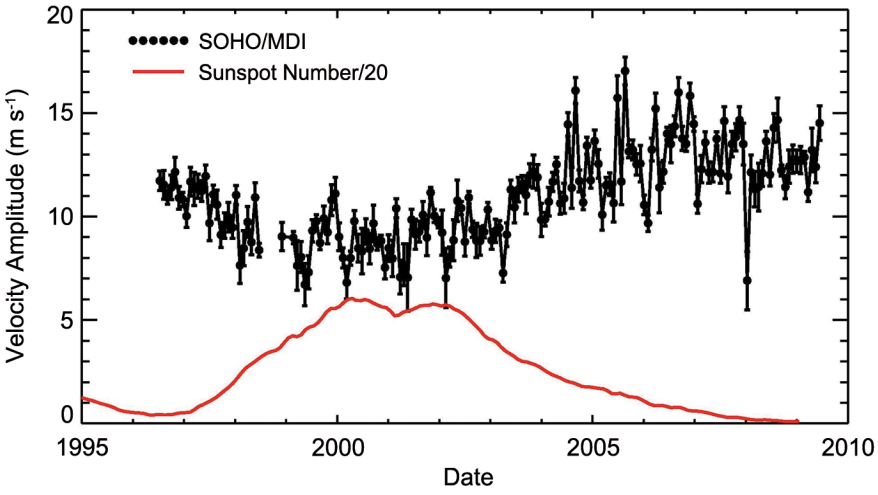

Figure 2.2.1. Variations in meridional flow from 1996 to 2009, as measured by SOHO/MDI. The scaled smoothed sunspot number is shown in red to indicate the phase of the solar activity cycle. Note the significantly higher meridional flow speed during the approach to the 2009 minimum compared with the previous minimum. (Hathaway & Rightmire, 2010)

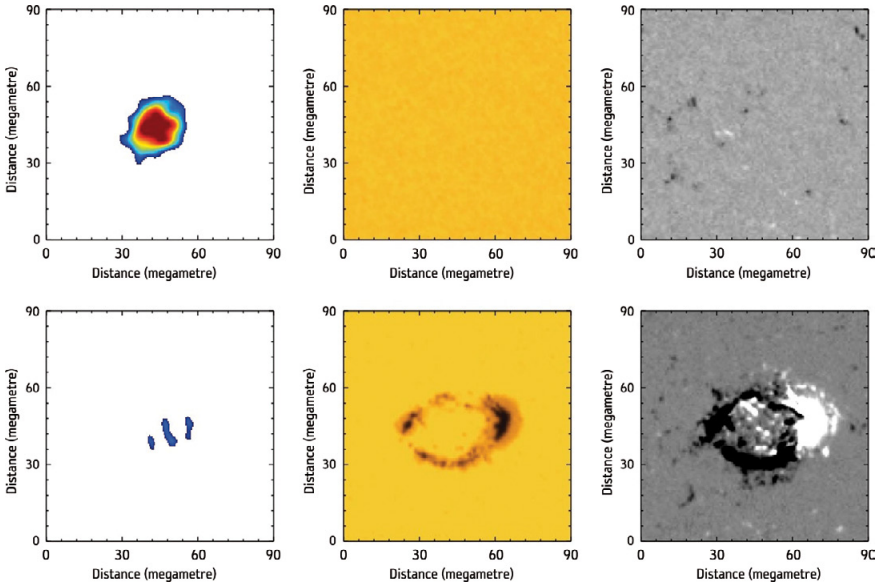

Figure 2.2.2. Acoustic travel time perturbations detected at a depth of about 60 000 km (*left*) and simultaneous observations of the photospheric intensity (*centre*) and magnetic field (*right*). The images in the upper row were taken at about 03:30 UT on 26 October 2003 and those in the lower row about 2 days later. (Ilinodis et al., 2011)

Solar irradiance

Kretzschmar et al. (2010) analysed 11 years of SOHO/VIRGO and Geostationary Operational Environmental Satellite (GOES) data to study the effects of flares on total solar irradiance. They find that the total energy radiated by flares (L_{bol}) exceeds the energy radiated in soft X-rays (L_X) by two orders of magnitude: $L_X/L_{bol} \approx 10^{-2}$. The results have implications for our understanding of solar flares and the variability of the Sun.

Solomon et al. (2010) studied the EUV irradiance and thermospheric density during the recent prolonged solar minimum (2007–09) using measurements from the Charge, Element, and Isotope Analysis System/Solar EUV Monitor (CELIAS/SEM) and Thermosphere, Ionosphere, Mesosphere Energetics and Dynamics (TIMED) satellite. Solar EUV irradiance levels were found to be lower than they were during the previous solar minimum, and the terrestrial thermosphere was cooler and lower in density than at any time since the beginning of the space age. From a comparison of circulation model simulations with thermospheric density measurements they conclude that the primary cause of the low thermospheric density was the unusually low level of solar EUV irradiance.

Chen et al. (2011) studied the relationship between the solar EUV flux during the recent solar minimum as measured by CELIAS/SEM and the $F_{10.7}$ index,

which has been routinely recorded since 1947 and is widely used in ionospheric physics as a proxy for the solar EUV flux. They find that the EUV irradiance measured by SEM was significantly lower during the recent minimum than during the previous one for the same $F_{10.7}$ level. The same was found for the critical frequency of the F_2 layer (f_0F_2) when compared with the $F_{10.7}$ index. This suggests that during the recent minimum the $F_{10.7}$ index was not a good proxy for the solar EUV flux, although it was adequate during previous minima. Solar irradiance models and ionospheric models will need to take this into account for solar cycle investigations.

Coronal Mass Ejections

Bemporad & Mancuso (2010) presented the first complete determination of plasma physical parameters across a CME-driven coronal shock, based on data from the UltraViolet Coronagraph Spectrometer (UVCS) and LASCO (Fig. 2.2.3). They found that the coronal plasma is heated across the shock from an initial temperature of 1.3×10^5K up to 1.9×10^6K, while at the same time the magnetic field undergoes a compression from a pre-shock value of ~0.02 G up to a post-shock field of ~0.04 G.

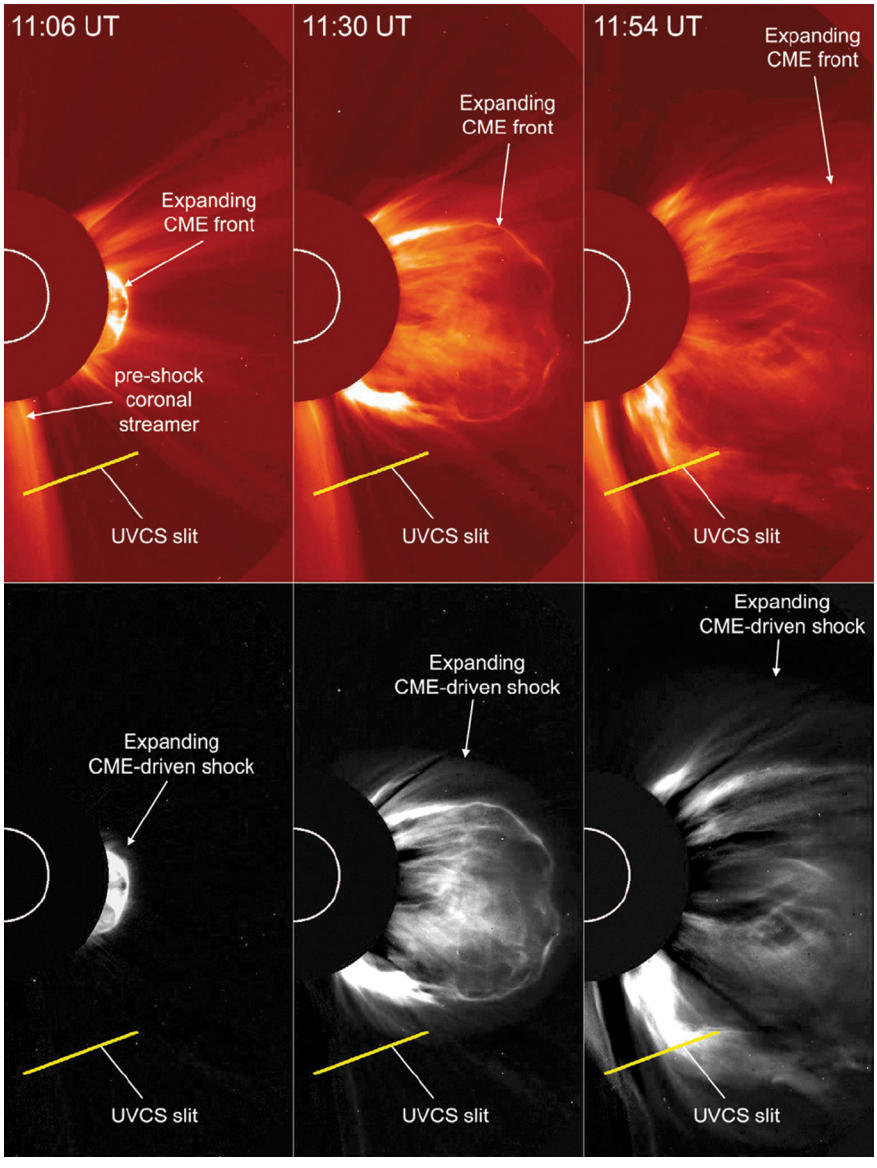

Figure 2.2.3. Sequence of LASCO/C2 standard (top) and base difference (bottom) images showing the evolution of the CME on 22 March 2002. The solid yellow line shows the position of the UVCS slit field of view (FOV), centred at 4.1 $R_\odot$. (Bemporad & Mancuso, 2010)

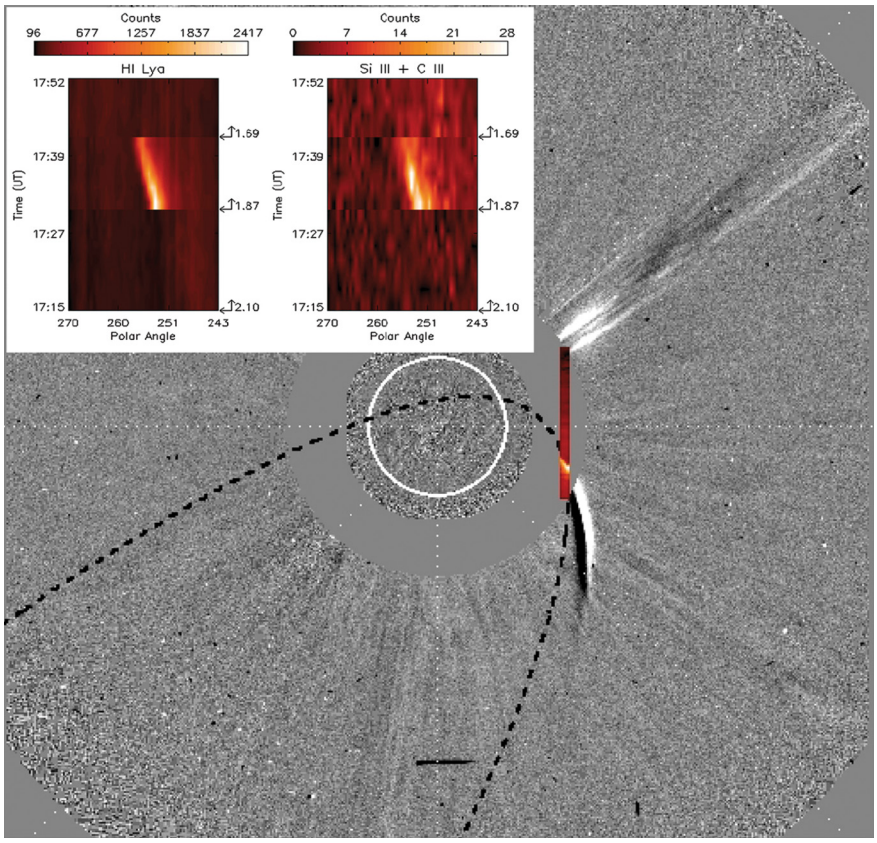

Figure 2.2.4. Composite image of LASCO-C2, UVCS slit, and the computed orbit of comet C 2003K7. The insets show the H I Lyman-α and Si III + C III UV images of the comet. (Ciaravella et al., 2010)

Comets

On 26 December 2010, SOHO discovered its 2000th comet. Drawing on help from citizen scientists around the world, SOHO has become the single greatest comet finder of all time. The 1999th and 2000th comets were both discovered on 26 December by M. Kusiak, an astronomy student at Jagiellonian University in Cracow, Poland. Kusiak found his first SOHO comet in November 2007 and has since found more than 100.

Combi et al. (2011) reported global water production rates of the comet 103P/Hartley 2, observed with the Solar Wind ANisotropies (SWAN) instrument around the time of the flyby by NASA's Extrasolar Planet Observation and Deep Impact Extended Investigation (EPOXI) spacecraft on 4 November 2010 (14 October to 2 December 2010). The water production was measured to be three times lower than during the 1997 apparition. On 30 September it increased by a factor of ~2.5 within one day, with a similar corresponding drop between 24 and 30 November. The high total surface area of sublimating water suggests that a significant fraction of Hartley 2's water production results from the extended halo of icy fragments that appear to be carried off the surface by CO_2 driven activity, rather than from the nucleus itself.

Ciaravella et al. (2010) reported on evidence for dust sublimation in UVCS spectra of Si III and C III lines from the bright sungrazing comet C 2003K7. The outgassing rate of $0.4–1.7 \times 10^{30}$ H atoms/s was determined to be more than a magnitude greater than that of other sungrazing comets observed with UVCS. The area and the rate of change of the nucleus area suggest that the comet broke apart into many fragments before it was observed by UVCS.

The unique feature of these serendipitous observations, which were taken as part of a synoptic scan of the corona, is the simultaneous detection of bright Si III 1206 Å and C III 977 Å lines, signatures of dust sublimation (Fig. 2.2.4). The detection of dust sublimation at such a low heliocentric distance (3.37 $R_\odot$) indicates a crystalline structure of the comet fragments. The observed intensities

in Si III and C III lines provide a Si III/C III ratio in the range 8–22, indicating a larger abundance of silicates in the cometary dust as compared with organic refractory materials. This result suggests that C 2003K7 may be part of a group of comets with strong silicate features.

References

Bemporad, A. & Mancuso, S. (2010). *Astrophys. J.* **720**, 130.
Chen, Y., Liu, L & Wan, W. (2011). *J. Geophys. Res.* **116**, A04304.
Ciaravella, A., Raymond, J.C. & Giordano, S. (2010). *Astrophys. J.* **713**, L69.
Combi, M.R., Bertaux, J.-L., Quemerais, E., Ferron, S. & Maekinen, J.T.T. (2011), *Astrophys. J.* **734**, L6.
Hathaway, D.M. & Rightmire, L. (2010). *Science* **327**, 1350.
Ilonidis, S., Zhao, J. & Kosovichev, A. (2011). *Science* **333**, 993.
Kretzschmar, M., de Wit, T.D., Schmutz, W., Mekaoui, S., Hochedez, J.-F. & Dewitte, S. (2010). *Nature Phys.* **6**, 690.
Solomon, S.C., Woods, T.N., Didkovsky, L.V., Emmert, J.T. & Qian, L. (2010). *Geophys. Res. Lett.* **37**, L16103.

2.3 Cassini-Huygens

Introduction

Cassini-Huygens is a NASA/ESA/ASI mission to explore the saturnian system. It was launched on 15 October 1997 on a Titan IVB Centaur rocket from Cape Canaveral Air Force Station in Florida. After a 6.7-year journey through interplanetary space, including gravity-assist manoeuvres at Venus, Earth and Jupiter, the spacecraft was inserted into the saturnian system on 1 July 2004.

The Cassini orbiter was carrying the Huygens probe, contributed by ESA, which entered the atmosphere of Saturn's largest moon, Titan, and descended under parachute down to the surface on 14 January 2005. The Huygens probe survived for 3 h on the surface of Titan, and delivered crucial data on the structure, winds and composition of the atmosphere of Titan, as well as surface imaging and state measurements.

The Cassini spacecraft is undertaking an extensive exploration of the saturnian system with its rings, icy satellites and magnetosphere. Cassini completed its initial four-year mission in June 2008, after 75 orbits around Saturn. The first extended mission, called the Cassini Equinox mission, ran from 1 July 2008 until September 2010. The Equinox mission was a unique opportunity to study the saturnian system as the Sun was crossing the equatorial plane from the southern to the northern hemisphere, a shift that occurs roughly every 14 years. In October 2010, a second extension to the mission, called the Cassini Solstice mission, was approved. It is intended to last until the northern summer solstice in September 2017.

Payload

Table 2.3.1 gives an overview of the Cassini orbiter payload.

Table 2.3.1. Overview of Cassini's instruments, measurements and resources.

Instrument/PI	Measurement	Technique	Mass (kg)	Power (W)	Participants
Optical remote sensing					
Composite Infrared Spectrometer (CIRS) M. Flasar, NASA/GFSC, CA, USA	High-resolution spectra 7–1000 μm.	Spectroscopy using three interferometric spectrometers.	43	43.3	US, FR, DE, IT, GB
Imaging Science Subsystem (ISS) C. Porco, SSI, Boulder, CO, USA	Photometric images through filters, 0.2–1.1 μm.	Imaging with CCD detectors: 1 wide-angle camera (61.2 mrad FOV) and 1 narrow-angle camera (6.1 mrad FOV).	56.5	59.3	US, FR, DE, GB
Ultraviolet Imaging Spectrometer (UVIS) L. Esposito, University of Colorado, Boulder, CO, USA	Spectral images, 0.35–1.05 μm; 0.85–5.1 μm occultation photometry.	Imaging spectroscopy; two spectrometers.	15.5	14.6	US, FR, DE
Visible and Infrared Mapper Spectrometer (VIMS) R. Brown, University of Arizona, Tucson, AZ, USA	Spectral images, 0.35–1.05 μm; occultation photometry 0.85–5.1 μm	Imaging spectroscopy; two spectrometers.	37.1	24.6	US, FR, DE, IT

Further information about the Cassini-Huygens mission can be found at *http://sci.esa.int/huygens*

Instrument/PI	Measurement	Technique	Mass (kg)	Power (W)	Participants
Radio remote sensing					
Cassini Radar (RADAR) C. Elachi/S. Wall, JPL, Pasadena, CA, USA	Ku-band radar images (13.8 GHz); radiometry, <0.5K resolution.	Synthetic aperture radar; radiometry with a microwave receiver.	43.3	108.4	US, FR, IT, GB
Radio Science Instrument (RSS) R. French, Wellesley College, USA	Ka-/S-/X-bands; frequency, phase, timing and amplitude.	X-/Ka-band uplink; Ka-/X-/S-band downlink.	14.4	82.3	US, IT
Particle remote sensing and *in situ* measurement					
Magnetospheric Imaging Instrument (MIMI) S. Krimigis, Johns Hopkins University, Baltimore, USA	Image energetic neutrals and ions at <10 keV to 8 MeV per nucleon; composition 10–265 keV/e ions; charge state; composition; directional flux mass range: 20 keV to 130 MeV ions; 15 keV to >11 MeV electrons; directional flux.	Particle direction and imaging; ion neutral camera (time-of-flight, total energy detector). Charge energy mass spectrometer. Solid-state detectors with magnetic focusing telescope and aperture-controlled ~45° FOV.	29	23.4	US, FR, DE
In situ measurements					
Cassini Plasma Spectrometer F. Crary, Southwest Research Institute, San Antonio, TX, USA	Particle energy/charge: 0.7–30 000 eV/e; 1–50 000 eV/e; 1–50 000 eV/e.	Particle detection and spectroscopy: Electron spectrometer; Ion-mass spectrometer; Ion-beam spectrometer.	23.8	19.2	US, FI, FR, HU, NO, GB
Cosmic Dust Analyzer R. Srama, MPIK, Heidelberg, Germany	Directional flux and mass of dust particles in the range 10^{-16}–10^{-6} g; chemical composition	Impact-induced currents.	16.8	19.3	DE, CZ, FR, NO, GB, US, ESA
Dual Technique Magnetometer (MAG) M. Dougherty, Imperial College, UK	B field: DC to 4 Hz up to 256 nT; scalar field DC to 20 Hz up to 44 000 nT.	Magnetic field measurements; flux gate magnetometer; vector scalar magnetometer .	8.8	12.4	GB, ES, US
Ion and Neutral Mass Spectrometer (INMS) J.H. Waite, Southwest Research Institute, San Antonio, TX, USA	Fluxes of positive ions and neutrals in mass range 2–66 Da.	Mass spectrometry Closed source and open source.	10.3	26.6	US, DE
Radio and Plasma Wave Science (RPWS) experiment D. Gurnett, University of Iowa, USA	E field: 10 Hz to 2 MHz B field: 1 Hz to 20 kHz; Plasma density and temperature.	Radio-frequency receivers; 3 electric monopole antennas; 3 magnetic search coils; Langmuir probe.	37.7	17.5	US, AT, FR, SW, GB, NO

Status

The spacecraft is in an excellent state of health and all subsystems are operating normally. One safe-mode occurred in November 2010, which was only the second since the beginning of the nominal mission in the saturnian system, and was probably caused by a corrupted radio link. The spacecraft was recovered without difficulty. One instrument, the Cassini Plasma Spectrometer (CAPS), was powered off in June 2011 following difficulties with interactions between the instrument and the spacecraft bus voltage. Scientists at the Jet Propulsion Laboratory (JPL) investigated the issue, and decided that it was not serious. CAPS was turned back on in March 2012, and will now be monitored for any unusual behaviour.

The Cassini Solstice mission has been approved until 2017, when the spacecraft will enter Saturn's atmosphere. This will provide a great opportunity for comparative planetology, with a coordinated observation campaign with NASA's Juno mission, which will be exploring similar regions at Jupiter at the same time.

ESA increased its participation in the Cassini Orbiter in 2010 by funding the UK-based Science Operations of the CAPS, Composite Infrared Spectrometer (CIRS) and Dual Technique Magnetometer (MAG) instruments, and which are now in principle ensured until the end of the mission.

The Cassini Participating Scientist Program was initiated in 2011, with the intention to broaden the Cassini scientific community by giving selected scientists an opportunity to join an instrument team and access the data. Around 20 Participating Scientists were selected through the Cassini Data Analysis Program (CDAP), managed by NASA, and have been appointed for a duration of three years. For 2011, four European scientists were selected, from France, Belgium and Italy.

Scientific Objectives

The scientific objectives of the Solstice mission are focused on studying seasonal–temporal changes of Titan, Saturn, the rings, the icy moons and the magnetosphere. On Titan, seasonal changes in the methane–hydrocarbon hydrological cycle will be studied by monitoring lakes, clouds, aerosols and their seasonal transport. Saturn's atmosphere will be observed for changes in temperature, clouds, storms and composition. The production, appearance and variability of 'spokes' on the rings will be studied in correlation with the varying solar elevation.

At the end of the Solstice mission, the magnetosphere of Saturn will have been observed during a whole solar cycle (11 years), from one solar minimum to the next. The long-term variability of the surfaces of Saturn's icy satellites will be monitored; in particular, measurements of seasonal variations in the cryovolcanic activity on Enceladus will provide new constraints on the mechanism of plume formation. The foreseen end of mission, with the spacecraft flying on highly inclined orbits with the periapse very close to Saturn (inside the D ring), will be a unique opportunity to obtain precise measurements of Saturn's internal magnetic field and to determine directly the mass of the ring.

Mission Phases and Events

The Solstice mission phases are defined by the orbit inclination (see Fig. 2.3.1) which is modified by Titan flybys. From October 2010 until early 2012, the spacecraft remained within the equatorial plane of Saturn. This period is favourable to studies of the moons by targeted flybys, as indicated in

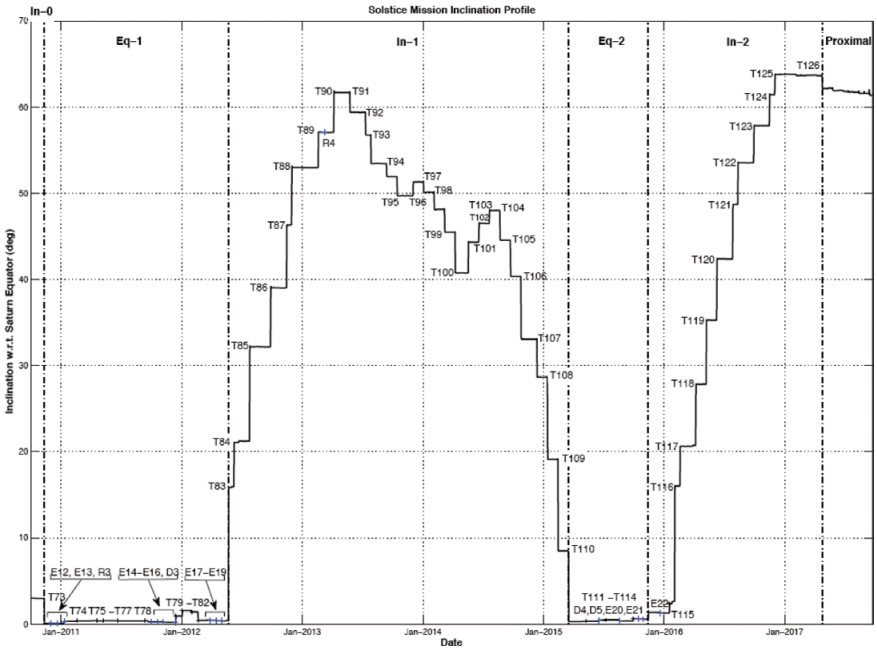

Figure 2.3.1. Cassini Solstice mission phases, defined by the varying inclination of the orbital plane. The successive Titan flybys are indicated.

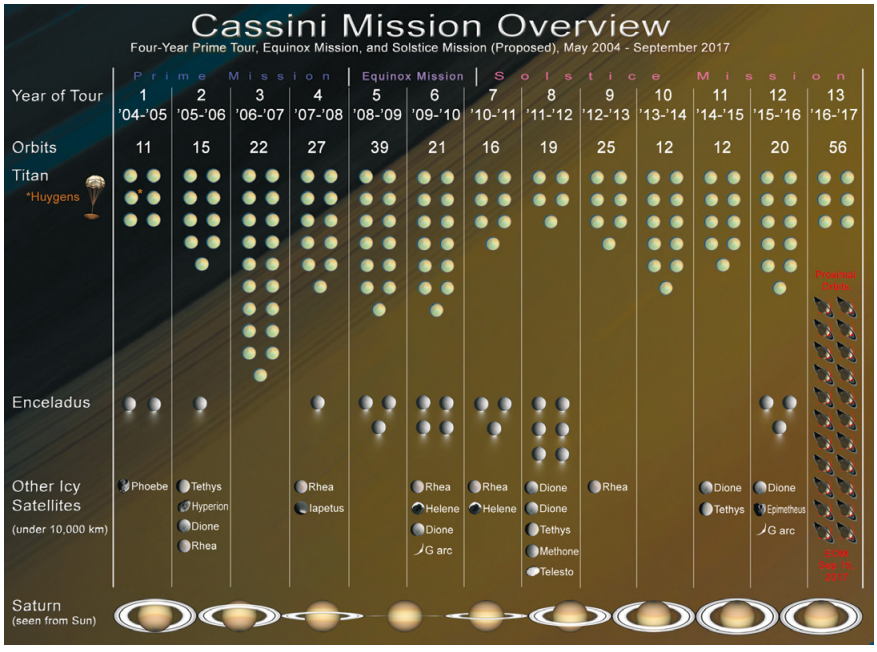

Figure 2.3.2. Major events in the Cassini mission (icy moons and Titan flybys) from orbit insertion to the end of the Solstice mission are indicated as function of time. The drawings of Saturn in the bottom row indicate the solar elevation above the ring plane.

Fig. 2.3.2. From 2012 onwards, the orbit inclination will be raised over 60° and lowered again such that the orbit is back in the equatorial plane in early 2015. This period will be favourable to studies of Titan and Saturn's rings and magnetosphere. The last mission phase will see the orbit inclination being raised again, until the final 'proximal orbits' can be flown, before the final disposal of the spacecraft in Saturn's atmosphere.

Scientific Highlights

The main scientific results of the Cassini-Huygens prime mission have been described in two reference books: *Saturn from Cassini-Huygens* (Dougherty et al., 2009) and *Titan from Cassini-Huygens* (Brown et al., 2009). As the most ambitious and interdisciplinary planetary exploration mission flown to date,

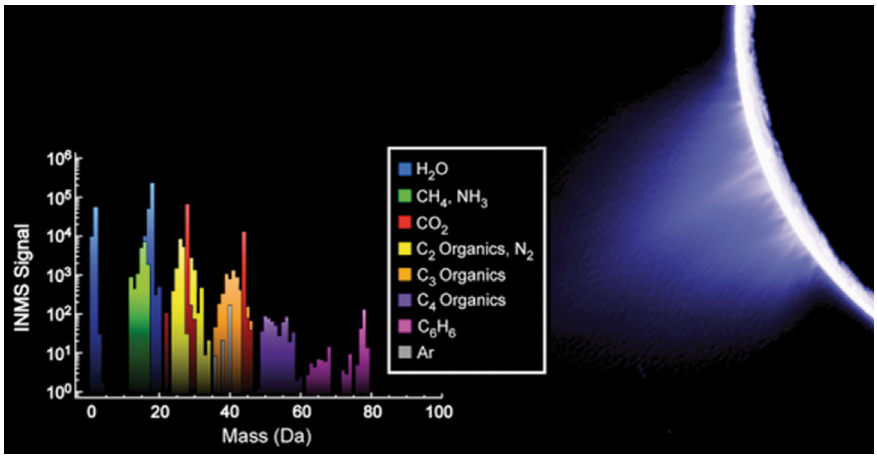

Figure 2.3.3. Composition of a plume (gas phase) escaping from the 'tiger stripes' fissures on Enceladus, as measured by the Ion and Neutral Mass Spectrometer (INMS) instrument. (NASA/JPL/Space Science Institute and NASA/JPL SWRI)

Cassini-Huygens has extended our knowledge of the saturnian system to levels of detail at least an order of magnitude beyond those gained from all previous missions to Saturn.

A selection of recent results per scientific discipline are summarised in the following paragraphs.

Icy Moons

A very detailed thermal map of Mimas, Saturn's innermost icy moon, 396 km diameter, was obtained in 2010. The temperature distribution is very different from the one theoretically expected. Rather than having a temperature distribution that is roughly axisymmetric around the moon–Sun line, Mimas appears to have a cold and a warm side separated by a V-shaped boundary. This temperature distribution is not understood so far.

Cryovolcanic activity on Enceladus was discovered in 2005, showing relatively warm fissures at the south pole that eject plumes of water vapour, icy grains and organics. During close flybys in 2008 and 2009, the Cosmic Dust Analyser (CDA) instrument was able to measure the chemical composition of large (a few tens of microns) icy grains in the plumes. It was found that the icy particles are rich in salts contained within the icy lattice (Fig. 2.3.3). Such a salt content cannot be achieved from a direct vaporisation of solid ice at the surface of Enceladus. This finding points to the existence of liquid water below the surface, possibly connected to an ocean in contact with a rocky core.

Titan

A recent study of the data obtained from the Chromatograph Gas Spectrometer on the Huygens probe addressed the mystery of the 'missing noble gases' in Titan's atmosphere. Only argon could be identified in the data. This study showed that the heavier noble gases can be trapped in clathrate hydrates if certain thermophysical conditions prevail at Titan's surface–atmosphere interface. Interestingly, such conditions could be met if a metre-thick layer of fresh lava is covering a significant part of Titan's surface, requiring recent cryovolcanic activity.

While active cryovolcanism has not been observed on Titan, in 2010 Cassini's RADAR instrument discovered the best candidate yet for an ice volcano, based on topographic mapping coupled with Visible and Infrared Mapper Spectrometer (VIMS) reflectance spectra (Fig. 2.3.4). Two peaks of up to 1000 m can be observed, as well as multiple craters (calderas?) as deep as 1500 m. The terrain around the peaks and the craters is covered by dunes. The

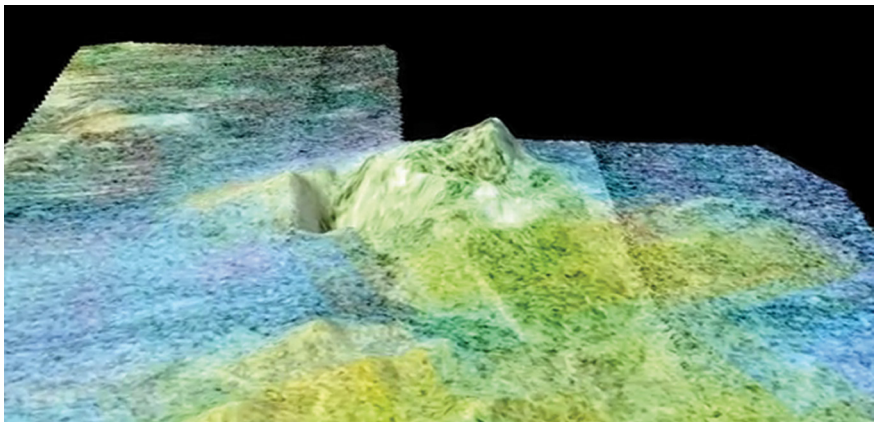

Figure 2.3.4. 3D topography of the area known as Sotra Facula on Saturn's moon Titan, obtained by Cassini's RADAR instrument. The topography has been vertically exaggerated by a factor of 10. Compositional differences inferred from the VIMS instrument data have been superimposed in false colour. (NASA–JPL–Caltech/UGSG/University of Arizona)

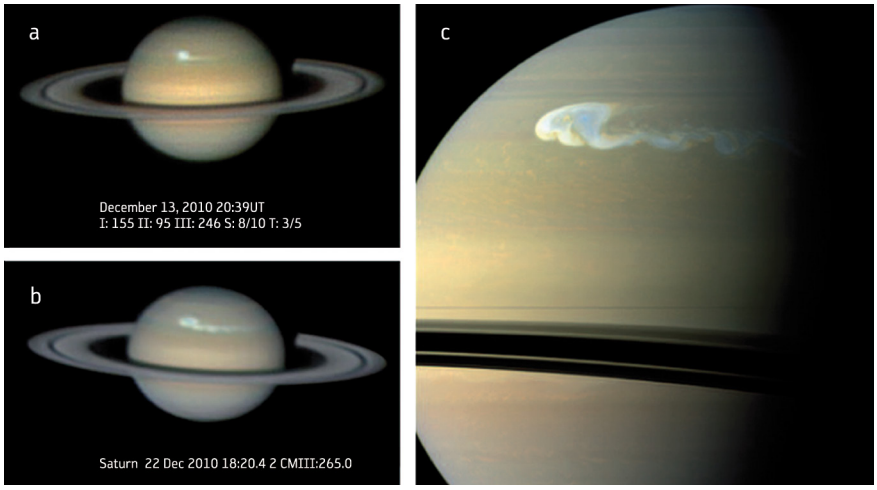

Figure 2.3.5. Images of a storm on Saturn taken in December 2010, (a, b) by ground-based telescopes (© C. Go, Cebu, the Philippines), and (c) by the wide-angle camera on Cassini (A. Wesley, Murrumbateman, Australia) (Fischer et al., 2011).

bluish dune regions represent exposed icy material, while the yellow-bright regions (peaks and calderas) are interpreted as being coated with organic material within the ice.

Evidence of cryovolcanism on Titan is actively being sought, as it could solve the 'methane mystery'. As methane is present in Titan's atmosphere but is rapidly destroyed by UV solar radiation, there must be a source for its replenishment elsewhere.

Saturn

A huge storm started to develop in the northern hemisphere of Saturn in December 2010 until it reached planetary scale a few months later (Fig. 2.3.5). It was first detected though its lightning events in the data from the Radio and Plasma Wave Science (RPWS) experiment, and quickly became the object of a multi-wavelength observation campaign. Measurements of strong winds were obtained through temperature measurements by the CIRS instrument, while VIMS reflectance spectra showed the upwelling of large icy grains of ammonia.

Rings

Data from the ISS camera trace telltale ripples in the rings of Saturn back to collisions with cometary fragments between 10 and 30 years ago, probably a cloud of cometary debris that plunged through the inner rings in late 1983.

Magnetosphere

Explosions of hot plasma were observed on the nightside of Saturn's magnetic field, resulting in a periodic inflation of the magnetic field lines every 10–11 h. The magnetic pressure resulting from the hot plasma density fluctuations at distances of 8–15 Saturn radii may explain the puzzling periodic variations in magnetic field signals known from previous measurements.

References

Brown, H., Waite, J.H. & Lebreton, J.-P. (Eds) (2009). *Titan from Cassini–Huygens*. Springer Science+Business Media. DOI: 10.1007/978-1-4020-9215-2.

Dougherty, M.K., Esposito, L.W. & Krimigis, S.M. (Eds) (2009). *Saturn from Cassini–Huygens*. Springer Science+Business Media. DOI: 10.1007/978-1-4020-9217-6.

Fischer, G., Kurth, W.S., Gurnett, D.A., Zarka, P., Dyudina, U.A., Ingersoll, A.P., Ewald, S.P., Porco, C.C., Wesley, A., Go, C. & Delcroix, M. (2011). A giant thunderstorm on Saturn, Letter to *Nature* **475**, 75–77. DOI: 10.1038/nature10205.

2.4 XMM-Newton

Introduction

The XMM-Newton observatory was launched on 10 December 1999 from Kourou in French Guiana on the first commercial Ariane 5 (V504) into a highly elliptical 48 h orbit. The mission is providing high-quality X-ray and optical/UV data from the European Photon Imaging Camera (EPIC), the Reflection Grating Spectrometer (RGS) and the Optical Monitor (OM). XMM-Newton is a 3-axis-stabilised satellite with a mass of about 4 t.

The satellite is dominated by a large carbon-fibre telescope tube attached to the Service Module (SVM) at one end and to the Focal Plane Assembly (FPA) at the other. The SVM is a platform that carries all the equipment for the power, data handling and attitude and orbit control subsystems, including the structure to support the solar arrays and antennas. The attitude control loop uses a startracker and momentum wheels, which allow for a slew rate of 90° per hour and a pointing reconstruction accuracy of a few arcsec. Gyros are used only in cases of eclipses or anomalies.

The operational efficiency allows for a maximum of 132 ks of science observations per revolution; the remaining 40 ks are spent inside the radiation belts. The mission routinely responds to Targets of Opportunity requests with response times as short as 5 h. This has been put to good use a number of times when XMM-Newton has performed rapid follow-up of gamma-ray bursts.

Mission Status

XMM-Newton continues to be in excellent health. Operations are approved until 31 December 2014, subject to a mid-term performance review to be held later this year. The status of the satellite, instruments and ground segment all remain excellent, and consistent with a lifetime well beyond that currently approved. Onboard consumables are sufficient to operate for at least up to 2019. The radiation-induced performance degradation has been largely ameliorated by allowing the X-ray detectors to operate at lower temperatures. Based on current knowledge, the instruments will be able to operate within specifications for the foreseeable future.

An EPIC detector is positioned behind each of the three X-ray mirror modules. Two MOS-CCD cameras share the mirrors with the grating array, and the pn-CCD detector is located behind the fully open telescope position. The in-orbit performance of the EPIC cameras is excellent, and the degradation of the camera owing to irradiation by (mostly solar) protons is as predicted pre-launch. A decision to lower the temperature of the detectors was taken at the end of 2002 in order to ameliorate the radiation damage. This action has been very successful: not only has the performance degradation since launch been recovered, but the rate of degradation has also decreased considerably.

The RGS is a powerful X-ray spectrometer with an $E/\Delta E$ of 300–700 (first order) in the 5–35 Å (0.35–2.4 keV) soft X-ray band. The effective area for the two grating arrays is in the range 40–200 cm^2 over this wavelength band. The instrument's performance is as predicted. The 2002 cooling exercise was as successful as with EPIC, ameliorating much of the incurred radiation damage and, most important, dramatically reducing the number of hot columns and hot pixels. The Optical Monitor is a powerful telescope in the 170–600 nm wavelength range, which can detect sources down to 24th magnitude in a few kiloseconds (depending on spectral type). This camera is powerful enough,

Further information about the XMM-Newton X-ray observatory can be found at *http://sci.esa.int/xmm*

in terms of both sensitivity and positional accuracy, to allow identification of counterparts of many of the new X-ray sources detected with XMM-Newton.

XMM-Newton operations are carried out via a Mission Operations Centre (MOC) at the European Space Operations Centre (ESOC) in Darmstadt, Germany, and a Science Operations Centre (SOC) at the European Space Astronomy Centre (ESAC) in Villanueva de la Cañada, near Madrid, Spain. The design of the satellite and its instruments is such that continuous realtime supervision of the operations is necessary. The ground segment also involves the Survey Science Consortium (SSC), an AO-selected, nationally funded, multinational consortium. The SSC pipeline processes raw science data and converts them into first-level science files and results. The PI teams, who designed and built the instruments, support the SOC in the areas of calibration and validation of changes to the onboard software. Both the PI teams and the SSC collaborated with ESA in the creation of the widely-used Science Analysis Software (SAS).

The analysis of XMM-Newton data is supported by the SAS software package, now at version 7.1, which is released approximately once a year. It allows scientific users to derive reliable and calibrated results for further analysis with standard X-ray astronomy spectral analysis packages. The derivation of accurate calibration data, and the proper incorporation of this knowledge into the SAS software, is a continuing process. The status of the calibration is now such that most (spectral) parameters can be derived to an absolute accuracy of around 12%, depending on the quantity. The XMM-Newton Science Archive (XSA), based on reusing technology from the ISO archive, was released in March 2002. The archive allows for flexible querying and retrieving of all XMM-Newton (public) data in a highly flexible and configurable way.

Impact of XMM-Newton

The scientific impact of XMM-Newton is high. So far, more than 3000 refereed articles based on XMM-Newton data have been published, at a rate that currently exceeds 300 per year. XMM-Newton publications are also highly cited; 38% of these publications belong to the top category of the 10% most cited articles published over the period 2007–09. The importance of XMM-Newton is now widely recognised not only in the scientific world in general, but also beyond the X-ray and even the astronomy communities.

As an illustration, *Nature* completed its cycle of review articles honouring the International Year of Astronomy with a description of the achievements of XMM-Newton (and of NASA's Chandra X-ray Observatory) (Santos-Lleo et al., 2009). The community using XMM-Newton is very large. All 11 XMM-Newton 'Calls for Observing Proposals' have resulted in an oversubscription of the available observing time by a factor of at least 6.6. Each call typically involves 1450 individual astronomers, or approximately 15% of all professional astronomers worldwide. XMM-Newton plays an important role in education as well; more than 108 doctorates have been based on XMM-Newton data.

Scientific Highlights

During the last two years, XMM-Newton has continued to break new ground in many areas of science as the following highlights illustrate.

XMM-Newton has contributed substantially to our knowledge of Young Stellar Objects (YSOs) and of their interaction with the surrounding circumstellar discs. During a deep observation of the ρ-Ophiuchi star forming region, XMM-Newton observed fluorescent iron emission lines for a period of four days following a large stellar flare. The iron lines trace magnetic field lines in accretion loops between the star and its disc. While most YSO flares are

similar to solar ones, some are occasionally large enough to span the star–disc separation.

Another important result was the first detection of faint, hard X-ray emission from a Wolf–Rayet star. The star, WR142, belongs to the rare WO category of stars characterised by strong oxygen lines in their optical spectra. Such stars are thought to be in an advanced evolutionary state shortly before their explosion as a supernovae or gamma-ray burst. The discovery of hard X-ray emission sheds new light on the properties of Wolf–Rayet stellar winds and on the last stages of massive star evolution.

Utilising XMM-Newton spectra, accurate relative elemental abundances could be measured in several supernovae remnants (SNRs), which in turn enabled detailed tests of type Ia supernovae explosion models. Among them is SNR 0509-67.5 in the Large Magellanic Cloud, for which both optical and X-ray data favour the delayed detonation model for an explosion that occurred some 400 yr ago.

Central Compact Objects (CCOs) are isolated neutron stars embedded in supernova remnants. XMM-Newton and Chandra data were used to infer the spin-down rate in the CCO pulsar PSR-J1852+0040. This led to the first determination of the magnetic field in a CCO of 3.1×10^{10} G, the smallest ever measured for a young neutron star. This provides strong support to the 'anti-magnetar' model whereby CCOs are born with a slow rotation rate, which prevents them from developing a strong magnetic field (see Fig. 2.4.1).

XMM-Newton monitoring of the active galactic nucleus of Mkn 509 over 100 days has demonstrated that most of the visible outflowing gas is blown off from a dusty gas torus surrounding the central region more than 15 light years away from the black hole.

Deep XMM-Newton observations of the Cosmos 2 deg^2 field led to the detection of 206 groups of galaxies with redshifts of up to 1. This large sample was used to investigate the scaling relation between the X-ray luminosity, L_X, and the halo mass, M_H, of the galaxy groups, where M_H represents the total (dark and baryonic) mass of the group inferred from weak gravitational lensing techniques. The L_X/M_H relation had so far been established only for large groups and clusters of galaxies in the local Universe. This new study extends its validity to much smaller halos and higher redshifts. The mass–luminosity relation is an important tool for cosmology and the study of structure evolution in the Universe.

Deep X-ray exposures from XMM-Newton combined with near-IR images from Subaru led to the discovery of SXDF-XCLJ0218-0510, the most distant galaxy cluster ever found at a redshift of 1.62. Using the newly released 'mosaic' observing mode, XMM-Newton recently mapped two new galaxy clusters, one of which, SPT-CL J2332-5358, is among the hottest and most massive clusters known to date. The clusters were tentatively discovered with the South Pole Telescope, but XMM-Newton observations were essential in confirming the discovery and characterising the cluster properties. This illustrates the power of combining millimetre and X-ray observations for finding and characterising clusters of galaxies.

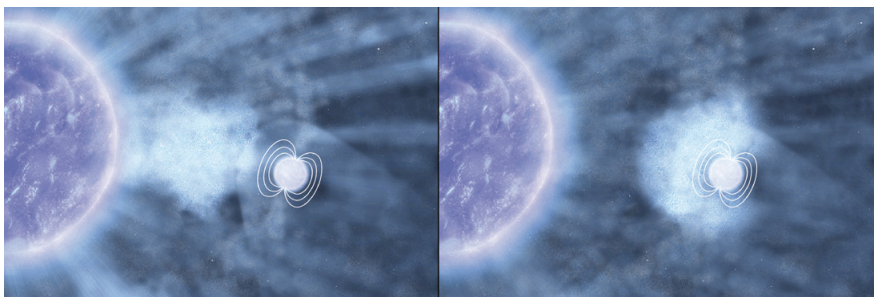

Figure 2.4.1. Data collected by ESA's XMM-Newton X-ray observatory appear to show that a denser patch in the stellar wind, released by the supergiant and accreted by the neutron star, contributed to boosting the X-ray luminosity of the source. This sequence of images illustrates the accretion of a clump of matter on the neutron star hosted in the supergiant fast X-ray transient, IGR J18410-0535. The neutron star is shown, on the right, with the field lines highlighting its intense magnetic field, while the companion, a blue supergiant, is represented as the large star on the left. The relative sizes of the objects shown here are purely indicative; in fact, the radius of the supergiant is about 2 million times larger than that of the neutron star. (AOES Medialab)

By combining high-resolution grating spectra from XMM-Newton and Chandra it has been possible for the first time to find direct and unambiguous observational evidence for the long sought after Warm–Hot Intergalactic Medium (WHIM). The cosmological importance of the WHIM is twofold: not only does it contain most of the baryonic mass in the local Universe, but it also acts as a tracer of large-scale structure. However, its temperature and very low density make it very difficult to detect with current facilities. The WHIM was detected by the O VII absorption line imprinted on the spectrum of a distant source, the blazar H 2356-309. At a redshift of 0.03, the absorption originates in the Sculptor Wall, a large-scale superstructure of galaxies in the nearby Universe.

Catalogues

Two catalogues of serendipitous sources are updated regularly. The 2XMM catalogue currently contains 353 000 X-ray detections of 263 000 individual sources, making it the largest X-ray catalogue ever. The X-ray Slew Catalogue contains 13 600 sources detected while XMM-Newton was manoeuvring between targets. It covers 70% of the entire sky. Finally, the XMM-OM Serendipitous Ultraviolet Source Survey contains 753 000 UV detections with the Optical Monitor from 624 000 unique sources.

Reference

Santos-Lleo, M., Schartel, N., Tananbaum, H., Tucker, W. & Weisskopf, M.C. (2009). *Nature* **462**, 997.

2.5 Cluster and Double Star

2.5.1 Cluster

After almost 12 years of operations, the four Cluster satellites continue to make great advances in magnetospheric physics, by probing Earth's magnetic environment for the first time in three dimensions. Results show that with four satellites, it is possible to obtain a detailed three-dimensional view of the Sun–Earth connection processes taking place at the interface between the solar wind and Earth's magnetic field.

Cluster is one of the two missions – the other being SOHO – that constitute the Solar Terrestrial Science Programme (STSP), the first cornerstone mission of ESA's Horizon 2000 programme. The Cluster mission was first proposed in November 1982 in response to an ESA call for proposals for the next series of scientific missions. After the Ariane 5 accident on 4 June 1996 and the destruction of the four original Cluster satellites, Cluster was rebuilt and launched in July and August 2000 on two Soyuz rockets.

In November 2010, ESA's Science Programme Committee (SPC) agreed to a third extension of the Cluster mission up to the end of December 2014, with a mid-term review in 2012.

Mission Status

The four satellites and 40 instruments (out of a possible 44) continue to work nominally, thanks to the efforts of the instrument teams, the science operation team at the Joint Science Operations Centre (JSOC) located at the Rutherford Appleton Laboratory, Didcot, UK, and the flight/mission control team at ESOC, in Darmstadt, Germany.

The Cluster payload consists of magnetometers (flux gate for the static magnetic field and search coil for the magnetic waves), wire booms, electron guns and wave receivers to measure electric fields and particle detectors to measure electrons and ions from a few eV to a few MeV (Table 2.5.1). The indium reservoirs of the Active Spacecraft Potential Control (ASPOC) instruments are now empty and are no longer functioning.

The goal of the Cluster mission is to measure magnetospheric structures and plasma phenomena at different scales, along a $4 \times 19.6\ R_E$ nominal orbit. To achieve this goal, about 150 kg of propellant was reserved to change the separation distance between the satellites during the constellation manoeuvres. Over 27 constellation manoeuvres have been performed so far to change the inter-satellite distance from 100 km up to 10 000 km in the first 'regular tetrahedron' phase (2001–04), and from 40 km to 10 000 km in the multiscale phase (2005 onwards) (Fig. 2.5.1).

As part of the current extension proposal, ESA issued an Announcement of Opportunity for special operations, opening the mission to the science community to suggest specific constellation configurations and instruments operation modes. As a result of this AO, six guest investigators were selected and over the next two years their specific science operations will be implemented. Already in 2011 a set of observations were implemented, running the electron instruments in a high-resolution mode to investigate energetic electrons at the high-latitude southern magnetopause.

The Cluster satellites are influenced by the perturbations from the Sun and the Moon, which have reduced the perigee and increased the apogee of the orbit. In addition, the apogee has drifted toward the southern hemisphere, accompanied by a decrease in the orbit inclination from ~90° to <40°. This

Further information about the Cluster mission can be found at *http://sci.esa.int/cluster*

Table 2.5.1 The Cluster payloads (identical on all four satellites).

Instruments	Principal Investigators
Fluxgate Magnetometer (FGM)	E. Lucek, Imperial College, London, UK
Spatio-Temporal Analysis of Field Fluctuation experiment (STAFF*)	N. Cornilleau-Wehrlin, CETP, France
Electric Field and Wave experiment (EFW*)	M. André, IRFU, Sweden
Waves of High Frequency and Sounder for Probing of Electron density by Relaxation (WHISPER*)	J.-G. Trotignon, LPCE, France
Wide Band Data (WBD*)	J. Pickett, University of Iowa, USA
Digital Wave Processing experiment (DWP*)	M. Balikhin, Sheffield University, UK
Electron Drift Instrument (EDI)	R. Torbert, University of New Hampshire, USA
Cluster Ion Spectrometry (CIS)	I. Dandouras, CESR, France
Plasma Electron and Current Experiment (PEACE)	A. Fazakerley, Mullard Space Science Laboratory, UK
Research with Adaptive Imaging Particle Detectors (RAPID)	P. Daly, MPAe, Germany
Active Spacecraft Potential Control (ASPOC)	K. Torkar, IWF, Austria
*Members of the Wave Experiment Consortium (WEC).	

Figure 2.5.1. Cluster inter-satellite distances from launch to late 2012. (ESA)

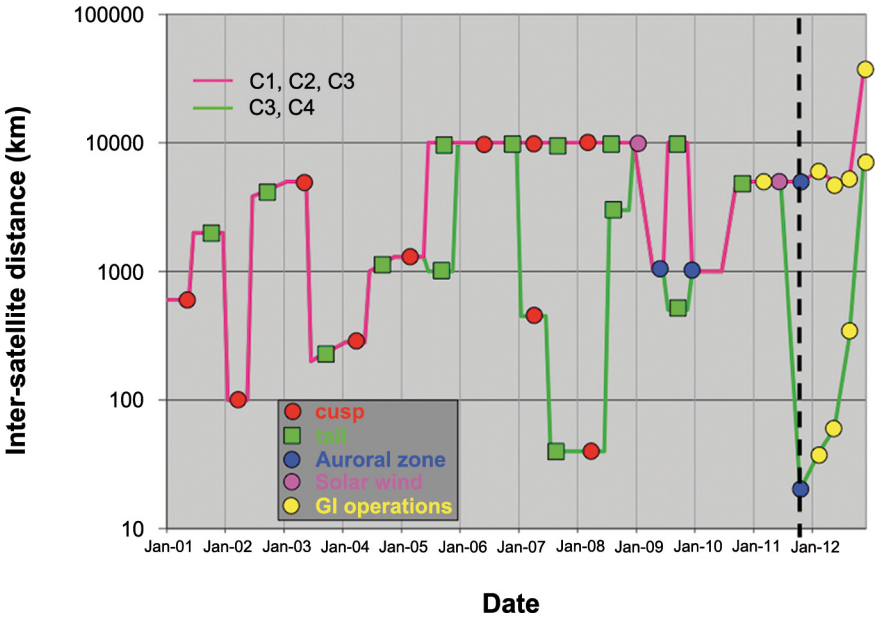

natural evolution has enhanced the science objectives by allowing Cluster to visit new regions, including the magnetopause subsolar point, the auroral acceleration region, the inner magnetosphere and plasmasphere and the southern high-altitude cusp and high-latitude magnetopause regions (Fig. 2.5.2). This evolution has also meant that the satellites cross various boundaries and plasma regions at different altitudes and latitudes, which, in combination with the evolving solar cycle, provide opportunities to make comparisons with earlier parts of the mission under different driving conditions.

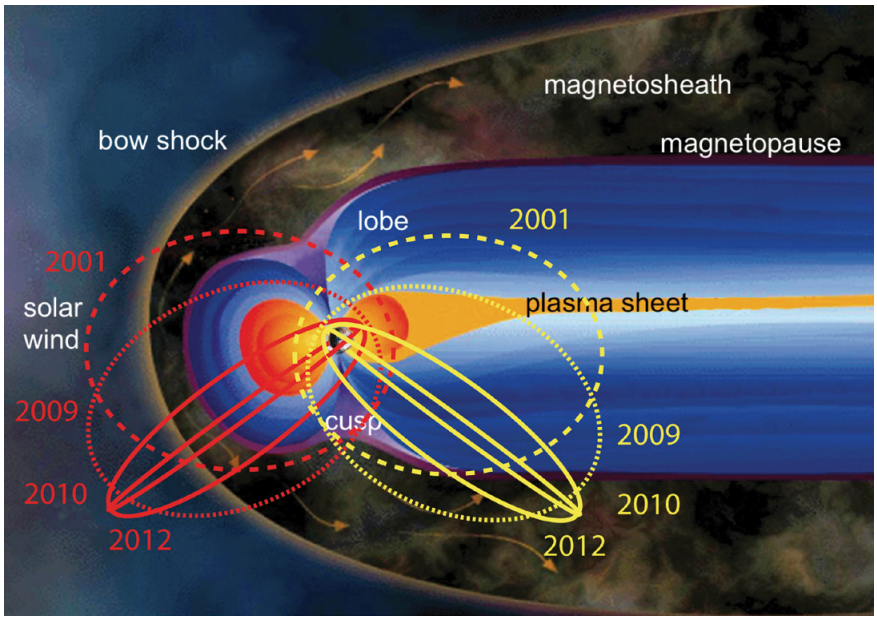

Figure 2.5.2. Cluster orbit evolution between 2001 and 2012 in winter (red) and summer (yellow). (NASA/ESA)

Scientific Highlights

Cluster continues to generate new and exciting science results, and is now at its most productive period in terms of refereed papers – more than 220 were published in 2011. Recent highlights include work examining the long journey that energetic ions undergo during geomagnetic storms and how they ultimately precipitate into Earth's atmosphere. Such precipitation affects the composition of the ionosphere, preventing GPS and communications satellites from operating correctly (Kistler et al., 2010).

In another study, a team of European scientists used observations from Cluster and Venus Express to improve models of the interactions of Earth and Venus with the solar wind, the perpetual stream of electrically charged particles emitted by the Sun. This work has implications for understanding the effects of charged particles on orbiting satellites (Echim et al., 2010).

Auroras, more commonly known as the northern and southern lights, are among the most beautiful and awe-inspiring natural phenomena. New insights into the processes that generate auroras on Earth and other planets were provided by Cluster during its current extension period. Owing to the orbit evolution discussed above, Cluster was able to make the first multi-satellite observations of the Auroral Acceleration Region (AAR) and revealed the temporal and spatial evolution of these regions, constraining the mechanisms responsible for the creation of these AAR structures (Fig. 2.5.3; Marklund et al., 2011). Cluster will continue to make important and unique observations in this region in the next few years.

At higher altitude in Earth's magnetotail, Cluster has been investigating high-speed plasma flows created by magnetic reconnection, often referred to as jets, which are extremely common across the Universe. Such jets are also observed in solar flares, and near various objects powered by black holes. New insights into the processes that modify these streams of ionised particles have been provided by rare *in situ* measurements of plasma flows made by Cluster. In a general astrophysical context, the observations suggest that one can expect particle acceleration anywhere that plasma jets are interacting with the local environment and braking (Khotyaintsev et al., 2011).

From time to time, sudden releases of energy in Earth's magnetosphere lead to major disturbances that result in bright auroral displays over the polar regions. These auroras are caused by a phenomenon known as a geomagnetic substorm. The precise cause of these substorms has been debated for decades, but new

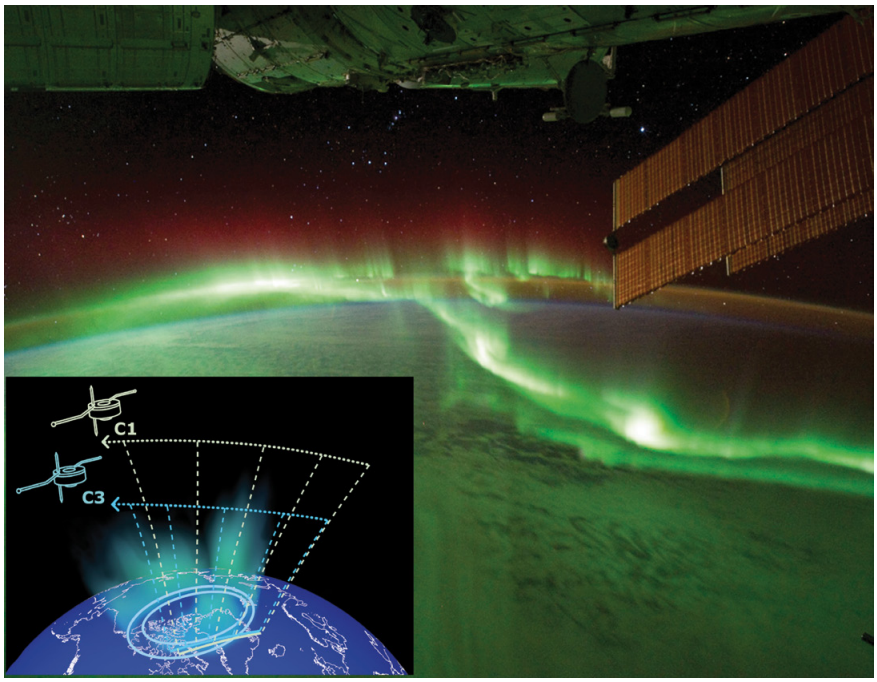

Figure 2.5.3. Frame from a video of the Aurora Australis (the southern lights) taken on the International Space Station on 17 September 2011. (NASA)
Inset: A schematic view of the Cluster C3 and C1 satellite trajectories during an AAR passage with C3 at an altitude of about 6400 km (one Earth radius, R_E), while C1 was flying at about 9000 km (1.4 R_E) and lagging about 5 min behind. The blue ovals indicate the poleward half of the auroral oval, which is characterised by upward currents flowing along in the dusk-side magnetic field. The measurements revealed the size and longevity of these regions. (ESA)

computer simulations, allied to analysis of data from the Cluster satellites have filled in many of the missing pieces of the puzzle (Shay et al., 2011).

Another Cluster highlight revealed that the bow shock formed by the solar wind as it encounters Earth's magnetic field is remarkably thin: it measures only 17 km across. Thin astrophysical shocks such as this are candidate sites for early phases of particle acceleration. The finding thus sheds new light on the much debated issue of particle injection in the context of cosmic ray acceleration (Schwartz et al., 2011).

Cluster Science Data System and the CAA

The Cluster Science Data System (CSDS) was designed as a distributed system to make possible the joint scientific analysis of data from all Cluster instruments. The general approach is to have national data centres located near the PIs and thus near the expertise required for processing the data. One of the major tasks of the CSDS is to offer, as a routine, products such as the Summary Parameter Database and the Prime Parameter Database.

The Cluster Active Archive (CAA) is the online depository of the calibrated data collected by the four Cluster satellites, including the highest-resolution data. It also provides access to the raw data, to some data analysis software modules (for example, interfaces to IDL and Matlab) and to supporting documentation such as instrument calibration reports and experiment user guides (Laakso et al., 2010).

The CAA is unique among data archives in the discipline of space physics, in terms of the breadth, quantity and quality of the data it contains. A continuous process of review and modification has focused on making the CAA interface and data products as easy to use as possible.

In summer 2010, more than 1000 scientists had registered to access data from the online CAA database of the Cluster mission; by mid-2012 the number had risen to 1275. Each month, these scientists download, on average, more than 1 TB of data. Current activities include work on the transition of the CAA to its final location at ESAC, near Madrid, Spain. In addition, data from the Double Star mission are currently being prepared for inclusion in the archive.

References

Echim, M. et al. (2010). *Planet. Space Sci*. DOI: 10.1016/j.pss.2010.04.019.
Khotyaintsev, Y.V. et al. (2011). *Phys. Rev. Lett.* **106**, 165001. DOI: 10.1103/PhysRevLett.106.165001.
Kistler, L.M. et al. (2010). *J. Geophys. Res.* **115**, A03209. DOI: 10.1029/2009JA014838.
Laakso, H. et al. (Eds.) (2010). *The Cluster Active Archive: Studying the Earth's Space Plasma Environment*. Springer, Dordrecht, the Netherlands.
Marklund, G.T. et al. (2011). *Phys. Rev. Lett.* **106**, 057204.
Schwartz, S. et al. (2011). *Phys. Rev. Lett.* **107**, 215002, DOI: 10.1103/PhysRevLett.107.215002.
Shay, M.A. et al. (2011). Super-Alfvénic propagation of substorm reconnection signatures and Poynting flux, *Phys. Rev. Lett.* **107**, 065001.

2.5.2 Double Star

The collaboration between China and ESA on Cluster began in 1992 when China proposed to set up a data centre to distribute Cluster data. In 1997, the Chinese Centre for Space Science and Applied Research (CSSAR) presented its new magnetospheric Double Star Programme (DSP) to the Cluster science working team. In July 2001, ESA and the China National Space Administration (CNSA) signed the DSP cooperation agreement. Within 2.5 years, on 29 December 2003, TC-1 (Tan Ce: Explorer) was launched from Xichang in southern China, into a 570×78 970 km, 28.5° orbit. TC-2 was launched six months later, on 25 July 2004, into a polar orbit of 680×38 300 km.

Following an initial mission extension up to December 2006, the Science Programme Committee approved a further mission extension up to September 2007, the projected end of life of TC-1. During the extension, the orbital planes of Cluster and TC-1 became separated by around 60° in azimuth or 'local time', providing new Cluster–Double Star conjunctions.

In early August 2007, contact with the TC-2 satellite was unexpectedly lost. Problems had been expected on the satellite due to the slow drift of the spin axis towards the Sun, and due to the failure of the attitude computer shortly after launch, increasing the temperature inside the satellite.

A more expected event occurred in the early morning of 14 October 2007, when the TC-1 satellite returned to Earth after completing its designed orbit lifetime, marking the completion the first Sino–European satellite mission. With the loss of contact with TC-2, it was thought that the reentry of TC-1 would mark the end of the Double Star programme altogether. However, tireless efforts by Chinese colleagues over the next months resulted in recontact with TC-2 in late November 2007. Operations continued up to December 2009, after which time it had been predicted that satellite operations would not be possible due to power limitations onboard satellite

Although the operational mission has ended, scientific results are still being published using Double Star data, both standalone and together with Cluster or other magnetospheric measurements. In one paper, data from the ion instruments on Double Star and Cluster were used to identify the locations of the inner and outer boundaries of the radiation belts. A novel data analysis technique was used based on instrument background contamination due to penetrating radiation in that region (Ganushkina et al., 2011).

Another study using TC-1-only data also looked at the average structure of large-scale electric fields in Earth's inner magnetosphere during different geomagnetic activities, finding them to be reasonably stable under moderate and low activity (He et al., 2010). In other studies, the data from Double Star were used in combination with Cluster and other observations to examine the phenomenon of magnetic reconnection at the boundary of Earth's magnetosphere, the magnetic bubble that protects us from the solar wind particles from the Sun (Wang et al., 2011; Zhang et al., 2011). These studies have provided constraints on the mechanisms and extent of reconnection in this region.

Since the end of active operations, the instrument teams have made a big effort to archive the Double Star data, using the Cluster Active Archive to allow wider and more frequent use of this unique and valuable dataset. To ensure that the best quality data were preserved in the archive, the Chinese Double Star team has made a huge effort to reprocess the raw dataset. This effort significantly improved the integrity of the raw data and established a good foundation for the archive products. At the time of writing, the teams have provided test data files and applicable documents to the CAA. The ingestion of

Further information about the Double Star mission can be found at *http://sci.esa.int/doublestar*

data files into the CAA is expected to begin in 2012, and should be available to the scientific community shortly thereafter.

References

Ganushkina, N.Y. et al. (2011). *J. Geophys. Res.* **116**, A09234. DOI: 10.1029/2010JA016376.
He, Z.H. et al. (2010). *Ann. Geophys.* **28**, 1625–1631. DOI: 10.5194/angeo-28-1625-2010.
Wang, J. et al. (2011). *Geophys. Res. Lett.* **38**, L10105. DOI: 10.1029/2011GL047125.
Zhang, Q.-H. et al. (2011). *Ann. Geophys.* **29**, 1827–1847. DOI: 10.5194/angeo-29-1827–2011.

2.6 Integral

The International Gamma-ray Astrophysics Laboratory (Integral) was launched on 17 October 2002 into a highly elliptical 72 h orbit with initial values for perigee: 9000 km, apogee: 154 000 km and inclination: 52°. Scientific observations are performed at nominal altitudes above about 40 000 km, resulting in about 210 ks per 3-day revolution.

Integral is performing hard X-ray/soft gamma-ray observations with high spatial and spectral resolution in the 15 keV–10 MeV energy range using two main instruments: the Spectrometer on Integral (SPI) and the Imager on Board the Integral Satellite (IBIS) (Table 2.6.1). Both instruments provide spectral and spatial information, with SPI optimised for high spectral resolution ($E/\Delta E \approx 500$) in the energy range 20 keV to 8 MeV, and IBIS optimised for high spatial resolution (source location accuracy of <1 arcmin). SPI utilises 19 large Ge detectors (15 are still active) cooled to 80K, while IBIS has an array of 16384 CdTe detectors (Integral Soft Gamma-ray Imager, ISGRI) sensitive at 15 keV to 1 MeV mounted above 4096 CsI crystals (Pixellated Imaging CaeSium Iodide Telescope, PICsIT) operating at 175 keV to 10 MeV. In addition, simultaneous X-ray (Joint European X-Ray Monitor, JEM-X; 3–35 keV) and optical V-band (Optical Monitoring Camera, OMC) monitoring is provided.

All three high-energy instruments use coded aperture masks to provide imaging information over large fields of view. A radiation monitor provides realtime information about the local satellite particle background. Mission operations, using ESA's Redu ground station in Belgium, are conducted from ESOC (Darmstadt, Germany) and scientific data products are provided to the scientific users community by the nationally funded Integral Science Data Centre (ISDC) in Versoix, Switzerland. The Integral Science Operations Centre (ISOC) is located at ESAC, near Madrid, Spain.

Integral has been operating since 2005. After a nominal mission of 2.2 years, it is now in its 'extended scientific mission operations phase', which has recently

Table 2.6.1. Performance characteristics of the Integral scientific payload.

	SPI	IBIS	JEM-X	OMC
Energy range	20 keV–8 MeV	15 keV–10 MeV	3–35 keV	500–850 nm
Detectors/ characteristics	19 Ge (each 6 × 7 cm) cooled @ 85K	16384 CdTe (each 4 × 4 × 2 mm); 4096 CsI (each 9 × 9 × 30 mm)	Microstrip Xe gas detector (1.5 bar)	CCD + V-filter
Detector area (cm^2)	500	2600 (CdTe) 3100 (CsI)	2 × 500	2048 × 1024s pixel
Spectral resolution	2.2 keV @ 1.33 MeV	9 keV @ 100 keV	1.3 keV @ 10 keV	–
FOV (fully coded)	16°	9 × 9°	4.8°	5 × 5°
Angular resolution (FWHM)	2°	12 arcmin	3 arcmin	17.6 arcsec/pixel
10σ source location	1.3°	< 1 arcmin	< 30 arcsec	6 arcsec
Continuum sensitivity*	3×10^{-6} @ 1 MeV	3×10^{-6} @ 100 keV	1.2×10^{-6} @ 6 keV	18.2^m (10^{-3} s)
Line sensitivity*	5×10^{-6} @ 1 MeV	2×10^{-5} @ 100 keV	1.7×10^{-6} @ 6 keV	–
Timing accuracy (3σ)	129 μs	62 μs–30 min	122 μs	Var. in units of 1 s
Mass (kg)	1309	628	65	17
Power (W)	250	220	52	12
Telemetry allocation (kbit/s)	45	57	4	2

*Sensitivities are 3σ in 10^5 s and $\Delta E/E = 0.5$, units ph cm^{-2} s^{-1} keV^{-1} (continuum) and ph cm^{-2} s^{-1} (line).

Further information about the Integral mission can be found at *http://sci.esa.int/integral*

been extended to 31 December 2014, subject to a mid-term technical status review at the end of 2012. The onboard consumables (fuel, power) technically allow an extension of Integral's operational lifetime beyond 2014.

Mission Status

Operations are running smoothly, with all systems of the flight and ground segments performing as expected. The perigee altitude varies due to solar–lunar gravitational disturbances; it reached a minimum of 2800 km in October 2011, and is now increasing again towards a maximum of about 10 000 km in October 2015. The increased exposure to proton radiation at low perigee altitudes has led to an accelerated rate of degradation of the solar array. This is being carefully monitored, but since the power margin is still very good, it is expected that it will not be necessary to constrain the solar aspect angle. No significant effects of the increased radiation on the instruments have been observed.

The particle background experienced by Integral is being monitored via a dedicated counter (the Integral Radiation Environment Monitor, IREM). Due to the extended solar minimum, particle background rates slowly increased up to the end of 2009 and are now slowly decreasing again. After many years of operating only one of the two identical JEM-X units at a time, the slow anode degradation rate and lowered background have permitted both units to be operated together again, increasing the sensitivity accordingly. The other instruments are working as expected, with performances in line with those predicted before launch.

The online data archive at the ISDC is regularly updated as new observations enter the public domain (1 yr after they are received by the observer). In collaboration with the ISDC, the ISOC Science Data Archive (ISDA) has been publicly available since July 2005. The ISDA is based on the technology used to create the ISOC and XMM-Newton ESA archives and provides users experienced with, for example, the XMM-Newton archive with a familiar interface to access Integral science products. Mirror public data archives exist at NASA's Goddard Space Flight Center (High-Energy Astrophysics Science Archive Research Center, HEASARC) and at the Space Research Institute's High-Energy Astrophysics Department (IKI/RSDC) in Moscow.

Scientific Highlights

Integral continues to provide an important resource to the astronomy community. This section presents a selection of recent scientific achievements.

The Centre of the Galaxy

The persistent hard X-ray emission from the centre of the Galaxy as observed by Integral is not due to the hot plasma seen at lower energies with Chandra or XMM-Newton, and neither is it due to the central black hole, Sgr A*. Integral's discovery of hard X-rays from the giant molecular cloud Sgr B2, which are best interpreted as scattering of radiation emitted by Sgr A* more than 100 years ago, shows that this nonthermal emission likely traces the past activity of Sgr A*. The most compelling evidence of such reflection is the Integral discovery of Sgr B2 fading in hard X-rays (Fig. 2.6.1). Along with XMM-Newton measurements of the Fe K-line variability from other clouds in this region, this discovery has allowed both the strength to be constrained and the duration of this past activity to be limited.

These results established that the behaviour of Sgr A* resembles that of a low-luminosity active galactic nucleus and that it might become brighter again in the future. During the continued monitoring of the current activity of Sgr A*,

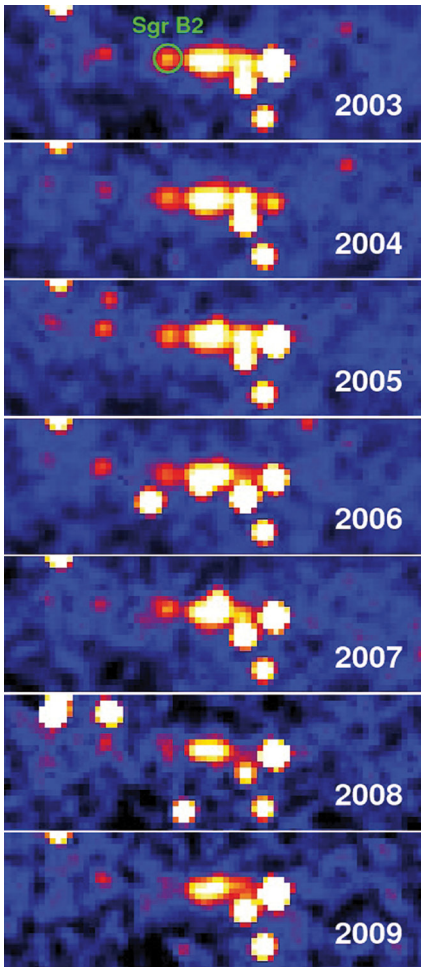

Figure 2.6.1. Integral IBIS 20–60 keV images of the galactic centre (7° × 2°), 2003–09. Most of the sources are X-ray binaries and display strong time variability. The green circle in the top panel corresponds to the position of the molecular cloud Sgr B2. The associated hard X-ray source, IGR J17475-2822, shows a clear decline in flux during the 7 years of monitoring. (Terrier et al., 2010).

Integral surveys of the galactic centre will also allow the past activity of the closest supermassive black hole to be monitored by detecting the Compton echo of its outburst radiation as it propagates through the molecular clouds of the region (Terrier et al., 2010).

The Crab Nebula: An Unreliable Calibration Source?

The Crab Nebula, a remnant of a supernova explosion in 1054, has for decades been used as a standard candle to calibrate most X-ray and gamma-ray telescopes once they have been launched. This is because its flux is both intense and steady. However, Integral has made a significant contribution to demonstrating that the Crab does not radiate entirely like a standard candle. Based on observations made by NASA's Fermi Gamma-ray Burst Monitor (GBM), the Swift Burst Alert Telescope (BAT), the Rossi X-ray Timing Explorer (RXTE) and Integral, a real, intrinsic decline in the Crab Nebula's flux of about 7% can be discerned since 2008 in the 15–50 keV energy band (Fig. 2.6.2). A similar decline can also be seen in the 50–100 keV band. Moreover, the Crab has brightened and faded by as much as 3.5% per year since 1999.

The flickering arises from the nebula, and not from the pulsar located inside, as no unexpected variations in the pulsed flux have been detected. Unlike the NASA satellites involved in the study, which are in relatively low orbits, Integral is operating in a highly eccentric orbit. Therefore, the Integral orbital environment has a different level of background radiation with respect to the other satellites, and this allows any orbit-induced background effect in the Crab Nebula's flickering to be excluded (Wilson-Hodge et al., 2011).

Polarised High-energy Emission from Cygnus X-1

The X-ray binary Cygnus X-1 is composed of a 35 $M_\odot$ supergiant O star and a ~10 $M_\odot$ black hole accreting matter that is either directly ejected from the companion star, or via an accretion disc. It was one of the first X-ray binaries discovered in our Galaxy soon after the advent of X-ray astronomy in the 1960s. Cygnus X-1 is also the first galactic source for which optical measurements (in the early 1970s) showed the presence of a black hole. Radio observations have shown that Cygnus X-1 is a source of powerful ejections, and is therefore

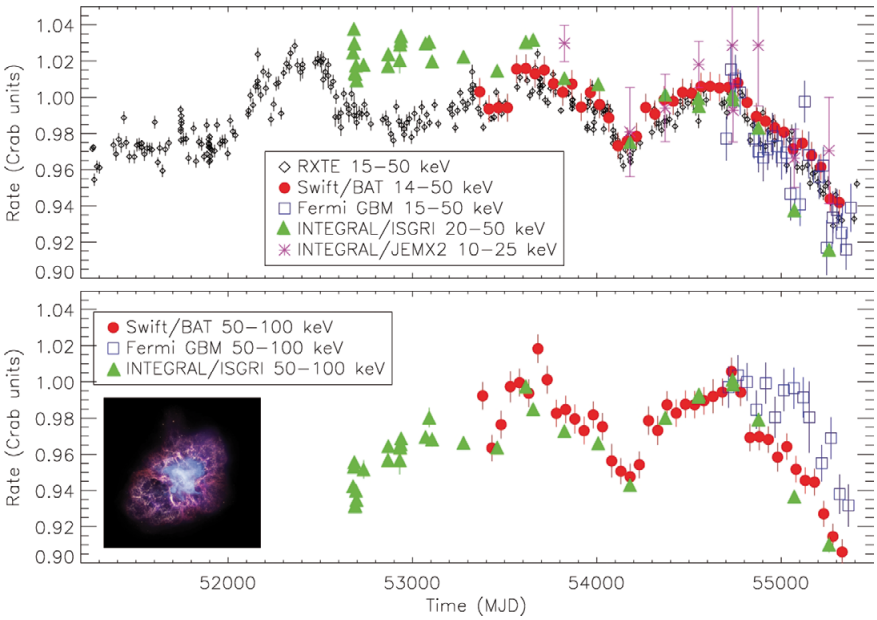

Figure 2.6.2. Normalised flux of the Crab nebula during the period MJD 52200–55400 (18 October 2001–23 July 2010) as observed by RXTE, Swift/BAT, Fermi/GBM and Integral (ISGRI, JEM-X). (Wilson-Hodge et al., 2011).

a 'micro-quasar', a galactic scaled-down version of the very massive black holes that power the nuclei of active galaxies. These jets are very important for the understanding of the accretion–ejection connections, that is, the physical mechanisms at work close to the black hole, since they can carry large quantities of matter at speeds close to the speed of light.

Integral has shown that the jets in Cygnus X-1 could also be responsible for the most energetic light emitted near the black hole. Using the Compton interactions between the two detector arrays of IBIS (ISGRI and PICSiT) the polarised gamma-rays emitted by Cygnus X-1 have been measured. Spectral modelling of the data reveals two emission mechanisms. First, the 250–400 keV data are consistent with emission dominated by Compton scattering on thermal electrons and are weakly polarised. Second, the spectral component seen in the 400–2000 keV band is, in contrast, strongly polarised (67 ± 30)%, revealing that the MeV emission is probably related to the jet first detected in the radio band (Laurent et al., 2011a).

Reflected Radiation from Seyfert-2 Galaxies

The unified model of Active Galactic Nuclei (AGNs) identifies the differences observed among different classes of AGN with an anisotropic obscuration: Seyfert 1 galaxies are being seen by the observer along a direct line of sight to the central engine, whereas the central engine is obscured in Seyfert-2 galaxies by a 'torus' of absorbing material.

According to this unification scheme, one should observe in hard X-rays, where absorption does not play an important role, on average the same emission from all classes of AGN. The average hard X-ray spectra of different classes of AGN have been produced using 7 years of Integral IBIS/ISGRI data, with a total effective exposure time of about 100 million seconds. Contrary to expectations, the average spectrum of mildly obscured Seyfert-2 galaxies shows an excess of between 30 and 60 keV with respect to that of Seyfert-1 galaxies. This excess is a characteristic of X-ray reflection by dense clouds of matter surrounding the X-ray source. The large reflection observed in mildly obscured Seyfert-2 galaxies might be the signature of the presence of more clouds of matter around the central engine in these objects compared with Seyfert-1 galaxies, indicating that the environments of these two classes of active galactic nuclei are different.

The Diffuse Cosmic X-ray Background

The observed diffuse cosmic X-ray background is due to the integrated emission of spatially unresolved AGNs, and while its shape is well reproduced by models below 10 keV, at higher energies a large number of heavily obscured ('Compton-thick') objects are required to explain the peak of that emission. But so far, only a handful of these heavily obscured AGNs have been found. The high reflection detected in mildly obscured Seyfert-2 might explain the peak of the cosmic X-ray background emission without the contribution of undetected heavily obscured AGN. In Fig. 2.6.3, the bottom panel shows that the peak of the cosmic X-ray background, as measured by Integral above 10 keV, can be explained by the contribution of obscured and reflective AGNs and that the contribution of heavily obscured Compton-thick objects might be much lower than has so far been assumed (Ricci et al., 2011).

Integral Tests Einstein's General Relativity

In the framework of Einstein's theory of general relativity, light propagates in the same way in all directions, whatever the photon energy. This invariance

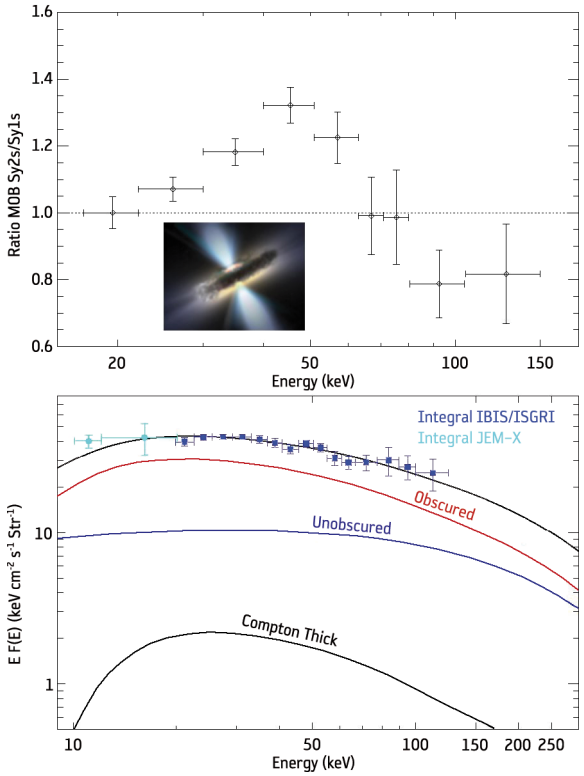

Figure 2.6.3. Ratio between the spectra of mildly obscured Seyfert-2 and Seyfert-1 galaxies. *Top panel:* Excess of radiation at 30–60 keV as observed by Integral in a sample of Seyfert-2 galaxies. *Bottom panel:* The observed diffuse cosmic background emission can be modelled (solid black line: obscured + unobscured + Compton-thick sources) by a smaller amount of Compton-thick sources than previously assumed. (Ricci et al., 2011)

is called 'Lorentz invariance' because it was described mathematically by the 1902 Nobel Prize winner H.A. Lorentz. However, according to some theorists who have tried to match general relativity and quantum mechanics, the two pillars of modern physics, this fundamental law could be violated. Investigating a possible violation of this Lorentz invariance has been an active area of physics research, in particular particle physics, for decades.

Various astrophysical tests have recently been proposed, in particular by analysing the properties of the radiation emitted by distant sources, such as gamma-ray bursts (GRBs). Integral has observed the gamma-ray burst GRB 041219A, which is at a distance of more than 300 million light years, and has put a very strong constraint on the possibility of obtaining such a violation of the Lorentz invariance. Indeed, the IBIS telescope on Integral, thanks to its Compton imaging mode, has measured the polarisation of the GRB gamma-ray emissions in two adjacent energy bands and has shown that there is statistically no difference between these two measurements. On the other hand, according to some quantum gravity theories, Lorentz invariance violation should induce an energy-dependent rotation of the linear polarisation during its long travel in the vacuum between the GRB and Earth. Integral observations have put a limit on this phenomenon – the 'vacuum birefringence effect' – of $\xi < 1.1 \times 10^{-14}$, that is 10^5 times more constraining than what was previously determined, thus reinforcing one of the pillars of Einstein's general relativity (Laurent et al., 2011a,b).

References

Laurent, P. et al. (2011a). *Science* **332**, 438.
Laurent, P. et al. (2011b). *Phys. Rev. D* **83**, 121301.
Ricci, C. et al. (2011). *Astron. Astrophys.* **532**, 102.
Terrier, R. et al. (2012). *Astrophys. J.* **719**, 143.
Wilson-Hodge, C.A. et al. (2011). *Astrophys. J.* **727**, 40.

2.7 Mars Express

Introduction

Mars Express was the first European mission to orbit another planet in our Solar System. The spacecraft was launched on 2 June 2003 from the Baikonur Cosmodrome in the Russian Federation on a Soyuz–Fregat vehicle, for an originally approved mission of 2.5 years. Subsequently, the mission operations have been extended on three occasions up to (currently) the end of 2014.

In addition to global studies of the surface, subsurface, atmosphere and upper atmosphere of Mars at unprecedented spatial, spectral and temporal resolution, the unifying theme of the mission is the search for water in its various states everywhere on the planet. Dedicated flybys of Phobos are also regularly planned, in order to gain new data on the largest martian moon.

The overall impact of the mission has been (and still is) very high and is best illustrated by the fact that more than 550 papers have published in international scientific journals, many of them in high-impact journals such as *Nature* and *Science*. The 17 December 2010 issue of *Science*, for example, included special sections highlighting the 'Breakthrough of the Year' and 'Insights of the Decade'. Mars Express was again honoured; one of the top 10 insights was 'Water on Mars'. The past decade's half-dozen missions to Mars (including Mars Express) have made it clear that early in martian history, liquid water on or just below the planet surface did indeed persist long enough to alter rocks and, possibly, sustain the evolution of life.

Over the past 10 years the planetary science literature has shown the very strong impact of the discovery, characterisation and mapping of hydrated minerals on Mars by the OMEGA instrument. This led to an in-depth reassessment of martian history, and demonstrated that liquid water once altered the planet on a planetary scale (Table 2.7.1 and Fig. 2.7.1).

Instrument	Acronym	Principal Investigators
High-Resolution Stereo Camera	HRSC	G. Neukum
Observatoire pour la Minéralogie, l'Eau, les Glaces et l'Activité (visible and near-infrared hyperspectral imager)	OMEGA	J.-P. Bibring
Planetary Fourier Spectrometer	PFS	D. Grassi
Analyser of Space Plasma and Energetic Atoms	ASPERA	S. Barabash
Mars Radio Science Experiment	MaRS	M. Pätzold
Spectroscopy for the Investigation of Characteristics of the Atmosphere of Mars (ultraviolet and infrared dual spectrometer)	SPICAM	F. Montmessin
Mars Advanced Radar for Subsurface and Ionospheric Sounding	MARSIS	G. Picardi, J. Plaut, R. Orosei

Table 2.7.1. Mars Express experiments.

Further information about the Mars Express mission can be found at *http://sci.esa.int/marsexpress*

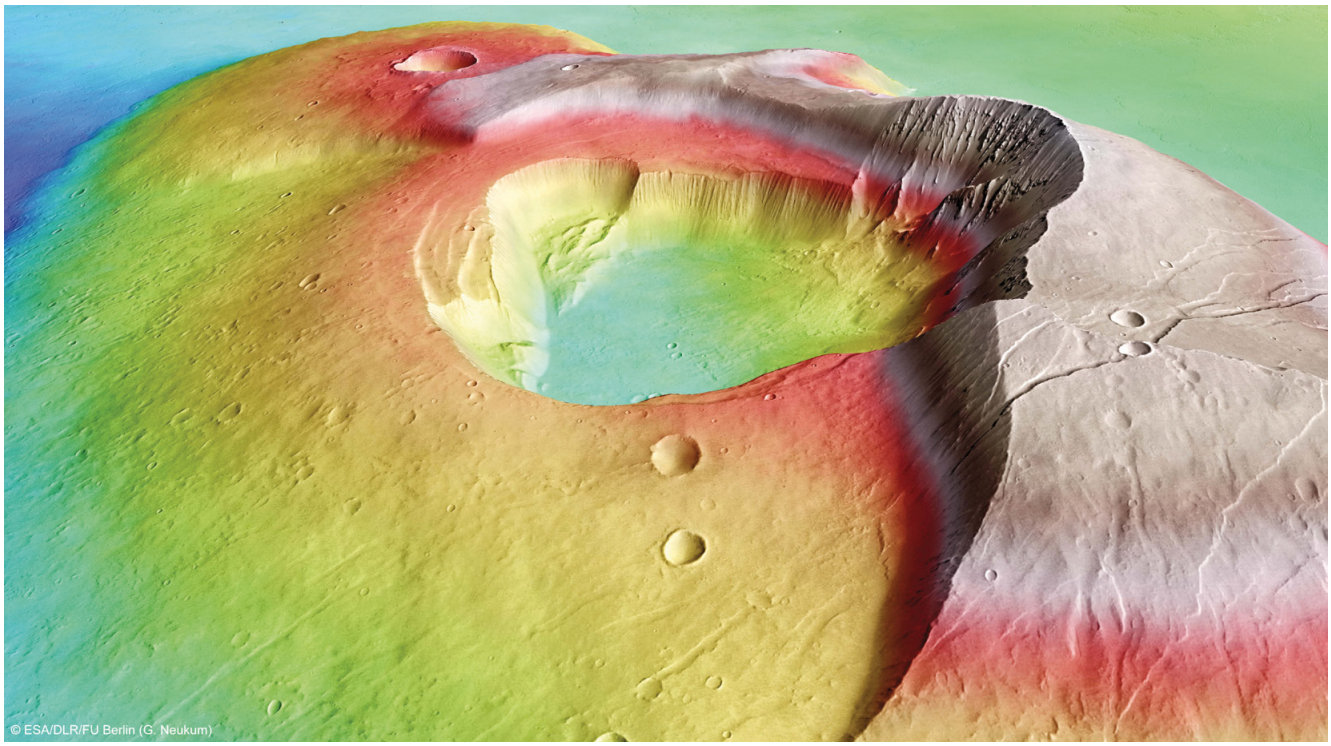

Figure 2.7.1. Image of the volcano Tharsis Tholis released by ESA in November 2011 on the occasion of the 10 000th orbit of Mars Express. The volcano is 8 km high with a base extending 155 × 125 km and a central caldera measuring 32 × 34 km. The image was created using a Digital Terrain Model (DTM). Elevation data from the DTM are colour coded: purple indicates the lowest-lying regions and beige the highest. The relief has been exaggerated by a factor of three. (©ESA/DLR/FU Berlin; G. Neukum)

Status

Two notable anomalies with the spacecraft and payload occurred during the reporting period.

First, in August 2010, an anomaly was detected in the OMEGA instrument, related to an end-of-life on the C-channel (infrared range 0.93–2.6 µm) cryocooler. The loss of the C-channel has in part been compensated by a close coupling between OMEGA and the Compact Reconnaissance Imaging Spectrometer for Mars (CRISM) on the Mars Reconnaissance Orbiter (MRO), while the two other instrument channels (0.35–1.05 µm and 2.5–5.1 µm) are still operating perfectly and delivering useful data.

Second, anomalies in the operation of the solid-state mass memory system caused science observations to be suspended for a few weeks between August and October 2011. A technical work-around was implemented that has allowed the full resumption of the observations.

Otherwise, preparations have begun for the coverage of the entry, descent and landing of NASA's Mars Science Laboratory in August 2012, at NASA's request.

Scientific Highlights

After more than eight years of operations and 10 000 orbits around the Red Planet, Mars Express is still delivering important results. The mission has provided a comprehensive and multidisciplinary view of Mars, including the subsurface structure, the surface geology and mineralogy, the evolution of the climate, the atmospheric dynamics and composition, and the interaction between the solar wind and the upper atmosphere. The regular Phobos flybys have also boosted studies of the origin of the martian moons.

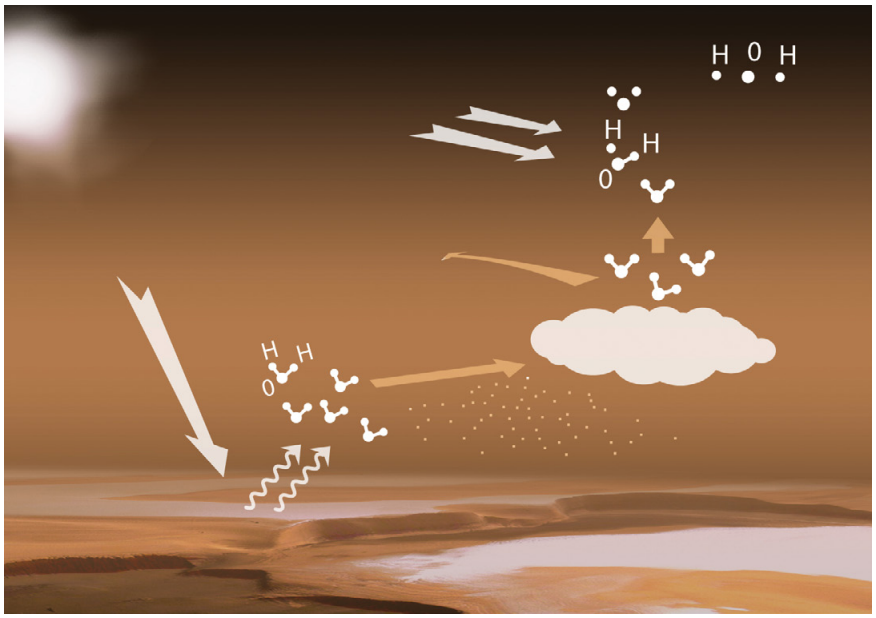

Figure 2.7.2. The water cycle in the atmosphere of Mars. When the polar caps are illuminated by the Sun during spring and summer, their water content progressively sublimates and is released into the atmosphere. The molecules are transported by winds to higher altitudes where, in the presence of dust and aerosols, they condense to form clouds. If there are too few dust particles, condensation is impeded, leaving substantial amounts of water vapour, i.e. the atmosphere is supersaturated. Supersaturated water vapour may be transported by winds to the southern hemisphere or carried high into the upper atmosphere, where solar radiation splits it into hydrogen and oxygen atoms, which can then escape into space. (ESA/AOES Medialab)

A selection of results achieved during the reporting period is provided below:

— The radar north polar nightside campaign, one of the major goals of the extended mission, took place mid-2011. The new data have higher signal-to-noise (better deep detections) and higher lateral resolution than previous north polar observations. The base of the basal unit is visible across the entire polar plateau; this allows better constraints on thickness and volume of the polar ice cap. A preliminary estimate of the refractive index implies that the composition is not pure water ice.

— OMEGA has detected, for the first time, the nightside emission of molecular oxygen at 1.27 μm (Bertaux et al., 2012). This emission, formed by the recombination of two oxygen atoms, is a clear diagnostic of the atmospheric circulation from dayside to nightside, similar to what occurs on Venus.

— Observations made by the SPICAM instrument have provided evidence, for the first time, of the existence of water vapour in excess of saturation, by an amount far surpassing that encountered in Earth's atmosphere (Maltagliati et al., 2011). This finding contradicts the assumption that atmospheric water on Mars cannot exist in a supersaturated state, directly affecting the long-term representation of water transport, accumulation, escape and chemistry on a planetary scale (Fig. 2.7.2).

— From measurements of α-particles (He^{2+} ions) with ASPERA, it has been concluded that α-particles in the solar wind contribute to the helium content observed in the martian atmosphere (Stenberg et al., 2011). Such studies of the helium balance in a planetary atmosphere are providing critical information on the formation of the Solar System.

— The detection of hydrated minerals on the surface of Phobos, by the Planetary Fourier Spectrometer (PFS) instrument, at wavelengths larger than 10 μm, (Giuranna et al., 2011) (see the image of Phobos acquired by Mars Express on 9 January 2011, Fig. 2.7.3), is now the subject of debate in the scientific community. This identification has not been confirmed by OMEGA in the near-infrared range.

Figure 2.7.3. Mars Express HRSC image of Phobos, taken on 9 January 2011, from a distance of 111 km. The image has been photometrically enhanced to illuminate darker areas. Resolution: 4.1 m per pixel. (©ESA/DLR/FU Berlin; G. Neukum)

References

Bertaux, J.-L. et al. (2012). *J. Geophys. Res.* **117**, E00J04.
Giuranna, M. et al. (2011). *Planet. Space Sci.* **59**(13), 1308–1325.
Maltagliati, L. et al. (2011). *Science* **333**(6051), 1868.
Stenberg, G. et al. (2011). *Geophys. Res. Lett.* **38**(9).

2.8 Rosetta

Introduction

The international Rosetta mission is the Planetary Cornerstone of ESA's Horizon 2000 long-term science programme. Rosetta was launched from Kourou in French Guiana on Ariane V158 on 2 March 2004, when it began its 10-year journey to the Jupiter-family comet 67P/Churyumov–Gerasimenko.

The scientific objective of the mission is to study the origin of comets, the relationship between cometary and interstellar material, and its implications with regard to the origin of the Solar System. En route to its rendezvous with its main target, Rosetta has also performed close flybys at two very different Main Belt asteroids, (2867) Steins and (21) Lutetia.

The principal mission milestones are listed in Table 2.8.1.

Scientific Objectives, Spacecraft and Payload

Rosetta will study the nucleus and environment of one comet in great detail by accompanying it for many months along its pre- and post-perihelion orbit. The scientific payload will obtain dedicated remote-sensing observations and *in situ* measurements from close orbit around the nucleus, starting at a heliocentric distance beyond 3.5 AU and continuing through perihelion and outbound to a heliocentric distance of about 2 AU. In addition, the lander Philae will land on the nucleus to perform an *in situ* analysis of its material, whereby the elemental, molecular and isotopic composition as well as many physical properties of the surface and subsurface will be determined.

Rosetta is a 3-axis stabilised spacecraft with a box-type main structure (Table 2.8.2). The primary structure consists of a central cylinder of aluminium honeycomb with shear panels, connecting the side panels on which the spacecraft and payload equipment are mounted. The main propulsion system is in the centre, where two propellant tanks are mounted around a vertical thrust tube. In addition, 24 thrusters each providing 10 N are available for trajectory and attitude corrections. The scientific payload is on the top panel (Payload Support Module) either body-mounted or attached to one of the deployable booms, while the steerable 2.2-m high-gain antenna and the lander

Milestone	Date
Launch	2 March 2004
Earth Gravity Assist #1	4 March 2005
Mars Gravity Assist	25 February 2007
Earth Gravity Assist #2	13 November 2007
Asteroid Steins flyby	5 September 2008
Earth Gravity Assist #3	13 November 2009
Asteroid Lutetia flyby	10 July 2010
Enter/exit hibernation	July 2011/January 2014
Rendezvous manoeuvre	May 2014
Start global mapping phase	August 2014
Lander delivery	November 2014
Perihelion passage	August 2015
End of mission	31 December 2015

Table 2.8.1. Rosetta mission milestones.

Further information about the Rosetta mission can be found at *http://sci.esa.int/rosetta*

Table 2.8.2 Rosetta spacecraft overview.

Spacecraft characteristics		
Dimensions	Main satellite dimensions Solar panel dimensions Total area of solar panels Total area of solar panels	2.8 m × 2.1 m × 2.0 m 14 m × 2.3 m 2 × 32 m^2 32 m
Mass	Total launch mass Propellant Science payload Philae Lander	~2900 kg ~1720 kg ~165 kg ~100 kg
Power	Solar array output	395 W at 5.25 AU 850 W at 3.40 AU
Lifetime	Operational	12 years

Table 2.8.3. The Rosetta Orbiter payload.

Instrument	Objective	Principal Investigators
Remote sensing		
ALICE	UV spectroscopy SRI (70–205 nm)	A. Stern, Southwest Research Institute, Boulder, CO, USA
OSIRIS	Multicolour imaging (narrow- & wide-angle cameras)	H. Sierks, MPS, Katlenburg-Lindau, Germany
VIRTIS	VIS and IR mapping spectroscopy (0.25–5 μm)	F. Capaccioni (acting), IAS-CNR, Rome, Italy
MIRO	Microwave spectroscopy (0.5 mm and 1.3 mm)	S. Gulkis, NASA–JPL, Pasadena, CA, USA
Mass spectrometers		
COSIMA	Dust mass spectrometer (SIMS, $m/\Delta m$ ~ 2000)	M. Hilchenbach, MPS, Katlenburg-Lindau, Germany
ROSINA	Gas and ion mass spectroscopy DFMS: 12–150 amu, $m/\Delta m \approx 3000$ RTOF: 1 ≥ 350 amu, $m/\Delta m > 500$ COPS: gas density and velocity	K. Altwegg, University of Bern, Switzerland
Dust flux and physical properties		
GIADA	Grain Impact Analyser and Dust Accumulator	A. Rotundi, Oss. Astro., Capodimonte, Italy
MIDAS	Grain morphology, nm resolution (atomic force microscope)	K. Torkar, IWF, Graz, Austria
Radio experiments		
CONSERT	Radio sounding Nucleus tomography	W. Kofman, CEPHAH, Grenoble, France
RSI	Radio Science Experiment	M. Pätzold, University of Cologne, Germany
Comet plasma environment, solar wind interaction		
RPC	Langmuir Probe (LP) Ion and Electron Sensor (IES) Flux Gate Magnetometer (MAG) Ion Composition Analyser (ICA) Mutual Impedance Probe (MIP) Plasma Interface Unit (PIU)	A. Eriksson, IRF, Uppsala, Sweden J. Burch, SRI, San Antonio, Texas, USA K.-H. Glassmeier, IGEP, Braunschweig, Germany H. Nilsson, IRF, Kiruna, Sweden J.G. Trotignon, LPCE/ CNRS, Orleans, France C. Carr, Imperial College, London, UK

Table 2.8.4. The Rosetta Lander (Philae) payload.

Instrument	Objective	Principal Investigators
Imaging		
CIVA	Panoramic imaging Vis–IR microscopic imaging of samples	J.P. Bibring, IAS, Orsay, France
ROLIS	Descent and down-looking camera	S. Mottola, DLR, Berlin, Germany
Composition		
APX	α–X-ray spectrometer Elemental surface composition	G. Klingelhöfer, University of Mainz, Germany
COSAC	Evolved gas analyser Molecular composition and chirality of samples	F. Goesmann, MPS, Katlenburg-Lindau, Germany
Ptolemy	Evolved gas analyser Isotopic composition of light elements in sample	I.P. Wright, Open University, UK
Physical properties		
MUPUS	Multipurpose sensor for (sub)surface science (density, porosity, thermal properties)	T. Spohn, DLR, Berlin, Germany
SESAME	Comet Acoustic Surface Sounding Experiment (CASSE) Dust Impact Monitor (DIM) Permittivity Probe (PP)	K.J. Seidensticker, DLR, Cologne, Germany I. Apathy, KFKI, Hungary W. Schmidt, FMI, Finland
SD2	Sampling, Drilling and Distribution device	A. Ercoli-Finzi, Politechnico Milano, Italy
ROMAP	Rosetta Lander Magnetometer and Plasma Monitor	U. Auster, IGEP, TU Braunschweig, Germany
CONSERT	Radio sounding, nucleus tomography	W. Kofman, CEPHAH, Grenoble, France

Philae are attached to two opposite sides of the spacecraft and the solar panel wings extend from the other two sides.

The spacecraft carries 11 scientific experiments, each provided by a Principal Investigator team, plus facility instruments, such as a navigation camera, startrackers and a radiation monitor (Table 2.8.3), and of course the lander Philae, which carries another 10 scientific experiments (Table 2.8.4). The Rosetta payload, with its remote sensing and *in situ* experiments, has unprecedented capabilities to fulfil the scientific objectives of the mission. A detailed overview of the mission can be found in Schulz et al. (2009).

Science Operations

Rosetta is a Principal Investigator-type mission, i.e. the individual experiment teams are responsible for defining the science operations timelines for their individual instruments. These requests are coordinated and merged into the Science Operations Plans by the Rosetta Science Operations Centre (RSOC) as part of the Science Operations Department at ESAC, near Madrid, Spain. For key mission phases (commissioning, nucleus rendezvous, Philae delivery), the RSOC is collocated with the Rosetta Mission Operations Centre (RMOC) at ESOC, in Darmstadt, Germany. ESOC is operating and controlling the spacecraft throughout the mission, working through ESA's 35 m Deep Space Antenna at New Norcia in Western Australia.

The Rosetta Science Data Archive is a major element of ESA's Planetary Science Archive (PSA) and will be prepared by RSOC in collaboration with the Primitive Bodies Node of the Planetary Data System at the University of Maryland, USA.

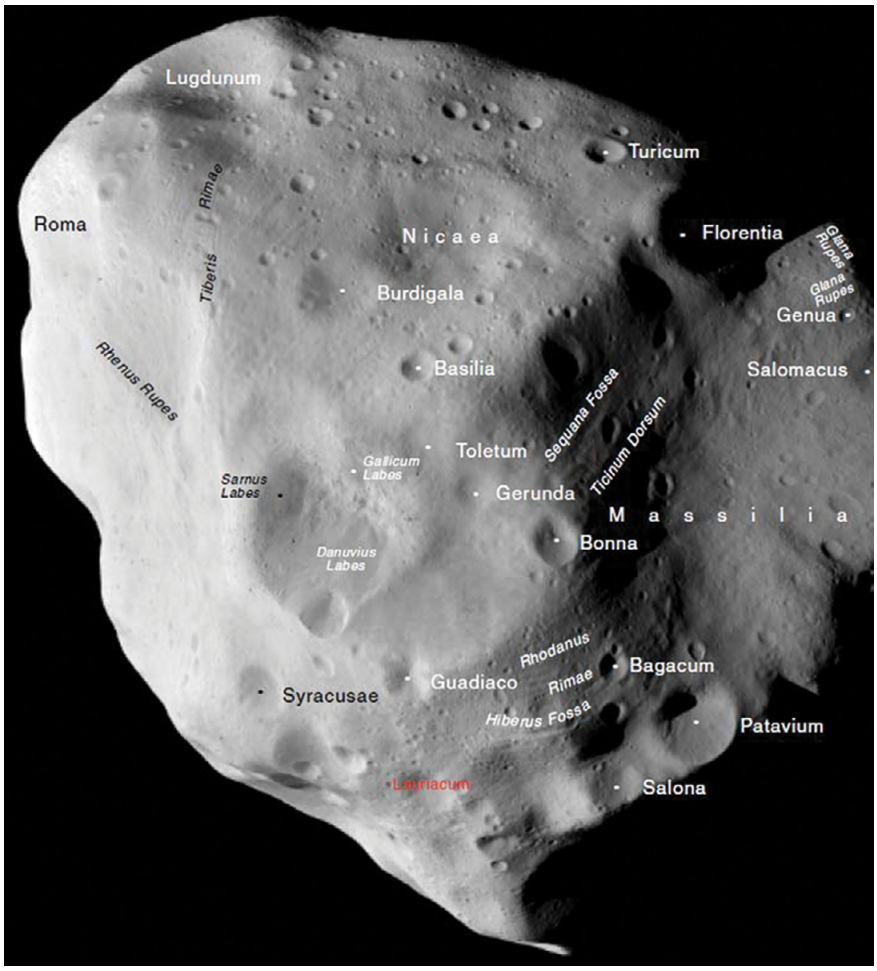

Figure 2.8.1. A map of (21) Lutetia. The craters on Lutetia have been named after European cities at the time when Paris was called Lutetia (53 BC to 360 AD). Regions are named after provinces at that time, curvilinear features by river names. The crater Lauriacum determines the zero meridian on Lutetia.

Status

In July 2010 Rosetta performed a successful close flyby at its main asteroid target, the main-belt asteroid (21) Lutetia. The encounter occurred at a heliocentric distance of 2.72 AU, and a geocentric distance of 3.05 AU, resulting in a signal travel time of some 20 min. Rosetta passed the asteroid with a relative flyby velocity of 15 km s^{-1}, with closest approach on 10 July 2010, 15:45 UT at a distance of 3168.2 km (Fig. 2.8.1). The spacecraft approached the asteroid at low phase angle and went through phase angle zero 18 min before closest approach at a distance of 16 400 km. The flyby strategy allowed continuous observations of (21) Lutetia before, during and for 30 min after closest approach, after which the spacecraft had to slew away from the asteroid as the minimum allowed solar aspect angle was reached.

Altogether 17 instruments were switched on during the flyby, obtaining spatially resolved imaging and spectral observations covering wavelengths from the UV to the radio, as well as *in situ* measurements of the asteroid and its direct environment (Fig. 2.8.2). The flyby results revealed that (21) Lutetia has one of the highest densities of any known asteroid, 3400 kg m^{-3}, implying that it contains significant quantities of iron. In spite of this, the asteroid has not formed a dense iron core as is the case for the terrestrial planets. Its surface composition remained primordial and does not show the rocky material expected for a fully differentiated body. This can only be explained if the asteroid was subjected to some internal heating early in its history, but did not melt completely and so did not end up with a well-defined iron core (Sierks et al., 2011; Pätzold et al., 2011; Coradini et al., 2011).

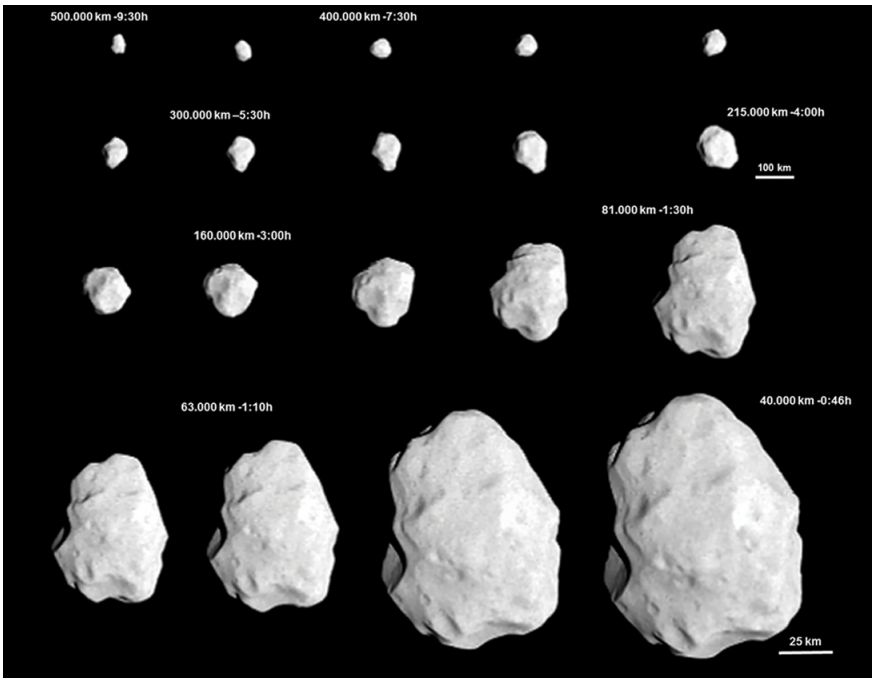

Figure 2.8.2. Series of images showing the approach to Lutetia taken with the OSIRIS narrow-angle camera from a distance of 500 000 km to 40 000 km, or 9 h 30 min to 46 min to closest approach. Lutetia is resolved to a few pixels in diameter already at a distance of 0.5 million km from the Rosetta spacecraft. The (pro-grade) rotation of Lutetia can be seen from the far distance.

On 8 June 2011, at 07:30 UTC, the Rosetta spacecraft was spun up to stabilise its attitude before the command to enter hibernation mode was released. The last radio-frequency pulse from the spacecraft was detected at about 14:12:00 UTC, as expected; but after that no further signal could be identified, confirming its successful entry into hibernation. The wake-up time has been set for 20 January 2014, at 10:00:00 UTC. After its exit from hibernation, at a distance of 5.39 AU from Earth and 4.49 AU from the Sun, Rosetta will proceed to its rendezvous with comet 67P/Churyumov–Gerasimenko.

References

Coradini, A., Capaccioni, F., Erard, S. et al. (2011). The surface composition and temperature of Asteroid 21 Lutetia as observed by ROSETTA/VIRTIS. *Science* **334**(6055), 492–494.

Pätzold. M., Andert, T.P., Asmar, S.W. et al. (2011). Asteroid (21) Lutetia – low mass, high density. *Science* **334**(6055), 491–492.

Schulz, R., Alexander, C., Boehnhardt, H. & Glassmeier, K.H. (Eds.) (2009). *Rosetta: ESA's Mission to the Origin of the Solar System*. Springer Science, New York.

Sierks, H., Lamy, P., Barbieri, C. et al., 2011. Images of Asteroid 21 Lutetia: A remnant planetesimal from the early Solar System. *Science* **344**(6055), 487–490.

2.9 Venus Express

Introduction

Venus Express was launched on a Soyuz–Fregat rocket from Baikonur in Kazakhstan on 9 November 2005 and arrived at Venus on 11 April 2006. Even during its very first orbit around the planet, the instruments on Venus Express captured stunning images of the southern hemisphere and of the giant vortex at the south pole. The mission had been developed in a record time of less than four years following the proposal to ESA and its selection in 2001. By December 2011 the spacecraft had transmitted more than 3 Tbit of high-quality science data to ground.

Venus Express orbits the planet in a 24 h period polar orbit, with a pericentre altitude of 165–250 km and an apocentre altitude of 66 000 km. The initial pericentre was located at 78°N latitude and initially drifted northwards at a rate of about 3° per year, until reaching the north pole in October 2009. The drift now continues southwards at the same rate. The scientific observations are shared between the pericentre part of the orbit, where high-resolution studies of small-scale features are carried out, and the near apocentre and intermediate regions, where global features and dynamical processes are studied.

The acquired data are transmitted to Earth in each orbit during the 8 h following the pericentre pass. ESA's deep-space tracking station at Cebreros, Spain, is the nominal ground station for spacecraft control and data downlink. The 35 m station at New Norcia, Australia, and NASA's Deep Space Network are used occasionally, mainly for radio-science support during dedicated campaigns at certain phases of the mission.

Scientific Objectives

The main scientific goal of the Venus Express mission is to conduct a comprehensive study of the atmosphere of Venus, particularly the plasma environment and the interaction between the upper atmosphere and the solar wind (Table 2.9.1). Several aspects of the surface and surface–atmosphere interactions are also being studied. Seven top-level science themes have been defined: atmospheric dynamics, atmospheric structure, atmospheric composition and chemistry, cloud layers and hazes, radiative balance, surface properties and geology, the plasma environment and escape processes.

Addressing these themes to a proper depth is providing answers to many fundamental open questions about Venus, including:

- the mechanism of the global atmospheric circulation;
- the mechanism and driving force behind the atmospheric super-rotation;
- the planet's chemical composition and its variations;
- the role of the cloud layers and trace gases in the thermal balance of the planet;
- the importance of the greenhouse effect;
- the origin and evolution of the atmosphere;
- the role of atmospheric escape for the state of the atmosphere;
- the role of the solar wind in the evolution of the atmosphere; and
- the presence of active volcanism and seismic activity.

Further information about the Venus Express mission can be found at *http://sci.esa.int/venusexpress*

Table 2.9.1. The Venus Express payload and Principal Investigators.

Acronym	Instrument/technique	Principal Investigators
ASPERA	Analyser of Space Plasma and Energetic Atoms	S. Barabash, IRF, Kiruna, Sweden
MAG	Magnetometer	T. Zhang, IFW, Graz, Austria
PFS	High-resolution IR Fourier spectrometer (non-operational from start of mission)	V. Formisano, IFSI-INAF, Rome, Italy
SPICAV/SOIR	Spectroscopy for the Investigation of Characteristics of the Atmosphere of Venus/Solar Occultation at Infrared – UV & IR atmospheric spectrometer for solar/stellar occultation and nadir observations	J.-L. Bertaux, SA/CNRS, Verrières-le-Buisson, France A.-C. Vandaele, BIRA-IASB, Brussels, Belgium
VeRa	Venus Express Radio Science Experiment	B. Häusler, Bundeswehr University Munich, Germany
VIRTIS	High-resolution Visible and Infrared Thermal Imaging Spectrometer	P. Drossart, CNRS/LESIA & Observatoire de Paris, France G. Piccioni, IASF-INAF, Rome, Italy
VMC	Wide-angle Venus Monitoring Camera	W. Markiewicz, MPS, Katlenburg-Lindau, Germany

Status

The spacecraft is in very good condition, with nominal performance of all subsystems and instruments except for the Visible and Infrared Thermal Imaging Spectrometer (VIRTIS), where the cooling of the infrared channels is no longer possible. In addition, the PFS instrument has been non-operational since the start of the mission.

About half of the available fuel has been used since orbit insertion. It is used to compensate for the lowering of the pericentre altitude, which occurs at a rate of up to 3 km per day. The remaining fuel should last until the end of 2015.

The mission operations are characterised by the different phases of the synodic year of Venus. The duration of this period is 584 Earth days, which is equal to the time between for example two superior conjunctions. During superior conjunction (when Venus is behind the Sun) communication with the spacecraft is inhibited and the spacecraft is left inactive with only essential systems in operation. At both the superior and inferior conjunctions the spacecraft is rotated 180° about the *z*-axis in order to avoid solar illumination of certain faces of the spacecraft.

Scientific Achievements

The mission has now entered a phase when thorough investigations are being made of selected topics, in which long-term studies are important elements. Great progress has been achieved in fields concerned with the dynamics of the atmosphere. The dynamics of clouds at the cloud tops, at ~70 km, has been studied at around 370 nm by the Venus Monitoring Camera (VMC) and VIRTIS, where a still-unknown substance in the clouds shows a strong absorption band. The UV band thus allows the tracking of the motion of clouds, and studies of the dynamics on global and local scales.

Three distinctly different dynamical regimes have been identified. At low latitudes, where the solar heating causes packets of air to rise due to convection, a mottled structure appears. In the polar region a vast permanent vortex, resembling an Earth hurricane, rotates above the pole. The eye of the vortex can take different shapes that change on timescales of less than a day. The intermediate latitudes show a banded structure that resembles a laminar flow. This region is dominated by high-altitude hazes, with small droplet sizes, that reside slightly above the main clouds and therefore obscure them. Mapping of the cloud altitudes has shown that the clouds in the vortex are located about 5 km lower than those covering the rest of the planet.

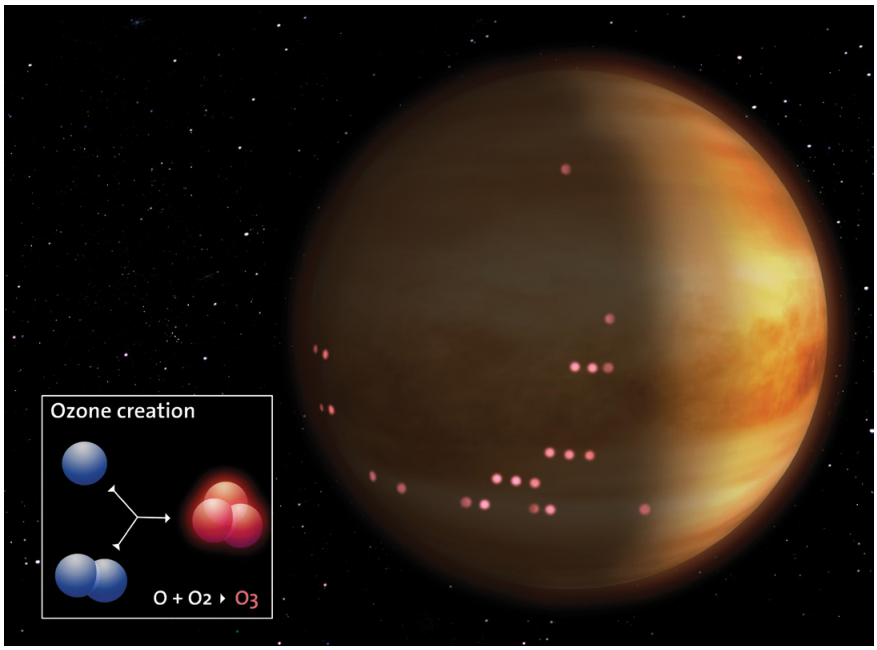

Figure 2.9.1. The locations where ozone has been detected on the nightside, indicated against an artist's impression of Venus. The current models of ozone formation and atmospheric dynamics predict a maximum of ozone at the anti-solar point, i.e. close to the local midnight. Surprisingly, however, no ozone has been detected in this region.

VIRTIS has also made extensive studies of the polar vortex region with several campaigns of four-dimensional data (two spatial, one spectral and time). The vortex rotates with a slightly variable period of around 2.5 days, while the rotation period of the atmosphere at mid- and low latitudes is about four days. These high values are referred to as a super-rotation, because the solid planet rotates with a period of 243 days. The energy to drive this super-rotation must be coming from solar heating, but the process is not yet fully understood. With the new data from Venus Express, the modelling of this phenomenon could be refined and the latest models are now for the first time very close to reproducing the observed super-rotation.

The thermal structure of the atmosphere has been investigated by the spectrometer SPICAV (altitude range 140–90 km) and the Venus Express Radio Science Experiment (VeRa; altitude range 45–90 km) through stellar/solar and Earth occultations, respectively. SPICAV has found a strong inversion layer on the nightside at 90–120 km altitude, which may be due to compressional heating by the downdraft of the air. The VeRa data show a less pronounced inversion associated with the main cloud layer between 62 km and 75 km altitude.

Ozone, O_3, was recently discovered by the SPICAV instrument (Fig. 2.9.1). Ozone was previously known to exist only on Earth and on Mars. Both ozone and hydroxyl (OH), which was also found at Venus for the first time by Venus Express, are highly reactive gases that play important roles in the chemistry of the upper atmosphere. Tracking these gases can help to understand the complex dynamics in this region. VIRTIS and SPICAV have identified various other minor species, including H_2O, HDO, CO, SO_2, HCl, HF and COS.

The ratio of HDO to H_2O is of particular interest since it gives a clue to the history of water on the planet. Thermal escape of hydrogen is more efficient than for deuterium and indeed there is an enhancement of deuterium found in the present atmosphere. The ASPERA instrument is detecting both hydrogen and oxygen in the exosphere at a ratio of 2:1, indicating that water is still being lost from the planet. A small amount of helium has also been seen to be escaping.

Different plasma regions and their borders, such as bow shock and induced magnetopause, have been characterised by the magnetometer. The data taken at around the solar minimum complement well the earlier data from Pioneer Venus taken at the solar maximum. Additional results from the magnetometer include the detection of lightning at a rate comparable with that on Earth.

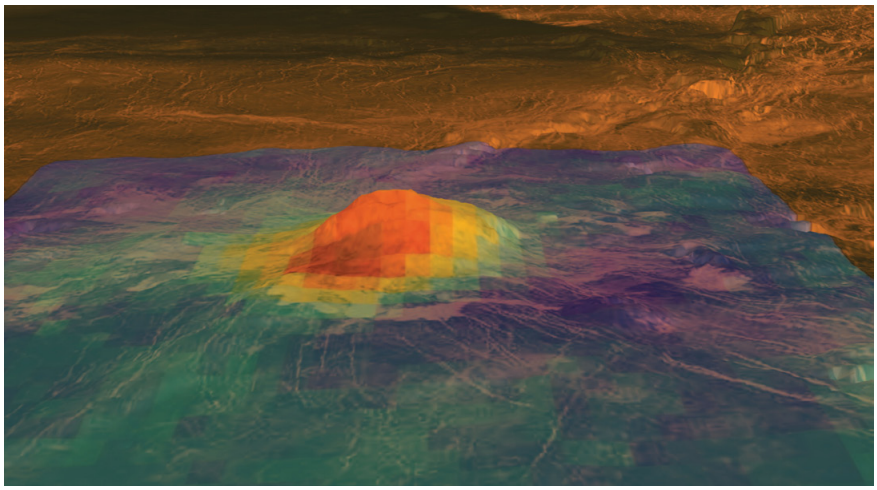

Figure 2.9.2. 3D image of a part of the Imdr Regio, which shows a clear excess in emissivity at Idunn Mons (centre of the image) compared with the surrounding terrain. The image is a combination of an SAR image from the Magellan spacecraft (greyscale) and emissivity from Venus Express/VIRTIS (colour scale). High emissivity indicates a young surface.

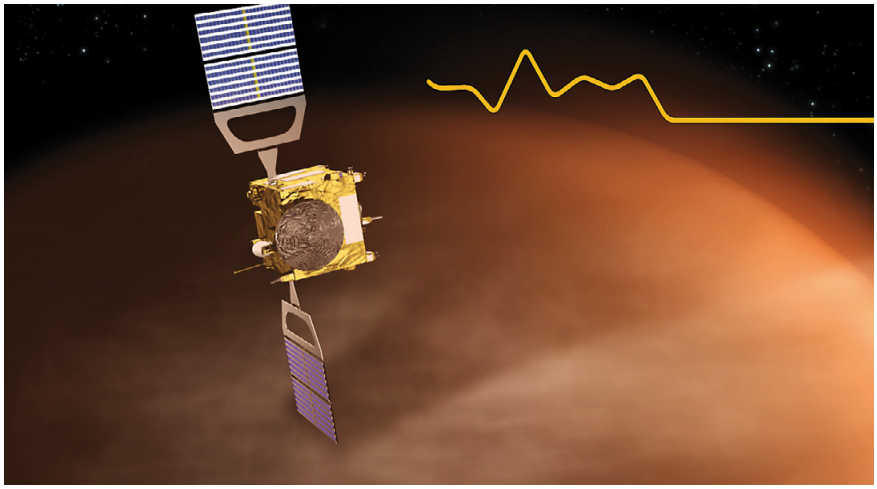

Figure 2.9.3. Highly sensitive measurements of the atmospheric density are made using the new torque technique whereby the two solar panels are rotated to form an asymmetric drag on the spacecraft.

By using the spectral windows at and near 1.0 µm it is possible to probe the lower atmosphere and the surface of Venus. Such mapping has revealed the surface temperature and emissivity of the whole southern hemisphere of the planet. When combining these data with those from the Magellan mission, it appears that some regions are relatively young, about 250 000 years, or possibly (much) younger (Fig. 2.9.2). This indicates that the planet is potentially still geologically active, and thus addresses one of the major questions about Venus.

Using a completely new technique developed by the Venus Express team, the upper atmosphere can now be probed at altitudes that are not accessible by conventional methods. During times of low pericentre altitude (165–200 km), atmospheric drag has traditionally been measured by monitoring small perturbations in the orbit as determined by tracking by the ground stations. Now, by turning one solar wing against the 'wind' and one parallel to it, a torque is felt by the spacecraft. This torque is compensated for by the reaction wheels. The control signals from the reaction wheels give a direct measure of the atmospheric density, allowing this to be monitored at altitudes as high as 200 km (Fig. 2.9.3). This complements the onboard remote sensing instruments that measure atmospheric density below 160 km. Surprising small-scale variations have been revealed using this novel method, and a new model of the venusian atmosphere is being constructed.

References

The results from Venus Express have been described in key papers published in special issues or sections of the following scientific journals:
Nature **450**, 29 November 2007.
Journal of Geophysical Research **113**, 2008, and **114**, 2009.
Planetary and Space Science **59**(10), August 2011.
Icarus **217**(2), February 2012.

2.10 Herschel

Introduction

The Herschel Space Observatory is the fourth of the original Cornerstone missions in the ESA Horizon 2000 science plan. It was launched on 14 May 2009 by an Ariane 5 ECA, together with Planck (see Section 2.11), from Europe's Spaceport in Kourou, French Guiana. Herschel is a space observatory mission (Pilbratt et al., 2010) providing unrivalled observing opportunities for the astronomy community in the relatively poorly explored part of the far-infrared (FIR) and submillimetre (sub-mm) spectral range, covering approximately 55–670 μm. It offers a much larger telescope and extends the spectral coverage to longer wavelengths compared with earlier infrared missions such as the Infrared Astronomical Satellite (IRAS), the Infrared Space Observatory (ISO), Akari and Spitzer, and bridges the wavelength gap to ground-based sub-millimetre observatories.

It is now foreseen that Herschel will offer in excess of 20 000 h for scientific observations, about two-thirds of which is open time that has been made available to the astronomy community through a standard competitive proposal process in three Announcements of Opportunity. Over 3000 astronomers from more than 40 countries have already applied for observing time on Herschel.

Scientific Objectives

Herschel is the first and only space facility dedicated to the FIR and sub-mm part of the spectrum. The major strengths of Herschel are its large telescope, its payload complement that provides a photometric large-area mapping capability for performing unbiased surveys, and its spectral coverage for follow-up observations.

About half the energy emitted in the Universe since the formation of the Cosmic Microwave Background (CMB) is today to be found in the part of the spectrum targeted by Herschel. Originally emitted at shorter wavelengths by stars or in accretion processes, the photons have been absorbed by dust in the Interstellar Medium (ISM) in galaxies, and emitted at the longer Herschel wavelengths appropriate to the ISM temperatures. Redshifted ultraluminous IR-dominated galaxies, with Spectral Energy Density functions (SEDs) that 'peak' in the 50–100 μm range in their rest frames, as well as Class 0 protostars and prestellar objects in our own and nearby galaxies, have SEDs that peak in the Herschel 'prime' band. Herschel is also well equipped to perform spectroscopic follow-up observations to characterise further particularly interesting individual objects.

The key science objectives emphasise the formation of stars and galaxies, and their interrelation. Examples of observing programmes being conducted with Herschel include:

— Broadband photometric extragalactic surveys of a variety of fields and depths. Herschel is further resolving the IR background into discrete sources, in order to investigate how the star formation rate and galaxy luminosity functions have evolved with cosmic time over the last 80% of the age of the Universe.

— Follow-up spectroscopy of especially interesting survey objects, including gravitationally lensed high-redshift galaxies. The FIR/sub-mm band contains the brightest cooling lines of interstellar gas, providing important

Further information about the Herschel Space Observatory can be found at *http://sci.esa.int/herschel* and *http://herschel.esac.esa.int/*

information on the physical processes and energy-production mechanisms (e.g. AGN versus star formation and feedback processes) in galaxies.

— Herschel is also investigating nearby resolved galaxies of different structure and composition, providing more detailed information at the level of individual galaxies using a combination of photometry and spectroscopy.

— Herschel is conducting broadband photometric galactic surveys of the galactic plane, the Gould Belt of nearby star-forming regions, and additional regions including regions of high-mass star formation, supernova remnants, and molecular clouds at a variety of galactic latitudes. Herschel is providing a much more detailed understanding of the physics of the early stages of star formation in molecular clouds in the interstellar medium.

— Observational astrochemistry (of gas and dust) as a quantitative tool for understanding the stellar/interstellar lifecycle and investigating the physical and chemical processes involved in star formation and in both early and late stages of stellar evolution in our own Galaxy.

— Herschel is providing unique information on the evolution of circumstellar discs, both during the early planet-forming era when they consist of gas and dust, and for mature stars and their dust 'debris discs' maintained from the continuous grinding down of planetesimals.

— Detailed high-resolution spectroscopy of a number of comets and the atmospheres of the cool outer planets and their satellites.

— Studies of Kuiper Belt objects, and comparisons with the global properties of those observed around nearby stars.

From experience, the discovery potential is significant when a new capability is being implemented for the first time. Observations have never before been performed in space in the prime band of Herschel; some examples of the scientific results are presented below.

Satellite, Telescope and Science Instruments

The Herschel satellite is dominated by its large 3.5 m-diameter telescope and superfluid helium cryostat containing the three science instruments, the Photodetector Array Camera and Spectrometer (PACS; Poglitsch et al., 2010), the Spectral and Photometric Imaging Receiver (SPIRE; Griffin et al., 2010), and the Heterodyne Instrument for the Far-Infrared (HIFI; de Graauw et al., 2010). The telescope is on top of the cryostat and is radiatively cooled to an operational temperature in the range 85–90K. The instruments are cooled by superfluid helium that is gradually evaporating and eventually released into space; 335 kg was carried at launch and this supply is determining the operational lifetime of the observatory.

The relevant details are summarised in Tables 2.10.1 and 2.10.2; see also Pilbratt et al. (2010) and ESA's Report to the 38th COSPAR Meeting (ESA, 2010).

Principal characteristics	
Type of mission	Far-infrared and submillimetre space observatory; ~2/3 open time available to the general user community; 4th ESA Cornerstone mission
Science goals	Star and galaxy formation and evolution, interstellar medium physics and chemistry, solar system body studies
Telescope	3.5 m-diameter Cassegrain telescope of silicon carbide
Satellite	3-axis stabilised satellite with superfluid helium cryostat for instrument focal plane unit cooling
Size	Height 7.4 m × width 4 m; launch mass 3400 kg
Science data rate	130 kbit/s average production rate
Lifetime	3 years of routine science operations
Operational orbit	Large Lissajous (halo) orbit around L2
Launch	Dual launch (with Planck) on Ariane 5 ECA on 14 May 2009

Table 2.10.1. The Herschel mission.

Table 2.10.2. Herschel's scientific payload.

Instrument	Objective	Principal Investigators
Photodetector Array Camera and Spectrometer (PACS)	Imaging camera and grating spectrometer, spectral coverage ~55–205 μm	A. Poglitsch, MPE, Garching, Germany
Spectral and Photometric Imaging Receiver (SPIRE)	Imaging camera and Fourier transform spectrometer, spectral coverage ~194–671 μm	M. Griffin, University of Cardiff, UK
Heterodyne Instrument for the Far-Infrared (HIFI)	High-resolution heterodyne spectrometer; spectral coverage 157–212 μm and 240–625 μm	F. Helmich, SRON, Groningen, the Netherlands

Mission and Science Ground Segment

Herschel is an observatory facility that is open to the general astronomy community. The available observing time is shared between guaranteed time (one third) owned by contributors to the Herschel mission (mainly by the PI instrument consortia), and open time allocated to the general community (including the guaranteed time holders) on the basis of calls for observing time.

The mission and science operations of Herschel are conducted in a decentralised manner. The operational ground segment comprises six elements:

- the Herschel Science Centre (HSC), provided by ESA;
- three dedicated Instrument Control Centres (ICCs), one for each instrument, provided by the respective PIs;
- the Mission Operations Centre (MOC), provided by ESA; and
- the NASA Herschel Science Center (NHSC), provided by NASA.

The HSC acts as the interface between the science community and the outside world, supported by the NHSC (primarily) for the US science community. The HSC provides information and user support related to the entire life cycle of an observation, from calls for observing time, the proposing procedure, proposal tracking, data access and data processing, as well as general and specific information about using Herschel and its instruments. All scientific data are archived and made available to the data owners. After the proprietary time has expired for a given observation, the data are made available to the entire astronomy community.

Status

Herschel is well into its third year inflight and, apart from the HIFI instrument that is operating on its redundant warm electronics, all systems are operating on their prime units.

Mission and science operations are working well according to established procedures. In the last year Herschel had a track record of conducting more than 19 h of science observing per day (in excess of the preflight mission design number of 18 h), and good science data and data products are routinely delivered to its observers.

All Herschel observing time has now been allocated to observers in a total of three Announcements of Opportunity, one conducted before launch, followed by inflight AOs in 2010 and 2011.

Scientific Results: A Few Tasters

Herschel observes the cool Universe near and far, in time as well as in space. A particularly far-reaching result is that galaxies with redshifts up to $z \approx 2.5$, corresponding to a lookback time of 11 billion years or 80% of the age of the Universe, appear to form stars in much the same spatially 'spread-out' manner as in our own Galaxy, the Milky Way, still does to this day (Elbaz et al., 2011; see Fig. 2.10.1). It was already known that galaxies on the average formed stars at higher rates in the past (a result that has been corroborated by Herschel in detail for last few billion years) but this result shows that the way this is happening has been much the same throughout and that the difference in rate is due to the fact that galaxies contained more gas (stellar raw material) in the past. This is quite a surprising result, as it was believed that merger-induced spatially compact 'bursts' of star formation played a much more prominent role.

Starbursts do occur, however. Another interesting Herschel result (Sturm et al., 2011) indicates a mechanism by which such starbursts can basically turn themselves off on short timescales. Observations of a sample ultraluminous infrared galaxies have shown them to exhibit outflows of molecular gas with

Figure 2.10.1. Herschel's deepest observations reveal the cosmic history of star formation. *Left:* The image shows a composite, three-colour view of the GOODS North field, observed with Herschel/PACS at 100 μm (blue) and 160 μm (green) and with Herschel/SPIRE at 250 μm (red), and based on 124 h of integration. *Right:* The 'infrared main sequence', the total infrared luminosity (an indicator of the amount of star formation) versus the amount of 8 μm emission (an indicator of the manner of star formation) form a straight line all the way to a lookback time of 11 billion years, corresponding to a redshift of $z \approx 2.5$. (ESA/GOODS–Herschel consortium/D. Elbaz)

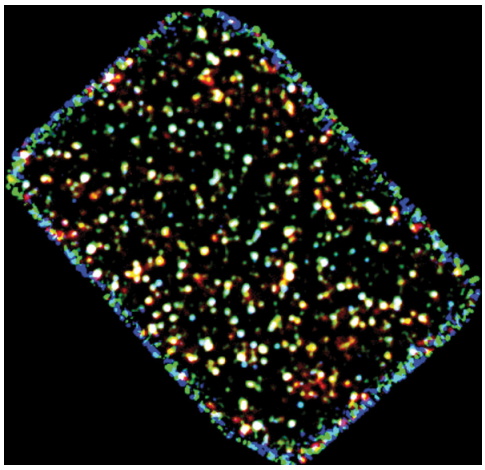

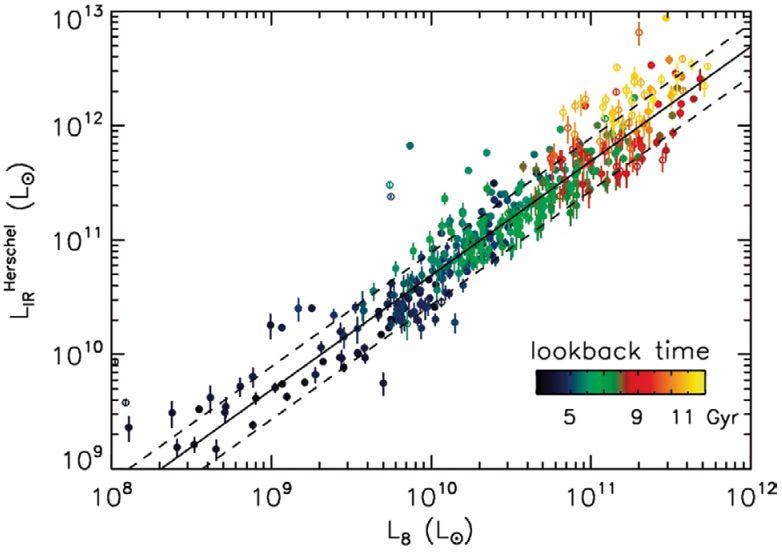

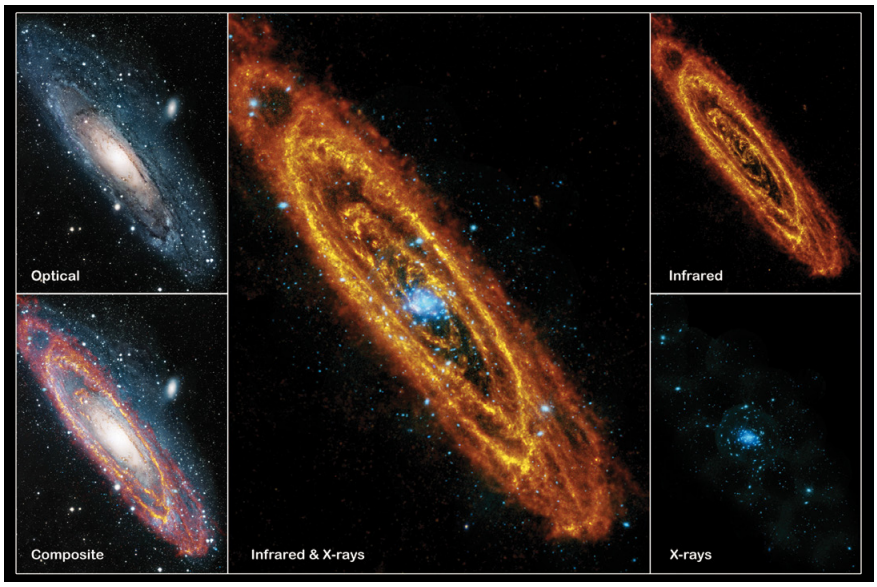

Figure 2.10.2. Infrared, X-ray and optical views of M31, showing how observations in the three spectral regions complement each other. In the optical, mainly starlight is seen with dark lanes where the stars are obscured. These dark lanes, filled with dust that traces the gas where new stars will be born, are glowing in the far-infrared. Finally, the X-rays provide a view of stars having reached their evolution endpoints as compact objects accreting material from their surroundings. (Infrared: ESA/Herschel/SPIRE/J. Fritz, University of Gent, Belgium; X-ray: ESA/XMM-Newton/EPIC/W. Pietsch, MPE; Optical: R. Gendler)

velocities in excess of 1000 km s^{-1} and rates up to 1200 solar masses per year, suggesting quenching of the ongoing star formation by expulsion of the molecular gas from the galactic centres on very short timescales, down to as little as millions of years, a cosmic instant.

A good global view of star formation in a galaxy similar to our own can be obtained from observations of the Andromeda galaxy, M31. In particular, by combining Herschel observations with observations in the optical and X-rays (from XMM-Newton) parts of the spectrum the full story emerges (see Fig. 2.10.2). Closer views of star formation obtained by Herschel were provided in ESA's Report to the 38th COSPAR meeting (ESA, 2010, pp.10 and 92).

A special talent of Herschel is its ability to observe water in gas form. Recently, this has enabled Herschel to produce a number of interesting results. Observations of the young (~10 Myr) nearby (~55 pc) T Tauri star TW Hydrae have led to the detection of cold water vapour in its protoplanetary disc (Hogerheijde et al., 2011; see Fig. 2.10.3). Modelling implies that the amount of detected water vapour is roughly equivalent to 0.005 Earth oceans. It results from photodesorption of water ice frozen onto dust grains in the disc, and implies an ice reservoir of thousands of Earth oceans in the giant planet formation zone and further out around TW Hydrae.

Water geysers are known to exist on Enceladus, one of the moons of the giant planet Saturn. There is also water in the upper atmosphere of Saturn, but its origin was always a mystery. Now Herschel has shown (Hartogh et al., 2011a) that water from geyser plumes ends up in a giant torus around Saturn centred on the orbit of Enceladus, and some if it finally ends up in the upper atmosphere of Saturn. This is the first time that a moon has been observed to alter the composition of the atmosphere of its host planet.

The origin of the water on Earth is also a subject of controversy. It is generally presumed that it was delivered from space by impacting bodies, but by which class of bodies is unclear, and sometimes passionately debated. Based on previously observed deuterium/hydrogen (D/H) ratios, it has been argued that asteroids fit the picture better than comets. However, Herschel observations now show that at least one comet, 103P/Hartley 2, has a very similar D/H ratio to those of the oceans on Earth (Hartogh et al., 2011b; see Fig. 2.10.3). The debate has been reopened.

More examples and additional information and links can be found on the Herschel Science Centre website (*http://herschel.esac.esa.int*), in particular under 'Latest News', while a full list of papers (including the references cited here) can be found under 'Scientific Publications'.

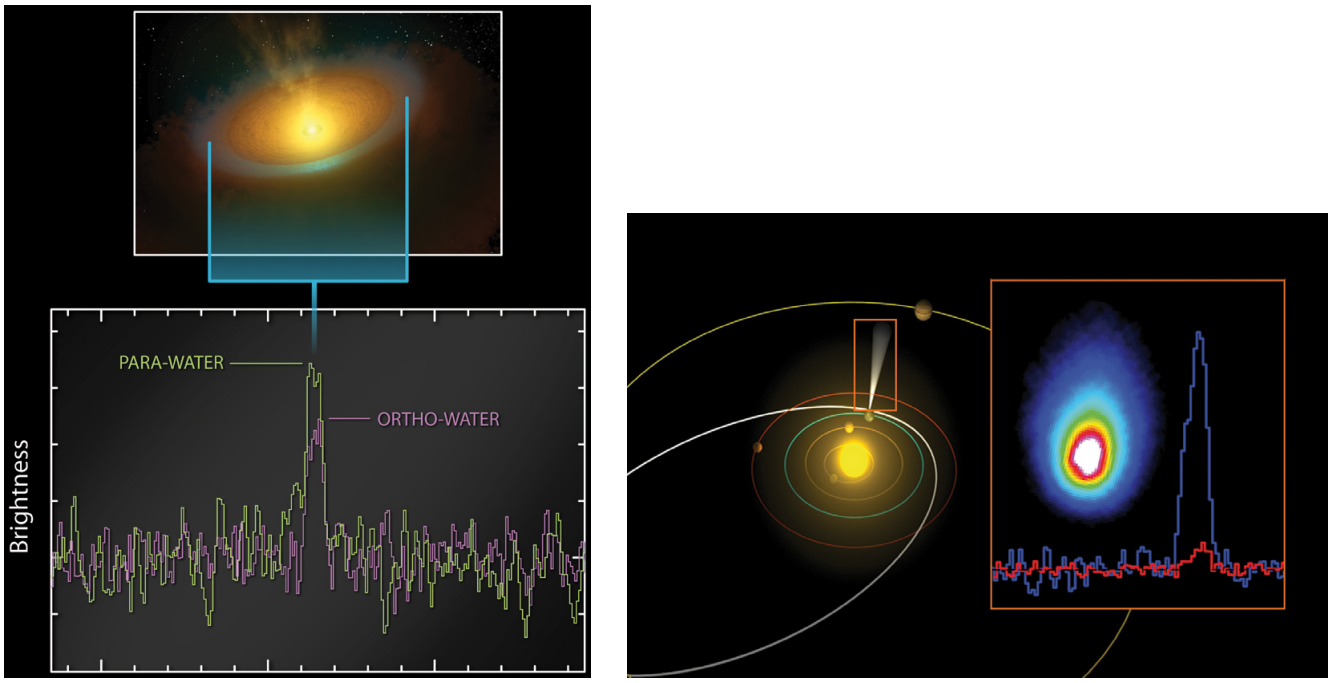

Figure 2.10.3. *Left:* Artist's impression of the icy protoplanetary disc around the young star TW Hydrae (upper panel) and the spectrum of the disc obtained using the Herschel HIFI spectrometer (*lower panel*). The ratio of ortho- to para-water observed in the disc points to the presence of cold water vapour. (ESA/NASA/JPL-Caltech/M. Hogerheijde, Leiden Observatory, the Netherlands)
Right: The orbit of the Jupiter-family comet 103P/Hartley 2 in relation to the orbits of the innermost five planets of the Solar System. *Inset, right:* The comet as viewed with the PACS instrument onboard Herschel. Also shown are two lines excerpted from the spectrum of the comet taken with HIFI and reflecting the presence of two different isotopologues of the water molecule. By comparing the D/H ratio measured across the Solar System to that measured in Earth's oceans, it is possible to constrain the nature of the bodies that contributed most to delivering water to our planet. (ESA/AOES Medialab; Herschel/HssO Consortium)

Looking to the Future

As part of the preparations for the last time allocation process in 2011, a reassessment of the predicted Herschel lifetime using all available information has been conducted. The conclusion is that around February 2013 is the most likely time that Herschel will run out of helium, precluding any further observing: there is no 'warm' Herschel mission.

The end of inflight operations is clearly a major milestone, but it is by no means the end of the Herschel mission. The observers will be working on their data for years to come, and the detailed planning for the 'post-operations phase' is now being performed.

References

Elbaz, D. et al. (2011). *Astron. Astrophys.* **533**, A119.
ESA (2010). *ESA's Report to the 38th COSPAR meeting*. ESA SP-1318, European Space Agency, Noordwijk, the Netherlands, p.88–90.
de Graauw, T. et al. (2010). *Astron. Astrophys.* **518**, L6.
Griffin, M.J. et al. (2010). *Astron. Astrophys.* **518**, L3.
Hartogh, P. et al. (2011a). *Astron. Astrophys.* **532**, L2.
Hartogh, P. et al. (2011b). *Nature* **478**, 218.
Hogerheijde, M.R. et al. (2011). *Science* **334**, 338.
Pilbratt, G. et al. (2010). *Astron. Astrophys.* **518**, L1.
Poglitsch, A. et al. (2010). *Astron. Astrophys.* **518**, L2.
Sturm, E. et al. (2011). *Astrophys. J.* **733**, L16.

2.11 Planck

Introduction

The Planck satellite was launched on 14 May 2009, and has been surveying the sky stably and continuously since 13 August 2009 (Tauber et al., 2010). The main objective of Planck is to measure the spatial anisotropies of the temperature of the Cosmic Microwave Background, with an accuracy set by fundamental astrophysical limits. Its level of performance will enable the extraction of essentially all the information in the CMB temperature anisotropies.

Planck will also measure to high accuracy the polarisation of the CMB anisotropies, which encodes not only a wealth of cosmological information, but also provides a unique probe of the thermal history of the Universe during the time when the first stars and galaxies formed. In addition, the Planck sky surveys will produce a wealth of information on the properties of extragalactic sources and on the dust and gas in our own Galaxy. The scientific objectives of Planck are described in detail in Planck Collaboration (2005).

Planck carries a scientific payload consisting of an array of 74 detectors sensitive to a range of frequencies between ~25 GHz and ~1000 GHz, which scan the sky simultaneously and continuously with an angular resolution varying between ~30 arcmin at the lowest frequencies and ~5 arcmin at the highest. The array is arranged into two instruments: the detectors of the Low-Frequency Instrument (LFI) are pseudo-correlation radiometers, covering three bands centred at 30, 44 and 70 GHz; and the detectors of the High-Frequency Instrument (HFI) are bolometers, covering six bands centred at 100, 143, 217, 353, 545 and 857 GHz.

The Planck satellite, its payload and its performance as predicted at the time of launch are described in 13 ‘pre-launch papers’ included in volume 520 of the journal *Astronomy & Astrophysics*.

The design of Planck allows it to image the whole sky approximately twice per year, with an unprecedented combination of sensitivity, angular resolution and frequency coverage. The high quality of the Planck data can be appreciated in Fig. 2.11.1, which is a composite of data acquired during the first complete all-sky survey.

On 14 January 2012, the supply of helium gas needed to cool the detectors of HFI was exhausted, as expected, and it stopped acquiring scientific data. Up to that moment, Planck had completed five surveys of the whole sky. The LFI will continue to operate as long as its cooling system is able to maintain 20K on the focal plane, currently predicted to be at least up to October 2012.

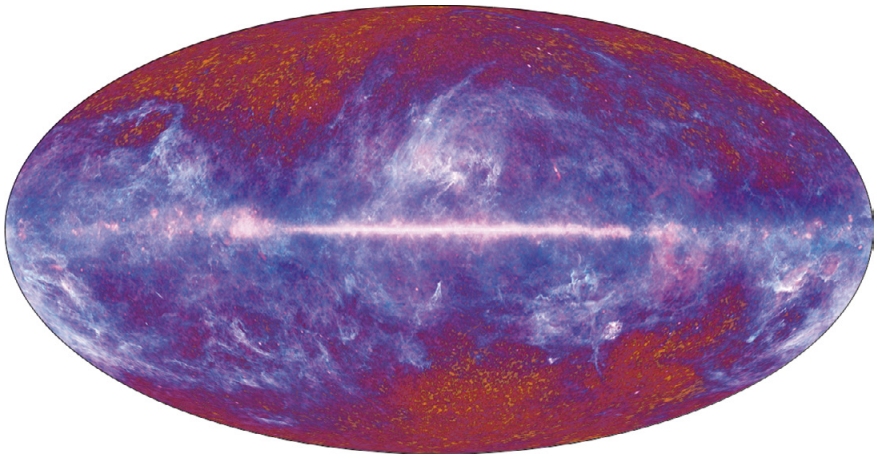

Figure 2.11.1. The microwave sky as seen by Planck. This multifrequency all-sky image of the microwave sky has been composed using data from Planck covering the electromagnetic spectrum from 30 GHz to 857 GHz.

Further information about the Planck mission can be found at *http://sci.esa.int/planck* and *www.rssd.esa.int/planck*

Scientific Results

In January 2011, ESA and the Planck Collaboration released to the public a first set of scientific data. This dataset, the Early Release Compact Source Catalogue (ERCSC), is a list of unresolved and compact sources extracted from the first complete all-sky survey carried out by Planck. The ERCSC (Planck Early Results VII) consists of:

— nine lists of sources, extracted independently from each of Planck's nine frequency bands; and
— two lists of sources extracted using multiband criteria targeted at selecting specific types of source, i.e. 'cold cores', cold and dense locations in the interstellar medium of the Milky Way based mainly on their estimated dust temperature, and clusters of galaxies, selected using the spectral signature left on the Cosmic Microwave Background by the Sunyaev–Zel'dovich effect.

The ERCSC is a highly reliable compilation of sources, released early to give the astronomy community a timely opportunity to follow up these sources using ground- or space-based observatories, in particular ESA's Herschel observatory, which has a limited lifetime. The ERCSC was released to the public through an online distribution system accessible via *www.rssd.esa.int/planck*.

At the same time as the ERCSC was released, the Planck Collaboration prepared a package of 26 papers that were published as a Special Feature of *Astronomy & Astrophysics* (volume 536, December 2011). The package consisted of:

— one paper (Planck Early Results I) describing the history and main performance elements of the Planck satellite in its first year of operation;
— two papers describing the performance of each of Planck's two instruments (LFI and HFI) within the same period (Planck Early Results III and IV);
— one paper describing the thermal performance of Planck in orbit (Planck Early Results II);
— two papers describing the processing that was applied to the data acquired by LFI and HFI to produce the maps used for the ERCSC and the scientific papers in the package (Planck Early Results V and VI);
— an Explanatory Supplement to the ERCSC (Planck Early Results XXVI) describing in detail the production and characteristics of the ERCSC;
— one paper summarising the production of the ERCSC, and the main characteristics of the sources it contains (Planck Early Results VII);
— 11 papers describing in more detail specific aspects of different source populations contained in the ERCSC (radio sources, infrared galaxies, galaxy clusters, cold cores, etc.), and cross-correlation analysis and follow-up observations that form part of the scientific validation and analysis of the ERCSC data. These papers are:
  – Planck Early Results VIII describes the physical properties of the sample of clusters included in the ERCSC;
  – Planck Early Results IX describes the validation of a subset of the cluster sample by follow-up observations with the XMM-Newton X-ray observatory;
  – Planck Early Results X analyses the statistical relationship between the SZ flux and X-ray luminosity of the ERCSC cluster sample;
  – Planck Early Results XI uses a high signal-to-noise subset of the ERCSC cluster sample to investigate the relationship between X-ray-derived masses and SZ fluxes;
  – Planck Early Results XII studies the relation between the SZ flux and optical properties of galaxy clusters by stacking Planck fluxes at the locations of the MaxBCG optical cluster catalogue;
  – Planck Early Results XIII analyses the statistical properties of a complete subsample of radio sources drawn from the ERCSC;

  - Planck Early Results XIV describes the spectral energy distributions and other properties of some extreme radio sources, using Planck ERCSC data and ground-based observations;
  - Planck Early Results XV presents the spectral energy distributions of a sample of extragalactic radio sources, based on the Planck ERCSC and simultaneous multifrequency data from a range of other observatories;
  - Planck Early Results XVI studies the dust properties of nearby galaxies ($z < 0.25$) present in the ERCSC;
  - Planck Early Results XXIII presents the statistical properties of cold cores as observed by Planck, in terms of spatial distribution, temperature, distance, mass and morphology;
  - Planck Early Results XII presents the physical properties and discusses the nature of a selection of interesting cold cores observed by Planck;
- seven papers describing in more detail selected science results, based on the maps that were used as inputs for the production of the ERCSC. The results addressed in these papers are characterised by their robustness, a critical element required for publication at a rather early stage in the reduction of the Planck data. These seven papers are:
  - Planck Early Results XVII presents estimates based on Planck and IRAS data for the apparent temperature and optical depth of interstellar dust in the Small and Large Magellanic Clouds, and investigates the nature of the millimetre-wavelength excess emission observed in these galaxies;
  - Planck Early Results XVIII presents estimates of the angular power spectrum of the Cosmic Infrared Background as observed by Planck in selected regions of the sky;
  - Planck Early Results XIX estimates over the whole sky the apparent temperature and optical depth of interstellar dust based on Planck and IRAS data, and investigates the presence of 'dark' gas, i.e. gas that is not spatially correlated with known tracers of neutral and molecular gas;
  - Planck Early Results XX constructs the spectral energy distributions of selected regions in the Milky Way, using Planck maps combined with ancillary multifrequency data, and investigates the presence of anomalous excess emission which can be interpreted as arising from small spinning grains;
  - Planck Early Results XXI estimates the radial distribution of molecular, neutral, and ionised gas in the Milky Way, using as spatial templates a wide variety of tracers of the different phases and components of the interstellar medium;
  - Planck Early Results XXIV presents a joint analysis of Planck, IRAS and 21 cm observations of selected high-galactic-latitude fields, and discusses the properties of dust in the diffuse interstellar medium close to the Sun and in the galactic halo;
  - Planck Early Results XXV presents Planck maps of a selection of nearby molecular clouds, and discusses the evolution of the emitting properties of the dust particles embedded in them.

The next package of Planck products will be released in January 2013, and will cover data acquired in the period up to 27 November 2010, including:

- temperature maps for each frequency band between 30 GHz and 857 GHz;
- catalogues of compact sources extracted from the frequency maps;
- maps of the main diffuse components separated from the maps, including the CMB; and
- scientific results based on the data released.

A third release of products is foreseen after January 2014, to cover the data acquired beyond November 2010 and up to the end of Planck operations. In addition to the products foreseen for the first release, it will include cleaned

and calibrated data timelines for each detector, polarised maps in each frequency band between 30 GHz and 353 GHz, and the corresponding polarised CMB and foreground maps.

References

Planck Collaboration (2005). *Planck: The Scientific Programme*. ESA-SCI(2005)1. European Space Agency, Noordwijk, the Netherlands.

Planck Early Results I: Planck Collaboration (2011). *Astron. Astrophys*. **536**, A1.

Planck Early Results II: Planck Collaboration (2011). *Astron. Astrophys*. **536**, A2.

Planck Early Results III: Mennella, A., Bersanelli, M., Butler, R.C. et al. (2011). Astron. Astrophys. 536, A3.

Planck Early Results IV: Planck HFI Core Team (2011). *Astron. Astrophys*. **536**, A4.

Planck Early Results V: Zacchei, A., Maino, D., Baccigalupi, C. et al. (2011). *Astron. Astrophys*. **536**, A5.

Planck Early Results VI: Planck HFI Core Team (2011). *Astron. Astrophys*. **536**, A6.

Planck Early Results VII: Planck Collaboration (2011). *Astron. Astrophys*. **536**, A7.

Planck Early Results VIII: Planck Collaboration (2011). *Astron. Astrophys*. **536**, A8.

Planck Early Results IX: Planck Collaboration (2011). *Astron. Astrophys*. **536**, A9.

Planck Early Results X: Planck Collaboration (2011). *Astron. Astrophys*. **536**, A10.

Planck Early Results XI: Planck Collaboration (2011). *Astron. Astrophys*. **536**, A11.

Planck Early Results XII: Planck Collaboration (2011). *Astron. Astrophys*. **536**, A12.

Planck Early Results XIII: Planck Collaboration (2011). *Astron. Astrophys*. **536**, A13.

Planck Early Results XIV: Planck Collaboration (2011). *Astron. Astrophys*. **536**, A14.

Planck Early Results XV: Planck Collaboration (2011). *Astron. Astrophys*. **536**, A15.

Planck Early Results XVI: Planck Collaboration (2011). *Astron. Astrophys*. **536**, A16.

Planck Early Results XVII: Planck Collaboration (2011). *Astron. Astrophys*. **536**, A17.

Planck Early Results XVIII: Planck Collaboration (2011). *Astron. Astrophys*. **536**, A18.

Planck Early Results XIX: Planck Collaboration (2011). *Astron. Astrophys*. **536**, A19.

Planck Early Results XX: Planck Collaboration (2011). *Astron. Astrophys*. **536**, A20.

Planck Early Results XXI: Planck Collaboration (2011). *Astron. Astrophys*. **536**, A21.

Planck Early Results XXII: Planck Collaboration (2011). *Astron. Astrophys*. **536**, A22.

Planck Early Results XXIII: Planck Collaboration (2011). *Astron. Astrophys*. **536**, A23.

Planck Early Results XXIV: Planck Collaboration (2011). *Astron. Astrophys*. **536**, A24.

Planck Early Results XXV Planck Collaboration (2011). *Astron. Astrophys*. **536**, A25.

Planck Early Results XXVI: Planck Collaboration (2011). *The Explanatory Supplement to the Planck Early Release Compact Source Catalogue*. European Space Agency, Noordwijk, the Netherlands.
www.sciops.esa.int/index.php?project=planck&page=Planck_Legacy_Archive

Planck Early Results XXVII: Planck Collaboration (2011). *Astron. Astrophys*. **536**, A26.

Tauber, J.A., Mandolesi, N., Puget, J.L. et al. (2010). *Astron. Astrophys*. **520**, A1.

2.12 Proba-2

Introduction

The Proba-2 satellite was launched as a co-passenger with the Soil Moisture and Ocean Salinity (SMOS) satellite, ESA's second Earth Explorer satellite, early in the morning of 2 November 2009 from Plesetsk Cosmodrome, Russian Federation. After the separation from the Russian Rokot vehicle, a third stage ejected SMOS and Proba-2 into their orbits. The checkout and commissioning of the Proba-2 satellite, its subsystems and instruments were executed by the Prime Contractor at the Mission Operations Centre, Redu, Belgium. Following commissioning, the two main scientific instruments – the EUV imager SWAP and the Large Yield Radiometer (LYRA) – are now operated by the Proba-2 Science Centre (P2SC) from the Royal Observatory of Belgium in Brussels.

Table 2.12.1 summarises the scientific experiments on Proba-2.

Mission Status

The first mission extension period started in November 2011 with the satellite in good health, all subsystems working normally and the orbital plane confirmed at least until 2020.

The Langmuir probe (DSLP) is working normally and will be in continuous operation during the extension period. The Thermal Plasma Measurement Unit (TPMU) will be operated once a month, ensuring the return of sufficient data for long-term trend analysis. DSLP and TPMU overview plots are available several days after acquisition, and preparations are being made to allow public access to raw and calibrated data files.

The LYRA radiometer is operating normally and continuously at 50 Hz using one of the three available units. The two long-wavelength channels of this unit are degraded and no longer support the scientific investigations. The two short-wavelength channels are still providing excellent data on solar background and flare activity. The two other backup units are used for dedicated observation campaigns with all channels providing valuable scientific data.

Since launch, the SWAP imager has provided a stream of continuous high-quality data with a cadence of about 110 s. The SWAP and LYRA data are made available as raw and calibrated FITS (Flexible Image Transport System) files, and a multitude of overview plots just 45 min after each of the 10 daily downlink passes.

A final, deep archive for Proba-2 data within ESAs archives at ESAC, near Madrid, Spain, is currently is preparation.

Table 2.12.1. The Proba-2 scientific experiments.

Experiment	Instrument	Principal Investigators	Participants
SWAP	Sun Watcher using Active Pixel System Detector and Image Processing	D. Berghmans, Royal Observatory of Belgium	IT, IE, DE
LYRA	Large Yield Radiometer	M. Dominique, Royal Observatory of Belgium	CH, FR, UK, US
DSLP	Dual Segmented Langmuir Probe	P. Travnicek, Astronomical Institute, Academy of Science, Czech Republic	IT, IE, DE, CH, FR, UK, US, JP
TPMU	Thermal Plasma Measurement Unit for Microsatellites	F. Hruska, Institute of Atmospheric Physics, Academy of Science, Czech Republic	NL

Further information about the Proba-2 mission can be found at *http://sci.esa.int/proba*

Scientific Highlights

The scientific investigations came up to speed slowly due to the rather small science consortium and the availability of excellent data from NASA's Solar Dynamics Observatory. The scientific highlights listed below show Proba-2's contributions to joint observation campaigns and the dedicated capabilities of the scientific instruments.

— LYRA has demonstrated, on several occasions, its backup capabilities to the recognised Geosynchronous Operational Environmental Satellite (GOES) solar flare detector; it complements and completes the flare measurements and statistics during GOES satellite maintenance or eclipses.

— It has been demonstrated that the four channels on LYRA are sufficient to reconstruct the UV solar irradiance at 28–280 nm with a relative error of about 20%.

— LYRA operates at 50 Hz and oscillations are regularly seen at the onset of and during solar flare events. It has been demonstrated that LYRA contributes to the solar seismology by deriving several flare plasma parameters as a result of the oscillation data analysis.

— SWAP images have been used for 3D reconstructions of solar events, together with images from the EUVI imagers on the Solar TErrestrial RElations Observatory satellites STEREO-A or STEREO-B.

— In 2010 and 2011, SWAP observed eight solar eclipses. The Sun was observed in up to 10 s cadence during these eclipses and a combined analysis of ground-based spectral imaging and SWAP images linked the white-light corona with the EUV corona for several coronal structures.

— A comparison of the ground-based 637.4 nm Fe X line and the 17.4 nm Fe X line of SWAP during a total eclipse demonstrated the unique diagnostic capabilities of coronal forbidden lines for exploring the evolution of the coronal magnetic field and thermodynamics of the coronal plasma.

— The SWAP field-of-view of 54 arcmin is larger than any other imager. The analysis of the as yet unexplored part of the corona in the EUV is inherently difficult, however, as SWAP can only provide a projected view of events in the corona. On several occasions, structures were observed in the full SWAP field-of-view leaving the Sun's surface and appearing in SOHO's coronograph images.

— Data products from SWAP and LYRA are contributing to space weather-related activities and, for example, are being used as additional inputs to space weather predictions or modelling tools.

Each year, the Guest Investigator programme provides support for up to 10 scientists to visit the Proba-2 Science Centre and to participate in operation campaigns.

Results from Proba-2, especially its SWAP movies, are often used in ESA's outreach activities, such as following solar events or solar eclipses.

2.13 Contributions to Nationally-Led Missions

2.13.1 Suzaku

Suzaku, previously called Astro-E2, is Japan's fifth X-ray astronomy satellite and was launched into a low-Earth orbit in July 2005. The mission was developed by the Japan Aerospace Exploration Agency and a number of institutes in Japan and the United States.

The Suzaku payload consists of three instruments: an imaging X-ray micro-calorimeter (XRS), four CCD detectors (X-Ray Imaging Spectrometer, XIS) and a non-imaging Hard X-ray Detector (HXD). Since November 2006, one of the XIS CCD cameras has not been operational and in June 2009 an outer region of one the other CCD cameras became unusable.

The 0.5–10 keV XIS provides high-sensitivity imaging, particularly for extended sources, as well as good spectral resolution. For soft X-rays below 0.8 keV, the XIS provides a capability better than those offered by Chandra and XMM-Newton. Above 10 keV, the non-imaging hard-X-ray detector provides spectral and timing information with high sensitivity to several hundred keV. Unfortunately, during the course of commissioning all the helium cryogen was lost from the XRS, the highest-resolution spectrometer flown to date.

With its imaging X-ray telescopes and hard X-ray response, Suzaku has brought many new capabilities to the observations of all classes of astronomical objects including active galactic nuclei, clusters of galaxies, stars, supernova remnants, X-ray binaries and Solar System objects.

After a nine-month performance verification phase, Suzaku began operating as an observatory open to the worldwide astronomy community. Since the start of open time observations, JAXA has kindly offered to allocate 8% of the open observing time to proposals from scientists from institutes in ESA Member States. In response to the most recent announcement of observing opportunity, AO-7, a total of 26 European proposals were received, corresponding to an oversubscription in time of 3.9. For comparison, 28 European proposals were received in response to AO-6, an oversubscription of 3.2, showing the continued high interest of European scientists in the mission. The European proposals are peer-reviewed by an ESA-appointed Time Allocation Committee and the recommended proposals are forwarded to JAXA to be merged with those received in response to the parallel Japanese and US calls.

Further information about the Suzaku mission can be found at *www.rssd.esa.int/suzaku*

2.13.2 Hinode

Introduction

Hinode (Japanese for 'sunrise'), known as 'Solar-B' before launch, is a Japanese mission with instrument contributions from the US and the UK, and ESA ground station support. It was launched into a dusk–dawn, polar, Sun-synchronous orbit on 23 September 2006. Using a combination of optical, EUV and X-ray instrumentation, Hinode studies the generation, transport and dissipation of magnetic energy from the photosphere to the corona, and how energy stored in the Sun's magnetic field is released as the field rises into the Sun's outer atmosphere.

The satellite consists of a Sun-pointing platform with three major instrument packages:

- Solar Optical Telescope (SOT), a high-resolution (0.25 arcsec) visual imaging system with a vector magnetograph and spectrograph;
- X-ray Telescope (XRT), which provides full- or partial-disc imaging with 1.0–2.5 arcsec resolution in the wavelength range 0.2–6 nm; and
- EUV Imaging Spectrometer (EIS), with wavelength ranges 17–21 nm and 25–29 nm, 2.0 arcsec resolution and a field of view of 360 × 512 arcsec.

Hinode's operations centre is located at JAXA's facility in Sagamihara, Japan.

ESA, in partnership with the Norwegian Space Centre, is providing ground station coverage through several KSAT stations (Svalbard Satellite Station, on the Norwegian Svalbard Islands, and Troll in Antarctica). In 2010 and 2011 (to October) these stations provided 4008 and 4124 successful passes, respectively. In addition, the two partners have established a European Hinode Science Data Centre at the Institute of Theoretical Astrophysics at the University of Oslo, Norway, providing scientists access to all the satellite's data. In 2010 (2011), 3685 (3822) distinct visitors accessed the site and 626 GB (353 GB) of data were downloaded.

Scientific Highlights

The origin of the solar wind is one of the most important unresolved problems in space and solar physics. A Chinese–German team (Tian et al., 2010) reported the first spectroscopic signatures of the nascent fast solar wind in a polar coronal hole at coronal temperatures ($\log(T/K) > 5.8$) in observations made by the EUV Imaging Spectrometer on Hinode (Fig. 2.13.2.1). The measured upflows are associated with open field lines in the coronal hole. They seem to start in the solar transition region and become more prominent with increasing temperature. The patches with significant upflows are still isolated in the upper transition region but merge in the corona, in agreement with the scenario of solar wind outflow being guided by expanding magnetic funnels.

Martinez Pillet et al. (2011) identified ubiquitous quiet-Sun jets in Hinode's Spectropolarimeter (SP) data. They often appear in pairs (both red- and blue-shifted components), mostly in the outer boundaries of granules next to regions of transverse magnetic fields. The authors suggest that these high-speed flows are driven by magnetic reconnection.

Harra et al. (2011) combined Hinode/EIS and SDO/AIA observations to determine for the first time with a high time cadence the spectroscopic signature of an EIT wave (large-scale coronal wave) as it propagates away from

Further information about the Hinode mission can be found at *www.esa.int/esaSC/SEM55CVHESE_index_0_m.html*

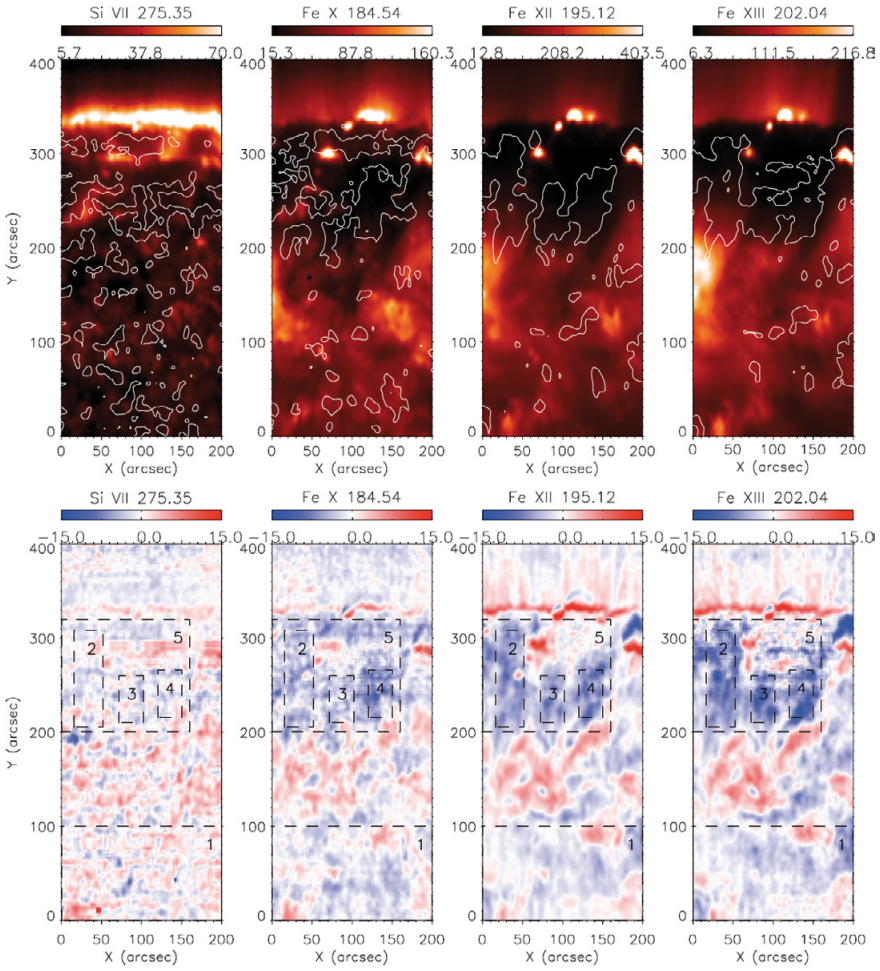

Figure 2.13.2.1. Maps of radiance and Doppler shift in a polar coronal hole in four emission lines as measured by Hinode/EIS. (Tian et al., 2010)

an active region. They found that the main wave front travels at ~500 km s^{-1} and is strongly redshifted, i.e. as the wave propagates it also pushes plasma down towards the solar chromosphere at a speed of ~20 km s^{-1}. After a low-velocity period they observed a second redshifted feature with velocities of 200–500 km s^{-1} and with a comparable or somewhat lower Doppler velocity.

De Pontieu et al. (2011) combined SDO/AIA and Hinode/SOT and EIS observations to reveal a ubiquitous coronal mass supply in which chromospheric plasma in fountain-like jets or spicules is accelerated to velocities of 50–100 km s^{-1} upwards into the corona, with much of the plasma heated to transition region temperatures (20 000–100 000K) and a small but significant fraction to temperatures above 1 MK (Fig. 2.13.2.2). They estimated that these events carry a mass flux density of 1.5×10^{-9} g cm^{-2} s^{-1} and an energy flux density of ~2×10^{6} erg cm^{-2} s^{-1} into the corona, which are of the order required to sustain the energy lost from the active region corona. The authors conclude that these events are likely to play a substantial role in the coronal energy balance, and highlight the importance of the chromosphere (the interface between the photosphere and corona) for a better understanding of heating in the solar atmosphere.

Socas-Navarro (2011) presented the first high-resolution 3D model of the solar photosphere that is based on the inversion of spectropolarimetric observations with Hinode/SP. Previous 3D models were all based on numerical radiation-hydrodynamic simulations. Due to the high spatial resolution of Hinode observations the major granular components are resolved. The derived model therefore does not require micro- or macroturbulence to properly fit the widths of the observed spectral lines. The model is available for use by others.

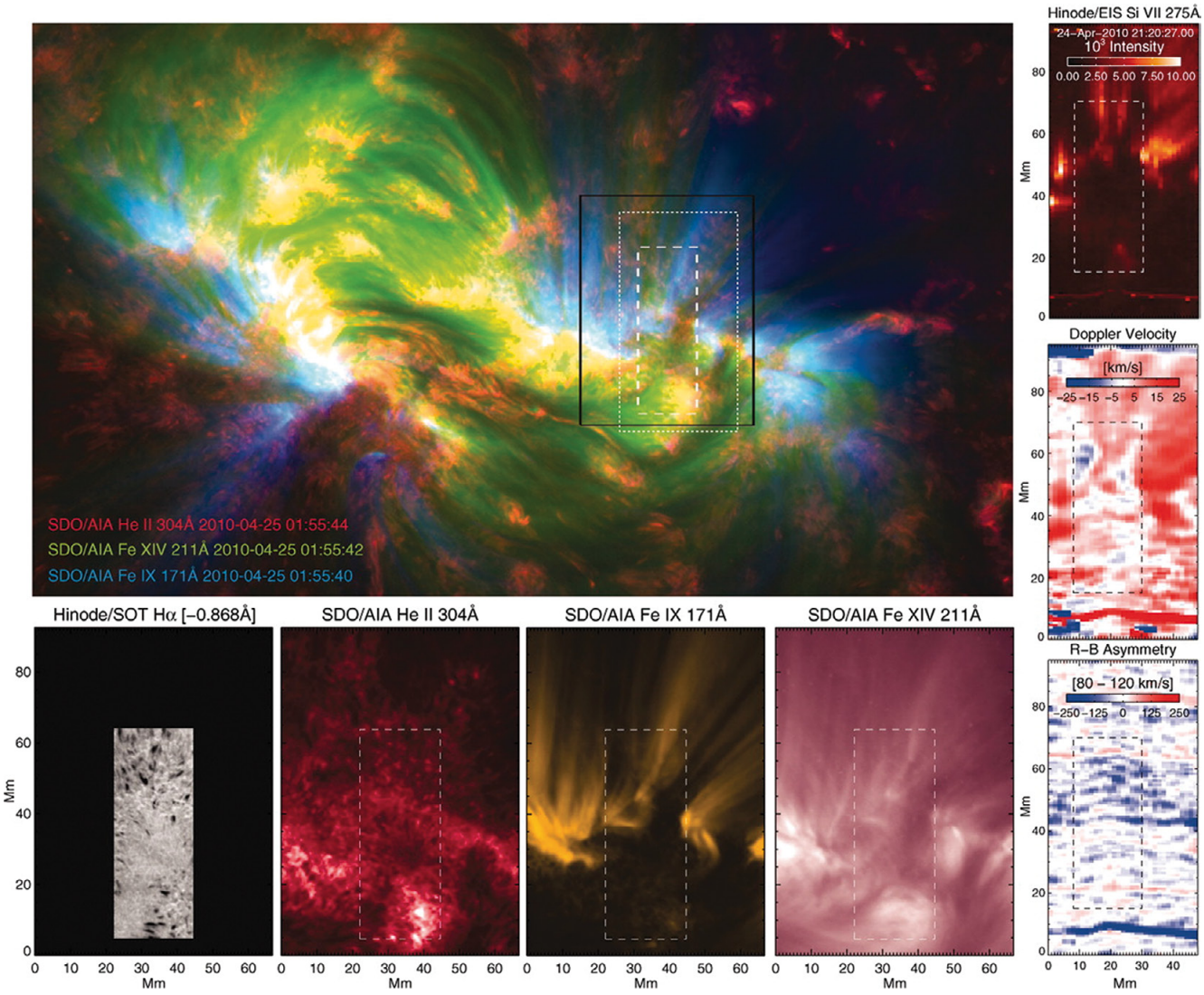

Figure 2.13.2.2. The chromosphere, transition region and corona of an active region as studied with SDO/AIA, Hinode/SOT and Hinode/EIS. (De Pontieu et al., 2011).

Berger et al. (2011) combined optical and EUV observations obtained with Hinode/SOT and SDO/AIA to study the thermodynamics of polar crown filaments (Fig. 2.13.2.3). They found that the low-density coronal cavity contains plasma at temperatures in the range $(2.5–12)\times10^5$K, which is 25–120 times hotter than the overlying prominence. These observations suggest that the coronal cavity–prominence system supports a novel form of magnetoconvection in the solar atmosphere, challenging current hydromagnetic concepts of prominences and their relation to coronal cavities.

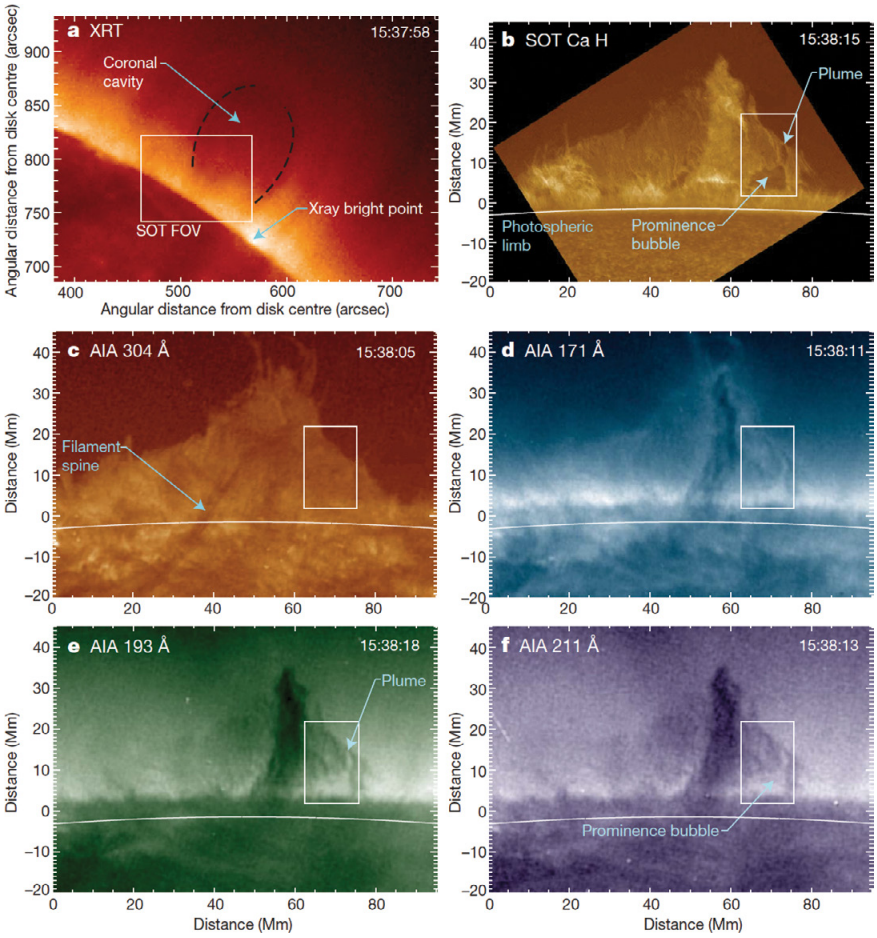

Figure 2.13.2.3. (a) Hinode XRT image of the region surrounding the prominence, which is transparent to X-rays and hence not seen. (b) SOT image in the Ca II H line, showing a bubble and a large rising plume on the right of the prominence. (c) SDO/AIA 304 Å-channel image. The bubble is not visible in this passband, indicating that optically thick emission is mostly from the sheath-like prominence–corona transition region surrounding the structure seen in (b). (d) AIA 171 Å-channel image. The prominence shows strong absorption along the spine region and weak emission from surrounding regions. (e) AIA 193 Å-channel image. This and (f) show strong absorption from neutral H and neutral and ionised He in all regions of the prominence. (f) AIA 211 Å-channel image. Note that the bubble and plume show up clearly in emission relative to the dark prominence. The darkened region above 30 Mm indicates the lower regions of the associated coronal cavity. Time (UT) is shown at top right in all panels. (Berger et al., 2011)

References

Berger, T., Testa, P., Hillier, A., Boerner, P., Low, B.C., Shibata, K., Schrijver, C., Tarbell, T. & Title, A. (2011). *Nature* **472**, 197.

De Pontieu, B., McIntosh, S.W., Carlsson, M., Hansteen, V.H., Tarbell, T.D., Boerner, P., Martinez-Sykora, J., Schrijver, C.J. & Title, A.M. (2011). *Science* **331**, 55.

Harra, L.K., Sterling, A.C., Goemoery, P. & Veronig, A. (2011). *Astrophys. J.* **737**, L4.

Martinez Pillet, V., del Toro Iniesta, J.C. & Quintero Noda, C. (2011). *Astron. Astrophys.* **530**, A111.

Socas-Navarro, H. (2011). *Astron. Astrophys.* **529**, A37.

Tian, H., Tu, C., Marsch, E., He, J. & Kamio, S. (2010). *Astrophys. J.* **709**, L88.

2.13.3 COROT

Introduction

The Convection, Rotation and planetary Transits (COROT) satellite was launched into a polar orbit at an altitude of 900 km on 27 December 2006. It is the first satellite dedicated to exoplanetary research and was specifically designed for this purpose, although its other main scientific purpose is asteroseismology (the detection of microvariability caused by, for example, acoustical p modes in stars). COROT was developed by the French Space Agency (CNES) with ESA, Austria, Belgium, Brazil, Germany and Spain as partners. The development of COROT is described in *The COROT Mission* (ESA, 2006). The COROT collaboration today consists of about 80 Co-Investigators and more than 60 associated scientists in Europe and Brazil.

COROT thus has two main scientific objectives: to detect planets of a size analogous to our own Earth through observing transits, and to study stellar interiors through the detection of acoustical p-modes and activity

The requirement that one needs to look at a large enough sample of stars for the longest possible uninterrupted period of time, set the constraint that COROT can observe only two oppositely located regions (with 10–15° diameter) on the sky at any given time. The maximum observation time of a field is about 155 days. The 2.5-yr nominal mission was extended for a further 3 years (end-of-mission in May 2013).

The detectors are four frame transfer CCDs (2048 × 4096), two of which are dedicated to the exoplanetary research, and the other two to the seismology programme. The readout from one each of these CCDs failed in April 2009 after a single event upset. A prism is mounted in front of the two CCDs involved in the search for exoplanets, providing very short spectra. The mission is supported by a massive ground-based programme, consisting so far of 320 nights of radial velocity observations as well as more than 140 nights of photometric data taking (including using adaptive optics).

Scientific Highlights

COROT has the capability to detect planets in short-period orbits. At the time of writing, the mission has been in operation for 1810 days, and has been obtaining data for more than 90% of this time. COROT has been pointed towards 22 fields of interest, and has acquired more than 155 000 light curves over periods of 20–150 days. During these observations, 3870 separate transiting events have been detected, of which 645 have been considered for ground-based follow-up. Among these, 236 are considered to have been solved in that 26 have been confirmed as planets, while the remaining 210 have been identified as eclipsing binary stars.

The investigation of p-mode variations in several solar type stars is continuing, together with a large number of studies of other variable objects such as the stars β Cephei (Degroote et al., 2010a) and δ Scuti (Poretti et al., 2011) and very large numbers of interesting eclipsing binaries (Maciel et al., 2011). A study of a massive B-type star has identified g-modes (i.e. acoustic waves where the restoring force is buoyancy and penetrating to the very centre of the star) and has measured both the level of hydrogen remaining in the stellar core, as well as the size of the transiting region between radiative and convective zones near the core (Degroote et al., 2010b).

During 2011, 89 refereed papers reporting different aspects of the mission were published.

Further information about the COROT mission can be found at *http://sci.esa.int/corot*

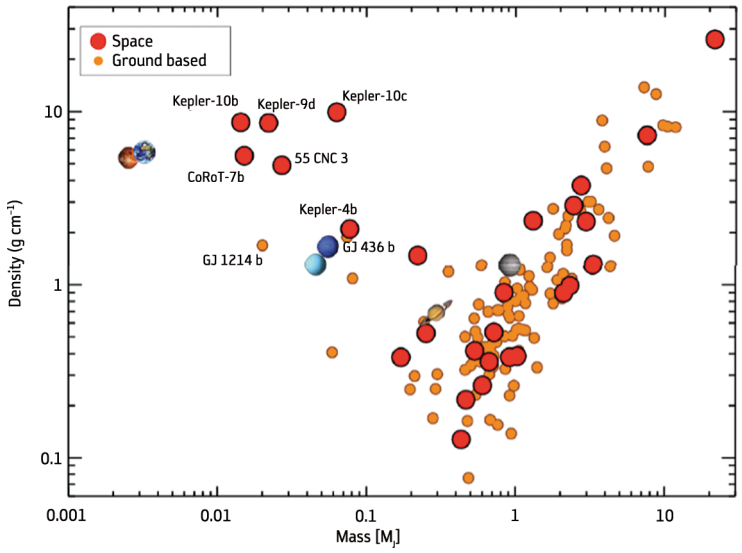

Figure 2.13.3.1. The exoplanets for which precise physical parameters have been determined. Almost all are due to the COROT, MOST (Microvariability and Oscillation of Stars) and Kepler missions. There is a clear range of densities for both gas giants (right upward-sloping arm), and for low-mass planets (left upward-sloping arm). (H. Rauer, DLR, Planetforschungs Institute, Berlin)

COROT is playing an important role in determining the first high-precision physical parameters for exoplanets. Figure 2.13.3.1 shows all known (at the time of writing) exoplanets for which well determined masses and radii exist. The figure clearly demonstrates the diversity in planets of all types. It indicates that there is a difference of two orders of magnitude in the densities of gas giants, while for low-mass planets the observed densities range from approximately 1 g cm^{-3} to 10 g cm^{-3}.

COROT is funded until May 2013. A proposal to extend the mission to 2017–18 has been submitted to the appropriate agencies. During this extension period, it has been suggested that COROT will increasingly focus on low-mass exoplanets.

References

Degroote, P. et al. (2010a). *Astron. Nachrichten* **331**, 1065D.
Degroote, P. et al. (2010b). *Nature* **464**, 259D.
ESA (2006). *The COROT Mission, Pre-Launch Status: Stellar Seismology and Planet Finding*. ESA SP-1306. European Space Agency, Noordwijk, the Netherlands.
Maciel, S.C., Osorio, Y.F.M. & de Mederios, J.R. (2011). *New Astron.* **16**, 68M.
Poretti, E. et al. (2011). *Astron. Astrophys.* **528A**, 97T.

→ MISSIONS IN THE POST-OPERATIONS AND ARCHIVING PHASES

3. Missions in the Post-Operations and Archiving Phases

3.1 Introduction

One of the main legacies of every mission is its archive of scientific data, both raw and processed, and often including links to the relevant refereed papers in the open scientific literature. The archive is usually finalised during the post-operations phase, although it is becoming more common to use the archive also for data distribution (and even processing, as in the case of the Herschel archive; see Fig. 3.1.1) during the active phase of the mission.

ESA is ensuring the long-term preservation of its scientific data holdings through a set of powerful and easy to use online science archives, sharing technologies and resources across multiple missions. Current data holdings at the ESA's European Space Astronomy Centre include the Planetary Science Archive (PSA), which includes data from the Rosetta, Mars Express, Venus Express, Huygens, SMART-1 and Giotto missions, as well as the archives of ExoSat, the Infrared Space Observatory, XMM-Newton, Integral, Herschel,

Figure 3.1.1. Role of the archive in Herschel data processing and distribution.

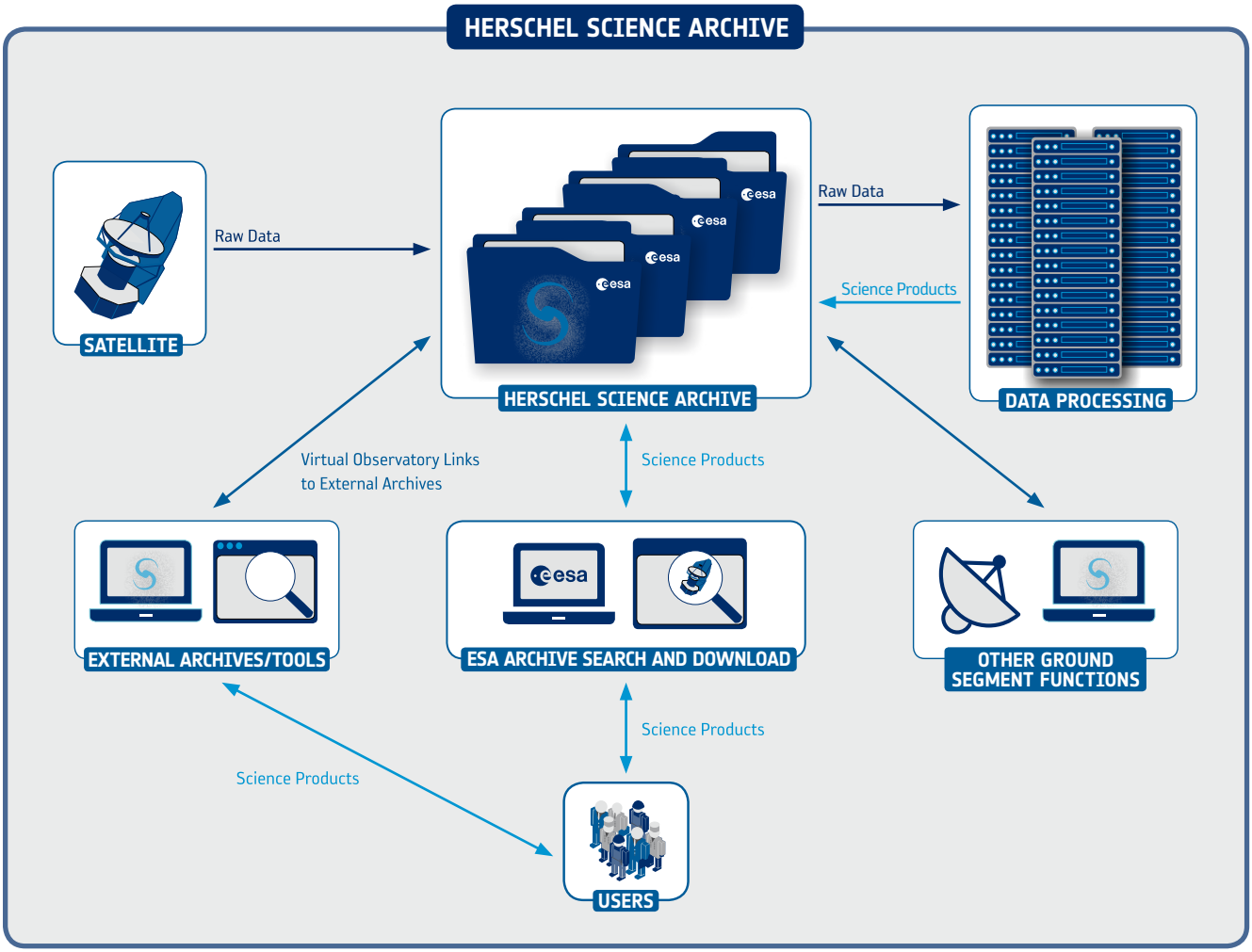

All of these science archives can be accessed at *http://archives.esac.esa.int*

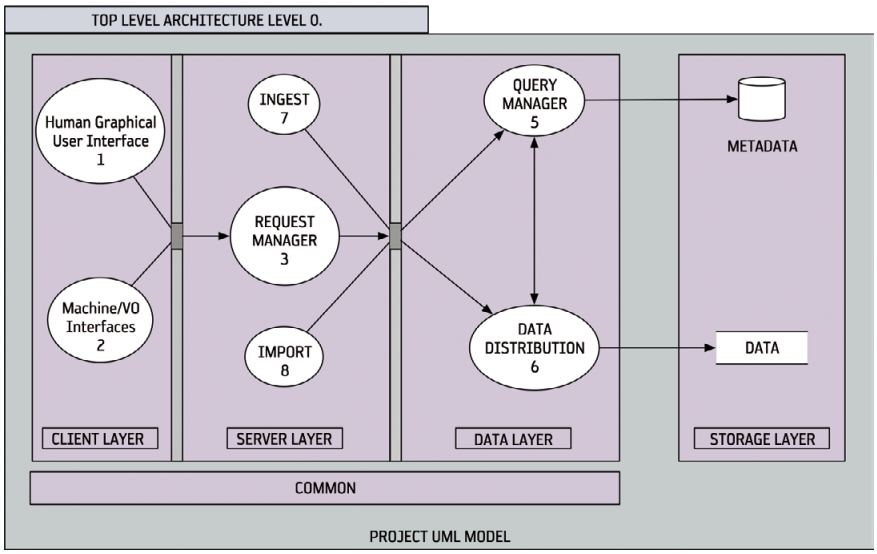

Figure 3.1.2. Architecture of ESA's science archives, shown as a Unified Modeling Language (UML) diagram (VO = virtual observatory).

Planck and SOHO. Archives under development at, or being transferred to ESAC include those of the Hubble Space Telescope, Cluster, Ulysses, Gaia and LISA Pathfinder. Work on the BepiColombo archive will start in the near future.

All the science archives at ESAC share the same technical framework, compatible with the Open Archival Information System (OAIS) standard. Their flexible multitier architecture (Fig. 3.1.2) separates the various archive functions into different modules.

The 'storage layer' consists of online data repositories on hard disks with data volumes ranging from a few dozen GB (for the older missions) to 100 TB (for Herschel, HST and Cluster). Keeping the data on hard disks greatly facilitates the archive operations and the migration process. Metadata are systematically extracted from the data and stored in a relational database, such as Sybase or Oracle, and more recently into open source databases like PostgreSQL.

The 'data layer' represents the software systems (Query Manager and Data Distribution) that access the Storage Layer. This provides independence in the way the data and metadata are stored, enabling the evolution towards new storage and database systems.

The 'server layer' can be seen as the 'engine' of the archive, connecting the front-end layer to the data layers. Together with some common libraries, it ensures proper access to the metadata and data (respecting the relevant project proprietary access period), logging and usage reporting functions, as well as other archive administration functions.

The 'client layer' offers front-end access to the archives. The main access can be a graphical user interface (through a rich internet client or a thin web client or, for some missions, a map-based interface; see Fig. 3.1.3) with powerful and friendly search, visualisation, selection and download facilities.

An additional alternative access is via a web service called the Archive Inter-Operability (AIO) system, which offers a scriptable interface with the archive. Interoperability with other archives can be built on top of the AIO, translating these web services into interoperability standards such as those of the International Virtual Observatory Alliance (IVOA) or International Planetary Data Alliance (IPDA).

Having a common archive technical framework across various archives enables faster and cheaper archive development cycles, more reliable software, as the code is reused, and knowledge transfer from project to project and person to person. Furthermore, corrections to and improvements made in one archive project are automatically carried over to other archive projects as they share the common framework. This also allows more efficient and cheaper long-term operation of the 'older' archives (for which no more project funds

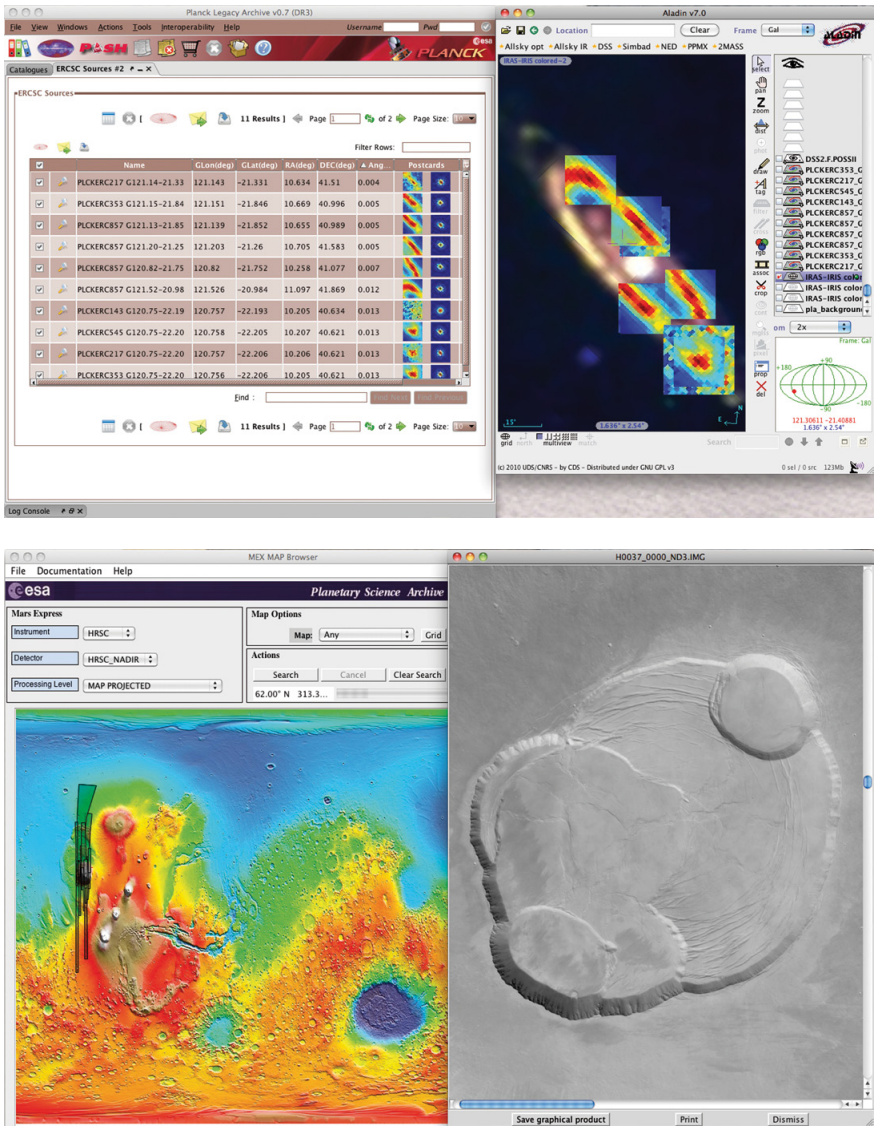

Figure 3.1.3. Examples of user interfaces. *Top:* Planck rich Internet client. *Bottom:* Mars Express map-based interface.

are available), as they are using similar technology and operating concepts to those of the more 'recent' archives.

Once in production, ESAC's science archives work 'autonomously', without the need for archive operators. Through their standard web browser, users can search the archives, visualise items of interest to them, and select them for immediate download (since all data are online on disks). All data are distributed through the internet via the standard FTP protocol.

3.2 Ulysses

Introduction

Launched in October 1990, the joint ESA–NASA Ulysses mission had as its primary objective the exploration of the uncharted high-latitude regions of the heliosphere within 5 AU of the Sun, under a wide range of solar activity conditions. Initially planned for a 5-year mission, satellite operations were finally terminated on 30 June 2009, after 18 years, 8 months and 22 days of almost continuous data acquisition. Ulysses made it possible, for the first time, to make *in situ* measurements far from the plane of the ecliptic and over the poles of the Sun. Its unique trajectory, which included a gravity-assist manoeuvre at Jupiter to incline the orbital plane by 80° with respect to the Sun's equator, literally took the satellite into the unexplored third dimension of the heliosphere.

The European contribution to the Ulysses programme consisted of the provision and operation of the satellite and about half of the experiments. NASA provided the launch aboard the Space Shuttle *Discovery* (together with the upper stage) and the satellite power generator, and was responsible for the remaining experiments. NASA also supported the mission using its Deep Space Network.

The broad range of phenomena that were studied by Ulysses included the solar wind, the heliospheric magnetic field, solar radio bursts and plasma waves, solar and interplanetary energetic particles, galactic cosmic rays, interstellar neutral gas, cosmic dust and gamma-ray bursts.

While the main focus of the mission was clearly the heliosphere and its variations in time and space, the investigations covered a wider range of scientific interests. Examples include studies related to Jupiter's magnetosphere (both *in situ* and via remote sensing), and radio-science investigations into the structure of the corona and a search for gravitational waves using the satellite and ground telecommunication systems. A major theme for Ulysses is the nature of the local Interstellar Medium and its interface with the heliosphere, and the mission has provided important contributions to our knowledge in this area, as well as to topics of a broad astrophysical nature.

During the operational phase of the mission, 1475 refereed papers using Ulysses data and four books summarising the scientific results were published, and more than 100 refereed papers have appeared since the termination of satellite operations.

Ulysses Data Archive

Data from the Ulysses investigations and flight project are currently archived and made accessible to the public through two channels: the ESA Ulysses Active Archive (UAA) at ESTEC, and NASA's National Space Science Data Center (NSSDC). Since there is no formal proprietary period for Ulysses data, the datasets are placed in these public archives immediately following verification by the PI teams. The ESA UAA archive provides a number of online facilities for browsing and downloading selected measurements made by the scientific instruments, including a web-based plotting interface that allows the user flexibility in defining start and end times and provides the capability to combine parameters from different experiments on the same plot. Definition and implementation of the Ulysses Final Archive at ESAC began in mid-2011 as a joint activity involving the UAA team and the ESAC Science Archive Team. As of mid-2012, significant progress had been made and it is envisaged that the Ulysses Final Archive will be fully operational by March 2013 at the latest.

Further information about the Ulysses mission can be found at *http://sci.esa.int/ulysses*

3.3 Chandrayaan-1

Introduction

Chandrayaan-1 was India's first mission to the Moon. It was launched on 22 October 2008 by the Indian Space Research Organisation (ISRO). It reached lunar orbit on 8 November 2008 and started its official science operations phase in January 2009. It was initially foreseen to operate the mission for two years. However, on 29 August 2009, ISRO lost communications with the satellite, most likely due to a failure of a power converter. Nevertheless, a large percentage of the science goals were achieved.

Europe contributed three instruments to the mission: the Chandrayaan-1 X-ray Spectrometer (C1XS; PI: M. Grande, UK), combined with the X-ray Solar Monitor (XSM; PI: J. Huevelin, Finland), the Sub-keV Reflecting Analyser (SARA; PI: S. Barabash, Sweden) and the SMART Infrared Spectrometer (SIR-2; PI: U. Mall, Germany). All instruments functioned well during the lifetime of the satellite. ESA supported the development, operations and data processing for all instruments, and assisted ISRO in the definition of the scientific data archive.

Scientific Highlights

Chandrayaan-1 was only 100 km away from the Moon for the first few months of its mission. It obtained very high-resolution data with its remote sensing instrumentation and was able, for example, to resolve the Apollo 15 lander on the lunar surface.

One of the highlights of the Chandrayaan-1 mission was that it contributed significantly to the understanding of the behaviour of hydrogen on the Moon. Measurements from Apollo 17 showed a much smaller abundance of hydrogen in the lunar exosphere than expected. For a long time these measurements were not understood; it was assumed that the solar wind ions impinging on the lunar surface are almost completely absorbed (see Wieser et al., 2009, and references therein). The SARA instrument was able to measure the flux of neutral hydrogen emerging from the lunar surface. The spectra observed by Wieser et al. (2009) can be explained by a solar wind–regolith interaction model developed by Hodges (2011). The main result is that the interaction of the solar wind creates a large fraction of neutral hydrogen atoms that are so fast that they quickly leave the Moon's gravitational influence. This explains both the low *in situ* abundance seen by Apollo 17 and the measurements made by SARA.

Status

ISRO is planning to produce a long-term archive using the standards of the US Planetary Data System and the European Planetary Science Archives. For the European instruments the data have been produced by the PI teams with the support of ESA personnel. ISRO is finalising the preparations for a process of peer-reviewing the data in order to finalise the long-term archive.

Further information about the Chandrayaan-1 mission can be found at *www.esa.int/esaSC/SEM5DO4N0MF_index_0_m.html* and *www.isro.org/chandrayaan*

References

Hodges, R.R. (2011). *Geophys. Res. Lett*. **38**, L06201.

Wieser, M., Barabash, S., Futaana, Y., Holmström, M., Bhardwaj, A.R. Sridharan, Dhanya, M.B., Wurz, P., Schaufelberger, A. & Asamura, K. (2009). *Planet. Space Sci*. **57**, 2131–2134.

3.4 Akari

Akari, previously called Astro-F, was developed by the Institute of Space and Astronautical Science (ISAS/JAXA) as the second Japanese space mission for IR astronomy. Its main objectives were to perform an all-sky survey (in six infrared bands) with better spatial resolution and wider wavelength coverage than IRAS and to complement this survey with pointed observations of objects of interest. Akari had a 68.5 cm-diameter telescope cooled to 6K to observe in the wavelength range 2–180 μm from a Sun-synchronous polar orbit at 700 km altitude. The payload consisted of two instruments, the Far-Infrared Surveyor (FIS) and the Infrared Camera (IRC). Further details of Akari's technical characteristics are presented in Table 3.4.1.

Akari was launched on an M-V rocket on 21 February 2006. More than 94% of the sky was covered twice before its cryogen supply ran out on 26 August 2007 – an in-orbit lifetime of 550 days as was expected. Akari also performed more than 5000 pointed observations in 13 bands over the wavelength range 2–180 μm, including dedicated mid-infrared surveys of the Large Magellanic Cloud and the north ecliptic pole. Akari also provided comprehensive multi-wavelength photometric and spectroscopic coverage of a wide variety of astronomical sources, including nearby Solar System objects, zodiacal light, brown dwarfs, young stars and debris discs, as well as evolved stars in our own Galaxy and in other galaxies of the Local Group.

Following the end of the cryogenic phase, Akari continued to observe in the near-infrared (1.8–5.5 μm) until May 2010, at which time scientific observations ceased. In late 2011, Akari was manoeuvred into a disposal orbit, from which it is expected to reenter Earth's atmosphere within 25 years.

The All-Sky Point Source Catalogues, released into the public domain on 30 March 2010 (*www.ir.isas.jaxa.jp/akari/observation/psc/public*), have been included in the Herschel Observation Planning Tool (HSPOT). A variety of additional catalogues (e.g. for the North Ecliptic Pole, for asteroids) have been published. The all-sky diffuse maps will enter the public domain by mid-2012. Akari's science results have been reported in over 170 refereed papers, including in a special issue of the journal *Astronomy & Astrophysics* (volume 514).

ESA collaborated with JAXA/ISAS in order to increase the scientific output of the mission by capturing all of the possible data with a second ground station in the cold phase, and to accelerate the production of the sky catalogues. In return, 10% of the observing opportunities in the non-survey phases of the mission were distributed to European astronomers. Tracking support was provided in the cold phase via ESOC and the Kiruna ground station in Sweden. ESAC provided expertise and support for the sky-survey data processing through the pointing reconstruction. The software, developed inhouse, correlated the Akari mid-infrared detections with existing catalogues, providing the required position accuracy of a few arcsec. ESAC also provided user support for European astronomers who were granted observing opportunities.

Further information about the Akari mission can be found at *www.rssd.esa.int/akari*

Table 3.4.1. The Akari mission.

Technical characteristics	
Satellite	Size: 3.3 × 2.0 m (3.3 × 5.5 m in orbit, with solar paddle open). Mass: 952 kg at launch.
Launch	21 February 2006 by a JAXA M-V8 rocket from Uchinoura Space Centre, Japan.
Orbit	Sun-synchronous polar, 100 min duration, 700 km altitude, 98.2° inclination.
Mission phases	Phase-1 (survey): from 8 May 2006. Phase-2 (pointed observations): from 10 November 2006 to 26 August 2007 (end of cryogen). Phase-3 (warm phase): completed in May 2010.
Science goals	IR astronomy (using imaging, photometry and spectroscopy), from comets to cosmology.
Operations	Institute of Space and Astronautical Science/JAXA.
Distribution of observing time for pointed observations	65% guaranteed time, 30% open time (20% Japanese–Korean, 10% European, via parallel AOs), 5% discretionary time.
Data transmission	S-band (uplink), S- and X- band (downlink). Ground stations: Uchinoura Space Centre (Japan), Kiruna (Sweden) and Svalbard (Norway). Data rate: 4 Mbit/s for scientific data.
Mission lifetime	550 days for the cold phase and ~32 months for the warm phase.
Cryogenics	Liquid-helium cryostat with Stirling-cycle coolers; 179 litres of superfluid liquid helium.
Instruments	
Far-Infrared Surveyor (FIS)	All-sky survey, imaging and spectroscopy with FTS bands: N60 (65 μm), Wide-S (90 μm), Wide-L (140 μm), N160 (160 μm). Detectors: 20 × 2 and 20 × 3 Ge:Ga arrays for N60 and Wide-S bands; 15 × 3 and 15 × 2 stressed Ge:Ga arrays for Wide-L, N160 bands. Pixel pitch: 29.5 arcsec for N60 and Wide-S bands; 49.1 arcsec for Wide-L and N160 bands. Resolution for spectroscopy: 0.19 cm^{-1}.
Infrared Camera (IRC)	All-sky survey, imaging and spectroscopy with grisms and a prism. Photometric bands: 9 bands in the wavelength range 2–26 μm. Detectors: one InSb 512 × 412 array for NIR; two 256 × 256 Si:As arrays for MIR-S and MIR-L. Pixel scale: 1.46 × 1.46 arcsec for NIR; 2.34 × 2.34 arcsec for MIR-S and 2.51 × 2.39 arcsec for MIR-L. Effective pixel scale in the all-sky survey: 10 arcsec (4 pixels are binned). Resolution for spectroscopy: 0.0097–0.17 μm.

→ PROJECTS UNDER DEVELOPMENT

4. Projects under Development

4.1 LISA Pathfinder

Introduction

LISA Pathfinder (formerly known as SMART-2, the second of ESA's Small Missions for Advanced Research in Technology), is a dedicated technology validation mission for future spaceborne gravitational wave detectors such as the New Gravitational wave Observatory (NGO).[1]

The technologies required for NGO are many and extremely challenging. Because of this, coupled with the fact that some flight hardware cannot be tested in a 1-*g* environment, the LISA Pathfinder (LPF) mission is being implemented to test the critical NGO technologies in space. The major scientific objective of the mission is to perform the first inflight test of low-frequency gravitational-wave detection metrology.

LISA Pathfinder mimics one arm of the NGO constellation by shrinking the 1 million km armlength down to a few tens of centimetres. The experimental concept is to measure the relative separation between two test masses nominally following their own geodesics, and thereby to determine the relative residual acceleration between them near 1 mHz, about a decade above the lowest frequency required by NGO.

To implement such a concept, disturbances on the test masses are kept very small through several design features, but chiefly by 'drag-free' flight. A drag-free spacecraft is one that follows a free-falling test mass (which it encloses), but has no mechanical connection to it. The spacecraft senses its orientation and separation with respect to the test mass, and its propulsion system is commanded to keep it about the test mass. Thus, the spacecraft shields the test mass from most external influences, and minimises the effects of force gradients arising from the spacecraft, and acting on the test mass. LISA Pathfinder will compare the geodesic of one test mass against that of the other.

LISA Pathfinder will carry two payloads: the LISA Technology Package (LTP), provided by a consortium of European national space agencies (France, Germany, Italy, Spain, Switzerland, the Netherlands and the United Kingdom) and ESA; and the Disturbance Reduction System (DRS), provided by NASA, and part of NASA's New Millennium Program.

Mission Goals

The concept that a particle falling under the influence of gravity alone should follow a geodesic in spacetime is one of the foundations of General Relativity. LISA Pathfinder will test this postulate to a precision two orders of magnitude better than any past, present or planned mission, with the exception of NGO itself. This will be achieved by tracking, using picometre-resolution laser interferometry, two test masses nominally in freefall, and by showing that their relative parasitic acceleration, at frequencies around 1 mHz, is at least two orders of magnitude smaller than anything demonstrated so far. As an

[1] When approved by the Science Programme Committee, LISA Pathfinder was a dedicated technology validation mission for the Laser Interferometer Space Antenna (LISA) mission. In the meantime, LISA has been descoped and renamed the New Gravitational wave Observatory. This new name is used throughout this section.

Further information about LISA Pathfinder mission can be found at *http://sci.esa.int/lisapathfinder*

inertial platform free of spurious accelerations, LISA Pathfinder will be the best laboratory ever created for fundamental physics experiments.

The LISA Pathfinder mission will test both General Relativity and precision metrology, pushing these disciplines several orders of magnitude beyond their current state. In doing so it will open up new ground for an entire class of missions in General Relativity, in fundamental physics at large, and in Earth observation. The high-resolution optical readout of test mass motion will allow test mass to test mass tracking even when they are located on different spacecraft, at large distances and in interplanetary space, e.g. NGO, or at short distances in low-Earth orbit, such as on future geodesy missions.

However, the objective of LISA Pathfinder is not to develop hardware, but to confirm the overall physical model of the forces that act on a test mass in interplanetary space. To fulfil this programme, the mission will not just measure acceleration, but will implement a full menu of measurements. At the end of this set of measurements, the residual acceleration noise model will be verified in painstaking detail.

The performance goals of LISA Pathfinder can be summarised as follows:

- to demonstrate that a test mass can be put in pure gravitational freefall within one order of magnitude of the requirement for NGO. The one order of magnitude rule also applies to frequency. Thus the flight test will be considered satisfactory if the freefall of one test mass is demonstrated to within 3×10^{-14} m s^{-2} Hz$^{-1/2}$ at 1 mHz, rising as f^2 between 3 mHz and 30 mHz;
- to demonstrate laser interferometry with a free-falling mirror (LTP test mass) with displacement sensitivity meeting the NGO requirements over the LTP measurement bandwidth. Thus the flight test of LTP will be considered satisfactory if the laser metrology resolution is demonstrated to within 9×10^{-12} m Hz$^{-1/2}$ between 3 mHz and 30 mHz, rising as $1/f^2$ down to 1 mHz; and
- to assess the lifetime and reliability of the µN thrusters, lasers and optics in a space environment.

LISA Technology Package

Unlike traditional observatory or planetary missions, the LISA Pathfinder payload cannot be regarded as a discrete piece of hardware carried by the spacecraft. Rather, during science operations, the payload and the spacecraft will act as a single unit: the attitude control of the spacecraft is driven by the payload.

The key elements of the LTP are two nominally free-flying (gold:platinum) test masses and a laser interferometer to read the distance between them (Fig. 4.1.1).

The two test masses are surrounded by position-sensing electrodes. These provide the position and rotation information to a drag-free control loop that, via a series of µN thrusters, keeps the spacecraft centred with respect to some fiducial point.

In NGO, the proper distance between the two free-falling test masses at the end of the interferometer arms would be measured via a three-step process: by measuring the distance between one test mass and the optical bench (known as the local measurement), by measuring the distance between optical benches (separated by 1 million km), and finally by measuring the distance between the other test mass and its optical bench. In LPF, the optical metrology system essentially makes two measurements: the separation of the test masses, and the position of one test mass with respect to the optical bench. The latter is identical to the NGO local measurement interferometer, thereby providing a flight validation of precision laser metrology directly applicable to NGO.

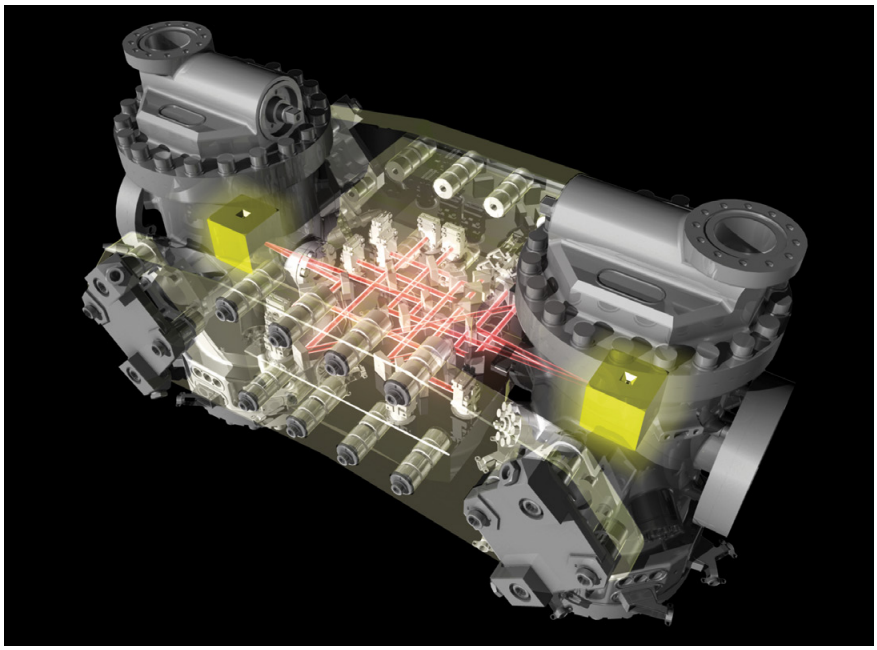

Figure 4.1.1. The LISA Technology Package core assembly, the heart of the LISA Pathfinder mission.

In both NGO and LPF, charging by cosmic rays is a major source of disturbance. Each test mass therefore carries a non-contacting charge measurement and neutralisation system based on UV photoelectron extraction. A flight test of this device is a key element of the overall LPF test.

All electronic units of the LISA Technology Package have been delivered to the LPF prime contractor and are now being integrated to the spacecraft. The LTP core assembly (Fig. 4.1.1) is scheduled to be delivered in September 2013.

Disturbance Reduction System (DRS)

The DRS, provided by NASA, consists of the μN colloidal thrusters, a Drag-Free and Attitude Control System (DFACS) and an onboard computer. The DRS will use the LTP inertial sensors as its drag-free sensors.

The primary goal of the DRS is to maintain the position of the spacecraft with respect to the proof mass to within 10 nm $Hz^{-1/2}$ over the frequency range 1–30 mHz.

Launch and Orbit

LISA Pathfinder is scheduled to be launched in mid-2014 on the new European small launcher, Vega. The spacecraft and expendable propulsion module will be injected into a low-Earth orbit (200×1600 km), from which, after a series of apogee raising manoeuvres, they will enter a transfer orbit towards the first Sun–Earth Lagrangian point (L1). After separation from the propulsion module, the LPF spacecraft will be stabilised using its μN thrusters, entering a Lissajous orbit around L1 (500 000×800 000 km orbit).

Following the initial in-orbit checkout and instrument calibration, the inflight demonstration of the NGO technology will take place. The nominal lifetime of the science operations is 180 days; this includes both the LISA Technology Package and the DRS operations.

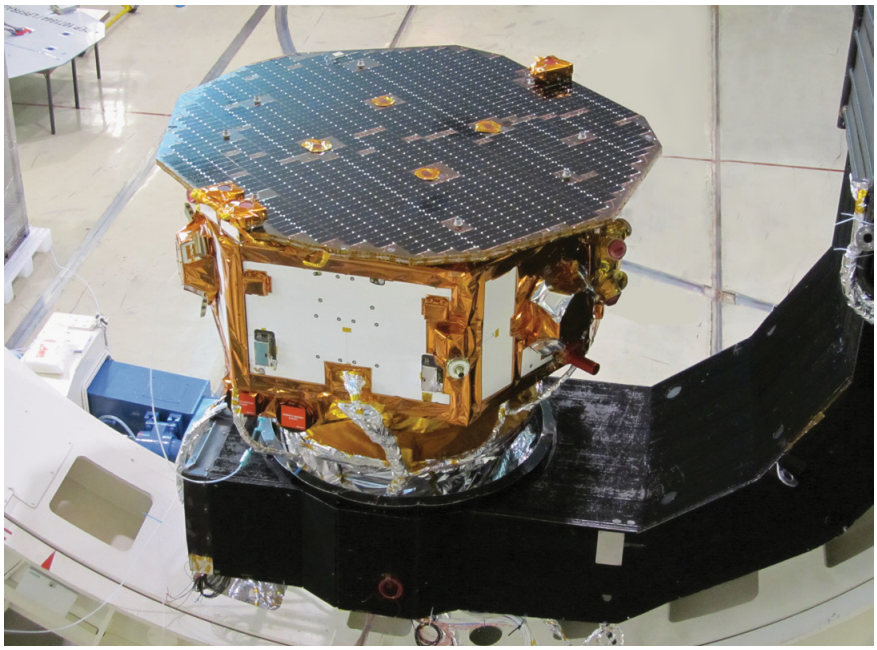

Figure 4.1.2. The LISA Pathfinder spacecraft being prepared for the On-Station Thermal Test at IABG, Germany.

Status

The LISA Pathfinder spacecraft has now completed the full suite of environmental test campaigns, culminating in the On-Station Thermal Test (OSTT) carried out at IABG, Germany (Fig. 4.1.2).

The OSTT examined both the functional and performance aspects of the flight system at the extremes of the operational temperature range. The performance tests focused on the Optical Metrology and the Diagnostics Systems, both made possible by the use of the Thermal Optical Qualification Model (TOQM) as a replacement for the LTP Core Assembly (LCA). The performance measured during the tests demonstrate that these systems not only meet, but exceed the requirements in all areas; for example,

- interferometric sensing of the test mass tilt and yaw angles shows a noise floor approximately two orders of magnitude lower than the requirements (~60 µarcsec $Hz^{-1/2}$ over 100 s);
- displacement sensing noise at a level of 3 pm $Hz^{-1/2}$ over 100 s; and
- the thermal stability of the optical bench was demonstrated to be lower than 100µK $Hz^{-1/2}$ over the measurement band.

These measurements exceed not only the LPF requirements, but also the more stringent NGO requirements.

With the completion of the environmental and integrated system test campaigns, the spacecraft and propulsion module will be put into storage awaiting the delivery of the LCA. Following delivery, the LCA will be integrated into the spacecraft, and a series of workmanship test campaigns (acoustic test, separation shock test, mass balancing) will take place, culminating in the Flight Acceptance Review in late 2014.

The mission and science ground segments are also proceeding as planned, and were successfully reviewed in 2011 as part of the Ground Segment Implementation Review.

4.2 Gaia

Introduction

After a detailed concept and technology study during 1998–2000, Gaia was selected as a confirmed mission within ESA's scientific programme in October 2000. It was confirmed by ESA's Science Programme Committee following a re-evaluation of the science programme in June 2002, and reconfirmed following another re-evaluation of the programme in November 2003. The project entered Phase-B2/C/D in February 2006. Gaia is currently in Phase-D (Qualification and Production) and will be launched in the second half of 2013.

Scientific Goals

Gaia will rely on the proven principles of ESA's Hipparcos mission to solve one of the most difficult yet deeply fundamental challenges in modern astronomy: to create an extraordinarily precise 3D map of about a billion stars throughout our Galaxy and beyond (see Table 4.2.1). In the process, Gaia will map their motions, which encode the origin and subsequent evolution of the Galaxy.

Through comprehensive photometric classification, Gaia will provide the detailed physical properties of each star observed, characterising their luminosity, temperature, gravity and elemental composition. This massive stellar census will provide the basic observational data needed to tackle an enormous range of important problems related to the origin, structure and evolutionary history of our Galaxy – a kind of 'Human Genome Project' for astronomy.

Gaia will achieve this by repeatedly measuring the positions of all objects down to $V = 20$ mag. Onboard object detection will ensure that variable stars, supernovae, burst sources, microlensing events and minor planets will all be detected and catalogued to this faint limit. Final accuracies of 12–25 μarcsec at 15 mag will provide distances accurate to 10% as far as the Galactic Centre, 30 000 light-years away. Stellar motions will be measured even in the Andromeda Galaxy.

	Hipparcos	Gaia
Magnitude limit	12	20
Completeness	7.3–9.0	20
Bright limit	0	6
Number of objects	120 000	26 million to $V = 15$ 250 million to $V = 18$ 1000 million to $V = 20$
Effective distance limit	1 kpc	1 Mpc
Quasars	None	500 000
Galaxies	None	10^6–10^7
Accuracy	1 milliarcsec	7 μarcsec at $V = 10$ 12–25 μarcsec at $V = 15$ 100–300 μarcsec at $V = 20$
Photometry	2-colour	Low-resolution spectra to $V = 20$
Radial velocity	None	15 km s^{-1} to $V = 16$–17
Observing programme	Preselected	Complete and unbiased

Table 4.2.1. Capabilities of Hipparcos and Gaia.

Further information about the Gaia mission can be found at *http://sci.esa.int/gaia*

Gaia's expected scientific harvest is enormous. Its main goal is to clarify the origin and history of our Galaxy, by providing tests of the various formation theories, and of star formation and evolution. This is possible because low-mass stars live for much longer than the present age of the Universe, and therefore retain in their atmospheres a detailed fossil record of their origin. The Gaia results will identify precisely the relics of tidally disrupted accretion debris, probe the distribution of dark matter, establish the luminosity function for pre-Main Sequence stars, detect and categorise rapid evolutionary stellar phases, place unprecedented constraints on the age, internal structure and evolution of all stellar types, establish a rigorous distance-scale framework throughout the Galaxy and beyond, and classify star formation and kinematical and dynamical behaviour within the Local Group of galaxies.

Gaia will pinpoint exotic objects in colossal and huge numbers: many thousands of extrasolar planets will be discovered, and their detailed orbits and masses determined; tens of thousands of brown dwarfs and white dwarfs will be identified; some 100 000 extragalactic supernovae will be discovered and details passed to ground-based observers for follow-up observations. Solar System studies will receive a massive impetus through the detection and orbit determination of many tens of thousands of minor planets. Inner Trojans and even new trans-neptunian objects, including plutinos, may be discovered.

Gaia will follow the bending of starlight by the Sun and major planets, over the entire celestial sphere, and therefore directly observe the structure of spacetime (the accuracy of its measurement of General Relativistic light bending may reveal the long-sought scalar correction to its tensor form). The parameterised post-Newtonian (PPN) parameters γ and β will be determined with unprecedented precision.

The Spacecraft

Gaia will carry the demonstrated Hipparcos principles to orders of magnitude improvements in terms of accuracy, number of objects and limiting magnitude, by combining them with state-of-the-art technology. It will be a continuously scanning spacecraft, accurately measuring 1D coordinates along great circles, and in two simultaneous fields of view, separated by a well-defined and well-known angle. These 1D coordinates will then be converted into the astrometric parameters in a global data analysis, in which distances and proper motions 'fall out' of the processing, as does information on double and multiple systems, photometry, variability, metric, planetary systems, etc. The Gaia payload is based on a large CCD focal plane assembly, with passive thermal control, and natural short-term instrument stability arising from the sunshield, selected orbit and robust payload design (Fig. 4.2.1).

The telescopes are moderate in size (1.45×0.5 m), manufactured from silicon carbide, with no specific design or manufacturing complexity. The system fits within a Soyuz–Fregat launch configuration, without deployment of any payload elements (moving from an Ariane to a Soyuz launch was one of the results of the 2002 redesign effort). A Lissajous orbit at L2 is the adopted operational orbit, from where about 1 Mbit/s of data will be returned to ground station throughout the five-year mission. The final astrometric accuracies will be evaluated through a comprehensive accuracy assessment programme; μarcsec accuracies will be possible partly by virtue of the unusual instrumental self-calibration achieved through the data analysis on the ground. This will ensure that final accuracies essentially reflect the photon noise limit for localisation accuracy, exactly as achieved with Hipparcos.

The Preliminary and Critical Design Reviews were completed in June 2007 and October 2010, respectively. At this phase of the project, as the hardware for the satellite is being built and qualified, many milestones are being achieved. Among them, it is possible to select three main achievements. All the mirrors

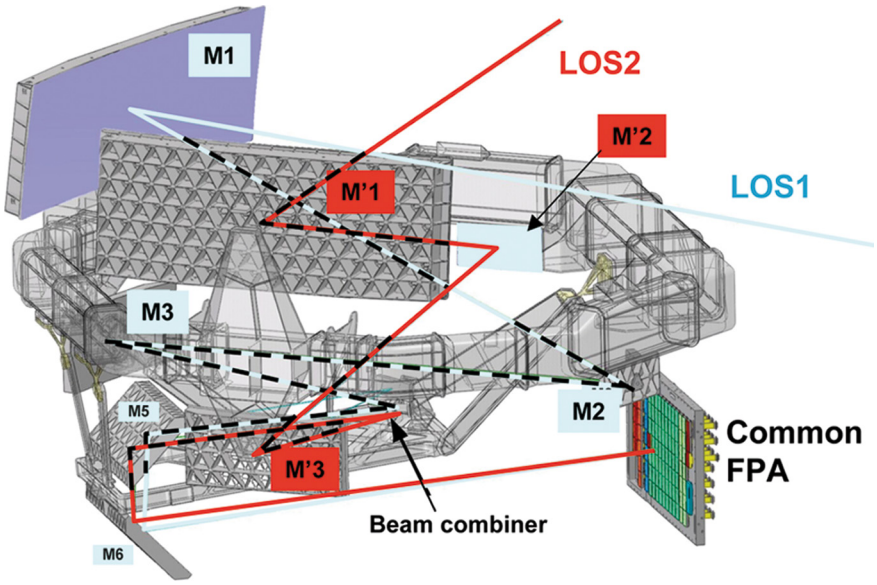

Figure 4.2.1. The mirrors (M1–M6) of the two telescopes providing the two lines of sight (LOS) in a combined Focal Plane Assembly form the core of the Gaia Payload Module.

Figure 4.2.2. The complete set of 106 CCDs that make up Gaia's focal plane. The CCDs are bolted to the CCD Support Structure (the grey plate beneath the CCDs), which weighs about 20 kg and is made of silicon carbide (SiC), a material that provides remarkable thermal and mechanical stability. The focal plane measures 1 × 0.5 m. (EADS Astrium)

for the two telescopes have been manufactured and integrated into the payload module. All CCDs and corresponding electronics have been integrated and aligned in the focal plane assembly. The impact of radiation effects on the data quality has been quantified based on laboratory test data revealing that the current estimated calibration errors are not at the level where they might endanger Gaia's scientific output. The 106 CCDs, yielding a total of almost one billion pixels, will form the largest focal plane in space (see Fig. 4.2.2).

Scientific Organisation and Progress

The participation of the wider European astronomy community in addressing the challenge of Gaia data processing has been formalised through the Gaia Data Processing and Analysis Consortium (DPAC), which was selected in 2007 following a call for proposals. DPAC is divided into nine coordination units (CUs; see Table 4.2.2) responsible for software development, and six data processing centres responsible for running the software, and thus cover the needs of the scientific ground segment data processing. The overall management of the consortium is entrusted to the DPAC Executive Committee (DPACE).

Table 4.2.2. Gaia DPAC coordination units (CUs).

Unit	Responsibilities
CU1 (System Architecture)	Addressing many issues common across DPAC and responsible for the overall architecture.
CU2 (Data Simulations)	Already operational, parallel to development, as simulated Gaia data are needed across DPAC for testing the data processing software.
CU3 (Core Processing)	Handling raw data and first look, in addition to the core task of providing the software for astrometric processing.
CU4 (Object Processing)	Dealing with more complicated sources, in particular binaries and Solar System targets.
CU5 (Photometric Processing)	Handling photometric data from the low-resolution spectrometer.
CU6 (Spectroscopic Processing)	Handling data from the radial velocity spectrometer.
CU7 (Variability Processing)	Developing software for variability analysis.
CU8 (Astrophysical Parameters)	Providing fundamental physical quantities to objects in the final Gaia Catalogue.
CU9 (Catalogue Access)	To be initiated in 2012.

DPAC passed the System Requirements Review in 2007 to ensure that the ongoing developments were based on a correct and complete set of requirements, and the Critical Design Review (CDR) in 2009 to ensure that the right design has been chosen for implementation, and also included ESA's Science Operations Centre. ESA Mission Operations Centre passed a separate CDR in 2009, thus completing the cycle of reviews of the Gaia ground segment elements. The mission-level CDR, which was successfully completed in April 2011, considered all the elements of Gaia to ensure that the space and ground segments function effectively together to fulfil the mission goals.

Once the spacecraft passed its preliminary design review and the DPAC was selected, the project entered a new phase. This phase included the selection of a new Gaia Science Team (GST) of seven scientists from the community and two ex officio members, the DPACE Chair and the ESA Project Scientist, who also chairs the GST. The GST began work in October 2007 and will continue to advise ESA on all scientific aspects of the Gaia mission.

4.3 James Webb Space Telescope

Introduction

NASA, ESA and the Canadian Space Agency have collaborated on the definition of a successor to the Hubble Space Telescope since 1996. Known initially as the Next Generation Space Telescope (NGST), this project for another 'great observatory' mission was renamed the James Webb Space Telescope (JWST) in 2002, in honour of NASA's second administrator, who led the agency during the Apollo programme.

The JWST observatory consists of a passively cooled, 6.55 m telescope, optimised for diffraction-limited performance in the near-IR (1–5 μm) region, but with extensions on either side into the visible (0.6–1 μm) and mid-IR (5–28 μm) regions. This combination of large aperture and IR coverage is first and foremost driven scientifically by the desire to follow the contents of the faint extragalactic Universe back in time and redshift to the epoch of 'First Light' and the ignition of the very first stars. Nonetheless, like its predecessor the HST, JWST will be a powerful general-purpose observatory and will carry a suite of instruments capable of addressing a very broad spectrum of outstanding problems in all fields of astronomy. In contrast with Hubble, however, JWST will be placed into a Sun–Earth L2 halo orbit 1.5 million km from Earth and will therefore not be serviceable after launch.

Scientific Themes

The scientific goals of the JWST mission can be grouped into four broad themes:

— First Light after the Big Bang;
— the assembly of galaxies;
— the birth of stars and protoplanetary systems; and
— planetary systems and the origins of life.

The first two themes are extragalactic and are concerned with exploring the formation of stars and galaxies in the remote Universe at the earliest times. These themes are nonetheless intimately linked to the latter two, mainly galactic, themes, which aim to improve understanding of the process of star and planet formation in our own Galaxy.

Observatory and Instruments

The JWST project has been facing severe schedule and cost difficulties in recent years, but is now well into its construction phase. Launch is presently scheduled for 2018 on a European Ariane 5. The JWST observatory will carry four main instruments:

— Near-IR Camera (NIRCam): a wide-field (2.2×4.4 arcmin) camera with coronagraphy and slitless-spectroscopy capabilities covering the wavelength range 0.6–5 μm;

— Near-IR Spectrometer (NIRSpec): a wide-field (3.41×3.56 arcmin) multi-object spectrometer covering the wavelength range 0.6–5.0 μm at spectral resolutions of $R \approx 100$, $R \approx 1000$ and $R \approx 2700$;

Further information about the James Webb Space Telescope can be found at *http://sci.esa.int/jwst*

Figure 4.3.1. The folded JWST observatory inside the fairing of the Ariane 5 ECA launcher.

— Mid-IR Instrument (MIRI): a combined camera (1.23×1.89 arcmin), spectrograph ($R \approx 100$ and $R \approx 3000$) and coronagraph covering the wavelength range 5–28.5 μm; and

— Fine Guidance Sensor/Near-Infrared Imager and Slitless Spectrograph (FGS/NIRISS): the observatory's Fine Guidance Camera that includes near-IR imaging and slitless spectrography capabilities.

The 6.55 m-diameter primary mirror of the JWST telescope is made up of 18 individual hexagonal segments that have already been manufactured and exhibit very good optical performance. The mirrors will be equipped with actuators that will allow their shape to be controlled once in orbit. The telescope and its associated near-infrared instruments will be passively cooled in bulk down to 35–40K by placing the observatory at L2 and keeping the telescope and its instrumentation in perpetual shadow behind a large, deployable sunshade.

In order to ensure optimal performance and to reduce parasitic thermal background emissions, the Mid-Infrared Instrument (MIRI) and its detectors will need to be cooled down to much lower temperatures. This will be achieved by means of a mechanical cryocooler. In order to fit into the fairing of the Ariane 5 launcher, the 6.55 m primary mirror will need to be folded (see Fig. 4.3.1) and deployed along with the sunshade in orbit.

ESA's Contributions

ESA's Science Programme Committee approved the key elements of Europe's contributions to JWST in February 2003. The level of participation closely follows that of the HST model, and consists of three components: scientific instrumentation, non-instrument flight hardware and contributions to operations.

ESA is providing the NIRSpec instrument (see Fig. 4.3.2) and, through special contributions from its member states, the optics module of the MIRI instrument. MIRI was delivered to NASA in May 2012 and NIRSpec will be delivered in early 2013. ESA will also provide the Ariane 5 ECA launcher that will place the observatory in orbit around the Earth–Sun Lagrangian point, L2.

Responsibility for the scientific operation of JWST lies with the Space Telescope Science Institute (STScI) in Baltimore, USA, working under contract to NASA. A number of ESA staff will be posted at STScI in support of the European payload components. The JWST observing programme will be determined by the astronomy community on the basis of periodic competitive peer reviews organised by the STScI. The overriding motivation for ESA's partnership in the mission is to secure full access for member-state scientists to compete for time on JWST on an equal footing with their US and Canadian counterparts.

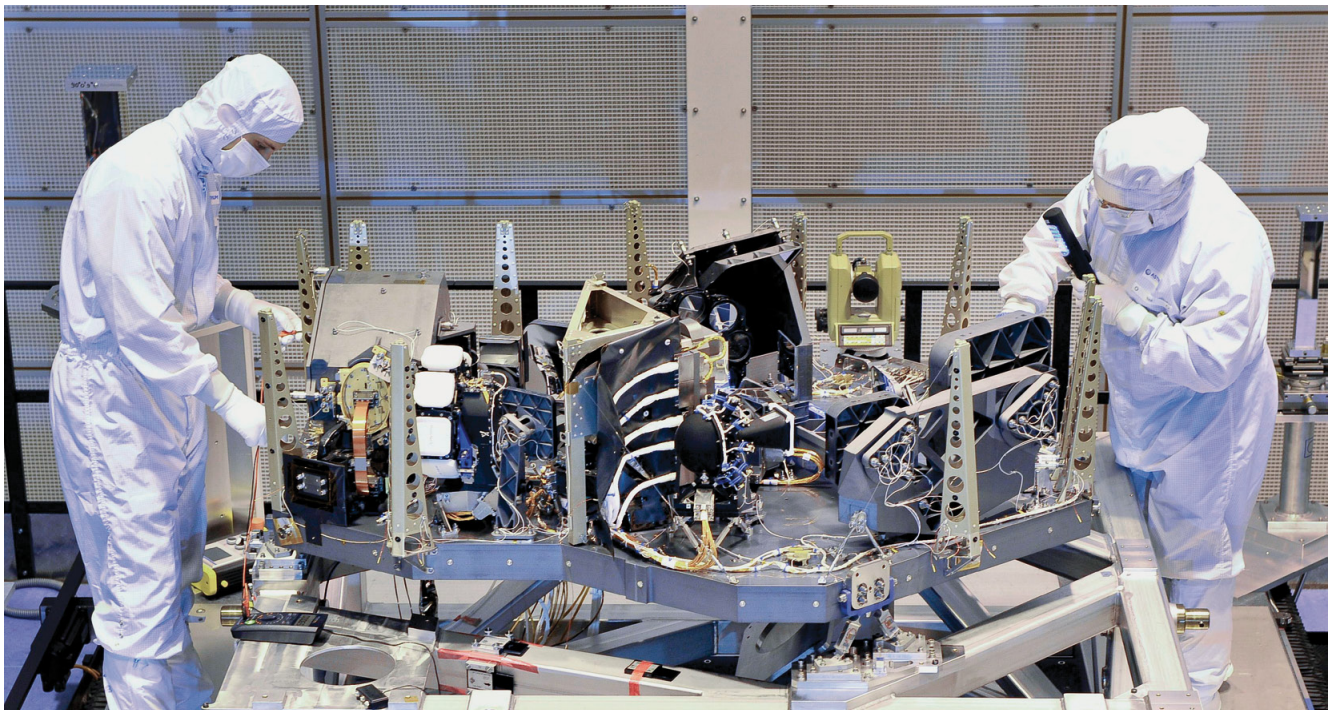

Figure 4.3.2. JWST/NIRSpec flight model 1 during its integration in a cleanroom of the prime contractor EADS Astrium. (EADS Astrium, 2011)

4.4 BepiColombo

Introduction

BepiColombo is an interdisciplinary mission to explore the planet Mercury through a partnership between ESA and JAXA. From separate orbits, two spacecraft, the ESA-provided Mercury Planetary Orbiter (MPO) and the JAXA-provided Mercury Magnetospheric Orbiter (MMO), will study the planet and its environment. The MPO will focus on a global characterisation of the planet itself, while the MMO will study the environment around Mercury, including the planet's exosphere and magnetosphere.

The two spacecraft of BepiColombo will be launched together in 2015. Upon arrival at Mercury in early 2022, after a cruise phase of about six and a half years, the Solar Electric Propulsion Module will be jettisoned and chemical propulsion will be used to inject both spacecraft into their dedicated polar orbits. The MMO will be released first, after which an additional thrust phase will insert the MPO into its final orbit. Both orbits will be elliptical with eccentricity and inclination optimised for the study of Mercury (MPO orbit: 400 × 1508 km) and its magnetosphere (MMO orbit: 400 × 11 824 km).

The BepiColombo mission will provide a rare opportunity to collect multipoint measurements in a planetary environment. This will be particularly important at Mercury because of the short temporal and spatial scales in its environment. The orbits of MPO and MMO have been selected in such a way to allow close encounters of the two spacecraft throughout the mission. Such opportunities are very important for the intercalibration of similar instruments on the two spacecraft. They also provide scientifically valuable opportunities to collect multipoint measurements in an environment where both spatial and temporal scales can be very short.

The mission has been named in honour of the Italian mathematician Giuseppe (Bepi) Colombo (1920–84), who made many contributions to planetary research, celestial mechanics, including the development of new space flight concepts. He is well known for explaining that Mercury rotates three times about its axis while it completes two orbits around the Sun.

Science Background

Compared with Earth, Mercury is a small planet, with a diameter of only 4878 km. It orbits the Sun in an elliptical orbit between 0.3 and 0.47 astronomical units (1 AU = 149 598 000 km) from the Sun. Mercury is difficult to observe from Earth because of its close proximity to the bright Sun.

BepiColombo will address a comprehensive set of scientific questions relevant to the origin and formation of terrestrial planets, and helping to answer the fundamental question of how Earth-like planets form and evolve in the Universe. A suite of state-of-art scientific instruments flying on the two spacecraft allow scientists to address a wide range of questions, including the origin and evolution of a planet so close to its parent star. It will also be possible to undertake detailed studies of Mercury's form, its interior structure and composition, and to investigate the interior dynamics and origin of Mercury's magnetic field.

Further science goals include trying to understand exo- and endogenic surface modifications, cratering, tectonics and volcanism. The composition, origin and dynamics of Mercury's exosphere and magnetosphere will be studied using combined measurements by both spacecraft. Last but not least, scientists believe they can also use BepiColombo as a laboratory to

Further information about the BepiColombo mission can be found at *http://sci.esa.int/bepicolombo*

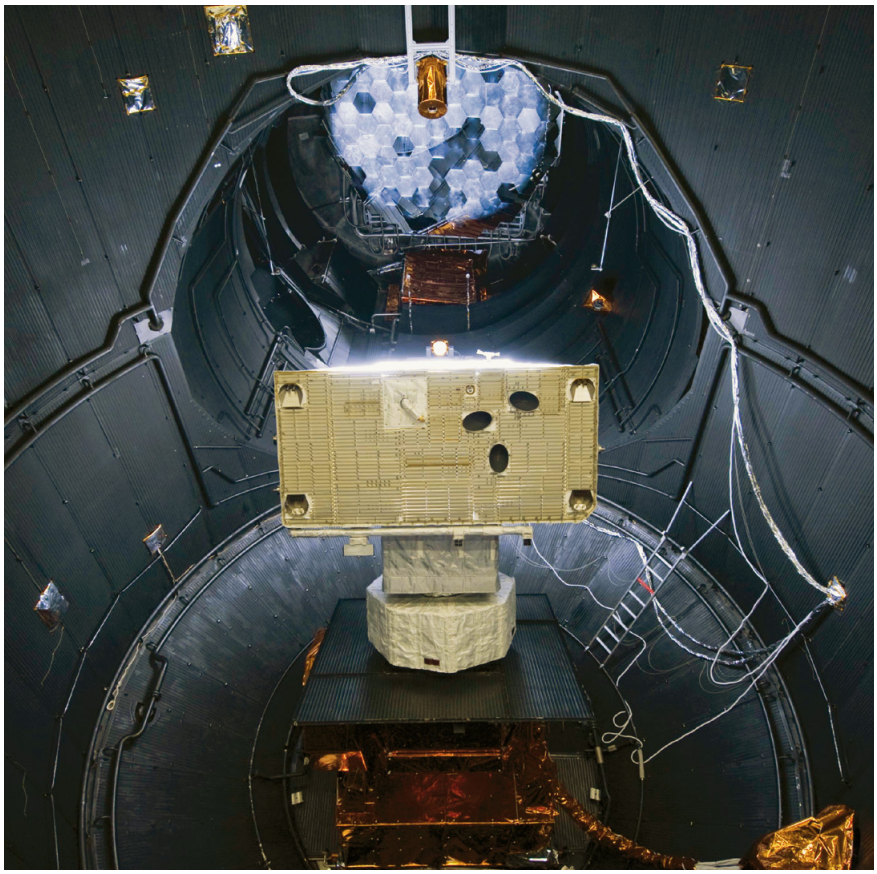

Figure 4.4.1. Structural/Thermal Model of the Mercury Planetary Orbiter during tests in ESTEC's Large Space Simulator.

test Einstein's theory of General Relativity by performing highly accurate positioning measurements of the spacecraft.

Mercury Planetary Orbiter

The Mercury Planetary Orbiter (Fig. 4.4.1) will carry a highly sophisticated suite of 11 scientific instruments, ten of which will be provided by Principal Investigators through national funding by ESA Member States and one from Russia (Table 4.4.1).

The MPO is designed to take scientific measurements in all parts of the orbit throughout the Mercury year, implying that the apertures of most of the remote sensing instruments are continuously nadir pointing. As a consequence, five out of six spacecraft faces may be illuminated by the Sun at some point. This leaves only one side of the spacecraft for a radiator to dump excess heat into space and to avoid solar exposure of the radiator. The heat load is tremendous: at the perihelion sub-solar point it is 14 kW m^{-2} from the Sun and 6 kW m^{-2} from Mercury.

Mercury Magnetospheric Orbiter

The Mercury Magnetospheric Orbiter (Fig. 4.4.2) is a spin-stabilised spacecraft that will separate from the MPO following Mercury orbit insertion. The MMO is optimised for *in situ* plasma and electromagnetic fields and waves measurements in Mercury orbit. The nominal spin rate is 15 rpm due to the scientific requirements. The spin axis is pointed nearly perpendicular to the Mercury orbital plane. The total mass of the MMO is about 270 kg, including the nitrogen gas for attitude control. It is octagonal in shape, about 1.8 m in diameter. Each of the eight side panels is 0.9 m high, 50% covered with solar cells and 50% with optical solar reflectors.

Table 4.4.1. The BepiColombo MPO payload.

Instrument	Science objective
BepiColombo Laser Altimeter (BELA)	Characterise the topography and surface morphology of Mercury.
Mercury Orbiter Radio Science Experiment (MORE)	Determine Mercury's gravity field as well as the size and physical state of its core.
Italian Spring Accelerometer (ISA)	Together, the ISA and MORE experiments will provide information on Mercury's interior structure and to test Einstein's theory of General Relativity.
Mercury Magnetometer (MERMAG-MAG)	Describe in detail Mercury's magnetic field and its source, to better understand the origin, evolution and current state of the planetary interior, as well as the interactions between Mercury and its magnetosphere and the solar wind.
Mercury Thermal Infrared Spectrometer (MERTIS)	Provide detailed information about the mineralogical composition of Mercury's surface layer, as well as global temperature maps.
Mercury Gamma-ray and Neutron Spectrometer (MGNS)	Determine the elemental composition of Mercury's surface and subsurface, and the regional distribution of volatile depositions in polar areas permanently shadowed from the Sun.
Mercury Imaging X-ray Spectrometer (MIXS)	Use X-ray fluorescence analysis to produce a global map of the surface atomic composition at high spatial resolution.
Probing of Hermean Exosphere by Ultraviolet Spectroscopy (PHEBUS)	The spectrometer is devoted to the characterisation of the composition and dynamics of Mercury's exosphere, and search for surface ice layers in permanently shadowed regions of high-latitude craters.
Search for Exosphere Refilling and Emitted Neutral Abundances (SERENA)	Study the gaseous interactions between the surface, exosphere, magnetosphere and the solar wind.
Spectrometers and Imagers for MPO BepiColombo Integrated Observatory System (SYMBIO-SYS)	Provide global, high-resolution, and IR imaging of the surface. Examine the surface geology, volcanism, global tectonics, surface age and composition, and geophysics.
Solar Intensity X-ray Spectrometer (SIXS)	Perform measurements of X-rays and particles of solar origin at high time resolution and over a very wide field of view.

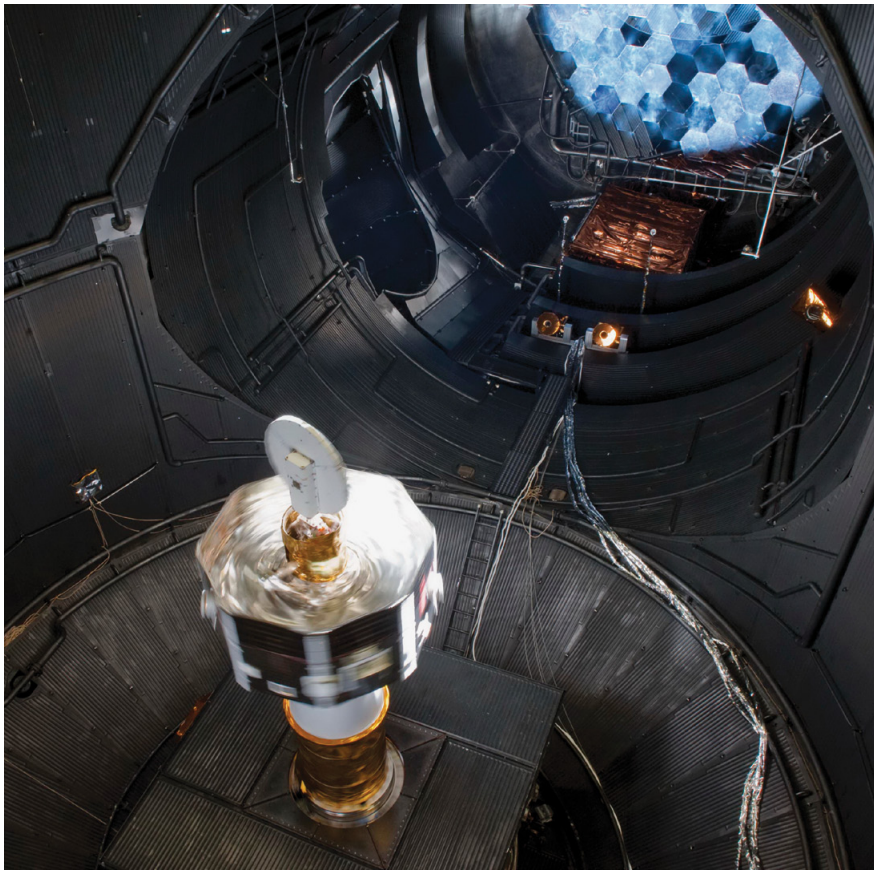

Figure 4.4.2. STM of the Mercury Magnetospheric Orbiter during tests in ESTEC's Large Space Simulator.

Instrument	Science Objective
Mercury Magnetometer (MERMAG-MGF)	Provide a detailed description of Mercury's magnetosphere and of its interaction with the planetary magnetic field and the solar wind.
Mercury Plasma Particle Experiment (MPPE)	Study low- and high-energetic particles in the magnetosphere.
Mercury Plasma Wave Instrument (PWI)	Make a detailed analysis of the structure and dynamics of the magnetosphere.
Mercury Sodium Atmospheric Spectral Imager (MSASI)	Measure the abundance, distribution, and dynamics of sodium in Mercury's exosphere.
Mercury Dust Monitor (MDM)	Study the distribution of interplanetary dust in the orbit of Mercury.

Table 4.4.2. The BepiColombo MMO payload.

For the high-gain antenna (HGA), a helical array antenna 80 cm in diameter is mounted on top of MMO. The HGA is pointed toward Earth. The scientific instruments are located on the upper and lower decks. The four deployment units of the electric probe antennas for the Plasma Wave Instrument sensors are installed on the lower side of the bottom deck.

The MMO will carry five advanced scientific experiments provided by nationally funded Principal Investigators, one European and four from Japan (Table 4.4.2).

Spacecraft Testing

In order to ensure the science and technical performance of the spacecraft, intense on-ground testing has to be performed. The environment around Mercury imposes strong requirements on the spacecraft design, particularly those elements that will be exposed to the Sun and Mercury, including the solar array mechanisms, antennas, multilayer insulation, thermal coatings and the radiator.

Recently, Structural/Thermal Models (STMs) of the two BepiColombo spacecraft have been tested in ESA's Large Space Simulator, which is capable of reproducing Mercury's thermal environment (see Figs 4.4.1 and 4.4.2). Both the MMO and MPO survived the simulated conditions in operation in orbit around the planet. During the six-year cruise to Mercury, the MMO will be covered by a sunshield (Fig. 4.4.3) to keep it cool. During the tests the two spacecraft and the sunshield withstood temperatures higher than 350°C. Once at Mercury, special thermal blankets will be deployed to protect BepiColombo from most of the Sun's heat (direct or reflected from the planet). These multilayer blankets consist of a white ceramic outer layer and several metallic layers to reflect as much heat as possible back into space. The performance of the thermal blankets was also measured and analysed during the tests.

Figure 4.4.3. STM of the Mercury Magnetospheric Orbiter covered by the sunshield during tests at ESTEC's Large Space Simulator to simulate environmental conditions during the cruise to Mercury.

4.5 ExoMars

Introduction

ESA's ExoMars programme is embedded in a wider international context. At the time of writing, ESA and the Russian Federal Space Agency, Roscosmos, are in the process of defining a joint programme for robotic Mars exploration.

The first stage of the ESA–Roscosmos programme includes two missions: the 2016 ExoMars Trace Gas Orbiter (TGO) mission and the 2018 Joint Rover mission. The two agencies are also undertaking a study of candidate missions to be considered for 2020 and beyond. The longer-term goal of the programme is the realisation of an international Mars Sample Return mission during the second half of the next decade.

2016 ExoMars Trace Gas Orbiter

The 2016 ExoMars TGO mission will include two elements: an orbiting satellite devoted to the study of atmospheric trace gases with the goal of acquiring information on possible ongoing geological or biological activity, and an Entry, Descent and Landing Demonstrator Module (EDM) to demonstrate the soft landing of a small payload on the surface of Mars (Fig. 4.5.1). TGO will also provide data communication services for all surface missions landing on Mars through 2022.

The goal of the 2016 ExoMars Trace Gas Orbiter is to gain a better understanding of trace and minor gases that are present in the martian atmosphere in small concentrations but which may nevertheless point to plausible biological or geological activities (or both). Investigations with Mars Express and ground-based observatories have detected the presence of small and variable amounts of methane in the atmosphere, implying the existence of an active and current source of methane. A neutron spectrometer will provide high-resolution information on the presence of water in the top 1 m of the martian subsurface.

The 2016 Orbiter will carry a scientific payload (Table 4.5.1) that will be capable of detecting and characterising the trace gases in the atmosphere, from

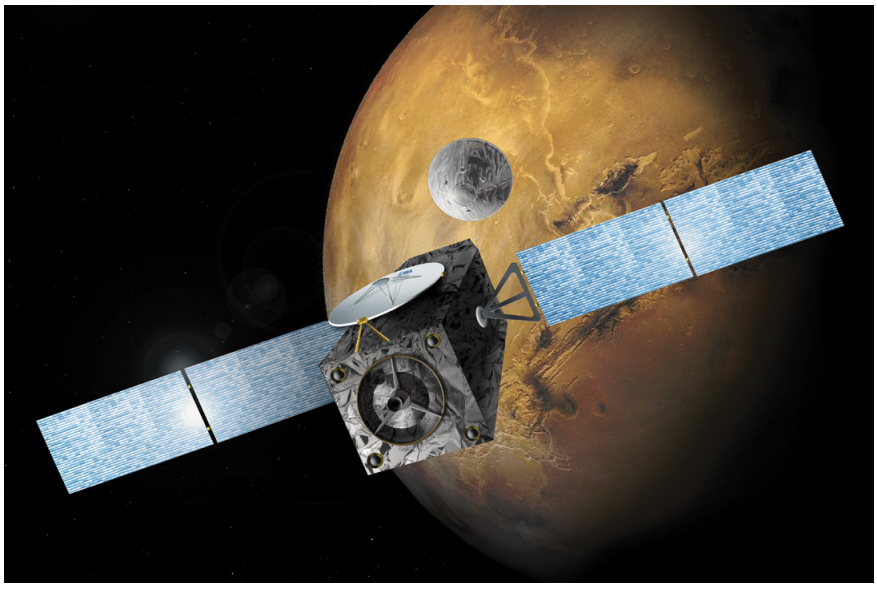

Figure 4.5.1. The 2016 ExoMars Trace Gas Orbiter mission approaching the red planet and releasing the Entry Descent and Landing Demonstrator Module.

Further information about the ExoMars mission can be found at *http://exploration.esa.int*

Table 4.5.1. The 2016 ExoMars Trace Gas Orbiter payload.

Instrument	Short description	Participants
Nadir and Occultation for MArs Discovery (NOMAD)	Solar occultation and nadir infrared spectrometer, ultraviolet spectrometer	BE, ES, IT, GB, CA, US
Atmospheric Composition Studies (ACS)	Cluster of solar occultation and nadir infrared spectrometers (complementary to NOMAD)	RU, FR
Fine Resolution Epithermal Neutron Detector (FREND)	Neutron spectrometer (subsurface water characterisation)	US, GB, FR
Colour and Stereo Surface Imaging System (CASSIS)	High-resolution stereo colour imager	CH, DE, SE, IT, FR, GB

its ~400 km altitude and 74° inclination orbit, with an improved accuracy of three orders of magnitude compared with previous measurements. The mission is planned to be launched in January 2016, and to be inserted into Mars orbit in October 2016.

The main objective of the EDM will be to demonstrate the landing of a small payload on the surface of Mars. Upon landing, a small environmental station will begin operations. It will be powered by a Radioisotope Thermoelectric Generator (RTG) for at least one martian year.

2018 ExoMars Rover

The 2018 mission will deliver a 300 kg-class rover to the surface of Mars using a landing system closely derived from the one used by the 2016 EDM.

The 2018 ExoMars rover will pursue one of the outstanding questions of our time by attempting to establish whether life ever existed or is still active on Mars today. The rover will travel several kilometres to explore the landing site's geological environment and conduct a search for signs of past and present life. It will collect and analyse samples from within rocky outcrops and from the subsurface, down to a depth of 2 m, using a drill. The ExoMars rover will carry a comprehensive suite of analytical instruments dedicated to exobiology and geochemistry research: the Pasteur payload (Table 4.5.2).

Table 4.5.2. The 2018 ExoMars rover's Pasteur payload.

Instrument	Description	Participants
PanCam	Panoramic Camera (high-resolution, wide-angle stereo camera)	GB, DE, AT, CH
MIR	Mast-mounted IR spectrometer for mineralogy	RU, FR
WISDOM	Water Ice and Subsurface Deposit Information On Mars (ground-penetrating radar)	FR, DE, US, NO
NS	Neutron Spectrometer for subsurface water	RU
CLUPI	Close-Up Imager	CH, FR
Ma_MISS	Mars Multispectral Imager for Subsurface Studies (IR spectrometer in subsurface drill)	IT
MicrOmega	VIS-IR micro-imaging spectrometer	FR, RU
Raman Laser Spectrometer	Raman spectrometer	ES, FR, GB
Mars-XRD	X-ray Diffractometer and X-ray fluorescence	IT, GB, PL
MOMA	Mars Organic Molecule Analyser (LDMS & pyr-GCMS)	DE, FR, US
LMC	Life Marker Chip	GB, NL, IT

Mars as an Astrobiology Target

If life ever arose on the red planet, it probably did so when Mars was warmer and wetter, sometime within the first billion years following planetary formation. Conditions then were similar to those when microbes gained a foothold on the young Earth. This marks Mars as a primary target in the search for signs of life in our Solar System. Unfortunately, on Earth, high-temperature metamorphic processes and plate tectonics have resulted in the reformation of most ancient terrains. Hence, the physicochemical record of the very early evolution of life on Earth is no longer accessible to us. Mars, on the other hand, has not suffered such widespread tectonic activity, so that well-preserved, ancient biomarkers may still be accessible for analysis. The study of ancient martian rocks may also provide important clues about deposition processes and habitable conditions on early Earth.

Subsurface Exploration

The ExoMars rover's surface mobility and the 2 m vertical reach of the drill are both crucial for the scientific success of the mission (Fig. 4.5.2). The ExoMars rover will search for two types of life-related signatures: morphological and chemical. This will be complemented by an accurate determination of the geological context.

Morphological information related to biological processes may be preserved on the surface of rocks. Possible examples include the biomediated deposition of sediments, fossilised bacterial mats and stromatolitic mounds. Such studies require mobility and an imaging system capable to cover from the metre scale down to sub-millimetre resolution (to discern microtextural information in rocks).

An effective chemical identification of biomarkers requires access to well-preserved organic molecules. Because the martian atmosphere is more tenuous than Earth's, three important physical agents reach the surface of Mars with adverse effects on the long-term preservation of biomarkers:

— The ultraviolet radiation dose is higher than on Earth and will quickly damage potential exposed organisms or biomolecules.

— UV-induced photochemistry is responsible for the production of reactive oxidant species that, when activated, can also destroy biomarkers; the diffusion of oxidants into the subsurface is not well characterised and constitutes an important measurement that the mission must perform.

— Ionising radiation penetrates into the uppermost metres of the planet's subsurface. This causes a slow degradation process that, over many millions of years, can alter organic molecules beyond the detection sensitivity of analytical instruments. Note that the ionising radiation effects are depth dependent: the material closer to the surface is exposed to a higher dose than that buried deeper.

A major goal of ExoMars is to study ancient (older than 3 billion years) sedimentary rock formations and evaporitic deposits. However, only if it has been trapped in the subsurface for long periods that the record of early martian life, if it ever existed, is likely to have escaped radiation and chemical damage. Studies show that a subsurface penetration in the range of 2 m is necessary to recover well-preserved organics from the very early history of Mars. In addition, it is essential to avoid loose dust deposits distributed by aeolian transport. While driven by the wind, this material has been processed by UV radiation, ionising radiation, and potential oxidants in the atmosphere and on the surface of Mars. Any organic biomarkers would be highly degraded in these

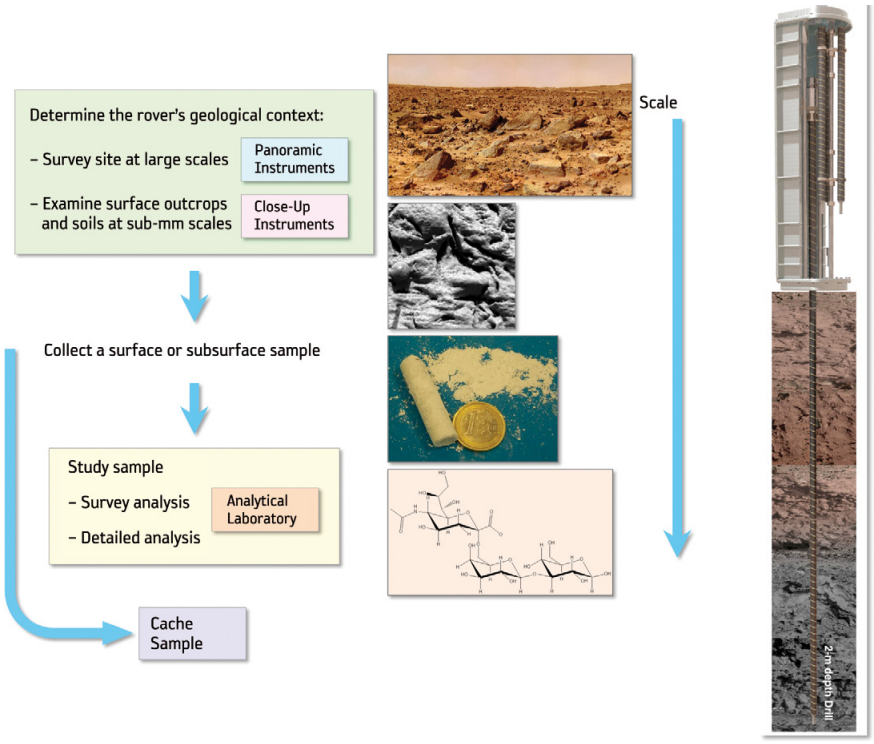

Figure 4.5.2. The 2018 Exomars rover must perform a range of measurements at multiple scales, from panoramic to molecular scale.

samples. For all these reasons, the ExoMars drill will be able to penetrate and obtain samples from well-consolidated (hard) formations, at various depths, down to 2 m.

The successful NASA Mars Exploration Rovers have demonstrated the past existence of wet environments on Mars using a geologically oriented instrument package. The results have persuaded the scientific community that mobility is a must-have requirement for future missions. Recent discoveries by ESA's Mars Express mission have revealed multiple deposits containing salt and clay minerals that can form only in the presence of liquid water. This reinforces the hypothesis that ancient Mars may have been wetter than it is today. NASA's Mars Science Laboratory, due to land in August 2012, will study surface geology and organics, with the goal of identifying habitable environments.

The 2018 rover constitutes the next logical step in Mars exploration. It will have instruments to investigate whether life ever arose on the red planet. It will also be the first mission to combine mobility and access to subsurface locations where organic molecules may be well preserved; thus allowing, for the first time, investigations of Mars's third dimension: depth. This alone is a guarantee that it will break new scientific ground.

4.6 Solar Orbiter

Introduction

Solar Orbiter, an international collaboration between ESA and NASA, is the first M-class mission in ESA's Cosmic Vision 2015–25 programme. Devoted to solar and heliospheric physics, the mission will provide unprecedented close-up and high-latitude observations of the Sun. With previously unavailable observational capabilities provided by the *in situ* and remote-sensing instruments, and the unique design of this inner-heliospheric mission, Solar Orbiter will address the central question in heliophysics: how does the Sun create and control the heliosphere?

This overarching scientific objective can be broken down into four interrelated scientific questions, all of which have strong, direct relevance to the Cosmic Vision theme 'How does the Solar System work?' Solar Orbiter is addressing four questions:

- How and where do the solar wind plasma and magnetic field originate in the corona?
- How do solar transients drive heliospheric variability?
- How do solar eruptions produce energetic particle radiation that fills the heliosphere?
- How does the solar dynamo work and drive the connections between the Sun and the heliosphere?

To answer these questions, it is essential to make *in situ* measurements of the solar wind plasma, fields, waves and energetic particles close enough to the Sun that they are still relatively pristine and have not had their properties modified by subsequent transport and propagation processes. This is one of the fundamental drivers for the Solar Orbiter mission, which will approach the Sun to within 0.28–0.30 AU. Relating these *in situ* measurements back to their source regions and structures on the Sun requires simultaneous, high-resolution imaging and spectroscopic observations of the Sun in and out of the ecliptic plane. The resulting combination of *in situ* and remote sensing instruments on the same spacecraft, together with the new, inner-heliospheric perspective, distinguishes Solar Orbiter from all previous and current missions, enabling breakthrough science that can be achieved in no other way.

In addition to delivering ground-breaking science in its own right, Solar Orbiter also has important synergies with NASA's Solar Probe Plus mission, and coordinated observations are expected to enhance greatly the scientific return of both missions. In the overall international context, Solar Orbiter is ESA's primary contribution to the International Living With a Star initiative; the joint studies incorporating data from all missions operating in the inner heliosphere (or providing remote-sensing observations of the near-Sun environment) will contribute greatly to our understanding of the Sun and its environment.

Spacecraft and Scientific Payload

The Solar Orbiter spacecraft (Fig. 4.6.1) is a Sun-pointed, 3-axis stabilised platform, with a dedicated heat shield to provide protection from the high levels of solar flux near perihelion. Feedthroughs in the heat shield provide the remote sensing instruments with their required fields-of-view to the Sun. Solar arrays provide the capability to produce the required power throughout

Further information about the Solar Orbiter mission can be found at *http://sci.esa.int/solarorbiter*

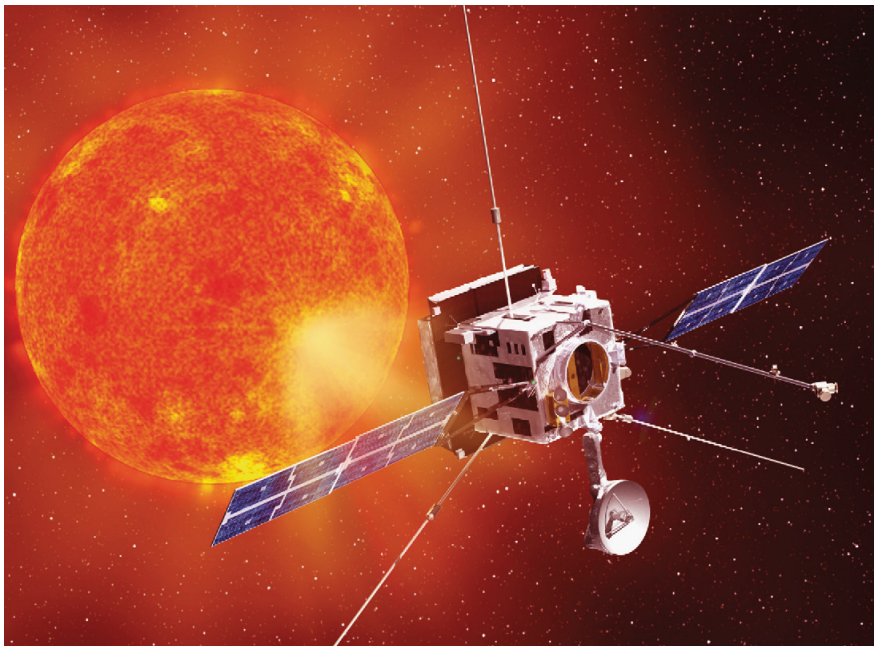

Figure 4.6.1. The Solar Orbiter spacecraft

the mission over the wide range of distances from the Sun using rotation about their longitudinal axis to change the solar aspect angle to control the array temperature, particularly during closest approach to the Sun. An articulated high-temperature high-gain antenna provides nominal communication with the ground station.

The design drivers for the Solar Orbiter spacecraft come not only from the need to satisfy the mission's technical and performance requirements, but also from the need to minimise the total cost of the mission. New technology developments have been avoided as far as possible and existing BepiColombo technology items incorporated where appropriate. Furthermore, heritage from the Express series of missions, with their goal of rapid and streamlined development, has also featured heavily in the Solar Orbiter spacecraft design.

The scientific payload of Solar Orbiter will comprise a sophisticated suite of 10 instruments, eight of which will be provided by Principal Investigators through national funding by ESA Member States. NASA will contribute one complete instrument and one sensor, and two European-led consortia supported by national funding and ESA contributions will provide one complete facility instrument and one sensor, respectively. The scientific payload is described in Table 4.6.1 and its accommodation on the spacecraft is depicted in Fig. 4.6.2.

A mission profile for Solar Orbiter has been developed that will, for the first time, make it possible to study the Sun with a full suite of *in situ* and remote sensing instruments from as close as 0.28 AU and provide imaging and spectral observations of the Sun's polar regions from out of the ecliptic. This proximity to the Sun will also have the advantage that the spacecraft will have periods of reduced angular velocity with respect to the solar surface, allowing observations of solar surface features and their connection to the heliosphere for significantly longer periods than from near-Earth vantage points.

The baseline mission is planned to start in January 2017 with a launch on a NASA-provided launch vehicle from Cape Canaveral, placing the spacecraft on a ballistic trajectory that will be combined with planetary gravity-assist manoeuvres (GAMs) at Earth and Venus (Fig. 4.6.2). The second Venus GAM will place the spacecraft into a 4:3 resonant orbit with Venus at a perihelion radius of 0.284 AU. The first perihelion at this close distance to the Sun will be reached 3.5 years after launch.

Table 4.6.1. Scientific payload of Solar Orbiter.

Experiment/PI	Goals
In situ instruments	
Energetic Particle Detector (EPD) J.R. Pacheco, Spain	Measure the properties of suprathermal and energetic particles.
Magnetometer (MAG) T.S. Horbury, UK	Provide detailed *in situ* measurements of the heliospheric magnetic field.
Radio and Plasma Waves (RPW) experiment M. Maksimovic, France	Measure magnetic and electric fields at high time resolution and determine the characteristics of waves in the solar wind.
Solar Wind Analyser (SWA) C.J. Owen, UK	Fully characterise the major constituents of the solar wind plasma between 0.28 AU and 1.2 AU.
Remote sensing instruments	
Extreme Ultraviolet Imager (EUI) P. Rochus, Belgium	Provide image sequences of the solar atmospheric layers from the photosphere into the corona.
Multi-Element Telescope for Imaging and Spectroscopy Coronagraph (METIS/COR) E. Antonucci, Italy	Perform broadband and polarised imaging of the visible K-corona and narrow-band imaging of the UV and EUV corona.
Polarimetric and Helioseismic Imager (PHI) S.K. Solanki, Germany	Provide measurements of the photospheric vector magnetic field and line-of-sight velocity as well as the continuum intensity.
Solar Orbiter Heliospheric Imager (SoloHI) R.A. Howard, USA	Image both the quasi-steady flow and transient disturbances in the solar wind over a wide field of view by observing visible sunlight scattered by solar wind electrons.
Spectrometer/Telescope for Imaging X-rays (STIX) S. Krucker, Switzerland	Provide imaging spectroscopy of solar thermal and non-thermal X-ray emission from ~4 keV to 150 keV.
Facility instruments	
Spectral Imaging of the Coronal Environment (SPICE) EUV Spectrograph	Provide spectral imaging to remotely characterise plasma properties of regions at and near the Sun.
Suprathermal Ion Spectrograph (EPD/SIS) sensor	Measure the properties of suprathermal ions.

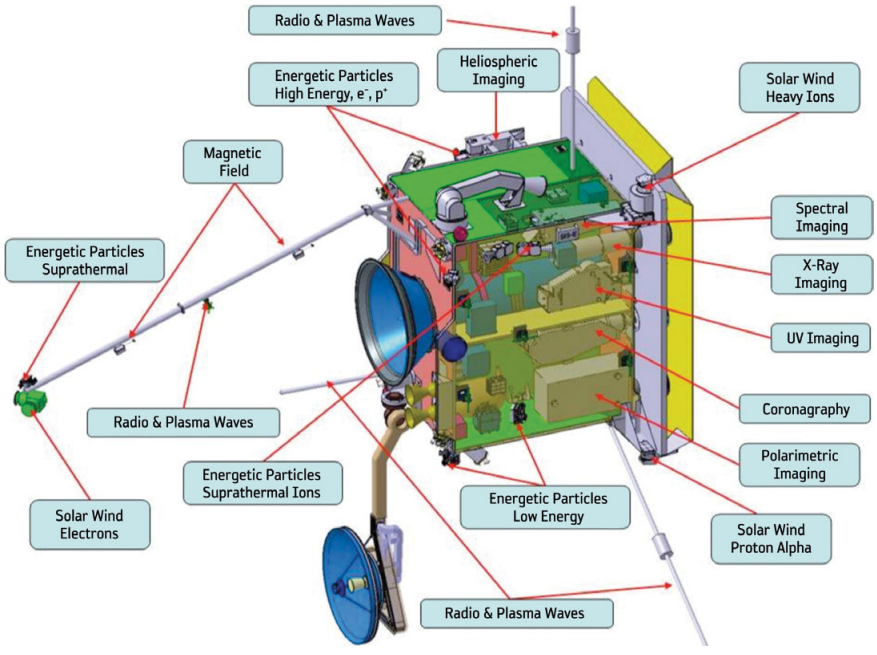

Figure 4.6.2. Payload accommodation on the Solar Orbiter spacecraft.

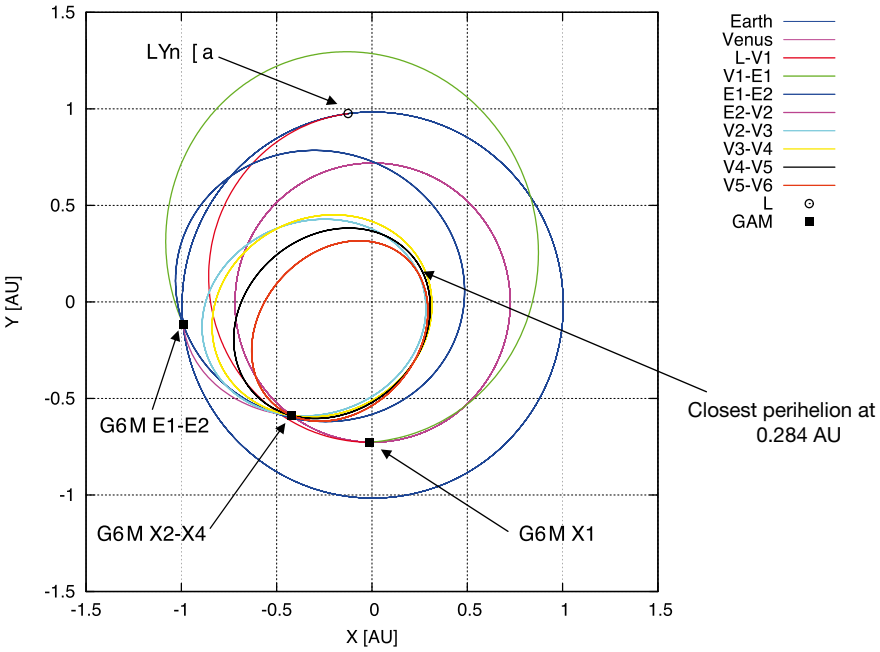

Figure 4.6.3. Solar Orbiter's trajectory viewed from above the ecliptic (January 2017 launch). The gravity-assist manoeuvres at Earth (E) and Venus (V) are indicated, along with the orbits of the two planets.

This orbit is the start of the sequence of resonances 4:3–4:3–3:2–5:3 that will be used to raise gradually the solar inclination angle at each Venus GAM. The resulting operational orbit has a period of 168 days during the nominal mission with a minimum perihelion radius of 0.28 AU. The nominal mission will end 7 years after launch, when the orbit inclination relative to the solar equator reaches 25°. The inclination may be further increased during an extended mission phase using additional Venus GAMs, to reach a maximum of 34° for the January 2017 baseline and 36° for a launch in March 2017.

Science Operations

One of the strengths of the Solar Orbiter mission is the synergy between *in situ* and remote-sensing observations, since each science objective requires coordinated observations between several *in situ* and remote-sensing instruments. Another unique aspect of the mission, in contrast to near-Earth or L1 observatory missions like SOHO, is that Solar Orbiter will operate much like a planetary encounter mission, with the main scientific activity and planning taking place during the near-Sun encounter part of each orbit. Specifically, observations with the remote-sensing instruments will be organised into three 10-day intervals centred on perihelion and either maximum latitude or maximum corotation passages. As a baseline, the *in situ* instruments will acquire data continuously during normal operations. Another important aspect of this mission, from a science operations standpoint, is that every science orbit is different, with different orbital characteristics (Sun–spacecraft distance, Earth–spacecraft distance, etc.).

Science and operations planning for each orbit is therefore critical, with specific orbits expected to be dedicated to specific science problems. This will be similar to what has been used successfully in the ESA/NASA SOHO mission's Joint Observation Programs.

Status

Solar Orbiter was selected and adopted as the first M-class Cosmic Vision mission by ESA's Science Programme Committee at its meeting on 4 October 2011. In

keeping with the ‘fast-track’ approach for the project that was agreed by SPC in 2010, the majority of the Phase-B1 activities (including the System Requirements Review) were completed by mid-2011 in order to begin Phase-B2 immediately after selection and adoption. A key driver in this respect is the January 2017 launch opportunity; Solar Orbiter employs Venus gravity-assist manoeuvres to reach the final operation orbit and Venus launch opportunities occur only once every 19 months.

In parallel with the industrial activities at spacecraft level, the instrument teams have continued to develop their instrument designs in preparation for the Preliminary Design Reviews that will take place over a period of about nine months starting in November 2011. The system-level PDR was completed in March 2012.

4.7 Contributions to Nationally-Led Projects

4.7.1 Astro-H

Astro-H is the sixth in a series of Japanese X-ray astronomy missions. Led by JAXA with contributions from both NASA and ESA, Astro-H aims to offer one of the first opportunities to carry out imaging and spectroscopic observations in the hard X-ray band, using a true focusing telescope (Fig. 4.7.1.1). It is expected to be the first observatory operating a high-spectral-resolution cryogenic X-ray microcalorimeter. A key feature of Astro-H will be the simultaneous wide-band operation between 30 keV and 600 keV.

A Memorandum of Understanding has been signed between ESA and JAXA for cooperation in the JAXA X-ray astronomy mission. This is a natural follow-on from the successful ESA participation in the Suzaku mission.

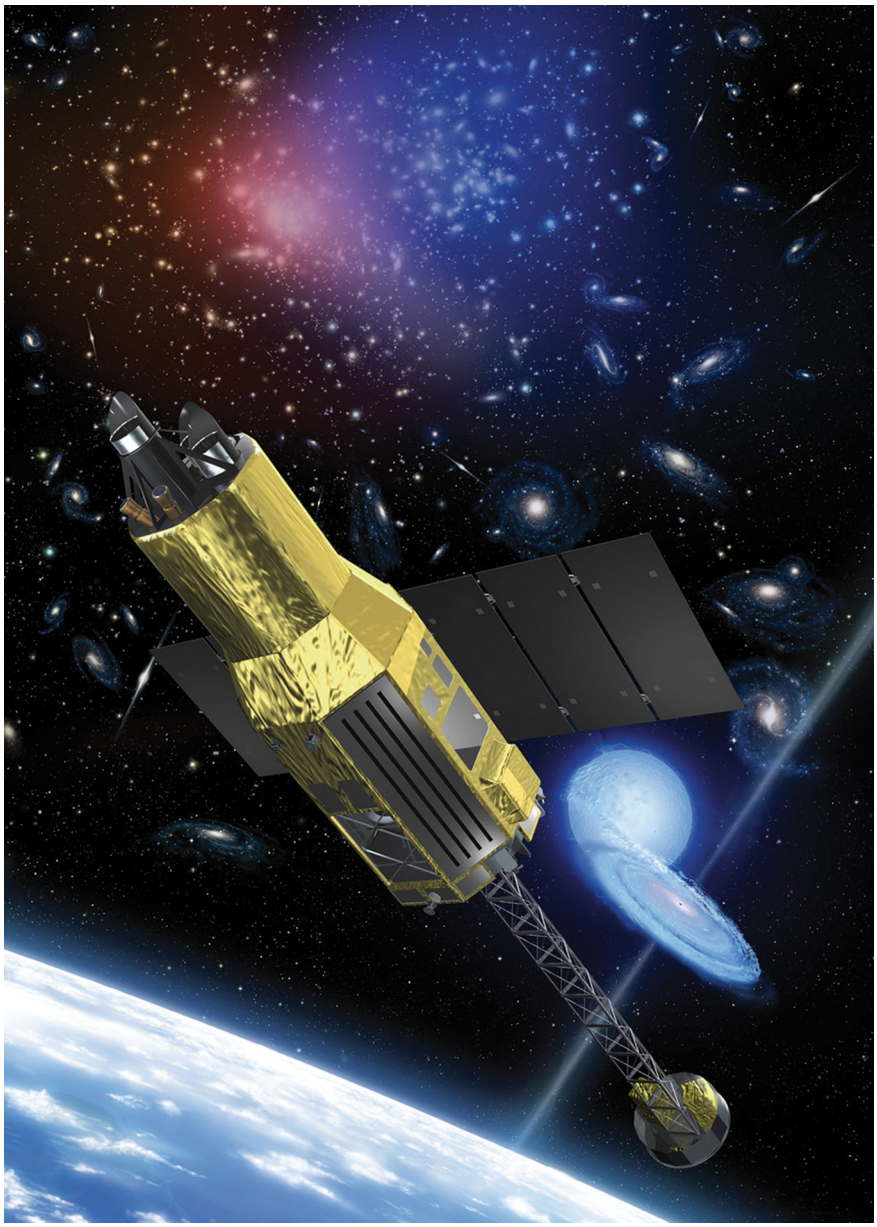

Figure 4.7.1.1. AThe Astro-H spacecraft. The extendable boom will allow a long focal length for the hard X-ray telescope. (A. Ikeshita/JAXA)

Further information about the Astro-H mission can be found at *www.esa.int/esaSC/SEM61VEWF0H_index_0.html* and *http://astro-h.isas.jaxa.jp*

For Astro-H, ESA will supply a number of components for various spacecraft and instrument subsystems, drawing on specific expertise in Europe. These include materials for fabricating mirrors and reflective coatings, scintillator components for anti-coincidence shields, high-voltage power supplies and loop heat pipes. In addition, ESA will provide access to test facilities to support radiation hardness testing of selected components. These activities complement existing bilateral agreements between JAXA and research groups in the Netherlands and Switzerland, where participation in development of scientific instruments has already begun.

ESA is also supporting the participation of three European scientists in the Astro-H Science Working Group, and will provide scientific support to supplement the science ground segment activities. This work will focus on areas such as user documentation, data analysis software testing and analysis of ground and inflight calibration.

Following the launch of Astro-H, anticipated in 2014, ESA will coordinate with JAXA (and NASA, as the other major international partner) on an international Announcement of Opportunity for guest observers. A fraction of observing time will be reserved for European participants in the programme.

→ MISSIONS UNDER STUDY

5. Missions under Study

5.1 NGO

Introduction

The New Gravitational wave Observatory (NGO) was an L1 candidate mission in ESA's Cosmic Vision 2015–25 programme. In April 2012, the Science Programme Committee selected JUICE (Section 5.3) as the L1 mission and thus the NGO study has been ended. It is possible that a gravitational wave mission may rejoin the competition for either the L2 or L3 slot.

NGO was derived from the Laser Interferometer Space Antenna (LISA), which was an L1 candidate mission that was to be undertaken in collaboration with NASA. Due to programmatic shifts within NASA, however, the collaboration ended in spring 2011 and NGO, a similar, ESA-led mission, has been studied that shares many of the science goals but differs in terms of the mission duration, architecture and payload.

NGO is a mission to detect and observe gravitational waves. Its science goals include:

- understanding the formation of massive black holes (10^4–10^8 solar masses);
- tracing the growth and merger history of massive black holes and their host galaxies; to explore stellar populations and dynamics in galactic nuclei;
- surveying compact stellar-mass binaries and study the structure of our Galaxy;
- confronting General Relativity with observations of gravitational waves and their sources;
- probing new physics and cosmology with gravitational waves; and
- searching for unforeseen sources of gravitational waves.

NGO's sensitivity range extends from 10^{-4} Hz to 10^{-1} Hz (Fig. 5.1.1), a frequency range inaccessible to ground-based interferometers partly due to the background of local gravitational noise such as seismic noise, anthropogenic

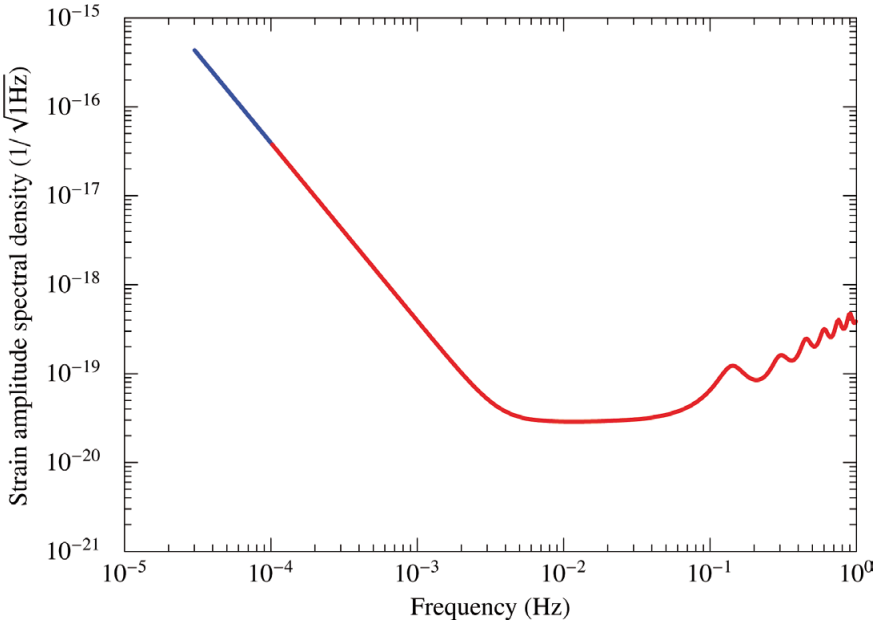

Figure 5.1.1. Sensitivity curve for NGO. Red indicates the science requirements, the blue extension at low frequencies indicate the goal.

Further information about the NGO mission can be found at *http://sci.esa.int/ngo*

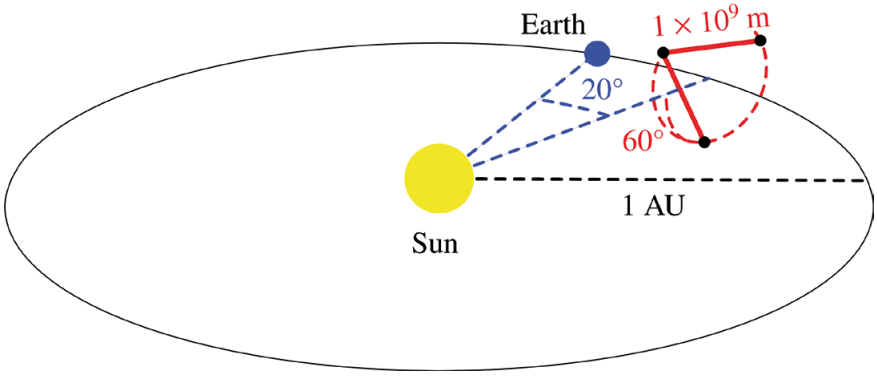

Figure 5.1.2. The NGO constellation trails Earth by about 20°, drifting slowly away over the mission lifetime.

noise, and gravity gradient noise; and partly because ground-based interferometers are limited in length to a few kilometres.

In the low-frequency band of NGO, potential sources are well known and signals should be stable over long periods (from many months to thousands of years). NGO would detect signals from numerous sources with signal-to-noise ratios of 50–1000 for massive black holes out to redshifts of z = 20, which would allow determination of the internal parameters of their sources, such as position, orientation, mass and distance. The coalescence of pairs of massive black holes are the most violent events in the Universe, setting free vast amounts of energy that renders them 'visible' through the emission of gravitational waves even from the farthest distances. Together with observations in the electromagnetic spectrum, these 'standard sirens' would provide important insights into the evolution of the Universe.

Configuration

NGO comprises three spacecraft positioned 1 million km apart in an equilateral triangle. The centre of the triangular formation is in the plane of the ecliptic, 1 AU from the Sun and trailing Earth between 10° and 20°. The plane of the triangle is inclined at 60° with respect to the ecliptic, resulting in a stable formation throughout the projected mission life. Owing to orbital mechanics, the formation appears to counter-rotate about its centre once per year (Fig. 5.1.2). Due to tidal forces, the spacecraft would oscillate around their nominal position that will cause the inter-spacecraft distance to change by many thousands of kilometres, resulting in relative velocities of up to 15 m s^{-1}. This oscillation is partly inherent to the chosen orbits, partly caused by the gravitational pull of the Earth–Moon system.

The range of the position of the formation behind Earth is a result of a trade-off between minimising the gravitational disturbances from the Earth–Moon system and the communication needs. While drifting farther away would further reduce the disturbances, the larger distance would require larger antennas or higher transmitter power.

Measurement Principle

While NGO provides interferometric measurements, the measurement principle is somewhat different from a ground-based interferometer. The laser light going from one spacecraft to another cannot be reflected directly back, because diffraction and the large separation would attenuate the beam by a factor of 10^{10}. In an analogy with an RF transponder scheme, the laser on the receiving spacecraft is phase-locked to the incoming light, effectively enabling a copy of the incoming light with full intensity to be sent back.

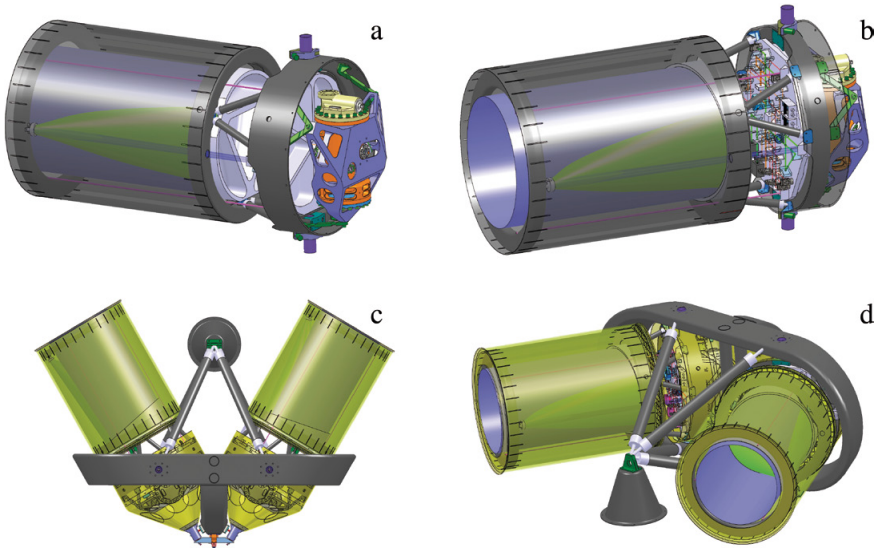

Figure 5.1.3. (a, b) Optical assembly with telescope, optical bench and inertial sensor. (c, d) Two optical assemblies mounted in the 'mother' configuration.

The transponded light from the far spacecraft is received and superposed with the onboard laser light that serves as the local oscillator in a heterodyne detection. This way, the change in armlength is measured individually for each arm. Heterodyne detection is chosen because the relative velocities of the spacecraft will cause a Doppler shift of the received light of up to 15 MHz, which does not allow for homodyne detection. In addition, heterodyne detection is self-calibrating, which allows accessing accurately the actual change in armlength from the optical signal. The Doppler shift, created by the tidal deformations of the constellation and changing on timescales of months, is not in the frequency band of NGO and therefore does not disturb the measurements. Subsequent data processing greatly reduces the effects of laser frequency noise.

Spacecraft

Each of the three spacecraft of NGO is slightly different. The 'mother' spacecraft, at the central position of the constellation, employs two optical assemblies (Fig. 5.1.3), while the two 'daughter' spacecraft, placed at the ends of the arms, include only one optical assembly. The launch masses of the spacecraft differ by about 1700 kg for the mother and about 1800 kg for the daughters, which are heavier under the current launch scenario because they have to carry more fuel to reach this operational orbit.

NGO would be launched on two Soyuz, one carrying the mother spacecraft, the other both daughters. After launch the spacecraft would use their propulsion modules to reach their operational orbits in about 14 months. There, they jettison their propulsion modules and attitude and drag-free control is left to μN thrusters.

Payload

The two optical assemblies on the mother spacecraft point towards an identical assembly on each of the two daughter spacecraft. A 2 W infrared laser beam (1064 nm wavelength) is transmitted to the corresponding remote spacecraft via a 25 cm aperture telescope. The same telescope is used to receive a small part of the light (about 200 pW) coming from the distant spacecraft and to direct the light to a sensitive photodetector (a quadrant photodiode), where it is superimposed with a fraction of the original local light.

At the heart of each assembly is a vacuum enclosure containing a free-flying, polished platinum–gold 40 mm cube (the test mass) that serves as an optical reference (mirror) for the light beams. A passing gravitational wave will change the length of the optical path between the proof masses of one arm of the interferometer relative to the other arm. The distance fluctuations are measured to a precision of 20 pm (averaged over 1 s) which, when combined with the large separation between the spacecraft, will allow NGO to detect gravitational wave strains down to a level of order $\Delta l/l = 10^{-23}$ in one year of observations with a signal to noise ratio of 5.

The spacecraft serves mainly to shield the test masses from the adverse effects of solar radiation pressure so that they follow a purely gravitational orbit. Although the position of the spacecraft does not enter directly into the measurement, it is nevertheless necessary to keep all spacecraft moderately accurately centred on their proof masses in order to reduce spurious local noise forces. This is achieved by a drag-free control system consisting of an accelerometer (or inertial sensor) and a system of μN thrusters.

Capacitive sensing in three dimensions and laser interferometry are used to measure the displacements of the test masses relative to the spacecraft. These position signals are used in a feedback loop to command the μN thrusters to follow the test masses precisely.

As the three-spacecraft constellation orbits the Sun in the course of a year, the observed gravitational waves are Doppler-shifted by the orbital motion and amplitude-modulated by the non-isotropic antenna pattern of the detector. This would allow determination of the direction of the source and assessment of some of its characteristics, e.g. its orientation, the mass and the distance. Depending on the strength of the source, positions can be determined to a precision of up to 1 arcmin.

5.2 ATHENA

Introduction

The Advanced Telescope for High-Energy Astrophysics (ATHENA) was an L1 candidate mission in ESA's Cosmic Vision 2015–25 programme. In April 2012, the Science Programme Committee selected JUICE (Section 5.3) as the L1 mission and thus the ATHENA study has been ended. It is possible that a high-energy astrophysics mission may rejoin the competition for either the L2 or L3 slot. Building on earlier studies for the International X-ray Observatory (IXO), ATHENA is an X-ray mission designed to address a suite of key questions in modern astrophysics. ATHENA would:

— determine how the process of accretion works by mapping the innermost flows around black holes, measure their spins, and determine the equation of state of ultradense matter in the cores of neutron stars;

— measure the energy flows giving rise to cosmic feedback, quantify the growth of supermassive black holes and the evolution of nuclear obscuration over cosmic time, and determine velocity and metallicity flows due to starburst superwinds;

— measure the evolution of the intracluster medium through temperature, metallicity and turbulent velocity changes with redshift, constrain dark energy as a function of redshift using clusters of galaxies and reveal the missing baryons at low redshift locked in the warm and hot intergalactic medium; and

— determine the physical conditions in hot plasmas covering a wide range of objects and phenomena, with profound impacts on astrophysics, from stars and planets, through supernovae and the galactic centre, out to other galaxies and the distant Universe.

Mission Scenario, Spacecraft and Payload

Thanks to its revolutionary optics technology and the most advanced X-ray instrumentation, ATHENA would deliver superior high-resolution X-ray imaging, timing and spectroscopy capabilities, far beyond those of any existing or approved future facilities.

The heart of the ATHENA mission is the X-ray optical system that will utilise the innovative silicon pore optics (SPO) technology pioneered in Europe. Addressing ATHENA's science goals would require a 1 m^2 effective collecting area with 10 arcsec angular resolution, and would be achieved using an assembly of two fixed 12 m focal length telescopes (Fig. 5.2.1). With respect to the current science goals, the science capabilities of ATHENA would be significantly boosted with a better angular resolution, and therefore a goal of 5 arcsec has been maintained. ESA has made a considerable investment in SPO technology and has already demonstrated an angular resolution of less than 10 arcsec in a flight-like assembly, consistent with the mission's scientific requirements and with a clear development plan towards the goal of 5 arcsec.

The baseline instrument complement consists of the X-ray Microcalorimeter Spectrometer (XMS) for high-resolution spectroscopic imaging, and a Wide-Field Imager (WFI) consisting of an active pixel sensor camera with high count-rate capability and moderate resolution spectroscopic capability.

Further information about the ATHENA mission can be found at *http://sci.esa.int/athena*

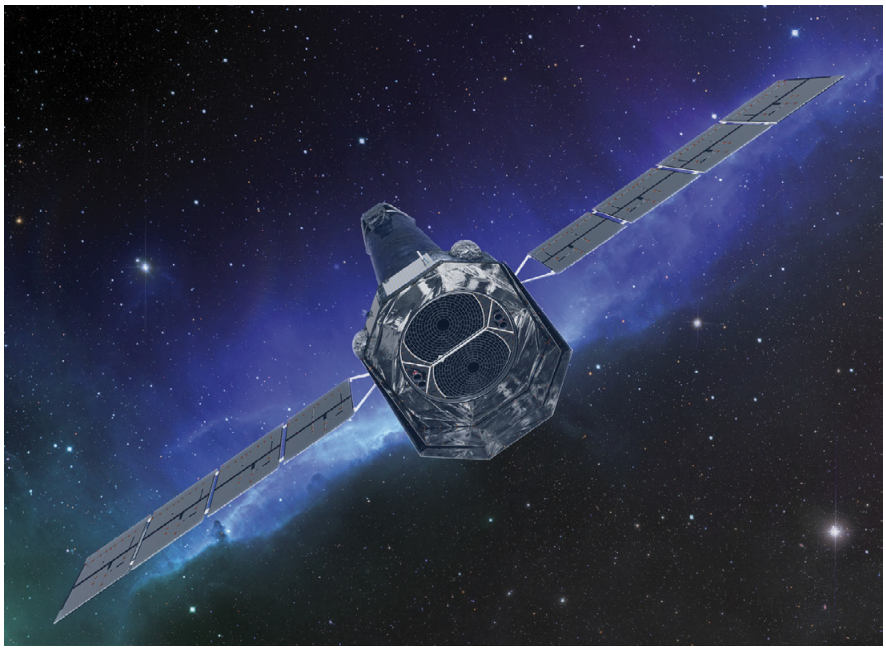

Figure 5.2.1. The ATHENA spacecraft. The two fixed telescopes can be seen at the centre, and a long 'fixed metering structure' extending to the rear would allow the 12 m focal length to be achieved.

ATHENA would be placed in orbit at L2, which will provide uninterrupted viewing and an ideal thermal environment. The design of the spacecraft assumes a five-year mission lifetime, but would carry consumables for at least 10 years. Studies by both ESA and industry have concluded that the ATHENA spacecraft can be built with mature technologies. The simpler design and technological progress will substantially reduce the estimated risk, and eliminate the need for major strategic investments from partner agencies.

Status

The instruments would be developed by ESA Member States. Although a clear path to a solely European solution had been defined, contributions from both NASA and JAXA to the XMS were baselined, particularly where their expertise would bring an improvement in Technology Readiness Level (TRL) and heritage. A Technology Development Plan is in place to improve the performance of the telescope optics towards the goal of 5 arcsec, and to ensure that TRL ≥ 5 will be achieved by the end of 2013.

5.3 JUICE

Introduction

The JUpiter ICy moon Explorer (JUICE) was an L1 candidate mission in ESA's Cosmic Vision 2015–25 programme. In April 2012, the Science Programme Committee selected JUICE as the L1 mission. JUICE is the result of the reformulation of the ESA–NASA Europa Jupiter System Mission (EJSM)–Laplace mission into a European-led concept, and is based on the original Jupiter Ganymede Orbiter – the ESA contribution to EJSM–Laplace. The JUICE mission will perform detailed investigations of Jupiter and its system in all their interrelations and complexity with particular emphasis on Ganymede as a planetary body and potential habitat. Investigations of Europa and Callisto will complete a comparative picture of the Galilean moons (Fig. 5.3.1).

JUICE builds on the outstanding heritage of past and current space missions to the outer planets. The NASA Galileo spacecraft provided the first comprehensive investigation of the Jupiter system in the footsteps of the Pioneer 10–11, Voyager 1–2 and Ulysses missions. In particular, Galileo revealed the galilean moons as unique worlds worthy of further in-depth exploration. The discovery of subsurface oceans on these moons led to the emergence of a new habitability paradigm that considers the icy satellites as potential habitats for life. Galileo also found an internal magnetic field at Ganymede, a unique feature for a planetary satellite in the Solar System. The Galileo results raised a new generation of key scientific questions related to the Jupiter system as a whole, its components and their interactions, origin, formation, evolution and, ultimately, their habitability.

Science Goals

The overarching theme of the JUICE mission has been formulated as 'The emergence of habitable worlds around gas giants'. The main science objectives for Ganymede, and to a lesser extent for Callisto, include:

- characterisation of the ocean layers and detection of putative subsurface water reservoirs;
- topographical, geological and compositional mapping of the surface;
- study of the physical properties of icy crusts;
- characterisation of the internal mass distribution, dynamics and evolution of the interiors;
- investigation of the exosphere; and
- studies of Ganymede's intrinsic magnetic field and how it interacts with the jovian magnetosphere.

For Europa, the JUICE mission will focus on the chemistry essential for life, including organic molecules, and on understanding the formation of surface features and the composition of the non-water-ice material. Furthermore, JUICE will provide the first subsurface sounding of Europa, including the first determination of the minimal thickness of the icy crust over the most recently active regions.

JUICE will perform a comprehensive investigation of the Jupiter system as an archetype for gas giants. The circulation, meteorology, chemistry and structure of Jupiter will be studied from the cloud tops to the thermosphere. These observations will be attained over a sufficiently long temporal baseline with broad latitudinal coverage to investigate evolving weather systems and

Figure 5.3.1. The JUICE spacecraft exploring the Jupiter system. (M. Carroll)

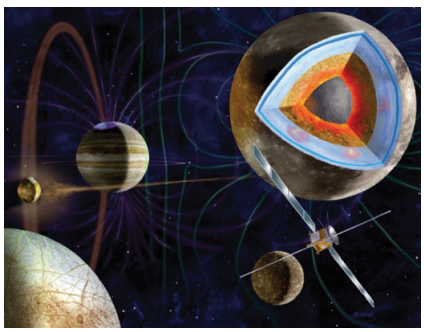

Further information about the JUICE mission can be found at *http://sci.esa.int/juice*

the mechanisms of transporting energy, momentum and material between the different layers.

The focus on Jupiter's magnetosphere will include an investigation of the three-dimensional properties of the magnetodisc and an in-depth study of coupling processes within the magnetosphere, ionosphere and thermosphere. Aurora and radio emissions and their response to the solar wind will be elucidated. Within Jupiter's satellite system, JUICE will study the moons' interactions with the magnetosphere, gravitational coupling and long-term tidal evolution of the galilean satellites. The mission investigations will help to improve mass determination, ephemerides and surface composition definition for small satellites, including possible new detections, and characterise physical and chemical properties of the ring system.

The study of the Jupiter system and its habitability has deep implications for understanding extrasolar planets and planetary systems. By performing detailed investigations of the jovian system in all its complexity, JUICE will address two key questions of ESA's Cosmic Vision programme: what are the conditions for planet formation and the emergence of life, and how does the Solar System work?

Mission Scenario, Spacecraft and Payload

The JUICE spacecraft will be launched in June 2022 on an Ariane 5 and will use several Venus and Earth gravity assists in its 7.6-year cruise to Jupiter. After orbit insertion in January 2030, the spacecraft will perform a 2.5-year tour of the jovian system focusing on continuous observations of Jupiter's atmosphere and magnetosphere (Fig. 5.3.2).

During the tour, gravity assists at Callisto will shape the trajectory to perform two targeted Europa flybys focused on composition of the non-water-ice material, and the first subsurface sounding of an icy moon. The Callisto gravity assists will also be used to raise the orbit inclination to 30° and to enable observations of Jupiter's polar regions. The Callisto flybys (13 in total) will enable unique remote observations of the moon and *in situ* measurements in its vicinity. The mission will culminate in a dedicated 8-month orbital tour around Ganymede, during which the spacecraft will perform a detailed investigation of the moon and its environment, before eventually impacting on it.

JUICE will be a 3-axis stabilised spacecraft with dry mass of about 1800 kg at launch. It will use chemical propulsion system and will be powered by 60–75 m^2 solar arrays. The high-gain antenna about 3 m in diameter will provide a downlink capability of not less than 1.4 Gbit/day. Special measures will be used to protect the spacecraft and payload from the harsh radiation environment at Jupiter.

Figure 5.3.2. Illustrative timeline for the JUICE baseline mission. The blue triangles mark perijoves and galilean moon flybys. The long blue bar at the end of the mission represents the Ganymede orbital tour. JOI = jovian orbit insertion.

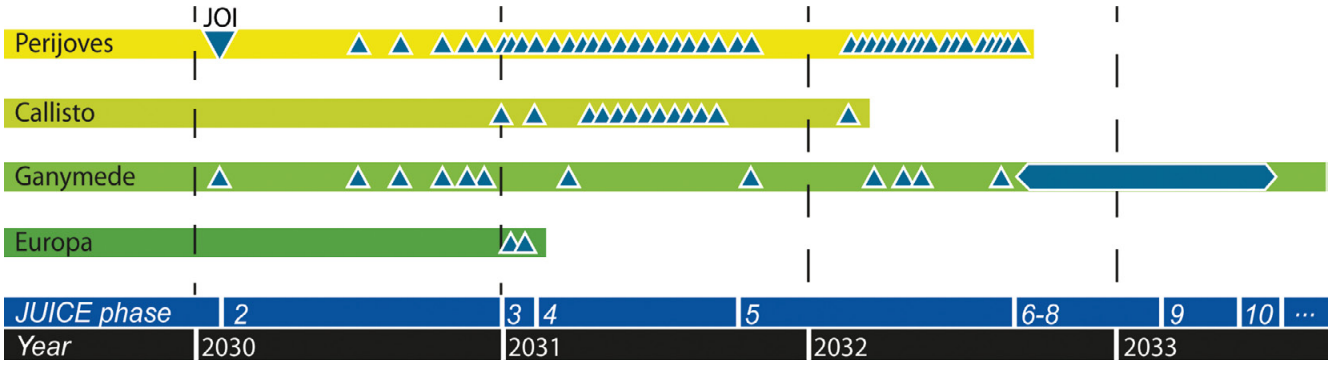

The spacecraft will carry a highly capable state-of-the-art scientific payload. The model payload, consisting of 11 instruments with total mass of ~104 kg, was identified by the ESA Science Study Team as a representative suite that will optimally address the JUICE science goals. The remote sensing package will include spectro-imaging capabilities from the ultraviolet to the near-infrared, wide- and narrow-angle cameras and a submillimetre wave instrument.

The geophysical package will include a laser altimeter and a radar sounder for exploring the surface and subsurface of Jupiter's moons. A radio science experiment will enable probing of the atmospheres of Jupiter and its satellites and measurements of the gravity fields. The model *in situ* package will comprise a magnetometer, radio and plasma wave instrument, including electric fields sensors and a Langmuir probe, complemented by a powerful particle package.

5.4 PLATO

Introduction

The PLAnetary Transits and Oscillations of stars (PLATO) mission builds on the highly successful small COROT mission (CNES/ESA/Europe/Brazil), and also on NASA's Kepler mission, but would offer more than two orders of magnitude improvement in the amount and quality of the science product.

The PLATO proposal was selected in 2008 for an assessment study as part of the ESA's Cosmic Vision 2015–25 scientific plan, and would require ESA to build and construct a satellite that can for the first time observe planetary transits of a large enough sample to:

— be statistically significant with respect to Earth-mass planets orbiting main sequence F-, G- and K-type (solar type) stars in the habitable zone;
— determine the radius and mass of both the parental star and the planet(s) orbiting it, with an accuracy of about 1%, as well as provide an age estimate of the detected exoplanetary systems to better than 10%; and
— provide a planetary mass function extending from brown dwarfs down to planets smaller than Earth.

The prime objective of the PLATO mission is to search for planetary transits (occultations) in front of stars that can be fully characterised in terms of fundamental physical parameters. This characterisation is done using the PLATO data themselves via asteroseismology, and supported from the ground using high resolution spectroscopy and some photometry. The priority is on the brighter stellar samples (even at the expense of the faint limit).

The asteroseismic data from PLATO would be needed in order to measure the stellar masses and ages, and the stars need to be relatively bright in order for PLATO to achieve the needed photometric accuracies. The stellar radius will already be known to a high degree of precision from data obtained with the Gaia spacecraft, but together with the asteroseismological data it will also allow studies of the internal structure and internal angular momentum of planet host stars to an unprecedented level. As has been shown repeatedly by NASA's Kepler spacecraft, the planetary parameters can be determined with a precision that is at least one order of magnitude higher than with any other method. Ground based high-resolution spectroscopy would be used to confirm or measure the star's fundamental parameters independently, as well as to detect and measure radial velocity variations due to the orbiting planet and to derive the planet/star mass ratio.

Mission Scenario, Spacecraft and Payload

PLATO was further selected for a definition study in late 2009. This involved two industrial contractors, as well as an outside scientific consortium led by the Observatoire de Paris, France, and eventually involving more than 215 scientists and engineers from essentially all ESA Member States.

The two spacecraft concepts studied consist of a platform on which 34 individual 120-mm telescopes of a refractive (six-element) design are mounted. Observing the same field in the sky, this construction would allow for a very large (>2500 deg^2) field of view (FOV) and, by adding the signal from each subaperture, one can also achieve a large collecting area (roughly equivalent to a single telescope with a 550 mm aperture). Two of the telescopes would be dedicated to the brightest of the stars in the sample. The mission is planned to be

Further information about the PLATO mission can be found at *http://sci.esa.int/plato*

launched on a Soyuz rocket to the L2 Lagrangian point in the Earth–Sun system. The mission is planned for an in-orbit lifetime of 6 years, extendable for several years after this.

The study progressed well and the industrial partners produced two very different but equally viable spacecraft on which to mount the telescopes. No significant problems were encountered during the study, and the results also indicated that the project could be carried out at a cost and in time for a launch in late 2018 or early 2019.

However, in the selection process carried out in early October 2011, PLATO was not selected for either the M1 or the M2 slots. The PLATO consortium was informed and the science team supporting the study was disbanded.

A joint recommendation from ESA's Astronomy Working Group and Space Science Advisory Committee proposed that PLATO should be brought into synchronisation with the M3 mission launch opportunity within the Cosmic Vision 2015–25 programme. As a consequence, ESA issued a letter soliciting a proposal from the PLATO consortium, detailing what this process would entail, and planning for a launch in 2024. During the consortium's discussions on how to respond to this positively, they had to judge if the PLATO science case would remain viable in 2024.

A decision on whether or not PLATO will enter the M3 competion is expected by mid-2012.

5.5 SPICA

Introduction

The Space Infrared Telescope for Cosmology and Astrophysics (SPICA) is a JAXA-led observatory that will operate in the mid- and far-infrared (MIR, FIR) wavelength range (5–210 μm). It will have unprecedented sensitivity, thanks to its cold (<6K), 3.0 m-class telescope and suite of advanced instruments. The combination of a new generation of high-sensitivity detectors and the low telescope temperature will enable sky-limited sensitivity over the ~35–210 μm band for the first time. SPICA will not only be one (spectroscopy) and two (photometry) orders of magnitude more sensitive than Herschel in the far-infrared band, but will also cover the missing 28–55 μm octave that is out of reach of both Herschel and the James Webb Space Telescope. SPICA will bridge the wavelengths covered by the JWST and the Atacama Large Millimeter Array (ALMA) with an observatory that is open to the worldwide community.

The SPICA waveband plays host to an extensive range of spectral features and photometric signatures that provide a unique view of the gaseous and dusty, often heavily obscured environments in which galaxies, stars and planets first form and subsequently evolve.

Science Goals

MIR and FIR fine-structure lines, and ratios thereof, provide the means by which to differentiate between gas excited by star formation and by accretion onto supermassive black holes, the two most energetic processes driving galaxy evolution. These line diagnostics are significantly less attenuated by dust than equivalents in the optical and near-IR, and can be detected to redshifts of ~1 in normal galaxies, and beyond (to $z \approx 3$) for luminous and ultraluminous infrared galaxies. Deep spectroscopic surveys with SPICA will reveal for the first time the interplay between star formation and mass accretion and its evolution with redshift, and as well as influences of the environment such as clustering.

The combination of sensitive FIR photometry with spectroscopic tracers of atomic/ionic and molecular gas, and solid state features from ice and magnesium-rich silicates, also provides a robust approach by which to determine the conditions under which planetary systems form. Locally, SPICA will significantly enhance our understanding of the formation and evolution of the Solar System by characterising outer Kuiper Belt objects as well as inner, hotter centaurs, comets and asteroids – determining the sizes, albedos, masses, surface conditions and distributions of different families of Solar System object, identifying mineral species and ices and establishing chemical composition.

The same spectroscopic tools will be used to trace the key chemical species and mineral components of hundreds of young protoplanetary discs in different star-forming regions at the time when planets form. They will also enable the first unbiased survey of dusty debris discs, searching for presence of zodiacal clouds and Kuiper belts in hundreds of exoplanetary systems around all stellar types, thus putting our own Solar System into a broader context.

SPICA will provide a unique view of young, giant gaseous exoplanets found in the outer regions of exoplanetary systems through direct imaging and low-resolution spectroscopy. Using MIR spectral signatures of molecules such as H_2O, CH_4, NH_3, CO and CO_2, it will be possible not only to establish the current chemical and physical conditions of the exoplanet atmospheres, but also to start to constrain both the history and the mechanisms of formation of the exoplanets themselves.

Further information about the SPICA mission can be found at *http://sci.esa.int/spica*

Mission Scenario, Spacecraft and Payload

A proposal for an ESA contribution to the 3-year (goal 5 years) SPICA mission was selected in October 2007 as a candidate M-class mission for ESA's Cosmic Vision 2015–25 programme, with the character of a 'mission of opportunity'. The contribution from ESA comprised the telescope assembly, provision of a European science ground segment and ground station support from the European Space Operations Centre in Darmstadt, Germany, and the interface management to JAXA of the European SPICA FAR-infrared Imaging instrument, SAFARI.

The three principal instruments in the scientific payload of SPICA will include:

— Mid-infrared Camera and Spectrometer (MCS), a combined spectrometer and imaging photometer. The WCS (Wide Field Camera) subinstrument will cover the 5–25 (S) and 20–38 (L) μm wavebands over fields of view of 5′ × 5′ in wideband photometry, with a filter wheel providing a range of broad (R ≈ 5–10)/narrowband (R ≈ 50) filters. Three spectroscopic modes are under consideration: high resolution, HRS (R ≈ 20–30 000) covering either 4–8/12–18 μm with slit lengths/widths of 3.5′ × 0.72′/6′ × 1.2′, respectively; medium resolution, MRS (R ≈ 1 to a few 1000s) covering 12.2–23.5/23–38 μm with slit lengths/widths of 12′ × 1.2′/2.5′ respectively, and an integral field unit providing ×5/×3 larger fields of view; and low-resolution, LRS (R ≈ 50–100) covering the (S)/(L) wavebands with slit length/widths of 2.5′ × 2.66′/1.4′.

— SPICA Coronographic Instrument (SCI), a mid-infrared coronograph, covering 5 μm (goal 3.5 μm) to 27 μm, with a resolving power of R ≈ 5–200, a baseline contrast of 10^{-4} (post-processing, 10^{-5}) and goal of 10^{-6}, and an inner/outer working angle of 2.2′ ($3.5l/D_{telescope}$)/10′ at 10 μm. The instrument also has a non-coronagraphic mode that will be used for transit spectroscopy.

— SPICA FAR-infrared Instrument (SAFARI), an imaging Fourier transform spectrometer with instantaneous and continuous spectral coverage (~35–210 μm), and variable resolving power (R ≈ 3/photometric to R ≈ 2000 at 100 μm) over a field of view of 2′ × 2′.

Two additional instruments are also under consideration: the scientific channel of the focal plane camera (provided by Korea), which will provide a NIR capability (photometry/wideband + linear variable filters) over a 5′ × 5′ field of view, and a far-infrared/submillimetre spectrometer optimised for observations of point sources and proposed by the US community.

SAFARI is under development by a consortium of institutes and universities in ESA member states, led by the Space Research Organisation Netherlands (SRON), with contributions from Canada and Japan. Significant progress has been made with the SAFARI design activities since the completion of the assessment phase in 2009.

A major milestone was the selection of the Transition-Edge Sensor (TES) detectors (transition edge sensor bolometers) in June 2010. These were selected from four candidates and are seen to be the only technology able to meet the stringent sensitivity requirements (goal 2×10^{-19} W Hz$^{-1/2}$) within the development schedule of SPICA. The detectors are being developed under an ESA Technology Research Programme (TRP) activity and at detector level are currently within a factor of 2.5 of the goal sensitivity. The detector array needs to be cooled to 50mK: the cooler ensemble comprising a ^{3}He sorption cooler (already developed and flown on Herschel) and a two-stage 50mK Adiabatic Demagnetisation Refrigerator (ADR) has already been demonstrated to breadboard level under a separate ESA TRP.

The baseline design of the instrument is converging: the front-end optical design is well established and a detector readout system featuring frequency

division multiplexing (FDM) has been validated with a 57-channel demonstrator. The conceptual design reviews at subsystem and system level are planned for 2012, with the detector system review having commenced in February 2012.

Status

At JAXA, SPICA has been in the pre-project phase (approximately equivalent to ESA's Phase-A) since July 2008. SPICA will enter the Risk Mitigation Phase in 2012 (similar to ESA's Phase-B1). This will be followed by the System Definition Review and Project Phase-up Review, both of which are expected to be carried out in 2013.

At ESA, SPICA is in an extended assessment/definition phase, with the decision on whether to adopt SPICA into the science programme to be taken on a timescale that is in line with JAXA's decision to adopt SPICA.

5.6 Euclid

Introduction

Euclid was proposed in 2007 as a candidate M-class mission in ESA's Cosmic Vision programme 2015–25 and, after study and definition phases, was selected for the M2 slot in 2011.

Euclid is designed to make accurate measurements of the expansion history of the Universe and the growth of cosmic structures using a large-area optical and near-infrared imaging survey and a massive spectroscopic survey in the wavelength range 1.1–2.0 μm. The mission will yield comprehensive maps of the Universe, tracing the distribution of both its luminous and dark components over more than one-third of the sky and out to epochs when the Universe was less than 3 billion years old. The statistical properties of these distributions will also constrain properties of dark matter, including the contribution from neutrinos.

Euclid is unique in the combination of its two primary dark energy probes, namely weak gravitational lensing and galaxy clustering. They will not only allow the experiment to reach unprecedented statistical precision, but will provide a crucial cross-check of systematic effects, which become dominant at these levels of precision. The mission will address the following key questions:

— *Dynamical dark energy*. Is the dark energy simply a cosmological constant, or is it a field that evolves dynamically with the expansion of the Universe?

— *Modification of gravity*. Alternatively, is the apparent acceleration instead a manifestation of a breakdown of General Relativity on the largest scales, or a failure of the cosmological assumptions of homogeneity and isotropy?

— *Dark matter*. What is dark matter? What is the absolute neutrino mass scale and what is the number of relativistic species in the Universe?

— *Initial conditions*. What is the power spectrum of primordial density fluctuations, which seeded large-scale structure, and are they described by a Gaussian probability distribution?

The last question will help to improve our understanding of the physics that caused inflation, the first period of accelerated expansion when the Universe was only a fraction of a second old. Euclid will complement the high-redshift picture of cosmology from the Planck mission by completing our census of the Universe at lower redshifts.

Beyond the foreseen breakthroughs in fundamental cosmology, the Euclid surveys will yield unique legacy science in various fields of astrophysics. In the area of galaxy evolution and formation, Euclid will deliver high-quality morphologies, masses, and star formation rates for billions of galaxies out to a redshift of $z \approx 2$, over the entire extragalactic sky, with a resolution four times better and three NIR magnitude fainter than ground-based surveys. The Euclid deep survey will probe the 'dark ages' of galaxy formation as it is predicted to find thousands of galaxies at $z > 6$, of which about 100 could be at $z > 10$; in other words, Euclid will probe the era of reionisation of the Universe. With Euclid, the majority of the new sources identified by future imaging observatories, from radio to X-rays, will be readily associated with a known redshift, out to a redshift of $z \approx 2$.

Further information about the Euclid mission can be found at *http://sci.esa.int/euclid*

Mission

Weak gravitational lensing requires a high image quality to perform accurate shear measurements, while galaxy clustering requires near-infrared spectroscopic capability to measure galaxies at redshifts $z > 0.7$. Both dark energy probes demand a very high degree of system stability in order to minimise systematic effects, and the ability to survey the entire extragalactic sky. Such a combination of requirements cannot be met from the ground, and demands a wide-field visible/near-infrared space mission. Central design drivers for Euclid are the need for tight control of systematic effects in space-based conditions and simultaneous measurements of weak gravitational lensing and galaxy clustering.

Euclid will be launched in 2019 on a Soyuz ST-2.1B rocket, with an all-year round launch window. A direct transfer of ~30 days is targeted to a large-amplitude free-insertion orbit at the L2 Lagrangian point of the Sun–Earth system, which will ensure stable thermal and observing conditions. It will take six years to complete a wide survey with the deep survey interspersed. Spacecraft commissioning, performance verification and initial calibration will require an additional 3–6 months. The sky mapping mode is step and stare. Image stability is maintained by scanning the sky along circles of nearly constant solar aspect angle. At least one ground station is available to receive the science data from the spacecraft at a rate of at most 850 Gbit over a daily pass time of 4 h.

The wide survey will cover 15 000 deg^2 of the extragalactic sky and is complemented by two 20 deg^2 deep fields observed on a monthly basis. For weak lensing, Euclid will measure the shapes of 30 resolved galaxies per $arcmin^2$ in one broad visible band (550–900 nm) down to AB mag 24.5 (10σ). The photometric redshifts for these galaxies reach a precision of $\sigma_z/(1 + z) < 0.05$. They are derived from three additional Euclid near-infrared bands (Y, J, H in the range 0.92–2.0 µm) reaching AB mag 24 (5σ) in each, complemented by ground-based photometry in visible bands.

To measure the shear from galaxy ellipticities, requirements are imposed on the point spread function such that it can be reconstructed with an error of $\leq 2\times10^{-4}$ in ellipticity and its dimension varies by less than 2×10^{-3} across the field of view. Galaxy clustering is determined from a spectroscopic survey with a redshift accuracy of $\sigma_z/(1 + z) \leq 0.001$. The slitless spectrometer, with $\lambda/\Delta\lambda \approx 250$, detects predominantly Hα emission line galaxies. The limiting line flux is 3×10^{-16} erg s^{-1} cm^{-2} (1 arcsec extended source, 3.5σ at 1.6 µm), yielding over 50 million galaxy redshifts with a completeness greater than 45%.

The deep survey will be two magnitudes deeper than the wide survey. This is needed for calibration of the slitless spectroscopy and is also unique as a self-standing survey. The deep survey will monitor the stability of the spacecraft and payload through repeated visits of the same regions.

Payload

The Euclid payload consists of a 1.2 m Korsch telescope designed to provide a large field of view. The telescope directs the light to two instruments via a dichroic filter placed in the exit pupil. The reflected light is led to the visual instrument (VIS) and the transmitted light from the dichroic feeds the near-infrared instrument (NISP) which contains a slitless spectrometer and a three-band photometer. Both instruments cover a common field of view of ~0.54 deg^2.

VIS is equipped with 36 CCDs. It measures the shapes of galaxies with a resolution better than 0.2 arcsec (PSF FWHM) with 0.1 arcsec pixels in one wide visible band (R + I + Z). The NISP photometer contains three NIR bands (Y, J, H), employing 16 HgCdTe NIR detectors with 0.3 arcsec pixels. The spectroscopic channel of NISP operates in the wavelength range 1.1–2.0 µm

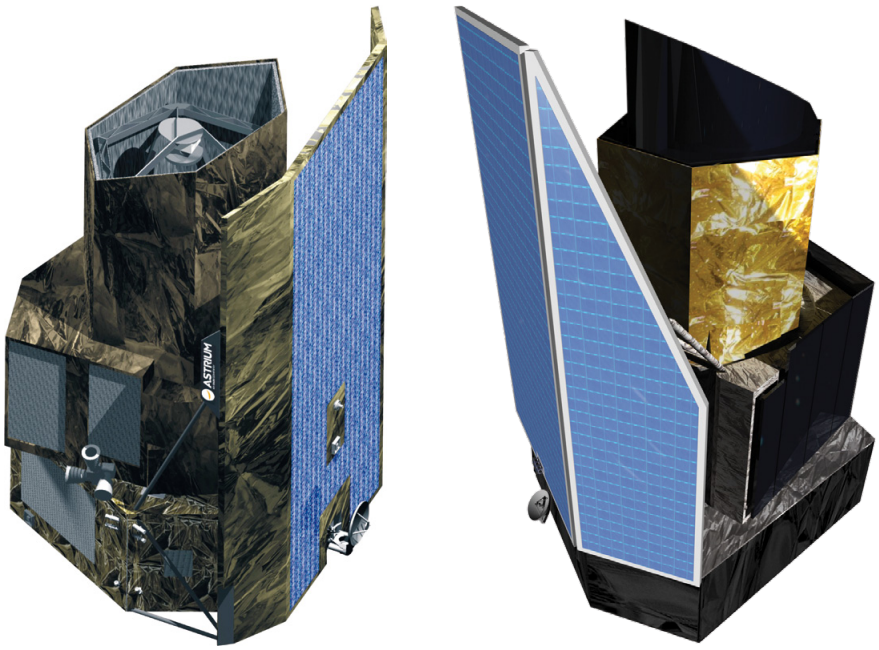

Figure 5.6.1. Designs of the Euclid spacecraft by Astrium (*left*) and by Thales Alenia Space (*right*) considered in the Phase-A studies.

at a mean spectral resolution $\lambda/\Delta\lambda \approx 250$, employing 0.3 arcsec pixels. While the VIS and NISP operate in parallel, the NISP performs the spectroscopy and photometry measurements in sequence by selecting a grism wheel in case of spectroscopy and a filter wheel in case of photometry.

Status

The Euclid Phase-A study was completed at the end of 2011 (Fig. 5.6.1). The adoption of the mission is foreseen for mid-2012, marking the end of the definition phase and the start of the implementation phase. For the space segment, ESA will provide the spacecraft and telescope through a selected industrial contractor, as well as the CCD and NIR detectors. A minor contribution from NASA towards the provision of the NIR detectors is also foreseen, subject to approval of a Memorandum of Understanding in mid-2012. The Euclid Mission Consortium (EMC), funded by national agencies, has been selected to provide the VIS and NISP instruments, and elements of the science ground segment (SGS) related to the scientific pipelines for generating the data products and the instrument in-orbit maintenance and operations.

The EMC is composed of about 800 members, including about 450 researchers, spread over 15 countries, most of them ESA member states, and over 100 institutes. The EMC is organised to support the instrument development, assessment of scientific requirements and performance, and the SGS. Together with ESA, the consortium has worked out the SGS operations concept, which has led to an agreed set of science implementation requirements for the SGS. The implementation encompasses the definition of tasks and interfaces of the science data centres and the architecture of the SGS that includes operation of the mission and the legacy archives.

5.7 MarcoPolo-R

Introduction

MarcoPolo-R is a candidate asteroid sample return mission. It was proposed for the M3 launch slot of ESA's Cosmic Vision programme and was selected as one of four candidate missions for a feasibility study. It is a follow-up of the original MarcoPolo proposal, which was studied for the M1/M2 launch slot but was not selected after the initial study phase. The main reason was that the cost was higher than the allocation. In the new proposal, the cost was reduced and US participation was proposed.

The MarcoPolo-R mission should answer a number of scientific questions:

— the processes that occurred in the early Solar System and accompanying planet formation;
— the physical properties and evolution of the building blocks of the terrestrial planets;
— whether near-Earth asteroids of primitive classes contain pre-solar material as yet unknown in meteoritic samples; and
— the nature and origin of organics in primitive asteroids and whether can they shed light on the origin of molecules necessary for life.

These questions will be addressed by analysing the material of a near-Earth object in the laboratory. As a target, the requirement is to go to a primitive asteroid, which means a low-albedo object of spectral types B, C, D, P or T according to the standard taxonomic asteroid classifications. The current baseline target is the binary asteroid 1996 FG3.

Configuration

The MarcoPolo-R spacecraft configuration was studied in an ESA internal study using its Concurrent Design Facility (CDF). The design assumes a spacecraft that will be launched on a Soyuz 2.1b/Fregat M from Kourou, French Guiana (Fig. 5.7.1). The most cost-effective solution found is based on using solar-electric propulsion. The spacecraft platform is based on the reuse of the Small GEO platform.

The baseline mission would be launched in April 2021 (backup February 2023) and reach the asteroid via two Venus swingbys (backup: no swingby). The return transfer would require an Earth swingby (Venus for the backup). Earth arrival would be in January 2029 (backup: March 2030). The spacecraft would be 1.9 × 2 × 3 m in size with a solar array wingspan of 12 m and a dry mass of about 1.2 t.

The sample would be acquired by a 'touch & go' scenario, which means that the spacecraft does not land on the asteroid. To put the returned sample in context, a small remote-sensing payload is foreseen, consisting mainly of cameras and IR/near-IR spectrometers to characterise the target body.

The sample will be returned in an Earth Reentry Capsule that would perform a passive entry into Earth's atmosphere. The capsule is designed such that it does not use a parachute; the landing shock will be dampened by crushable material.

Figure 5.7.1. The MarcoPolo-R concept as designed in ESA's internal CDF study, in the Soyuz fairing.

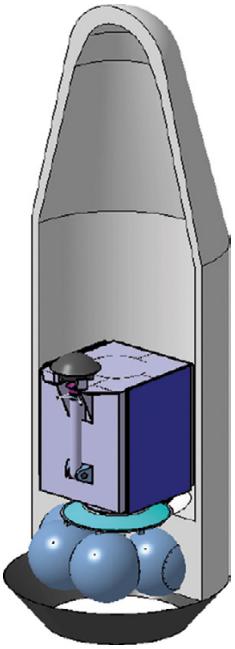

Further information about the MarcoPolo-R mission can be found at *http://sci.esa.int/marcopolo-r*

Status

The current study focuses on reducing the costs as much as possible, to be within the cost cap of the mission. The CDF study has shown that this is possible in many areas. Just to give two examples: the landing accuracy requirement was relaxed, resulting in a much simpler guidance and control system, and the touch and go sampling means that no landing legs will be required.

The mission will be further assessed in the industrial studies that began in early 2012 ahead of a downselection in 2013 and the start of a definition phase.

5.8 STE-QUEST

Introduction

The Space–Time Explorer and Quantum Equivalence Space Test (STE-QUEST) has been selected as one of the four candidate missions for the M3 slot in ESA's Cosmic Vision programme and is under study.

Einstein's theory of General Relativity is a cornerstone of our current understanding of the physical world. It is used to describe the flow of time in the presence of gravity, the motion of bodies from satellites to galaxy clusters, the propagation of electromagnetic waves in the presence of massive bodies, and the dynamics of the Universe as a whole. The measurement of general relativistic effects is very challenging, owing to their small size.

Although very successful so far, General Relativity, as well as numerous alternative or more general theories of gravitation, are classical theories. As such, they are fundamentally incomplete, because they do not include quantum effects. A theory that resolves this problem would represent a crucial step towards the unification of all fundamental forces of nature. Therefore, a full understanding of gravity will require observations or experiments able to determine the relationship of gravity with the quantum world. This topic is a prominent field of activity and includes the current studies of dark energy.

The STE-QUEST mission is designed to test the different aspects of Einstein's Equivalence Principle with quantum sensors.

Science Goals

The three main science goals of STE-QUEST are summarised in Table 5.8.1.

STE-QUEST also has applications in areas of research other than fundamental physics, such as time and frequency metrology, relativistic geodesy, cold-atom physics and matter-wave interferometry in weightlessness conditions, and optical and microwave ranging.

Payload

The satellite payload consists of two instruments: a cold-atom clock of highest performance and a differential atom interferometer.

The clock is derived from the microwave standard PHARAO (Projet d'Horloge Atomique par Refroidissement d'Atomes en Orbit), which is also the core instrument of the Atomic Clock Ensemble in Space (ACES) mission.

Scientific Objective	Target accuracy
Gravitational redshift tests	
Earth gravitational redshift	Measurement of Earth's gravitational redshift to a fractional frequency uncertainty better than 2×10^{-7}.
Sun gravitational redshift	Measurement of the Sun gravitational redshift to a fractional frequency uncertainty better than 6×10^{-7}.
Weak Equivalence Principle tests	
Universality of propagation of matter waves	Test the universality of the free propagation of matter waves to an uncertainty in the Eötvös parameter better than 1×10^{-15}.

Table 5.8.1. STE-QUEST primary mission objectives.

Further information about the STE-QUEST mission can be found at *http://sci.esa.int/ste-quest*

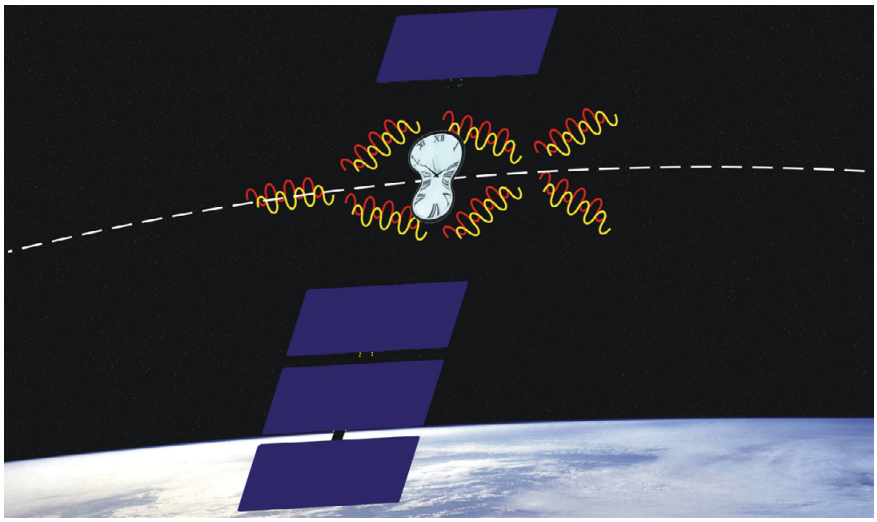

Figure 5.8.1. STE-QUEST.

The performance of the clock has been improved compared with the current implementation for ACES by an optically derived ultrapure microwave signal (Microwave–Optical Local Oscillator, MOLO) and by using the more favourable atomic species rubidium (PHARAO-Rb) rather than caesium. During the mission, the tick rate of the space clock will be nearly continuously compared with atomic clocks on Earth using precise microwave frequency transfer methods similar to those developed for the ACES mission (MWL), as well as using a laser coherent link based on the Laser Communication Terminal technology in use by ESA.

The differential atom interferometer will compare the free propagation of the coherent matter waves of the two rubidium isotopes (^{85}Rb and ^{87}Rb) under the influence of Earth's gravity. The use of ultracold matter close or down to quantum degeneracy (coherent atomic sources) and the long interrogation times possible in a freely falling laboratory will make it possible to go far beyond the current measurement accuracy.

Orbit and Measurement Strategy

The nature of the tests conducted by STE-QUEST requires a highly elliptical orbit with large variations in the gravitational potential, long contact times at perigee and long common-view durations from different continents.

Orbits with a 16 h period, a minimum perigee altitude of ~600 km and ~51 000 km of apogee altitude are being studied.

The ground track of the STE-QUEST orbit can be varied to maximise the visibilities at the STE-QUEST ground stations, which could possibly be located in Boulder (US), Turin (Italy) and Tokyo (Japan). These locations are particularly favourable because of their geographical position and their proximity to research laboratories operating highly stable and accurate atomic clocks.

The primary data product of the STE-QUEST mission will include

- space-to-ground comparisons between the STE-QUEST onboard clock and clocks on the ground; and
- atom interferometry measurements of the differential acceleration between ultracold samples of ^{85}Rb and ^{87}Rb.

Space-to-ground clock comparisons will be performed all along the orbit, in particular while the STE-QUEST spacecraft is orbiting around apogee and perigee. In this way, Einstein's prediction of the gravitational frequency shift will be verified both by an absolute measurement between space and ground

clocks, and by looking at the modulation of the redshift effect on the STE-QUEST clock between perigee and apogee. The STE-QUEST links will also allow a common-view comparison of terrestrial clocks. Common-view comparisons are used to measure the periodic effect of the gravitational frequency shift induced by the Sun.

The atom interferometer will perform differential acceleration measurements while the spacecraft is orbiting around perigee (spacecraft altitude below 3000 km), thus maximising the signal-to-noise ratio of an eventual violation of the Weak Equivalence Principle.

Status

The STE-QUEST assessment phase started in April 2011 and will be concluded in 2013.

STE-QUEST went through an internal study by the ESA Concurrent Design Facility in May 2011. The study concluded with the identification of a preliminary design of the STE-QUEST mission and its payload.

The industrial activities will have a typical duration of about 1 year. In parallel, studies of the STE-QUEST instruments will be carried out by consortia of scientific institutes selected by ESA through an open call and financially supported by ESA member states.

5.9 LOFT

Introduction

The Large (X-ray) Observing Facility for Timing (LOFT) has been selected as one of the four candidate missions for the M3 slot in the Cosmic Vision programme and is under study.

High-time-resolution X-ray observations of compact objects (galactic and extragalactic black holes and neutron stars) provide a unique tool to investigate strong-field gravity, as well as to measure black hole masses and spins, and the equation of state of ultradense matter. LOFT is specifically designed to exploit the diagnostics of very rapid X-ray flux and spectral variability that directly probe the motion of matter down to distances very close to these objects. In addition, LOFT will be a powerful tool for studying the X-ray variability and spectra of a wide range of objects, from accreting pulsars and bursters, to magnetar candidates (anomalous X-ray pulsars and soft gamma repeaters), cataclysmic variables, bright Active Galactic Nuclei, X-ray transients and the early afterglows of gamma-ray bursts. Through these studies it will be possible to address a variety of problems in the physics of these objects.

Mission Scenario, Spacecraft and Payload

An internal ESA study was conducted to confirm a technical approach that is feasible within the cost and technical constraints of the Cosmic Vision 'M-class' missions. This is now being followed by parallel competitive studies by two industry teams, leading to independent technical and peer science reviews to conclude the assessment.

LOFT will improve by a factor ~20 on the largest area X-ray instrument ever flown (the Rossi X-ray Timing Explorer's Proportional Counter Array, RXTE/PCA). The LOFT Large Area Detector (LAD; Fig. 5.9.1) also offers much improved energy resolution (better than 260 eV) that will allow the simultaneous exploitation of spectral diagnostics, in particular the relativistically broadened 6–7 keV Fe K lines. The LOFT scientific payload is completed by a coded-mask Wide Field Monitor (WFM), which will discover and localise X-ray transients and impulsive events and monitor spectral state changes with unprecedented sensitivity, triggering follow-up pointed observations and constituting an important resource in its own right.

The LOFT LAD covers a geometric area of ~20 m^2 with relatively low mass, employing large-area Silicon Drift Detectors (SDDs) designed on the heritage of the ALICE experiment at CERN's Large Hadron Collider, and a collimator based on lead-glass microcapillary plates. The detector drift concept makes the spectroscopic performance of the SDDs weakly dependent on the extent of the collecting surface: large-area (~70 cm^2) monolithic detectors can be designed, with only 256 readout anodes (thus low power requirements, ~60 W m^{-2}) but very good spectral performance. An unprecedentedly large throughput (~3×10^5 counts/s from the Crab Nebula) is achieved with a segmented detector, minimising the effects of pile-up and dead-time, which often limit focused experiments. The Wide Field Monitor, using the same type of detectors, will monitor a large fraction of the sky potentially accessible to LAD, to provide the history and context for the sources observed by LAD and trigger observations of their most interesting and extreme states.

The nominal operations assume a typical selected target will be observed by the LAD for some tens of kiloseconds. Due to Earth occultations in low-Earth orbit, depending on the source direction, it might be visible for <50%

Figure 5.9.1. The LOFT spacecraft with solar panels (blue) and Large Area Detector (pink) deployed. (S. Mangunsong/AOES)

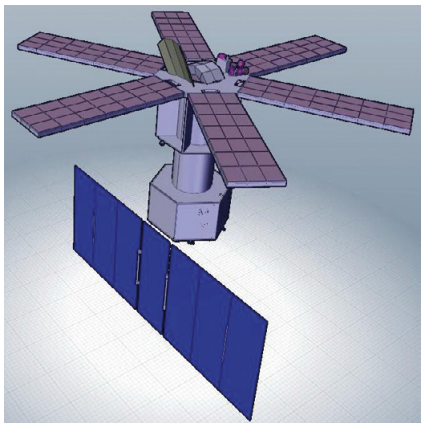

Further information about the LOFT mission can be found at *http://sci.esa.int/loft*

of each orbit, and therefore some slews between targets may occur each orbit. Otherwise, targets will be selected nearer the orbit poles for increased observing efficiency. The WFM will continuously scan a contiguous large area of sky for potential Targets of Opportunity, such as bright flares, from other sources. Following the alert of the Science Operations Centre, the spacecraft may slew within 8 h to the newly identified target.

5.10 EChO

Introduction

The Exoplanet Characterisation Observatory (EChO) is a dedicated mission to study the atmosphere of exoplanets. As part of ESA's Cosmic Vision 2015–25 programme, it is one of four medium (M-) class missions under assessment at ESA and is competing for the M3 slot in 2022–24.

EChO will exploit the technique of transit spectroscopy. By differencing the light originating from spatially unresolved observations of an exoplanet and its host star at different points in the planetary orbit, EChO will provide an unprecedented view of the atmospheres of exoplanets transiting nearby stars, measuring atmospheric transmission, reflection and emission spectra over a continuous wavelength range that spans 0.4–11 µm (goal 16 µm). This broad spectral coverage will provide access to an extensive range of spectral features from many key molecules that can be used to study the atmospheres of exoplanets covering a range of masses and physical temperatures. With coverage in the optical as well as in the near- and thermal-infrared, it will be possible to distinguish between changes in the combined host star + exoplanet signal that result from the change in exoplanet signal contribution as it moves around its orbit, and those due to the intrinsic variability in the output of the host star.

EChO will target a sample of ~100 exoplanets that cover a range of radii (Jupiter-class gas giants down to super-Earths) and temperatures (from a few 1000K down to a more temperate few 100K) orbiting a variety of host stars (of stellar types F, G, K and M). Through detailed measurements of the spectral energy distribution and spectral emission from molecules such as water, carbon monoxide, carbon dioxide, methane and ammonia, it will be possible to establish many critical atmospheric parameters, including chemical composition and abundances, energy budgets, thermal structure and, potentially, temporal and spatial variations in atmospheric structure. By considering properties over the sample as a whole, it will be possible not only to characterise the physics and chemistry of individual exoplanetary atmospheres, but also to start to determine the mechanisms that drive the formation of exoplanets themselves.

Through measurements of repeated transits, EChO will have the sensitivity to detect key spectral features in the atmospheres of hot Jupiter-like planets, and also of more temperate 'super-Earths' that are expected to be found around M-dwarfs. This offers the tantalising possibility of studying the habitable zones of planetary systems that are close cousins of our own Solar System.

Scientific Payload

The scientific payload of EChO will comprise a multichannel spectrometer with continuous and instantaneous spectral coverage over the 0.4–11 µm (goal 16 µm) waveband. The goal is to achieve a sensitivity that is limited only by astronomical noise (i.e. photon noise from the host star and/or zodiacal light). A resolving power of $R \approx 300$ or better will be required at wavelengths below 5 µm and $R \approx 30$ (goal $R \approx 300$) for wavelengths above 5 µm. In the current design, the spectrometer will be fed by a Cassegrain telescope that is diffraction-limited at visible wavelengths. The primary mirror has an entrance pupil diameter of 1.26 m (effective focal length of ~10.7 m), providing a collecting area of ~1.1 m^2 (Fig. 5.10.1).

Further information about the EChO mission can be found at *http://sci.esa.int/echo*

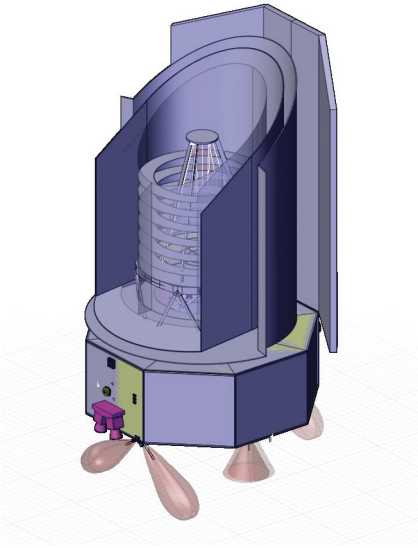

Figure 5.10.1. The ESA EChO CDF reference spacecraft. Passive cooling of the payload module down to ~45K will be achieved with a sunshield, two thermal shields and a telescope baffle.

EChO will be launched into a direct transfer orbit on a Soyuz MT Fregat from Europe's spaceport in Kourou, French Guiana. Its final orbit will be an eclipse-free, large-amplitude quasi-halo orbit around the Sun–Earth L2 point. This will provide an environment that is benign with regard to radiation exposure and, crucially for the photometric stability of EChO, is also thermally stable. The proposed orbit has the added benefits of being eclipse-free (Earth and Moon), and of offering instantaneous visibility of a large number of EChO targets at any one time.

Status

An internal ESA study was undertaken in mid-2011 at the Concurrent Design Facility at ESTEC to confirm a mission concept that is technically feasible within the programmatic constraints of the Cosmic Vision programme. The requirement of high photometric stability was identified as the most demanding, placing stringent constraints at the system level, including on pointing and thermal stability.

Two competitive, system-level studies of the mission by industry will run through 2012. Two studies of the scientific payload by consortia of research institutes and universities are also under way. Independent technical and scientific reviews of the mission will be carried out at the end of these studies in 2013.

5.11 Mars Network Science

Introduction

The Mars Network Science Mission (MNSM) is being studied within ESA's Mars Robotic Exploration Programme as a candidate mission together with a Martian Moon Sample Return (MMSR) mission. The selected mission would be a technological precursor to a Mars sample return mission in the 2020s. A Science Definition Team was formed in spring 2011 to define the top-level science goals and detailed science requirements for a first internal ESA study. Later, the candidate mission selected by the Human Spaceflight, Microgravity and Exploration Programme would further evolve into a more detailed industrial Phase-A study.

The proposed MNSM would focus on the early Mars, providing essential constraints on geophysical, geochemical and geological models of the evolution of Mars, and contributing to a better understanding of SNC meteorites and future returned martian samples. Measurements of the seismology, geodesy, magnetic field and surface heat flow would reveal the internal structure, activity and composition of Mars, its thermal structure and its magnetic evolution. Meteorological surface measurements would allow the monitoring of the atmospheric dynamics at the boundary layer (coupled with orbital measurements) to infer the climate patterns. Such a mission may also provide important insights into the astrobiological conditions on Mars, in particular its magnetic field, heat flow and climate evolution.

Configuration

Such a Mars Network Science Mission has been considered a significant priority by the planetary science community worldwide for the past two decades. In fact, a Mars Network mission concept has a long heritage, as it was studied a number of times by ESA, NASA and CNES (e.g. Marsnet, InterMarsNet, NetLander and MarsNEXT mission studies) since 1990. The current mission baseline includes three ESA-led small landers, each with a robotic arm, to be launched with a Soyuz rocket and with direct communications to Earth (no need for a dedicated orbiter). However, a larger network could be put in place through international collaboration, as several partners have expressed an interest in participating (e.g. Japan, Russia and China). Also, NASA's 2016 Gravity and Extreme Magnetism Small Mission Explorer (GEMS) one-station mission could be a very valuable precursor for MNSM, if selected as NASA's next Discovery mission.

Status

An internal ESA study, performed at its Concurrent Design Facility, concluded in December 2011 that the mission design is feasible and within an appropriate budgetary envelope. Together with the results of the MMSR mission and two other industrial studies (Mars precision landing and Mars Sample Return orbiter) the results have been presented to ESA's advisory structure. A decision on whether and how to continue this study is expected in mid-2012.

MNSM is a unique tool to perform new investigations of Mars, which could not be addressed by any other means. It would fill a longstanding gap in the scientific exploration of the Solar System by performing *in situ* investigations of the interior of an Earth-like planet other than our own and provide unique and critical information about the fundamental processes of terrestrial planetary formation and evolution. The long-term goal of Mars robotic exploration in Europe remains the return of rock, soil and atmospheric samples from the martian surface before humans explore the planet, but the Mars Network would provide the context in which the returned samples should be interpreted.

5.12 Martian Moon Sample Return

Introduction

The Martian Moon Sample Return mission aims to obtain and return a sample from one of the martian moons, Phobos. The mission is being studied within ESA's Mars Robotic Exploration Programme as a possible follow-up mission for the post-2018 period.

The design of the MMSR mission is heavily based on the experience gained with the MarcoPolo and MarcoPolo-R mission studies and is performed in parallel with the Mars Network Science Mission. A Science Definition Team was formed in spring 2011 to define the top-level science goals and detailed science requirements for a first internal ESA study. Later, if deemed interesting by the Human Spaceflight, Microgravity and Exploration Programme Board, the mission could be developed further in a more detailed industrial study.

Scientific Questions

Since the mission is part of the Mars Robotic Exploration Programme, it should act as a technological precursor to a Mars sample return mission. While the main aim would be to demonstrate the handling and return of a sample, a science justification is an important element of the mission. The Science Definition Team defined the top-level science goal for this mission as to 'understand the formation of the martian moons Phobos and Deimos and put constraints on the evolution of the Solar System'.

Currently, there are several possible scenarios to explain the formation of the martian moons: co-formation with Mars, the capture of objects coming close to Mars, or the impact of a large body on Mars and the formation of the moons from impact ejecta. In order to find out which of the three scenarios is the most probable, samples from one of the martian moons dating from the time of its formation would have to be returned to Earth. With better knowledge of the martian moon formation, the relevance of current formation models of the Solar System can be better assessed. Thus such a mission would address not only Mars science, but Solar System science in general.

The Science Definition Team concluded that Phobos would be the more interesting moon. Deimos seems to be covered with a thick layer of regolith that accumulated after its formation, thus covering the pristine material that would provide evidence of the formation history of the moons.

Mission Configuration

A previous ESA study of a Deimos sample return technology reference mission produced a design based on a Soyuz launcher, sending a spacecraft with a transfer stage and an Earth Reentry Capsule (ERC). The design was looked at again in an ESA-internal CDF study in 2011 in an attempt to adapt it to Phobos, but was found to be marginal with a Soyuz launch. A second CDF study in 2012 showed a feasible mission scenario based on an Ariane 5 launch. The spacecraft composite would land on Phobos, stay for just a few minutes on the surface, and lift off again after sampling. The landing spacecraft would stay in orbit around Phobos while a smaller return spacecraft made the journey back to Earth with the capsule. Finally, the ERC would bring the sample down through Earth's atmosphere.

Further information about the Martian Moon Sample Return mission can be found at *http://exploration.esa.int/science-e/www/object/index.cfm?fobjectid=44995*

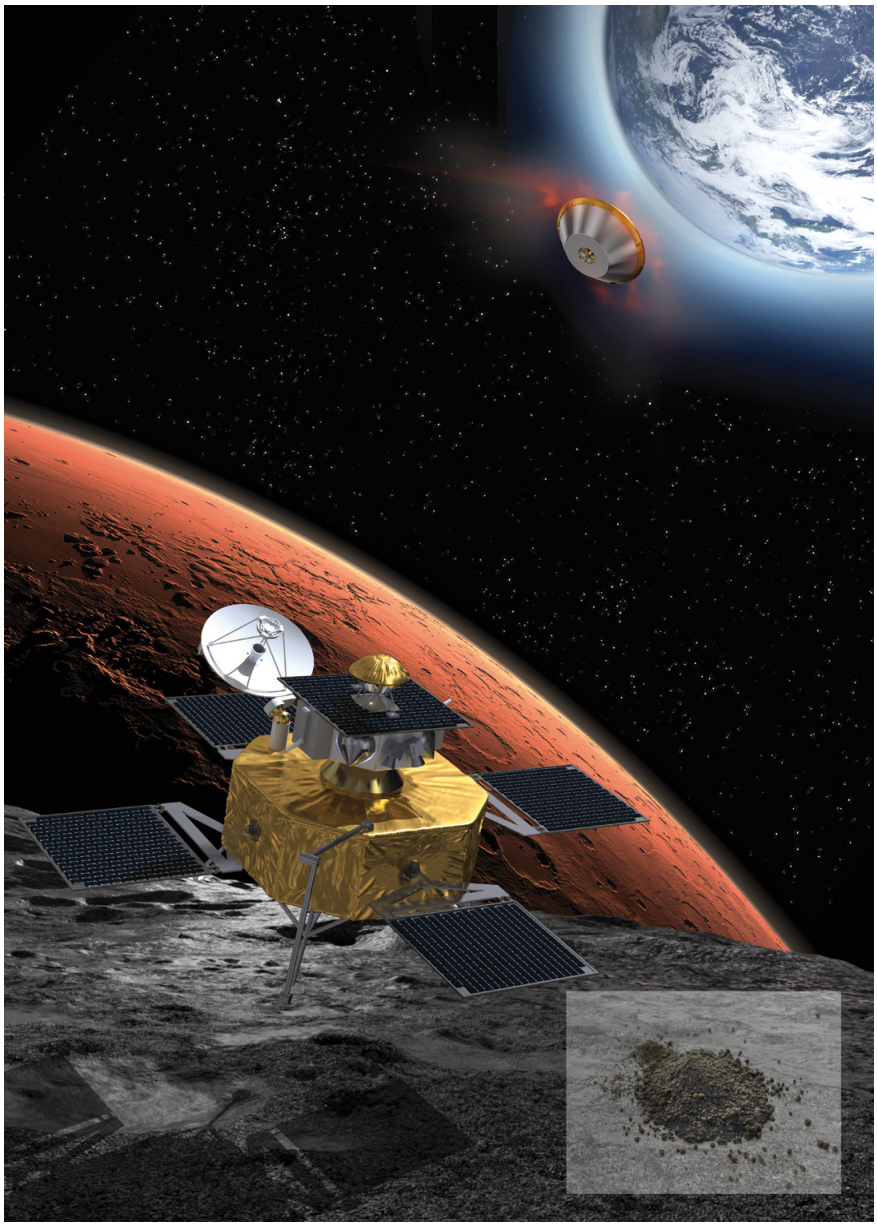

Figure 5.12.1. The Martian Moon Sample Return spacecraft at Phobos. The lander is at the bottom, with the Earth Return spacecraft above. The dome-shaped object at the very top is the Earth Reentry Capsule, which will bring the sample back through Earth's atmosphere.

Status

The results of the CDF study, together with those of the Mars Network Science Mission and two other industrial studies (Mars precision landing and Mars Sample Return orbiter), have been presented to ESA's advisory structure. A decision on whether and how to continue this study is expected in mid-2012.

→ ACRONYMS AND ABBREVIATIONS

Acronyms and Abbreviations

3DpQCT	Three-Dimensional peripheral Quantitative Computed Tomography
ACC	Accelerometer
ACES	Atomic Clock Ensemble in Space (ISS)
ACIA	Arctic Climate Impact Assessment
ACIS	Advanced CCD Imaging Spectrometer (ATHENA)
ACS	Advanced Camera for Surveys (HST); Atmospheric Composition Studies (ExoMars)
A-DCS	Advanced Data Collection System (MetOp)
ADM	Atmospheric Dynamics Mission – Aeolus
ADR	Adiabatic Demagnetisation Refrigerator (SPICA)
AGN	Active Galactic Nuclei
AIA	Atmospheric Imaging Assembly (SDO)
AIO	Archive Inter-Operability system
AIS	Automatic Identification System (ISS)
ALADIN	Atmospheric Laser Doppler Instrument (ADM-Aeolus)
ALICE	Rosetta Orbiter UV imaging spectrometer (Rosetta Lander)
ALMA	Atacama Large Millimetre Array
ALTEA	Anomalous Long-Term Effects in Astronauts' Central Nervous System(ISS)
AMI	Active Microwave Instrument (ERS)
AMSU	Advanced Microwave Sounding Unit (MetOp)
AO	Announcement of Opportunity
APXS	α-Particle X-ray Spectrometer (Rosetta)
aRED	advanced Resistance Exercise Device (ISS)
ARISS	Amateur Radio on the ISS (ISS)
ArtEMISS	Arthrospira sp. Gene Expression and mathematical Modelling in the ISS (ISS)
ASAR	Advanced Synthetic Aperture Radar (Envisat)
ASCAT	Advanced Scatterometer (ERS and MetOp)
ASCAT SAG	Advanced Scatterometer Science Advisory Group (ERS)
ASI	Agenzia Spaziale Italiana (Italian Space Agency)
ASIM	Atmosphere–Space Interactions Monitor (ISS)
ASM	Absolute Scalar Magnetometer (Swarm)
ASPERA	Analyser of Space Plasma and Energetic Atoms (Mars Express/Venus Express)
ASPOC	Active Spacecraft Potential Control (Cluster)
ATHENA	Advanced Telescope for High-Energy Astrophysics
ATLID	Atmospheric Lidar (EarthCARE)
ATOX	Atomic Oxygen
ATSR	Along Track Scanning Radiometer (ERS)
ATV	Automated Transfer Vehicle (ISS)
AU	Astronomical Unit
AVHRR	Advanced Very-High-Resolution Radiometer (MetOp)
BAT	Burst Alert Telescope (Swift)
BBR	Broad-Band Radiometer (EarthCARE)
BELA	BepiColombo Laser Altimeter (BepiColombo)
BIM-2	Biology in Microgravity experiment (ISS)
BIOMICS	BIO-Mimetic and Cellular Systems (Sounding Rockets)
BOF	Bogart Operations Facility (SOHO)
BUBSUS	Bubble Suspension in Microgravity (Drop Towers)
CAA	Cluster Active Archive
CADTS	Centre Aval de Traitement des Donnees SMOS (France)
CALIPSO	Cloud–Aerosol Lidar and Infrared Pathfinder Satellite Observation
Cal/Val	Calibration and Validation
CalTech	California Institute of Technology (USA)
CANDELS	Cosmic Assembly Near-infrared Deep Extragalactic Legacy Survey
CAPS	Cassini Plasma Spectrometer (Cassini-Huygens)
CarbonSat	Carbon Monitoring Satellite
CASSE	Comet Acoustic Surface Sounding Experiment (Rosetta)
CASSIS	Colour and Stereo Surface Imaging System (ExoMars)
CATDS	Centre Aval de Traitement des Données SMOS (France)
CCD	Charge-Coupled Device
CCO	Central Compact Object
CDA	Cosmic Dust Analyser (Cassini-Huygens)
CDAP	Cassini Data Analysis Program (NASA)
CDF	Concurrent Design Facility (ESTEC)
CDFS	Chandra Deep Field South
CDN	Content Delivery Network (ERS-2)
CDR	Critical Design Review
CDS	Coronal Diagnostics Spectrometer (SOHO)
CELIAS	Charge, Element and Isotope Analysis System (SOHO)
CERASP	Cellular Responses to Radiation in Space
CERN	Organisation Européenne pour la Recherche Nucléaire / European Organization for Nuclear Research (Geneva, Switzerland)
CESR	Centre d'Etude Spatiale des Rayonnements (Toulouse, France)

CETP	Centre d'Etude des Environnements Terrestre et Planétaires (France)
CETSOL	Columnar-to-Equiaxed Transition in Solidification Processing (ISS)
CIMEX	Convection and Interfacial Mass Exchange (ISS)
CIRS	Composite Infrared Spectrometer (Cassini-Huygens)
CIS	Cluster Ion Spectrometry
CIVA	Comet nucleus Infrared and Visible Analyzer (Rosetta Lander)
CLASH	Cluster Lensing And Supernova survey with Hubble
CLUPI	Close-Up Imager (ExoMars Rover)
CMB	Cosmic Microwave Background
CME	Coronal Mass Ejection
CNES	Centre National d'Etudes Spatiales (France)
CNR/IREA	Consiglio Nazionale delle Ricerche (National Research Council) / Institute for Electromagnetic Sensing of the Environment (Italy)
CNRS	Centre National de la Recherche Scientifique (France)
CNSA	China National Space Administration
Co-I	Co-Investigator
COBE	Cosmic Background Explorer (NASA)
COMSS	Coastal Oceans Monitoring Satellite System
CONSCIOUS	Consequences of Stress Challenges on Stress Response Systems and Immunity in Space (ISS)
CONSERT	Radio sounding, nucleus tomography (Rosetta)
CoReH$_2$O	Cold Regions Hydrology High-resolution Observatory
COROT	Convection, Rotation and Planetary Transits
COS	Cosmic Origins Spectrograph (HST)
COSAC	Comet Sampling and Composition Experiment (Rosetta)
COSIMA	Cometary Secondary Ion Mass Analyser (Rosetta)
COSPAR	Committee on Space Research
COSTEP	Comprehensive SupraThermal Energetic Particle analyser (SOHO)
CoSyMONa	Combustion Synthesis of Metal Oxide Nanoparticles processes (Drop Towers)
CPR	Cloud Profiling Radar
CP34	SMOS Level 3/4 Processing Centre (Spain)
CRISM	Compact Reconnaissance Imaging Spectrometer for Mars (MRO, Mars Express)
CSA	Canadian Space Agency
CSDS	Cluster Science Data System
CSRSR	Center for Space and Remote Sensing Research (Taiwan)
CSSAR	Centre for Space Science and Applied Research (China)
CSTARS	Center for Spatial Technologies and Remote Sensing (University of California, Davis)
C1XS	Chandrayaan-1 X-ray Spectrometer
DCS	Data Collection System (MSG)
DEBIE-2	DEBris In-orbit Evaluator-2 (ISS)
DEM	Digital Elevation Model
DEX	Dexterous Manipulation payload (Parabolic Flight)
DFACS	Drag-free and Attitude Control System (LISA Pathfinder)
DFVLR	now the German Aerospace Center, DLR
DIM	Dust Impact Monitor (Rosetta Lander)
DIRSOL	DIRectional SOLidification (ISS)
DLR	Deutsches Zentrum für Luft- und Raumfahrt / German Aerospace Center
DOBIES	Dosimetry for Biological Experiments in Space (ISS)
DORIS	Doppler Orbitography and Radio Positioning Integrated by Satellite (Envisat)
DOSIS	Dose Distribution inside the ISS (ISS)
DOSTEL	Dosimetric Telescope (ISS)
DPAC	Data Processing and Analysis Consortium (Gaia)
DPACE	DPAC Executive Committee (Gaia)
DPGS	Data Processing Ground Segment
DRS	Disturbance Reduction System (NASA)
DSC	Diffusion and Soret Coefficient measurements (SODI, ISS); Data Collection System (MSG)
DSLP	Dual Segmented Langmuir Probe (Proba-2)
DSN	Deep Space Network (NASA)
DSP	Double Star Programme (China)
DTM	Digital Terrain Model
DUST	Cosmic Dust experiment (Ulysses)
DWL	Doppler Wind Lidar
DWP	Digital Wave Processing experiment (Cluster)
EAF	Experimenters' Analysis Facility (SOHO)
EARSC	European Association of Remote Sensing Companies
EARSeL	European Association of Remote Sensing Laboratories
EarthCARE	Earth Cloud, Aerosol and Radiation Explorer
EChO	Exoplanet Characterisation Observatory
ECMWF	European Centre for Medium-Range Weather Forecasts
ECV	Essential Climate Variable (IPCC)
EDI	Electron Drift Instrument (Cluster)
EDM	Entry, Descent and Landing Demonstrator Module (ExoMars)
EDOS	Early Detection of Osteoporosis in Space (ISS)

EE	Earth Explorer
EEA	European Environment Agency
EEG	Electroencephalograph
EFI	Electrical Field Instrument (Swarm)
EFW	Electric Field and Wave experiment (Cluster)
EGG	Electrostatic Gravity Gradiometer (GOCE)
EIS	EUV Imaging Spectrometer (Hinode)
EIT	Extreme-ultraviolet Imaging Telescope (SOHO)
EJSM	Europa Jupiter System Mission; renamed Jupiter Icy moon Explorer (JUICE)
ELIPS	European Programme for Life and Physical Sciences in Space
EMC	Euclid Mission Consortium
EML	ElectroMagnetic Levitator (ISS)
ENSO	El Niño/La Niña–Southern Oscillation
EO	Earth observation
EOEP	Earth Observation Envelope Programme
EOF	Experimenters' Operations Facility (SOHO)
EPD	Energetic Particle Detector (Solar Orbiter)
EPIC	European Photon Imaging Camera (XMM-Newton)
EPOXI	Extrasolar Planet Observation and Deep Impact Extended Investigation (NASA)
EPS	Eumetsat Polar System (MetOp/IJPS)
ERB 2	Erasmus Recording Binocular 2 (ISS)
ERC	Earth Reentry Capsule (Martian Moon Sample Return mission)
ERCSC	Early Release Compact Source Catalogue (Planck)
ERNE	Energetic and Relativistic Nuclei and Electron experiment (SOHO)
ERNO	Entwicklungsring Nord (ERNO Raumfahrttechnik GmbH, Bremen, Germany)
ERS	European Remote Sensing satellites
ESA	European Space Agency
ESAC	European Space Astronomy Centre (Madrid, Spain)
ESO	European Southern Observatory
ESOC	European Space Operations Centre (Darmstadt, Germany)
ESRIN	European Space Research Institute (Frascati, Italy)
ESRO	European Space Research Organisation (forerunner of ESA)
ESTEC	European Space Research and Technology Centre (Noordwijk, the Netherlands)
EU	European Union
EuCPD	European Crew Personal Dosimeter (ISS)
EUI	Extreme Ultraviolet Imager (Solar Orbiter)
Eumetsat	European Organisation for the Exploitation of Meteorological Satellites
EuTEF	European Technology Exposure Facility (ISS)
EuTEMP	European temperature recording unit (ISS)
EUV	Extreme Ultraviolet
EUV-TEC	Extreme Ultraviolet –Total Electron Content
EVA	Extravehicular Activity
FAIR	Facility for Antiproton and Ion Research (GSI, Germany)
FAO	Food and Agriculture Organization (UN)
FASES	Fundamental and Applied Studies of Emulsion Stability (ISS)
FASTER	Facility for Adsorption and Surface Tension (ISS)
FCDP	Frequency Comparison and Distribution Package
FCI	Flexible Combined Imager (MTG)
FDM	frequency division multiplexing
FGM	Fluxgate Magnetometer
FGS	Fine Guidance Sensor (HST)
FGS/NIRISS	Fine Guidance Sensor/Near-Infrared Imager and Slitless Spectrograph (JWST)
FIPEX	Flux-(Phi)-Probe Experiment (ISS)
FIR	far infrared
FIS	Far-Infrared Surveyor (Akari)
FITS	Flexible Image Transport System
FLEX	Florescence Explorer
FoCUS	Foam Casting and Utilisation in Space (ISS)
FoV	Field of View
FPA	Focal Plane Assembly
FREND	Fine Resolution Epithermal Neutron Detector (ExoMars)
FSLP	First Spacelab Payload (ISS)
FTP	File Transfer Protocol
FTS	Fourier Transform Spectrometer
FUV	Far Ultraviolet
FWHM	Full Width at Half Maximum
GaAs	Gallium Arsenide
GAM	Gravity Assist Manoeuvre
GBM	Gamma-ray Burst Monitor (Fermi, NASA)
GBT	Green Bank Telescope (West Virginia, USA)
GCMS	Gas Chromatograph Mass Spectrometer (Cassini-Huygens)
GCOS	Global Climate Observing System
GEMS	Gravity and Extreme Magnetism Small Explorer (NASA)
GEOSS	Global Earth Observation System of Systems
GERB	Geostationary Earth Radiation Budget (MSG)
GIADA	Grain Impact Analyser and Dust Accumulator (Rosetta)
GMES	Global Monitoring for Environment and Security
GNSS	Global Navigation Satellite Systems
GOCE	Gravity field and steady-state Ocean Circulation Explorer
GOES	Geostationary Operations Environmental Satellite (NOAA)

GOLF	Global Oscillations at Low Frequencies (SOHO)
GOME	Global Ozone Monitoring Experiment (MetOp/ERS-2)
GOMOS	Global Ozone Monitoring through Occultation of Stars (Envisat)
GOODS	Great Observatories Origins Deep Survey
GOS	Global Observing System
GOSAT	Greenhouse Gases Observing Satellite
GPS	Global Positioning System
GRACE	Gravity Recovery and Climate Experiment
GRADECET	GRAvity Dependence of Columnar-to-Equiaxed Transition (ISS)
GRAS	GNSS Receiver for Atmospheric Sounding (MetOp)
GRB	Gamma-ray Burst
GSC	GMES Space Component
GSFC	Goddard Space Flight Center (NASA)
GST	Gaia Science Team
GSTP	General Support Technology Programme (SMOS)
GTS	Global Transmission Services experiment (ISS)
HEASARC	High-Energy Astrophysics Science Archive Research Center (NASA/ GSFC)
HGA	High-Gain Antenna
HFI	High-Frequency Instrument (Planck)
HICO	Hyperspectral Imager for the Coastal Ocean
HIFI	Heterodyne Instrument for the Far Infrared (Herschel)
HiLRS	High-LET Radiation Spectrometer (ISS)
HIRS	High-Resolution Infrared Radiation Sounder (MetOp)
HLOS	Horizontal Line-Of-Sight
HMI	Helioseismic and Magnetic Imager (SDO)
HPF	High-level Processing Facility
HRSC	High-Resolution Stereo Camera (Mars Express)
HSC	Herschel Science Centre
HSPOT	Herschel Observation Planning Tool
HST	Hubble Space Telescope
HTV	H-II Transfer Vehicle (ISS)
HUVEC	Human Umbilical Vein Endothelial Cell (ISS)
HXD	Hard-X-ray Detector (Suzaku)
IABG	Industrieanlagen-Betriebsgesellschaft mbH (Germany)
IAS	Institut d'Astrophysique Spatiale (CNRS, Orsay, France)
IASI	Infrared Atmospheric Sounding Interferometer (MetOp)
IBER	Investigations into Biological Effects of Radiation
IBIS	Imager on Board the Integral Satellite
IBMP	Institute for Biomedical Problems (Moscow, Russia)
ICA	Ion Composition Analyser (Rosetta)
ICE	Interférometrie Cohérente pour l'Espace
IES	Ion and Electron Sensor (Rosetta)
IFREMER	Institut Français de Recherche pour l'Exploitation de la Mer
IGACO	Integrated Global Atmospheric Chemistry Observations
IGOS	Integrated Global Observing Strategy
IJPS	Initial Joint Polar-Orbiting Operational Satellite System (NOAA/Eumetsat)
IKI	Space Research Institute (Moscow, Russian Federation)
ILSRA-09	International Life Science Research Announcement 2009
IMO	International Maritime Organization
IMPRESS	Intermetallic Materials Processing in Relation to Earth and Space Solidification (ISS)
INMS	Ion and Neutral Mass Spectrometer (Cassini-Huygens)
Integral	International Gamma-Ray Astrophysics Laboratory
IOC	Intergovernmental Oceanographic Commission
IPCC	Intergovernmental Panel on Climate Change
IPDA	International Planetary Data Alliance
IPEV	Institut Paul Emile Victor (France)
IR	Infrared
IRAS	Infrared Astronomy Satellite
IRC	Infrared Camera (Akari)
IREM	Integral Radiation Environment Monitor (Integral)
IRLS	Infrared Limb Sounder (PREMIER)
IRS	Infrared Sounding Instrument (MTG)
ISA	Italian Spring Accelerometer (BepiColombo)
ISAS/JAXA	Institute of Space and Astronautical Science, now part of JAXA (Japan)
ISDA	ISOC Science Data Archive (Integral)
ISDC	Integral Science Data Centre (Versoix, Switzerland)
ISEA	Icosahedral Snyder Equal Area (SMOS)
ISEE-2	International Sun–Earth Explorer 2
ISGRI	Integral Soft Gamma-Ray Imager
ISM	Interstellar Medium
ISO	Infrared Space Observatory
ISOC	Integral Science Operations Centre (ESAC, Madrid, Spain)
ISRO	Indian Space Research Organisation
ISS	Imaging Science Subsystem (Cassini-Huygens); International Space Station
IUE	International Ultraviolet Explorer
IVOA	International Virtual Observatory Alliance

IVIDIL	Influence of Vibrations on Diffusion in Liquids (ISS)
IWF	Institut für Weltraumforschung / Space Research Institute (Austria)
IXO	International X-ray Observatory
JAXA	Japanese Aerospace Exploration Agency
JEM-X	Joint European X-ray Monitor (Integral)
JEPPF	Joint European Partial-*g* Parabolic Flight Campaign
JEREMI	Japanese–European Research Experiments on Marangoni Instabilities
JPL	Jet Propulsion Laboratory (NASA)
JSOC	Joint Science Operations Centre (RAL, UK)
JUICE	Jupiter Icy moon Explorer
JWST	James Webb Space Telescope
KBO	Kuiper Belt Object
KSAT	Kongsberg Satellite Services (Hinode)
LAD	Large Area Detector (LOFT)
LASCO	Large-Angle and Spectrometric Coronagraph (SOHO)
LBR	Low Bit Rate
LCA	LISA Technology Package Core Assembly (LISA Pathfinder)
L-DAP	Lunar Dust Analysis Package (Lunar Lander)
L-DEPP	Lunar Dust Environment and Plasma Package (Lunar Lander)
LDMS	Laser Desorption Mass Spectroscopy (MOMA, ExoMars Rover)
L-VRAP	Lunar Volatiles Analysis Package (Lunar Lander)
LEOP	Launch and Early Orbit Phase
LET	Linear Energy Transfer (ISS)
LFI	Low-Frequency Instrument (Planck)
LI	Lightning Imager (MTG)
LIBS	Laser-Induced Breakdown Spectroscopy (Lunar Lander)
lidar	Light Detection And Ranging
LIFE	Lichens and Fungi Experiment (ISS)
LISA	Laser Interferometer Space Antenna; renamed the New Gravitational wave Observatory (NGO)
LLP	Living Planet Programme (ESA)
LMC	Large Magellanic Cloud; Life Marker Chip (ExoMars Rover)
LOFT	Large (X-ray) Observing Facility for Timing
LOS	Line Of Sight
LOSU	Level of Scientific Understanding
LPCE	Laboratoire de Physique et Chimie de l'Environnement et de l'Espace (France)
LPF	LISA Pathfinder; formerly SMART-2
LRM	Low-Resolution Mode (Cryosat-2)
LRR	Laser Retroreflector
LTP	LISA Technology Package (LISA Pathfinder)
LYRA	Large Yield Radiometer (Proba-2)
MAG	Dual Technique Magnetometer (Cassini-Huygens)
Ma_MISS	Mars Multispectral Imager for Subsurface Studies (ExoMars Rover)
MARES	Muscle Atrophy Research and Exercise System (ISS)
MARISS	Maritime Security Service (GMES/ERS-2)
MaRS	Radio Science Experiment (Mars Express)
MARSIS	Mars Advanced Radar for Subsurface and Ionosphere Sounding (Mars Express)
MarsXRD	Mars X-ray Diffractometer (ExoMars Rover)
MASER	Material Science Experiment Rocket (Sounding Rocket)
MCS	Mid-infrared Camera and Spectrometer (SPICA)
MDI	Michelson Doppler Imager (SOHO)
MDM	Mercury Dust Monitor (BepiColombo)
MEDET	Material Exposure and Degradation Experiment (ISS)
MEEMM	Multi-Electrode Encephalogram Measurement Module (ISS)
MELFI	Minus Eighty degree C Laboratory Freezer for the ISS
MERMAG-MGF	Mercury Magnetometer (BepiColombo)
MERIS	Medium-Resolution Imaging Spectrometer (Envisat)
MERTIS	Mercury Thermal Infrared Spectrometer (BepiColombo)
METCOMP	Metastable Solidification of Composites (ISS)
Meteosat	Meteorological satellite
METIS/COR	Multi-Element Telescope for Imaging and Spectroscopy Coronagraph (Solar Orbiter)
MetOp	Meteorological Operational Satellite
MGNS	Mercury Gamma-ray and Neutron Spectrometer (BepiColombo)
MHS	Microwave Humidity Sounder (MetOp)
MIA	Motion and Interact (ISS)
MICAST	Microstructure Formation in Casting of Technical Alloys under Diffusive and Magnetically Controlled Convective Conditions (ISS)
MicrOmega	Micro-imaging spectrometer (ExoMars Rover)
MIDAS	Micro-Imaging Dust Analysing System (Rosetta)
MIMI	Magnetospheric Imaging Instrument (Cassini–Huygens)
MIP	Mutual Impedance Probe (Rosetta); Moon Impact Probe (Chandrayaan-1)
MIPAS	Michelson Interferometer for Passive Atmospheric Sounding (Envisat)
MIRAS	Microwave Imaging Radiometer using Aperture Synthesis (SMOS)
MIRI	Mid-Infrared Instrument (JWST)
MIRO	Microwave Instrument for the Rosetta Orbiter (Rosetta)

MISSE	Materials ISS Experiment (NASA)
MIXS	Mercury Imaging X-ray Spectrometer (BepiColombo)
MNSM	Mars Network Science Mission
MOC	Mission Operations Centre
MOCISS	Monitoring the Cellular Immunity by in vitro Delayed Type Hypersensitivity assay on the ISS
MOLO	Microwave-Optical Local Oscillator (STE-QUEST)
MOMA	Mars Organic Molecule Analyser (ExoMars Rover)
MORABA	Mobile Rocket Base (DLR, Germany)
MORE	Mercury Orbiter Radio Science Experiment (BepiColombo)
MOS-CCD	Metal Oxide Semiconductor – Charge-Coupled Device
MOST	Microvariability and Oscillation of Stars (Canadian Space Agency)
MOU	Memorandum of Understanding
MMO	Mercury Magnetosphere Orbiter (BepiColombo)
MMSR	Martian Moon Sample Return mission
MPAe	Max-Planck-Institut für Aeronomy (Germany)
MPE	Max-Planck-Institut für Extraterrestrische Physik (Germany)
MPO	Mercury Planetary Orbiter (BepiColombo)
MPPE	Mercury Plasma Particle Experiment (BepiColombo)
MRI	Magnetic Resonance Imaging
MRO	Mars Reconnaissance Orbiter (NASA)
MSASI	Mercury Sodium Atmospheric Spectral Imager (BepiColombo)
MSG	Meteosat Second Generation; Microgravity Science Glovebox (ISS)
MSI	MultiSpectral Instrument (Sentinel-2)
MTG	Meteosat Third Generation
MTG-I/-S	MTG Imaging/Sounding satellites
MWL	MicroWave Link
MWR	Microwave Radiometer (ERS; Envisat)
M3	Moon Mineralogy Mapper (Chandrayaan-1)
NASA	National Aeronautics and Space Administration (USA)
NERC	Natural Environment Research Council (UK)
NGO	New Gravitational wave Observatory
NGST	Next Generation Space Telescope, renamed the James Webb Space Telescope (JWST)
NHSC	NASA Herschel Science Center
NICT	National Institute of Information and Communications Technology (Japan)
NIR	near infrared
NIRCam	Near-Infrared Camera (JWST)
NIRISS	Near-IR Imaging and Slitless Spectrograph (JWST)
NIRSpec	Near-Infrared Spectrometer (JWST)
NOAA	National Oceanic and Atmospheric Administration (USA)
NOMAD	Nadir and Occultation for MArs Discovery (ExoMars)
NORAIS	Norwegian Automatic Identification System
NRT	Near-Realtime
NS	Neutron Spectrometer (ExoMars Rover)
NSSDC	National Space Science Data Center (NASA)
N-USOC	Norwegian User Support and Operations Centre
NWP	Numerical Weather Prediction
OAIS	Open Archival Information System
OCO	Orbiting Carbon Observatory
OLCI	Ocean and Land Colour Instrument (Sentinel-3)
OM	Optical Monitor (XMM-Newton)
OMC	Optical Monitoring Camera (Integral)
OMEGA	Observatoire pour la Minéralogie, l'Eau, les Glaces et l'Activité (Mars Express)
OSIRIS	Optical and Spectroscopic Remote Imaging System (Rosetta)
OSTT	On-Station Thermal Test (LISA Pathfinder)
PACS	Photodetector Array Camera and Spectrometer (Herschel)
PADIAC	PAthway DIfferent Activators (ISS)
PAFs	Processing and Archiving Facilities (ERS-1)
PAIRITEL	Peters Automated IR Imaging Telescope
PanCam	Panoramic Camera (ExoMars Rover)
pc	parsec
PDR	Preliminary Design Review
PEACE	Plasma Electron and Current Experiment (Cluster)
PERWAVES	Percolating Reactive Waves in Particulate Suspensions (ISS)
PFS	Planetary Fourier Spectrometer (Mars Express, Venus Express)
PHARAO	Projet d'Horloge Atomique par Refroidissement d'Atomes en Orbit
PHEBUS	Probing of Hermean Exosphere by Ultraviolet Spectroscopy (BepiColombo)
PHI	Polarimetric and Helioseismic Imager (Solar Orbiter)
PI	Principal Investigator
PICsIT	Pixellated Imaging CaeSium Iodide Telescope (Integral)
PK	Plasma-Kristall experiment (ISS)
PLATO	PLAnetary Transits and Oscillations of Stars
PLEGPAY	Plasma Electron Gun Payload (ISS)

PMOD/WRC	Physikalisch–Meteorologischen Observatorium Davos und Weltstrahlungszentrum / Physical–Meteorological Observatory and World Radiation Centre (Davos, Switzerland)
PNTD	Plastic Nuclear Track Detector (ISS)
Pol-InSAR	Polarimetric Synthetic Aperture Radar Interferometry (Biomass)
PostgreSQL	Postgres Structured Query Language
PP	Permittivity Probe (SESAME, Rosetta)
PPN	Parameterised post-Newtonian (parameters) (Gaia)
PRARE	Precise Range and Range Rate Experiment (ERS)
PREMIER	PRocess Exploration through Measurement of Infrared and millimetre-wave Emitted Radiation
PRI	Photochemical Reflectance Index
Proba	Project for OnBoard Autonomy
PROCESS	PRebiotic Organic ChEmistry on the Space Station (ISS)
PromISSe	Programme for Research in Orbit Maximising the Inspiration from the Space Station for Europe (ISS)
PSA	Planetary Science Archive (ESA)
psu	Practical Salinity Unit
PWI	Plasma Wave Instrument (BepiColombo)
P2SC	Proba-2 Science Centre (Royal Observatory, Belgium)
QRT	Quasi-Realtime
QWEP	Quantum test of the Weak Equivalence Principle
QWG	Quality Working Group (ERS-2)
R3D	Radiation Risks Radiometer–Dosimeter (ISS)
RA-2	Radar Altimeter (Envisat)
RADAR	Cassini Radar instruments (Cassini-Huygens)
RAL	Rutherford Appleton Laboratory (UK)
RAPID	Research with Adaptive Imaging Particle Detectors (Cluster)
REDD	Reducing Emissions through Degradation and Deforestation (UN)
REXUS/BEXUS	Rocket and Balloon Experiments for University Students
RF	Radio Frequency; Radiative Forcing
RGS	Reflection Grating Spectrometer (XMM-Newton)
RHOCYT	Involvement of Rho family GTPases in gravity perception and reaction (ISS)
RINEX	Receiver-Independent Exchange Format (for raw satellite navigation system data)
RMOC	Rosetta Mission Operations Centre (ESOC, Darmstadt, Germany).
ROALD	ROle of Apoptosis in Lymphocyte Depression (ISS)
ROCC	Rover Operations Control Centre (Turin)
ROLIS	Rosetta Lander Imaging System (Rosetta Lander)
ROMAP	Rosetta Lander Magnetometer and Plasma Monitor (Rosetta)
ROSINA	Rosetta Orbiter Spectrometer for Ion and Neutral Analysis (Rosetta)
RPC	Rosetta Plasma Consortium
RPW	Radio and Plasma Waves Experiment (Solar Orbiter)
RPWS	Radio and Plasma Wave Science (Cassini-Huygens)
RSI	Radio Science Experiment (Rosetta)
RSOC	Rosetta Science Operations Centre (ESAC, Villafranca, Spain)
RSR	Rigid Solar Reflector (ISS)
RSS	Radio-Science Instrument (Cassini-Huygens)
RTG	Radioisotope Thermoelectric Generator (ExoMars)
RUBI	Reference multiscale Boiling Investigation (ISS)
RXTE	Rossi X-ray Timing Explorer
SAG	Science Advisory Group (ESA)
SAR	Synthetic Aperture Radar
SARA	Sub-keV Atom Reflecting Analyser (Chandrayaan-1)
SARIn	Synthetic Aperture Radar Interferometry (CryoSat)
SAS	Scientific Analysis Software (XMM-Newton)
SBAS–InSAR	Small Baseline Subset–Interferometric SAR (ERS-2)
SCI	SPICA Coronographic Instrument
SCIAMACHY	SCanning Imaging Absorption SpectroMeter for Atmospheric CartograpHY (Envisat)
SDD	Silicon Drift Detector (LOFT)
SDO	Solar Dynamics Observatory (NASA)
SD2	Sample acquisition system (Rosetta)
SEBA	Solidification along an Eutectic Path in Binary Alloys (ISS)
SEE	Solar EUV Experiment (NASA)
SEM	Solar EUV Monitor (SOHO)
SERENA	Search for Exosphere Refilling and Emitted Neutral Abundances (BepiColombo)
SESAME	Surface Electric, Seismic and Acoustic Monitoring Experiment (Rosetta)
SETA	Solidification along a Eutectic path in Ternary Alloys (ISS)
SEVIRI	Spinning Enhanced Visible and Infrared Imager (MSG)
SIDC	Solar Influence Data Centre (Brussels, Belgium)

SIR	SMART Infrared Spectrometer (SMART-1)
SIR-2	SMART Near-Infrared Spectrometer (Chandrayaan-1)
SIRAL	Synthetic Interferometric Radar Altimeter (CryoSat)
SIS	Superconductor–Insulator–Superconductor
SIXS	Solar Intensity X-ray Spectrometer (BepiColombo MPO)
SLSTR	Sea and Land Surface Temperature Radiometer (Sentinel-3)
SMART	Small Mission for Advanced Research in Technology
SMEs	Small and Medium Enterprises
SMILES	Superconducting SubMIllimeter-wave Limb-Emission Sounder (JAXA)
SMOS	Soil Moisture and Ocean Salinity
SMOV	Servicing Mission Orbital Verification (HST)
SNC	Shergotty, Nakhla, Chassigny (meteorites)
SNR	Supernova Remnant
SNSB	Swedish National Space Board
SOC	Science Operations Centre
SODI	Selectable Optical Diagnostic Instrument (ISS)
SOGS	Satellite Operations Ground Segment (SMOS)
SOHO	Solar and Heliospheric Observatory
SolACES	Solar Auto-Calibrating Extreme UV Spectrometer (ISS)
SOLO	SOdium LOading in Microgravity (ISS)
SoloHI	Solar Orbiter Heliospheric Imager (Solar Orbiter)
SOLSPEC	Solar Spectral irradiance experiment (ISS)
SORCE	Solar Radiation and Climate Experiment (NASA)
SOT	Solar Optical Telescope (Hinode)
SOURCE-2	SOUnding Rocket Compere Experiment-2
SOVIM	Solar Variability and Irradiance Monitoring instrument (ISS)
SP	Spectropolarimeter (Hinode)
SPC	Science Programme Committee
SPHINX	SPaceflight of Huvec: an Integrated eXperiment (ISS)
SPI	Spectrometer on Integral
SPICA	Space Infrared Telescope for Cosmology and Astrophysics (JAXA)
SPICAM	Spectroscopy for the Investigation of the Characteristics of the Atmosphere of Mars (Mars Express)
SPICAV/SOIR	Spectroscopy for the Investigation of Characteristics of the Atmosphere of Venus/Solar Occultation at Infrared (Venus Express)
SPICE	Spectral Imaging of the Coronal Environment (Solar Orbiter)
SPIRE	Spectral and Photometric Imaging Receiver (Herschel)
SPO	Silicon Pore Optics
SPORES	Small Probes for Orbital Return of Experiments
SPOT	Satellite pour l'Observation de la Terre
SREM	Space Radiation Environment Monitor (Rosetta)
SRON	Space Research Organisation Netherlands
SRTM	Shuttle Radar Topography Mission (ERS-2)
SSC	Survey Science Consortium (XMM-Newton); Swedish Space Corporation
SSD	Silicon Scintillator Device (ISS)
SSTI	Satellite-to-Satellite Tracking Instrument (GOCE)
STAFF	Spatio-Temporal Analysis of Field Fluctuations (Cluster)
STScI	Space Telescope Science Institute (USA)
STEAMR	Stratosphere–Troposphere Exchange And climate Monitor Radiometer (PREMIER)
STEREO-A/-B	Solar–Terrestrial Relations Observatory satellites (NASA)
STE-QUEST	Space–Time Explorer and Quantum Test of the Equivalence Principle
STIM	Signal Transduction in human T-cells In Microgravity (ISS)
STIS	Space Telescope Imaging Spectrograph (HST)
STIX	Spectrometer/Telescope for Imaging X-rays (Solar Orbiter)
STM	Structural/Thermal Model (BepiColombo)
STS	Space Transportation System (NASA)
STSP	Solar-Terrestrial Science Programme (ESA)
SUMER	Solar UV Measurements of Emitted Radiation (SOHO)
SuperSTAR	Super Space Three-axis Accelerometer for Research (GRACE)
SURE	Supporting the Use of Research Evidence
SVM	Service Module (XMM-Newton)
SWA	Solar Wind Analyser (Solar Orbiter)
SWAN	Solar Wind ANisotropies (SOHO)
SWAP	Sun Watcher using Active Pixel System Detector and Image Processing (Proba-2)
SWE	Snow Water Equivalent
SWIR	Short-Wave Infrared
SYMBIO-SYS	Spectrometers and Imagers for MPO BepiColombo Integrated Observatory System
TC	Tan Ce ('Explorer', China)
TEC	Total Electron Content
TEPC	Tissue-Equivalent Proportional Counter (ISS)
TES	Transition-edge sensor (SPICA)
Texus	Technologische EXperimente unter Schwerelosigkeit (Sounding Rockets)
TGO	Trace Gas Orbiter (ExoMars)
TIMED	Thermosphere, Ionosphere, Mesosphere Energetics and Dynamics satellite (NASA)
TIR	Thermal Infrared

TLD	Thermoluminescence Dosimeter (ISS)
TOA	Top Of the Atmosphere
TOQM	Thermal Optical Qualification Model (LISA Pathfinder)
TPMU	Thermal Plasma Measurement Unit for Microsatellites (Proba-2)
TRL	Technology Readiness Level
TRP	Technology Research Programme (ESA)
TSI	Total Solar Irradiance
TT&C	Telemetry, Tracking and Command
UAA	Ulysses Active Archive (ESTEC)
UKIDSS	UK Infrared Deep Sky Survey
UKIRT	UK Infrared Telescope (Hawaii)
ULF	Utilization and Logistics Flight
UML	Unified Modeling Language
UNDCP	United Nations International Drug Control Program
UNEP	United Nations Environment Programme
UNESCO	United Nations Educational, Scientific and Cultural Organization
UNFCCC	United Nations Framework Convention on Climate Change
UNILAC	Universal Linear Accelerator (GSI Helmholtz Centre, Germany)
UNOOSA	United Nations Office for Outer Space Affairs
UT	Universal Time
UTC	Coordinated Universal Time
UTLS	Upper Troposphere and Lower Stratosphere
UV	Ultraviolet
UVCS	Ultraviolet Coronagraph Spectrometer (SOHO)
UVIS	Ultraviolet Imaging Spectrometer (Cassini-Huygens)
UVN	Ultraviolet/Visible/Near-infrared instrument (Sentinel-4)
VeRa	Venus Express Radio Science Experiment (Venus Express)
VFM	Vector Field Magnetometer (Swarm)
VHF	Very High Frequency
VIMS	Visible and Infrared Mapper Spectrometer (Cassini-Huygens)
VIP-GRAN	Vibration-Induced Phenomena in GRANular media (ISS)
VIPIL	VIbrational Phenomena In Liquids (ISS)
VIRGO	Variability of Solar Irradiance and Gravity Oscillations (SOHO)
VIRTIS	Visible-Infrared Thermal Imaging Spectrometer (Rosetta/Venus Express)
VIS	Visible
VLT	Very Large Telescope (European Southern Observatory)
VMC	Video Monitoring Camera (Mars Express); Venus Monitoring Camera (Venus Express)
VNIR	Visible and Near-Infrared
VO	Virtual observatory
VO_2 Max	Maximum Volume of Oxygen (ISS)
VOC	Volatile Organic Compound
WAICO	Waving and Coiling of Arabidopsis Roots at Different *g*-levels (ISS)
WBD	Wide Band Data (Cluster)
WCRP	World Climate Research Programme
WEAR	Wearable Augmented Reality (ISS)
WEC	Wave Experiment Consortium (Cluster)
WFI	Wide Field Imager (ATHENA)
WFM	Wide Field Monitor (LOFT)
WHIM	Warm-Hot Intergalactic Medium
WHISPER	Waves of High Frequency and Sounder for Probing of Electron density by Relaxation (Cluster)
WHT	William Herschel Telescope (La Palma)
WISDOM	Water Ice and Subsurface Deposit Information On Mars (ExoMars Rover)
WMO	World Meteorological Organization
XIS	X-ray Imaging Spectrometer (Suzaku)
XMM	X-ray Multi-Mirror Mission; renamed XMM-Newton
XMS	X-ray Microcalorimeter Spectrometer (ATHENA)
XRMON	X-Ray Monitoring on sounding rockets
XRS	X-Ray Microcalorimeter (Suzaku)
XRT	X-Ray Telescope (Hinode)
XSA	XMM-Newton Science Archive
XSM	X-ray Solar Monitor (SMART-1; Chandrayaan-1)
YING	Yeast In No Gravity (ISS)
YSO	Young Stellar Object
ZARM	Zentrum für Angewandte Raumfahrttechnologie und Mikrogravitation / Center of Applied Space Technology and Microgravity (Germany)

ESA Member States

Austria
Belgium
Czech Republic
Denmark
Finland
France
Germany
Greece
Ireland
Italy
Luxembourg
Netherlands
Norway
Portugal
Romania
Spain
Sweden
Switzerland
United Kingdom

An ESA Communications Production